LEABHARLANN CHOLÁISTE NA TRÍONÓIDE, BAILE ÁTHA CLIATH | TRINITY COLLEGE LIBRARY DUBLIN
Ollscoil Átha Cliath | The University of Dublin

**Terms and Conditions of Use of Digitised Theses from Trinity College Library Dublin**

**Copyright statement**

All material supplied by Trinity College Library is protected by copyright (under the Copyright and Related Rights Act, 2000 as amended) and other relevant Intellectual Property Rights. By accessing and using a Digitised Thesis from Trinity College Library you acknowledge that all Intellectual Property Rights in any Works supplied are the sole and exclusive property of the copyright and/or other IPR holder. Specific copyright holders may not be explicitly identified. Use of materials from other sources within a thesis should not be construed as a claim over them.

A non-exclusive, non-transferable licence is hereby granted to those using or reproducing, in whole or in part, the material for valid purposes, providing the copyright owners are acknowledged using the normal conventions. Where specific permission to use material is required, this is identified and such permission must be sought from the copyright holder or agency cited.

**Liability statement**

By using a Digitised Thesis, I accept that Trinity College Dublin bears no legal responsibility for the accuracy, legality or comprehensiveness of materials contained within the thesis, and that Trinity College Dublin accepts no liability for indirect, consequential, or incidental, damages or losses arising from use of the thesis for whatever reason. Information located in a thesis may be subject to specific use constraints, details of which may not be explicitly described. It is the responsibility of potential and actual users to be aware of such constraints and to abide by them. By making use of material from a digitised thesis, you accept these copyright and disclaimer provisions. Where it is brought to the attention of Trinity College Library that there may be a breach of copyright or other restraint, it is the policy to withdraw or take down access to a thesis while the issue is being resolved.

**Access Agreement**

By using a Digitised Thesis from Trinity College Library you are bound by the following Terms & Conditions. Please read them carefully.

I have read and I understand the following statement: All material supplied via a Digitised Thesis from Trinity College Library is protected by copyright and other intellectual property rights, and duplication or sale of all or part of any of a thesis is not permitted, except that material may be duplicated by you for your research use or for educational purposes in electronic or print form providing the copyright owners are acknowledged using the normal conventions. You must obtain permission for any other use. Electronic or print copies may not be offered, whether for sale or otherwise to anyone. This copy has been supplied on the understanding that it is copyright material and that no quotation from the thesis may be published without proper acknowledgement.

# Molecular targeting of HPV oncogenes and oncogenic protein.

By

Cathy Spillane, B.Sc. (Hons)

Department of Histopathology and Morbid Anatomy,

Trinty College, Dublin.

A thesis submitted to Trinity College,

University of Dublin,

For the degree of

Doctor of Philosophy

November 2009

Under the supervision of Professor John O'Leary.

TRINITY COLLEGE
2 4 MAR 2011
LIBRARY DUBLIN
THESIS
8974

## Declaration

I declare that this is my own work and has not been submitted previously for a PhD degree at this or any other university. I agree that the library may lend or copy this thesis on request.

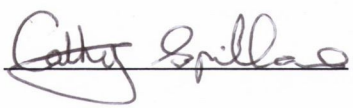

Cathy Spillane

Dedicated

to my beloved grandmother ‘Mo’

# Table of contents


Acknowledgements I

Summary III

Abbreviations V

Publications IX

**1.0 Introduction 1**

**1.1 Cervical Cancer 2**

**1.2 Cervical Cancer and Human Papillomavirus Infection 5**

**1.3 Natural HPV infection 8**

**1.4 HPV structure 10**

**1.5 The 'productive' HPV life cycle 12**

1.5.1 Infection 12

1.5.2 Genome maintenance 15

1.5.3 Genome amplification 16

1.5.4 Virus assembly and release 20

**1.6 HPV and carcinogenesis 22**

1.6.1 Integration 22

1.6.2 The E6 Protein 25

1.6.2.1 Structure 25

1.6.2.2 Apoptosis Inhibition 27

1.6.2.3 Induction of telomerase activity 29

1.6.2.4 Targeting and distruption of PDZ proteins 30

1.6.3 The E7 protein 32

1.6.3.1 Structure 32

1.6.3.2 Dysregulation of G1/S Checkpoint – Pocket Protein Family 33

1.6.3.3 Dysregulation of the cell cycle – Rb independent 34

1.6.3.4 Transcriptional regulation 36

1.6.4 The interplay between high-risk E6 and E7 37

**1.7 A new era in cervical cancer driven by molecular knowledge 40**

1.7.1 Therapeutic nucleic acids a treatment option for cervical cancer 42

1.7.1.1 RNA interference 44

1.7.2 Other gene targeted therapies for cervical cancer 49

**1.8 Summary 52**

**1.9 Study Aims 53**

**1.10 References 54**

**2.0 Materials and methods 91**

**2.1 Cell culture of cervical cancer cell lines 92**

2.1.1 Cell culture protocols 93

2.1.2 Mycoplasma testing 94

2.1.2.1 Mycoplasma detection assay 95

**2.2 Transfection of synthetic siRNA 96**

2.2.1 Transient transfection of cells in 96 well format 97

2.2.1.1 Lipofectamine™ RNAiMAX 98

2.2.1.2 NeoFx™ siPORT ™ 98

2.2.1.3 HIPERFECT 98

2.2.2 Transient transfection of SiHa cells in a 6-well format 99

**2.3 Total RNA extraction 100**

2.3.1 Cell-to-Signal™ Lysis Buffer 100

2.3.1.1 Protocol 100

2.3.2 mirVana™ miRNA Isolation Kit 101

2.3.2.1 Protocol 101

2.3.3 DNase digestion 102

**2.4 Nucleic acid quantification and quantitation** **103**

2.4.1 NanoDrop® ND-1000 103

2.4.1.1 Protocol 103

2.4.2 2100 Bioanalyzer 104

2.4.2.1 Protocol 105

**2.5 TaqMan® PCR** **106**

2.5.1 TaqMan® PCR primer and probes 108

2.5.2 TaqMan® two step RT-PCR 108

2.5.2.1 cDNA reaction 109

2.5.2.2 TaqMan® PCR 109

2.5.2.3 Reference genes 110

2.5.3 TaqMan® Low Density Arrays 110

2.5.3.1 cDNA reaction 110

2.5.3.2 TaqMan® Low Density Array RT-PCR 111

2.5.3.3 Reference genes 112

2.5.3 TaqMan® RT-PCR analysis – relative quantification 113

2.5.3.1 Comparative $C_T$ method 114

**2.6 Affymetrix microarray analysis** **115**

2.6.1 Affymetrix GeneChip® Gene 1.0 ST array technology 116

2.6.2 Affymetrix GeneChip® analysis protocol 119

2.6.2.1 Double stranded cDNA synthesis 119

2.6.2.2 cRNA synthesis and purificationDNA 120

2.6.2.3 Single stranded DNA synthesis and purification 120

2.6.2.4 Fragmentation and labelling of single stranded 121

2.6.2.5 Hybridisation to GeneChip® Gene 1.0 ST arrays 121

2.6.2.6 GeneChip® washing, staining and scanning 121

**2.7 Western blot analysis** **122**

2.7.1 Protein extraction using radioimmunoprecipitation buffer 122

2.7.2 Protein quantification 123

2.7.2.1 BCA™ assay protocol 123

2.7.3 SDS polyacrylamide gel electrophoresis 124

2.7.4 Transfer of proteins to membrane 124

2.7.5 Antibody blotting 124

**2.8 Flow cytometry 126**

2.8.1 Apoptosis detection analysis: FITC Annexin V / PI analysis 128

2.8.1.1 Assay protocol 129

2.8.1.2 Flow cytometry analysis 129

2.8.2 Cell Cycle Analysis: BrdU/PI Analysis 133

2.8.2.1 Assay protocol 133

2.8.2.2 Flow cytometry analysis 134

**2.9 $PGE_2$ immunoassay 135**

2.9.1 Assay protocol 135

**2.10 Analysis of *in vitro* cell growth 136**

2.10.1 Assay protocol 136

**2.11 References 137**

**3.0 Silecing of HPV16 oncogenes 139**

**3.1 Introduction 140**

**3.2 Chapter Aim 150**

**3.3 Materials and Methods 151**

3.3.1 Cell culture 151

3.3.2 siRNA design 151

3.3.2.1 Design of HPV16 E7 targeting siRNA 151

3.3.2.2 In-house designed HPV16 E7 siRNA 153

3.3.2.3 Ambion™ designed HPV16 E7 siRNA 155

3.3.3 Transfections 156

3.3.4 TaqMan® RT-PCR 157
3.3.5 Western Blot Analysis 159
3.3.6 Analysis of in vitro cell growth 160
3.3.6.1 Evaluating cell toxicity 160
3.3.6.2 Evaluating cell viability 160
3.3.7 Cell cycle analysis 160
3.3.8 Apoptosis analysis 161
3.3.9 Statistical analysis 161
**3.4 Results** **162**
3.4.1 Evaluation of optimal knockdown conditions for SiHa & HeLa cells 162
3.4.1.1 Assessment of transfection reagents 162
3.4.1.2 Assessment of negative control siRNA 167
3.4.1.3 Assessment of positive control siRNA 172
3.4.2 HPV16 E7 siRNA silence expression of both E6 and E7 174
3.4.3 E7 siRNA inhibit cell proliferation 179
3.4.4 E7 siRNA do not induce apoptosis in SiHa cells 183
**3.5 Discussion** **196**
**3.6 Reference** **204**

**4.0 Genome expression profiling of E6/E7 silenced cervical cancer cells** **211**
**4.1 Introduction** **212**
**4.2 Chapter Aim** **215**
**4.3 Materials and Methods** **216**
4.3.1 Samples 216
4.3.2 RNA quantity and quality 216
4.3.3 Affymetrix GenChip® Gene 1.0 ST microarray 216
4.3.4 Quality control analysis of microarrays 217
4.3.5 Data analysis of microarrays 221

4.3.5.1 Probe transformation and summarisation 221
4.3.5.2 Identification of expressed genes 222
4.3.5.3 Comparative analysis between groups 222
4.3.5.4 Analysis of gene target lists 224
4.3.6 TaqMan® low density arrays 225
**4.4 Results** **226**
4.4.1 Microarray quality control 226
4.4.1.1 RNA for microarray gene expression analysis 226
4.4.1.2 Initial quality control assessment of microarrays 228
4.4.1.3 Quality control assessment of microarrays by calculated quality metrics 229
4.4.4 Differential gene expression analysis 232
4.4.5 Comparative analysis of the differentially expressed genes 234
4.4.6 Validation of microarray results by TaqMan® RT-PCR 244
4.4.7 Gene ontology analysis 256
**4.5 Discussion** **260**
**4.6 References** **276**

**5.0 Sulindac induces apoptosis and E7 degradation in HPV18 cervical cancer cells** **287**
**5.1 Introduction** **288**
**5.2 Chapter Aim** **297**
**5.3 Methods** **298**
5.3.1 Cell culture 298
5.3.2 Drug treatment of cells 298
5.3.3 MTT assay 299
5.3.3.1 Defining the exponential growth phase 299
5.3.3.2 Cell viability 299

5.3.4 Cell cycle analysis 300

5.3.5 Apoptosis analysis 300

5.3.6 Determination of COX activity 300

5.3.7 TaqMan® RT-PCR 301

5.3.8 Western blot analysis 302

5.3.9 Stastical analysis 303

**5.4 Results 304**

5.4.1 Sulindac decreases cell viability of cervical cancer cell lines 304

5.4.2 The effect of sulindac derivatives on the growth of cervical cancer cells 312

5.4.3 Sulindac alters endogenous COX-2 activity and expression 314

5.4.4 Sulindac induces cell cycle dysregulation in HPV18 positive cells 316

5.4.5 Quantification of apoptosis 322

5.4.6 Sulindac treatment induces altered HPV18 oncogene expression 327

**5.5 Discussion 329**

**5.6 References 336**

**6.0 General Discussion 347**

**6.1 General discussion 348**

**6.2 Translation implications of this study 359**

**6.3 Future Work 361**

**6.4 Conclusion 363**

**6.5 References 365**

**Appendix 375**

## List of figures


| | | |
|---|---|---|
| Figure 1.1: | Worldwide prevalence of cervical cancer | 2 |
| Figure 1.2: | Worldwide age-specific HPV-DNA prevalence among women by country-specific development status. | 9 |
| Figure 1.3: | HPV Structure. | 11 |
| Figure 1.4: | HPV-mediated progression to cervical cancer. | 14 |
| Figure 1.5: | Schematic representation of the fragment of HPV genome integrated in the cellular genome. | 24 |
| Figure 1.6: | Splicing of HPV E6 mRNA. | 26 |
| Figure1.7: | Approaches to trigger the RNAi pathway in mammalian cells. | 48 |
| Figure 2.1: | Illustrating of a haemocytometer. | 94 |
| Figure 2.2: | Proposed mechanism of nucleotide entry into cells using cationic lipid formulations. | 96 |
| Figure 2.3: | Schematic representation of forward and reverse transfection protocols. | 97 |
| Figure 2.4: | NanoDrop® spectrophotometer sample pedestal. | 104 |
| Figure 2.5: | 2100 Bioanalyzer Electropherogram. | 105 |
| Figure 2.6: | Graphical representation of the process involved in the TaqMan® PCR. | 107 |
| Figure 2.7: | Representation of TaqMan® low density array and its features. | 111 |
| Figure 2.8: | Step by step instructions followed when performing TaqMan Low Density Array Card. | 112 |
| Figure 2.9: | An example of an amplification plot from a TaqMan® RT-PCR reaction. | 113 |
| Figure 2.10: | Types of transcripts captured by a whole-transcript assay. | 115 |
| Figure 2.11: | Affymetrix uses a combination of photolithography and combinatorial chemistry to manufacture GeneChip Arrays. | 116 |
| Figure 2.12: | Schematic of the procedure for gene expression analysis using Affymetrix. | 118 |

| | | |
|---|---|---|
| Figure 2.13: | Principle components of flow cytometer. | 127 |
| Figure 2.14: | Compensation of fluorescent signal due to annexin V-FITC and PI spectral overlap. | 131 |
| Figure 2.15: | Flow cytometry analysis of cells dual stained with annexin V-FITC and PI. | 132 |
| Figure 2.16: | Flow cytometry analysis of cells dual stained with anti-BrdU antibody-FITC and PI. | 134 |
| Figure 3.1: | Influence of siRNA and target mRNA structure on RNAi efficiency. | 145 |
| Figure 3.2: | Representation of the sequence alignment of HPV16 variants. | 153 |
| Figure 3.3: | Digramatic representation of the position of the five siRNA designed towards HPV16 E7. | 156 |
| Figure 3.4: | Evaluation of the efficiency of transfection with three different transfection reagents in SiHa and HeLa cervical cancer cells seeded at low cell concentrations. | 164 |
| Figure 3.5: | Evaluation of the efficiency of transfection with three different transfection reagents in SiHa and HeLa cervical cancer cells seeded at high cell concentrations. | 165 |
| Figure 3.6: | Effect of Lipofectamine™ RNAiMAX on cell viability. | 166 |
| Figure 3.7: | Evaluation of universal negative controls for use with SiHa and HeLa cells. | 169 |
| Figure 3.8: | Evaluation of universal negative controls for use with SiHa and HeLa cells. | 171 |
| Figure 3.9: | Silencing of GAPDH in the SiHa cell line. | 173 |
| Figure 3.10: | Silencing of HPV16 E6 and E7 RNA in the SiHa cell line. | 176 |
| Figure 3.11: | Silencing of HPV16 E6 and E7 protein in the SiHa cell line. | 178 |
| Figure 3.12: | SiHa cell viability over a 96hrs period post transfection with E7 siRNA. | 180 |
| Figure 3.13: | E7 siRNA induces significant alterations in the cell cycle of SiHa cells. | 181 |
| Figure 3.14: | Representative fluorocytograms of cell cycle analysis on SiHa cells 48hrs post E7 siRNA transfection. | 182 |

| | | |
|---|---|---|
| Figure 3.15: | E7 siRNA do not induce apoptosis by 96hrs. | 185 |
| Figure 3.16: | Representative fluorocytograms of apoptosis analysis of SiHa cells 48hrs post siRNA treatment. | 186 |
| Figure 3.17: | Representative fluorocytograms of apoptosis analysis of SiHa cells 96hrs post siRNA treatment. | 187 |
| Figure 3.18: | Representative fluorocytograms of side versus forward scatter analysis of SiHa cells 48hrs post siRNA treatment. | 188 |
| Figure 3.19: | Representative graphs of side scatter and forward scatter profiles of SiHa cells 48hrs post siRNA treatment. | 189 |
| Figure 3.20: | Representative fluorocytograms of side versus forward scatter analysis of SiHa cells 96hrs post siRNA treatment. | 190 |
| Figure 3.21: | Representative graphs of side scatter and forward scatter profiles of SiHa cells 96hrs post siRNA treatment. | 191 |
| Figure 3.22: | Light microscopic findings 24hrs post transfection. | 192 |
| Figure 3.23: | Light microscopic findings 48hrs post transfection. | 193 |
| Figure 3.24: | Light microscopic findings 72hrs post transfection. | 194 |
| Figure 3.25: | Light microscopic findings 96hrs post transfection. | 195 |
| Figure 3.26: | Effect of repressing HPV E6 and E7 genes on apoptosis. | 201 |
| Figure 4.1: | A histogram of the GC content range of the probes on the Affymetrix GeneChip® Gene 1.0 ST microarray. | 222 |
| Figure 4.2: | Assessment of the RNA quality. | 227 |
| Figure 4.3: | Diagrammatic representation of B2 illuminated regions of an Affymetrix GeneChip microarray. | 228 |
| Figure 4.4: | Quality control metrics of microarrays performed on siRNA transfected SiHa cells. | 231 |
| Figure 4.5: | Correlation between the gene expression profiles of SiHa cells transfected with E7#1, E7#3 or negative control siRNA. | 236 |
| Figure 4.6: | Comparison of the 168 differentially expressed genes identified on both the E7#1 and E7#3 microarrays. | 238 |
| Figure 4.7: | Venn diagrams illustrating the number of differentially expressed unique andcommon genes between E7#1 and E7#3 transfection in SiHa cells | 239 |

| | | |
|---|---|---|
| Figure 4.8: | Evaluating the correlation between Affymetrix microarray derived and TaqMan® RT-PCR derived gene expression values for 8 up-regulated genes. | 245 |
| Figure 4.9: | Evaluating the correlation between Affymetrix microarray derived and TaqMan® RT-PCR derived gene expression values for 24 down-regulated genes. | 246 |
| Figure 4.10: | Evaluating the correlation between Affymetrix microarray derived and TaqMan® RT-PCR derived gene expression values for 23 down-regulated genes. | 247 |
| Figure 4.11: | Evaluating the validity of 8 genes which did not meet significance parameters in E7#3 samples when analysed by TaqMan® RT-PCR but did when analysed by Affymetrix microarray analysis. | 249 |
| Figure 4.12: | Evaluating the validity of Group II and Group III differentially expressed genes. | 252 |
| Figure 4.13: | Evaluating the correlation between TaqMan® fold change values when untreated cells were applied as a calibrator and when negative control cells were applied as the calibrator. | 254 |
| Figure 4.14: | Evaluation of the gene expression profile of 68 genes in SiHa cells transfected with negative control siRNA compared to untreated SiHa. | 255 |
| Figure 4.15: | DNA replication – the formation of the licensing complex. | 266 |
| Figure 4.16: | Representative illustrations of (A) the BRCA1-dependent ubiquitin-ligase activity pathway and (B) the role of BRCA1, BRCA2 and ATR in cancer susceptibility pathway. | 272 |
| Figure 5.1: | Representative diagram of arachadonic acid cascade. | 291 |
| Figure 5.2: | Determining seeding concentration for exponential growth. | 306 |
| Figure 5.3 | Effect of sulindac on cervical cell lines. | 307 |
| Figure 5.4: | HeLa cells 24hrs after treatment with sulindac. | 308 |
| Figure 5.5: | HeLa cells 48hrs after treatment with sulindac. | 309 |
| Figure 5.6: | SiHa cells 24hrs after treatment with sulindac. | 310 |
| Figure 5.7: | SiHa cells 48hrs after treatment with sulindac. | 311 |
| Figure 5.8: | The effect of sulfide and sulfone on cervical cancer cells. | 313 |

Figure 5.9: Effect of sulindac on endogenous COX-2 expression and activity in HeLa cells. 315

Figure 5.10: Sulindac induces alterations in the cell cycle of HeLa cells. 319

Figure 5.11: Representative fluorocytograms of cell cycle analysis on HeLa cells 24hrs post sulindac treatment. 320

Figure 5.12: Representative fluorocytograms of cell cycle analysis on HeLa cells 48hrs post sulindac treatment. 321

Figure 5.13: Sulindac induces apoptosis in HeLa cells. 324

Figure 5.14: Representative fluorocytograms of apoptosis analysis on HeLa cells 24hrs post sulindac treatment. 325

Figure 5.15: Representative fluorocytograms of apoptosis analysis on HeLa cells 48hrs post sulindac treatment. 326

Figure 5.16: Effect of sulindac on endogenous HPV18 E6 and E7 expression in HeLa cells. 328

## List of tables


| | | |
|---|---|---|
| Table 1.1: | Classification of HPV types based on oncogenic potential. | 6 |
| Table 2.1: | Description of cell lines used in this study. | 92 |
| Table 3.1: | Suggested parameters for optimal design of siRNA by Ui-Tei *et al.* & *Reynolds et al.* | 143 |
| Table 3.2: | Online siRNA design tools utilised. | 154 |
| Table 3.3: | Criteria used in the selection of in-house designed HPV16 E7 targeting siRNA. | 155 |
| Table 3.4: | Description of all five siRNA designed towards HPV16 E7. | 156 |
| Table 3.5: | Transfection conditions applied for optimisation experiments | 157 |
| Table 3.6: | HPV16 E6 and E7 primer and probe sequences. | 158 |
| Table 3.7: | Antibody and corresponding dilutions used in the study. | 159 |
| Table 4.1: | 260/280 ratios and RIN numbers of RNA samples deemed suitable for microarray analysis. | 226 |
| Table 4.2: | Genes differentially regulated upon E7#1 or E7#3 siRNA induced silencing of the E6/E7 oncogenes in SiHa cells. | 233 |
| Table 4.3: | The 10 genes up-regulated by both E7#1 and E7#3 siRNA induced silencing of E6/E7. | 240 |
| Table 4.4: | The top 20 genes down-regulated by both E7#1 and E7#3 siRNA silencing of E6/E7. | 241 |
| Table 4.5: | Genes differentially regulated upon E7#1 or E7#3 siRNA induced silencing of the E6/E7 oncogenes in SiHa cells. | 243 |
| Table 4.6: | Three groups of differentially expressed genes upon E7#1 or E7#3 siRNA induced silencing of the E6/E7 oncogenes in SiHa cells. | 243 |

Table 4.7: Pearson correlation between expression values as determined by Affymetrix microarrays and TaqMan® RT-PCR. 244

Table 4.8: Pearson correlation between expression values as determined by Affymetrix microarrays and TaqMan® RT-PCR for E7 siRNA transfected SiHa cells. 248

Table 4.9: Differential gene expression of group II and III gens as determined by Affymetrix microarrays and TaqMan® RT-PCR for E7 siRNA transfected SiHa cells. 251

Table 4.10: Significantly overrepresented biological processes as defined by the DAVID database. 257

Table 4.11: Significantly overrepresented biological processes as defined by the PANTHER database. 259

Table 4.12: Significantly overrepresented pathways as defined by the PANTHER and DAVID databases. 259

Table 4.17: Centromeric proteins, kinetochore associated proteins and members of the spindle checkpoint identified within the list of 168 differentially expressed genes. 270

Table 5.1: HPV18 E6 and E7 primer and probe sequences. 302

Table 5.2: Antibody and corresponding dilutions used in the study. 303

## Acknowledgements

Firstly I would like to extend my sincerest and most heartfelt thanks to my supervisor Professor John O'Leary. His endless support, encouragement and especially his enthusiasm were and are greatly appreciated.

I would also like to extend a huge thank you to Dr. Cara Martin. Her constant support, encouragement and guidance made the work in this thesis possible.

A special thank you must also go to Professor Orla Sheils who was always there providing an open ear and invaluable advice.

To everyone in the laboratory at the Coombe Women's hospital: Louise, Jamie, Helen, Mic, Lorretto, Catriona, Sahla, Sebastain, Yvonne, Adele and Grainne. It has been a pleasure working and getting to know each and everyone one of you. Thank you for all your support and advice and for making the last three years full of fun and laughter.

To those in the Laboratory in James', thank you for looking after me and making me feel so welcome when I was working down there with you. Paul thank you for all the statistical advice, it often was sought and always provided along with a big smile.

To the girls from the PhD programme: Sinead, Therese and Christine. Starting this PhD programme four years ago I anticipated coming away with a PhD but never imagined the lifelong friends I would make in the process. For the chats, friendship and support thank you.

Michelle, your support and friendship as always makes things easier and so much more fun, thank you for being there through everything. And to all my other friends thank you for your listening ear throughout my years of study.

To Paul, where do I begin, you have been rock for the last four years, every tear and triumph you have shared with me, standing beside me supporting me when I needed it and as importantly celebrating when things went well. Thank you.

Finally, a very special thank you to my parents without your constant encouragement, support and love I would not be where I am or who I am.

## Summary

Worldwide cervical cancer is the second most common cause of cancer related death in women. Over the last three decades high-risk HPV has been conclusively established as the major etiological factor in cervical cancer and the expression of its two oncogenes, E6 and E7, are critical to the neoplastic progression. Integration of high-risk HPV and subsequent permanent expression of E6 and E7 are key events in the pathogenesis of cervical cancer. While E6 and E7 expression is necessary for the neoplastic progression of cervical cancer, their expression alone is not sufficient to induce tumourigenesis. However it is believed that the expression of these viral oncogenes produces an environment in which other pro-oncogenic alterations occur at an increased rate. The purpose of this study was to further substantiate this view, and to investigate novel pathways involved in the pathogenesis of cervical cancer, this study aimed to examine the effect of suppressing the expression of endogenously expressed viral oncogenes. To achieve this goal, two independent approaches were pursued; firstly, the RNA of the E6/E7 oncogenes was targeted using siRNA, secondly, the protein product of the E7 oncogenes was targeted using the NSAID, Sulindac. The final objective was to establish the downstream effects of these silencing events.

The introduction of E7 targeting siRNA into a HPV16 positive cervical cancer model system resulted in a concomitant reduction in E7 and E6 expression. This was validated both at the RNA level, using TaqMan® RT-PCR, and at the protein level by western blot analysis. The silencing of E6 and E7 expression induced significant alterations in the phenotype of these cells; cells were observed to stall in the G1 phase of the cell cycle, morphologically they appeared to have increased cytoplasmic granularity, to have lost contact inhibition and were enlarged and flattened. In addition the flow cytometry analysis indicated that they may be auto-fluorescing. These are all changes indicative of the induction of cellular senescence.

To evaluate the downstream effects of E6/E7 silencing at the trancripstome, genome-wide microarray analysis was performed. In total 168 differentially expressed genes with a fold change values above 2 and FDR below 0.05 were identified. Within this set of genes there was a significant over-representation of both mitotic spindle genes and members of the FA-BRCA pathway, both of which play a role in chromosomal maintenance. This is potentially important as one mechanism by which E6 and E7 are believed to augment the accumulation of pro-oncogeneic alterations is thorough chromosomal instability.

While RNAi technology was exploted to silence the expression of E6/E7 mRNA in a HPV16 positive cervical cancer model system, a complimentary study was performed where the expression of the protein product of the E7 oncogene was degraded. Sulindac a NSAID, which has been previously demonstrated to have anti-neoplastic activities, was observed to degrade E7 post-transcriptional in a dose dependent manner. In addition sulindac induced a time and dose dependent decrease in cell viability of cervical cancer cells of different origins, HPV status and viral DNA content. The most efficacious response was observed in the HPV 18 positive cervical cell line HeLa, where it was demonstrated to both induce cell cycle arrest and apoptosis.

The approaches used in this study have a potential role in gene-specific therapy in HPV associated cervical cancer. Additionally, it was demonstrated that in combination with high-throughput analysis the identification of a subset of dysregulated genes in cervical cancer was possible. While over the last 25 years been many important insights into the functionality of E6 and E7 have been discovered, a complete understanding still eludes us. A thorough knowledge of the interaction of these oncoproteins with their numerous cellular partners, as well as the consequences of these interactions, would allow for the possibility of developing novel therapeutic approaches that would impede the activity of the oncoproteins.

## Abbreviations

| | |
|---|---|
| 2'-O-Me | 2'-O-methyl |
| 2'-F | 2'-fluoro |
| 4-NPP | 4-Nitrophenylphosphate |
| Ad | Adenovirus |
| APE1 | Apurinic/Apyrimidinic Endonuclease 1 |
| AP | Alkaline Phosphatase |
| ATCC | American Type Culture Collection |
| AUC | Area Under the Curve |
| B2M | Beta-2-Microglobulin |
| BCA | Bicinchoninic Acid |
| BGP | Background Probes |
| BRCA | Breast Cancer Associated Gene |
| Brd4 | Bromodomain Protein 4 |
| BrdU | Bromodeoxyuridine |
| Cdks | Cyclin Dependent Knases |
| cDNA | Complementary DNA |
| cGIN | Cervical Glandular Intraepithelial Neoplasia |
| CIN | Cervical Intraepithelial Neoplasia |
| COX | Cyclooxygenase |
| $C_T$ | Threshold Cycle |
| DAVID | Database for Annotation, Visualization and Integrated Discovery |
| DDBI | DNA Data Bank of Japan |
| DNA | Deoxyribonucleic acid |
| E6AP | E6 Associated Protein |
| EBI | European Bioinformatics Institute |
| ECL | Enhanced Chemiluminesence |
| EGF | Epidermal Growth Factor |
| EGFR | Epithelial Growth Factor Receptor |

| | |
|---|---|
| EMBL | European Molecular Biology Laboratory |
| EMT | Epithelial-to-Mesenchymal Transition |
| FA | Fanconi Anaemia |
| FANC | Fanconi Anemia, Complementation Group |
| FDR | False Discovery Rate |
| FRET | Forster Resonance Energy Transfer |
| GAPDH | Glyceraldehyde-3-Phosphate Dehydrogenase |
| HATs | Histone Acetyl Transferases |
| HLA | Human Leukocyte Antigen |
| HPV | Human Papillomavirus |
| HSV-2 | Herpes Simplex Type 2 |
| hTERT | Human Telomerase Reverse Transcriptase |
| iVT | In Vitro Transcription |
| KIR | Killer Immunoglobulin-like Receptor |
| LCR | Long Control Region |
| LNA | Locked Nucleic Acid |
| MCM's | Minichromosome Maintenance Proteins |
| MEM | Modified Eagle Medium |
| MGB | Minor Groove Binding |
| MYBL2 | Myeloblastosis Viral Oncogene Homolog (avian)-like 2 |
| NCBI | National Centre for Biotechnology Information |
| ND-10 | Nuclear Dot-10 |
| NMR | Nuclear Magnetic Resonance |
| NSAID | Non streodial anti-infalmmatory drug |
| ORC | Origin of Replication |
| ORFs | Open Reading Frames |
| PAP | Papanicolaou |
| PAE | Early Polyadenylation Site |
| PAL | Late Polyadenylation Site |
| PCAF | P300/CBP-Associated Factor |

| | |
|---|---|
| PGs | Prostaglandins |
| PI | Propidium Iodide |
| $PLA_2$ | Phospholipase $A_2$ |
| PM | Perfect Match |
| PML | Promyelocytic Leukaemia |
| PMSF | Phenylmethanesulponylfluoride |
| Rb | Retinoblastoma |
| PVDF | Polyvinylidene Diflouride |
| RIPA | Radioimmunoprecipitation |
| RIN | RNA Integrity Number (RIN) |
| RLE | Relative Log Expression |
| RNA | Ribonucleic acid |
| RNAi | RNA interference |
| RPA | Replication Protein A |
| RT | Real-Time |
| SA-β-gal | Senescence-Associated-β-Galactosidase |
| SDS | Sodium Dodecyl Sulphate |
| siRNA | small interfering RNA |
| StDev | Standard Deviation |
| TA | Transit-amplifying |
| T Ag | T Antigens |
| TdT | Terminal Deoxynucleotidyl Transferase |
| TLDAs | TaqMan® Low Density Arrays |
| TLR | Toll-like receptors |
| Tm | Melting Temperature |
| $TXA_2$ | Thromboxane $A_2$ |
| UDG | Uracil DNA Glycosylase |
| URR | Upstream Regulatory Region |
| VLPs | Virus-like Particles |
| WT | Whole Transcript |

# Publications

## Journal Articles

Martin CM, Kehoe L, **Spillane C**, O'Leary JJ. Gene discovery in cervical cancer : towards diagnostic and therapeutic biomarkers. Mol Diagn Ther. 2007;11(5):277-90. Review. Erratum in: Mol Diagn Ther. 2007;11(6):411. PMID: 17963416

**CD Spillane**, Kehoe L, Smyth P, Sheils O, Martin CM, O'Leary JJ. Gene expression profiling of HPV16 E6/E7 silenced cervical cancer cells. *Manuscript in preparation*

**CD Spillane**, Kehoe L, McEliggott T, Sheils O, Martin CM, O'Leary JJ. Sulindac induces apoptosis and E7 degradation in a HPV18 model system. *Manuscript in preparation*

## Published Abstracts

**CD Spillane**, L Kehoe, O Sheils, CM Martin, JJ O'Leary. Transcriptome analysis of oncogene silenced HPV16 positive carcinoma cells. Accepted for European Research Organisation on Genital Infection and Neoplasia (Eurogin) 2009. (Platform presentation)

**CD Spillane**, L Kehoe, O Sheils, CM Martin, JJ O'Leary. Novel Molecular Treatment Options for Cervical Cancer. The British Society for Colposcopy & Cervical Pathology Annual Scientific Meeting. 2009. (Platform presentation)

L Kehoe, **CD Spillane**, Gallagher M, CM Martin, JJ O'Leary. The p16INK4A Pathway in Cervical Cancer. Accepted for The British Society for Colposcopy & Cervical Pathology (BSCCP) Annual Scientific Meeting 2009.

**CD Spillane**, L Kehoe, O Sheils, CM Martin, JJ O'Leary. Silencing of HPV Viral Oncogenes E6 and E7 in Cervical Cancer. European Research Organisation on Genital Infection and Neoplasia (Eurogin) 2008. (Platform presentation)

L Kehoe, **CD Spillane**, Gallagher M, CM Martin, JJ O'Leary. Elucidation of the Role of the p16INK4A Pathway in the Cell Cycle and its relationship with the Human Papilloma Virus in Cervical Cancer. European Research Organisation on Genital Infection and Neoplasia (Eurogin) 2008.

**CD Spillane**, L Kehoe, O Sheils, CM Martin, JJ O'Leary. siRNA targeting of HPV viral oncogenes E6 and E7 in cervical cancer. *Invited speaker* ABI RNA Symposium 2007 (Dublin, Irealnd)

**CD Spillane**, L Kehoe, O Sheils, CM Martin, JJ O'Leary. Silencing of HPV Viral Oncogenes E6 and E7 in Cervical Cancer. International Papillomavirus Meeting 2009 (Malmo, Sweden).

L Kehoe, **CD Spillane**, Gallagher M, CM Martin, JJ O'Leary. The p16INK4A Pathway in Cervical Cancer. Accepted for the International Papillomavirus (IPV) Meeting 2009.

**CD Spillane**, L Kehoe, H Keegan, O Sheils, CM Martin, JJ O'Leary. Silencing of HPV Viral Oncogenes E6 and E7 in Cervical Cancer. 5th Annual Cancer Conference 2008.

**CD Spillane**, L Kehoe, H Keegan, O Sheils, CM Martin, JJ O'Leary. Silencing of HPV Viral Oncogenes E6 and E7 in Cervical Cancer. Irish Association of Cancer Research (IACR) Annual Meeting 2008 .

# Chapter One

# Introduction

## 1.1 Cervical Cancer

Worldwide, cervical cancer is the second most common cause of cancer related death in women (Parkin *et al*, 2006). The prevalence rate in developed nations has shown a tendency to decrease year on year mainly, due to early diagnosis, as a result of the introduction of cervical screening programs based on the Papanicolaou (Pap) smear method (Bray *et al.*, 2005; Parkin *et al*, 2005; Wang *et al.*, 2004). In contrast, however, cervical cancer continues to be a leading cause of mortality in developing countries (Parkin *et al.*, 2002; Pisani et la., 1999) where screening programmes are not well established and the situation is confounded by a lack of treatment facilities. In 2005, there were over half a million new cases of cervical cancer, of which over 90% were in developing countries, and almost 260,000 women died of this cancer, 95% of them in developing countries (WHO, 2006). Ireland, unlike many of its European neighbours has seen a slow increasing trend in mortality rates, approximately 1.5% per year (Comber and Gavin, 2004). However, the recent introduction of the national screening program in late 2008 is anticipated to reverse this trend.

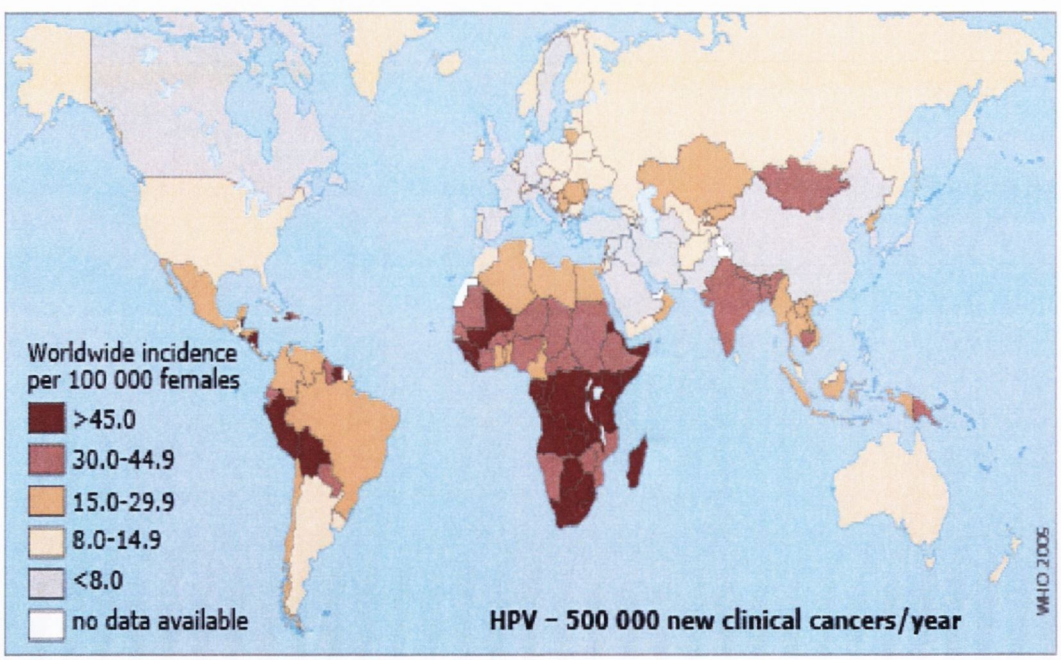


**Figure 1.1: Worldwide prevalence of cervical cancer.** (reproduced from WHO, 2006)

There are two predominant forms of cervical cancer, squamous cell carcinoma and adenocarcinoma, with the former accounting for approximately 60% of cases (Muñoz *et al.*, 2004). Squamous cell carcinomas arise in immature cells of the transformation zone of the cervix; this is the region where the columnar (glandular) epithelium of the endocervix meets the stratified squamous epithelium of the ectocervix. Adenocarcinoma a glandular lesion, occurs in the columnar cell of the endocervical canal. Worryingly even in developed countries, despite the introduction of screening programs, the incidence of adenocarcinoma has increased significantly over recent years, now accounting for approximately 25% of all cervical cancers (Bray *et al.*, 2005; Schorge *et al.*, 2004). The reason for this is unclear, but it may, in part, be due to difficulties detecting its precursor form with conventional screening methods (Bulk *et al*, 2005; Smith *et al.*, 2000). Since adenocarcinomas show greater malignancy than squamous cell carcinomas and have a poor prognosis, this trend is of grave concern (Hopkins and Morely, 1991; Kim *et al.*, 2004).

Cervical cancer is characterized by a well defined pre-malignant phase, based on a series of dysplastic changes which occur over a period of many years and signify the malignant progression of lesions (Wright *et al.*, 1994). The classification of cervical dysplasias is cervical intraepithelial neoplasia (CIN) grades I, II and III, which correspond to mild, moderate and severe dysplasia in the case of squamous cell carcinomas and cGIN (cervical glandular intraepithelial neoplasia) in adenocarcinoma. CIN III also encompasses in situ carcinoma. These dysplastic grades relate to the degree to which the epithelium is replaced by epithelial cells and for the most severe dysplasias, CIN III, epithelial cells will have replaced the entire thickness of the lesion.

Although screening programmes have been effective in reducing the incidence of cervical cancer, it is well recognised that there are limitations to existing PAP smear screening procedures. These include a significant incidence of false positive and false negative results (Nanda *et al.*, 2000). Approximately one-third of errors can be attributed to slide misinterpretation, which strongly reflects the subjectivity of

cytological diagnosis. Improvements to current cervical screening programmes have been made through the introduction of liquid based cytology and advances in computerisation technologies (Bolger *et al.*, 2006). Currently, in an effort to further reduce the error rate, the focus has turned to the utilisation of molecular biomarkers as adjuncts to existing screening procedures. In recent years the discovery of a number of disease biomarkers, such as cdc6, mcm5 and $p16^{INK4a}$ through immunohistochemical and mRNA studies, has enhanced the diagnostic accuracy of both cervical cytology and histology (Murphy *et al.*, 2005a; Murphy *et al.*, 2005b).

## 1.2 Cervical Cancer and Human Papillomavirus Infection

As early as the 1840's, it was postulated that there was a relationship between cervical cancer and sexually transmitted infectious events. This was based on the observations of an Italian physician, Rigoni-Stern, who studied death certificates of women in Verona during the period 1760 - 1839 and noted that a high frequency of cancer of the womb occurred in married women, widows and prostitutes, but it was a rare occurrence in virgins and nuns (Rigoni-Stern, 1987). However, it was not until the late 1960's that reproducible data was obtained linking cervical cancer and sexual transmitted infection (Nahmias *et al.*, 1970; Naib *et al.*, 1969; Rawls *et al.*, 1968). At that time, the first reports of an association with viral infection were also published; though the virus in question was speculated to be the Herpes simplex type 2 (HSV-2) (Nahmias *et al.*, 1970; Naib *et al.*, 1969; Rawls *et al.*, 1968). In the 1970's, stemming from negative attempts to isolate HSV-2 DNA from cervical cancer biopsies (zur Hausen *et al.*, 1974), the attention turned to the Human papillomavirus (HPV). It was postulated by Harald zur Hausen in 1976 that cervical cancer may arise from HPV, the virus found in condylomas (commonly known as genital warts). He based this hypothesis on the knowledge of the localization of condylomas, their sexual mode of transmission, a number of anecdotal reports in the medical literature of rare malignant transition of condylomas and the relationship between condylomas and papillomaviruses, a well characterised group of oncogenic DNA viruses (zur Hausen 1976).

With the advent of molecular biology, specific types of papillomavirus were isolated from condylomas and laryngeal papillomas, HPV6 and HPV11 respectively (Gissmann and zur Hausen, 1980; Gissmann *et al.*, 1982). The subsequent application of nucleic acid hybridisation techniques at low stringency allowed for the screening of related but not identical HPV types (Law *et al.*, 1979) and for the first time, the presence of papillomavirus-related DNA sequence in biopsies of cervical cancer was proven (Boshart *et al.*, 1984; Dürst *et al.*, 1983). The first HPV types isolated directly from cancer biopsies of the cervix were HPV16 and HPV18, cloned in 1983 and 1984

respectively (Boshart *et al.*, 1984; Dürst *et al.*, 1983). Over the past three decades, evidence has accumulated implicating HPV as the major etiological factor in cervical cancer. HPV DNA is now known to be present in virtually all (99%) cervical cancer tumours (Walboomers *et al.*, 1999). In addition, studies on the incidence of viral DNA in cervical cancer precursor lesions has supported the conclusion that all cervical cancer cases can be linked with HPV DNA (Gargiulo *et al.*, 2007; Poljak *et al.*, 2005). The presence of HPV DNA has been detected in 86-100% of CIN III; 69-91% of CIN II and in a smaller fraction (44-77%) of CIN I cases (Gargiulo *et al.*, 2007; Poljak *et al.*, 2005).

**Table 1.1: Classification of HPV types based on oncogenic potential.** (adapted from Munoz *et al.*, 2003)

| Oncogenic Potential | HPV types |
|---|---|
| High-risk | 16, 18, 31, 33, 35, 39, 45, 51, 52, 56, 58, 59, 68, 73, 82. |
| Probable high-risk | 26, 53, 66. |
| Low-risk | 6, 11, 40, 42, 43, 44, 54, 61, 70, 72, 81, CP6108. |
| Un-defined risk | 34, 55, 57, 62, 64, 67, 69, 71, 74, 83, 84. |

Over a hundred different types of HPV have been identified, of which about 40 infect the genital mucosa (de Villers *et al.*, 2004). These viruses have been classified into high-risk or low-risk groups depending on the propensity for malignant progression of their associated lesions (Table 1.1). While there are 16 HPV types considered high risk, the most predominant strains are HPV16 and HPV18, which are associated with 70% of cervical tumours (Walboomers *et al.*, 1999). HPV18 is the type most strongly associated with adenocarcinoma of the cervix, whereas HPV16, followed by HPV18, is the most frequently detected when squamous cell carcinoma is diagnosed (Clifford *et al.*, 2003; Muñoz *et al.*, 2003). The frequency with which HPV16 is found integrated into the host genome increases with the severity of cervical neoplasia, although in some women with invasive disease only episomal forms are detected (Corden *et al.*, 1999; Cullen *et al.*, 1991; Pirami *et al.*, 1997). By contrast, HPV18 is almost always

found in integrated forms in women with high-grade cervical intraepithelial neoplasia and invasive disease (Cullen *et al.*, 1991; Melsheimer *et al.*, 2004; Pirami *et al.*, 1997). The carcinogenic potential of both HPV16 and HPV18 should be seen as highly significant. A meta analysis of squamous cell carcinomas pooled from 11 case studies (1918 cases versus 1928 controls) determined the odds ratio for developing HPV16 associated cervical cancer was 434 and for developing HPV18 associated cervical cancer was 248 (Muñoz *et al.*, 2003). These are among the highest odds ratios for human carcinogens.

## 1.3 Natural HPV infection

HPV infection of the genital tract is thought to be the most common sexually transmitted infection, with more than 75% of sexually active women showing evidence of infection at some stage in their life (Baseman and Koutsky, 2005; Cates, 1999; Ho *et al.*, 1998, Liaw *et al.*, 2001). The prevalence of HPV infection is age dependent in most populations, with the age specific prevalence trend showing higher proportions among young age groups, a decline in young adults and an increase again in post-menopausal women (Figure 1.2). The initial decrease observed with increasing age is likely due to a combination of decreased HPV exposure, the self-limited nature of most infections, and a resistance to re-infection. The reason for the second increase in the older age groups is unclear. Two explanations have been proposed to explain this phenomenon: one, it translates to biological changes related to menopause-hormonal and immunological status that facilitates HPV DNA detection from exposures earlier in life that remained silent or undetectable for a number of years (Bosch and Sanjose, 2007; Boxman *et al.*, 1999; Maran *et al.*, 1995) or two, it constitutes a genuine infection incident. This second argument is based on evidence from individual cohort studies and sexual behaviour surveys which indicate that a genuine infection occurs due to the number of new sexual partners in middle age and above (Khan *et al.*, 2005; Muñoz *et al.*, 2004).

Despite the unusually high prevalence of HPV infection, nearly 90% of detectable HPV infections are resolved spontaneously by the host immune system (Bosch *et al.*, 2002; Elfgren *et al.*, 2000; Moscicki *et al.*, 2006). The half-life of HPV infections has been estimated at approximately 10 months for high risk types and half that for low risk viral types (Castellsague, 2008). Interestingly, infections by HPV16 appear to have prolonged longevity, persisting for on average 16 months (Woodman *et al.*, 2001). The majority of women clear the infection spontaneously, but where HPV infection persists, there is a high risk of progression and development of severe dysplasia and malignancy (Walboomers *et al.*, 1999). The risk is so great that screening programs are increasingly incorporating HPV testing in an effort to improve accuracy. Given the prevalence of genital HPV types in the general population and the high life-time risk of

infection, the incidence of cervical cancer is very low, typically 0.03% in the absence of screening (Parkin *et al.*, 2005). Thus, while HPV infection is a necessary agent for cervical carcinogenesis it is not sufficient. Host and environmental factors have been studied for their potential influence on the occurrence of cervical cancer and precursor lesions. Factors such as pregnancy, high parity, long duration of oral contraceptive use, smoking, micronutrients, and other sexually transmitted diseases have been independently associated with an increased risk after adjustment for HPV infection (Castellsague *et al.*, 2003; Castellsague *et al.*, 2006; Garcia-Closas *et al.*, 2005; Smith *et al.*, 2002; Smith *et al.*, 2004). In addition, a hereditary contribution to cervical cancer risk has been demonstrated, it would appear that specific alleles of certain immune response genes are associated with protection from or susceptibility to infection with HPV (Carrington *et al.*, 2005; Hemminki *et al.*, 1999; Hildesheim and Wang, 2002; Magnusson *et al.*, 2000). Such alleles are from human leukocyte antigen (HLA) class I and II genes and killer immunoglobulin-like receptor (KIR) genes, which recognise HLA antigen class I alleles (Carrington *et al.*, 2005; Hildesheim and Wang, 2001).

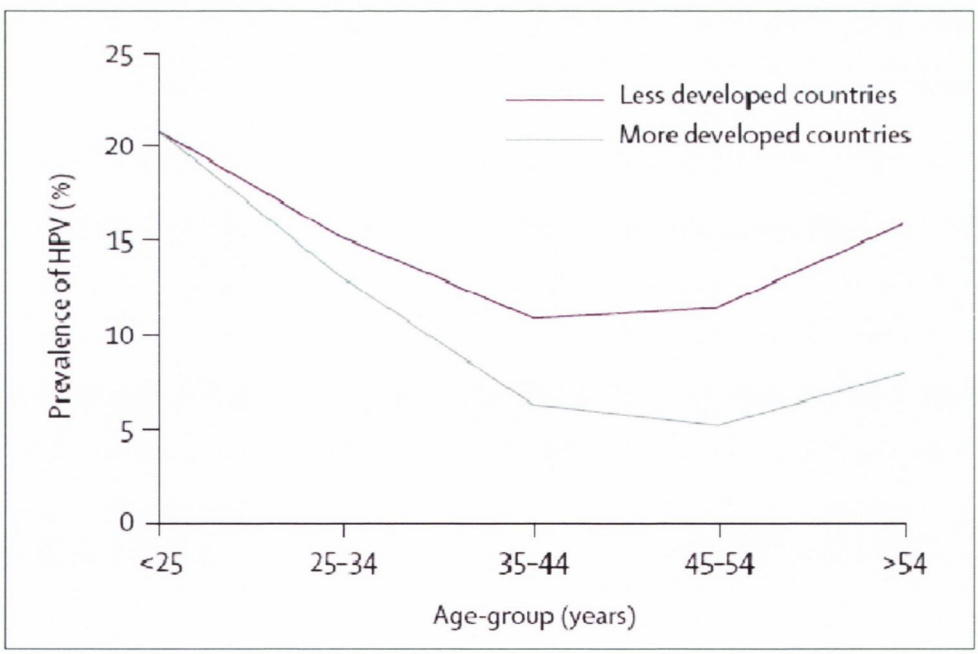


**Figure 1.2: Worldwide age-specific HPV-DNA prevalence among women by country-specific development status.** (reproduced from de Sanjosé *et al.*, 2007)

## 1.4 HPV structure

HPVs are small non-enveloped viruses with a 55nm diameter icosahedral caspid, composed of 72 star shaped capsomers (Figure 1.3 A). A single viral protein the major caspid protein, L1, is both necessary and sufficient to form the caspid (Kirnbauer *et al.*, 1992). A second caspid protein, the minor caspid protein, L2, while still unclear on its arrangement within the viron is required for several important functions, including that of genome packaging and viral entry into the host cell (Buck *et al.*, 2005; Day *et al.*, 2003). Encapsulated within the caspid is a circular double stranded DNA genome of approximately 8,000bp which contains one coding sequence (Longworth and Lamins, 2004). Genomic organisation is highly conserved across all types of papillomaviruses and can be divided into 3 regions (Figure 1.3 B); the early (E), the late (L) and the upstream regulatory region (URR) or long control region (LCR). The early region encodes non-structural proteins required for viral transcription and replication. Within this region resides the carcinogenic potential of HPVs. The late region encodes the two caspid proteins. The LCR contains a variety of *cis*-regulatory elements necessary for viral replication and gene expression, including the origin of replication (ORC) and the early promoter, known as p97. The HPV genome encodes a second promoter located within the E7 gene, known as the late promoter or p670 (Figure 1.3 B). The early open reading frames (ORFs) can be expressed from either promoter depending on environmental factors (Spink and Laimins, 2005). The late ORFs are solely expressed from the late promoter, following a change in splicing, and a shift in polyadenylation site usage from the early polyadenylation site (PAE) to the late polyadenylation site (PAL). The early and late genes are numbered according to their size; the higher the number the smaller the corresponding open reading frame. The L1 and L2 proteins are conserved across widely divergent papillomaviruses and along with E1 and E2 are key viral genes that are thought to have been present in the common ancestor of all animal papillomaviruses (Teri *et al.*, 2002). Other viral genes have been acquired or significantly altered during evolution, such as E4, E5, E6 and E7, and are not necessarily present in all papillomavirus types (de Villiers *et al.*, 2004). All HPV types have E6 and E7 ORFs but not necessarily E5 ORF.

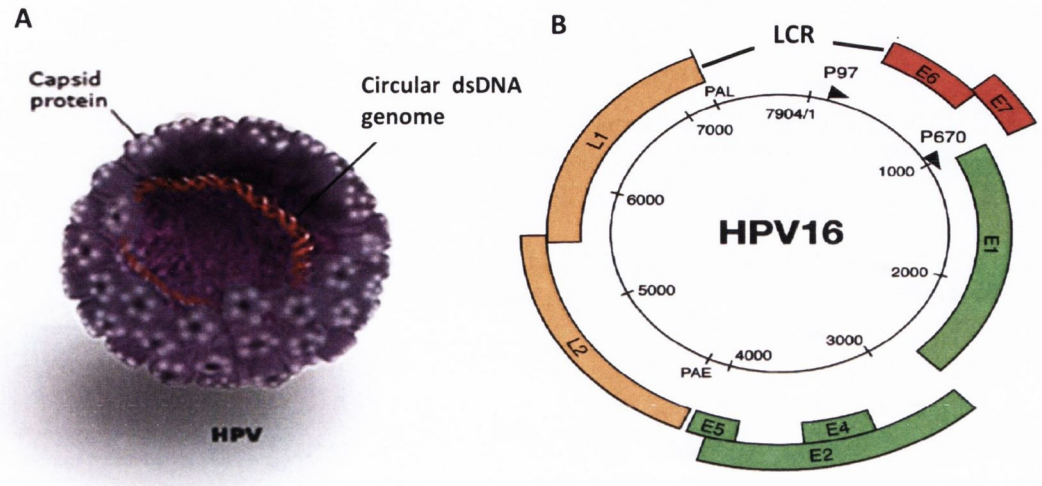


**Figure 1.3: HPV Structure. (A)** Depicts the composition of a HPV viron. The nonenveloped papillomavirus consists of only three components; it has a circularly closed, double-stranded DNA genome in the form of chromatin and two capsid proteins, L1 and L2. The major capsid protein, L1, is the main structural component of the viral protein shell. Three hundred sixty L1 copies assemble to form 72 pentamers, called capsomers, whereas each virion probably contains only 12 copies of the minor capsid protein, L2. **(B)** Depicts the HPV 16 genomic structure. The ORFs E6, E7, E1, E2 E4 and E5 encode proteins required for regulation of viral DNA replication and viral gene expression, the L1 and L2 ORFs encode the viral caspid proteins. Only one strand of the double-stranded DNA serves as the template for viral gene expression, coding for a number of polycistronic mRNA transcripts. Transcription is regulated by enhancer sequences located in the long control region (LCR), which are bound by a number of cellular factors as well as the viral E2 product. The transcription start site of viral promoters differs depending on the virus type. HPV16 contains two promoters the early promoter, p97, and the late promoter, p670, both which are responsible for expression of ORF E1, E2, E4, E5, E6 and E7, while L1 and L2 are expressed solely from the late promoter. (Reproduced from Doorbar, 2006)

## 1.5 The 'productive' HPV life cycle

### *1.5.1 Infection*

The 'productive' life cycle of HPV begins with the infection of the stratified squamous epithelia, where the process of epithelium differentiation is employed by the virus to regulate its own replication (Stubenrauch and Laimins, 1999; zur Hausen, 2002). Cervical epithelium is formed of stratified layers of keratinocytes that serve predominantly as a protective barrier against the external environment (Figure 1.4). The proliferation of keratinocytes is confined to the basal layer adjacent to the basement membrane, whereas differentiation occurs in the suprabasal layers. Within the basal membrane, there is a sub-population of stem cells which retain a high capacity for self-renewal (Hummel *et al.*, 1992). These stem cells can undergo asymmetric division allowing simultaneous regeneration and production of a differentiated daughter cell, known as a transit-amplifying (TA) cell (Lehrer *et al.*, 1998). TA cells migrate laterally to populate the basal layer and are its main constituent. They undergo a limited number of rapid cell divisions before withdrawing from the cell cycle, detaching from the basement membrane and moving into the suprabasal layers, where they are committed to undergoing terminal differentiation (Lehrer *et al.*, 1998). As they move up through the suprabasal layer to the mucosal surface, the cells undergo a process of sequential terminal differentiation acquiring the characteristics that are necessary for their protective role. Changes include the physical cross-linking of keratin intermediate filaments, the formation of cornified envelopes, and the secretion of lipids, which together allow the epithelial surface to form a physical barrier against the environment (Madison, 2003). Keratinocytes are continually shed at the mucosal surface; therefore renewal of the epithelium is constantly required to maintain structural integrity. The basal subpopulations of stem cells are ultimately responsible for this, and thus play a vital role in the epithelial homeostasis.

Successful infection requires the penetration of the epithelium and infection of the epithelial basal cells. HPV infection occur either at sites where columnar and stratified

epithelial cells meet each other, such as at the cervical transformation zone, facilitating access to the basal cells or due to a break in the integrity of the stratified epithelium, which may occur through micro-abrasions that exposes the basal layer to viral entry (Figure 1.4). There is much controversy as to the precise mechanism of viral entry into the host cell. It would appear that different types of papillomavirus use different cell receptors and hence there are a range of entry mechanisms depending on the papillomavirus type. It is thought that host cell entry is initiated by binding of the virus particles to specifically modified heparin sulphate pretoglycans, which induces a conformational change in both L1 and L2 caspid proteins (Giroglou *et al.*, 2001; Joyce *et al.*, 1999; Selinka *et al.*, 2003; Yang *et al.*, 2003). As with other viruses, it is believed that a secondary receptor is then required. Initial experimental evidence suggested for HPV16 that the secondary receptor was the cell surface protein α6 integrin (Bossis *et al* 2005; Evander *et al.*, 1997; McMillan *et al.*, 1999), whose binding was believed to facilitate endocytosis via clatharin-coated vesicles (Bousarghin *et al.*, 2003; Day *et al.*, 2003). However, a recent report now suggests that while α6 integrin may be involved, it is not the main target of HPV16 and that endocytosis is via a clatharin independent pathway, potentially involving a novel endocytic mechanism related to tetraspanin proteins (Spoden *et al.*, 2008). This is consistent with the observation that the length of time required for HPV16 endocytosis was much greater than was usually observed for clatharin dependent entry (Culp *et al.*, 2004). For HPV31 it has been proposed that it may gain entry via caveolae, a mechanism that has been ruled out for HPV16 (Bousarghin *et al.*, 2003; Smith *et al.*, 2007). Once host entry is achieved, the papillomavirus particles disassemble in late endosomes and/or lysosomes, with the transfer of viral DNA to the nucleus being facilitated by the minor caspid protein L2 (Day *et al.*, 2003; Day *et al.*, 2004).

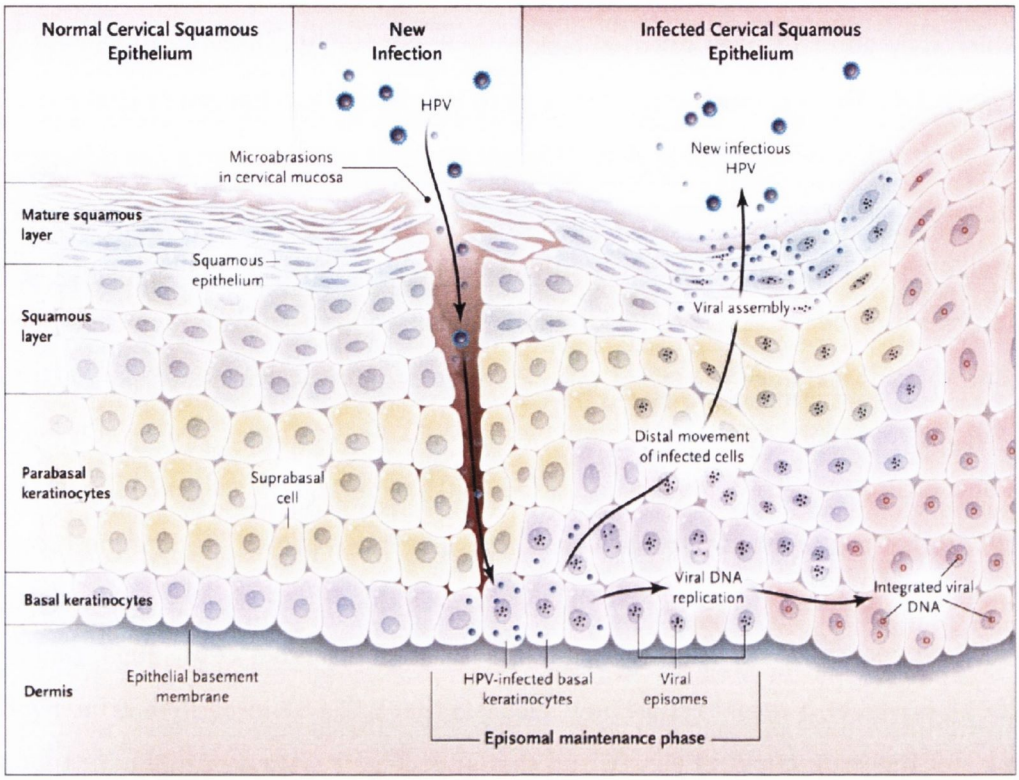


**Figure 1.4: HPV-mediated progression to cervical cancer.** Basal cells in the cervical epithelium rest on the basement membrane, which is supported by the dermis. Human papillomavirus (HPV) is thought to access the basal cells through micro-abrasions in the cervical epithelium. Following infection, the early HPV genes E1, E2, E4, E5, E6 and E7 are expressed and the viral DNA replicates from episomal DNA. In the upper layers of epithelium (parabasasl keratinocytes and squamous layer) the viral genome is replicated further, and the late genes L1 and L2, and E4 are expressed. The L1 and L2 proteins encapsidate the viral genomes to form progeny virions in the nucleus. The shed virus can then initiate a new infection. Low-grade intraepithelial lesions support productive viral replication. An unknown number of high-risk HPV infections progress to high-grade cervical intraepithelial neoplasia. The progression of untreated lesions to microinvasive and invasive cancer is associated with the integration of the HPV genome into the host chromosomes, with associated loss or disruption of E2, and subsequent up-regulation of E6 and E7 oncogene expression. (reproduced from Kahn, 2009).

### *1.5.2 Genome maintenance*

In the 'productive' HPV life cycle, infection leads to the establishment of the HPV genome as a stable episome that is maintained at a low copy number without integration into the host genome. The viral genome is thought to be maintained at between 50 and 200 copies per cell in the basal layer throughout infection (Bedell *et al.*, 1991; De Geest *et al.*, 1993). Maintenance of the viral genome in the cells of the basal layer, both stem and TA cells, requires replication of the HPV genome and subsequent genome segregation. With the exception of two virally encoded early proteins, E1 and E2, HPV DNA replication is performed entirely by the host cellular replication machinery (Stubenrauch and Laimins, 1999). This is achieved in the basal layer by viral replication accompanying cellular DNA replication as the cells naturally progress through the S phase of the cell cycle.

The requirement of the early proteins, E1 and E2, for HPV replication is well established (Frattini *et al.*, 1996; Stubenrauch *et al.*, 1998). The E2 is a multifunctional protein that regulates both viral replication and transcription. The protein has N-terminal transactivation domain linked by a relatively unstructured hinge region to a well-characterized C-terminal DNA binding domain, which interacts with $ACCN_6GGT$ DNA motifs (Dell *et al.*, 2003). One such motif is located adjacent to the viral ORC and it is believed that E2, through a direct interaction, recruits E1 to the viral origin (Frattini and Laimins, 1994; Lusky *et al.*, 1994; Mohr *et al*, 1990). The C-terminal of E1 has an ATP-dependent DNA helicase domain, which allows E1 to use ATP to catalyse the unwinding of double stranded DNA, thus preparing the viral genome for replication (Hughes and Romanos, 1993). The E1 protein forms a double hexameric ring at the HPV origin, the assembly of which is promoted by the protein-folding activities of cellular chaperone proteins (Lee *et al.*, 1999). This results in the displacement of E2, allowing extensive bidirectional unwinding from the ORC of the viral DNA template by E1 (Titolo *et al.*, 1999). In addition to its helicase activity E1, also binds host cellular proteins required for DNA replication, including replication protein A (RPA) and DNA polymerase α primase (Conger *et al.*, 1999; Han et la., 1999; Loo *et al.*, 2004). The final step in the process is to ensure faithful distribution of viral genomes to each daughter

cell after cell division. This is accomplished by E2, which tethers viral genomes to mitotic chromosomes (Bastien and McBride, 2000; Skiadopoulos and McBride, 1998). The association of HPV E2 with mitotic chromosomes is mediated by a direct interaction with C-terminal of the bromodomain protein 4 (Brd4; You *et al.*, 2004).

### 1.5.3 Genome amplification

The objective of the 'productive' life cycle of HPV is to produce infectious virions, which can re-infect the basal epithelium or spread to a new host. In order to achieve this, genome amplification must occur, followed by assembly of mature virions and subsequent virion release. There is a spatial and temporal pattern of HPV gene expression in the infected epithelium. HPV genome maintenance occurs in the basal layer of the epithelium, as discussed in section 1.5.2. Genome amplification arises in the suprabasal layer and assembly and release occurring in the superficial layer (Peh *et al.*, 2002). The exact mechanism underlying the induction of these different HPV life cycle stages is not completely understood but it would appear that it depends at least in part on changes in the cellular environment induced with the movement of keratinocytes from the basal to the suprabasal and eventually to the superficial layer. For example, once a TA cell exits the basal layer and enters the suprabasal layer, it becomes quiescent and begins the process of terminal differentiating (Lehrer *et al.*, 1998). This environment causes a significant problem for the virus as it is dependent on the host cellular replication machinery for its own replication, which is active only in mitotic cells. To solve this problem, there is a dramatic up regulation in expression of the early viral proteins which reactivate cellular DNA synthesis, inhibit apoptosis and delay the differentiation programme, creating a replication competent environment in the infected keratinocytes (Cheng *et al.*, 1995; Dyson *et al.*, 1992; Werness *et al.*, 1990).

The subversion of the normal terminal differentiation process and induction of a proliferative phenotype is attributed to the expression of the viral oncogenes, E6 and E7. The activity of these proteins induces unscheduled re-entry into S phase of the cell cycle, thus delaying cell cycle arrest and activating the host replication machinery. This

facilitates both an expansion in the number of infected cells in the suprabasal layer, and also amplification of the viral genome. Both E6 and E7 stimulate cell cycle progression by association with regulators of the cell cycle. The principal and most extensively characterised effect of E7, is its association with members of the cell cycle regulatory family of pocket proteins, retinoblastoma (pRb), p107 and p130 (Dyson *et al.*, 1992). A negative regulator of the cell cycle, pRb controls S phase entry by associating with members of the E2F family of DNA-binding transcription factors (Edmonds and Vousden, 1989; Weintraub *et al*, 1995); E7 disrupts this function by binding to pRb and displacing E2F proteins (Dyson *et al.*, 1992). Cells therefore enter S phase and activate the cellular replication factors required for both cellular proliferation and viral replication. The E6 and E7 proteins work in a cooperative manner; while E7 drives proliferation E6 counteracts the apoptotic response to these abnormal growth stimuli. Therefore, the major function of E6 during natural infection is as an anti-apoptotic protein. The primary activity through which E6 fulfils this role is by it binding to the tumour suppressor p53 and targeting p53 for proteosomal degradation (Huibregtse *et al.*, 1991; Huibregtse *et al.*, 1993a; Scheffner *et al.*, 1990; Scheffner *et al.*, 1993; Werness *et al.*, 1990). In addition, E6 and E7 bind to a variety of other cellular proteins and the consequences of some of these interactions will be discussed in detail in section 1.6.

Activation of the late differentiation-dependent promoter during HPV genome amplification results in an up-regulation in E1, E2, E4 and E5 expression (Nakahara *et al.*, 2005; Spink *et al.*, 2005; Wilson *et al.*, 2005). Though expression of E6 and E7 is necessary to induce the replicative competent environment, they themselves are not directly involved in the process of replication. The key players in this regard are E2 and E1, and the molecular basis for their role in replication is well understood (section 1.5.2). While the assumption had been, that after the virus induced the S phase of the cell cycle its DNA was amplified concurrently with the process of host DNA replication, recent publications have suggested otherwise (Chow *et al.*, 2009; Wang *et al.*, 2008). These reports come from work performed in an organotypic raft culture system which recreated the HPV18 life cycle. In this system, it was observed that genome

amplification, rather than occurring during S phase of the cell cycle, actually occurred subsequent to the host DNA replication in a prolonged G2 arrest phase (Chow *et al.*, 2009; Wang *et al.*, 2008). It appears that E7 expression causes the cells to re-enter the cell cycle and proliferate, but as they move towards the epithelial surface they arrest in G2. The continued expression of E7 in cells arrested in G2 is thought to create a pseudo-S phase state, which facilitates viral genome amplification rather than cell proliferation. Therefore, what seems to be occurring in the suprabasal layer is an initial stage of infected cell expansion, followed by a stage of viral genome amplification.

HPV E4 and E5 are also believed to contribute to the process of genome amplification, as the disruption of either gene leads to a reduced level of genome amplification (Fehrmann *et al.*, 2003; Genther *et al.*, 2003; Nakahara *et al.*, 2005; Peh *et al.*, 2004). However, the mechanism by which they contribute to the process is not fully understood. HPV E5 is a hydrophobic protein that resides predominantly in the endoplasmic reticulum (Conrad *et al.*, 1993). It has been suggested that E5 activity is based on its association with the epidermal growth factor (EGF) receptor, which leads to increased EGF signalling and subsequently may result in maintenance of the proliferative environment. This is based in part on the observation that over-expression of E5 increases the phosphorylation of the EGF receptor as well as inhibiting its degradation (Conrad *et al.*, 1993; del Mar Pena and Lamins, 2001; Solinas-Toldo *et al.*, 1997). The E4 ORF is translated from spliced transcripts as a fusion with the first 5 amino acids of E1 to generate full-length proteins, also called E1^E4. It has been shown *in vivo* that viral genome amplification coincides with E4 and E7 expression (Doorbar *et al.*, 1997; Peh *et al.*, 2002). The E4 protein encoded by several HPV types prevents the nuclear accumulation of Cdk1/cyclin B1 that is required for mitosis by binding to the complex and tethering it to cytoplasmic keratins (Davy *et al.*, 2002; Knight *et al.*, 2004; Nakahara *et al.*, 2002). Initial investigations into the G2 arrest associated with genome amplification focused on E4. However, the theory that high levels of E4 could cause this event has not been supported by experimental data and recent studies have not been able to demonstrate the co-localisation of E4 with cyclin B1 (Chow *et al.*, 2009; Wang *et al.*, 2008).

During the 'productive' infection, expression levels of E6 and E7 is tightly regulated to ensure they do not pose a carcinogenic threat, which is detrimental to the viral life cycle. One approach utilised is simply by limiting high-level expression of the oncogenic proteins to the suprabasal post-mitotic keratinocytes. These cells are destined to be lost from the cervical squamous epithelium and as such any pro-carcinogenic alterations that occur will be eliminated. The second approach involves the E2 protein. Not only is this protein involved in viral replication and genome segregation but in addition it plays a role as a transcription factor, regulating the viral early promoter and hence controlling expression of the viral oncogenes (Longworth and Laimins 2004). It has been proposed that at early stages of infection, low levels of E2 acts as a transcriptional activator, whereas at later times of infection and higher E2 protein levels, E2 might lead to the repression of transcription (Hines *et al.*, 1998; Steger and Corbach, 1997). The mechanism by which repression is brought about has been elucidated in detail. There are two-binding sites for E2 proximal to the early promoter, and binding within this region causes the displacement of the transcription activator Sp1 leading to transcription repression (Romanczuk *et al.*, 1990). In addition to competing with Sp1, E2 can also interact with this protein. Furthermore, E2 is capable of interacting directly with both E6 and E7, resulting in the modulation of their functions (Gammoh *et al.*, 2006; Grm *et al.*, 2005). The regulatory effects of E2 on the viral oncogenes is so extensive that the reintroduction of E2 into cervical carcinoma cells has been shown to repress transcription of integrated E6 and E7 genes and induce growth arrest, apoptosis and cellular senescence (DeFilippis *et al.*, 2003; Goodwin and DiMaio 2001). An interesting point to note in relation to the viral 'productive' life cycle is that it would appear that the increase in E2 repression that is important in stimulating viral genome amplification will lead eventually to the down regulation of E6 and E7 expression, and to the eventual loss of the replicative environment necessary for viral DNA synthesis.

### 1.5.4 Virus assembly and release

The final steps in the HPV 'productive' life cycle involve the assembly, maturation and release of the infectious virus, which occur in the terminal differentiated cells of the superficial layers (Hummel *et al.*, 1992). The main requisite proteins for these processes are the viral structural proteins, L1 and L2, though E2 and E4 may also be required. The accumulation of L1 and L2 proteins within infected cells is observed after the cells have undergone viral genome amplification; with L2 expression preceding that of L1 (Doorbar and Gallimore, 1987; Florin *et al.*, 2002). The activation of the late differentiation-dependent promoter during HPV genome amplification results not only in the increased expression of the early proteins, E1, E2, E4 and E5, but also the late proteins, L1 and L2. The expression of L1 and L2 during the early phases of the HPV life cycle is controlled both at RNA and protein level. In proliferating cells, there is a negative regulatory element located in the coding regions that destabilises the late transcripts (Cumming *et al.*, 2003; McPhillips *et al.*, 2004), as well as a splicing silencer in the L1 gene that allows preferential transcription of the early genes (Zhao *et al.*, 2004). Furthermore, the pattern of codon usage within the late genes is distinct from that of the host cell and it is believed this may contribute to the suppression of the late genes (Zhao *et al.*, 2003; Zhou *et al.*, 1999).

Once the differentiation of replicating epithelial cells to non-replicating mature keratinocytes eventually occurs, virus assembly initiates in the cell nucleus. L2 relocates from the cytoplasm to the nucleus by virtue of its NLS located in its N- and C-termini, and after an initial phase of capsomer formation in the cytoplasm L1 also localises to the nucleus again via its NLS (Klucevsek *et al.*, 2006). Although viral assembly occurs in the absences of L2, there is a reduction in the efficiency of DNA packaging and the level of viral infectivity of these viral particles (Roden *et al.*, 2001; Stauffer *et al.*, 1998). One mechanism that has been proposed to explain the process of viral assembly involves sub-nuclear domains, nuclear dot-10 (ND-10). In this model, once localised to the nucleus L2 is believed to associate with promyelocytic leukaemia (PML), a biomarker and critical scaffold protein of the ND-10s (Day *et al.*, 1998). The

ability of E2 to bind to specific motifs in the viral genome is believed to be utilised in the system to convey genomic DNA to the ND-10 bodies and L2 (Florin *et al.*, 2002). Following L2 binding and the subsequent displacement of the sp100 protein, L1 capsomers are recruited to the ND-10 bodies (Day *et al.*, 1998). This model implies that the concentration of components at the ND-10 drives viral assembly. However, some researchers have suggested that ND-10 is not physiologically important in viral assembly. Instead it has been proposed that ND-10 bodies act as nuclear dumps for overexpressed and/or misfolded proteins, including L2 (Kieback and Muller, 2006). Indeed L2 targets to discrete sub-nuclear domains most efficiently when expressed to a high level in cultured cells via plasmid transfection or as transgenes in recombinant viruses (Day *et al.*, 1998; Florin *et al.*, 2002; Kieback and Muller, 2006), whereas recruitment to ND-10 is inefficient at lower L2 expression levels in stably transduced cell lines (Kieback and Muller, 2006).

The assembly of the caspids in the nucleus requires the C-terminus of the L1 protein, which is essential for capsomer interactions. As the infected cells reach the epithelial surface, before release from the cells, the capsids undergo a maturation process involving stabilisation of the virion components by disulphide cross-linking of the proteins. It is believed that initially the shed virus is still contained within a cornified squame and that the E4 is required for release. E4 proteins from high-risk types associate with keratin networks in cells and, when overexpressed in transient-transfection assays, can induce their collapse (Doorbar *et al.*, 1991). Therefore E4 could affect the integrity of the cornified envelope (Bryan and Brown, 2004; Doorbar *et al.*, 1991), facilitating realise from the cornified envelope. In essence, the HPV natural infection cycle the virus is basically a hitchhiker joining the keratinocytes at the start of its journey as a primitive basal cell in the epithelium through to its end as a terminally differentiated squame.

## 1.6 HPV and carcinogenesis

The relationship between HPV and cervical cancer hinges on the production of the viral early oncoproteins E6 and E7 (Snijders *et al.*, 2006). Cervical neoplastic progression requires both spatial and quantitative deregulation of the tight transcriptional control, such that viral oncogene expression occurs at a high level throughout the epithelium (Cheng *et al.*, 1995; Durst *et al.*, 1992; Stoler *et al.*, 1992). Clinically, the HPV E6 and E7 genes are expressed at low levels in low-grade CIN but are abundantly expressed in high-grade malignant lesions (zur Hausen, 2000), consistent with deregulated expression being a key element in neoplastic development. Elucidating the underlying molecular events in the association between the aberrant expression of these high-risk HPV genes and the shift from infection to pre-neoplasia and cancer in the cervix has been the focus of research for over 25 years. While our understanding of this carcinogenic process is in no means complete in this short period of time, there have been significant advances in our basic knowledge and this information will be presented within this section.

### *1.6.1 Integration*

One of the key events in HPV induced carcinogenesis is said to be the integration of the HPV genome into a host chromosome. In almost 90% of cervical carcinomas a truncated form of the HPV genome can be detected which is integrated into the host genome (Pett and Coleman, 2007). Integration is not a normal part of the productive life cycle of HPV and appears to confer no advantage to the virus. Indeed it results in an abortive viral infection, in which the virus persist in its cellular host but cannot complete its life cycle as late events of the life cycle are not supported due to deletion of viral genes required for synthesis of an infectious virion. Mechanisms of integration are not well understood, but the process most likely involves double-strand breaks (DSB) in viral and host genomes, followed by DNA ligation by host proteins (Winder *et al.*, 2007). While integration can occur randomly throughout the host genome, a clear preference for common fragile sites (CFS) has been demonstrated, with 50% of the naturally occurring HPV16 integration events isolated from CFS (Thorland *et al.*, 2003;

Yu *et al.*, 2004; Wentzensen *et al.*, 2004). There is a definite pattern with respect to integration of the HPV genome, characterised by the retention of the E6 and E7 oncogenes along with the viral LCR containing at least the early promoter. Disruption often occurs within the E2 viral gene and/or the E1; loss of E1 consequently results in the loss of E2 expression as well (Finzer *et al.*, 2002; Hebner and Laimins, 2006). In general, integration leads to increased expression and stability of transcripts encoding E6 and E7 proteins, owing mainly to the loss of E2 mediated transcriptional repression and potentially also to increased mRNA stability (Jeon *et al.*, 1995) and alterations in host cellular transcription (Alazawi *et al.*, 2002). As a result, HPV-infected cells with integrated HPV DNA acquire extended life spans, retain the capacity to proliferate, and tend to develop and perpetuate mutations in the germline DNA attributable to the actions of E6 and E7 proteins.

Not only is integration detected in the vast majority of cervical carcinomas, but also in subsets set of high grade lesions and even in some CIN I lesions. However, transcriptional activity is only rarely observed in high grade lesions and not at all in CIN I lesions (Evans *et al.*, 2004; Melsheimer *et al.*, 2004; Woodman *et al.*, 2007; Klase *et al.*, 1999) indicating, that an intermediate stage in cervical carcinogenesis could be characterised by transcriptionally silent HPV integrants. This has lead to the theory that the process of integration and clonal selection of the integrant cells may be two independent events in neoplastic progression. Since integration must occur in cells containing a background of episomal viruses (Durst *et al.*, 1985), and the expression of E2 protein inhibits integrant transcription of E6 and E7, this could account for the clinical phenotype seen in some lesions of transcriptional inactive integrants. This model contends that at some later point in the carcinogenic progression clearance of episomes occurs, e.g. by the host innate immunity, and this is associated with loss of integrant silencing and subsequent clonal selection of the integrant cells. Indeed, integrated HPV may be viewed as selectable because it represents a form of the virus that is resistant to host mechanisms of viral clearance, enabling infected cells to maintain viral oncogene expression and avoid cell death.

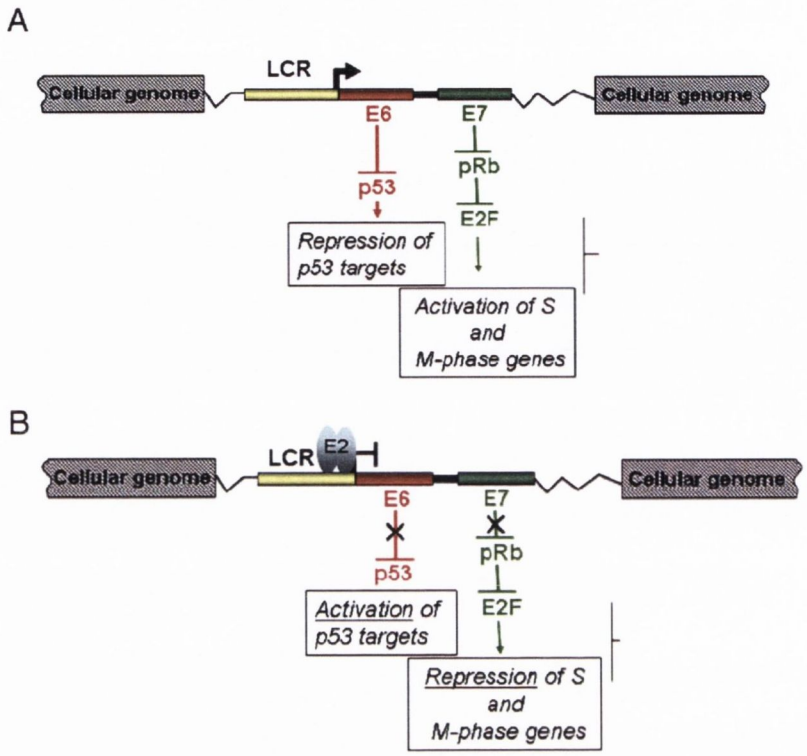


**Figure 1.5 Schematic representation of the fragment of HPV genome integrated in the cellular genome.** (A) The E6 and E7 genes are transcribed from the early promoter and the products of these genes negatively interfere with p53 and pRB respectively, thus inducing cell cycle deregulation and cell transformation. (B) When integration occurs in cells with a background of episomal HPV gene expression the viral E2 transcription factor represses the E6 and E7 transcription. (Adapted from Thierry, 2009).

### *1.6.2 The E6 Protein*

#### 1.6.2.1 Structure

The E6 protein is approximately 150 amino acids in length, composed of two zinc-like fingers linked by 36 amino acids and flanked by short N- and C-terminal domains of variable lengths. Determining the crystal structure of E6 has been problematic due to the inability to isolate the protein in a native, soluble form. Recently, however, the structure of the C-terminal half of HPV16 E6 was solved by nuclear magnetic resonance (NMR) and was used as the basis from which to construct a model for the whole protein (Figure 1.6) (Nomine *et al.*, 2006). The availability of the three dimensional structure allows for the visualisation of potential residues that mediate binding to its cellular targets. Unfortunately, it has also revealed that many of the mutations previously described, that were used to ascertain domain specific functions of E6, likely disrupted the global integrity of the structure instead of interfering with specific protein-protein interactions. Although E6 dimerises at high salt and protein concentrations, it is thought in physiologic conditions to be monomeric (Lipari *et al.*, 2001). The E6 proteins from low-risk types are predominantly found in the cytoplasm, while the E6 from high-risk HPV types, which contain two nuclear localisation signals, are located in the nucleus and the cytoplasm (Tao *et al.*, 2003).

All HPV E6 and E7 are expressed from a single promoter, producing a single polycistronic mRNA which encodes both E6 and E7 (Stacey *et al.*, 2000). For high-risk HPV, there is a conserved splice donor site within the E6 transcript, which allows the generation of either full-length E6 or its splice variant, E6*(Figure 1.5; Inagaki *et al* 1988; Schneider-Gadicke *et al.*, 1988; Sedman *et al.*, 1991; Stacey *et al.*, 1995; Vaeteewoottacharn *et al.*, 2005). The E6* proteins are C-terminally truncated versions of the full-length E6 proteins. This phenomenon is a common feature of the early transcripts of high-risk HPVs as opposed to the low-risk counterparts, who lack the essential splice donor site for this pattern of splicing. The alternatively spliced E6* mRNA is found at much higher levels compared with the full-length E6 transcripts (Tang *et al.*, 2006; Smotkin and Wettstein 1986; Zheng and Baker 2006). Recent

evidence from cell line studies suggests that, at least for HPV types 16 and 18, unspliced mRNA encodes mostly full length E6, whilst spliced mRNA encodes both E7 and also the splice variant E6* proteins (Tang *et al.*, 2006). Whilst some papillomavirus types, such as HPV16 seem to have splicing patterns that allow the expression of up to four E6* species, others like HPV18 appears to transcribe only one mRNA species that is capable of expressing E6*. Recent evidence would suggest that the functions of E6* may vary depending on the ratio of the E6 to E6* transcripts (Pim *et al.*, 2009). High E6* protein levels may allow targeting of cellular proteins whose phosphorylation-dependent localisation makes them inaccessible to full length E6 (Pim *et al.*, 2009). Additionally, interaction of E6* with full-length E6 may either inhibit or enhance some of the functions of the later (Pim *et al.*, 2009).

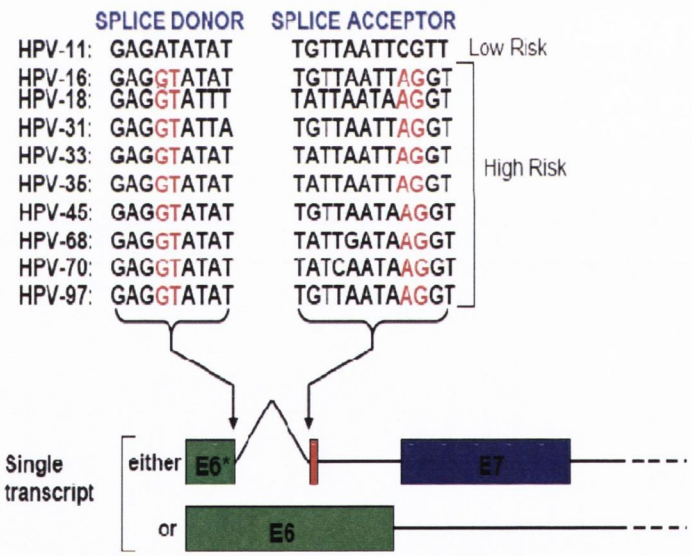


**Figure 1.6: Splicing of HPV E6 mRNA.** High-risk E6 mRNAs undergo alternative splicing resulting in generation of smaller E6* protein. This phenomenon of alternative splicing has been reported in high-risk HPV types only; the low-risk types do not show alternative splicing. This is because the low-risk types lack the essential dinucleotides (GT) of splice consensus sequences that are present in the high-risk types. (adapted from Pim *et al.*, 2009).

### 1.6.2.2 Apoptosis Inhibition

As E6 lacks intrinsic enzymatic and specific DNA binding activities, it is accepted that its biological effects are mediated by protein–protein interactions. The first function identified for the E6 protein, and arguably the most important, was its ability to induce the degradation of p53 (Schneffer *et al.*, 1990; Werness *et al.*, 1990). Cellular damage and improper simulation of DNA synthesis result in the activation of p53; which in turn, depending upon the type and extent of the damage, initiates pathways for DNA repair, cell cycle arrest or apoptosis (El-Deiry *et al.*, 1993; Harper *et al.*, 1993; Lowe *et al.*, 1994; Wu and Levine, 1994). The importance of p53 is exemplified by the observation that approximately one-half of all human cancers harbour mutations in the p53 gene (Beroud and Soussi, 2003; Olivier *et al.*, 2002). Unlike most other cancers cervical carcinomas generally harbour wild-type p53 (Crook *et al.*, 1991a; Scheffner *et al.*, 1991) and have instead evolved mechanisms to inhibit p53 activity through the action of E6. For HPV, blocking the apoptotic signal from p53 is essential, as otherwise the virally infected cell would be eliminated.

The first protein shown to interact with E6 was E6 associated protein (E6AP), an E3 ubiquitin ligase (Huibregtse *et al.*, 1991; Huibregtse *et al.*, 1993a; Scheffner *et al.*, 1993). The ubiquitin cascade functions to target proteins for proteasomal degradation by means of adding multiple ubiquitin monomers to the protein destined to be destroyed. E6 mediated degradation of p53 requires the formation of a protein complex consisting of E6, E6AP and p53 (Huibregtse *et al.*, 1993a; Huibregtse *et al.*, 1993b). Since E6AP does not bind to p53 normally, the sequence of events is believed to involve an initial interaction between E6 and the N-terminal of the E6AP before p53 can be bound and subsequently ubiquitinated (Huibregtse *et al.*, 1993a; Huibregtse *et al.*, 1993b). An interesting insight into the different mechanism of action between high-risk and low-risk HPV types is observed with p53 degradation. While both types interact with p53, high-risk types bind to the C-terminal and core domain of p53, whereas low–risk types bind solely to the C-terminal. Only the high-risk E6-p53 core domain interaction targets p53 for degradation (Crook *et al.*, 1991b; Li and Coffino, 1996).

Although the main mechanism of action of E6 on p53 is to induce its degradation, this does not remove all p53 from the cells. Since the abolishment of p53 activity is essential, E6 has evolved other mechanism to circumvent its activity (Cooper *et al.*, 1993; Lechner *et al.*, 1992; Lie *et al.*, 1999; Mantovani and Banks, 1999). These effects are mediated through several different methods all of which appear to be E6-AP independent. First it has been shown that by inducing a conformational change in p53, E6 can inhibit its binding to site-specific DNA sequences and can even cause dissociation of p53-DNA complexes, inhibiting p53 transactivation (Lechner and Laimins,1994; Thomas *et al.*, 1995). These effects have been shown correlate with the affinity that different types of HPV E6 have for p53, and that this affinity correlates with the ability to inhibit transcription of p53 responsive genes (Lechner and Laimins, 1994). Additionally aberrant p53 localisation has been proposed as a mechanism of E6 regulation. Evidence for mislocalisation of p53 by E6 comes from cell line experiments where E6 degradation of p53 was blocked but normal nuclear localisation of p53 did not occur (Mantovani and Banks, 1999). This activity has been postulated to be mediated through the interaction of E6 to the C-terminal of p53, where a nuclear localisation signal resides. The final mechanism employed by E6 is post-transcriptional modification. HPV E6 is believed to abrogate the transactivation of p53 responsive genes through its interaction with histone acetyltransferases, p300 and hADA3 (Kumar *et al.*, 2002; Patel *et al.*, 1999; Zimmermann *et al.*, 2000). Acetylation of p53 by p300 following DNA damage is known to occur and enhance the ability of p53 to induce the expression of responsive genes. The E6 proteins have been shown to bind to p300, and this interaction inhibits p53 acetylation at p300-dependent sites, leading to decreased expression from p53 responsive genes (Patel *et al.*, 1999; Zimmermann *et al.*, 2000). The E6 interaction with hADA3, in contrast to that of p300, results in hADA3 degradation (Kumar *et al.*, 2002). This degradation has been shown to diminish p53 mediated transactivation (Kumar *et al.*, 2002; Zeng *et al.*, 2002).

The apoptotic effects of E6, primarily involve p53 but are not limited to this pathway. In the late 1990's two studies in systems that lacked p53 expression demonstrated that E6 mediated inhibition of apoptosis could occur in a p53 independent manner (Pan and Griep, 1995; Steller *et al.*, 1996). Subsequently, it was discovered that cellular

targets of E6 included several pro-apoptotic factors, including Bak, c-myc, FADD, procaspase 8 and TNFR-1 (Filippova *et al.*, 2002; Filippova *et al.*, 2004; Garnett *et al.*, 2006; Kinoshita *et al.*, 1998; Thomas *et al.*, 2002). There are two major apoptotic pathways that can be triggered by different stresses, the extrinsic and the intrinsic pathway, both of which E6 disrupts by interacting with the above mentioned factors. The fact that E6 disrupts both pathways is interesting, as one pathway can activate the other and thus amplify the apoptotic signal. Thus, E6 not only protects an infected cell from multiple apoptotic stimuli but also from cross activation between pathways. Moreover, E6 has been shown to interact with proteins that are involved in apoptotic signalling at the crossroads where the intrinsic and extrinsic pathways join, downstream of the effector caspases. HPV16 E6 has been shown to up-regulate the expression of two inhibitor of apoptosis (IAP) proteins, c-IAP2 (James *et al.*, 2006; Yuan *et al.*, 2005) and survivin (Borbely *et al.*, 2006), which inactive the executioner caspase 3 and caspase 7. One can conclude that E6 is a multi functional anti-apoptotic protein.

### 1.6.2.3 Induction of telomerase activity

Human Telomerase Reverse Transcriptase (hTERT) is the catalytic subunit of telomerase, a ribonucleoprotein that extends the repetitive telomeric DNA of chromosomes in eukaryotes. Telomerase is active only in stem cells and during embryonic development, with hTERT gene expression mirroring this pattern of activity (Bryan and Cech, 1999). Along with the inactivation of p53 and pRb pathways, activation of telomerase is a commonly observed event in human cancers. In somatic cells, chromosomal telomeres shorten with each round of cell division, eventually resulting in chromosomal instability and senescence (Hahn and Weinberg, 2002). However, in cancerous cells reactivation of telomerase confers an immortalised phenotype, as there is little to no shortening of the telomere, thus allowing cells to avoid senescence once a replicative competent environment is maintained (Meyerson *et al.*, 1997; Shay and Bacchetti, 1997).

In 1996, Klingelhutz *et al.*, observed that the E6 protein of high-risk HPVs could induce telomerase activity. Subsequent investigations demonstrated that this activity of E6 was due to an increase in expression of hTERT and dependent on its interaction with E6AP (Gewin *et al.*, 2004; Liu *et al.*, 2005). The promoter region of hTERT is known to be regulated by a number of transcription activators and repressors, including the transcription activator c-myc (Wang *et al.*, 1998). While investigations demonstrated that c-myc was required for E6 mediated activation of hTERT (Oh *et al.*, 2001; Veldman *et al.*, 2003), neither increased c-myc protein level nor enhanced myc/max complex formation was detected with E6 expression (Gewin and Galloway, 2001, Veldman *et al.*, 2003). Recently a novel transcription repressor of hTERT has been described, NFX-91 (Xu *et al.*, 2008), and it is believed this protein may hold the key to understanding the mechanism of action of E6 on hTERT. Like p53, NFX-91 appears to be poly-ubiquitinated and targeted for degradation by the E6/E6AP complex (Gewin *et al.*, 2004). In HPV16 E6 expressing cells, a reduced level of NFX–91 has been observed to correspond with decreased occupancy at the hTERT promoter and with signs of transcriptional activity, for instance an increase in the acetylation of the hTERT gene (Gewin *et al.*, 2004; Xu *et al.*, 2008). It has now been hypothesised that E6 stimulates hTERT expression by inducing the degradation of NFX-91, which in turn allows the recruitment of myc/max complex to the promoter region of hTERT, thus explaining the initial findings for a requirement of c-myc.

### 1.6.2.4 Targeting and disruption of PDZ proteins

High-risk HPV E6 proteins contain a conserved class I PDZ motif (X-S/T-X-V) at their extreme C-terminal (Songyang ete al., 1997), which facilitates their binding to specific domains of cellular proteins known as PDZ proteins. Interestingly, this protein interaction domain is a unique characteristic of high-risk HPV types, with none of the low-risk HPV E6 proteins having this motif (Gardiol *et al.*, 1999; Kiyono *et al.*, 1997; Lee *et al.*, 1997; Pim *et al.*, 2000). The PDZ domain has been demonstrated to be essential for the transforming capabilities of E6, an activity which is independent of E6's inhibition of the p53 pathway (Nguyen *et al.*, 2003; Simonson *et al.*, 2005; Shai *et al.*, 2008). For instance, mice expressing a version of E6 which lacks the C-terminal five

amino acids that mediate binding to PDZ proteins renders these mice unable to trigger unregulated cellular proliferation, highlighting the requirement of the PDZ domain in directing E6 induced hyperplasia (Gardiol *et al.*, 2002; Lee *et al.*, 2004; Nguyen *et al.*, 2003). Additionally, both HPV16 and HPV18 can induce epithelial-to-mesenchymal transition (EMT) like changes in keratinocytes *in vitro*, a hallmark of cancer development. This ability was found to be dependent on an intact PDZ-binding motif (Spanos *et al.*, 2008; Watson *et al.*, 2003). The importance of this domain to EMT provides a strong indication of the nature of the targets with which E6 interacts through this motif.

The first PDZ protein which was shown to be targeted by E6 was the human homolog of the *Drosophila* discs large tumour suppressor protein (Dlg) (Kiyono *et al.*, 1997; Lee *et al.*, 1997). hDlg functions as a tumour suppressor required at epithelial tight junctions, where it is involved in regulating cell-cell adhesion, epithelial polarity and cellular proliferation. Subsequently many more PDZ proteins involved in the maintenance of the epithelial cell junctions were observed to be targeted by E6 through this C-terminal domain, including hScrib (Nakagawa and Huibregste, 2000), MUPP1 (Lee *et al.*, 2000), MAGI (Glaunsinger *et al.*, 2000; Thomas *et al.*, 2002) and PATJ (Latorre *et al.*, 2005; Storrs *et al.*, 2007). Epithelial structure is important for the maintenance of correct regulation of cell proliferation and differentiation. Consequently, the establishment of cell-ECM (extra cellular matrix) adhesion, cell-cell contact, cytoskeletal organisation and polarity of epithelial cells is essential and tightly regulated (Bilder, 2004). Proper cervical epithelial structure, restricting cell proliferation to matrix-interacting cells, would therefore hamper E6 activity. High-risk E6 is believed to circumvent this problem by interacting with the previously named PDZ proteins. These proteins are thought to have roles in maintenance of cell polarity, formation of cell-cell adherence junctions and organisation of multi-protein signalling complexes as scaffolding proteins. Consequently their functional inhibition by E6 would results in loss of cell polarity or morphological conversion associated with EMT leading to transformation and carcinogenesis. Supporting this view are the findings in various human cancers, such as cervical (Nakagawa *et al.*, 2004), breast (Martin *et al.*,

2004) and colon (Gardiol *et al.*, 2006), that decreased expression of hDlg, hScrib and MUPP1 proteins correlates with malignancy. In addition potential tumour suppressor activities have been described *in vitro* for hDlg, MAG1 and MUPP1 (Massimi *et al*, 2004). However, though we know that E6 interacts with these PDZ domains and in some cases degrades them, their role in the neoplastic progression has still to be conclusively demonstrated.

### *1.6.3 The E7 protein*

#### 1.6.3.1 Structure

The E7 protein was the first oncogene of the high-risk HPVs to be discovered. The HPV E7 proteins are small, acidic polypeptides of approximately 100 amino acids in length. Within the N-terminal domain of E7 lies two conserved regions called CR1 and CR2, which are homologous to sequences found in SV40 large T antigens (T Ag) and adenovirus (Ad) E1A proteins (Figge *et al.*, 1988; Phelps *et al.*, 1988; Vousden and Jat 1989). As with SV40 T Ag and AD E1A, these two conserved regions significantly contribute to the transforming activities of high risk HPV E7 oncoprotein (Edmonds and Vousden, 1989; Jewers *et al.*, 1992; Phelps *et al.*, 1992; Storey *et al.*, 1990; Watanabe *et al.*, 1990). The C-terminus contains a zinic binding domain consisting of two copies of a Cys-X-X-Cys sequence motif separated by 29 amino acid residues (Barbosa *et al.*, 1989). This region of E7 functions as a dimerisation domain (Clemens *et al.*, 1995; Liu *et al.*, 2006; McIntyre *et al.*, 1993; Ohlenschlager *et al.*, 2006), although there is no compelling evidence that E7 exists as a dimer *in vivo* or that dimerisation is necessary for its biological activity. Intriguingly, the C-terminal zinc binding domains have sequence similarity to those of E6, indicating that the E6 and E7 genes may have arisen from a common ancestor (Cole and Danos, 1987). The structure of HPV E7 proteins has been solved by NMR (Liu *et al.*, 2006) and X-ray crystallography (Ohlenschlager *et al.*, 2006). These studies have revealed that the amino terminal domain is unfolded, whereas the C-terminal domain forms a unique, tightly packed zinc-binding fold (Liu *et al.*, 2006; Ohlenschlager *et al.*, 2006). HPV E7 is primarily located within the cytoplasm (Huh *et al.*, 2005; Nguyen *et al.*, 2007; Ressler *et al.*, 2007) but nuclear pools have also

been observed (Greenfield *et al.*, 1991; Sato *et al.*, 1989; Smith-McCune *et al.*, 1999). Although E7 does not have a prototypical nuclear targeting sequence, it is actively transported into the nucleus through a novel Ran-dependent import receptor (Angeline *et al.*, 2003). Like E6, E7 lacks intrinsic enzymatic activities and specific DNA binding activities and it is widely accepted that its biological activities are linked to its ability to associate with and subvert the normal activities of cellular regulatory complexes.

### 1.6.3.2 Dysregulation of G1/S Checkpoint – Pocket Protein Family

The most characterised property of HPV E7 protein is its ability to subvert the activity of the members of the pocket protein family, Rb, p107 and p130. These proteins function primarily as regulators of the cell cycle and while, Rb is constitutively expressed throughout all phases of the cell cycle, p107 is synthesized predominantly during the S phase and p130 predominates at $G_0$ (Berezutskaya *et al.*, 1997; Classon and Dyson 2002). The subsequent discussion is focused on Rb rather than Rb family members, but the actions described are usually equally applicable to all three.

The Rb protein functions primarily through inhibiting the activity of the E2F transcription factor. Hypophosphorylated Rb binds to E2F forming a transcriptional repressor complex (Edmonds and Vousden, 1989; Weintraub *et al*, 1995). The E2F transcription factor can be found bound to promoters of genes involved in S phase entry and progression; as such then hypophosphorylated Rb suppress the expression of genes required for the movement from the G1 to the S phase (Edmonds and Vousden, 1989; Weintraub *et al*, 1995). During the normal cell cycle, in late G1, Rb is phosphorylated by cyclin D1/cyclin-dependent kinase (cdk)4 and cyclin E/cdk2 complexes producing a hyperphosphorylated form of the protein and causing the dissociation of Rb from E2F thereby allowing normal S phase progression (Munger and Howley 2002).

HPV E7 preferentially associates with the hypophosphorylated form of Rb preventing its interaction with E2F (Dyson *et al.*, 1992). Therefore, in cells expressing the E7 protein, the checkpoint control at the G1/S transition is lost leading to uncontrolled cellular proliferation. The association of E7 with Rb occurs through a conserved Leu-X-Cys-X-Glu (LXCXE) motif in its CR2 homology domain (Dyson *et al.*,1992; Munger *et al.*, 1989). Both high- and low-risk HPV types bind to Rb but the binding affinity of the high-risk E7 is approximately 10-fold higher (Gage *et al.*,1990; Munger *et al.*,1989). This difference has been attributed to a single amino acid difference in E7, Asp21 in HPV16 E7 versus Gly22 in HPV6 E7 (Heck *et al.*, 1992; Sang and Barbosa, 1992). High-risk E7 proteins not only sequester Rb, but also induce its degradation via a proteasome dependent pathway, whereas low-risk E7 proteins do not target Rb for degradation (Boyer *et al.*, 1996; Giarre *et al.*, 2001). It is postulated that rather than these two processes of E7 mediated Rb regulation simply evolving to control Rb functionality, that they are actual required for functionally different tasks. For example, during the HPV16 life cycle the ability of E7 to allow suprabasal cells to support DNA synthesis is linked to E7's ability to bind Rb family members but not with its ability to induce their degradation (Collins *et al.*, 2005). On the other hand, its capacity to perturb differentiation correlates with both E7's binding to and degradation of Rb (Collins *et al.*, 2005), suggesting that different key stages of the 'productive' HPV16 life cycle rely on different functions of E7.

### 1.6.3.3 Dysregulation of the cell cycle – Rb independent

Like the E6 protein, E7 does not rely on the exploitation of a single protein to disrupt a pathway but rather to ensure continuity of the alteration it targets several proteins within the pathway. Therefore, in addition to inducing cell cycle dysregulation through the interaction with Rb, E7 targets other proteins involved in this pathway. For instance HPV E7 not only augments the expression of the E2F responsive genes by sequestering Rb but it has also been demonstrated to bind directly to E2F1 and in this manner enhance its transcriptional activity (Hwang *et al.*, 2002). This ability of E7 appears to be important in tumourigenesis, as the affinity of E7 for E2F1 appears to correlate with the oncogenic potential of the virus, with high-risk E7 reported to have a

greater affinity for E2F1 than low-risk E7 (Hwang *et al.*, 2002). Furthermore, E7 interacts with the E2F6 (McLaughlin-Drubin *et al.*, 2008), which functions as a transcriptional repressor at the promoters of E2F1 responsive (Lyons *et al.*, 2006). In fact this protein itself is an E2F1 responsive gene and is found to be up-regulated at the G1/S transition. Thus it is part of the regulatory machinery by which the cell controls the cell cycle, involved in directing appropriate cell cycle exit and differentiation. The interaction between E7 and E2F6 abrogates its function as a transcriptional repressor (McLaughlin-Drubin *et al.*, 2008), thus E7 is counteracting the up-regulation induced by increased activity of E2F1 ensuring continuous cell proliferation.

In proliferating cells, cyclin dependent kinases (cdks) are the motors that drive the cell cycle progression. Multiple mechanisms, most importantly association with positive regulatory subunits, cyclins, and negative regulators, cdk inhibitors, regulate the activity of cdks. In addition to interacting with members of the pocket protein and E2F families E7 associates with cyclins A and E (Tommasino *et al.*, 1993) as well as the cdk inhibitors p21 (Funk *et al.*,1997; Jones *et al.*, 1997) and p27 (Zerfass-Thome *et al.*, 1996). Cyclins A and E are the regulators of cdk2, which is essential for DNA synthesis and progression from G1 through S Phase of the cell cycle. In normal proliferating cells the transcription of these cyclins is increased through phosphorylation of Rb and subsequent activation of E2F. In turn, in order to drive the cell cycle, they also induce phosphorylation and inactivation of Rb. In E7 expressing cells, not only is increased expression level of these two cyclins observed (Zerfass *et al.*, 1995), moreover the activity of the cyclin/cdk complexes is enhanced (He *et al.*, 2003). High risk E7 can directly associate with cyclin A/cdk2 and cyclin E/cdk2 complexes (He *et al.*, 2003; McIntyre *et al.*, 1996; Nguyen and Munger, 2008; Tommasino *et al.*, 1993), which results in increased cdk2 activity. Furthermore, E7 interacts with p21 (Funk *et al.*, 1997; Jones *et al.*, 1997) and p27 (Zerfass-Thome *et al.*, 1996), overriding their growth inhibitory activities on cdk2. The activity of p21 and p27 is essential for normal cellular proliferation and they respond to multiple anti-proliferative signals, including growth factor withdrawal (Firpo *et al.*, 1994), activation of p53 (el-Deiry *et al.*, 1993), and loss

of cellular adhesion (Assoian, 1997; Fang *et al.*, 1996). Therefore, it is unsurprising that E7 has learnt to abrogate the activities of these proteins as either one could severely hamper the 'productive' HPV infection or HPV driven carcinogenesis. Part of the mechanism of E7 on p21 has been delineated, demonstrating that E7 binding prevents p21 from inhibiting proliferating cell nuclear antigen (PCNA) dependent replication and also from directly inhibiting E2F activity (Funk *et al.*, 1997). Interestingly, p21 levels are increased further through a non-transcriptional mechanism in the presence of HPV E7. Although high-risk HPV E7 expression increases p21 levels through protein stabilization (Jian *et al.*, 1998, Jones *et al.*, 1999 and Noya *et al.*, 2001), cdk2 remains active in HPV E7-expressing cells (Funk *et al.*, 1997, Jones *et al.*, 1997; Ruesch and Laimins, 1997). The reason behind this observation has yet to be explained.

### 1.6.3.4 Transcriptional regulation

An important mechanism of transcriptional regulation is chromatin remodelling through histone acetylation. Actively transcribed genes have a high level of histone acetylation (Grunstein 1997). E7 has been demonstrated to indirectly induce chromatin remodelling and this activity requires its zinc finger domain (Brehm *et al.*, 1999; Longworth and Laimins, 2004). Histone deacetylases (HDACs) are expressed in all tissues and function as transcriptional co-repressors by removing acetyl groups from lysine rich amino terminal tails of the histone proteins in nucleosomes inducing chromatin remodelling. High-risk E7 proteins bind indirectly with HDAC-1 through mi2β, a component of a nucleosome remodelling deacetylation complex (Brehm *et al.*, 1999). The importance of this interaction is demonstrated by the observation that E7 mutants that fail to bind Mi2β but which bind Rb normally fail to overcome cell cycle arrest. The underlying mechanism probably relates to the association between HDAC-1 and Rb. These proteins are believed to work in a cooperative manner to repress E2F mediated transcription (Brehm *et al.*, 1998; Wells *et al.*, 2000). This is supported by the fact that the association between E7 and HDAC-1 results in increased levels of E2F2 mediated transcription in differentiating cells (Longworth *et al.*, 2005), potentially influencing S phase progression. Both high-risk and low-risk E7 displaces HDAC-1 from Rb and the E7 HDAC-1 interaction is independent of Rb (Brehm *et al.*, 1998).

Additionally E7 can also associate with histone acetyl transferases (HATs), including p300 and p300/CBP-associated factor (PCAF) (Avvakumov *et al.*, 2003; Bernat *et al.*, 2003; Huang and McCance, 2002). HATs function in the opposite manner to HDACs and thus are transcriptional co-activators. PCAF and p300 have been observed to acetylate Rb and this modification is required for Rb to mediate terminal cell cycle exit (Nguyen *et al.*, 2004; Nguyen and McCance 2005). Therefore, unsurprisingly it has been reported that the interaction between E7 and PCAF reduces its acetyltransferases activity (Avvakumov *et al.*, 2003). Targeting of histone acetylation thus provides another method by which E7 can alter gene transcription, in particular that of E2F responsive genes by inhibiting Rb activity. It is also a potential explanation why the zinc finger domain is essential in activating E2F-regulated genes as well as immortalising keratinocytes (Avvakumov *et al.*, 2003; Huang *et al.*, 1993; Jewers *et al.*, 1992).

### *1.6.4 The interplay between high-risk E6 and E7*

The high-risk E6 and E7 oncogenes are independently able to immortalise various cell types in tissue culture (White *et al.*, 1994), but efficiency is exponentially increased when they are expressed together (Song *et al.*, 2000). Immortalisation occurs when cells become capable of continuous proliferation and proliferate indefinitely. From the preceding descriptions of the functions of these oncogenes, it is clear that working in a cooperative manner they can efficiently trigger cell immortalisation, with E7 driving cellular proliferation and E6 eliminating the apoptotic signals due to E7 activity, as well as inducing telomerase activity. However, although continuous expression of E6 and E7 induces cell immortalisation by disrupting key tumour suppressor pathways and can predispose to the development of cervical cancer, this alone is not sufficient for tumourigenesis. At low passage, keratinocytes immortalised through the introduction of high-risk HPV are non-tumorigenic (DiPaolo *et al.*, 1989; Durst *et al.*, 1989; Hurlin 1991; Pei *et al.*, 1993). They can undergo malignant progression after extended growth in tissue culture (Durst *et al.*, 1989; Hurlin 1991) or when additional oncogenes such a ras or fos are expressed (DiPaolo *et al.*, 1989; Pei *et al.*, 1993). Evidently, additional oncogenic events are necessary in E6/E7 expressing cells to yield full transformation. Consistent with this concept, cervical carcinomas contain chromosomal abnormalities,

in particular specific gains of chromosome 3q have been observed to occur at the transition from high-risk HPV associated severe dysplasia to invasive carcinoma (Habermann *et al.*, 2004; Heselmeyer *et al.*, 1996).

While the high-risk oncogenes may not be able to fully transform cells, potentially they may facilitate the acquisition of the additional genetic changes required to drive neoplastic procession. As a consequence of their ability to interact with host cellular proteins, the expression of high-risk HPV E6 and E7 proteins in cultured cells causes disruption of cell cycle checkpoint controls, which directly results in increased rates of mutagenesis and genetic instability (Duensing and Munger, 2004). Genomic instability is a hallmark of the carcinogenic process (Klausner, 2002). Though not necessarily the end result of oncogenic transformation, it is believed to be involved in the acquisition of genetic alterations that are necessary for survival and clonal expansion of tumour cells within the microenvironment of an emerging neoplasm. Both high-risk E6 and E7 have been demonstrated *in vivo* to work in a cooperative manner to induce genomic instability in normal cells (White *et al* 1994) through the induction of chromosomal rearrangements and abnormal centrosome numbers, which results in the generation of mitotic defects and aneuploidy (Duensing *et al.*, 2000; Plug-DeMaggio *et al.*, 2004).

Accurate chromosome segregation relies on correct formation of the bipolar mitotic spindle poles, which in turn relies on the precise single duplication of the centrosome. High-risk but not low-risk E7 induces centrosome over-duplication resulting in the creation of multipolar mitotic spindle poles that give rise to aberrant chromosome segregation (Duensing *et al.*, 2000). It is proposed that this activity of E7 is Rb independent and mediated through the dysregulation of cyclinA and E/cdk2 complexes (Duensing *et al.*, 2006; Duensing and Munger, 2003; Southern *et al.*, 2004), which are known to regulate normal centrosome duplication. Though no direct effect of E6 on centrosome numbers has been observed (Duensing *et al.*, 2000), its inhibition of cell cycle checkpoints is required to allow cells to enter mitosis in the presence of centrosome abnormalities and proceed to rounds of DNA replication (Ciciarello *et al.*,

2001; Lanni and Jacks, 1998; Thompson *et al.*, 1997; Thomas and Laimins, 1998; Vogel *et al.*, 2004). In addition, E6 and/or E7 oncoprotein expressing cells have been observed to exhibit centrosome independent mechanisms of genomic instability through chromosomal rearrangements (Duensing and Munger, 2002; Plug-DeMaggio *et al.*, 2004), chiefly anaphase bridges. Anaphase bridges can be generated between unprotected chromosome ends caused by DNA breakage, which likely accumulate in E6 and E7 expressing cells by abrogation of multiple checkpoint controls and DNA damage responses (Thompson *et al.*, 1997; Thomas and Laimins, 1998). The chromosomal breakage-fusion-bridge cycle is considered to give rise to chromosomal rearrangement, including translocations, additions and deletions (Gisselsson *et al.*, 2000).

## 1.7 A new era in cervical cancer driven by molecular knowledge

Our understanding of the involvement of HPV in cervical cancer has allowed us to investigate and identify some of the molecular pathways and targets implicated in this carcinogenic process. With our increased knowledge of the molecular mechanisms that underlie this disease, we can now begin to exploit this information to design preventative and therapeutic agents that specifically target the genes and gene products involved. One major advance has been the introduction of prophylactic HPV vaccines, which utilise L1 virus-like particles (VLPs) to block HPV infection. The driving force behind this momentous progress was the molecular knowledge of the structure of the viral caspid and the subsequent development of VLPs that are morphologically and immunologically similar to native virions (Kirnbauer *et al.*, 1992; Zhou *et al.*, 1991). These vaccines are considered to be molecularly targeted, because they generate immune responses against specific proteins, the HPV major viral caspid protein. Two vaccines are presently available and in clinical use; one is a quadrivalent vaccine containing VLPs of HPV6, 11, 16 and 18, Gardisil® developed by Merck and the other a bivalent vaccine covering HPV16 and 18, Cerarix produced by Glaxo-Smith-Kline. Randomized Phase III clinical trials in women with no evidence of prior HPV infection have demonstrated that both these vaccines are extremely successful in inducing nearly complete protection from persistent HPV16 and 18 infections (Kjaer *et al.*, 2009; Paavonen *et al.*, 2007; Paavonen *et al.*, 2009; The FUTURE II Study Group, 2007). Since HPV16 covers slightly more than 50% of all cervical cancer and HPV18 close to 20%, it is anticipated that these vaccines should protect against at least 70% of cervical carcinomas and their precursor lesions (Muñoz *et al.*, 2003). However, the growing expectation is that this figure could be even higher, as recent data from the clinical trials have indicated that there is cross-protection for several non-vaccine oncogenic HPV types (Brown *et al.*, 2009; Jenkins, 2008; Paavonen *et al.*, 2009). In particular high levels of protection against HPV31 (most closely related to HPV16) and HPV45 (most closely related to HPV18) were consistently noted, which may bring the protection rate close to 80%.

Although HPV vaccines are a hugely significant development in reducing the burden of cervical cancer, there are still a number of issues that need to be addressed. Both vaccines are very effective over approximately a 6 year period (Kjaer *et al.*, 2009; Paavonen *et al.*, 2009), but the longevity of protection and possible need for booster immunisations remain important questions. While initial indications show high cross-protection for other oncogenic HPV types, the degree to which this occurs and again the duration of the effect needs to be evaluated. In addition, immunosuppressed patients such as organ recipients and HIV infected patients have a greater propensity for cervical cancer and their response to an HPV vaccine is unknown. The current high costs of the vaccines have made them prohibitive for global application. This is extremely important as approximately 90% of all cervical cancers occur in resource-constraint developing countries (WHO, 2006), i.e. the countries that cannot afford the vaccines are those that most require them. Unfortunately, these vaccines have not been shown to accelerate HPV clearance and are unlikely to be of significant benefit to the large number of individuals with established lesions who are already infected with oncogenic HPV (Hildesheim *et al.*, 2007). This is an important issue, because of the wide prevalence of HPV infection and the considerable burden of established HPV-related disease worldwide. Furthermore, preventive vaccines will not impact cervical cancer rates for several decades from the implementation of mass vaccination because of existing infections and slow process of carcinogenesis. Therefore, it is essential that we continue efforts to develop effective therapies for cervical cancer, such as low cost prophylactic vaccines to aid worldwide distribution, and novel therapeutic agents to treat women that present with high grade lesions.

With the identification of genes involved in the neoplastic progression of cervical cancer, and concurrent advances in molecular targeting approaches, novel therapeutic development is focused on targeting genes that contribute to the carcinogenic process, with the expectation that such approaches may lead to selective and specific inhibition of tumour growth with minimal untoward side effects on normal cells. In general, it is easier to repress the function of a gene rather than to reactivate a functionally inactive gene and therefore the dominant approach taken is to down-

regulate gene activity. Since the presence of E6 and E7 is necessary for the malignant phenotype of the cervical cancer cell, much of the effort to develop targeted therapy has focused on interfering with their activity. This will potentially result in growth arrest of infected cells and may lead to apoptosis (Desaintes *et al*, 1997). Although, the majority of the research has focused on the HPV viral oncogenes, the advent of gene expression profiling and the subsequent identification of many differentially expressed genes has meant there has been a broadening of focus with investigators also examining these genes as alternative potential novel therapeutics targets.

### *1.7.1 Therapeutic nucleic acids a treatment option for cervical cancer*

Over the last 30 years, much effort has gone into developing and optimising genomic based strategies for cancer therapy. The ambition has been to use nucleotide sequences, known as therapeutic nucleic acids (TNAs) of relevant cancer genes, as tailored anticancer agents that lack many of the toxic side effects of traditional cytotoxic drugs. The idea dates back to the 1960's when RNA sequences were shown to serve as endogenous inhibitors of gene expression in prokaryotes. The TNAs now available include ribozymes, anti-gene oligonucleotides, antisense oligonucleotides, aptamers and small interfering RNA (siRNA). The majority of these TNAs work on the basic principles of Waston-Crick base pairing, binding to a cellular DNA/RNA target which results in inhibition of the expression of the protein coded for by the target. Until recently, the most effective TNA applications in cervical cancer involved antisense oligonucleotides and ribozymes.

Antisense oligonucleotides hybridise to complementary sequences forming DNA-RNA heteroduplex helices and through this action not only physically block translation but also activate endogenous RNaseH causing cleavage of the target mRNA (Bonham *et al.*, 1995). There are several generations of antisense oligonucleotides, as initial forms experienced problems with *in vivo* instability, and alterations to increase stability lead to loss of RNaseH induction (Agrawal and Zhang, 2000; Mercatante and Kole, 1997). The current class includes peptide nucleic acids (PNAs), phosphorodiamidate

morpholino oligomers (PMOs) and locked nucleic acids (LNAs), which are all nuclease resistant and highly effective, efficiently recruiting RNaseH. Ribozymes are naturally occurring catalytic oligonucleotides discovered in the 1980's (Inoue *et al.*, 1985). Once hybridised with a complementary sequence, the catalytic core of these molecules cleave the RNA (Sheldon and Symons, 1989; Uhlenbeck, 1987; Walter and Burke, 1997). Two recombinant ribozymes have been extensively used as TNAs, the hairpin and the hammerhead ribozymes.

Both antisense and ribozyme technologies have been used to target HPV16 and HPV18 E6/E7 transcripts and *in vitro* have been demonstrated to efficiently cleave these transcripts inhibiting cellular proliferation and promoting apoptosis (Chen *et al.*, 1996; Guapillo *et al.*, 2006; Venturini et la., 1999). These initial studies resulted in the application into nude mice where they were shown to suppress tumour growth (Venturini et la., 1999; Zheng *et al.*, 2002; Zheng *et al.*, 2004). A particularly interesting study was where E6/E7 expression was inhibited by a triplex expression system which allowed the production of multiple ribozymes directed against alternative target sites. Such an approach may result in the abrogation of highly variable HPVs (Aquino-Jarquin *et al.*, 2008). The use of antisense oligonucleotides and ribozymes has also been extended to proteins that are associated with the activities of the oncogenes, for example E6-AP. Targeting of E6-AP *in vitro* was observed to reduce its expression in high-risk HPV infected cells resulting in increased p53 levels (Beer-Romero *et al.*, 1997; Kim *et al.*, 2003). In addition, one study demonstrated that the reduction enhanced the apoptotic response of HPV18 positive cervical cancer cells to mitomycin C-induced DNA damage, indicating the possibility of suppressing E6-AP expression as a possible adjunct therapy (Kim *et al.*, 2003).

### 1.7.1.1 RNA interference

RNA interference (RNAi) is considered the most powerful discovery of recent times for the manipulation of gene expression, with far reaching applications from target validation to pharmacological agents for human disease. It is an evolutionary conserved post-transcriptional gene silencing mechanism triggered by the presence of double-stranded RNA (dsRNA) (Cerrutti 2003; Denli and Hannon 2003; Dykxhoorn *et al.*, 2003). During RNAi, long transcripts of dsRNA are rapidly processed into small interfering RNAs (siRNAs), which represent RNA duplexes of specific length and structure that finally guide sequence-specific degradation of mRNAs homologous in sequence to the siRNAs (Elbashir *et al.*, 2001). This naturally occurring phenomenon was first observed in the late 1980's by plant biologists working with petunias. They found that the introduction of a purple pigment-producing gene under the control of a promoter resulted unexpectantly in a white coloured flower (Napoli *et al.*, 1990). Thus, the introduction of this exogenous gene led to the silencing of both itself and the homologous endogenous gene. However, the molecular mechanism underlying this phenomenon, known at this point as "cosurpression", remained unclear until the late 1990's, when work by Fire and Mello showed that injecting of dsRNA into the nematode *Caenorhabditis elegans* resulted in the silencing of a gene whose sequence was complimentary to that of the introduced dsRNA (Fire *et al.*, 1998). This silencing response has subsequently been found to occur in other eukaryotes, from yeast to mammals (Hammond *et al.*, 2000; Hannon 2002).

In recent times, genetic and biochemical studies have rapidly increased our knowledge of the molecular mechanisms driving RNAi. It is recognised that RNAi works at multiple different sites within a cell and can suppress gene expression by inhibiting transcription (in the nucleus), by degrading messenger mRNA (in the cytoplasm) or by indirectly suppressing translation (in the cytoplasm). RNAi is achieved through complex interactions of many different proteins. In the cytoplasm long dsRNA is processed into 21 nucleotide siRNAs, which have 2-nucleotide 3' overhangs and 5' phosphates, by the ribonuclease III (RNase III)-like protein, Dicer (Bernstein *et al.*, 2001). Dicer is part of a heterodimer complex composed of itself and the HIV-1 TAR RNA-binding protein

(TRBP; Preall and Sontheimer, 2005). Argonaute 2 (Ago2) is then recruited to the TRBP/Dicer/siRNA complex, forming the RNA-induced silencing complex (RISC; Preall and Sontheimer, 2005). Once the complex has formed the siRNA is transferred from the TRBP/Dicer complex to Ago2, where it unwinds and a single strand, known as the sense or passenger strand, is degraded or discarded (Matranga *et al.*, 2005; Rand *et al.*, 2005). The remaining single stranded RNA (ssRNA), known as the anti-sense or guide strand, stabilized within a pocket in Ago2 drives sequence specific silencing by RISC. This guide strand directly interacts with sequence complimentary mRNA (Martinez *et al.*, 2002) and the RNaseH-like PIWI domain of Ago 2 subsequently cleaves the target mRNA (Liu *et al.*, 2004) between the $10^{th}$ and $11^{th}$ base relative to the 5' end of the siRNA antisense strand (Elbashir *et al.*, 2001). Cleaved mRNA cannot be translated and its encoded protein is therefore not produced. Afterwards the RISC complex dissociates from the target mRNA which allows it to bind to a new target; a single RISC complex can direct multiple round of mRNA silencing (Hutvagner and Zamore, 2002).

Ago2 is one of four ubiquitously expressed Ago proteins found in mammalian cells (Carmell *et al.*, 2002). While Ago2 seems to be the only one of this family of proteins with nuclease ability, it would appear the other three also contribute to RISC activity (Liu *et al.*, 2004). In particular it has been suggested that Ago1 is involved in the translational repression arm of RNAi. In mammalian cells, although any RNA loaded into the RISC complex has the capability of inducing translation suppression, the main mediators of this activity are endogenous microRNA (miRNA). These small RNA are the predominant species found in somatic mammalian cells and are natural regulatory molecules that employ the RNAi machinery to control gene expression (Bartel, 2004). Mature miRNA loaded in the RISC complex trigger the translation repression activity of RISC by imperfect base pairing between the target mRNA and the miRNA (Liu *et al.*, 2005). While miRNA predominantly function as translational repressors, they can on, occasion, like siRNA, cause mRNA cleavage. Furthermore, imperfect base pairing between an siRNA and a target mRNA can result in translational suppression of that target. This is generally unintended and can cause undesired side effects, referred to as off-target effects (Doench *et al.*, 2003; Saxena *et al.*, 2003).

Originally the application of RNAi in mammalian cells demonstrated a particular challenge, since the introduction of exogenous long dsRNA activates the interferon response in higher eukaryotes, resulting in the activation of two enzymes PKR and RNaseL which inhibit protein translation and induce degradation of all mRNA respectively (Bass, 2001). However, a solution to this problem came with the discovery that 21–23 bp long dsRNA fragments with 3' overhangs of two nucleotides efficiently trigger sequence-specific mRNA degradation (Elbashir *et al.*, 2001). Subsequently the specific nature of these siRNA to mediate post-transcriptional gene silencing without inducing the interferon response has been demonstrated in global genetic profiling studies (Chi *et al.*, 2003). There are now two main methods applied for introducing siRNAs into mammalian cells, direct transfer and endogenous delivery. Direct transfer utilises chemically synthetic siRNAs, which as the name suggests are directly transfected intracellularly. Alternatively, endogenous delivery involves inserting DNA templates for siRNAs into vectors. The constitutes of the expression system are either sense and antisense strands of the siRNA duplex transcribed from individual promoters (Lee *et al.*, 2002; Miyagishi *et al.*, 2002; Yu *et al.*, 2002), or siRNAs expressed as fold-back stem-loop structures, known as short hairpin RNAs (shRNAs), that give rise to siRNAs after intracellular processing by Dicer (Brummelkamp *et al.*, 2002; Dykxhoorn *et al.*, 2003; Paul *et al.*, 2002; Sui *et al.*, 2002).

Not surprisingly, due to its unparalleled specificity and efficacy, there has been immense interest in developing RNAi-based pharmaceutical agents for clinical applications. In fact, the use of RNAi has rapidly progressed beyond an *in vitro* research tool with hundreds of reports already having been published describing its use in animal models and several siRNA compounds are currently undergoing clinical trials (reviewed in Castanotto and Rossi, 2009 and Kurreck, 2009). The potential for RNAi-therapy in cancer is enormous. A major advantage of RNAi for cancer therapy is that it can potentially silence a disease allele specifically without affecting the wild type allele, therefore achieving tumour specific therapy (Martinez *et al.*, 2002). Thus far, various

individual genes have been targeted using RNAi techniques in different tumour cell models and their knockdown have led to profound biological consequences. These genes include oncogenes/anti-apoptotic molecules, telomerase, growth factor receptor genes, signalling molecules and some other genes (Fu *et al.*, 2005; Lee *et al.*, 2004; Ling and Li, 2004; Pichler *et al.*, 2005; Sumimoto *et al.*, 2005). In particular, viral oncogenic proteins are considered to be a very promising set of targets for clinical knockdown by RNAi, as they have no human counterpart. In recent years several studies have been published in relation to the inhibition of HPV E6 and E7 expression using RNAi technology. The first report was in 2002 when Jiang and Milner demonstrated that it was feasible to silence E6 and E7. However, there is much controversy over the phenotypic outcome after silencing of the oncogenic genes, though all studies to date have observed inhibition of the cell proliferation, some in addition describe the induction of apoptosis and others not (Butz *et al.*, 2003; Koivusalo *et al.*, 2005; Koivusalo *et al.*, 2006; Yoshinouchi *et al.*, 2003). Obviously the ideal situation in relation to application of these siRNA in a therapeutic setting would be that they would induce apoptosis and further investigation will be required to determine this conclusively. However, even if it emerges that they are unable to cause cell death, their ability to induce growth arrest may still be beneficial. A study by Koivusalo *et al.* in 2006 demonstrated the utility of siRNA targeting of E6 and E7 as an adjunct to chemotherapy. They were able to demonstrate that with the majority of chemotherapeutic agents tested, there was a synergistic increase in the cytotoxicty of the drugs post siRNA silencing of E6 and E7.

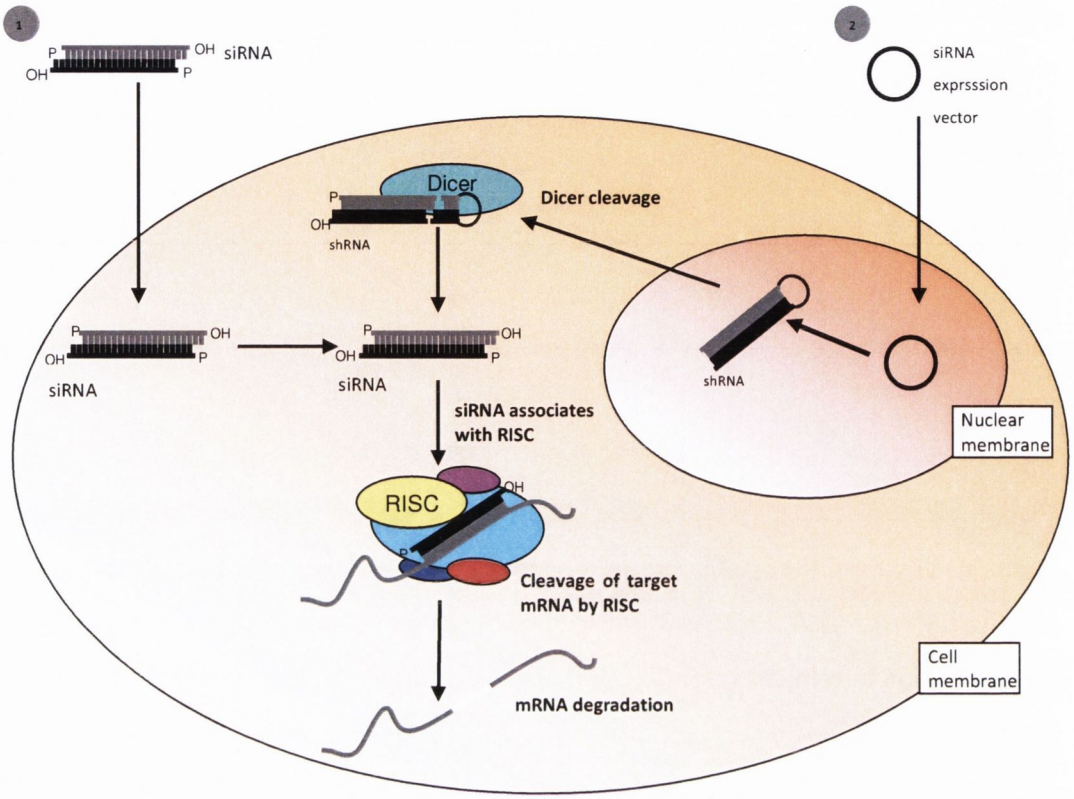


**Figure 1.7: Approaches to trigger the RNAi pathway in mammalian cells.** In mammalian systems, RNAi can be triggered (1) by synthetic short interfering RNA (siRNA) molecules or (2) by DNA based expression vectors designed to express short hairpin RNA (shRNA) molecules. These shRNA are cleaved by the cytoplasmic ribonuclease III (RNase III)-like protein, Dicer, into dsRNA fragments of about 21 nuceotides in length, i.e. siRNA. The siRNA molecule created by Dicer or the synthetic siRNA assembles with proteins to form a RNA-induced silencing complex (RISC). Once the complex has formed the siRNA unwinds and RISC deciphers between the different siRNA strands. The sense strand (grey) is degraded, while the antisense strand (black) is used to target genes for silencing. The antisense strand interacts with the catalytic protein of RISC, Argonaute 2 (Ago 2). Stabilised within a pocket in Ago 2, the antisense strand of the siRNA identifies the target mRNA and a catalytic domain of Ago 2 cleaves the mRNA. Cleaved mRNA cannot be translated and its encoded protein is not produced. RISC then dissociates from its target, to repeat this process.

### *1.7.2 Other gene targeted therapies for cervical cancer*

While genomic based strategies hold much promise, there are still major obstacles that need to be overcome for pharmacologically wide application, including such issues as efficient and safe delivery, poor cellular uptake and the possibility of off-target effects. Therefore the pursuit of additional approaches is required. The introduction of the prophylactic vaccine has produced much anticipation that the development of antigen-specific immunotherapies, i.e. therapeutic vaccines, may only be around the corner. Indeed many in this research field believe that HPV-associated neoplasia is the ideal disease to determine the proof-of-principle of immune based therapeutic interventions for epithelial cancers. The idea of antigen-specific immunotherapies for the treatment of cervical cancer would seem rational since the majority of genital HPV infections clear without any intervention (Baseman and Koutsky, 2005; Cates, 1999; Ho *et al.*, 1998; Liaw *et al.*, 2001) and clearance correlates with the development of specific CD4-T cell immunity to the papillomavirus E2 and E6 (Welters *et al.*, 2006). Even though high-grade dysplasia is associated with integration of the viral genome into the host genome, there is evidence that such an approach could be effective. For instance a proportion of established cervical high-grade lesions undergo regression over a relatively short timeframe (Melnikow *et al.*, 1998; Trimble *et al.*, 2005). This has been highlighted in both retrospective and prospective studies, which suggest that across all HPV types, the rate of regression of cervical high-grade squamous intraepithelial lesions (HSIL) in 4–6 months is approximately 35%. Moreover, a subset of persistent HPV disease is susceptible to immune manipulation; topical application of an inducer of innate immune responses, imiquimod, a toll-like receptor (TLR) 7 agonist, is approved by the US Food and Drug Administration (FDA) as first-line therapy for external genital warts, most of which are caused by HPV-6 and 11 (Trimble and Frazer, 2009). A number of therapeutic vaccine approaches have been tested in preclinical trials such as fusion proteins, recombinant viruses, DNA constructs and chimeric VLPs (Roden *et al.*, 2007). As with all targeted therapies, they have predominantly been designed towards the HPV oncogenes. However, this is not only because of their functional role in carcinogenesis but also because natural immune responses to these antigens have been identified in relation to disease (Trimble and Frazer, 2009). The

targeting of E6 and E7 has had only limited success and instead an E2 recombinant vaccine, MVA E2, is showing much promise (Garcia-Hernandez *et al.*, 2006). The results of a phase II clinical trial of MVA E2 has demonstrated significant efficacy in eliminating CIN II and III (Garcia-Hernandez *et al.*, 2006). Not only did the entire treated group have antibodies against the E2 protein, but regression of CIN II, III was observed in all of these women, of whom approximately 50% had complete histological regression. Furthermore, none of the women in the MVA E2 group had developed recurrent disease 1 year after treatment. In contrast, in the control group, although conization eliminated the lesion in 80% of the women, this procedure did not completely eradicate the HPV DNA virus, resulting in 15% of the women having recurrent CIN III after 1 year (Garcia-Hernandez *et al.*, 2006).

An alternative immune based strategy being pursued is the application of the commonly used non steroidal anti-inflammatory drugs (NSAIDs). These drugs are known to hamper inflammation through the inhibition of cyclooxygenase (COX) enzyme activity. The initial basis for this line of investigation was the up-regulation of COX2 in both pre-invasive and invasive cervical cancer and its established association with metastasis and poor prognosis (Ferrandina *et al.*, 2002; Kim *et al.*, 2003). A COX2 specific NSAID, celecoxib, has been evaluated in many different studies with mixed results. Unfortunately though promising evidence emerged from early studies, it would appear that the toxicity of this drug outweighs any benefit from its use in patients with locally advanced cervical cancer (Gaffney *et al.*, 2007; Herrera *et al.*, 2007). Despite this, it has shown potential as a medical treatment for pre-invasive disease (Powell *et al.*,2003; Farley *et al.*, 2006; Hefler *et al.*, 2006). Interestingly sulindac, a non selective COX, has recently been shown to induce growth arrest in HPV18 infected HeLa cells and cause strong inhibition of the G1 to S transition of the cell cycle (Karl *et al.*, 2005). It was demonstrated that sulindac-induced G1 arrest is preceded by suppression of cyclins E and A, inactivation of cdk2, and complete loss of the viral oncoprotein E7, despite ongoing HPV transcription (including E7). These results suggest that sulindac may offer new perspectives as a chemopreventative or supplementary therapeutic for cervical cancer.

Finally, some of the most interesting targets are genes that have been shown to be differentially expressed but as yet have no assigned role; a classic example is the epithelial growth factor receptor (EGFR) (Woodworth *et al.,* 2005). EGFR is a member of tyrosine kinase receptor family. All proteins of this family possess an extracellular ligand-binding domain, a single hydrophobic transmembrane domain, and a cytoplasmic tyrosine kinase-containing domain. On endogenous ligand-binding to the extracellular domain, EGFR forms receptor homo- or heterodimers and activates the intrinsic tyrosine kinase-containing domain (Citri *et al.*, 2006). Subsequently, a complex network of signal transduction pathways that promote proliferation, motility, invasion, and angiogenesis is induced, including the phosphatidylinositol 3'-kinase/Akt/mTOR pathway and the Erk1/2 mitogen-activated protein kinase pathway (Hynes *et al.*, 2005). Currently clinical trials are being undertaken involving two EGFR-tyrosine kinase inhibitors, gefitinib and erlotinib (Li *et al.*, 2007; Woodworth *et al.*, 2005), and two monoclonal antibodies directed against the extracellular domain of the receptor, cetuximab and matuzumab (Blohmer *et al.*, 2005). This work stemmed from two independent observations: 1, EGFR is overexpressed in up to 85% of cervical cancer cases, being associated with higher stage and poor prognosis (Hale *et al.*, 1993; Kim *et al.*, 2005; Oh *et al.*, 2000) and, 2, that the use of antibodies against EGFR as an adjunt to tranditional radiation therapy could improve the effectiveness of radiotherapy to cure tumours and delay the appearance of recurrent tumours not cured by radiation treatment (Nasu *et al.*, 2001).

## 1.8 Summary

High-risk HPVs are the main etiological factors in invasive cancer of the cervix; their oncogenic actions are primarily mediated through the dysregulated activity of two early proteins E6 and E7. The function of these proteins in the 'productive' life cycle is to maintain a replicative competent environment in the suprabasal layer of the epithelium. Through a cooperative manner, they appear to achieve this by altering the activity of cell cycle proteins, such that proteins involved in cell cycle progression have enhanced activity while regulatory elements are neutralised. Integration of high-risk HPV and subsequent permanent expression of E6 and E7 results in continuous cell proliferation, which enables the progression towards malignancy. While the expression of E6 and E7 alone is not sufficient to induce tumourigenesis, it is believed they produce an environment in which other pro-oncogenic alterations occur at an increased rate.

## 1.9 Study aims

The hypothesis holds that progression to malignancy in cervical cancer is a result of continuous expression of the HPV viral oncoproteins, E6 and E7. The premise, is that the expression of these oncoproteins provides an environment whereby malignant transformation can occur at higher rates than normally observed. To further substantiate this view, and to investigate novel pathways involved in the pathogenesis of cervical cancer, this study aims to examine the effect of suppressing the expression of endogenously expressed viral oncogenes. To achieve this goal, two independent approaches are being pursued; firstly, the RNA of the E6/E7 oncogenes is being targeted using siRNA, secondly, the protein product of the E7 oncogenes is being targeted using the NSAID, Sulindac. The final objective will be to establish the downstream effects of these silencing events using gene expression microarray analyses. These approaches may have a potential role for gene-specific therapy in HPV associated cervical cancer and additionally, will allow the identification of a subset of dysregulated genes in cervical cancer. While over the last 25 years been many important insights into the functionality of E6 and E7 have been discovered, a complete understanding still eludes us. A thorough knowledge of the interaction of these oncoproteins with their numerous cellular partners, as well as the consequences of these interactions, would allow for the possibility of developing novel therapeutic approaches that would impede the activity of the oncoproteins.

## 1.10 References

Agrawal and Zhang. 1997. Pharmacokinetics of oligonucleotides. *Ciba. Found. Symp.* 209, 60.

Alazawi, William, Mark Pett, Barbara Arch, Laurie Scott, Tom Freeman, Margaret A Stanley, and Nicholas Coleman. 2002. Changes in cervical keratinocyte gene expression associated with integration of human papillomavirus 16. *Cancer Research* 62, no. 23 (December 1): 6959-6965.

Angeline, Michael, Eric Merle, and Junona Moroianu. 2003. The E7 oncoprotein of high-risk human papillomavirus type 16 enters the nucleus via a nonclassical Ran-dependent pathway. *Virology* 317, no. 1 (December 5): 13-23.

Anon. 2007. Quadrivalent vaccine against human papillomavirus to prevent high-grade cervical lesions. *The New England Journal of Medicine* 356, no. 19 (May 10): 1915-1927.

Aquino-Jarquin, Guillermo, María Luisa Benítez-Hess, Joseph A DiPaolo, and Luis M Alvarez-Salas. 2008. A triplex ribozyme expression system based on a single hairpin ribozyme. *Oligonucleotides* 18, no. 3: 213-224.

Assoian, R K, and X Zhu. 1997. Cell anchorage and the cytoskeleton as partners in growth factor dependent cell cycle progression. *Current Opinion in Cell Biology* 9, no. 1 (February): 93-98.

Avvakumov, Nikita, Joe Torchia, and Joe S Mymryk. 2003. Interaction of the HPV E7 proteins with the pCAF acetyltransferase. *Oncogene* 22, no. 25 (June 19): 3833-3841.

Bartel, David P. 2004. MicroRNAs: genomics, biogenesis, mechanism, and function. *Cell* 116, no. 2 (January 23): 281-297.

Baseman, Janet G, and Laura A Koutsky. 2005. The epidemiology of human papillomavirus infections. *Journal of Clinical Virology: The Official Publication of the Pan American Society for Clinical Virology* 32 Suppl 1 (March): S16-24.

Bastien, N, and A A McBride. 2000. Interaction of the papillomavirus E2 protein with mitotic chromosomes. *Virology* 270, no. 1 (April 25): 124-134.

Bedell, M A, J B Hudson, T R Golub, M E Turyk, M Hosken, G D Wilbanks, and L A Laimins. 1991. Amplification of human papillomavirus genomes in vitro is dependent on epithelial differentiation. *Journal of Virology* 65, no. 5 (May): 2254-2260.

Beer-Romero, P, S Glass, and M Rolfe. 1997. Antisense targeting of E6AP elevates p53 in HPV-infected cells but not in normal cells. *Oncogene* 14, no. 5 (February 6): 595-602.

Bernat, Agnieszka, Nikita Avvakumov, Joe S Mymryk, and Lawrence Banks. 2003. Interaction between the HPV E7 oncoprotein and the transcriptional coactivator p300. *Oncogene* 22, no. 39 (September 11): 7871-7881.

Bernstein, E, A A Caudy, S M Hammond, and G J Hannon. 2001. Role for a bidentate ribonuclease in the initiation step of RNA interference. *Nature* 409, no. 6818 (January 18): 363-366.

Bilder, David. 2004. Epithelial polarity and proliferation control: links from the Drosophila neoplastic tumor suppressors. *Genes & Development* 18, no. 16 (August 15): 1909-1925.

Blohmer, J, Gore, M, Kuemmel, S, Verheijen, RH, Kimmig R and. Massuger L. 2005. Phase II study to determine response rate, pharmacokinetics (PK), pharmacodynamics (PD), safety, and tolerability of treatment with the humanized anti-epidermal growth factor receptor (EGFR) monoclonal antibody EMD 72000 (matuzumab) in patients with recurrent cervical cancer. *Proc Am Assoc Cancer Res Am Soc Clin Oncol* 16, no. 23 (abstr 2534).

Bolger, Noel, Cynthia Heffron, Irene Regan, Mary Sweeney, Sinead Kinsella, Mary McKeown, Grace Creighton, Joan Russell, and John O'Leary. 2006. Implementation and evaluation of a new automated interactive image analysis system. *Acta Cytologica* 50, no. 5 (October): 483-491.

Bonham, M A, S Brown, A L Boyd, P H Brown, D A Bruckenstein, J C Hanvey, S A Thomson, A Pipe, F Hassman, and J E Bisi. 1995. An assessment of the antisense properties of RNase H-competent and steric-blocking oligomers. *Nucleic Acids Research* 23, no. 7 (April 11): 1197-1203.

Borbély, Agnes A, Melinda Murvai, József Kónya, Zoltán Beck, Lajos Gergely, Fengzhi Li, and György Veress. 2006. Effects of human papillomavirus type 16 oncoproteins on survivin gene expression. *The Journal of General Virology* 87, no. Pt 2 (February): 287-294.

Bosch, F Xavier, and Nubia Muñoz. 2002. The viral etiology of cervical cancer. *Virus Research* 89, no. 2 (November): 183-190.

Bosch, F Xavier, and Silvia de Sanjosé. 2002. Human papillomavirus in cervical cancer. *Current Oncology Reports* 4, no. 2 (March): 175-183.

Bosch, F Xavier, and Silvia de Sanjosé. 2007. The epidemiology of human papillomavirus infection and cervical cancer. *Disease Markers* 23, no. 4: 213-227.

Boshart, M, L Gissmann, H Ikenberg, A Kleinheinz, W Scheurlen, and H zur Hausen. 1984. A new type of papillomavirus DNA, its presence in genital cancer biopsies and in cell lines derived from cervical cancer. *The EMBO Journal* 3, no. 5 (May): 1151-1157.

Bossis, Ioannis, Richard B S Roden, Ratish Gambhira, Rongcun Yang, Mitsuo Tagaya, Peter M Howley, and Patricio I Meneses. 2005. Interaction of tSNARE syntaxin 18 with the papillomavirus minor capsid protein mediates infection. *Journal of Virology* 79, no. 11 (June): 6723-6731.

Bousarghin, Latifa, Antoine Touzé, Pierre-Yves Sizaret, and Pierre Coursaget. 2003. Human papillomavirus types 16, 31, and 58 use different endocytosis pathways to enter cells. *Journal of Virology* 77, no. 6 (March): 3846-3850.

Boxman, I L, A Hogewoning, L H Mulder, J N Bouwes Bavinck, and J ter Schegget. 1999. Detection of human papillomavirus types 6 and 11 in pubic and perianal hair from patients with genital warts. *Journal of Clinical Microbiology* 37, no. 7 (July): 2270-2273.

Boyer, S N, D E Wazer, and V Band. 1996. E7 protein of human papilloma virus-16 induces degradation of retinoblastoma protein through the ubiquitin-proteasome pathway. *Cancer Research* 56, no. 20 (October 15): 4620-4624.

Bray, Freddie, Bendix Carstensen, Henrik Møller, Marco Zappa, Maja Primic Zakelj, Gill Lawrence, Matti Hakama, and Elisabete Weiderpass. 2005. Incidence trends of adenocarcinoma of the cervix in 13 European countries. *Cancer Epidemiology, Biomarkers & Prevention: A Publication of the American Association for Cancer Research, Cosponsored by the American Society of Preventive Oncology* 14, no. 9 (September): 2191-2199.

Brehm, A, E A Miska, D J McCance, J L Reid, A J Bannister, and T Kouzarides. 1998. Retinoblastoma protein recruits histone deacetylase to repress transcription. *Nature* 391, no. 6667 (February 5): 597-601.

Brehm, A, S J Nielsen, E A Miska, D J McCance, J L Reid, A J Bannister, and T Kouzarides. 1999. The E7 oncoprotein associates with Mi2 and histone deacetylase activity to

Brown, C R, M L Leon, K Muñoz, A Fagioni, L G Amador, B Frain, W Tu, B Qadadri, and D R Brown. 2009. Human papillomavirus infection and its association with cervical dysplasia in Ecuadorian women attending a private cancer screening clinic. *Brazilian Journal of Medical and Biological Research = Revista Brasileira De Pesquisas Médicas E Biológicas / Sociedade Brasileira De Biofísica ... [et Al* 42, no. 7 (July): 629-636.

Brummelkamp, Thijn R, René Bernards, and Reuven Agami. 2002. A system for stable expression of short interfering RNAs in mammalian cells. *Science (New York, N.Y.)* 296, no. 5567 (April 19): 550-553.

Bryan, J T, and D R Brown. 2000. Association of the human papillomavirus type 11 E1()E4 protein with cornified cell envelopes derived from infected genital epithelium. *Virology* 277, no. 2 (November 25): 262-269.

Bryan, T M, and T R Cech. 1999. Telomerase and the maintenance of chromosome ends. *Current Opinion in Cell Biology* 11, no. 3 (June): 318-324.

Buck, Christopher B, Diana V Pastrana, Douglas R Lowy, and John T Schiller. 2005. Generation of HPV pseudovirions using transfection and their use in neutralization assays. *Methods in Molecular Medicine* 119: 445-462.

Bulk, Saskia, Otto Visser, Lawrence Rozendaal, René H M Verheijen, and Chris J L M Meijer. 2005. Cervical cancer in the Netherlands 1989-1998: Decrease of squamous cell carcinoma in older women, increase of adenocarcinoma in younger women. *International Journal of Cancer. Journal International Du Cancer* 113, no. 6 (March 1): 1005-1009.

Butz, Karin, Tutik Ristriani, Arnd Hengstermann, Claudia Denk, Martin Scheffner, and Felix Hoppe-Seyler. 2003. siRNA targeting of the viral E6 oncogene efficiently kills human papillomavirus-positive cancer cells. *Oncogene* 22, no. 38 (September 4): 5938-5945.

Carmell, Michelle A, Zhenyu Xuan, Michael Q Zhang, and Gregory J Hannon. 2002. The Argonaute family: tentacles that reach into RNAi, developmental control, stem cell maintenance, and tumorigenesis. *Genes & Development* 16, no. 21 (November 1): 2733-2742.

Carrington, Mary, Sophia Wang, Maureen P Martin, Xiaojiang Gao, Mark Schiffman, Jie Cheng, Rolando Herrero, et al. 2005. Hierarchy of resistance to cervical neoplasia mediated by combinations of killer immunoglobulin-like receptor and human leukocyte antigen loci. *The Journal of Experimental Medicine* 201, no. 7 (April 4): 1069-1075.

Castanotto, Daniela, and John J Rossi. 2009. The promises and pitfalls of RNA-interference-based therapeutics. *Nature* 457, no. 7228 (January 22): 426-433.

Castellsagué, Xavier, F Xavier Bosch, and Nubia Muñoz. 2002. Environmental co-factors in HPV carcinogenesis. *Virus Research* 89, no. 2 (November): 191-199.

Castellsagué, Xavier, and Nubia Muñoz. 2003a. Chapter 3: Cofactors in human papillomavirus carcinogenesis--role of parity, oral contraceptives, and tobacco smoking. *Journal of the National Cancer Institute. Monographs*, no. 31: 20-28.

Cates, W. 1999. Estimates of the incidence and prevalence of sexually transmitted diseases in the United States. American Social Health Association Panel. *Sexually Transmitted Diseases* 26, no. 4 Suppl (April): S2-7.

Cerutti, Heriberto. 2003. RNA interference: traveling in the cell and gaining functions? *Trends in Genetics: TIG* 19, no. 1 (January): 39-46.

Chen, R J, Y H Lin, C A Chen, S C Huang, S N Chow, and C Y Hsieh. 1999. Influence of histologic type and age on survival rates for invasive cervical carcinoma in Taiwan. *Gynecologic Oncology* 73, no. 2 (May): 184-190.

Chen, Z, P Kamath, S Zhang, L St John, K Adler-Storthz, and E J Shillitoe. 1996. Effects on tumor cells of ribozymes that cleave the RNA transcripts of human papillomavirus type 18. *Cancer Gene Therapy* 3, no. 1 (February): 18-23.

Cheng, S, D C Schmidt-Grimminger, T Murant, T R Broker, and L T Chow. 1995. Differentiation-dependent up-regulation of the human papillomavirus E7 gene reactivates cellular DNA replication in suprabasal differentiated keratinocytes. *Genes & Development* 9, no. 19 (October 1): 2335-2349.

Chi, Jen-Tsan, Howard Y Chang, Nancy N Wang, Dustin S Chang, Nina Dunphy, and Patrick O Brown. 2003. Genomewide view of gene silencing by small interfering RNAs. *Proceedings of the National Academy of Sciences of the United States of America* 100, no. 11 (May 27): 6343-6346.

Chow, Louise T, Aaron A Duffy, Hsu-Kun Wang, and Thomas R Broker. 2009. A highly efficient system to produce infectious human papillomavirus: Elucidation of natural virus-host interactions. *Cell Cycle (Georgetown, Tex.)* 8, no. 9 (May 1): 1319-1323.

Ciciarello, M, R Mangiacasale, M Casenghi, M Zaira Limongi, M D'Angelo, S Soddu, P Lavia, and E Cundari. 2001. p53 displacement from centrosomes and p53-mediated G1 arrest following transient inhibition of the mitotic spindle. *The Journal of Biological Chemistry* 276, no. 22 (June 1): 19205-19213.

Citri, Ami, and Yosef Yarden. 2006. EGF-ERBB signalling: towards the systems level. *Nature Reviews. Molecular Cell Biology* 7, no. 7 (July): 505-516.

Classon, M, and N Dyson. 2001. p107 and p130: versatile proteins with interesting pockets. *Experimental Cell Research* 264, no. 1 (March 10): 135-147.

Clemens, K E, R Brent, J Gyuris, and K Münger. 1995. Dimerization of the human papillomavirus E7 oncoprotein in vivo. *Virology* 214, no. 1 (December 1): 289-293.

Clifford, G M, J S Smith, M Plummer, N Muñoz, and S Franceschi. 2003. Human papillomavirus types in invasive cervical cancer worldwide: a meta-analysis. *British Journal of Cancer* 88, no. 1 (January 13): 63-73.

Cole, S T, and O Danos. 1987. Nucleotide sequence and comparative analysis of the human papillomavirus type 18 genome. Phylogeny of papillomaviruses and repeated structure of the E6 and E7 gene products. *Journal of Molecular Biology* 193, no. 4 (February 20): 599-608.

Collins, Asha S, Tomomi Nakahara, Anh Do, and Paul F Lambert. 2005. Interactions with pocket proteins contribute to the role of human papillomavirus type 16 E7 in the papillomavirus life cycle. *Journal of Virology* 79, no. 23 (December): 14769-14780.

Comber, H, and A Gavin. 2004. Recent trends in cervical cancer mortality in Britain and Ireland: the case for population-based cervical cancer screening. *British Journal of Cancer* 91, no. 11 (November 29): 1902-1904.

Conger, K L, J S Liu, S R Kuo, L T Chow, and T S Wang. 1999. Human papillomavirus DNA replication. Interactions between the viral E1 protein and two subunits of human dna polymerase alpha/primase. *The Journal of Biological Chemistry* 274, no. 5 (January 29): 2696-2705.

Conrad, M, V J Bubb, and R Schlegel. 1993. The human papillomavirus type 6 and 16 E5 proteins are membrane-associated proteins which associate with the 16-kilodalton pore-forming protein. *Journal of Virology* 67, no. 10 (October): 6170-6178.

Cooper, K, C S Herrington, M F Evans, K C Gatter, and J O McGee. 1993. p53 antigen in cervical condylomata, intraepithelial neoplasia, and carcinoma: relationship to HPV infection and integration. *The Journal of Pathology* 171, no. 1 (September): 27-34.

Corden, S A, L J Sant-Cassia, A J Easton, and A G Morris. 1999. The integration of HPV-18 DNA in cervical carcinoma. *Molecular Pathology: MP* 52, no. 5 (October): 275-282.

Crook, T, J A Tidy, and K H Vousden. 1991. Degradation of p53 can be targeted by HPV E6 sequences distinct from those required for p53 binding and trans-activation. *Cell* 67, no. 3 (November 1): 547-556.

Crook, T, D Wrede, and K H Vousden. 1991. p53 point mutation in HPV negative human cervical carcinoma cell lines. *Oncogene* 6, no. 5 (May): 873-875.

Cullen, A P, R Reid, M Campion, and A T Lörincz. 1991. Analysis of the physical state of different human papillomavirus DNAs in intraepithelial and invasive cervical neoplasm. *Journal of Virology* 65, no. 2 (February): 606-612.

Culp, Timothy D, and Neil D Christensen. 2004. Kinetics of in vitro adsorption and entry of papillomavirus virions. *Virology* 319, no. 1 (February 5): 152-161.

Cumming, Sarah A, Maria G McPhillips, Thanaporn Veerapraditsin, Steven G Milligan, and Sheila V Graham. 2003. Activity of the human papillomavirus type 16 late negative regulatory element is partly due to four weak consensus 5' splice sites that bind a U1 snRNP-like complex. *Journal of Virology* 77, no. 9 (May): 5167-5177.

Davy, Clare E, Deborah J Jackson, Qian Wang, Kenneth Raj, Phillip J Masterson, Nicola F Fenner, Shirley Southern, Scott Cuthill, Jonathan B A Millar, and John Doorbar. 2002. Identification of a G(2) arrest domain in the E1 wedge E4 protein of human papillomavirus type 16. *Journal of Virology* 76, no. 19 (October): 9806-9818.

Day, P M, R B Roden, D R Lowy, and J T Schiller. 1998. The papillomavirus minor capsid protein, L2, induces localization of the major capsid protein, L1, and the viral transcription/replication protein, E2, to PML oncogenic domains. *Journal of Virology* 72, no. 1 (January): 142-150.

Day, Patricia M, Carl C Baker, Douglas R Lowy, and John T Schiller. 2004. Establishment of papillomavirus infection is enhanced by promyelocytic leukemia protein (PML) expression. *Proceedings of the National Academy of Sciences of the United States of America* 101, no. 39 (September 28): 14252-14257.

Day, Patricia M, Douglas R Lowy, and John T Schiller. 2003. Papillomaviruses infect cells via a clathrin-dependent pathway. *Virology* 307, no. 1 (March 1): 1-11.

De Geest, K, M E Turyk, M I Hosken, J B Hudson, L A Laimins, and G D Wilbanks. 1993. Growth and differentiation of human papillomavirus type 31b positive human cervical cell lines. *Gynecologic Oncology* 49, no. 3 (June): 303-310.

DeFilippis, Rosa Anna, Edward C Goodwin, Lingling Wu, and Daniel DiMaio. 2003. Endogenous human papillomavirus E6 and E7 proteins differentially regulate proliferation, senescence, and apoptosis in HeLa cervical carcinoma cells. *Journal of Virology* 77, no. 2 (January): 1551-1563.

Dell, Ghislaine, Kay W Wilkinson, Rebecca Tranter, Joanna Parish, R Leo Brady, and Kevin Gaston. 2003. Comparison of the structure and DNA-binding properties of the E2 proteins from an oncogenic and a non-oncogenic human papillomavirus. *Journal of Molecular Biology* 334, no. 5 (December 12): 979-991.

Denli, Ahmet M, and Gregory J Hannon. 2003. RNAi: an ever-growing puzzle. *Trends in Biochemical Sciences* 28, no. 4 (April): 196-201.

Desaintes, C, and C Demeret. 1996. Control of papillomavirus DNA replication and transcription. *Seminars in Cancer Biology* 7, no. 6 (December): 339-347.

DiPaolo, J A, C D Woodworth, N C Popescu, V Notario, and J Doniger. 1989. Induction of human cervical squamous cell carcinoma by sequential transfection with human papillomavirus 16 DNA and viral Harvey ras. *Oncogene* 4, no. 4 (April): 395-399.

Doench, John G, Christian P Petersen, and Phillip A Sharp. 2003. siRNAs can function as miRNAs. *Genes & Development* 17, no. 4 (February 15): 438-442.

Doorbar, J, S Ely, J Sterling, C McLean, and L Crawford. 1991. Specific interaction between HPV-16 E1-E4 and cytokeratins results in collapse of the epithelial cell intermediate filament network. *Nature* 352, no. 6338 (August 29): 824-827.

Doorbar, J, C Foo, N Coleman, L Medcalf, O Hartley, T Prospero, S Napthine, J Sterling, G Winter, and H Griffin. 1997. Characterization of events during the late stages of HPV16 infection in vivo using high-affinity synthetic Fabs to E4. *Virology* 238, no. 1 (November 10): 40-52.

Doorbar, J, and P H Gallimore. 1987. Identification of proteins encoded by the L1 and L2 open reading frames of human papillomavirus 1a. *Journal of Virology* 61, no. 9 (September): 2793-2799.

Doorbar, John. 2006. Molecular biology of human papillomavirus infection and cervical cancer. *Clinical Science (London, England: 1979)* 110, no. 5 (May): 525-541.

Duensing, A, Y Liu, M Tseng, M Malumbres, M Barbacid, and S Duensing. 2006. Cyclin-dependent kinase 2 is dispensable for normal centrosome duplication but required for oncogene-induced centrosome overduplication. *Oncogene* 25, no. 20 (May 11): 2943-2949.

Duensing, S, L Y Lee, A Duensing, J Basile, S Piboonniyom, S Gonzalez, C P Crum, and K Munger. 2000. The human papillomavirus type 16 E6 and E7 oncoproteins cooperate to induce mitotic defects and genomic instability by uncoupling centrosome duplication from the cell division cycle. *Proceedings of the National Academy of Sciences of the United States of America* 97, no. 18 (August 29): 10002-10007.

Duensing, Stefan, and Karl Münger. 2002. The human papillomavirus type 16 E6 and E7 oncoproteins independently induce numerical and structural chromosome instability. *Cancer Research* 62, no. 23 (December 1): 7075-7082.

Duensing, Stefan, and Karl Münger. 2003. Human papillomavirus type 16 E7 oncoprotein can induce abnormal centrosome duplication through a mechanism independent of inactivation of retinoblastoma protein family members. *Journal of Virology* 77, no. 22 (November): 12331-12335.

Duensing, Stefan, and Karl Münger. 2004. Mechanisms of genomic instability in human cancer: insights from studies with human papillomavirus oncoproteins. *International Journal of Cancer. Journal International Du Cancer* 109, no. 2 (March 20): 157-162.

Dürst, M, D Gallahan, G Jay, and J S Rhim. 1989. Glucocorticoid-enhanced neoplastic transformation of human keratinocytes by human papillomavirus type 16 and an activated ras oncogene. *Virology* 173, no. 2 (December): 767-771.

Dürst, M, L Gissmann, H Ikenberg, and H zur Hausen. 1983. A papillomavirus DNA from a cervical carcinoma and its prevalence in cancer biopsy samples from different geographic regions. *Proceedings of the National Academy of Sciences of the United States of America* 80, no. 12 (June): 3812-3815.

Dürst, M, D Glitz, A Schneider, and H zur Hausen. 1992. Human papillomavirus type 16 (HPV 16) gene expression and DNA replication in cervical neoplasia: analysis by in situ hybridization. *Virology* 189, no. 1 (July): 132-140.

Dürst, M, A Kleinheinz, M Hotz, and L Gissmann. 1985. The physical state of human papillomavirus type 16 DNA in benign and malignant genital tumours. *The Journal of General Virology* 66 ( Pt 7) (July): 1515-1522.

Dykxhoorn, Derek M, Carl D Novina, and Phillip A Sharp. 2003. Killing the messenger: short RNAs that silence gene expression. *Nature Reviews. Molecular Cell Biology* 4, no. 6 (June): 457-467.

Dyson, J E, J Daniel, and C R Surrey. 1992. The effect of sodium butyrate on the growth characteristics of human cervix tumour cells. *British Journal of Cancer* 65, no. 6 (June): 803-808.

Dyson, N. 1998. The regulation of E2F by pRB-family proteins. *Genes & Development* 12, no. 15 (August 1): 2245-2262.

del Mar Peña, L M, and L A Laimins. 2001. Differentiation-dependent chromatin rearrangement coincides with activation of human papillomavirus type 31 late gene expression. *Journal of Virology* 75, no. 20 (October): 10005-10013.

de Sanjosé, Silvia, Mireia Diaz, Xavier Castellsagué, Gary Clifford, Laia Bruni, Nubia Muñoz, and F Xavier Bosch. 2007. Worldwide prevalence and genotype distribution of cervical human papillomavirus DNA in women with normal cytology: a meta-analysis. *The Lancet Infectious Diseases* 7, no. 7 (July): 453-459.

de Villiers, Ethel-Michele, Claude Fauquet, Thomas R Broker, Hans-Ulrich Bernard, and Harald zur Hausen. 2004. Classification of papillomaviruses. *Virology* 324, no. 1 (June 20): 17-27.

de Villiers, Ethel-Michele, Karin Gunst, Harald Stein, and Hans Scherübl. 2004. Esophageal squamous cell cancer in patients with head and neck cancer: Prevalence of human papillomavirus DNA sequences. *International Journal of Cancer. Journal International Du Cancer* 109, no. 2 (March 20): 253-258.

Edmonds, C, and K H Vousden. 1989a. A point mutational analysis of human papillomavirus type 16 E7 protein. *Journal of Virology* 63, no. 6 (June): 2650-2656.

Elbashir, S M, W Lendeckel, and T Tuschl. 2001. RNA interference is mediated by 21- and 22-nucleotide RNAs. *Genes & Development* 15, no. 2 (January 15): 188-200.

el-Deiry, W S, T Tokino, V E Velculescu, D B Levy, R Parsons, J M Trent, D Lin, W E Mercer, K W Kinzler, and B Vogelstein. 1993. WAF1, a potential mediator of p53 tumor suppression. *Cell* 75, no. 4 (November 19): 817-825.

Elfgren, K, M Kalantari, B Moberger, B Hagmar, and J Dillner. 2000. A population-based five-year follow-up study of cervical human papillomavirus infection. *American Journal of Obstetrics and Gynecology* 183, no. 3 (September): 561-567.

Evander, M, I H Frazer, E Payne, Y M Qi, K Hengst, and N A McMillan. 1997. Identification of the alpha6 integrin as a candidate receptor for papillomaviruses. *Journal of Virology* 71, no. 3 (March): 2449-2456.

Evans, Mark F, and Kumarasen Cooper. 2004. Human papillomavirus integration: detection by in situ hybridization and potential clinical application. *The Journal of Pathology* 202, no. 1 (January): 1-4.

Fang, F, G Orend, N Watanabe, T Hunter, and E Ruoslahti. 1996. Dependence of cyclin E-CDK2 kinase activity on cell anchorage. *Science (New York, N.Y.)* 271, no. 5248 (January 26): 499-502.

Farley, John H, Vu Truong, Elwin Goo, Catherine Uyehara, Christina Belnap, and Wilma I Larsen. 2006. A randomized double-blind placebo-controlled phase II trial of the cyclooxygenase-2 inhibitor Celecoxib in the treatment of cervical dysplasia. *Gynecologic Oncology* 103, no. 2 (November): 425-430.

Fehrmann, Frauke, David J Klumpp, and Laimonis A Laimins. 2003. Human papillomavirus type 31 E5 protein supports cell cycle progression and activates late viral functions upon epithelial differentiation. *Journal of Virology* 77, no. 5 (March): 2819-2831.

Ferrandina, G, L Lauriola, M G Distefano, G F Zannoni, M Gessi, F Legge, N Maggiano, et al. 2002. Increased cyclooxygenase-2 expression is associated with chemotherapy resistance and poor survival in cervical cancer patients. *Journal of Clinical Oncology: Official Journal of the American Society of Clinical Oncology* 20, no. 4 (February 15): 973-981.

Figge, J, T Webster, T F Smith, and E Paucha. 1988. Prediction of similar transforming regions in simian virus 40 large T, adenovirus E1A, and myc oncoproteins. *Journal of Virology* 62, no. 5 (May): 1814-1818.

Filippova, Maria, Helen Song, Jodi L Connolly, Terence S Dermody, and Penelope J Duerksen-Hughes. 2002. The human papillomavirus 16 E6 protein binds to tumor necrosis factor (TNF) R1 and protects cells from TNF-induced apoptosis. *The Journal of Biological Chemistry* 277, no. 24 (June 14): 21730-21739.

Finzer, Patrick, Adriana Aguilar-Lemarroy, and Frank Rösl. 2002. The role of human papillomavirus oncoproteins E6 and E7 in apoptosis. *Cancer Letters* 188, no. 1-2 (December 15): 15-24.

Fire, A, S Xu, M K Montgomery, S A Kostas, S E Driver, and C C Mello. 1998. Potent and specific genetic interference by double-stranded RNA in Caenorhabditis elegans. *Nature* 391, no. 6669 (February 19): 806-811.

Florin, Luise, Cornelia Sapp, Rolf E Streeck, and Martin Sapp. 2002. Assembly and translocation of papillomavirus capsid proteins. *Journal of Virology* 76, no. 19 (October): 10009-10014.

Frattini, M G, and L A Laimins. 1994. Binding of the human papillomavirus E1 origin-recognition protein is regulated through complex formation with the E2 enhancer-binding protein. *Proceedings of the National Academy of Sciences of the United States of America* 91, no. 26 (December 20): 12398-12402.

Frattini, M G, H B Lim, and L A Laimins. 1996. In vitro synthesis of oncogenic human papillomaviruses requires episomal genomes for differentiation-dependent late expression. *Proceedings of the National Academy of Sciences of the United States of America* 93, no. 7 (April 2): 3062-3067.

Fu, Geng-Feng, Xue-Hong Lin, Qing-Wang Han, Yan-Rong Fan, Ye-Fen Xu, Dan Guo, Gen-Xing Xu, and Ya-Yi Hou. 2005. RNA interference remarkably suppresses bcl-2 gene expression in cancer cells in vitro and in vivo. *Cancer Biology & Therapy* 4, no. 8 (August): 822-829.

Funk, J O, S Waga, J B Harry, E Espling, B Stillman, and D A Galloway. 1997. Inhibition of CDK activity and PCNA-dependent DNA replication by p21 is blocked by interaction with the HPV-16 E7 oncoprotein. *Genes & Development* 11, no. 16 (August 15): 2090-2100.

Gaffney, David K, Kathryn Winter, Adam P Dicker, Brigitte Miller, Patricia J Eifel, Janice Ryu, Vilija Avizonis, Mitch Fromm, and Kathryn Greven. 2007. A Phase II study of acute toxicity for Celebrex (celecoxib) and chemoradiation in patients with locally advanced cervical cancer: primary endpoint analysis of RTOG 0128. *International Journal of Radiation Oncology, Biology, Physics* 67, no. 1 (January 1): 104-109.

Gage, J R, C Meyers, and F O Wettstein. 1990. The E7 proteins of the nononcogenic human papillomavirus type 6b (HPV-6b) and of the oncogenic HPV-16 differ in retinoblastoma protein binding and other properties. *Journal of Virology* 64, no. 2 (February): 723-730.

Gammoh, Noor, Helena Sterlinko Grm, Paola Massimi, and Lawrence Banks. 2006. Regulation of human papillomavirus type 16 E7 activity through direct protein interaction with the E2 transcriptional activator. *Journal of Virology* 80, no. 4 (February): 1787-1797.

García-Closas, Reina, Xavier Castellsagué, Xavier Bosch, and Carlos A González. 2005. The role of diet and nutrition in cervical carcinogenesis: a review of recent evidence. *International Journal of Cancer. Journal International Du Cancer* 117, no. 4 (November 20): 629-637.

García-Hernández, E, J L González-Sánchez, A Andrade-Manzano, M L Contreras, S Padilla, C C Guzmán, R Jiménez, et al. 2006. Regression of papilloma high-grade lesions (CIN 2 and CIN 3) is stimulated by therapeutic vaccination with MVA E2 recombinant vaccine. *Cancer Gene Therapy* 13, no. 6 (June): 592-597.

Gardiol, D, C Kühne, B Glaunsinger, S S Lee, R Javier, and L Banks. 1999. Oncogenic human papillomavirus E6 proteins target the discs large tumour suppressor for proteasome-mediated degradation. *Oncogene* 18, no. 40 (September 30): 5487-5496.

Gardiol, Daniela, Silvina Galizzi, and Lawrence Banks. 2002. Mutational analysis of the discs large tumour suppressor identifies domains responsible for human papillomavirus type 18 E6-mediated degradation. *The Journal of General Virology* 83, no. Pt 2 (February): 283-289.

Gargiulo, F, M A De Francesco, C Schreiber, G Ciravolo, F Salinaro, B Valloncini, and N Manca. 2007. Prevalence and distribution of single and multiple HPV infections in cytologically abnormal cervical samples from Italian women. *Virus Research* 125, no. 2 (May): 176-182.

Garnett, T O, M Filippova, and P J Duerksen-Hughes. 2006. Accelerated degradation of FADD and procaspase 8 in cells expressing human papilloma virus 16 E6 impairs TRAIL-mediated apoptosis. *Cell Death and Differentiation* 13, no. 11 (November): 1915-1926.

Genther, Sybil M, Stephanie Sterling, Stefan Duensing, Karl Münger, Carol Sattler, and Paul F Lambert. 2003. Quantitative role of the human papillomavirus type 16 E5 gene during the productive stage of the viral life cycle. *Journal of Virology* 77, no. 5 (March): 2832-2842.

Gewin, L, and D A Galloway. 2001. E box-dependent activation of telomerase by human papillomavirus type 16 E6 does not require induction of c-myc. *Journal of Virology* 75, no. 15 (August): 7198-7201.

Gewin, Lindy, Hadley Myers, Tohru Kiyono, and Denise A Galloway. 2004. Identification of a novel telomerase repressor that interacts with the human papillomavirus type-16 E6/E6-AP complex. *Genes & Development* 18, no. 18 (September 15): 2269-2282.

Giarrè, M, S Caldeira, I Malanchi, F Ciccolini, M J Leão, and M Tommasino. 2001. Induction of pRb degradation by the human papillomavirus type 16 E7 protein is essential to efficiently overcome p16INK4a-imposed G1 cell cycle Arrest. *Journal of Virology* 75, no. 10 (May): 4705-4712.

Giroglou, T, L Florin, F Schäfer, R E Streeck, and M Sapp. 2001. Human papillomavirus infection requires cell surface heparan sulfate. *Journal of Virology* 75, no. 3 (February): 1565-1570.

Gisselsson, D, L Pettersson, M Höglund, M Heidenblad, L Gorunova, J Wiegant, F Mertens, P Dal Cin, F Mitelman, and N Mandahl. 2000. Chromosomal breakage-fusion-bridge events cause genetic intratumor heterogeneity. *Proceedings of the National Academy of Sciences of the United States of America* 97, no. 10 (May 9): 5357-5362.

Gissmann, L, and H zur Hausen. 1980. Partial characterization of viral DNA from human genital warts (Condylomata acuminata). *International Journal of Cancer. Journal International Du Cancer* 25, no. 5 (May 15): 605-609.

Goodwin, E C, and D DiMaio. 2000. Repression of human papillomavirus oncogenes in HeLa cervical carcinoma cells causes the orderly reactivation of dormant tumor suppressor pathways. *Proceedings of the National Academy of Sciences of the United States of America* 97, no. 23 (November 7): 12513-12518.

Greenfield, I, J Nickerson, S Penman, and M Stanley. 1991. Human papillomavirus 16 E7 protein is associated with the nuclear matrix. *Proceedings of the National Academy of Sciences of the United States of America* 88, no. 24 (December 15): 11217-11221.

Grm, Helena Sterlinko, Paola Massimi, Noor Gammoh, and Lawrence Banks. 2005. Crosstalk between the human papillomavirus E2 transcriptional activator and the E6 oncoprotein. *Oncogene* 24, no. 33 (August 4): 5149-5164.

Guapillo, Mario R, Miguel A Márquez, María L Benítez-Hess, and Luis M Alvarez-Salas. 2006. A bacterial reporter system for the evaluation of antisense oligodeoxynucleotides directed against human papillomavirus type 16 (HPV-16). *Archives of Medical Research* 37, no. 5 (July): 584-592.

Habermann, Jens K, Kristina Hellman, Sandra Freitag, Kerstin Heselmeyer-Haddad, Ann-Cathrin Hellström, Keerti Shah, Gert Auer, and Thomas Ried. 2004. A recurrent gain of chromosome arm 3q in primary squamous carcinoma of the vagina. *Cancer Genetics and Cytogenetics* 148, no. 1 (January 1): 7-13.

Hahn, William C, and Robert A Weinberg. 2002. Modelling the molecular circuitry of cancer. *Nature Reviews. Cancer* 2, no. 5 (May): 331-341.

Hale, R J, C H Buckley, W J Gullick, H Fox, J Williams, and F L Wilcox. 1993. Prognostic value of epidermal growth factor receptor expression in cervical carcinoma. *Journal of Clinical Pathology* 46, no. 2 (February): 149-153.

Hamid, N Abdul, C Brown, and K Gaston. 2009. The regulation of cell proliferation by the papillomavirus early proteins. *Cellular and Molecular Life Sciences: CMLS* 66, no. 10 (May): 1700-1717.

Hammond, S M, E Bernstein, D Beach, and G J Hannon. 2000. An RNA-directed nuclease mediates post-transcriptional gene silencing in Drosophila cells. *Nature* 404, no. 6775 (March 16): 293-296.

Han, Y, Y M Loo, K T Militello, and T Melendy. 1999. Interactions of the papovavirus DNA replication initiator proteins, bovine papillomavirus type 1 E1 and simian virus 40 large T antigen, with human replication protein A. *Journal of Virology* 73, no. 6 (June): 4899-4907.

Hannon, Gregory J. 2002. RNA interference. *Nature* 418, no. 6894 (July 11): 244-251.

Harper, J W, G R Adami, N Wei, K Keyomarsi, and S J Elledge. 1993. The p21 Cdk-interacting protein Cip1 is a potent inhibitor of G1 cyclin-dependent kinases. *Cell* 75, no. 4 (November 19): 805-816.

He, Wanxia, Doug Staples, Clark Smith, and Chris Fisher. 2003. Direct activation of cyclin-dependent kinase 2 by human papillomavirus E7. *Journal of Virology* 77, no. 19 (October): 10566-10574.

Hebner, Christy M, and Laimonis A Laimins. 2006. Human papillomaviruses: basic mechanisms of pathogenesis and oncogenicity. *Reviews in Medical Virology* 16, no. 2 (April): 83-97.

Heck, D V, C L Yee, P M Howley, and K Münger. 1992. Efficiency of binding the retinoblastoma protein correlates with the transforming capacity of the E7 oncoproteins of the human papillomaviruses. *Proceedings of the National Academy of Sciences of the United States of America* 89, no. 10 (May 15): 4442-4446.

Hefler, Lukas A, Christoph Grimm, Paul Speiser, Gerhard Sliutz, and Alexander Reinthaller. 2006. The cyclooxygenase-2 inhibitor rofecoxib (Vioxx) in the treatment of cervical dysplasia grade II-III A phase II trial. *European Journal of Obstetrics, Gynecology, and Reproductive Biology* 125, no. 2 (April 1): 251-254.

Hemminki, K, C Dong, and P Vaittinen. 1999. Familial risks in cervical cancer: is there a hereditary component? *International Journal of Cancer. Journal International Du Cancer* 82, no. 6 (September 9): 775-781.

Herrera, Fernanda G, Philip Chan, Corinne Doll, Michael Milosevic, Amit Oza, Amy Syed, Melania Pintilie, Wilfred Levin, Lee Manchul, and Anthony Fyles. 2007. A prospective phase I-II trial of the cyclooxygenase-2 inhibitor celecoxib in patients with carcinoma of the cervix with biomarker assessment of the tumor microenvironment. *International Journal of Radiation Oncology, Biology, Physics* 67, no. 1 (January 1): 97-103.

Heselmeyer, K, E Schröck, S du Manoir, H Blegen, K Shah, R Steinbeck, G Auer, and T Ried. 1996. Gain of chromosome 3q defines the transition from severe dysplasia to invasive carcinoma of the uterine cervix. *Proceedings of the National Academy of Sciences of the United States of America* 93, no. 1 (January 9): 479-484.

Hildesheim, Allan, Rolando Herrero, Sholom Wacholder, Ana C Rodriguez, Diane Solomon, M Concepcion Bratti, John T Schiller, et al. 2007. Effect of human papillomavirus 16/18 L1 viruslike particle vaccine among young women with preexisting infection: a randomized trial. *JAMA: The Journal of the American Medical Association* 298, no. 7 (August 15): 743-753.

Hildesheim, Allan, and Sophia S Wang. 2002. Host and viral genetics and risk of cervical cancer: a review. *Virus Research* 89, no. 2 (November): 229-240.

Hines, C S, C Meghoo, S Shetty, M Biburger, M Brenowitz, and R S Hegde. 1998. DNA structure and flexibility in the sequence-specific binding of papillomavirus E2 proteins. *Journal of Molecular Biology* 276, no. 4 (March 6): 809-818.

Ho, G Y, R Bierman, L Beardsley, C J Chang, and R D Burk. 1998. Natural history of cervicovaginal papillomavirus infection in young women. *The New England Journal of Medicine* 338, no. 7 (February 12): 423-428.

Hopkins, M P, and G W Morley. 1991. A comparison of adenocarcinoma and squamous cell carcinoma of the cervix. *Obstetrics and Gynecology* 77, no. 6 (June): 912-917.

Huang, P S, D R Patrick, G Edwards, P J Goodhart, H E Huber, L Miles, V M Garsky, A Oliff, and D C Heimbrook. 1993. Protein domains governing interactions between E2F, the retinoblastoma gene product, and human papillomavirus type 16 E7 protein. *Molecular and Cellular Biology* 13, no. 2 (February): 953-960.

Hughes, F J, and M A Romanos. 1993. E1 protein of human papillomavirus is a DNA helicase/ATPase. *Nucleic Acids Research* 21, no. 25 (December 25): 5817-5823.

Huh, Kyung-Won, Joseph DeMasi, Hidesato Ogawa, Yoshihiro Nakatani, Peter M Howley, and Karl Münger. 2005. Association of the human papillomavirus type 16 E7 oncoprotein with the 600-kDa retinoblastoma protein-associated factor, p600. *Proceedings of the National Academy of Sciences of the United States of America* 102, no. 32 (August 9): 11492-11497.

Huibregtse, J M, M Scheffner, and P M Howley 1991. A cellular protein mediates association of p53 with the E6 oncoprotein of human papillomavirus types 16 or 18. *The EMBO Journal* 10, no. 13 (December): 4129-4135.

Huibregtse, J M, M Scheffner, and P M Howley.. 1993a. Cloning and expression of the cDNA for E6-AP, a protein that mediates the interaction of the human papillomavirus E6 oncoprotein with p53. *Molecular and Cellular Biology* 13, no. 2 (February): 775-784.

Huibregtse, J M, M Scheffner, and P M Howley. 1993b. Localization of the E6-AP regions that direct human papillomavirus E6 binding, association with p53, and ubiquitination of associated proteins. *Molecular and Cellular Biology* 13, no. 8 (August): 4918-4927.

Hummel, M, J B Hudson, and L A Laimins. 1992. Differentiation-induced and constitutive transcription of human papillomavirus type 31b in cell lines containing viral episomes. *Journal of Virology* 66, no. 10 (October): 6070-6080.

Hurlin, P J, P Kaur, P P Smith, N Perez-Reyes, R A Blanton, and J K McDougall. 1991. Progression of human papillomavirus type 18-immortalized human keratinocytes to a malignant phenotype. *Proceedings of the National Academy of Sciences of the United States of America* 88, no. 2 (January 15): 570-574.

Hutvágner, György, and Phillip D Zamore. 2002. RNAi: nature abhors a double-strand. *Current Opinion in Genetics & Development* 12, no. 2 (April): 225-232.

Hwang, Sun Gwan, Daeyoup Lee, Jiyun Kim, Taegun Seo, and Joonho Choe. 2002. Human papillomavirus type 16 E7 binds to E2F1 and activates E2F1-driven transcription in a retinoblastoma protein-independent manner. *The Journal of Biological Chemistry* 277, no. 4 (January 25): 2923-2930.

Hynes, Nancy E, and Heidi A Lane. 2005. ERBB receptors and cancer: the complexity of targeted inhibitors. *Nature Reviews. Cancer* 5, no. 5 (May): 341-354.

Inagaki, Y, Y Tsunokawa, N Takebe, H Nawa, S Nakanishi, M Terada, and T Sugimura. 1988. Nucleotide sequences of cDNAs for human papillomavirus type 18 transcripts in HeLa cells. *Journal of Virology* 62, no. 5 (May): 1640-1646.

Inoue, T, F X Sullivan, and T R Cech. 1985. Intermolecular exon ligation of the rRNA precursor of Tetrahymena: oligonucleotides can function as 5' exons. *Cell* 43, no. 2 Pt 1 (December): 431-437.

James, Michael A, John H Lee, and Aloysius J Klingelhutz. 2006. Human papillomavirus type 16 E6 activates NF-kappaB, induces cIAP-2 expression, and protects against apoptosis in a PDZ binding motif-dependent manner. *Journal of Virology* 80, no. 11 (June): 5301-5307.

Jenkins, David. 2008. A review of cross-protection against oncogenic HPV by an HPV-16/18 AS04-adjuvanted cervical cancer vaccine: importance of virological and clinical endpoints and implications for mass vaccination in cervical cancer prevention. *Gynecologic Oncology* 110, no. 3 Suppl 1 (September): S18-25.

Jeon, S, B L Allen-Hoffmann, and P F Lambert. 1995. Integration of human papillomavirus type 16 into the human genome correlates with a selective growth advantage of cells. *Journal of Virology* 69, no. 5 (May): 2989-2997.

Jewers, R J, P Hildebrandt, J W Ludlow, B Kell, and D J McCance. 1992. Regions of human papillomavirus type 16 E7 oncoprotein required for immortalization of human keratinocytes. *Journal of Virology* 66, no. 3 (March): 1329-1335.

Jian, Y, D C Schmidt-Grimminger, W M Chien, X Wu, T R Broker, and L T Chow. 1998. Post-transcriptional induction of p21cip1 protein by human papillomavirus E7 inhibits unscheduled DNA synthesis reactivated in differentiated keratinocytes. *Oncogene* 17, no. 16 (October 22): 2027-2038.

Jones, D L, R M Alani, and K Münger. 1997. The human papillomavirus E7 oncoprotein can uncouple cellular differentiation and proliferation in human keratinocytes by abrogating p21Cip1-mediated inhibition of cdk2. *Genes & Development* 11, no. 16 (August 15): 2101-2111.

Jones, D L, D A Thompson, E Suh-Bürgmann, M Grace, and K Münger. 1999. Expression of the HPV E7 oncoprotein mimics but does not evoke a p53-dependent cellular DNA damage response pathway. *Virology* 258, no. 2 (June 5): 406-414.

Joyce, J G, J S Tung, C T Przysiecki, J C Cook, E D Lehman, J A Sands, K U Jansen, and P M Keller. 1999. The L1 major capsid protein of human papillomavirus type 11 recombinant virus-like particles interacts with heparin and cell-surface glycosaminoglycans on human keratinocytes. *The Journal of Biological Chemistry* 274, no. 9 (February 26): 5810-5822.

Kahn, Jessica A. 2009. HPV vaccination for the prevention of cervical intraepithelial neoplasia. *The New England Journal of Medicine* 361, no. 3 (July 16): 271-278.

Karl, Theresia, Nadine Seibert, Michael Stöhr, Hans Osswald, Frank Rösl, and Patrick Finzer. 2007. Sulindac induces specific degradation of the HPV oncoprotein E7 and causes growth arrest and apoptosis in cervical carcinoma cells. *Cancer Letters* 245, no. 1-2 (January 8): 103-111.

Khan, Michelle J, Philip E Castle, Attila T Lorincz, Sholom Wacholder, Mark Sherman, David R Scott, Brenda B Rush, Andrew G Glass, and Mark Schiffman. 2005. The elevated 10-year risk of cervical precancer and cancer in women with human papillomavirus (HPV) type 16 or 18 and the possible utility of type-specific HPV testing in clinical practice. *Journal of the National Cancer Institute* 97, no. 14 (July 20): 1072-1079.

Kieback, Elisa, and Martin Müller. 2006. Factors influencing subcellular localization of the human papillomavirus L2 minor structural protein. *Virology* 345, no. 1 (February 5): 199-208.

Kim, Gwi Eon, Yong Bae Kim, Nam Hoon Cho, Hyun-Cheol Chung, Hong Ryull Pyo, Jong Doo Lee, Tchan Kyu Park, Woong Sub Koom, Mison Chun, and Chang Ok Suh. 2004. Synchronous coexpression of epidermal growth factor receptor and cyclooxygenase-2 in carcinomas of the uterine cervix: a potential predictor of poor survival. *Clinical Cancer Research: An Official Journal of the American Association for Cancer Research* 10, no. 4 (February 15): 1366-1374.

Kim, Hooja, Kyung-Ja Lee, Sun-Ock Lee, and Sungjae Kim. 2004. Cervical cancer screening in Korean American women: findings from focus group interviews. *Taehan Kanho Hakhoe Chi* 34, no. 4 (June): 617-624.

Kim, Yoonah, Murray J Cairns, Rita Marouga, and Lun-Quan Sun. 2003. E6AP gene suppression and characterization with in vitro selected hammerhead ribozymes. *Cancer Gene Therapy* 10, no. 9 (September): 707-716.

Kinoshita, T, H Shirasawa, Y Shino, H Moriya, L Desbarats, M Eilers, and B Simizu. 1997. Transactivation of prothymosin alpha and c-myc promoters by human papillomavirus type 16 E6 protein. *Virology* 232, no. 1 (May 26): 53-61.

Kirnbauer, R, F Booy, N Cheng, D R Lowy, and J T Schiller. 1992. Papillomavirus L1 major capsid protein self-assembles into virus-like particles that are highly immunogenic. *Proceedings of the National Academy of Sciences of the United States of America* 89, no. 24 (December 15): 12180-12184.

Kiyono, T, A Hiraiwa, M Fujita, Y Hayashi, T Akiyama, and M Ishibashi. 1997. Binding of high-risk human papillomavirus E6 oncoproteins to the human homologue of the Drosophila discs large tumor suppressor protein. *Proceedings of the National Academy of Sciences of the United States of America* 94, no. 21 (October 14): 11612-11616.

Kjaer, Susanne K, Kristján Sigurdsson, Ole-Erik Iversen, Mauricio Hernandez-Avila, Cosette M Wheeler, Gonzalo Perez, Darron R Brown, et al. 2009. A pooled analysis of continued prophylactic efficacy of quadrivalent human papillomavirus (Types 6/11/16/18) vaccine against high-grade cervical and external genital lesions. *Cancer Prevention Research (Philadelphia, Pa.)* 2, no. 10 (October): 868-878.

Klausner, Richard D. 2002. The fabric of cancer cell biology-Weaving together the strands. *Cancer Cell* 1, no. 1 (February): 3-10.

Klingelhutz, A J, S A Foster, and J K McDougall. 1996. Telomerase activation by the E6 gene product of human papillomavirus type 16. *Nature* 380, no. 6569 (March 7): 79-82.

Klucevsek, K, J Daley, M S Darshan, J Bordeaux, and J Moroianu. 2006. Nuclear import strategies of high-risk HPV18 L2 minor capsid protein. *Virology* 352, no. 1 (August 15): 200-208.

Knight, Gillian L, John R Grainger, Phillip H Gallimore, and Sally Roberts. 2004. Cooperation between different forms of the human papillomavirus type 1 E4 protein to block cell cycle progression and cellular DNA synthesis. *Journal of Virology* 78, no. 24 (December): 13920-13933.

Kumar, Ajay, Yongtong Zhao, Gaoyuan Meng, Musheng Zeng, Seetha Srinivasan, Laurie M Delmolino, Qingshen Gao, et al. 2002. Human papillomavirus oncoprotein E6 inactivates the transcriptional coactivator human ADA3. *Molecular and Cellular Biology* 22, no. 16 (August): 5801-5812.

Kurreck, Jens. 2009. RNA interference: from basic research to therapeutic applications. *Angewandte Chemie (International Ed. in English)* 48, no. 8: 1378-1398.

Lanni, J S, and T Jacks. 1998. Characterization of the p53-dependent postmitotic checkpoint following spindle disruption. *Molecular and Cellular Biology* 18, no. 2 (February): 1055-1064.

Latorre, Isabel J, Michael H Roh, Kristopher K Frese, Robert S Weiss, Ben Margolis, and Ronald T Javier. 2005. Viral oncoprotein-induced mislocalization of select PDZ proteins disrupts tight junctions and causes polarity defects in epithelial cells. *Journal of Cell Science* 118, no. Pt 18 (September 15): 4283-4293.

Law, M F, W D Lancaster, and P M Howley. 1979. Conserved polynucleotide sequences among the genomes of papillomaviruses. *Journal of Virology* 32, no. 1 (October): 199-207.

Lechner, M S, and L A Laimins. 1994. Inhibition of p53 DNA binding by human papillomavirus E6 proteins. *Journal of Virology* 68, no. 7 (July): 4262-4273.

Lechner, M S, D H Mack, A B Finicle, T Crook, K H Vousden, and L A Laimins. 1992. Human papillomavirus E6 proteins bind p53 in vivo and abrogate p53-mediated repression of transcription. *The EMBO Journal* 11, no. 8 (August): 3045-3052.

Lee, D, H Sohn, G V Kalpana, and J Choe. 1999. Interaction of E1 and hSNF5 proteins stimulates replication of human papillomavirus DNA. *Nature* 399, no. 6735 (June 3): 487-491.

Lee, Nan Sook, Taikoh Dohjima, Gerhard Bauer, Haitang Li, Ming-Jie Li, Ali Ehsani, Paul Salvaterra, and John Rossi. 2002. Expression of small interfering RNAs targeted against HIV-1 rev transcripts in human cells. *Nature Biotechnology* 20, no. 5 (May): 500-505.

Lee, S S, B Glaunsinger, F Mantovani, L Banks, and R T Javier. 2000. Multi-PDZ domain protein MUPP1 is a cellular target for both adenovirus E4-ORF1 and high-risk papillomavirus type 18 E6 oncoproteins. *Journal of Virology* 74, no. 20 (October): 9680-9693.

Lee, S S, R S Weiss, and R T Javier. 1997. Binding of human virus oncoproteins to hDlg/SAP97, a mammalian homolog of the Drosophila discs large tumor suppressor protein. *Proceedings of the National Academy of Sciences of the United States of America* 94, no. 13 (June 24): 6670-6675.

Lehrer, M S, T T Sun, and R M Lavker. 1998. Strategies of epithelial repair: modulation of stem cell and transit amplifying cell proliferation. *Journal of Cell Science* 111 ( Pt 19) (October): 2867-2875.

Li, X, and P Coffino. 1996. High-risk human papillomavirus E6 protein has two distinct binding sites within p53, of which only one determines degradation. *Journal of Virology* 70, no. 7 (July): 4509-4516.

Li, Y, H Li, G Yao, W Li, F Wang, Z Jiang, and M Li. 2007. Inhibition of telomerase RNA (hTR) in cervical cancer by adenovirus-delivered siRNA. *Cancer Gene Therapy* 14, no. 8 (August): 748-755.

Liaw, K L, A Hildesheim, R D Burk, P Gravitt, S Wacholder, M M Manos, D R Scott, et al. 2001. A prospective study of human papillomavirus (HPV) type 16 DNA detection by polymerase chain reaction and its association with acquisition and persistence of other HPV types. *The Journal of Infectious Diseases* 183, no. 1 (January 1): 8-15.

Lie, A K, S Skarsvåg, H Skomedal, O A Haugen, and R Holm. 1999. Expression of p53, MDM2, and p21 proteins in high-grade cervical intraepithelial neoplasia and relationship to human papillomavirus infection. *International Journal of Gynecological Pathology: Official Journal of the International Society of Gynecological Pathologists* 18, no. 1 (January): 5-11.

Ling, Xiang, and Fengzhi Li. 2004. Silencing of antiapoptotic survivin gene by multiple approaches of RNA interference technology. *BioTechniques* 36, no. 3 (March): 450-454, 456-460.

Lipari, F, G A McGibbon, E Wardrop, and M G Cordingley. 2001. Purification and biophysical characterization of a minimal functional domain and of an N-terminal Zn2+-binding fragment from the human papillomavirus type 16 E6 protein. *Biochemistry* 40, no. 5 (February 6): 1196-1204.

Liu, Jidong, Michelle A Carmell, Fabiola V Rivas, Carolyn G Marsden, J Michael Thomson, Ji-Joon Song, Scott M Hammond, Leemor Joshua-Tor, and Gregory J Hannon. 2004. Argonaute2 is the catalytic engine of mammalian RNAi. *Science (New York, N.Y.)* 305, no. 5689 (September 3): 1437-1441.

Liu, Jidong, Marco Antonio Valencia-Sanchez, Gregory J Hannon, and Roy Parker. 2005. MicroRNA-dependent localization of targeted mRNAs to mammalian P-bodies. *Nature Cell Biology* 7, no. 7 (July): 719-723.

Liu, Xin, Adrienne Clements, Kehao Zhao, and Ronen Marmorstein. 2006. Structure of the human Papillomavirus E7 oncoprotein and its mechanism for inactivation of the retinoblastoma tumor suppressor. *The Journal of Biological Chemistry* 281, no. 1 (January 6): 578-586.

Liu, Xuefeng, Hang Yuan, Baojin Fu, Gary L Disbrow, Tania Apolinario, Vjekoslav Tomaic, Melissa L Kelley, Carl C Baker, Jon Huibregtse, and Richard Schlegel. 2005. The E6AP ubiquitin ligase is required for transactivation of the hTERT promoter by the human papillomavirus E6 oncoprotein. *The Journal of Biological Chemistry* 280, no. 11 (March 18): 10807-10816.

Longworth, Michelle S, and Laimonis A Laimins. 2004a. The binding of histone deacetylases and the integrity of zinc finger-like motifs of the E7 protein are essential for the life cycle of human papillomavirus type 31. *Journal of Virology* 78, no. 7 (April): 3533-3541.

Longworth, Michelle S, and Laimonis A Laimins. 2004b. Pathogenesis of human papillomaviruses in differentiating epithelia. *Microbiology and Molecular Biology Reviews: MMBR* 68, no. 2 (June): 362-372.

Longworth, Michelle S, Regina Wilson, and Laimonis A Laimins. 2005. HPV31 E7 facilitates replication by activating E2F2 transcription through its interaction with HDACs. *The EMBO Journal* 24, no. 10 (May 18): 1821-1830.

Loo, Yueh-Ming, and Thomas Melendy. 2004. Recruitment of replication protein A by the papillomavirus E1 protein and modulation by single-stranded DNA. *Journal of Virology* 78, no. 4 (February): 1605-1615.

Lowe, S W, T Jacks, D E Housman, and H E Ruley. 1994. Abrogation of oncogene-associated apoptosis allows transformation of p53-deficient cells. *Proceedings of the National Academy of Sciences of the United States of America* 91, no. 6 (March 15): 2026-2030.

Lusky, M, J Hurwitz, and Y S Seo. 1994. The bovine papillomavirus E2 protein modulates the assembly of but is not stably maintained in a replication-competent multimeric E1-replication origin complex. *Proceedings of the National Academy of Sciences of the United States of America* 91, no. 19 (September 13): 8895-8899.

Lyons, Tarrah E, Maysoon Salih, and Balwant S Tuana. 2006. Activating E2Fs mediate transcriptional regulation of human E2F6 repressor. *American Journal of Physiology. Cell Physiology* 290, no. 1 (January): C189-199.

Madison, Kathi C. 2003. Barrier function of the skin: "la raison d'être" of the epidermis. *The Journal of Investigative Dermatology* 121, no. 2 (August): 231-241.

Magnusson, P K, P Lichtenstein, and U B Gyllensten. 2000. Heritability of cervical tumours. *International Journal of Cancer. Journal International Du Cancer* 88, no. 5 (December 1): 698-701.

Mantovani, F, and L Banks. 1999. Inhibition of E6 induced degradation of p53 is not sufficient for stabilization of p53 protein in cervical tumour derived cell lines. *Oncogene* 18, no. 22 (June 3): 3309-3315.

Mantovani, F, and L Banks. 2001. The human papillomavirus E6 protein and its contribution to malignant progression. *Oncogene* 20, no. 54 (November 26): 7874-7887.

Maran, A, C A Amella, T P Di Lorenzo, K J Auborn, L B Taichman, and B M Steinberg. 1995. Human papillomavirus type 11 transcripts are present at low abundance in latently infected respiratory tissues. *Virology* 212, no. 2 (October 1): 285-294.

Martin, Tracey A, Gareth Watkins, Robert E Mansel, and Wen G Jiang. 2004. Loss of tight junction plaque molecules in breast cancer tissues is associated with a poor prognosis in patients with breast cancer. *European Journal of Cancer (Oxford, England: 1990)* 40, no. 18 (December): 2717-2725.

Martinez, Javier, Agnieszka Patkaniowska, Henning Urlaub, Reinhard Lührmann, and Thomas Tuschl. 2002. Single-stranded antisense siRNAs guide target RNA cleavage in RNAi. *Cell* 110, no. 5 (September 6): 563-574.

May, E, J R Jenkins, and P May. 1991. Endogenous HeLa p53 proteins are easily detected in HeLa cells transfected with mouse deletion mutant p53 gene. *Oncogene* 6, no. 8 (August): 1363-1365.

McIntyre, M C, M G Frattini, S R Grossman, and L A Laimins. 1993. Human papillomavirus type 18 E7 protein requires intact Cys-X-X-Cys motifs for zinc binding, dimerization, and transformation but not for Rb binding. *Journal of Virology* 67, no. 6 (June): 3142-3150.

McLaughlin-Drubin, Margaret E, Kyung-Won Huh, and Karl Münger. 2008. Human papillomavirus type 16 E7 oncoprotein associates with E2F6. *Journal of Virology* 82, no. 17 (September): 8695-8705.

McMillan, N A, E Payne, I H Frazer, and M Evander. 1999. Expression of the alpha6 integrin confers papillomavirus binding upon receptor-negative B-cells. *Virology* 261, no. 2 (September 1): 271-279.

McPhillips, Maria G, Thanaporn Veerapraditsin, Sarah A Cumming, Dimitra Karali, Steven G Milligan, Winifred Boner, Iain M Morgan, and Sheila V Graham. 2004. SF2/ASF binds the human papillomavirus type 16 late RNA control element and is regulated during differentiation of virus-infected epithelial cells. *Journal of Virology* 78, no. 19 (October): 10598-10605.

Melnikow, J, J Nuovo, A R Willan, B K Chan, and L P Howell. 1998. Natural history of cervical squamous intraepithelial lesions: a meta-analysis. *Obstetrics and Gynecology* 92, no. 4 Pt 2 (October): 727-735.

Melsheimer, Peter, Svetlana Vinokurova, Nicolas Wentzensen, Gunther Bastert, and Magnus von Knebel Doeberitz. 2004. DNA aneuploidy and integration of human papillomavirus type 16 e6/e7 oncogenes in intraepithelial neoplasia and invasive squamous cell carcinoma of the cervix uteri. *Clinical Cancer Research: An Official Journal of the American Association for Cancer Research* 10, no. 9 (May 1): 3059-3063.

Mercatante, D, and R Kole. 2000. Modification of alternative splicing pathways as a potential approach to chemotherapy. *Pharmacology & Therapeutics* 85, no. 3 (March): 237-243.

Meyerson, M, C M Counter, E N Eaton, L W Ellisen, P Steiner, S D Caddle, L Ziaugra, et al. 1997. hEST2, the putative human telomerase catalytic subunit gene, is up-regulated in tumor cells and during immortalization. *Cell* 90, no. 4 (August 22): 785-795.

Miyagishi, Makoto, and Kazunari Taira. 2002. Development and application of siRNA expression vector. *Nucleic Acids Research. Supplement (2001)*, no. 2: 113-114.

Mohr, I J, R Clark, S Sun, E J Androphy, P MacPherson, and M R Botchan. 1990. Targeting the E1 replication protein to the papillomavirus origin of replication by complex formation with the E2 transactivator. *Science (New York, N.Y.)* 250, no. 4988 (December 21): 1694-1699.

Moscicki, Anna-Barbara, Mark Schiffman, Susanne Kjaer, and Luisa L Villa. 2006. Chapter 5: Updating the natural history of HPV and anogenital cancer. *Vaccine* 24 Suppl 3 (August 31): S3/42-51.

Münger, K, B A Werness, N Dyson, W C Phelps, E Harlow, and P M Howley. 1989. Complex formation of human papillomavirus E7 proteins with the retinoblastoma tumor suppressor gene product. *The EMBO Journal* 8, no. 13 (December 20): 4099-4105.

Münger, Karl, and Peter M Howley. 2002. Human papillomavirus immortalization and transformation functions. *Virus Research* 89, no. 2 (November): 213-228.

Muñoz, Nubia, F Xavier Bosch, Silvia de Sanjosé, Rolando Herrero, Xavier Castellsagué, Keerti V Shah, Peter J F Snijders, and Chris J L M Meijer. 2003. Epidemiologic classification of human papillomavirus types associated with cervical cancer. *The New England Journal of Medicine* 348, no. 6 (February 6): 518-527.

Muñoz, Nubia, Fabián Méndez, Héctor Posso, Mónica Molano, Adrian J C van den Brule, Margarita Ronderos, Chris Meijer, and Alvaro Muñoz. 2004. Incidence, duration, and determinants of cervical human papillomavirus infection in a cohort of Colombian women with normal cytological results. *The Journal of Infectious Diseases* 190, no. 12 (December 15): 2077-2087.

Murphy, N, M Ring, C C B B Heffron, B King, A G Killalea, C Hughes, C M Martin, E McGuinness, O Sheils, and J J O'Leary. 2005a. p16INK4A, CDC6, and MCM5: predictive biomarkers in cervical preinvasive neoplasia and cervical cancer. *Journal of Clinical Pathology* 58, no. 5 (May): 525-534.

Murphy, Niamh, Martina Ring, Cynthia C B B Heffron, Cara M Martin, Eamon McGuinness, Orla Sheils, and John J O'Leary. 2005b. Quantitation of CDC6 and MCM5 mRNA in cervical intraepithelial neoplasia and invasive squamous cell carcinoma of the cervix. *Modern Pathology: An Official Journal of the United States and Canadian Academy of Pathology, Inc* 18, no. 6 (June): 844-849.

Nahmias, A J, W E Josey, Z M Naib, C F Luce, and B A Guest. 1970. Antibodies to Herpesvirus hominis types 1 and 2 in humans. II. Women with cervical cancer. *American Journal of Epidemiology* 91, no. 6 (June): 547-552.

Naib, Z M, A J Nahmias, W E Josey, and J H Kramer. 1969. Genital herpetic infection. Association with cervical dysplasia and carcinoma. *Cancer* 23, no. 4 (April): 940-945.

Nakagawa, S, and J M Huibregtse. 2000. Human scribble (Vartul) is targeted for ubiquitin-mediated degradation by the high-risk papillomavirus E6 proteins and the E6AP ubiquitin-protein ligase. *Molecular and Cellular Biology* 20, no. 21 (November): 8244-8253.

Nakagawa, S, T Yano, K Nakagawa, S Takizawa, Y Suzuki, T Yasugi, J M Huibregtse, and Y Taketani. 2004. Analysis of the expression and localisation of a LAP protein, human scribble, in the normal and neoplastic epithelium of uterine cervix. *British Journal of Cancer* 90, no. 1 (January 12): 194-199.

Nakahara, Tomomi, Woei Ling Peh, John Doorbar, Denis Lee, and Paul F Lambert. 2005. Human papillomavirus type 16 E1circumflexE4 contributes to multiple facets of the papillomavirus life cycle. *Journal of Virology* 79, no. 20 (October): 13150-13165.

Nanda, K, D C McCrory, E R Myers, L A Bastian, V Hasselblad, J D Hickey, and D B Matchar. 2000. Accuracy of the Papanicolaou test in screening for and follow-up of cervical cytologic abnormalities: a systematic review. *Annals of Internal Medicine* 132, no. 10 (May 16): 810-819.

Napoli, C., C. Lemieux, and R. Jorgensen. 1990. Introduction of a Chimeric Chalcone Synthase Gene into Petunia Results in Reversible Co-Suppression of Homologous Genes in trans. *The Plant Cell* 2, no. 4 (April): 279-289.

Nasu S, Ang KK, Fan Z, Milas L. 2001. C225 antiepidermal growth factor receptor antibody enhances tumor radiocurability. *International Journal of Radiation Oncology, Biology, Physics* 51, no.2 (October): 474-7.

Nguyen, Christine L, Catherine Eichwald, Max L Nibert, and Karl Münger. 2007. Human papillomavirus type 16 E7 oncoprotein associates with the centrosomal component gamma-tubulin. *Journal of Virology* 81, no. 24 (December): 13533-13543.

Nguyen, Christine L, and Karl Münger. 2008. Direct association of the HPV16 E7 oncoprotein with cyclin A/CDK2 and cyclin E/CDK2 complexes. *Virology* 380, no. 1 (October 10): 21-25.

Nguyen, Don X, Laurel A Baglia, Shih-Min Huang, Christina M Baker, and Dennis J McCance. 2004. Acetylation regulates the differentiation-specific functions of the retinoblastoma protein. *The EMBO Journal* 23, no. 7 (April 7): 1609-1618.

Nguyen, Don X, and Dennis J McCance. 2005. Role of the retinoblastoma tumor suppressor protein in cellular differentiation. *Journal of Cellular Biochemistry* 94, no. 5 (April 1): 870-879.

Nguyen, Marie L, Minh M Nguyen, Denis Lee, Anne E Griep, and Paul F Lambert. 2003. The PDZ ligand domain of the human papillomavirus type 16 E6 protein is required for E6's induction of epithelial hyperplasia in vivo. *Journal of Virology* 77, no. 12 (June): 6957-6964.

Nominé, Yves, Murielle Masson, Sebastian Charbonnier, Katia Zanier, Tutik Ristriani, François Deryckère, Annie-Paule Sibler, et al. 2006. Structural and functional analysis of E6 oncoprotein: insights in the molecular pathways of human papillomavirus-mediated pathogenesis. *Molecular Cell* 21, no. 5 (March 3): 665-678.

Nourse, J, E Firpo, W M Flanagan, S Coats, K Polyak, M H Lee, J Massague, G R Crabtree, and J M Roberts. 1994. Interleukin-2-mediated elimination of the p27Kip1 cyclin-dependent kinase inhibitor prevented by rapamycin. *Nature* 372, no. 6506 (December 8): 570-573.

Noya, F, W M Chien, T R Broker, and L T Chow. 2001. p21cip1 Degradation in differentiated keratinocytes is abrogated by costabilization with cyclin E induced by human papillomavirus E7. *Journal of Virology* 75, no. 13 (July): 6121-6134.

Oh, M J, J H Choi, I H Kim, Y H Lee, J Y Huh, Y K Park, K W Lee, et al. 2000. Detection of epidermal growth factor receptor in the serum of patients with cervical carcinoma. *Clinical Cancer Research: An Official Journal of the American Association for Cancer Research* 6, no. 12 (December): 4760-4763.

Oh, S T, S Kyo, and L A Laimins. 2001. Telomerase activation by human papillomavirus type 16 E6 protein: induction of human telomerase reverse transcriptase expression through Myc and GC-rich Sp1 binding sites. *Journal of Virology* 75, no. 12 (June): 5559-5566.

Ohlenschläger, O, T Seiboth, H Zengerling, L Briese, A Marchanka, R Ramachandran, M Baum, et al. 2006. Solution structure of the partially folded high-risk human papilloma virus 45 oncoprotein E7. *Oncogene* 25, no. 44 (September 28): 5953-5959.

Olivier, Magali, Ros Eeles, Monica Hollstein, Mohammed A Khan, Curtis C Harris, and Pierre Hainaut. 2002. The IARC TP53 database: new online mutation analysis and recommendations to users. *Human Mutation* 19, no. 6 (June): 607-614.

Paavonen, Jorma, David Jenkins, F Xavier Bosch, Paulo Naud, Jorge Salmerón, Cosette M Wheeler, Song-Nan Chow, et al. 2007. Efficacy of a prophylactic adjuvanted bivalent L1 virus-like-particle vaccine against infection with human papillomavirus types 16 and 18 in young women: an interim analysis of a phase III double-blind, randomised controlled trial. *Lancet* 369, no. 9580 (June 30): 2161-2170.

Parkin, D Max, Freddie Bray, J Ferlay, and Paola Pisani. 2005. Global cancer statistics, 2002. *CA: A Cancer Journal for Clinicians* 55, no. 2 (April): 74-108.

Parkin, D Maxwell, and Freddie Bray. 2006. Chapter 2: The burden of HPV-related cancers. *Vaccine* 24 Suppl 3 (August 31): S3/11-25.

Patel, D, S M Huang, L A Baglia, and D J McCance. 1999. The E6 protein of human papillomavirus type 16 binds to and inhibits co-activation by CBP and p300. *The EMBO Journal* 18, no. 18 (September 15): 5061-5072.

Paul, Cynthia P, Paul D Good, Ira Winer, and David R Engelke. 2002. Effective expression of small interfering RNA in human cells. *Nature Biotechnology* 20, no. 5 (May): 505-508.

Peh, Woei L, Janet L Brandsma, Neil D Christensen, Nancy M Cladel, Xing Wu, and John Doorbar. 2004. The viral E4 protein is required for the completion of the cottontail rabbit papillomavirus productive cycle in vivo. *Journal of Virology* 78, no. 4 (February): 2142-2151.

Peh, Woei Ling, Kate Middleton, Neil Christensen, Philip Nicholls, Kiyofumi Egawa, Karl Sotlar, Janet Brandsma, et al. 2002. Life cycle heterogeneity in animal models of human papillomavirus-associated disease. *Journal of Virology* 76, no. 20 (October): 10401-10416.

Pei, X F, J M Meck, D Greenhalgh, and R Schlegel. 1993. Cotransfection of HPV-18 and v-fos DNA induces tumorigenicity of primary human keratinocytes. *Virology* 196, no. 2 (October): 855-860.

Pett, M, and N Coleman. 2007. Integration of high-risk human papillomavirus: a key event in cervical carcinogenesis? *The Journal of Pathology* 212, no. 4 (August): 356-367.

Phelps, W C, K Münger, C L Yee, J A Barnes, and P M Howley. 1992. Structure-function analysis of the human papillomavirus type 16 E7 oncoprotein. *Journal of Virology* 66, no. 4 (April): 2418-2427.

Phelps, W C, C L Yee, K Münger, and P M Howley. 1988. The human papillomavirus type 16 E7 gene encodes transactivation and transformation functions similar to those of adenovirus E1A. *Cell* 53, no. 4 (May 20): 539-547.

Pichler, Andrea, Noam Zelcer, Julie L Prior, Annemieke J Kuil, and David Piwnica-Worms. 2005. In vivo RNA interference-mediated ablation of MDR1 P-glycoprotein. *Clinical Cancer Research: An Official Journal of the American Association for Cancer Research* 11, no. 12 (June 15): 4487-4494.

Pim, D, M Thomas, R Javier, D Gardiol, and L Banks. 2000. HPV E6 targeted degradation of the discs large protein: evidence for the involvement of a novel ubiquitin ligase. *Oncogene* 19, no. 6 (February 10): 719-725.

Pim, David, Vjekoslav Tomaic, and Lawrence Banks. 2009. The human papillomavirus (HPV) E6* proteins from high-risk, mucosal HPVs can direct degradation of cellular proteins in the absence of full-length E6 protein. *Journal of Virology* 83, no. 19 (October): 9863-9874.

Pisani, P, D M Parkin, F Bray, and J Ferlay. 1999. Estimates of the worldwide mortality from 25 cancers in 1990. *International Journal of Cancer. Journal International Du Cancer* 83, no. 1 (September 24): 18-29.

Plug-DeMaggio, Annemieke W, Terri Sundsvold, Michelle A Wurscher, Jennifer I Koop, Aloysius J Klingelhutz, and James K McDougall. 2004. Telomere erosion and chromosomal instability in cells expressing the HPV oncogene 16E6. *Oncogene* 23, no. 20 (April 29): 3561-3571.

Poljak, M, K Fujs, K Seme, B J Kocjan, and E Vrtacnik-Bokal. 2005. Retrospective and prospective evaluation of the Amplicor HPV test for detection of 13 high-risk human papillomavirus genotypes on 862 clinical samples. *Acta Dermatovenerologica Alpina, Panonica, Et Adriatica* 14, no. 4 (December): 147-152.

Powell MPJ, Buttin BB, Gibb RK, Luck MD, Rader JS. 2003. A pilot study of celecoxib in the treatment of patients with cervical and vaginal intraepithelial neoplasia. *American Society of Clinical Oncology*. Abstract 1830.

Preall, Jonathan B, and Erik J Sontheimer. 2005. RNAi: RISC gets loaded. *Cell* 123, no. 4 (November 18): 543-545.

Rand, Tim A, Sean Petersen, Fenghe Du, and Xiaodong Wang. 2005. Argonaute2 cleaves the anti-guide strand of siRNA during RISC activation. *Cell* 123, no. 4 (November 18): 621-629.

Rawls, W E, W A Tompkins, M E Figueroa, and J L Melnick. 1968. Herpesvirus type 2: association with carcinoma of the cervix. *Science (New York, N.Y.)* 161, no. 847 (September 20): 1255-1256.

Ressler, Sigrun, René Scheiden, Kerstin Dreier, Andreas Laich, Elisabeth Müller-Holzner, Haymo Pircher, Dieter Morandell, et al. 2007. High-risk human papillomavirus E7 oncoprotein detection in cervical squamous cell carcinoma. *Clinical Cancer Research: An Official Journal of the American Association for Cancer Research* 13, no. 23 (December 1): 7067-7072.

Rigoni-Stern. 1987. Statistical facts about cancers on which Doctor Rigoni-Stern based his contribution to the Surgeons' Subgroup of the IV Congress of the Italian Scientists on 23 September 1842. (translation). *Statistics in Medicine* 6, no. 8 (December): 881-884.

Roden, R B, P M Day, B K Bronzo, W H Yutzy, Y Yang, D R Lowy, and J T Schiller. 2001. Positively charged termini of the L2 minor capsid protein are necessary for papillomavirus infection. *Journal of Virology* 75, no. 21 (November): 10493-10497.

Roden, Richard B S, Archana Monie, and T-C Wu. 2007. Opportunities to improve the prevention and treatment of cervical cancer. *Current Molecular Medicine* 7, no. 5 (August): 490-503.

Romanczuk, H, F Thierry, and P M Howley. 1990. Mutational analysis of cis elements involved in E2 modulation of human papillomavirus type 16 P97 and type 18 P105 promoters. *Journal of Virology* 64, no. 6 (June): 2849-2859.

Sang, B C, and M S Barbosa. 1992. Single amino acid substitutions in "low-risk" human papillomavirus (HPV) type 6 E7 protein enhance features characteristic of the "high-risk" HPV E7 oncoproteins. *Proceedings of the National Academy of Sciences of the United States of America* 89, no. 17 (September 1): 8063-8067.

Sato, H, A Furuno, and K Yoshiike. 1989. Expression of human papillomavirus type 16 E7 gene induces DNA synthesis of rat 3Y1 cells. *Virology* 168, no. 1 (January): 195-199.

Saxena, Sandeep, Zophonías O Jónsson, and Anindya Dutta. 2003. Small RNAs with imperfect match to endogenous mRNA repress translation. Implications for off-target activity of small inhibitory RNA in mammalian cells. *The Journal of Biological Chemistry* 278, no. 45 (November 7): 44312-44319.

Scheffner, M, J M Huibregtse, R D Vierstra, and P M Howley. 1993. The HPV-16 E6 and E6-AP complex functions as a ubiquitin-protein ligase in the ubiquitination of p53. *Cell* 75, no. 3 (November 5): 495-505.

Scheffner, M, K Münger, J C Byrne, and P M Howley. 1991. The state of the p53 and retinoblastoma genes in human cervical carcinoma cell lines. *Proceedings of the National Academy of Sciences of the United States of America* 88, no. 13 (July 1): 5523-5527.

Scheffner, M, B A Werness, J M Huibregtse, A J Levine, and P M Howley. 1990. The E6 oncoprotein encoded by human papillomavirus types 16 and 18 promotes the degradation of p53. *Cell* 63, no. 6 (December 21): 1129-1136.

Schneider-Gädicke, A, S Kaul, E Schwarz, H Gausepohl, R Frank, and G Bastert. 1988. Identification of the human papillomavirus type 18 E6 and E6 proteins in nuclear protein fractions from human cervical carcinoma cells grown in the nude mouse or in vitro. *Cancer Research* 48, no. 11 (June 1): 2969-2974.

Schorge, John O, Lynne M Knowles, and Jayanthi S Lea. 2004. Adenocarcinoma of the cervix. *Current Treatment Options in Oncology* 5, no. 2 (April): 119-127.

Sedman, S A, M S Barbosa, W C Vass, N L Hubbert, J A Haas, D R Lowy, and J T Schiller. 1991. The full-length E6 protein of human papillomavirus type 16 has transforming and trans-activating activities and cooperates with E7 to immortalize keratinocytes in culture. *Journal of Virology* 65, no. 9 (September): 4860-4866.

Selinka, Hans-Christoph, Tzenan Giroglou, Thorsten Nowak, Neil D Christensen, and Martin Sapp. 2003. Further evidence that papillomavirus capsids exist in two distinct conformations. *Journal of Virology* 77, no. 24 (December): 12961-12967.

Shay, J W, and S Bacchetti. 1997. A survey of telomerase activity in human cancer. *European Journal of Cancer (Oxford, England: 1990)* 33, no. 5 (April): 787-791.

Sheldon, C C, and R H Symons. 1989. Mutagenesis analysis of a self-cleaving RNA. *Nucleic Acids Research* 17, no. 14 (July 25): 5679-5685.

Skiadopoulos, M H, and A A McBride. 1998. Bovine papillomavirus type 1 genomes and the E2 transactivator protein are closely associated with mitotic chromatin. *Journal of Virology* 72, no. 3 (March): 2079-2088.

Smith, H O, M F Tiffany, C R Qualls, and C R Key. 2000. The rising incidence of adenocarcinoma relative to squamous cell carcinoma of the uterine cervix in the United States--a 24-year population-based study. *Gynecologic Oncology* 78, no. 2 (August): 97-105.

Smith, Jennifer S, Cristina Bosetti, Nubia Muñoz, Rolando Herrero, F Xavier Bosch, José Eluf-Neto, Chris J L M Meijer, Adriaan J C Van Den Brule, Silvia Franceschi, and Rosanna W Peeling. 2004. Chlamydia trachomatis and invasive cervical cancer: a pooled analysis of the IARC multicentric case-control study. *International Journal of Cancer. Journal International Du Cancer* 111, no. 3 (September 1): 431-439.

Smith, Jennifer S, Rolando Herrero, Cristina Bosetti, Nubia Muñoz, F Xavier Bosch, José Eluf-Neto, Xavier Castellsagué, et al. 2002. Herpes simplex virus-2 as a human papillomavirus cofactor in the etiology of invasive cervical cancer. *Journal of the National Cancer Institute* 94, no. 21 (November 6): 1604-1613.

Smith, Jessica L, Samuel K Campos, and Michelle A Ozbun. 2007. Human papillomavirus type 31 uses a caveolin 1- and dynamin 2-mediated entry pathway for infection of human keratinocytes. *Journal of Virology* 81, no. 18 (September): 9922-9931.

Smith-McCune, K, D Kalman, C Robbins, S Shivakumar, L Yuschenkoff, and J M Bishop. 1999. Intranuclear localization of human papillomavirus 16 E7 during transformation and preferential binding of E7 to the Rb family member p130. *Proceedings of the National Academy of Sciences of the United States of America* 96, no. 12 (June 8): 6999-7004.

Smotkin, D, and F O Wettstein. 1986. Transcription of human papillomavirus type 16 early genes in a cervical cancer and a cancer-derived cell line and identification of the E7 protein. *Proceedings of the National Academy of Sciences of the United States of America* 83, no. 13 (July): 4680-4684.

Snijders, Peter J F, Renske D M Steenbergen, Daniëlle A M Heideman, and Chris J L M Meijer. 2006. HPV-mediated cervical carcinogenesis: concepts and clinical implications. *The Journal of Pathology* 208, no. 2 (January): 152-164.

Solinas-Toldo, S, M Dürst, and P Lichter. 1997. Specific chromosomal imbalances in human papillomavirus-transfected cells during progression toward immortality. *Proceedings of the National Academy of Sciences of the United States of America* 94, no. 8 (April 15): 3854-3859.

Song, S, A Liem, J A Miller, and P F Lambert. 2000. Human papillomavirus types 16 E6 and E7 contribute differently to carcinogenesis. *Virology* 267, no. 2 (February 15): 141-150.

Songyang, Z, A S Fanning, C Fu, J Xu, S M Marfatia, A H Chishti, A Crompton, A C Chan, J M Anderson, and L C Cantley. 1997. Recognition of unique carboxyl-terminal motifs by distinct PDZ domains. *Science (New York, N.Y.)* 275, no. 5296 (January 3): 73-77.

Soussi, Thierry, and Christophe Béroud. 2003. Significance of TP53 mutations in human cancer: a critical analysis of mutations at CpG dinucleotides. *Human Mutation* 21, no. 3 (March): 192-200.

Spanos, William C, Jeremy Geiger, Mary E Anderson, George F Harris, Aaron D Bossler, Russell B Smith, Aloysius J Klingelhutz, and John H Lee. 2008. Deletion of the PDZ motif of HPV16 E6 preventing immortalization and anchorage-independent growth in human tonsil epithelial cells. *Head & Neck* 30, no. 2 (February): 139-147.

Spink, Kathryn M, and Laimonis A Laimins. 2005. Induction of the human papillomavirus type 31 late promoter requires differentiation but not DNA amplification. *Journal of Virology* 79, no. 8 (April): 4918-4926.

Stacey, S N, D Jordan, P J Snijders, M Mackett, J M Walboomers, and J R Arrand. 1995. Translation of the human papillomavirus type 16 E7 oncoprotein from bicistronic mRNA is independent of splicing events within the E6 open reading frame. *Journal of Virology* 69, no. 11 (November): 7023-7031.

Stacey, S N, D Jordan, A J Williamson, M Brown, J H Coote, and J R Arrand. 2000. Leaky scanning is the predominant mechanism for translation of human papillomavirus type 16 E7 oncoprotein from E6/E7 bicistronic mRNA. *Journal of Virology* 74, no. 16 (August): 7284-7297.

Stauffer, Y, K Raj, K Masternak, and P Beard. 1998. Infectious human papillomavirus type 18 pseudovirions. *Journal of Molecular Biology* 283, no. 3 (October 30): 529-536.

Steger, G, and S Corbach. 1997. Dose-dependent regulation of the early promoter of human papillomavirus type 18 by the viral E2 protein. *Journal of Virology* 71, no. 1 (January): 50-58.

Stoler, M H, C R Rhodes, A Whitbeck, S M Wolinsky, L T Chow, and T R Broker. 1992. Human papillomavirus type 16 and 18 gene expression in cervical neoplasias. *Human Pathology* 23, no. 2 (February): 117-128.

Storey, A, N Almond, K Osborn, and L Crawford. 1990. Mutations of the human papillomavirus type 16 E7 gene that affect transformation, transactivation and phosphorylation by the E7 protein. *The Journal of General Virology* 71 ( Pt 4) (April): 965-970.

Storrs, Carina H, and Saul J Silverstein. 2007. PATJ, a tight junction-associated PDZ protein, is a novel degradation target of high-risk human papillomavirus E6 and the alternatively spliced isoform 18 E6. *Journal of Virology* 81, no. 8 (April): 4080-4090.

Stubenrauch, F, and L A Laimins. 1999. Human papillomavirus life cycle: active and latent phases. *Seminars in Cancer Biology* 9, no. 6 (December): 379-386.

Stubenrauch, F, H B Lim, and L A Laimins. 1998. Differential requirements for conserved E2 binding sites in the life cycle of oncogenic human papillomavirus type 31. *Journal of Virology* 72, no. 2 (February): 1071-1077.

Sui, Guangchao, Christina Soohoo, El Bachir Affar, Frédérique Gay, Yujiang Shi, William C Forrester, and Yang Shi. 2002. A DNA vector-based RNAi technology to suppress gene expression in mammalian cells. *Proceedings of the National Academy of Sciences of the United States of America* 99, no. 8 (April 16): 5515-5520.

Sumimoto, Hidetoshi, Makoto Miyagishi, Hiroyuki Miyoshi, Shizuko Yamagata, Ayako Shimizu, Kazunari Taira, and Yutaka Kawakami. 2004. Inhibition of growth and invasive ability of melanoma by inactivation of mutated BRAF with lentivirus-mediated RNA interference. *Oncogene* 23, no. 36 (August 12): 6031-6039.

Tang, Shuang, Mingfang Tao, J Philip McCoy, and Zhi-Ming Zheng. 2006. The E7 oncoprotein is translated from spliced E6*I transcripts in high-risk human papillomavirus type 16- or type 18-positive cervical cancer cell lines via translation reinitiation. *Journal of Virology* 80, no. 9 (May): 4249-4263.

Tao, Mingfang, Michael Kruhlak, Shuhua Xia, Elliot Androphy, and Zhi-Ming Zheng. 2003. Signals that dictate nuclear localization of human papillomavirus type 16 oncoprotein E6 in living cells. *Journal of Virology* 77, no. 24 (December): 13232-13247.

Thierry, Françoise. 2009. Transcriptional regulation of the papillomavirus oncogenes by cellular and viral transcription factors in cervical carcinoma. *Virology* 384, no. 2 (February 20): 375-379.

Thomas, J T, and L A Laimins. 1998. Human papillomavirus oncoproteins E6 and E7 independently abrogate the mitotic spindle checkpoint. *Journal of Virology* 72, no. 2 (February): 1131-1137.

Thomas, M, and L Banks. 1998. Inhibition of Bak-induced apoptosis by HPV-18 E6. *Oncogene* 17, no. 23 (December 10): 2943-2954.

Thomas, M, P Massimi, J Jenkins, and L Banks. 1995. HPV-18 E6 mediated inhibition of p53 DNA binding activity is independent of E6 induced degradation. *Oncogene* 10, no. 2 (January 19): 261-268.

Thomas, Miranda, Richard Laura, Karin Hepner, Ernesto Guccione, Charles Sawyers, Laurence Lasky, and Lawrence Banks. 2002. Oncogenic human papillomavirus E6 proteins target the MAGI-2 and MAGI-3 proteins for degradation. *Oncogene* 21, no. 33 (August 1): 5088-5096.

Thompson, D A, G Belinsky, T H Chang, D L Jones, R Schlegel, and K Münger. 1997. The human papillomavirus-16 E6 oncoprotein decreases the vigilance of mitotic checkpoints. *Oncogene* 15, no. 25 (December 18): 3025-3035.

Thorland, Erik C, Shannon L Myers, Bobbie S Gostout, and David I Smith. 2003. Common fragile sites are preferential targets for HPV16 integrations in cervical tumors. *Oncogene* 22, no. 8 (February 27): 1225-1237.

Titolo, S, A Pelletier, F Sauvé, K Brault, E Wardrop, P W White, A Amin, M G Cordingley, and J Archambault. 1999. Role of the ATP-binding domain of the human papillomavirus type 11 E1 helicase in E2-dependent binding to the origin. *Journal of Virology* 73, no. 7 (July): 5282-5293.

Tommasino, M, J P Adamczewski, F Carlotti, C F Barth, R Manetti, M Contorni, F Cavalieri, T Hunt, and L Crawford. 1993. HPV16 E7 protein associates with the protein kinase p33CDK2 and cyclin A. *Oncogene* 8, no. 1 (January): 195-202.

Trimble, Cornelia L, and Ian H Frazer. 2009. Development of therapeutic HPV vaccines. *The Lancet Oncology* 10, no. 10 (October): 975-980. Trimble, Cornelia L, Steven Piantadosi, Patti Gravitt, Brigitte Ronnett, Ellen Pizer, Andrea Elko, Barbara Wilgus, et al. 2005. Spontaneous regression of high-grade cervical dysplasia: effects of human papillomavirus type and HLA phenotype. *Clinical Cancer Research: An Official Journal of the American Association for Cancer Research* 11, no. 13 (July 1): 4717-4723.

Uhlenbeck, O C. 1987. A small catalytic oligoribonucleotide. *Nature* 328, no. 6131 (August 13): 596-600.

Vaeteewoottacharn, Kulthida, Siriphatr Chamutpong, Mathurose Ponglikitmongkol, and Peter C Angeletti. 2005. Differential localization of HPV16 E6 splice products with E6-associated protein. *Virology Journal* 2: 50.

Veldman, Tim, Xuefeng Liu, Hang Yuan, and Richard Schlegel. 2003. Human papillomavirus E6 and Myc proteins associate in vivo and bind to and cooperatively activate the telomerase reverse transcriptase promoter. *Proceedings of the National Academy of Sciences of the United States of America* 100, no. 14 (July 8): 8211-8216.

Venturini, F, J Braspenning, M Homann, L Gissmann, and G Sczakiel. 1999. Kinetic selection of HPV 16 E6/E7-directed antisense nucleic acids: anti-proliferative effects on HPV 16-transformed cells. *Nucleic Acids Research* 27, no. 7 (April 1): 1585-1592.

Vousden, K H, and P S Jat. 1989. Functional similarity between HPV16E7, SV40 large T and adenovirus E1a proteins. *Oncogene* 4, no. 2 (February): 153-158.

Walboomers, J M, M V Jacobs, M M Manos, F X Bosch, J A Kummer, K V Shah, P J Snijders, J Peto, C J Meijer, and N Muñoz. 1999. Human papillomavirus is a necessary cause of invasive cervical cancer worldwide. *The Journal of Pathology* 189, no. 1 (September): 12-19.

Walter, and Burke. 1998. The hairpin ribozyme: structure, assembly and catalysis . *Current Opinion in Chemical Biology* 2, no. 2 (April): 303.

Wang, Hsu-Kun, Aaron A Duffy, Thomas R Broker, and Louise T Chow. 2009. Robust production and passaging of infectious HPV in squamous epithelium of primary human keratinocytes. *Genes & Development* 23, no. 2 (January 15): 181-194.

Wang, J, L Y Xie, S Allan, D Beach, and G J Hannon. 1998. Myc activates telomerase. *Genes & Development* 12, no. 12 (June 15): 1769-1774.

Wang, Sophia S, Mark E Sherman, Allan Hildesheim, James V Lacey, and Susan Devesa. 2004. Cervical adenocarcinoma and squamous cell carcinoma incidence trends among white women and black women in the United States for 1976-2000. *Cancer* 100, no. 5 (March 1): 1035-1044.

Watanabe, S, T Kanda, H Sato, A Furuno, and K Yoshiike. 1990. Mutational analysis of human papillomavirus type 16 E7 functions. *Journal of Virology* 64, no. 1 (January): 207-214.

Watson, Richard A, Miranda Thomas, Lawrence Banks, and Sally Roberts. 2003. Activity of the human papillomavirus E6 PDZ-binding motif correlates with an enhanced morphological transformation of immortalized human keratinocytes. *Journal of Cell Science* 116, no. Pt 24 (December 15): 4925-4934.

Weintraub, S J, K N Chow, R X Luo, S H Zhang, S He, and D C Dean. 1995. Mechanism of active transcriptional repression by the retinoblastoma protein. *Nature* 375, no. 6534 (June 29): 812-815.

Wells, S I, D A Francis, A Y Karpova, J J Dowhanick, J D Benson, and P M Howley. 2000. Papillomavirus E2 induces senescence in HPV-positive cells via pRB- and p21(CIP)-dependent pathways. *The EMBO Journal* 19, no. 21 (November 1): 5762-5771.

Welters, Marij J P, Pauline van der Logt, Susan J F van den Eeden, Kitty M C Kwappenberg, Jan Wouter Drijfhout, Gert Jan Fleuren, Gemma G Kenter, Cornelis J M Melief, Sjoerd H van der Burg, and Rienk Offringa. 2006. Detection of human papillomavirus type 18 E6 and E7-specific CD4+ T-helper 1 immunity in relation to health versus disease. *International Journal of Cancer. Journal International Du Cancer* 118, no. 4 (February 15): 950-956.

Wentzensen, Nicolas, Svetlana Vinokurova, and Magnus von Knebel Doeberitz. 2004. Systematic review of genomic integration sites of human papillomavirus genomes in epithelial dysplasia and invasive cancer of the female lower genital tract. *Cancer Research* 64, no. 11 (June 1): 3878-3884.

Werness, B A, A J Levine, and P M Howley. 1990. Association of human papillomavirus types 16 and 18 E6 proteins with p53. *Science (New York, N.Y.)* 248, no. 4951 (April 6): 76-79.

World Health Organization. 2006. Comprehensive cervical cancer control; a guide to essential practice. http://whqlibdoc.who.int/publications/2006/9241547006_eng.pdf.

White, A E, E M Livanos, and T D Tlsty. 1994. Differential disruption of genomic integrity and cell cycle regulation in normal human fibroblasts by the HPV oncoproteins. *Genes & Development* 8, no. 6 (March 15): 666-677.

Wilson, Regina, Frauke Fehrmann, and Laimonis A Laimins. 2005. Role of the E1--E4 protein in the differentiation-dependent life cycle of human papillomavirus type 31. *Journal of Virology* 79, no. 11 (June): 6732-6740.

Winder, D M, M R Pett, N Foster, M K K Shivji, M T Herdman, M A Stanley, A R Venkitaraman, and N Coleman. 2007. An increase in DNA double-strand breaks, induced by Ku70 depletion, is associated with human papillomavirus 16 episome loss and de novo viral integration events. *The Journal of Pathology* 213, no. 1 (September): 27-34.

Woodman, C B, S Collins, H Winter, A Bailey, J Ellis, P Prior, M Yates, T P Rollason, and L S Young. 2001. Natural history of cervical human papillomavirus infection in young women: a longitudinal cohort study. *Lancet* 357, no. 9271 (June 9): 1831-1836.

Woodman, Ciaran B J, Stuart I Collins, and Lawrence S Young. 2007. The natural history of cervical HPV infection: unresolved issues. *Nature Reviews. Cancer* 7, no. 1 (January): 11-22.

Woodworth, Craig D, Evan Michael, Dan Marker, Sarah Allen, Laura Smith, and Matthias Nees. 2005. Inhibition of the epidermal growth factor receptor increases expression of genes that stimulate inflammation, apoptosis, and cell attachment. *Molecular Cancer Therapeutics* 4, no. 4 (April): 650-658.

Wright, T C, T V Ellerbrock, M A Chiasson, N Van Devanter, and X W Sun. 1994. Cervical intraepithelial neoplasia in women infected with human immunodeficiency virus: prevalence, risk factors, and validity of Papanicolaou smears. New York Cervical Disease Study. *Obstetrics and Gynecology* 84, no. 4 (October): 591-597.

Wu, X, and A J Levine. 1994. p53 and E2F-1 cooperate to mediate apoptosis. *Proceedings of the National Academy of Sciences of the United States of America* 91, no. 9 (April 26): 3602-3606.

Xu, Mei, Weifeng Luo, David J Elzi, Carla Grandori, and Denise A Galloway. 2008. NFX1 interacts with mSin3A/histone deacetylase to repress hTERT transcription in keratinocytes. *Molecular and Cellular Biology* 28, no. 15 (August): 4819-4828.

Yang, Rongcun, Patricia M Day, William H Yutzy, Ken-Yu Lin, Chien-Fu Hung, and Richard B S Roden. 2003. Cell surface-binding motifs of L2 that facilitate papillomavirus infection. *Journal of Virology* 77, no. 6 (March): 3531-3541.

You, Jianxin, Jennie L Croyle, Akiko Nishimura, Keiko Ozato, and Peter M Howley. 2004. Interaction of the bovine papillomavirus E2 protein with Brd4 tethers the viral DNA to host mitotic chromosomes. *Cell* 117, no. 3 (April 30): 349-360.

Yu, Jenn-Yah, Stacy L DeRuiter, and David L Turner. 2002. RNA interference by expression of short-interfering RNAs and hairpin RNAs in mammalian cells. *Proceedings of the National Academy of Sciences of the United States of America* 99, no. 9 (April 30): 6047-6052.

Yu, Tingxi, Matthew J Ferber, Tak Hong Cheung, Tong Kwok Hung Chung, Yick Fu Wong, and David I Smith. 2005. The role of viral integration in the development of cervical cancer. *Cancer Genetics and Cytogenetics* 158, no. 1 (April 1): 27-34.

Yuan, Huidong, Fenghua Fu, Jiaying Zhuo, Wei Wang, Junko Nishitani, Dong Sung An, Irvin S Y Chen, and Xuan Liu. 2005. Human papillomavirus type 16 E6 and E7 oncoproteins upregulate c-IAP2 gene expression and confer resistance to apoptosis. *Oncogene* 24, no. 32 (July 28): 5069-5078.

Zeng, Musheng, Ajay Kumar, Gaoyuan Meng, Qingshen Gao, Goberdhan Dimri, David Wazer, Hamid Band, and Vimla Band. 2002. Human papilloma virus 16 E6 oncoprotein inhibits retinoic X receptor-mediated transactivation by targeting human ADA3 coactivator. *The Journal of Biological Chemistry* 277, no. 47 (November 22): 45611-45618.

Zerfass, K, A Schulze, D Spitkovsky, V Friedman, B Henglein, and P Jansen-Dürr. 1995. Sequential activation of cyclin E and cyclin A gene expression by human papillomavirus type 16 E7 through sequences necessary for transformation. *Journal of Virology* 69, no. 10 (October): 6389-6399.

Zerfass-Thome, K, W Zwerschke, B Mannhardt, R Tindle, J W Botz, and P Jansen-Dürr. 1996. Inactivation of the cdk inhibitor p27KIP1 by the human papillomavirus type 16 E7 oncoprotein. *Oncogene* 13, no. 11 (December 5): 2323-2330.

Zhao, Kong-Nan, Wen Jun Liu, and Ian H Frazer. 2003. Codon usage bias and A+T content variation in human papillomavirus genomes. *Virus Research* 98, no. 2 (December): 95-104.

Zhao, Xiaomin, Margaret Rush, and Stefan Schwartz. 2004. Identification of an hnRNP A1-dependent splicing silencer in the human papillomavirus type 16 L1 coding region that prevents premature expression of the late L1 gene. *Journal of Virology* 78, no. 20 (October): 10888-10905.

Zheng, Yanfang, Jiren Zhang, and Zhiguo Rao. 2004. Ribozyme targeting HPV16 E6E7 transcripts in cervical cancer cells suppresses cell growth and sensitizes cells to chemotherapy and radiotherapy. *Cancer Biology & Therapy* 3, no. 11 (November): 1129-1134.

Zheng, Yan-Fang, Zhi-Guo Rao, and Ji-Ren Zhang. 2002. Effects of anti-HPV16 E6-ribozyme on the proliferation and apoptosis of human cervical cancer cell line CaSKi. *Di 1 Jun Yi Da Xue Xue Bao = Academic Journal of the First Medical College of PLA* 22, no. 6 (June): 496-498.

Zheng, Zhi-Ming, and Carl C Baker. 2006. Papillomavirus genome structure, expression, and post-transcriptional regulation. *Frontiers in Bioscience: A Journal and Virtual Library* 11: 2286-2302.

Zhou, J, W J Liu, S W Peng, X Y Sun, and I Frazer. 1999. Papillomavirus capsid protein expression level depends on the match between codon usage and tRNA availability. *Journal of Virology* 73, no. 6 (June): 4972-4982.

Zhou, J, X Y Sun, D J Stenzel, and I H Frazer. 1991. Expression of vaccinia recombinant HPV 16 L1 and L2 ORF proteins in epithelial cells is sufficient for assembly of HPV virion-like particles. *Virology* 185, no. 1 (November): 251-257.

Zimmermann, H, C H Koh, R Degenkolbe, M J O'Connor, A Müller, G Steger, J J Chen, Y Lui, E Androphy, and H U Bernard. 2000. Interaction with CBP/p300 enables the bovine papillomavirus type 1 E6 oncoprotein to downregulate CBP/p300-mediated transactivation by p53. *The Journal of General Virology* 81, no. Pt 11 (November): 2617-2623.

zur Hausen, H. 2000. Papillomaviruses causing cancer: evasion from host-cell control in early events in carcinogenesis. *Journal of the National Cancer Institute* 92, no. 9 (May 3): 690-698.

zur Hausen, H, and E M de Villiers. 1994. Human papillomaviruses. *Annual Review of Microbiology* 48: 427-447.

zur Hausen, J, H Schulte-Holthausen, H Wolf, K Dörries, and H Egger. 1974. Attempts to detect virus-specific DNA in human tumors. II. Nucleic acid hybridizations with complementary RNA of human herpes group viruses. *International Journal of Cancer. Journal International Du Cancer* 13, no. 5 (May 15): 657-664.

# Chapter Two

# Materials and Methods

## 2.0 Materials and methods

This chapter provides a full description of the methodologies employed in this thesis. For some newer techniques some background information is also provided. Several of the techniques are used in a number of chapters. Where this occurs, the full description of the technique is restricted to this chapter, with specifics appearing in the relevant chapters only.

## 2.1 Cell culture of cervical cancer cell lines

Three cervical cancer cell lines were utilised during this thesis, the HPV16 positive cell line SiHa, the HPV18 positive cell line HeLa and the HPV negative cervical cancer cell line C33A; Table 2.1 provides more detailed information. All cell lines were obtained from the American Type Culture Collection (ATCC) and maintained in Modified Eagle Medium (MEM) supplemented with L-glutamine (2mmol/L), penicillin (200U), streptomycin (200µg), 10% non-essential amino acids and 10% heat-inactivated fetal bovine serum (Lonza Group Ltd, Switzerland) at 37°C in a humidified 5% $CO_2$ atmosphere.

**Table 2.1: Description of cell lines used in this study.**

| Cell Line | Description |
|---|---|
| SiHa | Squamous Cell Carcinoma, grade II. HPV 16 positive, 1-2 copies per cell. p53+, Rb+. |
| HeLa | Adenocarcinoma. HPV 18 positive, 20-50 copies per cell. p53+, Rb+. |
| C33A | Derived from cervical cancer biopsy. Negative for HPV DNA and RNA. p53+, Rb+. |

### *2.1.1 Cell culture protocols*

All cell lines were thawed from 1ml, containing $1x10^6$cells, stocks by gentle agitation in a 37°C water bath. The thawed cells were equally split (500μL) between two sterile flat bottomed 25cm$^2$ cell culture flasks containing complete cell culture media. Media was changed the following day and afterwards every 2-3 days. Cells were grown to 80% confluency where upon they were transferred to a 75cm$^2$ and then a 175cm$^2$ flat bottomed cell culture flask.

All cells were passaged using trysin-EDTA (0.05mg/ml). Briefly, old cell media was removed, cells were washed with 3-5ml of phosphate buffered saline (PBS) and subsequently removed from the flask surface by incubation with 3-5ml of trypsin-EDTA for 5mins at 37°C. 6ml of complete medium was added to the cells. They were then transferred to a 15ml falcon tube and centrifuged at 1200rpm for 5mins. For all cell lines after centrifugation the supernatant was removed and the cells were resuspended in 1ml of complete medium, prior to being placed in the appropriate tissue culture flask. 75cm$^2$ flasks contained in total 15ml of complete media and 175cm$^2$ flasks 50ml.

For storage, cells were pelleted by centrifugation at a concentration of $1x10^6$, re-suspended in 1ml of Cell Recovery freezing media (Invitrogen, Life Technologies, Maryland, USA) and placed in a cryovial. The cryovial was placed overnight at -80°C and transferred the following day to a liquid nitrogen storage tank for long-term storage.

Cell counting was performed using the vital dye trypan blue, a haemocytometer and a bright light microscope. Cells were diluted in trypan blue, which stains dead cells blue and are excluded from live cells. The cell/trypan blue solution was then mounted on a haemocytometer and the number of viable cells within one of the nine 1mm$^2$ square of the haemocytometer was determined (Figure 2.1). The number of cells per ml was

calculated by multiplying this figure by the dilution factor of the cells in the trypan blue and then by the conversion factor of $10^4$, which corresponds to one $1mm^2$ haemocytometer square containing $10^{-4}ml$ of solution.

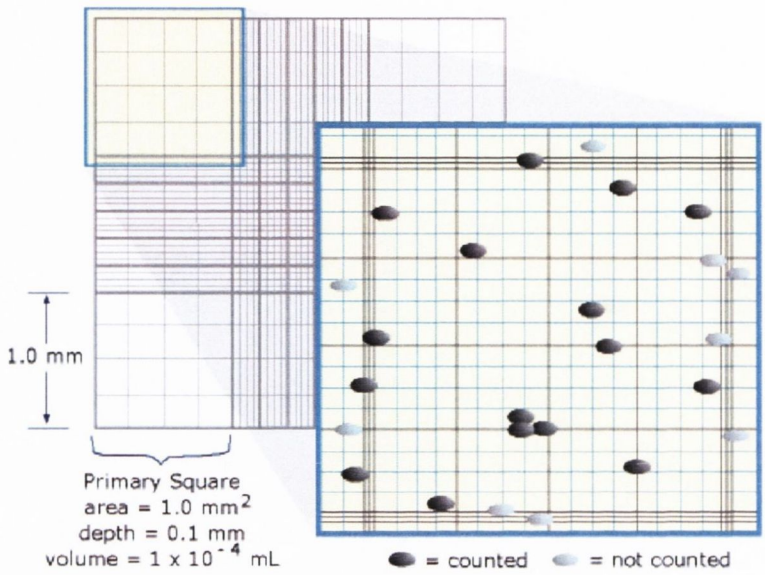


**Figure 2.1: Illustration of a haemocytometer.** A haemocytometer is composed of nine $1mm^2$ squares. These squares have a depth of 0.1mm allowing a volume of $1x10^{-4}ml$ to be contained within each $1mm^2$ square. Cells mounted on the slide are firstly stained with trypan blue, which stains dead cells blue ( ) and is excluded from live cells ( ). A cell count is based on the number of viable cells within one of the nine $1mm^2$ square of the haemocytometer. The number of cells per ml is calculated by multiplying the number of viable cells by the dilution factor of the cells in the trypan blue and then by the conversion factor of $1x10^{-4}ml$. (http://toolboxes.flexiblelearning.net.au/demosites/series4/412/laboratory/studynotes/SNHaemo.htm)

### *2.1.2 Mycoplasma testing*

First discovered as the aetiological agent of contagious bovine pleuropneumonia in 1898 and classified in the mid 1950s, mycoplasma was found to have a broad range of hosts, including humans, animals, insects, and plants. Mycoplasma infection of cell cultures are persistent, difficult to detect and tricky to remedy. Statistics prove that 30 to 60% of all cell cultures are contaminated with mycoplasma, resulting in alterations of growth rates, morphology, and cell viability. Furthermore this may have an effect on experimental results and can lead to findings that do not reflect true experimental variation.

### 2.1.2.1 Mycoplasma detection assay

Mycoplasma detection was performed using the Roche Mycoplasma detection Kit (Roche Diagnostics, IN, USA). This kit is based on the Sandwich ELISA technique and detects the most common mycoplasma species contaminating mammalian cell cultures (*M. arginini, M. hyorhinis, A. laidlawii, M. orale*). Primary polyclonal antibodies specific for the 4 different mycoplasma strains are coated onto the wells of a 96-well microplate. To eliminate non specific binding, a blocking solution is added prior to the prepared samples being added to the wells. The polyclonal antibodies will capture any corresponding antigens present in the prepared sample. Next biotin labelled secondary antibodies are added. These antibodies like the primary antibodies are also specific for the 4 different mycoplasma strains and detect any antigens bound to the primary antibody. Then a streptavidin-alkaline phosphatase (AP) conjugate is applied, which binds to the biotin-labelled secondary antibody, followed by a substrate solution, containing 4-nitrophenylphosphate (4-NPP). The presence of mycoplasma antigens results in the hydrolysis of 4-NPP by the alkaline phosphatase of the streptavidin-AP conjugate, which induces the conversion of the colourless liquid to yellow. The results can be evaluated visually, where yellow colour is positive and colourless negative, and by absorbance at 405nm.

Mycoplasma testing of the cell lines was performed according to the manufacturer's protocol. Colour changes were read on the microplate reader at 405nm (Sunrise plate reader, Tecan Trading AG, Switzerland). Positive controls were provided in the kit and negative controls consisted of complete but unused media.

## 2.2 Transfection of synthetic siRNA

There are several different techniques which can be utilised to introduce siRNA into cells, including electroporation and chemical transfection. In this study, chemical transfection methodology was employed by means of commercially available lipid based transfection agents. All transfection agents used were cationic lipid formulations and employed the mechanism of cationic lipid-mediated transfection. This mechanism of transfection relies on the structure of cationic lipids, a positively charged head group and one or two hydrocarbon chains. Cationic lipids are often formulated with a neutral co-lipid, which results in a unilamellar liposomal structure with a positive surface charge when formulated in water (Figure 2.2). The positively charged surface allows for the interaction between the lipid and the phosphate backbone of the nucleic acid, known as the transfection complex. Additionally, the positive surface charge of the liposomes also mediates the interaction of the nucleic acid and the cell membrane, allowing for fusion of the transfection complex with the negatively charged cell membrane. The transfection complex is then thought to enter the cell through endocytosis. Endocytosis is the process where a localised region of the cellular membrane uptakes the transfection complex by forming a membrane bound/intracellular vesicle.

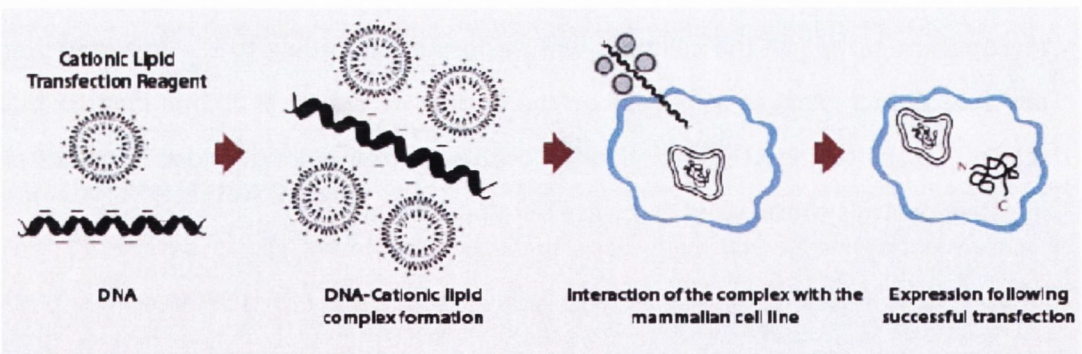


**Figure 2.2: Proposed mechanism of nucleotide entry into cells using cationic lipid formulations.** Cationic and neutral lipids in water form structures called liposomes, which have a positive surface charge. The positive surface charge of the liposomes mediates the interaction of the nucleic acid and the cell membrane, allowing for fusion of the liposome/nucleic acid (transfection complex) with the negatively charged cell membrane. The transfection complex is thought to enter the cell through endocytosis. (https://www.geneseesci.com/jetpei.php)

Several different methods have been developed for chemical transfection of siRNA into cells, primarily falling into the forward or reverse transfection categories (Figure 2.3). Throughout this study the reverse transfection technique was employed as it is faster and more convenient with cells seeded and transfected on the same day. Briefly, this procedure involves preparing transfection complexes inside individual wells, after which cells and medium are added.

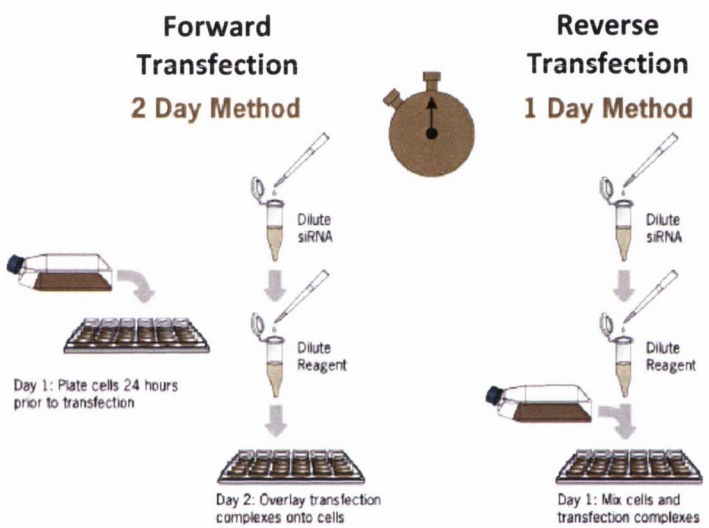


**Figure 2.3: Schematic representation of forward and reverse transfection protocols.** (www.ambion.com)

### *2.2.1 Transient transfection of cells in 96 well format*

Transfections of siRNA in 96-well plate were performed using three different transfection agents: Lipofectamine™ RNAiMAX (Invitrogen, Life Technologies, Maryland, USA), NeoFx™ siPORT ™ (Ambion at Applied Biosystems, Foster City, CA, USA) and HIPERFECT (Qiagen, Crawley, West Sussex, UK) according to the manufacturer's instructions for the reverse transcription technique. The techniques are described briefly below.

### 2.2.1.1 Lipofectamine™ RNAiMAX (Invitrogen, Life Technologies, Maryland, USA)

Cells were diluted in 100µl of complete MEM with or without antibiotics at a defined seeding concentration ($4x10^3$-$1x10^4$). For each transfection sample a reaction mixture was formed, composed of 20µl Opti-MEM® I Reduced Serum Media (Invitrogen, Life Technologies, Maryland, USA), siRNA (final concentration of 10nM) and Lipofectamine™ RNAiMAX (0.1 - 0.3µl). After 20mins incubation at room temperature, which facilitates formation of transfection complexes, 100µl of the diluted cells was added to each reaction mixture. Cells were incubated over time periods of 24 - 96hrs at 37°C in a humidified 5% $CO_2$ atmosphere prior to experimental analysis.

### 2.2.1.2 NeoFx™ siPORT ™ (Ambion at Applied Biosystems, Foster City, CA, USA)

Cells were diluted in 80µl of complete MEM with antibiotics at a defined seeding concentration ($4x10^3$ - $8x10^3$). A 30µl reaction mixture, made of Opti-MEM® I Reduced Serum Media (Invitrogen, Life Technologies, Maryland, USA) and transfection agent (0.3 – 1.2µl), was incubated at room temperature for 10min. The 30µl reaction mixture was then added to the siRNA (final concentration of 10nM) mixed gently and incubated at room temperature for a further 10mins. To each transfection complex mixture 80µl of the diluted cells was added. Cells were incubated for 48hrs at 37°C in a humidified 5% $CO_2$ atmosphere prior to experimental analysis.

### 2.2.1.3 HIPERFECT (Qiagen, Crawley, West Sussex, UK)

Cells were diluted in 175µl of complete MEM with antibiotics at a defined seeding concentration ($1x10^4$ - $3x10^4$). A reaction mixture, composed of 25µl of Opti-MEM® I Reduced Serum Media (Invitrogen, Life Technologies, Maryland, USA), transfection agent (0.25 – 1.125µl) and siRNA (final concentration 10nM), was incubated at room temperature for 20min. To each transfection complex solution 175µl of the diluted cells was added. Cells were incubated for 48hrs at 37°C in a humidified 5% $CO_2$ atmosphere prior to experimental analysis.

### *2.2.2 Transient transfection of SiHa cells in a 6-well format*

Lipofectamine™ RNAiMAX was used to transfect siRNA in 6-well plates. Cells ($1x10^5$ - $2x10^5$ cells) were diluted in 2.5 ml of complete MEM with or without antibiotics and stored at 37°C in a humidified 5% $CO_2$ atmosphere until required. For each transfection sample, 500µl Opti-MEM® I Reduced Serum Media (Invitrogen, Life Technologies, Maryland, USA) was added to each well and the appropriate amount of siRNA (final concentration of 1nM – 50nM per well) was then diluted in it and mixed gently. To this mix Lipofectamine™ RNAiMAX was added (3µl – 5µl) and the reaction mixed gently. The reaction mixture was incubated at room temperature for 20min, which facilitated formation of transfection complexes. To each well 2.5ml of the diluted cells was added. Cells were incubated for 24 - 96hrs at 37°C in a humidified 5% $CO_2$ atmosphere prior to experimental analysis.

## 2.3 Total RNA extraction

The extraction of RNA with high quantity and quality is important in a variety of molecular biological techniques, and is essential for gene expression analysis. RNA is susceptible to degradation by RNases, which are naturally occurring enzymes found in the environment and are also released from cells on cell lysis. In order to minimise RNA degradation, a number of precautions were taken using the following procedures. All water, salt based solutions and plasticware was certified RNase-free. Before commencing, equipment was wiped with the RNase decontamination solution, RNase Zap (Ambion at Applied Biosystems, Foster City, CA, USA). Gloves were worn at all times and regularly changed to avoid contamination. Where possible, procedures were carried out in hoods.

### *2.3.1 Cell-to-Signal™ Lysis Buffer (Ambion at Applied Biosystems, Foster City, CA, USA)*

Cell-to-Signal™ technology was developed for high throughput PCR analysis. It uses a chemical lysis method to create cell lysates in less than 5 minutes at room temperature that can then be used directly for RT-PCR, bypassing RNA isolation altogether. One caveat is that PCR primers must be designed to span exon-exon boundaries. This ensures RNA specific PCR amplification, as the intervening intron will inhibit undesired amplification of genomic DNA in the cell lysate.

#### 2.3.1.1 Protocol

The Cell-to-Signal™ Lysis Buffer (Ambion at Applied Biosystems, Foster City, CA, USA) was used to extract RNA from cell cultures in 96-well plates. Briefly, cell culture media was removed from all wells, cells were then washed with 200µl of PBS prior to 100µl of the Cell-to-Signal™ Lysis Buffer being added to each well. The solution was mixed by vigorous pipetting and then placed on a shaker at a low setting for 2mins. The lysate was then removed from the wells placed in PCR tubes and stored -80°C until required.

### *2.3.2 mirVana™ miRNA Isolation Kit (Ambion at Applied Biosystems, Foster City, CA, USA).*

Historically variations of two standard methods are used to isolate RNA from cell cultures, chemical extraction and immobilization on glass, often referred to as solid-phase extraction. The mirVana™ miRNA Isolation Kit employs a combination of both these techniques and has been optimised to effectively recovers all RNA, from large mRNA and ribosomal RNA down to 10mer miRNA. The sample is first lysed in a denaturing lysis solution which stabilizes RNA and inactivates RNases. To this lysate phenol:chloroform is added. The addition of chloroform yields a biphasic solution with a clear aqueous upper phase containing RNA, an interphase containing DNA and a lower organic phase containing proteins dissolved in phenol and lipids dissolved in chloroform. The upper phase is removed leaving a semi-pure RNA sample, which is further purified over a glass-fibre filter. Nucleic acids bind to the filter depending on the pH and the concentration of the buffers used. Binding is also dependant on charge; nucleic acids being negatively charged while the glass-fibre filter is positively charged. DNA and RNA are hydrophilic and can be absorbed onto the membrane, while hydrophobic lipids and proteins pass through, aided by washing buffers. The glass-fiber filter procedure uses solutions formulated specifically for miRNA retention to avoid the loss of small RNAs that is typically seen with glass-fibre filter methods.

#### 2.3.2.1 Protocol

Total RNA was extracted from the cervical cancer cell lines in all instances using the Ambion *mir*Vana™ miRNA Isolation protocol (Ambion at Applied Biosystems, Foster City, CA, USA), with the exception of when cells were grown on a 96-well plates. The protocol employed was the total RNA isolation protocol, which was performed according to the manufacturer's instructions. Total RNA was eluted in 100µl of nuclease-free water and stored at -80°C until required.

### *2.3.3 DNase digestion*

To ensure that RNA did not contain DNA contamination, DNase digestion was performed on all RNA extracted using the mirVana™ miRNA Isolation Kit (Ambion at Applied Biosystems, Foster City, CA, USA). DNase digestion was performed on RNA samples by incubating the RNA with 1X TURBO DNase buffer (Ambion at Applied Biosystems, Foster City, CA, USA) and 4U of TURBO DNase enzyme (Ambion at Applied Biosystems, Foster City, CA, USA) at 37°C for 30mins. The reaction was stopped by incubating the sample at 75°C for 10mins with EDTA (Sigma-Aldrich, St. Louis, MO, USA) at a final concentration of 15mM. The RNA was then purified out of this solution using the RNeasy Minikit (Qiagen, Crawley, West Sussex, UK) RNA clean up protocol. This was performed as per manufacturer's instructions with one exception - the volume of ethanol used was 700µl rather than the stated 350µl. This modification is suggested by Qiagen when looking to retain small RNAs. RNA was eluted in 50µl of nuclease-free water and stored at -80°C until required.

## 2.4 Nucleic acid quantification and quantitation

Due to the presence of RNases, and the instability of RNA, integrity checks and sample quantitation are essential steps before any RNA dependent application.

### *2.4.1 NanoDrop® ND-1000*

Nucleic acid concentration and quality was determined using the NanoDrop® ND-1000 spectrophotometer (Thermofisher Scientific In., Waltham, MA, USA). The NanoDrop® ND-1000 is a full-spectrum (220-750nm) spectrophotometer that measures 1-2μl samples with high accuracy and reproducibility. It utilises a patented sample retention technology that employs surface tension alone to hold the sample in place. In addition, the ND-1000 has the capability to measure highly concentrated samples without dilution (50X higher concentration than the samples measured by a standard cuvette spectrophotometer).

#### 2.4.1.1 Protocol

The NanoDrop® ND-1000 consists of upper and lower measurement pedestal (Figure 2.4). RNA samples were pipetted onto the lower measurement pedestal and the sample arm was closed. A sample column is automatically drawn between the upper and lower pedestals, which facilitates spectral measurement. RNase/DNase free water was used for blank measurements. The concentration of RNA was calculated by the operating software based on absorbance at 260 nm and the selected analysis constant, which in the case of RNA was 40μg/ml. The software also determined the ratio of sample absorbance at 260nm and 280nm. The 260/280 ratio is used to assess the purity of nucleic acids. A ratio of approximately 2.0 is generally accepted as "pure" for RNA. If the ratio is appreciably lower, it may indicate the presence of protein, phenol or other contaminants that absorb strongly at or near 280nm.

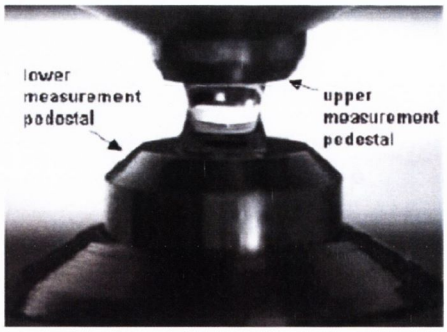


**Figure 2.4: NanoDrop® spectrophotometer sample pedestal.** (www.nanodrop.com)

### *2.4.2 2100 Bioanalyzer*

RNA integrity was analysed using the 2100 Bioanalyser from Agilent (Santa Clara, CA, USA). The Agilent 2100 Bioanalyzer is a microfluidics-based platform for sizing, quantification and quality control of RNA, DNA and proteins through electrophoretic separation. It was the first commercial analytical instrument based on lab-on-a-chip technology and has proven to be an excellent alternative to labour intensive gel electrophoresis techniques; delivering fast, automated, high quality digital data instead of the subjective, time-consuming results associated with gels. Samples are loaded into a chip and placed into the Bioanalyzer, where they are individually analysed and a pseudo gel image is created and bands are sized and quantified.

The 2100 Bioanalyzer has become the standard for RNA quality analysis and is seen as essential part of any work prior to running a microarray experiment, as it ensures the use of intact RNA. The 2100 Bioanalyzer Expert software allows visual inspection of RNA integrity. It generates ribosomal ratios and in addition contains a unique algorithm for total RNA integrity assessment, the output of which is a RNA Integrity Number (RIN). The RIN calculation is based on several critical features of RNA integrity that can be extrapolated from electrophoretic traces (Figure 2.5 A). The algorithm design means that RIN can be considered as a standard integrity measure that is independent of concentration, instrument or analyst. The RIN scale is from 1 to 10, with 1 being the most degraded and 10 being the most intact (Figure 2.5 B).

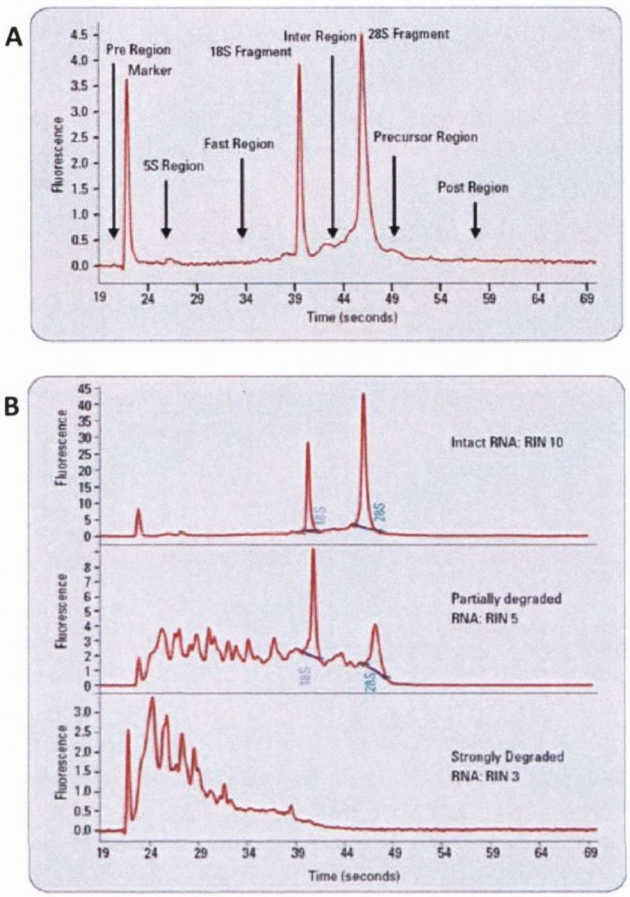


**Figure 2.5: 2100 Bioanalyzer Electropherogram. (A)** Electropherogram detailing the regions that are indicative of RNA quality. **(B)** Examples of electropherograms from samples with varying level of RNA integrity. (www.chem.agilent.com)

### 2.4.2.1 Protocol

The RNA integrity of samples for use in microarray analysis was assessed on the 2100 Bioanalyzer using the RNA Nano 6000 kit (Aglient, Santa Clara, CA, USA). The protocol followed was as per manufacturer's instructions. Visual assessment of gel images and RIN values calculated by the 2100 Bioanalyzer Expert software were used to assess the RNA integrity of samples.

## 2.5 TaqMan® PCR

A TaqMan® PCR-based system was selected for mRNA quantification in this study, due to its requirement for relatively small amounts of input material and its high specificity and sensitivity. TaqMan® PCR is a quantitative real-time (RT) PCR technique, which exploits the dual 5' polymerisation and exonuclease functionality of certain DNA polymerases. It detects the amplification of PCR product in real time by hybridisation and cleavage of a dual labelled fluorogenic probe. The TaqMan® probe is composed of a short oligonucleotide sequence, 20 - 25 bases in length, a 5' and 3' fluorescent molecule and a 3' blocking phosphate that prevents nucleotide extension. The probe is designed to hybridise within the target sequence of the forward and reverse primers. While the probe is intact the proximity of the 5' end fluorescent molecule, known as the reporter dye, to the 3' end fluorescent molecule, known as the quencher dye, results in energy transfer between the two molecules which suppresses the fluorescent emission from the reporter dye. This phenomenon is known as Forster resonance energy transfer (FRET; Forster, 1948; Lakowicz, 1983). On binding of the primers to target sequence, sequence elongation occurs resulting in cleavage of the probe due to the 5'-3' exonuclease activity of the polymerase used (Figure 2.6). Consequently there is a separation of the reporter and quencher molecules, which results in an increased fluorescent emission from the reporter molecule. Therefore the accumulation of PCR product is directly proportional to the increase in the fluorescent emission from the reporter dye, which can be monitored in real time using the 7900HT sequence detection system (Applied Biosystems, Foster City, CA, USA).

The most commonly used enzyme for TaqMan® PCR is Taq polymerase, which was isolated from *Thermus aquaticus.* This is used due to its ability to function in temperatures over 70°C and its 5' exonuclease activity. The exonuclease activity of this enzyme is double strand specific and thus will only act when the probe is hybridised to the target molecule. Detection of target molecule amplification relies on probe binding and subsequent release of the reporter molecule. Therefore hybridisation of the probe prior to primer binding and elongation is critical. For this reason, the melting

temperature (Tm) of the probe is approximately 10°C higher than that of the primers, which ensures the probes remains bound to the target molecule (Livak *et al.*, 1995) and prevents the generation of PCR products without fluorescence. In addition, TaqMan® probes are designed as minor groove binding probes. This consists of a probe conjugated to a minor groove binder at the 5' end, which can be a naturally occurring antibiotic like distamycin A or synthetic molecules. The incorporation of a minor groove binding (MGB) molecule allows the formation of extremely stable hybrids with complementary DNA. MGB probes also allow for higher melting temperatures as they bind more tightly to their targets.

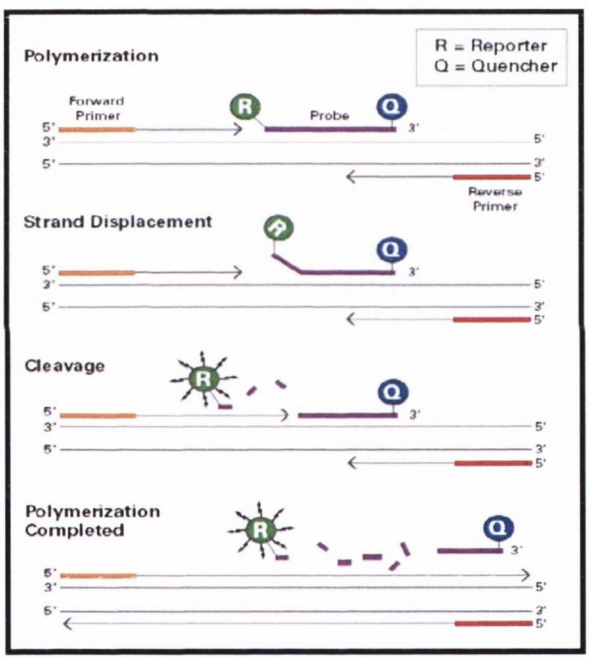


**Figure 2.6: Graphical representation of the process involved in the TaqMan® PCR.** Once bound to the target sequence, elongation occurs between the forward and reverse primers. At this initial point, the bound probe with its fluorescent 5' reporter (R) dye and 3' quencher (Q) remains intact and thus the reporter dye emission is quenched. During the process of elongation/polymerisation, however, the 5'-3' exonuclease activity of *Taq* polymerase acts to cleave the probe. This results in the separation of the reporter and quencher molecules and therefore allows the reporter dye to emit its characteristic fluorescence. It is this fluorescence which is recorded by 7900HT sequence detection system (Applied Biosystems, Foster City, CA, USA) and subsequently analysed. (www.appliedbiosystems.com)

### *2.5.1 TaqMan® PCR primer and probes*

HPV16 and 18 E6 and E7 specific TaqMan® primers and probes were designed using Primer Express Software Version 3.0 (Applied Biosystems, Foster City, CA USA). The following criteria were adhered for primer design; runs of identical nucleotide were avoided, Tm was kept between 58-60°C, the guanine and cytosine content was kept within 20–80% and the last five nucleotides at the 3′ end contained no more than two guanine and cytosine residues. For probe design the criteria were similar except; the Tm was kept as close to 68-70°C as possible, the guanine and cytosine content was kept between 30-80%, no guanines were present at the 5′ end and the probe was not shorter than 13 nucleotides. The specificity of the selected sequences was checked using the NCBI program BLASTN (http://www.ncbi.nlm.nih.gov/blast/). These sets of TaqMan® primers and probes were synthesised by Applied Biosystems (Foster City, CA USA).

All other primers and probes, including gene targets of interest and endogenous controls, used throughout this study were commercial pre-designed primer and probe mixes (20X) obtained from Applied Biosystems (Foster City, CA, USA).

### *2.5.2 TaqMan® two step RT-PCR*

All TaqMan® PCRs were performed using a two step method where messenger RNA (mRNA) is converted firstly to complementary DNA (cDNA) and this is then used as the template in the TaqMan® PCR reaction. All cDNA and PCR reactions were prepared in a dedicated area in a class II laminar flow hood using aerosol resistant pipette tips and dedicated pipettors. Template RNA and cDNA was added to the reaction mixes in a separate area.

### 2.5.2.1 cDNA reaction

Generation of cDNA was performed using the High Capacity cDNA Archive kit (Applied Biosystems, Foster City, CA, USA) according to the manufacturer's protocol. Each cDNA reaction contained 1X reverse transcription buffer, 25mM deoxynucleotide triphosphate (dNTP) mix, 1X random primers and 2.5U multiscribe reverse transcription enzyme. Multiscribe reverse transcriptase is a recombinant Moloney murine leukaemia virus reverse transcriptase and is an RNA dependant DNA polymerase which uses single stranded RNA in the presence of primer to generate cDNA. 500ng of template RNA was used in each 100µl cDNA reaction. The cDNA reaction was performed on the 9600 Thermal Cycler (Applied Biosystems, Foster City, CA, USA) as follows: 25°C for 10mins, 37°C for 120mins, 85°C for 5mins to deactivate the enzyme, and cooling to 4°C.

### 2.5.2.2 TaqMan® PCR

TaqMan® PCR was performed using 2X Universal Master Mix (Applied Biosystems, Foster City, CA, USA), which contains AmpliTaq Gold® DNA polymerase, dNTPs with dUTP, Amperase UNG® and passive reference 1. The use of Amperase UNG® prevents the re-amplification of PCR products containing dUTP as these are digested by the enzyme uracil N-glycolase (UNG). The passive reference is an internal control that can correct for inter well signal variation. RT-PCR reactions were performed in triplicate and per 20µl reaction contained: 4µl of cDNA, 1X Universal Master Mix and 1X pre-designed primers and probe mix or 300nM of in-house designed primers and 200-250nM of in-house designed probes. The RT-PCR reaction was performed on the 7900HT (Applied Biosystems, Foster City, CA, USA) under the following thermal cycling conditions: 50°C for 1min (UNG activation), 95°C for 10mins (AmpliTaq Gold® activation) and 40 cycles of 95°C for 15secs and 1 min at 60°C (melting and annealing/extension).

Controls included in each TaqMan® PCR were a no template control and a cDNA negative control, which were prepared for each primer and probe set.

#### 2.5.2.3 Reference genes

Endogenous controls used in this study included a FAM labelled β-actin or beta-2-microglobulin (B2M) TaqMan® primers and probe. All were assayed in a separate TaqMan® PCR reaction to the target gene. All reactions were performed in triplicate using Universal Master Mix (2X) and primers and probe mix (20X) at a concentration of 1X. The thermal cycling conditions on the 7900HT (Applied Biosystems, Foster City, CA, USA) were as follows: 50°C for 1min (UNG activation), 95°C for 10mins (AmpliTaq Gold® activation) and 40 cycles of 95°C for 15secs and 1 min at 60°C (melting and annealing/extension).

### *2.5.3 TaqMan® Low Density Arrays*

TaqMan® Low Density Arrays (TLDAs) are 384-well micro-fluidic cards, supplied by Applied Biosystems (Foster City, CA, USA), which enable 384 simultaneous TaqMan® RT-PCR reactions to be performed in a high throughput manner. Figure 2.7 shows a representative picture of a TLDA, which is composed of 8 loading ports that feed into forty eight separate wells. Each well contains dried TaqMan® primers and probes for one mRNA target. Thus, a single TLDA can evaluate from one to eight cDNA samples generated from total RNA in a two step RT-PCR experiment. Relative levels of gene expression are determined from the fluorescence data generated during PCR using the Applied Biosystems Prism® 7900HT Sequence detection System (Foster City, CA, USA). Custom designed TLDAs were used in this thesis to validate targets identified by microarray analysis. These TLDAs were comprised of ninety three microarray related targets and three endogenous controls.

#### 2.5.3.1 cDNA reaction

As for section 2.5.2.1

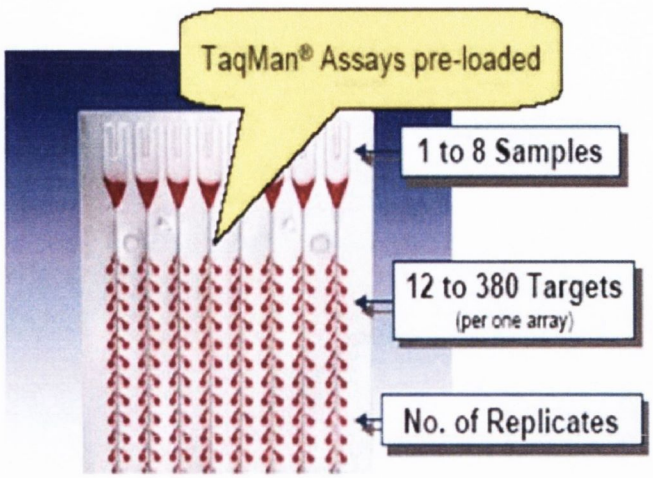


**Figure 2.7: Representation of TaqMan® low density array and its features.** (www.appliedbiosystems.com)

### 2.5.3.2 TaqMan® Low Density Array RT-PCR

130µl of cDNA sample was added to 325µl of TaqMan® Universal Master Mix and 195µl of nuclease free water. This was mixed by vortexing and briefly centrifuged. The reaction mixes were kept on ice while the TLDA cards were prepared. All cards were allowed to come to room temperature before use. Figure 2.8 gives a schematic representation of each step involved in the preparation of the cards. Briefly, the cards were placed foil side down and 100µl of sample was added to each of the 8 loading ports at the top left hand corner of each fill reservoir. The cards were then placed in centrifuge buckets containing custom made TaqMan® Low Density Array holders. The cards were spun at 1200rpm, with an up and down ramp rate of 9 for 2 sets of 1 minute spins. The reservoirs were then checked to ensure filling of the cards was complete. Next the cards were sealed using a specially designed sealer (Applied Biosystems, Foster City, CA , USA). Once the card was sealed the fill reservoirs were trimmed off. The TLDA card was then run on the 7900HT (Applied Biosystems, Foster City, CA , USA) using the TaqMan® Array cycling block, under the following conditions: 50°C for 1min (UNG activation), 95°C for 10mins (AmpliTaq Gold® activation) and 40 cycles of 95°C for 15secs and 1 min at 60°C (melting and annealing/extension).

### 2.5.3.3 Reference genes

Endogenous controls assayed on the TLDAs included FAM labelled TaqMan® primers and probe sets towards Glyceraldehyde-3-phosphate dehydrogenase (GAPDH), B2M and cyclin-dependent kinase inhibitor 2A (CDKN2A).

**Figure 2.8: Step by step instructions followed when performing TaqMan Low Density Array Card.** (www.appliedbiosystems.com)

### *2.5.4 TaqMan® RT-PCR analysis – relative quantification*

TaqMan® RT-PCR is a real time PCR technique and therefore data is collected throughout the PCR process, rather than at the end of the PCR. Consequently reactions are characterised by the point in time during cycling when amplification of a target is first significantly detected. The higher the starting copy number of the nucleic acid target, the sooner a significant increase in fluorescence is observed. A typical amplification plot generated during this process is shown in Figure 2.9.

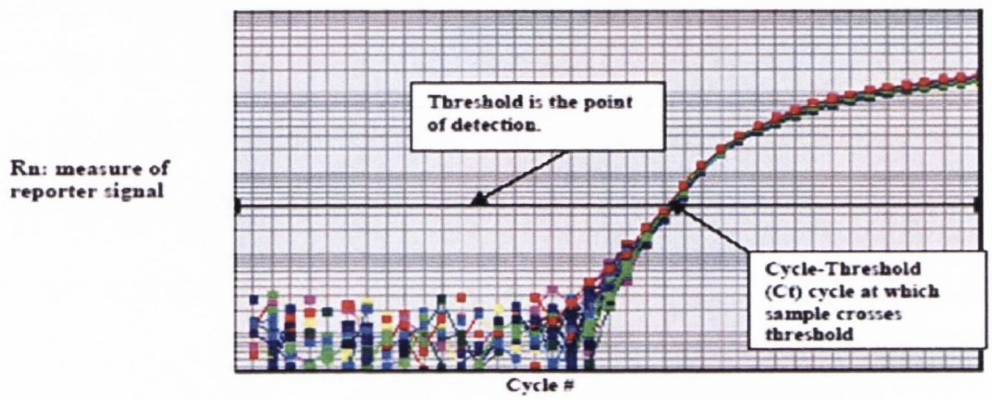


**Figure 2.9: An example of an amplification plot from a TaqMan® RT-PCR reaction.** (www.appliedbiosystems.com)

In the analysis, the initial cycles of PCR, where there is little change in the fluorescent signal, are used to define the baseline for the amplification plot. An increase in fluorescence above the baseline indicates the detection of accumulated target and a fixed fluorescence threshold is set above this baseline. The threshold is set at the point where a statistically significant increase in the fluorescent signal, i.e. the PCR product, is first detected (Figure 2.9). The cycle at which the sample crosses this threshold is determined by the analytical software (Applied Biosystems RQ Manager V1.2), this is known as the threshold cycle ($C_T$) and is used to calculate the relative expression levels. Relative quantification relates the $C_T$ of a target transcript to that of a control transcript, known as the calibrator. This allows the expression of the data as a fold change of expression levels and can be achieved either using the standard curve method or the comparative $C_T$ method. In this study the comparative $C_T$ method was used.

### 2.5.4.1 Comparative $C_T$ method

Relative quantification of the target genes using the comparative $C_T$ method was first described by Livak and Schmittgen in 2001. The comparative $C_T$ method calculates relative gene expression using the following equation:

$$\text{Relative Quantity} = 2^{-\Delta\Delta CT}$$

Initially, the mean $C_T$ value is calculated for each sample along with the standard deviation (StDev; all StDev were below .25). The $\Delta C_T$ is then calculated by normalising the $C_T$ of the target sample with the $C_T$ of the endogenous control ($C_T$ target – $C_T$ endogenous control). Next the $\Delta\Delta C_T$ is calculated by subtracting the $\Delta C_T$ for the calibrator sample from the $\Delta C_T$ for the test sample. In this study the $\Delta C_T$ for the calibrator sample represented an average value of at least three biological replicates, the StDev between these $\Delta C_T$ values was below .25. Finally the relative levels of the target gene expression can be calculated with the above formula.

## 2.6 Affymetrix microarray analysis

Microarray technology is a powerful tool for exploring genome wide expression profiles. It offers unique opportunities to study the interactions of genes and pathways, to characterise gene regulatory networks and to identify novel genes implicated in diseases. In this study the human Affymetrix GeneChip® Gene 1.0 ST array system was utilised. This array system is part of the Affymetrirx new-generation of gene expression profiling tools. It is designed to measure the gene expression of well-annotated genes, using a single probe set per gene comprised of multiple probes that are distributed along the entire length of the genomic locus. Historically, Affymetrix microarrays have interrogated the few hundred bases proximal to the 3' end of each gene, and used expression at the 3' end to approximate expression of the entire gene. However, this approach assumes that the 3' end of each gene is clearly defined, that each transcript has an intact poly-A tail and that the entire length of the gene is expressed as a single unit, e.g. no alternative splicing (figure 2.10). This approach was taken as sample preparation involved 3' oligo(dT)-based priming and labelling assays. The development by Affymetrix of a new target preparation protocol, the Whole Transcript (WT) Assay, which generates labelled target across the entire transcript has removed the need to anchor probes to the 3' end of genes, and opened the door to improved gene-level estimates with probes covering the entire gene, as well as the opportunity for exon level analysis of splice variants.

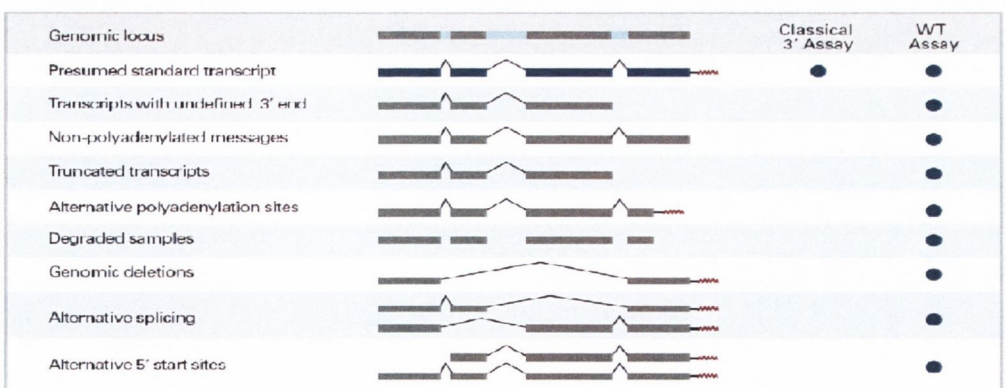


**Figure 2.10: Types of transcripts captured by a whole-transcript assay.** (www.affymetrix.com/index.affx)

### *2.6.1 Affymetrix GeneChip® Gene 1.0 ST array technology*

Both traditional and new generation Affymetrix oligonuceotide arrays are synthesised using a process combining photolithography and combinatorial chemistry (Pease *et al.*, 1994). The arrays are composed of a quartz wafer, which is naturally hydroxylated. A set of photolithographic masks are manufactured that allow the sequential addition of specific nucleotides to particular locations on the chip. When ultraviolet light is shone over the mask in the first step of synthesis the exposed linkers become deprotected and are available for nucleotide coupling. The single type nucleotide solution is then washed over the wafers surface and attaches to the activated linkers. In the next step another mask is placed over the wafer for the next round of deprotection and coupling. The process is sequentially repeated until the probes reach their full length. Figure 2.11 illustrates the process.

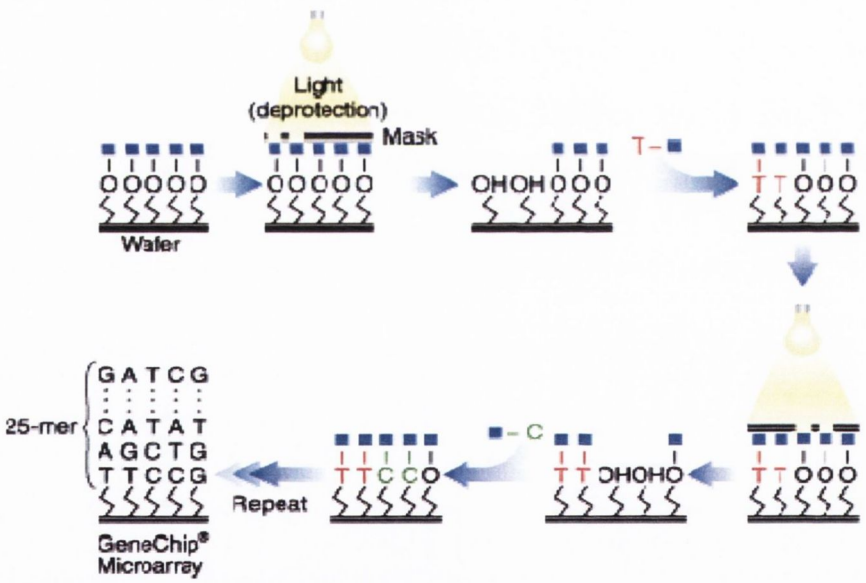


**Figure 2.11: Affymetrix uses a combination of photolithography and combinatorial chemistry to manufacture GeneChip Arrays.** (www.affymetrix.com/index.affx)

The GeneChip® Human Gene 1.0 ST Array interrogates 28,869 well-annotated genes with 764,885 distinct probes. The design of this array was based on the March 2006 human genome sequence assembly (UCSC Hg18, NCBI build 36) with comprehensive coverage of RefSeq, Ensembl and putative complete CDS GenBank transcripts. As of January, 2007, 99.7% of sequences present in RefSeq database are covered by four or more probes on this array.

On the GeneChip® 1.0 ST array individual genes are represented using a series (median of 26) of different 25-mer perfect match (PM) oligonucleotides. The probe sets are designed to be distributed across the transcribed regions of each gene. The Gene 1.0 ST Array System uses a PM-only design with probes that hybridize to sense targets. Background is estimated using a set of approximately 17,000 generic background probes (BGP). This is a collection of probes that were selected based on the fact that they are not present in the human genome and are not expected to cross-hybridize to transcribed human sequences. Background is calculated by subtracting the mean BGP intensity of the BGP probes with the same GC content as the PM probe. For each of the possible 26 bins of varying GC count (from zero G/Cs out of a 25-mer sequence, to all 25 bases being G/Cs), there are approximately 1,000 25-mer probes representing each bin. Standard poly-A controls and hybridization controls are also represented on the arrays to allow convenient troubleshooting along the entire experimental process.

Sample preparation using the Affymetrix WT assay starts with synthesis of double-stranded cDNA is from mRNA by reverse transcription with random oligo d(T) primers engineered to contain a T7 RNA promoter site. The double stranded cDNA is subsequently used as a template by T7 RNA polymerase producing many copies of antisense cRNA. In the second cycle of cDNA synthesis, random primers are used for reverse transcription of the cRNA to produce single stranded DNA in the sense orientation. During this process dUTP is incorporated into the DNA. This single-stranded DNA sample is then treated with a combination of uracil DNA glycosylase (UDG) and apurinic/apyrimidinic endonuclease 1 (APE 1) that specifically recognizes

the unnatural dUTP residues and breaks the DNA strand. DNA is labelled by terminal deoxynucleotidyl transferase (TdT) with the Affymetrix® proprietary DNA Labelling Reagent that is covalently linked to biotin. The fragmented labelled DNA sample is then hybridised onto the GeneChip® Gene 1.0 ST array. Figure 2.12 outlines the procedure involved.

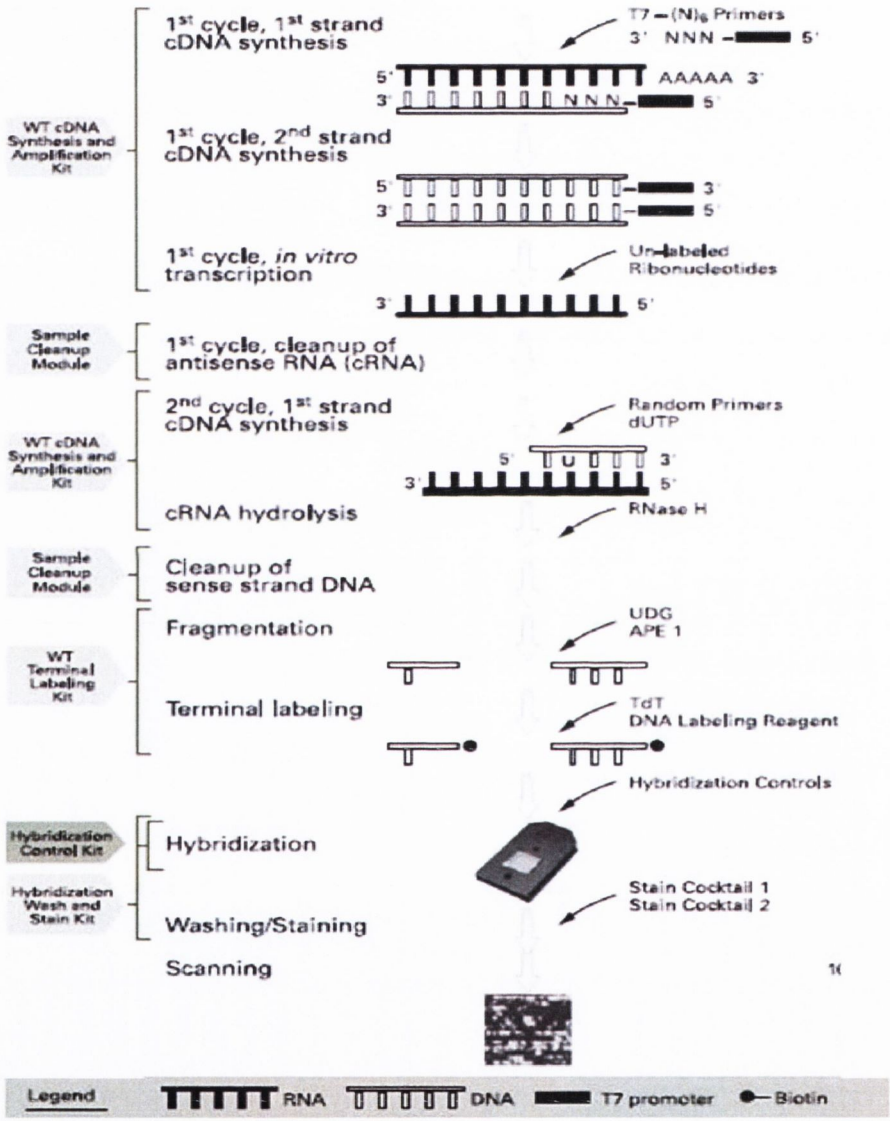


**Figure 2.12: Schematic of the procedure for gene expression analysis using Affymetrix.** (www.affymetrix.com/index.affx)

### *2.6.2 Affymetrix GeneChip® analysis protocol*

All thermal cycle reactions were performed on a 9600 Thermal Cycler (Applied Biosystems, Foster City, CA, USA) with a heated lid unless stated otherwise. Before the commencement of any thermal cycle reactions samples were flick-mixed and spun down.

#### 2.6.2.1 Double stranded cDNA synthesis

Double stranded cDNA was prepared from 200ng of total RNA using the GeneChip® WT cDNA synthesis kit (Affymetrix, Santa Clara, CA, USA). Firstly the Poly-A RNA controls were prepared as per the 1μg protocol in the GeneChip® WT Sense Target Labelling Assay Manual (Affymetrix, Santa Clara, CA, USA). Next the T7-$(N)_6$ primers were prepared by dilution in the diluted Poly-A RNA controls solution to a final concentration of 2.5μg/μl as per protocol.

The T7-$(N)_6$ primers/Poly-A RNA controls mix solution and total RNA were mixed, spun-down and incubated at 70°C for 5mins and cooled on ice for 2mins. For first strand cDNA synthesis the following reagents were added to the total RNA/T7-$(N)_6$ primers/Poly-A RNA controls mix, 1X $1^{st}$ strand buffer, 0.1M DTT, and 10 mM dNTP mix, RNase inhibitor and SuperScript™ II reverse transcriptase. The reaction was performed under the following thermal cycling conditions: 25°C for 10mins, 42 °C for 1hr, 70°C for 10 mins and 4°C for 2 mins.

For second strand cDNA synthesis the following reagents were added to the first stand synthesis reactions, RNase-free water, 17.5mM $MgCl_2$, 10mM dNTP mix, DNA polymerase I and RNase H. The reaction was performed under the following thermal cycling conditions: 16°C for 2hrs without a heated lid and then for at 75°C for 10mins and 4°C for 2mins with a heated lid.

### 2.6.2.2 cRNA synthesis and purification

This procedures required the use of the GeneChip® WT cDNA amplification kit (Affymetrix, Santa Clara, CA, USA). For cRNA synthesis reactions the following reagents were added to the double stranded cDNA synthesis reactions, 1X *in vitro* transcription (IVT) buffer, IVT NTP mix and IVT enzyme mix. The cRNA reaction was performed under the following thermal cycling conditions: 37°C for 16hrs and cooling to 4°C.

The purification procedure required the use of the GeneChip® sample clean up module (Affymetrix, Santa Clara, CA, USA). The protocol was carried out as outlined in the GeneChip® WT Sense Target Labelling Assay Manual. The cRNA was eluted in RNase-free water and the final volume was approximately 13.5µl. The cRNA yield was determined on the NanoDrop ND-1000 spectrophotometer (section 2.4.1), using the RNA setting.

### 2.6.2.3 Single stranded DNA synthesis and purification

Single strand cDNA was synthesised from cRNA using the GeneChip® WT cDNA synthesis kit (Affymetrix, Santa Clara, CA, USA). A cRNA/random primer mix was prepared. 10µg of cRNA was added to random primers (3µg/µl) and RNase-free water, final volume 8µl. The single stranded DNA reaction was performed under the following thermal cycling conditions: 70°C for 5mins, 25°C for 5mins and 4°C for 2mins.

The purification procedure required the use of the GeneChip® sample clean up module (Affymetrix, Santa Clara, CA, USA). The protocol was carried out as outlined in the GeneChip® WT Sense Target Labelling Assay Manual. The single stranded DNA was eluted in RNase-free water and the final volume was approximately 28µl. The single stranded DNA yield was determined on the NanoDrop ND-1000 spectrophotometer (section 2.4.1), using the ssDNA setting.

### 2.6.2.4 Fragmentation and labelling of single stranded DNA

DNA fragmentation and labelling was carried out using the GeneChip® WT Terminal Labelling Kit. For the DNA fragmentation reaction, single stranded DNA (5.5µg) was added to 16.8µL of fragmentation master mix (1X cDNA fragmentation buffer, 10U/µl UDG, 1000U/µl APE 1 and RNase-free water). The fragmentation reaction was performed under the following thermal cycling conditions: 37°C for 1hr, 93°C for 2mins and 4°C for 2mins.

For the labelling reaction, fragmented single stranded DNA (45µl) was added to 15µL of labelling master mix (1X TdT buffer, TdT and 1mM DNA labelling reagnet). The labelling reaction was performed under the following thermal cycling conditions: 37°C for 1hr, 70°C for 10mins and 4°C for 2mins.

### 2.6.2.5 Hybridisation to GeneChip® Gene 1.0 ST arrays

Labelled fragmented single stranded DNA (27µl) was added to 73µl of hybridisation cocktail (1X hybridisation mix, 1 X Eukaryotic hybridisation controls, 3nM control oligonucleotides, DMSO). The cocktail was heated to 99°C for 5mins, 45°C for 5mins and then hybridised to GeneChip® Gene 1.0 ST arrays. 100µl of each specific sample was injected into the array cartridges. Hybridisation was performed at 45°C for 18hrs in a GeneChip® Hybridization Oven 640 (Affymetrix, Santa Clara, CA, USA).

### 2.6.2.6 GeneChip® washing, staining and scanning

After hybridisation, each chip was washed and stained with streptavidin phycoerythrin. This was followed by a second cycle of washes and by signal amplification with biotin labelled anti streptavidin phycoerythrin antibodies. The arrays were then restained with streptavidin phycoerythrin and a final cycle of washes were performed. This entire procedure was carried out using the GeneChip® Fluidics station 450 (Affymetrix, Santa Clara, CA, USA). Fluorescent signals were measured on the arrays using the GeneChip® Scanner 3000 7G (Affymetrix, Santa Clara, CA, USA). Images were analysed using the Expression Console™ software (Affymetrix, Santa Clara, CA, USA).

## 2.7 Western blot analysis

Western blotting is an analytical technique used to detect specific proteins in a given sample of tissue homogenate or cell extract. It uses gel electrophoresis to separate denatured proteins by the length of the polypeptide. The proteins are then transferred to a membrane (typically nitrocellulose or PVDF), where they are detected using antibodies specific to the target protein (Towbin *et al.*, 1979; Renart *et al.*, 1979).

### *2.7.1 Protein extraction using radioimmunoprecipitation buffer*

Directly before use radioimmunoprecipitation (RIPA) buffer was prepared as follows, to 1ml of 10X RIPA buffer (Upstate, Temecula, CA, USA; final concentration 0.05M Tris-HCL, 0.15M NaCl, 0.25% deoxycholic acid, 1.0% NP-40, 1.0 mM EDTA) 100µl of protease inhibitor cocktail (Sigma-Aldrich, St. Louis, MO, USA), 100µl of phospatase inhibitor cocktail (Sigma-Aldrich, St. Louis, MO, USA), 100µl of phenylmethanesulponylfluoride (PMSF) (final concentration 2mM) was added. The solution was made up to 10ml with $H_2O$.

Cells were seeded in a 6 well plate (3ml) and following a defined time period, depending on experimental conditions, medium was removed from the cells. Cells were immediately placed on ice and then washed twice with ice cold PBS (1ml). RIPA buffer was then added to each well. Cells were scraped and placed into pre-chilled eppendorfs which were shaken for 30 min on ice. Samples were spun at 4°C at 10,000rpm for 15mins to collect debris, and supernatants transferred to fresh pre-chilled eppendorfs which were stored at -20°C. Just prior to electrophoresis, samples were mixed with 2X Lammeli buffer (Sigma-Aldrich, St. Louis, MO, USA) to a final concentration of 1X and boiled for 5mins.

### *2.7.2 Protein quantification*

Protein content of BSA standards and cell extracts were measured using the BCA™ Protein Assay Kit (Thermo Fisher Scientific, Rockford, IL, USA). The Thermo Scientific Pierce BCA™ Protein Assay is a detergent-compatible formulation based on bicinchoninic acid (BCA) for the colorimetric detection and quantitation of total protein. The assay involves a two step process: one, the chelation of copper with protein in an alkaline environment, which results in the reduction of copper ($Cu^{2+}$) to cuprous cation ($Cu^{1+}$), and the formation of a light blue complex and two, the chelation of the cuprous cation ($Cu^{1+}$) from step one with BCA producing an intense purple colour. The BCA/copper complex is water-soluble and exhibits a strong linear absorbance at 562 nm with increasing protein concentrations.

#### 2.7.2.1 BCA™ assay protocol

Initial set up involved diluting protein extracts samples 1:5 with $H_2O$ and preparing BSA standards with $H_2O$ as per manufacturer's instructions. An additional sample included was RIPA buffer diluted 1:5 with $H_2O$ which was used as a blank for the protein extracts. The BCA™ working reagent was prepared by mixing 50 parts of BCA™ Reagent A with 1 part BCA™ reagent B. Each of the standards and extracts (10µl) were pipetted into the wells of a 96-well plate in triplicate and mixed with BCA™ working reagent (200µl). The plate was incubated at 37°C for 30mins. The plate was cooled to room temperature prior to absorbance being measured using the Sunrise TECAN microplate reader at 562nm. Protein standards were used to construct a standard curve, which was subsequently used to determine protein concentration of the cell extracts.

### *2.7.3 SDS polyacrylamide gel electrophoresis*

SDS-PAGE was conducted according to the method of Laemmli (Laemmli, 1970), as modified by Studier (Studier, 1973). Protein extract samples (30µg) and appropriate prestained (Lonza Group Ltd, Switzerland) and biotinylated (Bio-Rad, Hercules, CA 94547, USA) protein markers were loaded into separate wells. Gel electrophoresis was performed at a constant current of 120mV. Samples were first run through an upper gel, known as the stacking gel (1.3ml 30 % bisacrylamide mix, 1ml 1M Tris pH 6.8, 80µl of 10% sodium dodecyl sulphate (SDS), 80µl 10 % ammonium persulphate (APS) and 8µl TEMED made up to 8ml with $H_2O$), which condenses the proteins to form a thin, sharply defined bands. Then the samples were resolved by size using 8-12% polyacrylamide gels (required volume of 30% bisacrylamide mix, 2.5ml 1.5M Tris pH 8.8, 100µl of 10% SDS, 100µl 10% APS, 6µl TEMED made up to 10ml with $H_2O$).

### *2.7.4 Transfer of proteins to membrane*

The resolved proteins were transferred to Immobilon™ polyvinylidene diflouride (PVDF) membrane (Millipore, Billerica, MA 01821, USA) using a wet transfer system, with all components soaked beforehand in cold transfer buffer (25mM Tris-HCl pH8.0, 0.2M glycine, 20 % methanol). The gel was placed on a layer of filter paper and sponge overlaid with the membrane. A second piece of filter paper was placed on top followed by a second sponge. The entire assembly was placed in a cassette, the chamber filled with transfer buffer and a constant current of 100mV was applied for 1hr.

### *2.7.5 Antibody blotting*

Prior to antibody blotting, the membranes were blocked in blocking buffer (5 % (w/v) non-fat dried milk in 1 % (v/v) Tris Buffered Saline (TBS)-Tween) for 1hr at room temperature to remove non-specific binding. Primary antibodies were prepared with blocking buffer using a 1:250000 – 1:100 dilution as appropriate. The membranes were either left shaking in the primary antibody for 1hr at room temperature or overnight at 4°C. After the appropriate incubation period the membranes were washed in 1% TBS-Tween for 5 minutes on a rocking platform at room temperature three times. The

secondary antibodies were prepared in blocking buffer using 1:1000 dilutions, to this solution a biotinylated secondary antibody for marker detection was also added. The membranes were left shaking in the secondary antibody solution for 1hr at room temperature. The membranes were then washed in 1% TBS-Tween for 5 minutes on a rocking platform at room temperature three times. Blots were developed by enhanced chemiluminesence (ECL). The membranes were placed in a cassette, SuperSignal West Pico Substrate (ThermoFisher Scientific, Rockford, IL, USA) chemiluminesence reagent was added and the membranes were covered with an acetate. In a darkroom the membranes were exposed to Kodak X-Omat LS Scientific Imaging Film (Sigma-Aldrich, St. Louis, MO, USA) for various time periods and the film was then developed.

## 2.8 Flow cytometry

Flow cytometry is a powerful technique which allows simultaneous multi-parametric analysis of the physical and/or chemical characteristics of individual cells within heterogeneous populations. The flow cytometer performs this analysis by passing thousands of cells per second through a light source (usually a laser beam) and capturing the light that emerges from each cell as it passes through. The data gathered through this process can be analysed statistically by flow cytometry software to report cellular characteristics such as size, complexity and phenotype.

Figure 2.13 shows the primary systems of the flow cytometer. The interrogation point, where the laser beam and the sample intersect, is the heart of the system. A number of detectors are aimed at this point: one in line with the light beam (forward scatter) and several perpendicular to it (side scatter and one or more fluorescent detectors). As a cell passes through the laser it will refract or scatter light, and fluorescent molecules found in or attached to the cell may be excited into emitting light at a longer wavelength than the light source. This combination of scattered and fluorescent light is picked up by the detectors, and by analysing fluctuations in brightness at each detector it is then possible to derive various types of information about the physical and/or chemical structure of each individual cell. In essence flow cytometry instruments generate three types of data:

- **Forward scatter** is the amount of light that is scattered in the forward direction as laser light strikes the cell. The magnitude of forward scatter is roughly proportional to the size of the cell, and this data can be used to quantify that parameter.
- **Side scatter** is the light that is reflected 90 degrees to the laser beam. It is caused by the inner complexity of the cell, e.g. the shape of the nucleus, the amount and type of cytoplasmic granules or the membrane roughness. The side scattered is focused through a lens system and collected by a detector perpendicular to the light path.

- **Fluorescence** is the most common way to study cellular characteristics using flow cytometry. Generally it involves the use of fluorescent molecules such as fluorescently-labelled proteins or organic fluorescent dyes. In these experiments, the fluorescent molecule is added to the cell sample where it binds to a specific molecule on the cell surface or inside the cell. When laser light of the right wavelength strikes the fluorophore, a fluorescent signal is emitted and detected by the flow cytometer. The fluorescent light coming from labelled cells as they pass through the laser travels along the same path as the side scatter signal. As the light travels along this path, it is directed through a series of filters and mirrors, so that particular wavelength ranges are delivered to the appropriate detectors.

Modern flow cytometry instruments usually have multiple lasers and fluorescence detectors. The instrument used in this study was the Cyan™ ADP (Beckman Coulter), which has two laser and nine detectors. Increasing the number of lasers and detectors allows the use of multiple protein markers and therefore a more precise identification of target populations by their phenotypic markers.

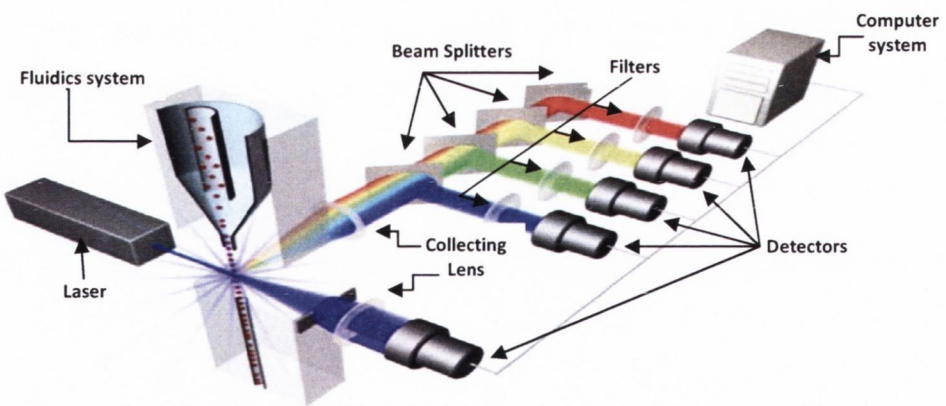


**Figure 2.13: Principle components of flow cytometer.** A flow cytometer has five main components these are: the fluidic system, which presents samples to the interrogation point and takes away the waste; the lasers, which are the light source for scatter and fluorescence; the optics, which gather and direct the light; the detectors, which receive the light; and, the electronics and the peripheral computer system, which convert the signals from the detectors into digital data and perform the necessary analyses. (http://flow.csc.mrc.ac.uk)

### *2.8.1 Apoptosis detection analysis: FITC Annexin V / PI analysis*

Apoptosis is the most common and well defined form of programmed cell death. It is a normal physiologic process which is essential for embryonic development, immune system function and in maintenance of tissue homeostasis (Kerr *et al.*, 1972; Jacobson *et al.*, 1997). The apoptotic program is characterised by a series of biochemical events that lead to a variety of morphological changes, including loss of membrane asymmetry and attachment, cell shrinkage, nuclear fragmentation, chromatin condensation, and chromosomal DNA fragmentation (reviewed in Saraste and Pulkki, 2000). In this study the apoptotic profile of cells was evaluated by flow cytometry analysis using annexin V-FITC and propidium iodide (PI) dual staining.

Loss of plasma membrane asymmetry is one of the earliest features of apoptosis and is accompanied by the translocation of the membrane phospholipid phosphatidylserine (PS) from the inner to the outer surface of the plasma membrane, thereby exposing PS to the external cellular environment (Fadok *et al.*, 1992). Annexin V is a 35-36 kDa calcium dependent phospholipid-binding protein that has a high affinity for PS, and binds to cells with exposed PS. Thus, annexin V-FITC can be used to quantitatively determine the percentage of cells within a population that are actively undergoing apoptosis. Its staining precedes the loss of membrane integrity which accompanies the later stages of cell death resulting from either apoptotic or necrotic processes. Therefore, staining with annexin V-FITC is typically used in conjunction with a vital dye, such as PI to allow the differentiation between late and early apoptotic cells. PI is a standard flow cytometric viability probe and is used to distinguish viable from nonviable cells. Viable cells with intact membranes exclude PI, whereas the membranes of dead and damaged cells are permeable to PI. Cells that stain positive for annexin V-FITC and negative for PI are undergoing apoptosis. Cells that stain positive for both Annexin V-FITC and PI are either in the end stage of apoptosis, are undergoing necrosis, or are already dead. Cells that stain negative for both Annexin V-FITC and PI are alive and not undergoing measurable apoptosis.

### 2.8.1.1 Assay protocol

Cell were seeded in 6-well dishes and incubated as per experimental conditions. After a defined time period all cells (adherent and non-adherent) were collected and pelleted by centrifugation at 1000rpm for 5mins. Cells were then washed twice in ice cold PBS (Lonza Group Ltd, Switzerland). An aliquot of the cells resuspended in PBS was taken and used to determine the cells number in each cell pellet, see section 2.1.1 for cell counting protocol. After the second wash the cells were resuspended in 1X binding buffer (BD Biosciences, San Jose, California, USA) such that there were $1x10^5$cells per 100µl. To 100µl of the cell suspension 5µl of annexin V-FITC (BD Biosciences, San Jose, California, USA) was added, and the cells were incubated in the dark at room temperature for 15mins. Next 5µl of PI (BD Biosciences, San Jose, California, USA) along with 400µl of 1X binding buffer was added. The samples were incubated in the dark on ice for a further 10mins and then analysed by flow cytometry within 1hr.

### 2.8.1.2 Flow cytometry analysis

Flow cytometry analysis was performed on the CyAn™ ADP flow cytometry instrument (Beckman Coulter®) with data acquisition and analysis carried out on the Summit V4.8 software (Beckman Coulter®). One of the important issues with this assay on the flow cytometer is correct instrument setup. Ideally the fluorescence emission profile for individual fluorescent probes would be a very intense, narrow peak well separated from all other emission peaks. In reality, organic dyes and fluorescent proteins have broad emission peaks which can overlap with each other. In this assay the FITC signal from the annexin V-FITC probe overlaps with the PI dye signal and vice versa. Looking at annexin V-FITC stained cells what one would preferably like to see is a population with bright fluorescence in the annexin V-FITC channel only. However, these same cells also emit fluorescence into the PI channel, which results in an apparent upward shift of this population (Figure 2.14 A). This signal occurs because the tail of the annexin V-FITC emission has the right wavelength range to be collected in the PI channel. This incidental collection of annexin V-FITC fluorescence by the PI filter would erroneously increase the magnitude of the PI signal assigned to annexin V-FITC labelled cells if left

uncorrected. Therefore for meaningful data analysis, the emission values must be corrected for the spectral overlap to remove the annexin V-FITC contribution to the PI fluorescence. The same situation exists for PI stained cells, with the tail of the PI emission having the right wavelength range to be collected by the annexin V-FITC channel (Figure 2.14 C). Though, as can be seen from Figure 2.14 C the overlap in emission spectra is significantly less.

To accurately record the fluorescence signal, an adjustment to the emission signal of each fluorescent probe needs to be made. This correction is called compensation. In order to determine the amount of compensation required to correct fluorescence, samples stained which each of the individual fluorescent probes is required. These are known as fluorescent compensation controls. They are run before the experimental samples are analysed to set up the flow cytometer. Focusing again first on the annexin V-FITC labelled population; it is compensated so that the mean fluorescence values in both the annexin positive and negative populations are equal in the PI channel. Practically, this is achieved by bringing the positive population in line with the negative population, such that an imaginary line drawn across the top of the two populations would be level (Figure 2.14 A - B). The same procedure is applied for PI compensation (Figure 2.14 C - D). Subsequently compensation is performed by the computer software for each event by subtracting a percentage of the fluorescence in the annexin V-FITC channel from the fluorescence in the PI channel and vice versa (Figure 2.14 E - F).

The analysis of the apoptotic profile of cells dual stained with annexin V-FITC and PI is achieved by defining and quantifying the different sub-populations of cells. This is achieved by gating subpopulations of cells with common phenotypic signatures as defined by the presence or absence of annexin V and PI, see Figure 2.15.

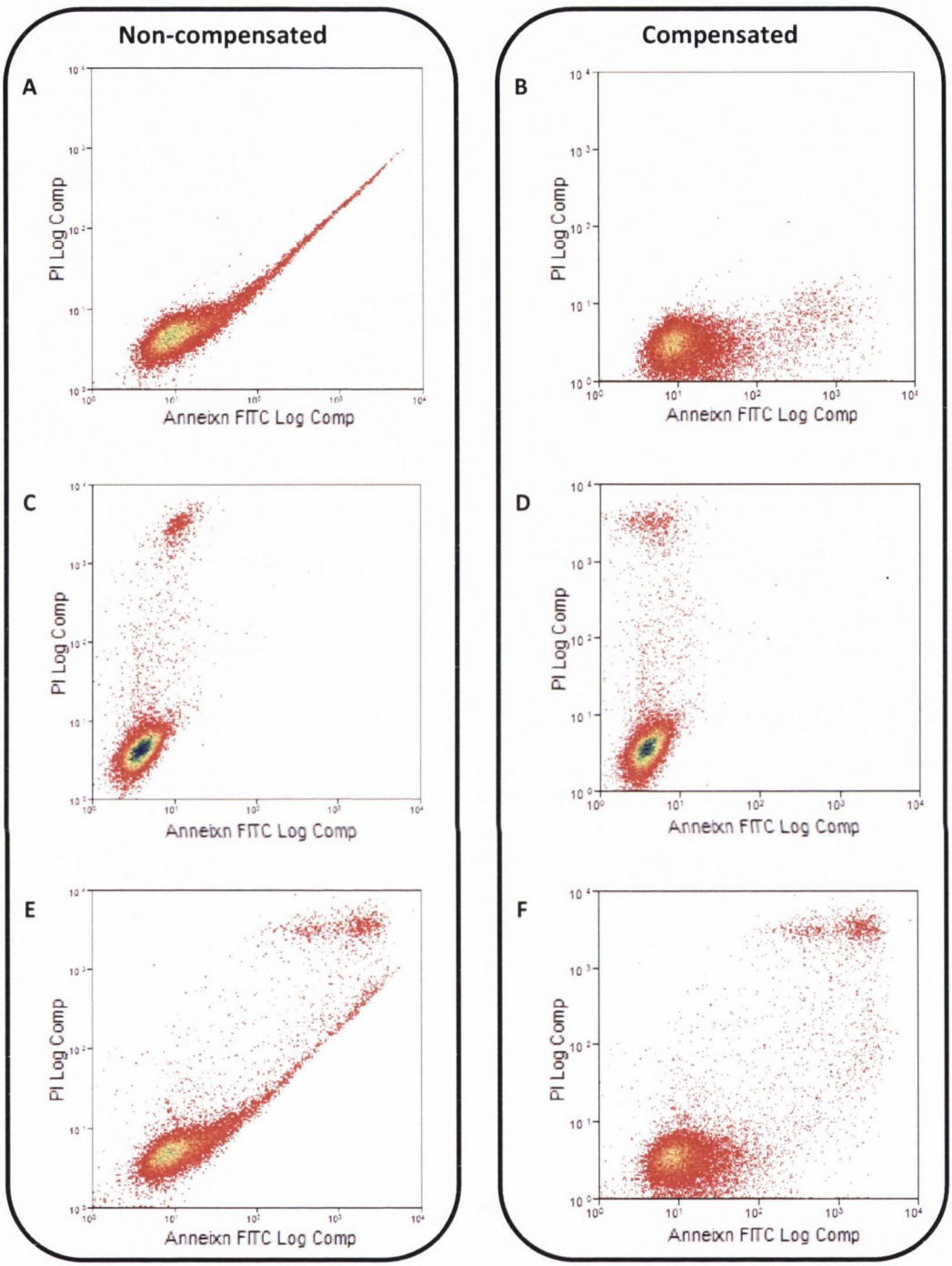


**Figure 2.14: Compensation of fluorescent signal due to annexin V-FITC and PI spectral overlap.** Fluorescent compensation controls are cells stained solely with either annexin V-FITC (A – B) or PI (C – D). They are used to correct the fluorescent signal of the individual emission profiles. Compensation is achieved by bringing the cell population positive for the fluorescent marker in line with the negative population (B and D). Figures E and F represent a sample pre- and post-compensation, respectively, it is easy to appreciate that without compensation the magnitude of the signal attributed to the individual fluorescent markers would be under or over appreciated.

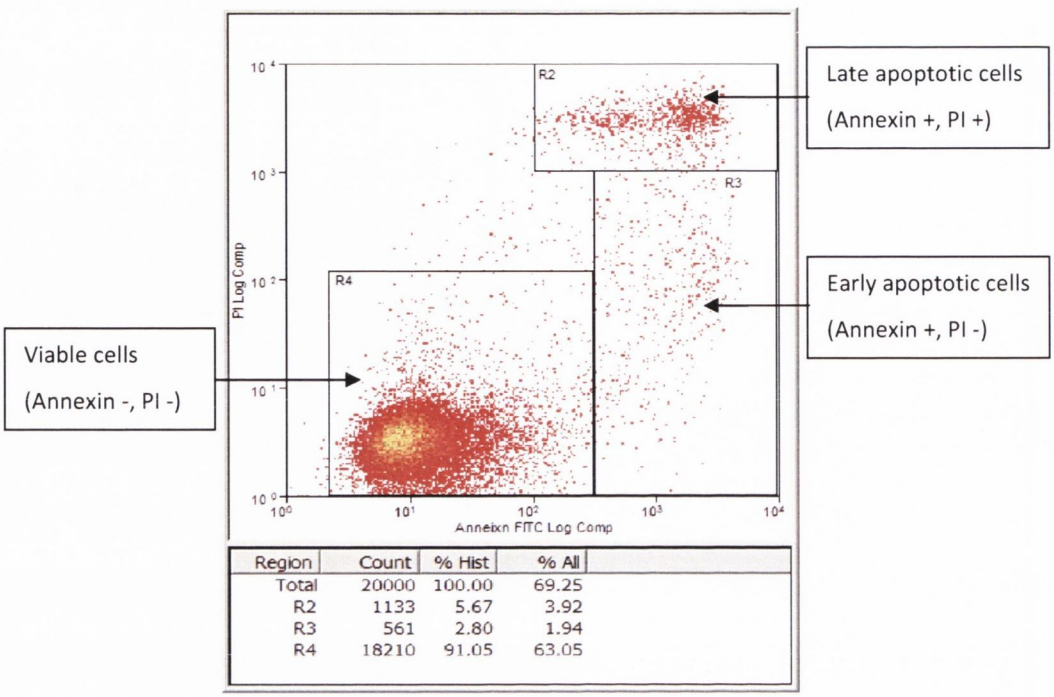


**Figure 2.15: Flow cytometry analysis of cells dual stained with annexin V-FITC and PI.** Cells gated into subpopulations as defined by the presence and/or absence of annexin V-FITC and PI. Annexin V-FITC staining is represented on the X-axis and PI staining along the Y-axis. Three subpopulations can be defined: lower left quadrant annexin and PI negative viable cells (R4), upper right quadrant annexin and PI positive late apoptotic/dead cells (R2) and lower right quadrant annexin positive and PI negative early apoptotic cells (R3). Below the fluorocytogram, the software provides values for the % of cells within each quadrant calculated in reference to the number of cells represented by the fluorocytogram, labelled % Hist.

### *2.8.2 Cell Cycle Analysis: BrdU/PI Analysis*

Flow cytometry may be used to analyse cellular proliferation by determining the stages of the cell cycle within a population of cells. In this study, cell cycle distribution was determined using the BD Pharmigen BrdU Flow Kit (BD Biosciences, San Jose, CA, USA). This kit is based on a two-colour flow cytometric analysis where DNA staining is coupled with anti-bromodeoxyuridine (BrdU) fluorescent antibody staining. BrdU is an analog of the DNA precursor thymidine. The rate of cell division can be monitored by pulsing cells with BrdU. BrdU becomes incorporated into newly synthesised DNA by cells entering and progressing through the S phase of the cell cycle. The cells can then be stained with a monoclonal FITC labelled anti-BrdU antibody and any cell having incorporated BrdU will stain positive. Cells are subsequently stained with a DNA dye, such as PI. PI binds to the DNA in the nucleus of the cell, therefore the intensity of the cell's PI fluorescence is proportional to the amount of DNA in the cell. Because cells contain different amounts of DNA depending on where they are in the cell cycle, it can thus be determined what percentage of cells are in the different parts of the cell cycle based on the intensity of fluorescence of the nuclei. This combination of BrdU and PI permits the characterisation of cells that are actively synthesising DNA (BrdU incorporation) in terms of their cell cycle position (G1, S, or G2/M phases defined by DNA staining intensities).

#### 2.8.2.1 Assay protocol

Cell were seeded in 6-well dishes and incubated as per experimental conditions. After a defined time period 30µl of 1mM BrdU solution (BD Biosciences, San Jose, CA, USA) was added to each well of a 6-well dish. The cells were incubated for a further 2hrs and afterwards all cells (adherent and non-adherent) were collected and pelleted by centrifugation at 1000rpm for 5mins. They were then resuspended in 1ml of staining buffer (BD Biosciences, San Jose, CA, USA). Cell were fixed using paraformaldehyde and stained with anti-BrdU FITC-labelled antibodies as manufacturer's instructions. Subsequently total cellular DNA was stained by resuspending the cells in 300µl of 1X DPBS containing PI and RNase (at final concentrations of 10µg and 100µg respectively).

Cells were then stored over night in the dark at 4°C, prior to analysis by flow cytometry.

### 2.8.2.2 Flow cyto metry analysis

Flow cytometry analysis was performed on the CyAn™ ADP flow cytometry instrument (Beckman Coulter®) with data acquisition and analysis carried out on the Summit V4.8 software (Beckman Coulter®). The final analysis involves defining and quantifying the different sub-populations of cells. This is achieved by gating populations of cells with common phenotypic signatures as defined by the presence or absence of BrdU and the quantity of the PI emission signal, see Figure 2.13.

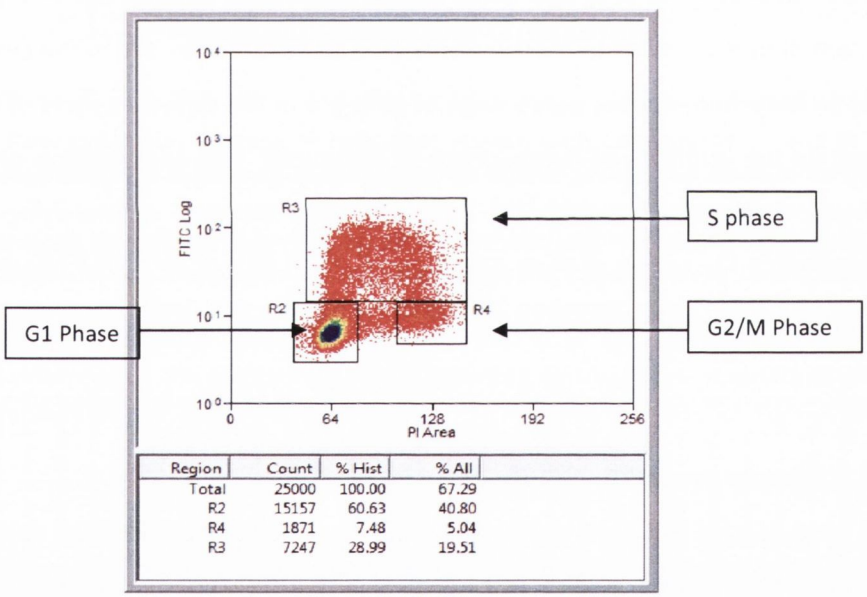


| Region | Count | % Hist | % All |
|---|---|---|---|
| Total | 25000 | 100.00 | 67.29 |
| R2 | 15157 | 60.63 | 40.80 |
| R4 | 1871 | 7.48 | 5.04 |
| R3 | 7247 | 28.99 | 19.51 |

**Figure 2.16: Flow cytometry analysis of cells dual stained with anti-BrdU antibody-FITC and PI.** Cells gated into subpopulations as defined by the presence and/or absence of anti-BrdU antibody-FITC and PI. Anti-BrdU antibody-FITC staining is represented on the Y-axis and PI staining along the X-axis. Three subpopulations can be defined: lower left quadrant BrdU and PI negative G1 phase cells (R2), upper quadrant BrdU and PI positive S phase cells (R3) and lower right quadrant BrdU negative and PI positive G2/M phase cells (R4). Below the fluorocytogram, the software provides values for the % of cells within each quadrant calculated in reference to the number of cells represented by the fluorocytogram, labelled % Hist.

## 2.9 $PGE_2$ immunoassay

Prostaglandins $E_2$ ($PGE_2$) expression level were determined using a $PGE_2$ immunoassay kit (R&D Systems, Minn., USA). $PGE_2$ expression is indicative of cyclooxygenases (COX) activity. When arachidonic acid is liberated from membrane phospholipids by the action of phospholipases, it is metabolised into $PGG_2$ and $PGH_2$ by the COX-1 and COX-2 enzymes, and subsequently converted into $PGE_2$ by prostaglandin E synthetase (Helliwell *et al.*, 2004; Ivanov and Romanovsky, 2004; Murakami and Kudo, 2004). Thus there is a correlation between $PGE_2$ expression levels and COX activity.

R&D Systems $PGE_2$ Immunoassay is performed in a 96-well plate, which comes pre-coated with goat anti-mouse antibody. It is based on the competitive binding technique in which $PGE_2$ present in a sample competes with a fixed amount of horseradish peroxidise-labelled $PGE_2$ for sites on a mouse monoclonal antibody. During the incubation, the mouse monoclonal antibody becomes bound to the goat anti-mouse antibody coated onto the 96-well plate. Following a wash to remove excess conjugate and unbound sample, a substrate solution is added to the wells to determine the bound enzyme activity. The colour development is stopped, and the absorbance is read at 450 nm. The intensity of the colour is inversely proportional to the concentration of $PGE_2$ in the sample.

### *2.9.1 Assay protocol*

Cells were seeded in 6-well dishes and incubated as per experimental conditions. After a defined time period cell culture supernatants were collected. $PGE_2$ quantification in these samples was determined as per the manufacture's high sensitivity protocol. Absorbance readings were made on the Sunrise microplate reader at 450nm (Tecan Trading AG, Switzerland). $PGE_2$ standards were used to construct a standard curve, which was subsequently used to determine $PGE_2$ concentration (pg/ml) in the cell supernatants.

## 2.10 Analysis of *in vitro* cell growth

During this study, cell viability was evaluated using the standard MTT assay. The MTT assay is a simple non-radioactive colorimetric assay used to measure cell cytotoxicity, proliferation or viability. It was first described by Mosmann *et al.* in 1983 and has been improved upon since but the principle remains the same. The principle is that only viable/metabolically active cells have the ability to cleave the tetrazolium rings of the the yellow water soluble tetrazolium salt, MTT, forming a purple formazon crystal. Solubilisation of the cells by the addition of a detergent results in the liberation of the crystals, which go into solution. The colour can be quantified by reading the plate on a multi-well scanning spectrophotometer and the absorbance is directly proportional to the number of viable/metabolically activated cells in the sample.

### *2.10.1 Assay protocol*

Cells were seeded in triplicate into 96 well plates and incubated as per experimental conditions. After a defined time period 10 µl of 5mg/ml MTT reagent (Roche diagnostics) was added to each well and the plate was incubated for a further 4hrs at 37°C. Next a 100 µl of the solubilisation buffer (Roche diagnostics) was added to each well and incubated overnight at 37°C. Absorbance at 595nm with a reference wavelength of 690nm was measured on a Sunrise microplate reader (Tecan Trading AG, Switzerland).

## 2.11 References

Berry, Elicia B E, Timothy A Sato, Murray D Mitchell, R Stewart Gilmour, and Rachel J A Helliwell. 2004. Differential effects of serum constituents on apoptosis induced by the cyclopentenone prostaglandin 15-deoxy-delta12,14-prostaglandin J2 in WISH epithelial cells. *Prostaglandins, Leukotrienes, and Essential Fatty Acids* 71, no. 3 (September): 191-197.

Fadok, V A, D R Voelker, P A Campbell, J J Cohen, D L Bratton, and P M Henson. 1992. Exposure of phosphatidylserine on the surface of apoptotic lymphocytes triggers specific recognition and removal by macrophages. *Journal of Immunology (Baltimore, Md.: 1950)* 148, no. 7 (April 1): 2207-2216.

Glantz,S. 1996. Primer of Bio-Statistics. *McGraw Hill* 4th Edition.

Ivanov, Andrei I, and Andrej A Romanovsky. 2004. Prostaglandin E2 as a mediator of fever: synthesis and catabolism. *Frontiers in Bioscience: A Journal and Virtual Library* 9 (May 1): 1977-1993.

Jacobson, M D, M Weil, and M C Raff. 1997. Programmed cell death in animal development. *Cell* 88, no. 3 (February 7): 347-354.

Kerr, J F, A H Wyllie, and A R Currie. 1972. Apoptosis: a basic biological phenomenon with wide-ranging implications in tissue kinetics. *British Journal of Cancer* 26, no. 4 (August): 239-257.

Laemmli, U K, E Mölbert, M Showe, and E Kellenberger. 1970. Form-determining function of the genes required for the assembly of the head of bacteriophage T4. *Journal of Molecular Biology* 49, no. 1 (April 14): 99-113.

Livak, K J, S J Flood, J Marmaro, W Giusti, and K Deetz. 1995. Oligonucleotides with fluorescent dyes at opposite ends provide a quenched probe system useful for detecting PCR product and nucleic acid hybridization. *PCR Methods and Applications* 4, no. 6 (June): 357-362.

Livak, K J, and T D Schmittgen. 2001. Analysis of relative gene expression data using real-time quantitative PCR and the 2(-Delta Delta C(T)) Method. *Methods (San Diego, Calif.)* 25, no. 4 (December): 402-408.

Mosmann, T. 1983. Rapid colorimetric assay for cellular growth and survival: application to proliferation and cytotoxicity assays. *Journal of Immunological Methods* 65, no. 1-2 (December 16): 55-63.

Mountgomery, DC. 2006. Design and Analysis of Experiments. *Wiley and Sons* 5th Edition.

Murakami, Makoto, and Ichiro Kudo. 2004. Secretory phospholipase A2. *Biological & Pharmaceutical Bulletin* 27, no. 8 (August): 1158-1164.

Renart, J, J Reiser, and G R Stark. 1979. Transfer of proteins from gels to diazobenzyloxymethyl-paper and detection with antisera: a method for studying antibody specificity and antigen structure. *Proceedings of the National Academy of Sciences of the United States of America* 76, no. 7 (July): 3116-3120.

Saraste, A, and K Pulkki. 2000. Morphologic and biochemical hallmarks of apoptosis. *Cardiovascular Research* 45, no. 3 (February): 528-537.

Studier, F W. 1973. Analysis of bacteriophage T7 early RNAs and proteins on slab gels. *Journal of Molecular Biology* 79, no. 2 (September 15): 237-248.

Towbin, H, T Staehelin, and J Gordon. 1979. Electrophoretic transfer of proteins from polyacrylamide gels to nitrocellulose sheets: procedure and some applications. *Proceedings of the National Academy of Sciences of the United States of America* 76, no. 9 (September): 4350-4354.

# Chapter Three

# Silencing of HPV16 oncogenes

## 3.1 Introduction

Human papillomavirus (HPV) infection is the single most important etiological agent in the pathogenesis of cervical cancer (Kirwan and Herrington, 2001). A small subgroup of HPV types have been designated as high risk in cervical cancers, being associated with more than 99% of cervical carcinomas (Bosch and Sanjose, 2002; Walboomers *et al.*, 1999). Among these HPV types, HPV16 and HPV18 are the most frequently detected in clinical cervical carcinomas (Clifford *et al.*, 2003; Munoz *et al.*, 2003; Walboomers *et al.*, 1999). The oncogenic potential of these viruses is dependent on two of their early proteins, E6 and E7 (Snijders *et al.*, 2006). The overexpression of these oncoproteins, predominantly a consequence of integration of the HPV DNA in the host genome (Pett and Coleman 2007), allows for progression towards malignancy (zur Hausen and deVillers, 1994). During the malignant transformation process, these oncoproteins work in a cooperative manner, with E7 driving cell proliferation and E6 counteracting the apoptotic response to the abnormal growth stimuli induced by E7. The protein products of E6 and E7 mediate these activities thorough protein-protein interactions and one of their primary sites of action is on critical cell cycle pathways including those governed by tumour suppressor proteins, p53 and Rb (Dyson *et al.*, 1992; Scheffner *et al.*, 1990; Werness *et al.*, 1990). This results in the dysregulation of the cell cycle in the infected cells and in combination with additional activities, such as the induction genomic instability (White *et al.*, 1994), it is believed these oncoproteins aid the accumulation of genetic alterations, which ultimately leads to a malignant phenotype. A more extensive discussion on the current state of knowledge of the oncogenic attributes of HPV E6 and E7 can be found in Chapter 1.

In light of the central role HPV E6 and E7 play in cervical carcinogenesis, several different techniques have been employed to specifically target these genes both in an attempt to further dissect the downstream regulatory pathways that are affected by their actions and as a means to develop novel therapeutics. Studies using antisense oligonucleotides and ribozymes established the utility of such approaches by demonstrating effective reduction in the expression of these oncogenes (Chen *et al.*,

1996; Guapillo *et al.*, 2006; Venturini et la., 1999). Additionally, they demonstrated that decreased expression inhibited proliferation of cervical cancer cells, however, their effectiveness has been limited due to unacceptable side effects. Since the discovery of RNAi, there has been a shift in molecular research away from employing traditional antisense oligonucleotides and ribozymes to this new technology base. This is due to two factors; the higher efficiency of siRNAs compared to traditional approaches (Bertrand *et al.*, 2002; Grunweller *et al.*, 2003; Miyagishi *et al.*, 2003) and the relative ease of RNAi mediated knockdown of target gene expression compared to knockout by homologous recombination.

RNAi is a naturally occurring phenomenon of RNA mediated post-transcriptional gene silencing that is highly conserved among multicellular organisms (Cerrutti 2003; Denli and Hannon 2003; Dykxhoorn *et al.*, 2003). During RNAi, long transcripts of dsRNA are rapidly processed into siRNA by the enzyme Dicer (Bernstein *et al.*, 2001). Once processed by Dicer, one of the strands in the small RNA duplex is incorporated into RISC and binds to the target mRNA by complementary base pairing, which subsequently suppresses gene expression either by cleavage or by translational repression (Elbashir *et al.*, 2001; Martinez *et al.*, 2002). In mammalian systems, it is possible to initiate the endogenous RNAi gene regulatory machinery by introducing chemical synthesised siRNA, composed of 19 base pairs, a two base 3' overhang and 5' phosphate group (Elbashir *et al.*, 2001). This process is comprehensively discussed in Chapter 1.

Since gene silencing performed by RNAi is mediated through the introduction of artificially synthesized small RNAs into cells, a crucial part of any knockdown study is the design of highly efficient siRNA. Initial expectations were that there was no need to select for optimal siRNA target sequences (Stein, 2001) but this view soon became redundant as extreme variations in silencing efficiency were observed for different siRNAs directed against the same target RNA (Holen *et al.*, 2002). It became clear that

both factors intrinsic to the siRNA and properties of the targeted mRNA were critical to the design of potent siRNA and hence the success of RNAi approaches.

An early set of criteria for siRNA sequence selection was described in 2002 by Elbashir *et al.* They recommended that siRNA should be designed towards a coding region, be at least 50 nucleotides downstream of the start codon, that the GC content should be approximately 50% and a sequence motif AA-$N_{19}$-TT was suggested to be advantageous. These early guidelines were employed with a considerable degree of success. However, the rapid increase in the use of this technology and the extension to therapeutic avenues meant there was a rising demand for parameters that significantly increased the probability of identifying potent siRNA. The initial breakthrough came with the identification of the first intrinsic property of siRNA; described by two independent studies in the same issue of Cell in 2003 (Khvorova *et al.*, 2003; Schwarz *et al.*, 2003). These studies demonstrated that for synthetic siRNA and the naturally occurring miRNAs, there was a strand bias in the duplexes such that one strand, the antisense strand, was preferentially incorporated into the RISC complex over the other, the sense strand (Khvorova *et al.*, 2003; Schwarz *et al.*, 2003). Analysis of effective siRNA and known miRNA sequences revealed that the 5'end of the antisense strand was of lower stability compared to the 5' end of the sense strand (Khvorova *et al.*, 2003; Schwarz *et al.*, 2003). This lead to the hypothesis that relative stability at the 5' terminal biased the steps involved in duplex unwinding and strand retention by RISC, which implies that the design of active siRNA required the antisense strand to be of lower thermodynamic stability at the 5' end than the sense. Indeed it was demonstrated that non-functional duplexes had a higher relative thermodynamic stability at the 5' end of the antisense strand than functional duplexes (Khvorova *et al.*, 2003).

Subsequent studies analysing the sequence of active and non-functional siRNA have both further validated this design feature and refined upon it, by identifying base preferences at certain positions of the siRNA duplex (Amarzguioui and Prydz, 2004; Hsieh *et al.*, 2004; Jagla *et al.*, 2005; Reynolds *et al.*, 2004; Shabalina *et al.*, 2006; Ui-Tel

*et al.*, 2004). Initial studies of this type were performed by Ui-Tel *et al.* and Reynolds *et al.*, who individually set out criteria they believed governed siRNA sequence preference and would hence result in the production of potent siRNA (Table 3.1). There was a high degree of overlap between the two sets of parameters and indeed additional independent studies analysing the activities of siRNAs against different mRNAs have confirmed the basic outcome of these two studies (Amarzguioui and Prydz, 2004; Jagla *et al.*, 2005; Hsieh *et al.*, 2004; Shabalina *et al.*, 2006). Predictably, there has been some divergence of opinion, with some questioning base preferences at certain positions and others adding to the list. On the whole, however, the conditions described by these studies suggest the need for the presence of higher A/U content at the 5' end and higher G/C content at the 3' end of the antisense strand, thus verifying the relative thermodynamic stability of the siRNA termini as a major determinant of the functionality of siRNAs.

**Table 3.1 Suggested parameters for optimal design of siRNA by Ui-Tei *et al.* & *Reynolds et al.***

| Ui-Tei *et al.*, 2004 | Renolds *et al.*, 2004 |
|---|---|
| $10^{th}$ and $19^{th}$ bases of SS should be A or U | GC content of the SS should be 30-50% |
| The 5' end (7 bases) of AS should be AU rich | Stable hairpin-like 2° structures should be avoided |
| The $1^{st}$ bases if SS Should be G/C | The melting temperature should be less than 20°C |
| The SS should have more than 3 A/U bases between the $13^{th}$ and $19^{th}$ bases | The presence of more than 3 A/U bases between the $15^{th}$ and $19^{th}$ bases |
| Absence of GC stretch of more than 9 nt in length | The $3^{rd}$ and $19^{th}$ base of SS should be A |
| | The $10^{th}$ bases of SS should be U |
| | The $13^{th}$ base of SS should not be G |
| | The $19^{th}$ base of SS should be G/C |

Although the design criteria based on thermodynamic stability undoubtedly increases the success rate in generating potent siRNA, they do not guarantee functionality. Therefore, other features must be considered to ensure efficiency of RNAi. Current parameters known to influence the efficiency of siRNA mediate gene silencing is RNA

secondary structures (Patzel *et al.*, 2005). As far as siRNAs themselves are concerned, intramolecular secondary structures, such as hairpins, and intermolecular interactions, such as stable duplex formation, should be avoided. As these duplexes have a higher stability and thus can hamper the dissociation and binding of siRNAs to their respective targets (Figure 3.1). Unsurprisingly, the structure of the siRNA antisense strand is particularly crucial for efficiency (Patzel *et al.*, 2005). It has been demonstrated that there is an inverse correlation between the degree of antisense siRNA secondary structure and the strength of gene silencing, where the degree is determined by the availability of terminal nucleotides within the antisense siRNA structures (Patzel *et al.*, 2005). In addition, the local structure of the targeted RNA is also important because this determines accessibility to the siRNAs (Figure 3.1). A very rigid secondary structure might render the siRNA-binding region inaccessible, thus preventing efficient silencing. A clear example of where such an issue arose was with RNA viruses. Many researchers failed to identify efficient siRNAs against the 5' untranslated region of plus-stranded RNA viruses. However this is a highly structured region and when the less tightly arranged coding region of the viruses were targeted, successful silencing was achieved (Phipps *et al.*, 2004; Schubert *et al.*, 2005; Werk *et al.*, 2005; Wilson *et al.*, 2003; Yuan *et al.*, 2005). Many algorithms used to design siRNA today not only include thermodynamic stability criteria, but also these secondary structure features. It is however clear, that all of these features still do not provide an exhaustive description of the determinants of siRNA potency. We can therefore expect additional factors to be identified that contribute to the activity of siRNAs.

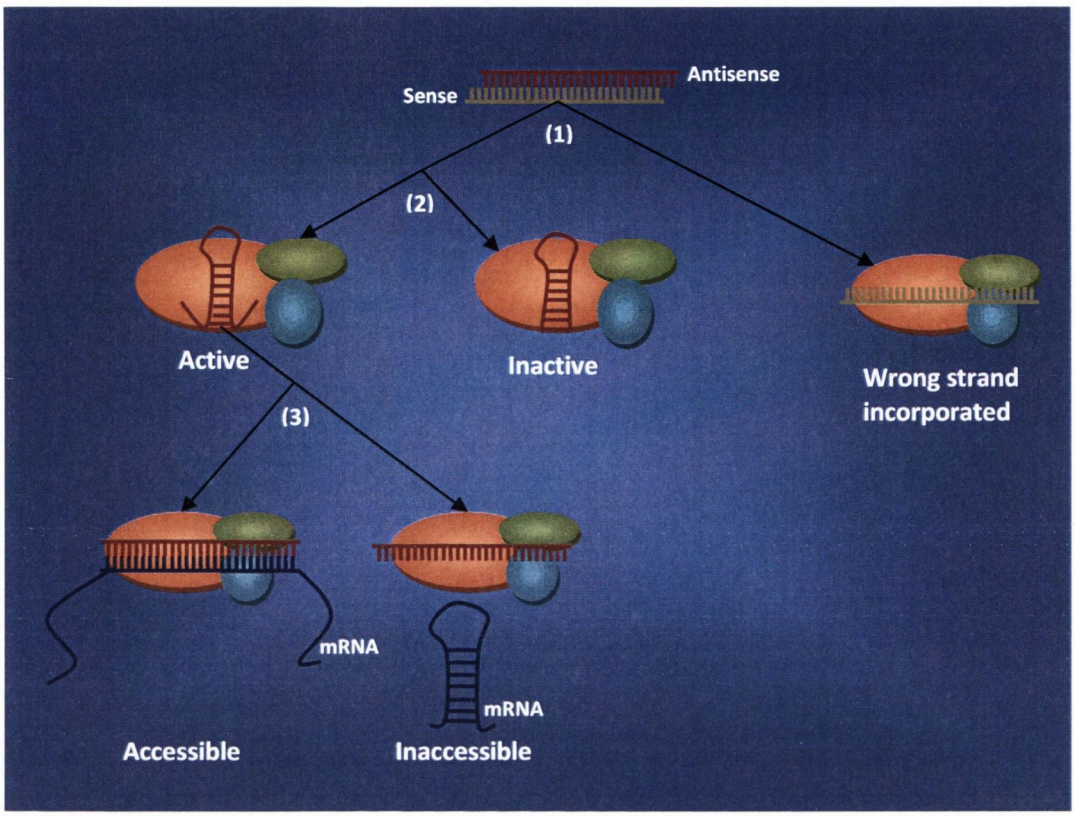


**Figure 3.1: Influence of siRNA and target mRNA structure on RNAi efficiency.** Efficiency of an siRNA is thus far known to be determined at three points of the RNAi pathway. (1) A strand bias exists that is defined by the intrinsic thermodynamic properties of the siRNA duplex. (2) siRNA guide strands with base-paired termini are found to be inactive, whereas guide RNAs with freely accessible ends (mainly 3'ends) are highly efficient. (3) A highly ordered target mRNA structure may have a detrimental influence on the hybridisation of the siRNA/RISC to its target site and may therefore reduce the efficiency of the silencing process.

Although siRNA are designed to be sequence specific and while it was originally assumed that siRNA were highly sequence specific, in recent years it has become clear that siRNA can have unintended effects, which are commonly known as off-target effects (Bagga *et al.*, 2005; Doench *et al.*, 2003; Saxena *et al.*, 2003). These off-target effects can be mediated in one of two manners, by the binding of siRNA with unintended target genes, hence suppressing their expression or by activation of the innate immune response by type I interferon and inflammatory cytokines. It is important to acknowledge that these effects are not solely due to the antisense strand but that if the sense strand is mistakenly incorporated into RISC, it too can cause its own set of off-target effects through the mechanisms just described (Jackson *et al.*, 2003).

While it is possible to achieve single base pair discrimination with selective siRNA, single or double base pair mismatches are often tolerated and can still lead to a significant reduction in gene expression levels (Birmingham *et al.*,2006; Dahlgren *et al.*, 2008; Du *et al.*, 2005; Schwarz *et al.*, 2006). Homology screening of candidate siRNA is an essential component of any design protocol as it allows for the elimination of regions of homology. However, even the most extensive screening program does not guarantee siRNA of high specificity, with on occasion changes in expression levels of unrelated genes still observed. There are different schools of thought regarding the factors responsible for these off-target silencing events. Some reports suggest that the reason behind these events is the unintended participation of the siRNA in the miRNA pathway, occurring due to strand complementarity over the seed sequence (nucleotides 2 to 8 from the antisense strand 5' end) to mRNA 3' untranslated regions (Birmingham *et al.*, 2006; Jackson *et al.*, 2006). Others have reported that it is due to overall homology between the siRNAs and targets, with Jackson *et al.* demonstrating as few as 11 nucleotides homology can result in off target silencing (Jackson *et al.*, 2003). Alternatively, it can be due to the assembly of RISC with the sense strand.

In mammals, the innate immune system provides the body's first line of defence and is capable of discriminating between self and non-self, or foreign, nucleic acids. There are two different types of receptors present in cells that recognise foreign DNA and RNA motifs, those in the endosomes and those within the cytoplasm (Marques and Williams, 2005; Schlee *et al.*, 2006). Toll like receptors (TLR) 3, 7 and 8 are located predominately in endosomes compartments. All three are activated by dsRNA and produce proinflammatory cytokines upon activation. The manner of delivery of synthetic siRNA is particularly important in relation to these TLRs, as lipid based delivery systems exposes the endosomal compartment and are known to increase the risk of triggering an immune response (Sioud, 2005; Sioud and Sorensen, 2003). Triggering of TLR 7 and 8 signalling can also be induced in a sequence dependent manner, and certain immunostimulatory RNA sequences have been described like 5'-UGUGU-3' or a 9 nucleotide motif, 5'-GUCCUUCAA-3' (Judge *et al.*, 2005; Heil *et al.*, 2004; Hornung *et al.*, 2005). Unfortunately, avoiding these sequences does not prevent immune activation as many other sequences, which do not have any GU bases, have also been observed to induce a response. In addition, cytoplasmic RNA receptors such as PKR, OAS and RIG-1 may be important in a siRNA mediated innate immune response. However, it would appear that these receptors maximally respond to longer RNA duplexes (greater than 30 base pairs) and therefore, it is only a rare incident that siRNA induce a response through these receptors (Marques *et al.*, 2006).

The use of chemically modified siRNA has shown promise as a mechanism to overcome the unwanted effects of siRNA (Jackson *et al.*, 2006). It has been demonstrated that modifications of the 2'-position of the ribose can improve nuclease resistance of the RNA duplex and at the same time lower the incidence of off-target events. Commonly reported chemical modifications include 2'-O-methyl (2'-O-Me), 2'-fluoro (2'-F) and locked nucleic acid (LNA). For example the 5'-phosphate group is essential for the siRNA strand to act as a guide strand. So, modification of the 5'-phosphate group of the sense strand to a 5'-O-Me group, can effectively avoid sense strand RISC formation (Chen *et al.*, 2008). In avoiding sense strand and promoting antisense strand incorporation into the RISC complex, off-target effects can be reduced. Modifications

of the antisense strand of the siRNA duplex have also been demonstrated to be helpful. A study by Jackson *et al.* in 2006 demonstrated that the use of two 2'-O-Me nucleotides at the 5' end of the antisense strand reduced miRNA-type off-target effects, without compromising silencing of the intended targets. These modifications have also been used effectively to reduce immune associated off-target effects. For example, the end of the sense strand of a siRNA containing an immunostimulatory motif was modified with a LNA residue; this abrogated the IFNα immunostimulatory activity of the duplex without affecting the silencing activity (Hornung *et al.*, 2005).

In experimental situations to ensure that the effect observed is specific to the targeted gene and not due to off-target effects, the use of multiple controls is recommended (Cullen, 2006; nature editorial, 2003). Essential controls are mock-transfected and negative siRNA controls. A mock-transfected control is where the system is treated with the transfection agent solely, while a negative control is where a siRNA known to have no homology to any gene within the system is transfected. The output from both these controls should be identical to their untreated counterparts. An additional control is the multiplicity control which involves the application of at least two different siRNA targeting different regions of the same gene. The end result from these independent siRNA should be identical therefore indicating the effect seen is due to specific reduction in the target gene expression and not an off-target effect. A supplementary control, generally used when doubts exist over the specificity of the observed response, is a rescue control. This is where the targeted gene is reintroduced into the system in a form that is functionally active but which is not targeted by the siRNA. If the observed result is due to siRNA specific reduction of the intended target then the effect should be reversed by the introduced gene (e.g. Kittler *et al.*, 2005 and Wu *et al.*, 2006). Another important consideration is that overexpression of siRNAs can lead to saturation of the RNAi pathway, which in turn can result in the deregulation of vital pathways dependent on the endogenous RNAi machinery (Grimm *et al.*, 2006). Therefore, it is recommended that the smallest concentration to elicit the maximum response is used.

Even though we still have much to learn about the mechanism, biogenesis and requirements for efficiency, RNAi mediated gene silencing has become an essential tool in present day molecular research. In gene functional studies, it is providing the research tools for target validation and genome-wide screens for assessing gene function. Functional genetic approaches can provide insights into assigning function to cancer genes and delineate molecular pathways by which these genes act in normal as compared to malignant cells. There has also been an enormous amount of research into therapeutic applications of RNAi, which has already resulted in several siRNA candidate pharmaceutical agents reaching clinical trials. The idea of treating cervical cancer in such a manner is highly enticing, not only because the overexpression of the HPV E6 and E7 oncogenes results in the development of cancer, which makes them ideal targets, but in addition these genes are not present in normal cells. Therefore RNAi based therapies would not affect them. A number of groups have shown that the viral oncogenes can be targeted by RNAi, resulting in slowed growth (Yoshinouchi *et al.*, 2003), apoptosis (Butz *et al.*, 2003; Jiang and Milner, 2002) or senescence (Hall and Alexander, 2003) of the target cell. However, of particular concern are recent reports demonstrating that the success of siRNA-based therapy in some clinical cases was due to the induction of an immune response by the siRNAs and not due to their RNAi-dependent activity (Kleinman *et al.*, 2008; Robbins *et al.*, 2008). This emphasises the importance of the inclusion of proper controls, such as those described above, in the design of RNAi based studies. Through the use of appropriate controls it should be possible to identify highly active siRNA which induce minimal off-target effects. For the purposes of any application of RNAi technology, whether it is gene functional studies or therapeutics, this must be seen as essential.

## 3.2 Chapter Aim

The aim of this chapter was to develop a protocol for the simultaneous suppression of HPV E6 and E7 oncogenes in an *in vitro* cervical cancer cell line model. This was facilitated by using the post transcriptional silencing method RNAi and in particular siRNA specifically targeting the E7 coding region of the E6/E7 bicistonic mRNA. Therefore, a major emphasis of the work in this chapter was the design and validation of highly effective siRNA towards the E6/E7 mRNA transcript. It is intended that the developed system would become the foundation of future research within the laboratory. Such assessment of the novel functions of the E6 and E7 proteins and how these activities contribute to the oncogenic process, will greatly increase our understanding of cervical carcinogenesis.

## 3.3 Materials and Methods

### *3.3.1 Cell culture*

The HPV18 positive HeLa and the HPV16 positive SiHa cervical cancer cell lines were used in this chapter (see section 2.1 for a detailed description). All cell lines were grown in at 37°C in a humidified 5% $CO_2$ atmosphere and cultured as described in section 2.1.1.

### *3.3.2 siRNA design*

Today, there are many companies providing predesigned and validated siRNA, such as Ambion, Dharmacon and Sigma-Aldrich. However, these siRNA primarily target human, mouse and rat genomes and since this study looked to silence viral genes custom design of siRNA was required. As described in section 3.1, several parameters have been highlighted to contribute to the efficacy of siRNAs to induce RNAi and these criteria have become the basis of many online design tools. However, the perfect algorithm for siRNA design has not yet been developed. The complexity of predicting the various criteria affecting siRNA function has meant that we are still unaware of many of these criteria. Therefore, a sensible approach is to follow the siRNA design guidelines defined in various pieces of software and literature, in an effort to include the maximum possible crucial parameters for improving the efficiency of siRNA. However the real efficiency of siRNA can only be validated experimentally.

#### 3.3.2.1 Design of HPV16 E7 targeting siRNA

HPV16 expresses E6 and E7 proteins from a single polycistronic mRNA (Stacey *et al.*, 1995; Stacey *et al.*, 2000). In this study, it was decided to design siRNA towards the HPV16 E7 coding region and theoretically, such a siRNA should inhibit the expression of both E6 and E7 simultaneously. In total five siRNA were designed towards the coding region of HPV16 E7 and two independent approaches were taken in the design the process; one set of three siRNA were in-house designed, and the second set of two siRNA were designed by Ambion.

Prior to initiating either design protocol, sequence divergence among HPV16 variants within the E7 coding region was determined. This was achieved by use of the National Centre for Biotechnology Information (NCBI) online sequence alignment search tool BLAST (http://www.ncbi.nlm.nih.gov/blast/). There are several different BLAST programmes and the one utilised throughout this study was BLASTN. This tool searches a nucleotide database based on a nucleotide query sequence. The nucleotide database in question is the GenBank sequence database, which is an annotated collection of all publicly available nucleotide sequences and their protein translations. This database is produced at NCBI as part of an international collaboration with the European Molecular Biology Laboratory (EMBL) Data Library from the European Bioinformatics Institute (EBI) and the DNA Data Bank of Japan (DDBJ). The initial query sequence input into this tool was the HPV16 complete genomic sequence between nucleotides 562 and 585 (Genbank accession number K02718.1), which represents the coding region of HPV16 E7. From the output list of this search, both HPV16 variants with identical and divergent sequences were identified and these sequences were extrapolated. In turn each of these variants was used to identify any additional variants through BLASTN. In total, 132 different variants were identified and of these 32 were determined to represent the entire divergence among the 132 over the E6 coding region. These 32 sequences were aligned using the online tool ClustalW (www.ebi.ac.uk/Tools/clustalw). Based on this alignment conserved and divergent regions were identified (Figure 3.2). The aim of this work was to determine regions of homology within the HPV16 E7 coding sequence such that the siRNA would be designed towards these regions. This would ensure that any HPV16 variant would be targeted by these siRNAs.

**Figure 3.2: Representation of the sequence alignment of HPV16 variants.** This figure represents part of the HPV16 E7 coding region of several different variants. The sequences were aligned and regions of homology and divergence among the HPV16 variants were identified using the online tool ClusatlW (www.ebi.ac.uk/Tools/clustalw). Sequence homology is indicated by * under the nucleotide, while points of divergence are highlighted in blue.

### 3.3.2.2 In-house designed HPV16 E7 siRNA

The in-house design process involved the use of four different design tools (Table 3.2), along with literature defined criteria (Table3.3), in an effort to include the maximum possible number of crucial parameters. The siRNA sequences were synthesised by Ambion®. It should be noted that none of the designed siRNA contained any chemical modifications, as all the design parameters used were developed based on data from studies performed with unmodified siRNA.

**Table 3.2: Online siRNA design tools utilised.**

| siRNA design tool provider | Website |
|---|---|
| Whitehead Institute | (http://jura.wi.mit.edu/bioc/siRNAext/) |
| EMBOSS | (http://www.hgmp.mrc.ac.uk/Software/EMBOSS/Apps/sirna.html) |
| Hannon Laboratory | (http://katahdin.cshl.org:9331/RNAi_web/scripts/main2.pl) |
| MWG | (http://ecom.mwgdna.com/cgi/sirna_design.cgi) |

To begin with, the HPV16 E7 coding sequence (nucleotides 562-585 of Genbank accession number K02718.1) was input into each of the individual online design algorithms. The prediction tools varied in the number of siRNA they identified, ranging from 8 to 80, and also in the information they provided. Particularly useful were the Whitehead and the MWG tools, which provided data on the thermodynamic stability of the siRNA ends and the secondary structure of the target mRNA respectively. A general parameter provided by all the tools was the percentage GC content. The output lists from these algorithms were cross compared and only siRNA common to at least two design tools were further evaluated. Firstly, it was determined whether these siRNA fell within a conserved E7 coding region, as defined by the analysis described in section 3.3.2.1, and secondly, whether they shared any homology to human genes. The homology search was performed using NCBI's BLASTN search algorithm (http://www.ncbi.nlm.nih.gov/blast/). Only siRNAs that fell within a conserved E7 coding region and were demonstrated to be unique were considered for further analysis. This list was ranked based on their appliance with the criteria set out in Table 3.3, which are a combination of those described by Ui-Tel *et al.* (2004) and Reynolds *et al.* (2004). These were the most referenced design criteria at the time that this work was completed. Additionally, the thermodynamic properties and the secondary structure of the mRNA target sequence were also considered. Based on these parameters, three siRNAs were chosen, one targeting the 5' region of E7, one the 3' region and one a central region, E7#3 – E7#5 Figure 3.3 and Table 3.4.

**Table 3.3: Criteria used in the selection of in-house designed HPV16 E7 targeting siRNA.**

| Criterion | Description (based on sense strand) |
|---|---|
| I | G/C content of 30-52%. |
| II | Low internal stability at the 3' end, i.e. A/U rich between point 1 to 7. |
| III | U or A at point 1. |
| IV | G or C (more often C) at point 19. |
| V | A or U (more often A) at point 10. |
| VI | Avoid extended run of alternating GC, more than 7. |
| VII | Avoid runs of greater than 3 G's. |
| VIII | U at point 17. |
| IX | Absence of C at point 7. |

### *3.3.2.3 Ambion™ designed HPV16 E7 siRNA*

Subsequent to the in-house design process being undertaken, Ambion® introduced a new range of siRNA, Silencer® Select siRNAs. These are designed using a new algorithm that was developed utilising the latest in machine-learning methods, and is said to produce siRNA that require 5 to 20 fold lower concentrations to elicit a potent silencing event compared to previous generations. In addition to a new algorithm, the design process also includes a five-step bioinformatic filtering procedure and incorporates chemical modifications. The five-step bioinformatic filtering process involves a mismatch filter, a silencer® select toxicity classifier, a natural miRNA seed region filter, an antiviral response motif filter and a siRNA seed region ranking. This procedure is said to eliminate siRNAs predicted to elicit off-target effects. To ensure elimination of off-target effects the siRNA are chemically modified with LNA®, which Ambion® believe reduce off-target effects by up to 90%.

The HPV16 E7 coding region (Genbank accession number K02718.1) with highlighted conserved regions was supplied to Ambion®. Two additional siRNA, specific for HPV16 E7 conserved regions were identified using the silencer select design protocol, E7#1 and E7#2 Table 3.4 and Figure 3.3. These siRNA were subsequently synthesised by Ambion®.

**Table 3.4: Description of all five siRNA designed towards HPV16 E7.**

| siRNA | Nucleotide position | Sense strand sequence | Antisense strand sequence |
|---|---|---|---|
| E7#1 | 493-518 | 5'-CACCTACATTGCATGAATA-3' | 5'-TATTCATGCAATGTAGGTG-3' |
| E7#2 | 545-563 | 5'-CTACTGTTATGAGCAATTA-3' | 5'-TAATTGCTCATAACAGTAG-3' |
| E7#3 | 538-556 | 5'-CTGATCTCTACTGTTATGA-3' | 5'-TCATAACAGTAGAGATCAG-3' |
| E7#4 | 730-748 | 5'-TGGGCACACTAGGAATTGT-3' | 5'-ACAATTCCTAGTGTGCCCA-3' |
| E7#5 | 623-641 | 5'-CTGATCTCTACTGTTATGA-3' | 5'-TCATAACAGTAGAGATCAG-3' |

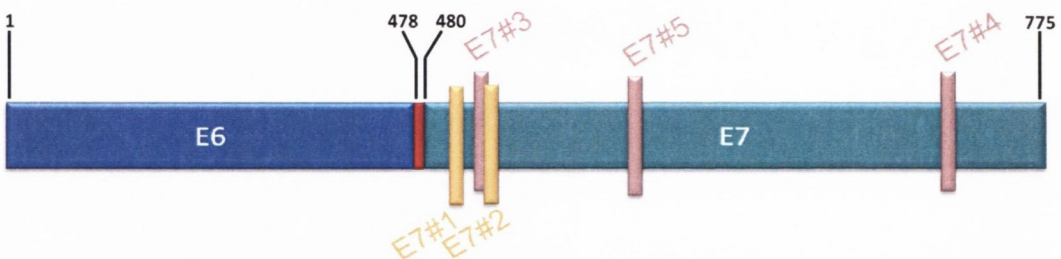


**Figure 3.3: Diagrammatic representation of the positions of the five siRNA designed towards HPV16 E7.**

### *3.3.3 Transfections*

Transfections involving the identification of the most suitable transfection agent were performed in 96-well plates supplied by Ambion (at Applied Biosystems, Foster City, CA, USA) which contained GAPDH and a universal negative control siRNA lyophilised to the bottom of the wells at a concentration of 10nM. Transfections were performed on HeLa and SiHa cells, using three different transfection agents: Lipofectamine™ RNAiMAX (Invitrogen, Life Technologies, Maryland, USA), NeoFx™ siPORT™ (Ambion at Applied Biosystems, Foster City, CA, USA) and HIPERFECT (Qiagen, Crawley, West Sussex, UK). For each transfection agent, cells were seeded at a low and high concentration and a range of transfection agent volumes were applied, depending on the manufacturer's recommendations (Table 3.5). The protocols for these transfections are as described in section 2.2.1.

All other transfections were performed with Lipofectamine™ RNAiMAX (Invitrogen, Life Technologies, Maryland, USA) and were carried out in 96-well plates as per section 2.2.1.1 and in 6-well plates as per section 2.2.2.

**Table 3.5: Transfection conditions applied for optimisation experiments.**

| Transfection agents | Cell seeding Concentration (per well) | | Transfection agent vol (µl) | | |
|---|---|---|---|---|---|
| | Low | High | Low | Avg | High |
| Lipofectamine™ RNAiMAX | $4x10^3$ | $1x10^4$ | 0.100 | 0.200 | 0.300 |
| NeoFx™ siPORT ™ | $4x10^3$ | $8x10^3$ | 0.300 | 0.600 | 1.200 |
| HIPERFECT | $1x10^4$ | $3x10^4$ | 0.375 | 0.750 | 1.125 |

### *3.3.4 TaqMan® RT-PCR*

GAPDH, HPV16 E6 and E7 mRNA expression was detected by TaqMan® RT-PCR. SiHa cells ($1.5x10^5$cells/well) were left untreated, treated with transfection agent or transfected with 10nM of negative control or experimental siRNA. Total RNA was extracted from these cells following a further 48hrs incubation using the Ambion MirVanna kit (section 2.3.2) and subjected to DNase digestion (section 2.3.3). The 260/280 nm ratio and the concentration of the extracted total RNA was determined using the NanoDrop® ND-1000 (section 2.4.1). TaqMan® two step RT-PCR was performed as per section 2.5.2 using the below primer and probe sets. The relative quantity of gene expression was calculation using the $2^{-\Delta\Delta CT}$ comparative $C_T$ method as described in section 2.5.4.1, where β-actin or B2M gene expression was used as the endogenous control and gene expression of untreated or negative control cells were used as the calibrator sample.

PCR primers and probes towards HPV16 E6 and E7 were designed using Primer Express Software Version 3.0 (Applied Biosystems, Foster City, CA USA) as described in section 2.5.1. Two sets of primers and probes towards E6 were designed, one targeting all forms of E6 and the second targeting solely the full-length. These were designed based

on the E6 coding region (nucleotides 83–559) of the HPV16 complete genomic sequence (Genbank accession number K02718.1). Primers and probes towards E7 were designed based on the E7 coding region (nucleotides 562–858) of the HPV16 complete genomic sequence (Genbank accession number K02718.1). Table 3.6 shows the HPV16 E6 and E7 primer and probe sequences and amplicon sizes. The concentration of HPV16 E6 and E7 primers and probes used in each assay was optimised on controls by performing PCR titrations of each primer set, 50-900nM, and probe, 50-250nM. The optimal combination of primer and probes for the TaqMan® RT-PCR assay were chosen based on those that generated the lowest threshold cycle and maximum ΔRn, see Table 3.6 for optimal concentrations.

The utilised primers and probes specific for GAPDH, β-actin and B2M were commercial pre-designed sets obtained from Applied Biosystems (Foster City, CA, USA). They were provided in 20X mixes and were used as per manufacturer's instructions at a concentration of 1X.

**Table 3.6: HPV16 E6 and E7 primer and probe sequences.**

| PCR Target | Nucleotide position | Amplicon size | Sequence | Concentrations | |
|---|---|---|---|---|---|
| | | | | Primers | Probes |
| E7 | 619-684 | 66 | F:5'-CGGACAGAGCCCATTACAATATT-3'<br>R:5'-TCTACGCTTCGGTTGTGCG-3'<br>P:5'-TAACCTTTTGTTGCAAGTGTGA-3' | 300nM | 250nM |
| E6 | 344-415 | 72 | F:5'-AGCCACTGTGTCCTGAAGAAAAG-3'<br>R:5'-AGATTCCATAATATAAGGGGTCGGT-3'<br>P:5'-ACATCTGGACAAAAAG-3' | 300nM | 200nM |
| E6* | 133-218 | 86 | F:5'-CTGCGACGTGAGGTATATGACTTTGC-3'<br>R:5'-GGAATCCATATGCTGTATGTGATAAATG-3'<br>P: 5'-TTTTCGGGATTTATGC-3' | 300nM | 200nM |

E6 primers and probe target all form of HPV16 E6. E6* primers and probe target specifically full-length HPV16 E6. Symbols: F represents forward primer, R represents reverse primer and P represents probe.

### *3.3.5 Western Blot Analysis*

Protein cell extracts were prepared 48hrs after transfection by lysing cells with 30µl of RIPA buffer (section 2.7.1). The concentration of recovered protein in each lysate was determined using the Pierce BCA™ protein assay kit (section 2.7.2). Equal amounts of protein (30µg/lane) were resolved by 10-12% SDS-PAGE and electrotransferred to PVDF membranes. After blocking, the membranes were incubated with anti-Rb, anti-p53, anti-p21, anti-β-actin and anti-GAPDH antibodies (Table 3.7). Subsequently, the membranes were washed and incubated with the appropriate peroxidise-conjugated secondary antibody (Table 3.7). The immunoreactivity was detected with the ECL system. GAPDH or β-actin were used to asses protein loading.

**Table 3.7: Antibody and corresponding dilutions used in the study.**

| Primary Antibodies | Supplied by | Antibody Type | Species Raised in | Dilution factor |
|---|---|---|---|---|
| GAPDH | Abcam (Cambridge, CB4 0WN, UK) | Monoclonal | Mouse | 1/250000 |
| B-actin | Abcam (Cambridge, CB4 0WN, UK) | Monoclonal | Mouse | 1/1000 |
| Rb | BD Pharmigen™ (at BD Biosciences, San Jose, CA, USA) | Monoclonal | Mouse | 1/100 |
| p53 | BD Pharmigen™ (at BD Biosciences, San Jose, CA, USA) | Monoclonal | Mouse | 1/1000 |
| p21 | BD Pharmigen™ (at BD Biosciences, San Jose, CA, USA) | Monoclonal | | |
| **Secondary Antibodies** | | | | |
| Mouse | Jackson Immuno Research (West Grove, PA, USA) | | Goat | 1/1000 |

### *3.3.6 Analysis of in vitro cell growth*

#### 3.3.6.1 Evaluating cell toxicity

Certain experimental procedures can cause high levels of cells toxicity. To assess whether the transfection agent Lipofectaimne™ RNAi Max or the transfection of cells with negative control siRNA induced cell toxicity, a standard MTT assay used. HeLa and SiHa cells were seeded at $1x10^4$cells per well in 200µl of complete growth medium. The cells were treated with a range of Lipofectaimne™ RNAi Max volumes (0.05µl-0.3µl) or transfected with increasing concentrations of negative control siRNA (10nM – 20nM). After incubation for 48hrs at 37°C in a humidified 5% $CO_2$ atmosphere, a MTT assay was performed (described section 2.10). All assays were performed in triplicate and repeated three times.

#### 3.3.6.2 Evaluating cell viability

The effect of functional E7 siRNA on the viability of the cervical cell line SiHa was determined using the standard MTT assay. SiHa cells were plated at $6x10^3$cells per well in 200µl of complete growth medium in a 96-well plate, and left untreated, treated with transfection agent or transfected with 10nM of negative control or experimental siRNA. After incubation for 24 - 96hrs at 37°C in a humidified 5% $CO_2$ atmosphere, cell viability was determined by means of the MTT assay, as described in section 2.10. Cell viability rate was calculated as the percentage MTT absorption as follows: % cell viability = (mean absorbance/mean control absorbance) x 100. All assays were performed in triplicate and repeated three times.

### *3.3.7 Cell cycle analysis*

Cell cycle status was evaluated by flow cytometry by means of dual BrdU and PI staining. 48hrs post transfection, BrdU was added to the growth media of the SiHa cells. After 2hrs growth in the presence of BrdU, all cells were collected (adherent and non adherent). Subsequent cell staining procedures and flow cytometry analysis was performed as described in section 2.8.2.

### *3.3.8 Apoptosis analysis*

The apoptotic profile of cells was determined by flow cytometry by means of annexin V-FITC and PI counter staining. 48hrs or 96hrs post transfection, all SiHa cells were collected (adherent and non adherent) and subjected to annexin V-FITC/PI staining and flow cytometry analysis as described in section 2.8.1.

### *3.3.9 Statistical analysis*

Data is expressed as means ± the standard deviation from at least three biological replicates. For all measurements as needed, a Student *t* test was used to assess the statistical significance of treated groups versus control groups. Student *t* test was performed using the GraphPad Prim version5 software (GraphPad Software, CA, USA). A statistically significant difference was considered to be present at $P < 0.05$.

## 3.4 Results

Throughout the study, the SiHa and HeLa cell lines are being used as an *in vitro* model system for HPV16 and HPV18 positive cervical cancer respectively. In this section of work, initial optimisations were performed for both model systems. However, the experimental focus was placed on the HPV16 infected SiHa cells.

### *3.4.1 Evaluation of optimal knockdown conditions for SiHa & HeLa cells*

#### 3.4.1.1 Assessment of transfection reagents

Since transfection technology had not been applied in this laboratory prior to the beginning of this work, the first objective was to determine the most efficient transfection reagent for both the HeLa and SiHa cervical cancer cell lines. This was established using a high throughput 96-well set up. Cells were transfected with either GAPDH siRNA or a human universal negative control siRNA using either Lipofectamine™ RNAiMax, siPORT™ NeoFX™ or HiPerFect. For each transfection reagent, three different concentrations were applied and two different cell seeding concentrations were employed, based on manufacture's recommendations. 48hrs post transfection total RNA was prepared and subjected to TaqMan® RT-PCR using primers and probes selective for GAPDH mRNA. The negative control siRNA was found to have no effect on GAPDH mRNA levels when compared to mRNA assessed from untransfected cells and was thus used as a calibrator in the final calculations. Overall the data demonstrated Lipofectamine RNAiMax to be the most efficient transfection reagent, giving the highest knockdown rates and lowest standard deviation between biological replicates (Figure 3.4, 3.5). In excess of 90% knockdown of GAPDH was achieved using the highest concentration of Lipofectamine™ RNAiMAX (Figure 3.4, 3.5). While siPORT™ NeoFx™ gave a similar result in the HeLa cells when seeded at a low concentration, the standard deviation was extremely high (Figure 3.4), the result was below 60% at the higher seeding concentration (Figure 3.5) and its effect on the SiHa cells was minimal (Figure 3.4, 3.5). Hiperfect was the least effective of the three transfection agents, with modest and highly variable results (Figure 3.4, 3.5). The analysis also established that for both cell types, lower seeding concentrations of cells

with medium to high concentrations of transfection reagent allowed for substantially more effecient silencing events over high cell seeding and low transfection reagent concentrations (Figure 3.4, 3.5).

Transfection agents can be highly toxic to cells. Therefore, to evaluate the toxicity of Lipofectamine™ RNAiMax, cell viability was assessed in a 96-well format using the standard MTT assay for both cell lines and also in a 6-well format using trypan blue staining for the HPV16 positive cell line, SiHa. The MTT assay results indicate that for both cell lines, there is a trend of decreasing cell viability with increasing transfection agent concentration (Figure 3.6 A). The trend though not significant, was slightly more severe for the SiHa cell line. However, when analysis was performed with these cells in a 6-well format, the trend completely disappeared (Figure 3.6 B). Since the experimental transfections will be carried out in a 6-well format, this result demonstrated that transfection toxicity should not be a concern for future work. Based on the toxicity results and the efficiency with which Lipofecatime™ RNAiMax silenced GAPDH in both the SiHa and HeLa cell line, it was determined to be the transfection agent of choice for all subsequent RNAi experiments.

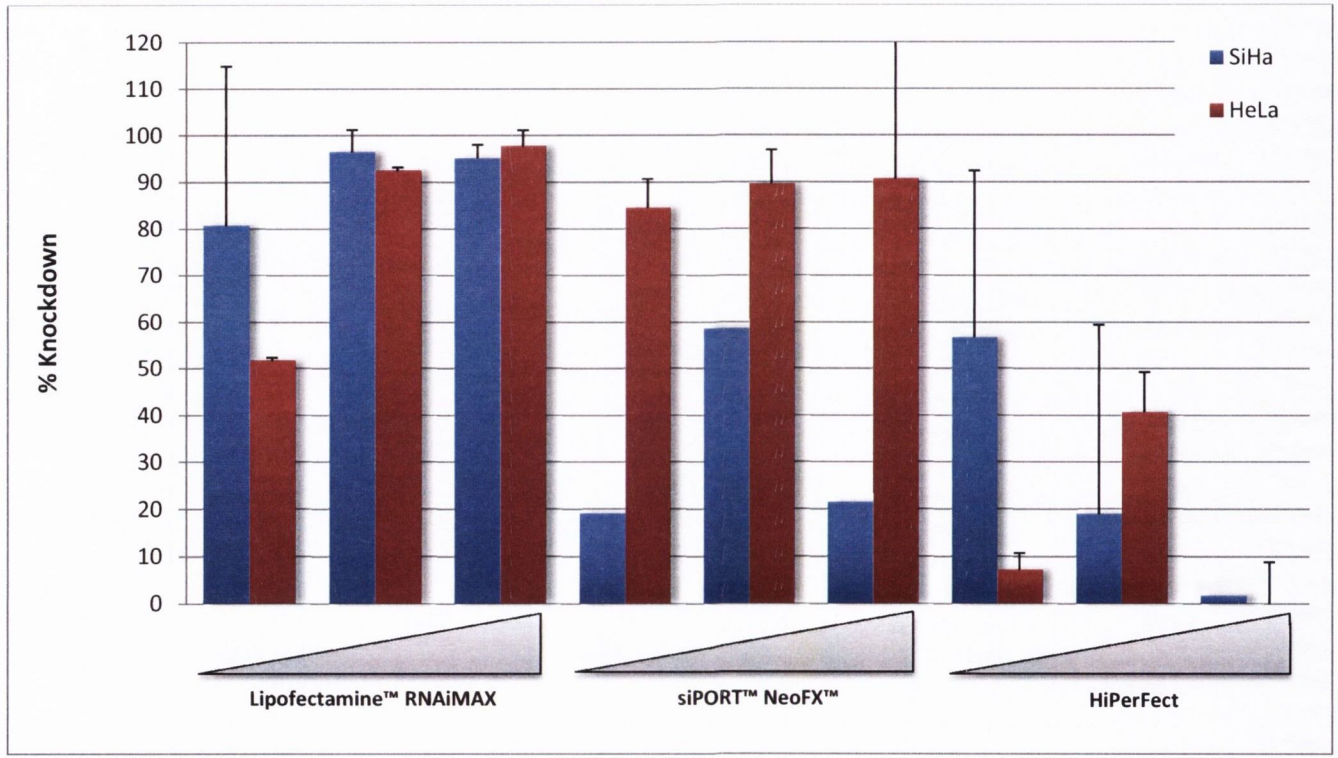


**Figure 3.4: Evaluation of the efficiency of transfection with three different transfection reagents in SiHa and HeLa cervical cancer cells seeded at low cell concentrations.** GAPDH (10nM) and negative control (10nM) siRNA were transfected into SiHa (blue) and HeLa (red) cells using increasing concentrations of three different transfection reagents, Lipofectamine™ RNAiMAX , siPORT™ NeoFX™ and HiPerFect. After 48hrs incubation total RNA was extracted and mRNA expression levels were assessed by TaqMan® RT-PCR using primers and probes selective for GAPDH and β-actin mRNA. The GAPDH mRNA expression was normalised to that of β-actin and calibrated to that of the negative control transfected cells to establish the relative level of mRNA expression.

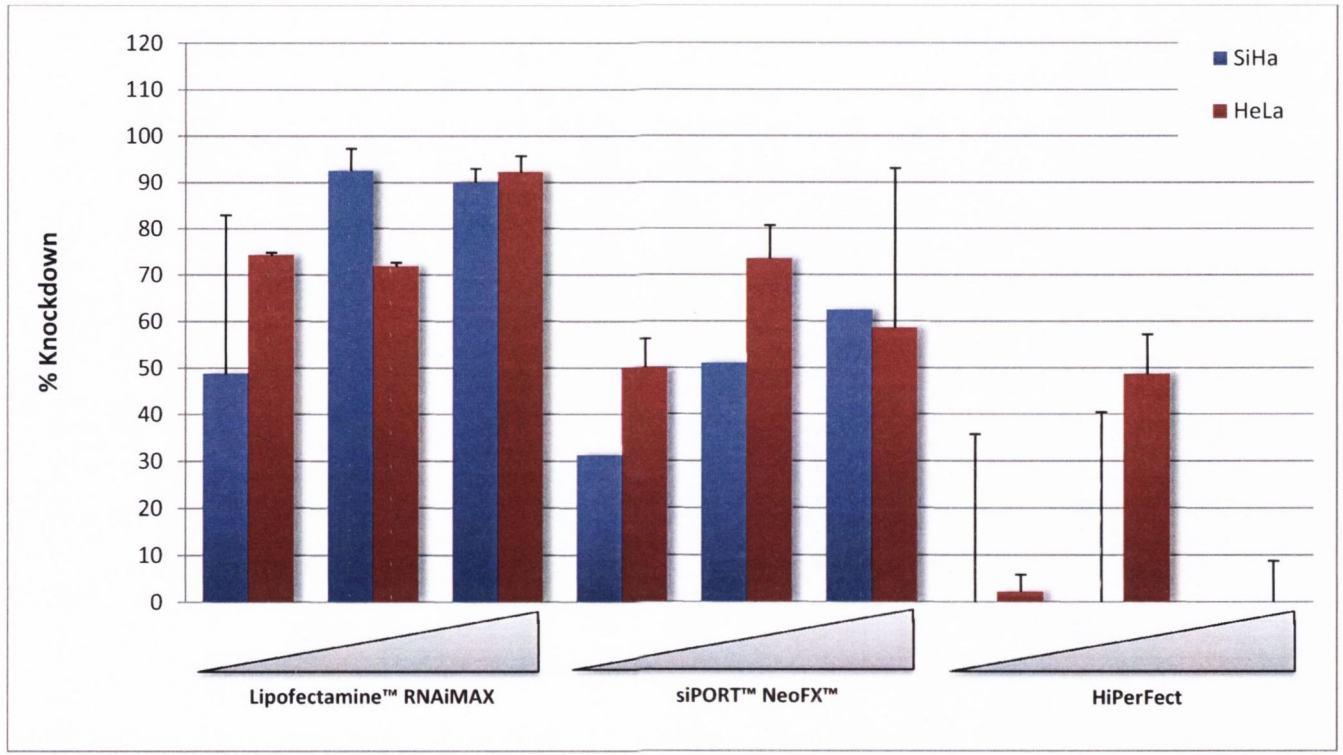


**Figure 3.5: Evaluation of the efficiency of transfection with three different transfection reagents in SiHa and HeLa cervical cancer cells at high cell seeding concentrations.** GAPDH (10nM) and negative control (10nM) siRNA were transfected into SiHa (blue) and HeLa (red) cells using increasing concentrations of three different transfection reagents, Lipofectamine™ RNAiMAX , siPORT™ NeoFX™ and HiPerFect. After 48hrs incubation total RNA was extracted and mRNA expression levels were assessed by TaqMan® RT-PCR using primers and probes selective for GAPDH and β-actin mRNA. The GAPDH mRNA expression was normalised to that of β-actin and calibrated to that of the negative control transfected cells to establish the relative level of mRNA expression.

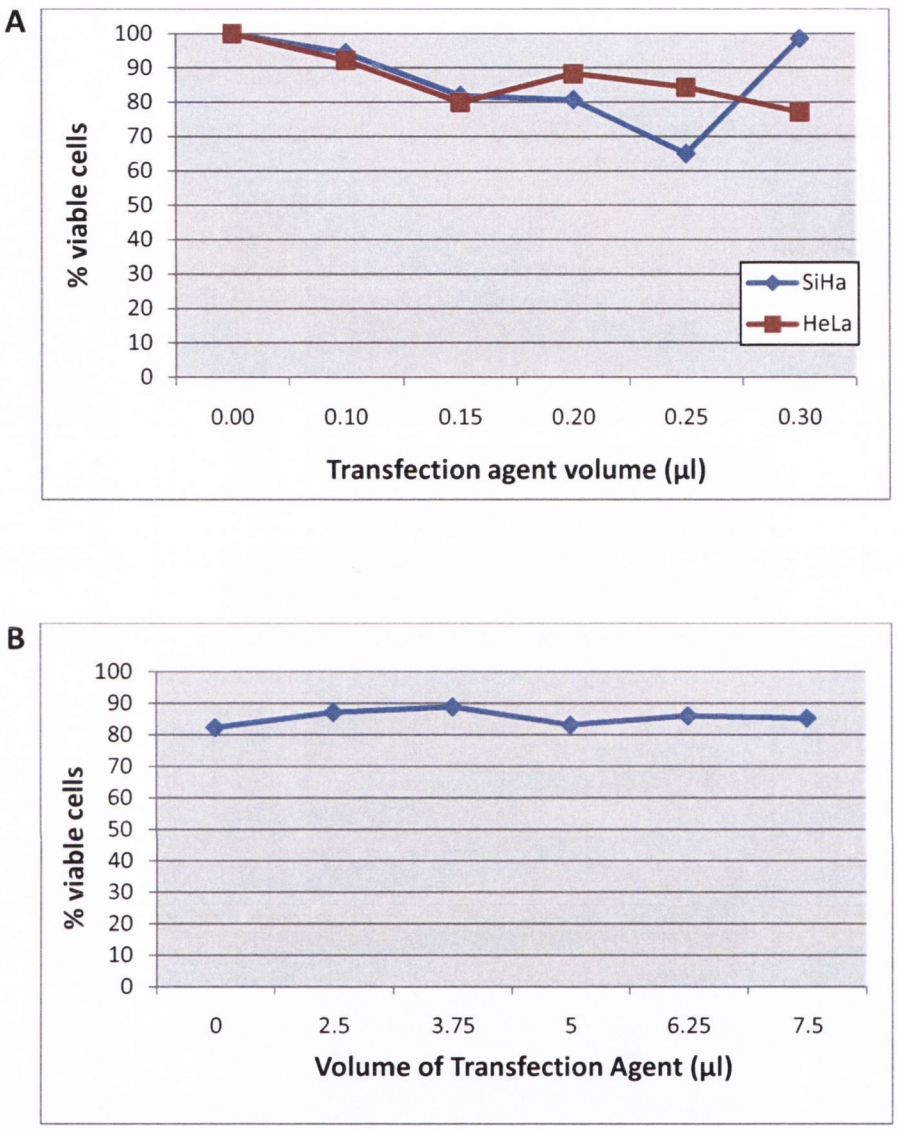


**Figure 3.6: Effect of Lipofectamine™ RNAiMAX on cell viability. (A)** SiHa ($1x10^4$) cells and HeLa ($1x10^4$) were treated in a 96-well dish, with increasing concentrations of Lipofectamine™ RNAiMAX, based on the upper and lower limits of the manufacturer's recommendations (0.1µl – 0.3µl). After 48 hours incubation, cell viability was assessed by means of the MTT assay. Cell viability rate was calculated as the percentage MTT absorption as follows: % cell viability = (mean mock transfected cell absorbance/mean untreated cell absorbance) x 100. All experiments were performed in triplicate. **(B)** SiHa ($1.5x10^5$) cells were treated in a 6-well dish with increasing concentrations of Lipofectamine™ RNAiMAX, based on the upper and lower limits of the manufacturer's recommendations (2.5µl – 7.5µl). After 48 hours incubation, cell viability was assessed using trypan blue dye. Trypan blue stains dead cells blue and are excluded from live cells. Cells were counted using a haemocytometer and a light microscope. Cell viability rate was calculated as the percentage live number of cells as follows: % cell viability = (mean viable cell count/mean total cell count) x 100. All experiments were performed in triplicate.

### 3.4.1.2 Assessment of negative control siRNA

With controls a central issue in RNAi experiments, it was essential to identify a negative control siRNA for the cervical cancer systems. The issue that arose was that while there are many commercial available human universal negative controls, at that time none had been applied to human cell line systems infected with HPV or taken into consideration the effect on HPV gene expression. A panel of three universal negative controls were identified by Ambion to contain an adequate number of mismatches to the HPV genome to result in a null effect; silencer #1 (s#1), silencer select #1 (ss#1) and silencer select #2 (ss#2).

To evaluate whether these negative control siRNA had any effect on the HPV infected cells at the RNA level, TaqMan® RT-PCR specific for the HPV oncogenes and also for the house keeping gene GAPDH was performed. Using Lipofectamine™ RNAiMax, both SiHa and HeLa cells were transfected with 10nM or 15nM of these siRNA. Cells transfected with a transfection agent alone (mock-transfected) were used as a control. Total RNA was extracted and by means of GAPDH, HPV16 E6, HPV16 E7, HPV18 E6 and HPV18 E7 specific TaqMan® RT-PCR, the ability of the negative control siRNA to affect the HPV genome was assessed. The mock-transfected control was found to have no effect on GAPDH, E7 or E6 mRNA levels by comparison to mRNA assessed from untransfected cells (Figure 3.7 A-C). The results showed that the effect of any of the three negative controls on HPV16/18 E6 mRNA expression was no greater than that expected for biological variation between biological replicates (Figure 3.7 B). Biological variation when using the $\Delta\Delta C_T$ relative expression calculation is defined as relative expression values within two-fold up or down regulation of the calibrator samples (between 0.5 and 2 on Figure 3.7's scale). Whereas there was no effect on HPV16 E7 levels (Figure 3.7 C), there was a significant effect on the expression of both GAPDH and HPV18 E7 when using the negative control s#1 in the HeLa cells (Figure 3.7 A, C respectively). While the results of the ss#1 and ss#2 are all within biological variation, a comparison between the two sets of data would indicate that ss#2 has the smallest outcome on E7 and E6 expression levels and a similar effect on GAPDH expression to

ss#1. This data indicates that the siRNA negative control ss#2 has the least impact on the HPV infected cell systems

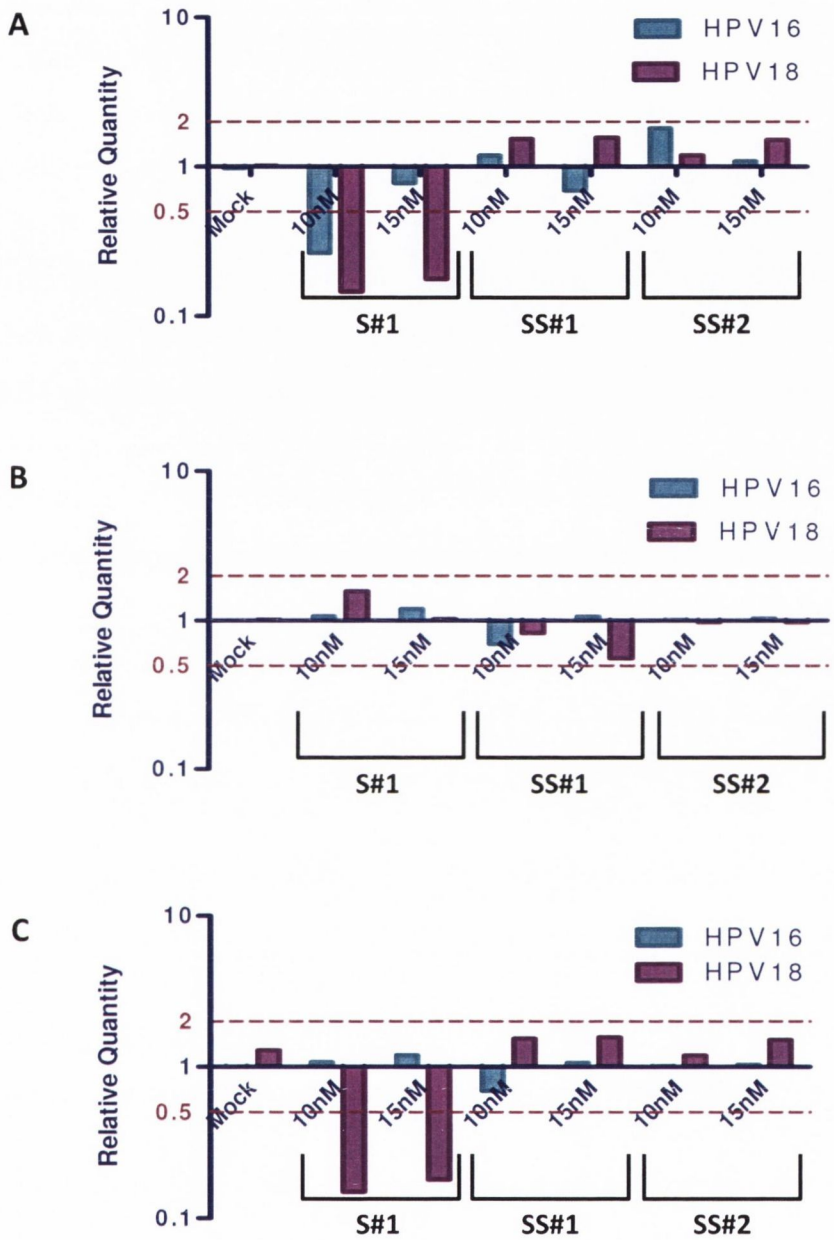


**Figure 3.7: Evaluation of universal negative controls for use with SiHa and HeLa cells.** SiHa ($1.5x10^5$) and HeLa ($1.5x10^5$) cells were left untreated, mock-transfected or transfected with negative control siRNA s#1, ss#1 or ss#2. After 48hrs, total RNA was extracted and mRNA expression was evaluated by TaqMan® RT-PCR using primers and probes selective for GAPDH, β-actin, HPV18 E6, HPV16 E6 and HPV16 E7 mRNA. The GAPDH (**A**), HPV18 E6 (**B**), HPV16 E6 (**B**), HPV16 E7 (**C**) and the HPV18 E7 (**C**) mRNA expression was normalised to that of β-actin and calibrated to that of the untransfected cells to establish the relative level of mRNA expression. Marked on the graphs are the considered limits of biological variation, from 0.5 to 2.

To further appraise the negative controls, their effect on cell growth was assessed, as alterations in cellular proliferation are indicative of changes in E6 and/or E7 expression. An MTT assay was performed on the HPV positive cell lines 48hrs post transfection with the individual negative controls. Figure 3.8 A, C and E show that in comparison to the cell growth rates of the untreated cells, there are minor reductions post negative control siRNA transfection. It would appear that the SiHa cells have a more pronounced effect, though this is probably attributed to the transfection agent rather than any consequence of the negative control. When the mock-transfected sample is used as the control sample for the cell viability calculation (Figure 3.8 B, D, F), the cell viability value is 100% or above for all treatments with the exception of 20nM of s#1. In fact, the graphs indicate that in nearly all instances, the transfection agent on its own is more toxic to the cells than in combination with the negative control. When the mock-transfected sample is employed as the control, the cell viability values are generally greater than 100%. Though there is no significant difference between the negative control siRNA, the data demonstrates that ss#2 had a slightly reduced effect on the rate of cell proliferation than the other two, with all cell viability values when compared to the mock-transfection samples being above 100%.

The negative control ss#2 was determined by the TaqMan® RT-PCR analysis to produce no alterations at the RNA level on the HPV genome or the GAPDH housekeeping gene, and the MTT assay results indicate that introduction of this siRNA has no effect on cell viability beyond the effect of the transfection agent. Thus, based on these two sets of data, it was deemed to be the most suitable negative control for the proceeding experimental work in the HPV systems.

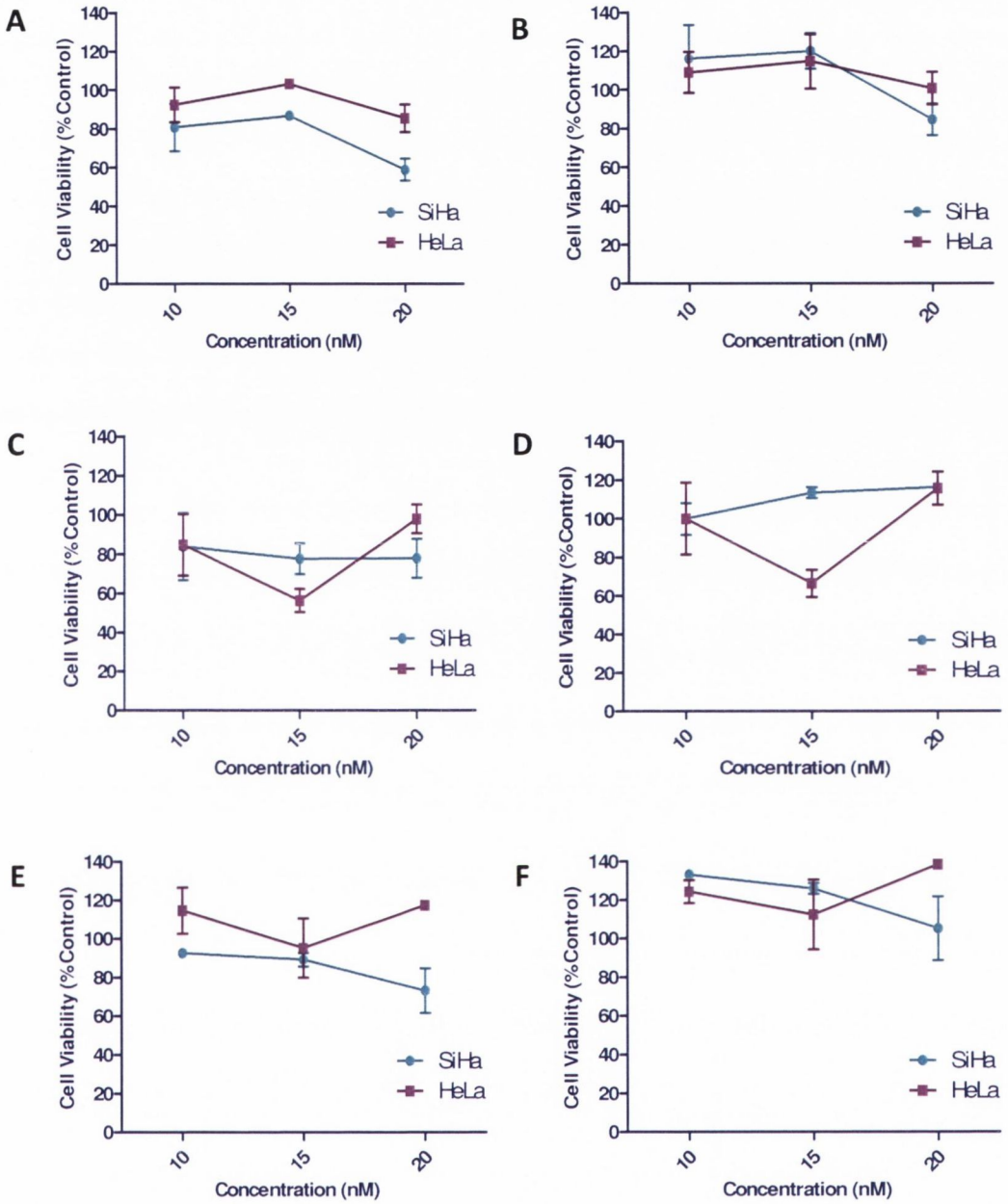


**Figure 3.8: Evaluation of universal negative controls for use with SiHa and HeLa cells.** SiHa ($1x10^4$) and HeLa ($1x10^4$) cells were transfected in a 96-well dish with 10, 15 or 20nM of negative control siRNA s#1 (**A** - **B**), ss#1 (**C** - **D**) or ss#2 (**E** - **F**) using 0.2µl Lipofectamine™ RNAiMAX. After 48 hours incubation, cell viability was assessed by means of the MTT assay. Cell viability rate was calculated as the percentage MTT absorption as follows: cell viability (% control) = (mean transfected cell absorbance/mean control cell absorbance) x 100. Graphs **A**, **C**, **E** represent where untreated cell absorbances were used as control value in cell viability (% control) calculation. Graphs **B**, **D**, **F** represent where mock treated absorbances were used as control value in cell viability (% control) calculation. All experiments were performed in triplicate.

### 3.4.1.3 Assessment of positive control siRNA

There are many different factors that can influence the efficiency of transfection, including cell seeding concentration, transfection agent concentration, siRNA concentration, the presence of antibiotics and the duration of transfection. Prior to transfecting the SiHa cells with the experimental siRNA, favourable transfection conditions were determined using a validated siRNA towards GAPDH. Using the previous knockdown experiment, Section 3.4.1.1, and published data as a guide different cell seeding concentrations ($1.0x10^5$ - $1.5x10^5$), transfection agent volumes (1µl - 5µl) and siRNA concentrations (1nM – 20nM) were evaluated. After 48 hours transfection, the efficiency of the knockdown process on GAPDH was either validated at RNA or protein level, using TaqMan® RT-PCR and western blotting respectively. In all experiments, there were no significant differences observed between the untreated cells and those mock-transfected or transfected with negative control siRNA. The final results showed that the most efficient silencing event was achieved with 1.5 $x10^5$ cells using 5µl of transfection reagent and 10nM of GAPDH siRNA (Figure 3.9), with a knockdown of on average 91% at the RNA level achieved when compared to the negative control siRNA. In addition, to indicating conditions for efficient transfection, these experiments also conclusively demonstrated that this stock of SiHa cells were vulnerable to the introduction of siRNA.

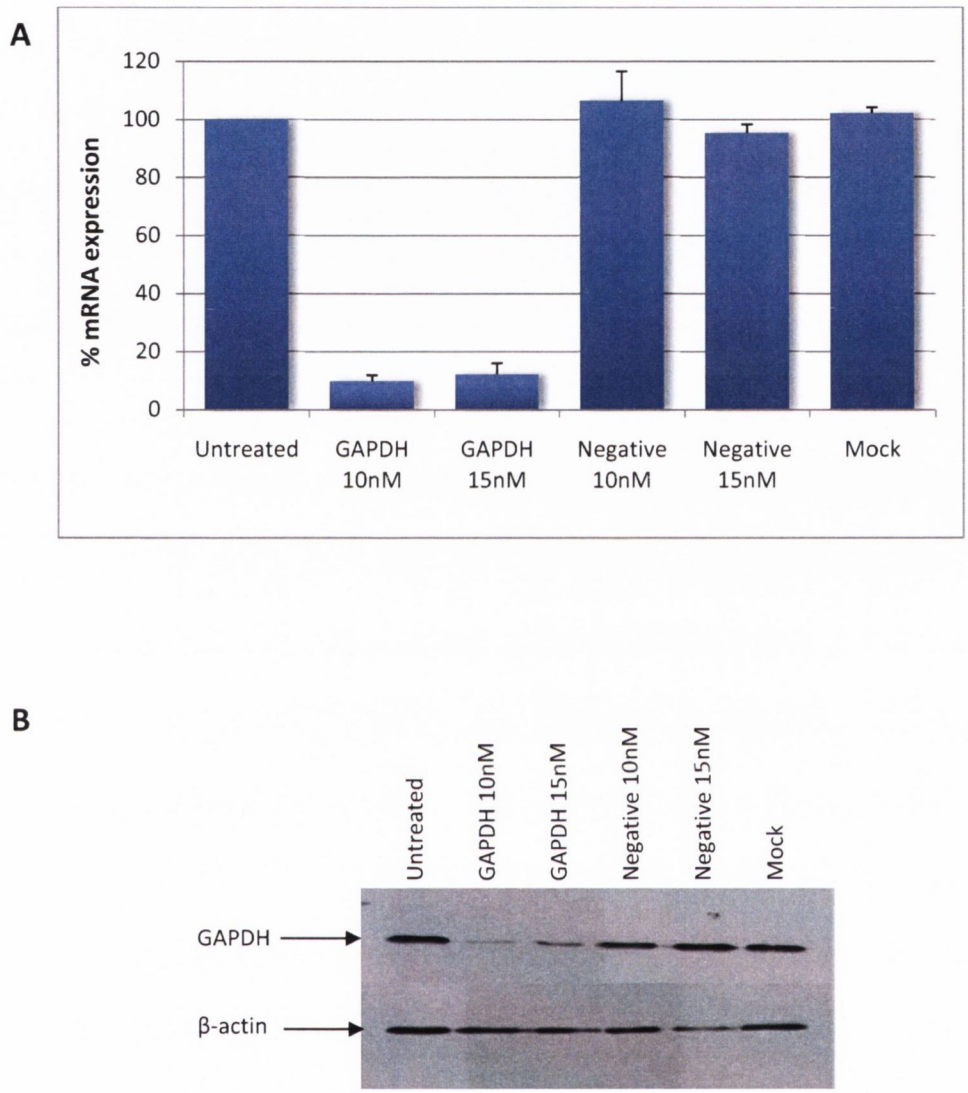


**Figure 3.9: Silencing of GAPDH in the SiHa cell line.** SiHa ($1.5x10^5$) cells were left untreated, mock-transfected, transfected with negative control siRNA or transfected with GAPDH targeting siRNA for 48hrs. **(A)** Total RNA was extracted and mRNA expression levels were assessed by TaqMan® RT-PCR using primers and probes selective for GAPDH and β-actin mRNA. The GAPDH mRNA expression was normalised to that of β-actin and calibrated to that of the untransfected cells to establish the relative level of mRNA expression. This figure was then multiplied by 100 to give the % mRNA expression. **(B)** Cells were lysed with RIPA buffer. The lysate samples (30μg) were then resolved by SDS PAGE electrophoresis and transferred to a PVDF membrane. The membrane was firstly blocked in blocking buffer and then immunoblotted for GAPDH (top panel) and β-actin (bottom panel). β-actin was used as a loading control.

### *3.4.2 HPV16 E7 siRNA silence expression of both E6 and E7*

To silence endogenous HPV16 E6/E7 expression in the SiHa cells, five siRNA were designed towards sequence motifs within E7 common to all classes and subclasses of HPV16. These siRNA will be referred to as E7#1, E7#2, E7#3, E7#4 and E7#5 siRNA. Two of the siRNA were designed by Ambion (E7#1 and E7#2) and three were designed in-house (E7#3, E7#4 and E7#5).

The SiHa cells were transfected independently with all five siRNA, initially using the conditions determined during the optimisation with the positive control siRNA, GAPDH. 48hrs after transfecting the cells, total RNA was extracted and the level of E7 expression was evaluated using E7 specific TaqMan® RT-PCR. At first with these conditions, none of the five siRNA gave consistently significant silencing events, even though there was a consistent potent reduction in the mRNA expression level with the positive control siRNA. Following a period of troubleshooting, it was determined that while the presence of antibiotics did not perturb the transfection and/or potency of the GAPDH siRNA, it had significant inhibitory activities on the efficacy of transfection and the silencing ability of the experimental E7 siRNA. Figure 3.10 demonstrates the result of treating the SiHa cells with just 10nM of siRNA for 48hrs in media lacking antibiotics. The first three siRNA demonstrate significant potency in their ability to reduce mRNA expression levels of E7, with knockdown values ranging from 70% to 75%. While, E7#4 did not induce a significant effect on E7, it did cause a 50% knockdown. E7#5 on the other had appeared to cause no alterations in the expression of E7. During the troubleshooting period, different time points, concentrations of siRNA and concentrations of transfection agent were analysed, both with and without antibiotics, and none of these alterations were observed to potentiate the effect of E7#5. Therefore, it was determined that E7#5 was a non-functional siRNA and no further evaluation of its effects on the HPV16 positive cell system was performed. There was no significant difference in mRNA expression levels between SiHa cells treated with negative control siRNA, mock-transfected and untreated cells. All

expression values were within biological variation (between 50% and 200% on Figure 3.10's scale).

The introduction of the functional E7 siRNA into the SiHa cells resulted in an equivalent concomitant reduction in E6 expression (Figure 3.10). The aim of this work was to establish a system, in which there was simultaneous repression of both E6 and E7 oncogene expression. Since it has been shown that E7 is expressed predominantly from the E6*I splice form of E6 (Tang *et al.*, 2006) and that the principal E6 transcripts in these cells is E6*I (Smotkin and Wettstein 1986; Zheng and Baker 2006) it was decided to ensure that the expression of full-length E6 was also being silenced to a similar extent and a null effect was not being masked by the reduction in the more abundant E6*I. A second primer probe set was designed within the intronic region of E6 and would thus solely identify full-length E6. Figure 3.10 shows that there is a minor increase in full-length E6 expression compared to the total E6 expression level but that ultimately the E7 siRNA induce a concomitant silencing of E7 and all forms of E6.

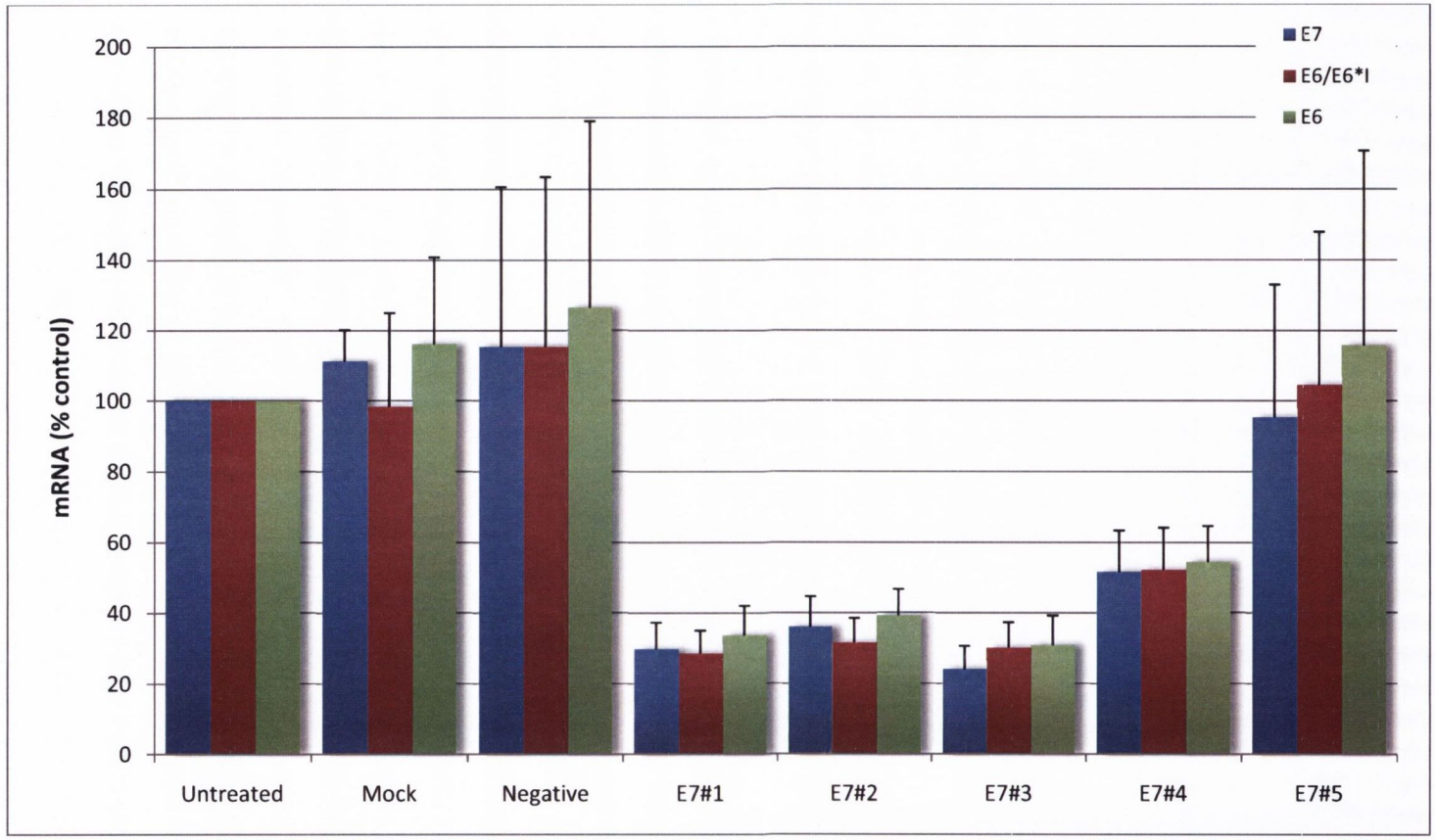


**Figure 3.10: Silencing of HPV16 E6 and E7 RNA in the SiHa cell line.** SiHa (1.5x105) cells were left untreated, mock-transfected, transfected with negativecontrol siRNA or transfected with E7 targeting siRNA (labelled #1 - #5) for 48hrs. Total RNA was extracted and mRNA expression levels were evaluated by TaqMan® RT-PCR using primers and probes selective for all forms of HPV16 E6, full-length HPV16 E6, HPV16 E7 and B2M mRNA. The HPV16 E6 and E7 mRNA expression was normalised to that of B2M and calibrated to that of untransfected cells to establish the relative level of mRNA expression. This figure was then multiplied by 100 to give the % mRNA expression. For this graphs the considered limits of biological variation are from 50% to 200%

As at the time of this work, there were no high-affinity antibodies available to reliably detect HPV16 E6 and/or E7. Inhibition at the protein level was assessed functionally by investigating the expression level of E6 and E7 targeted proteins, p53, Rb respectively and the p53 downstream target p21. As anticipated from the mRNA results, there was a change in the form of Rb detected, with a switch from a system where the hyperphosphorylated form of Rb was dominant to a system where there was a dramatic decrease in this form and an increase in the hypophosphorylated form (Figure 3.11 A). In addition, there was a substantial increase in the accumulation of p53 and p21 in the cells transfected with E7 targeting siRNA compared with those treated with negative control siRNA (Figure 3.11 B, C respectively). While the overall picture from the Western blot analysis concurs with that of the RNA results, the potency of the knockdown levels does not correspond. The E7#3 siRNA induced the most significant reduction in the E7 mRNA expression with a decrease in E6, which appeared at least as efficient as that of E7#1 and E7#2 siRNA. However, the protein analysis indicates that E7#3 is not as potent as either of these two siRNA. The level of p53 and p21 accumulation in these cells was significantly less than those transfected with either E7#1 or E7#2. As anticipated from the RNA analysis, the result of transfecting E7#4 into the cells induced the smallest alterations at the protein level.

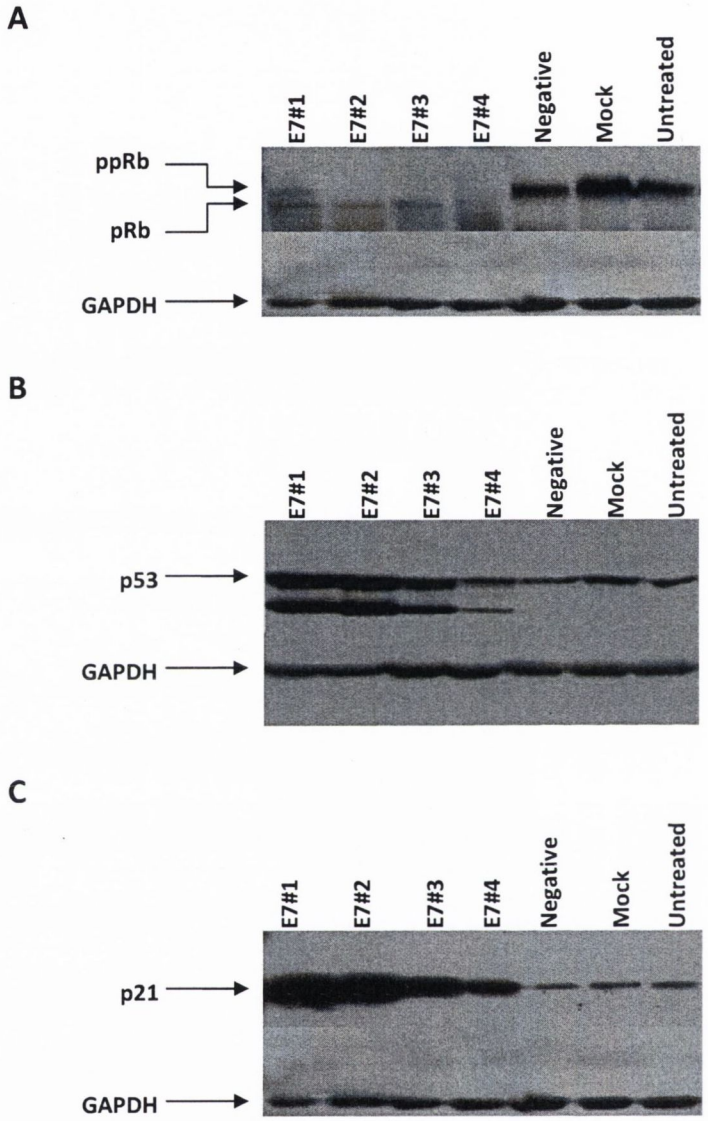


**Figure 3.11 Silencing of HPV16 E6 and E7 protein in the SiHa cell line.** SiHa ($1.5x10^5$) cells were left untreated, mock-transfected, transfected with negative control siRNA or transfected with E7 targeting siRNA (#1 - #4) for 48hrs. Cells were lysed with RIPA buffer. The lysate samples (30µg) were resolved by SDS PAGE electrophoresis and transferred to a PVDF membrane. The membrane was firstly blocked in blocking buffer and then immunoblotted for hyperphosphorylated Rb (ppRb) and hypophosphorylated Rb (pRb; upper panel **A**), p53 (upper panel **B**), p21 (upper panel **C**). All membranes were stripped and re-immunoblotted for GAPDH (lower panel **A – C**), which was used as a loading control.

### *3.4.3 E7 siRNA inhibit cell proliferation*

Previous studies that targeted the expression of E6 and/or E7, observed a growth inhibitory effect after efficient repression (Butz *et al.*, 2003; Koivusalo *et al.*, 2005; Koivusalo *et al.*, 2006; Yoshinouchi *et al.*, 2003). In order to examine if the silencing of E6 and E7 by these E7 siRNA affected the proliferation of these cells, a standard MTT assay was performed. The assay was conducted over a 96hr period and demonstrated that from 48 and 96hrs, there was a decrease in cell viability compared to negative and mock-transfection controls (Figure 3.12). The strongest effect was observed with the E7#1 and E7#2 siRNA, which is consistent with the results seen at the protein level post knockdown.

Since the primary function attributed to HPV E7 is to drive the cell cycle, it was decided to assess whether the decrease in cell proliferation post transfection corresponded with alterations in the cell cycle. SiHa cells were transfected independently with the four active siRNA for 48hrs before being harvested for flow cytometry analysis. Flow cytometry analysis was based on the dual staining of cells for BrdU incorporation and propidium iodide (PI). Figure 3.13 demonstrates that while the controls induced no significant changes in the cell cycle, in comparison, all four siRNA had highly significant effects on the progression of the cells through the phase of the cell cycle. All were observed to increase the number of cells found in the G1 phase which corresponded to a reciprocal decrease in the numbers in the S phase (Figure 3.13, 3.14). Therefore, the E7 siRNA in suppressing the expression of the E6 and E7 oncogenes induces a G1 arrest in the cells 48hrs post transfection. Clearly evident from this data is the variation in the potency of the siRNA, which correlates closely with that seen at the protein level. The E7#1 and E7#2 siRNA have a more pronounced effect on the cell cycle, increasing the number of cells in the G1 phase by 28% and 25% respectively, than E7#3 or E7#4 siRNA. The fluorocytograms in figure 3.14 probably demonstrate this potency distinction among the siRNA most clearly. Focussing on the S phase cells (region highlighted in purple), one can see a very apparent dramatic loss in numbers in this phase with E7#1 and E7#2, which is less pronounced with E7#3 and smaller again with E7#4.

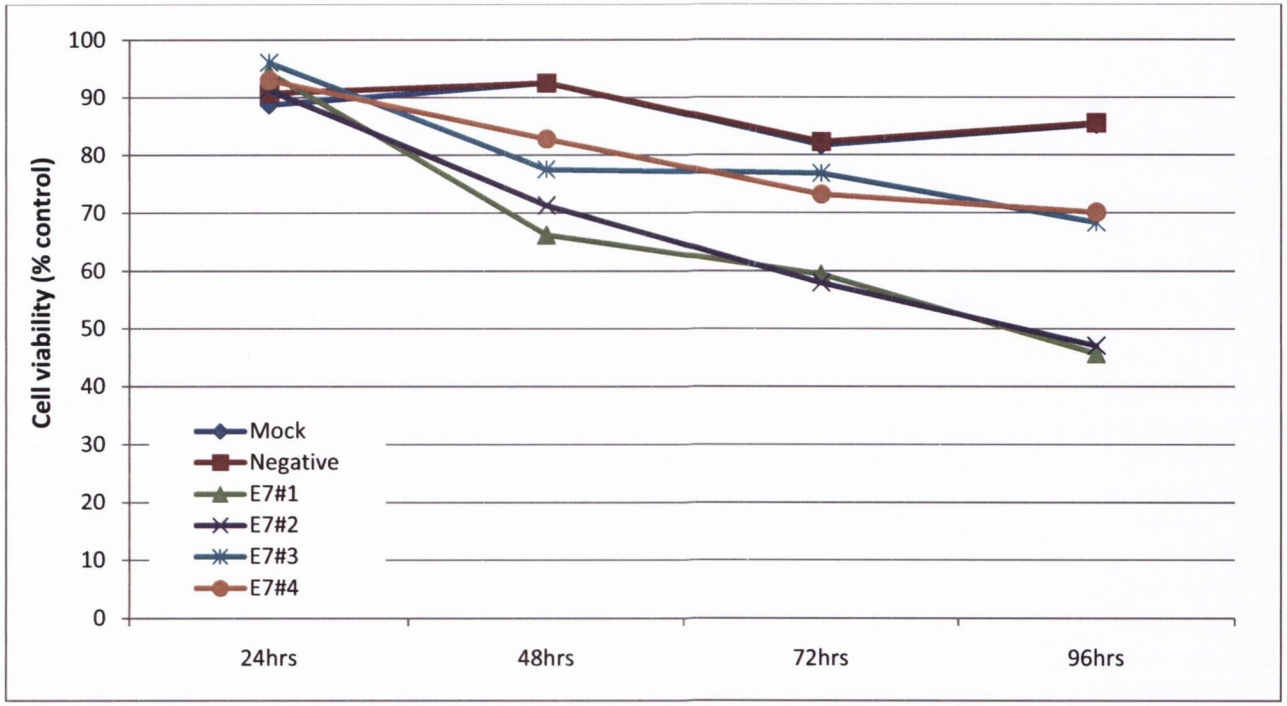


**Figure 3.12: SiHa cell viability over a 96hrs period post transfection with E7 siRNA.** SiHa ($6x10^3$) cells were left untreated, mock-transfected, transfected with negative control siRNA or transfected with E7 targeting siRNA (#1 - #4). After defined time intervals, cell viability was assessed by means of the MTT assay. Cell viability rate was calculated as the percentage MTT absorption as follows: cell viability (% control) = (mean transfected cell absorbance/mean control cell absorbance) x 100, where untreated cell absorbance values were used as the control. All experiments were performed in triplicate, thrice.

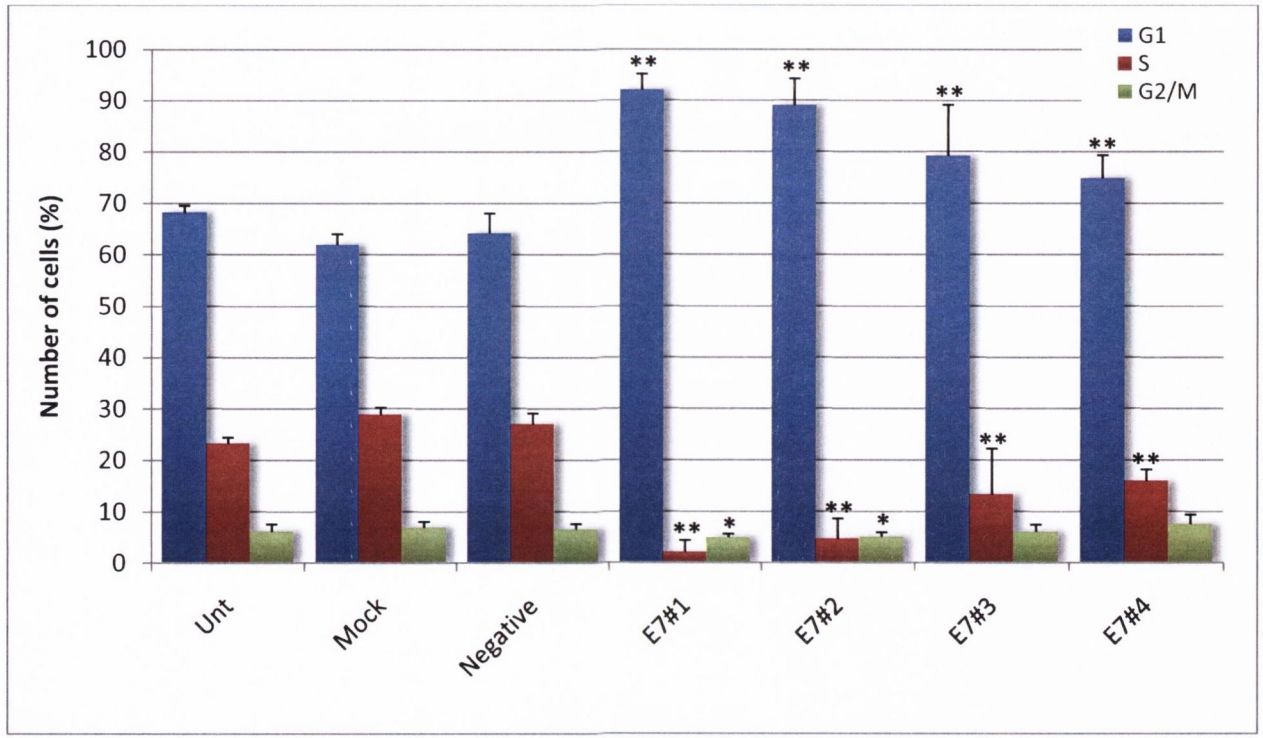


**Figure 3.13: E7 siRNA induces significant alterations in the cell cycle of SiHa cells.** SiHa ($1.5x10^3$) cells were left untreated (Unt), mock-transfected, transfected with negative control siRNA or transfected with E7 targeting siRNA (#1 - #4). After 48hrs BrdU was added to the cell culture media. After 2hrs incubation, all cells (adherent and non-adherent) were collected, stained with both FITC labelled anti-BrdU antibody and PI. Finally the cells were analysed by flow cytometry. The Histograms represent the cell cycle distribution after treatment with E7 siRNA. Results are representative of three independent experiments. Values are expressed as mean + SD. P values were calculated compared to negative control; *$p<0.05$, **$p<0.01$.

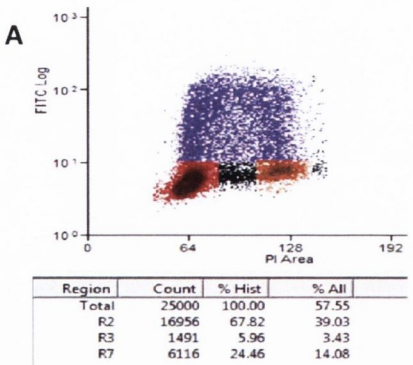


| Region | Count | % Hist | % All |
|---|---|---|---|
| Total | 25000 | 100.00 | 57.55 |
| R2 | 16956 | 67.82 | 39.03 |
| R3 | 1491 | 5.96 | 3.43 |
| R7 | 6116 | 24.46 | 14.08 |

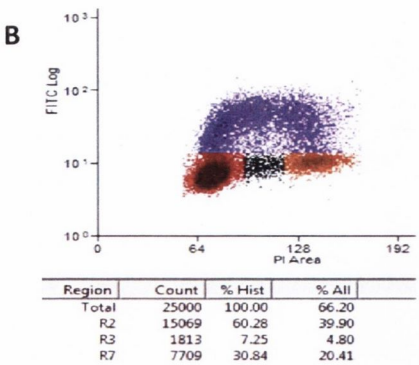


| Region | Count | % Hist | % All |
|---|---|---|---|
| Total | 25000 | 100.00 | 66.20 |
| R2 | 15069 | 60.28 | 39.90 |
| R3 | 1813 | 7.25 | 4.80 |
| R7 | 7709 | 30.84 | 20.41 |

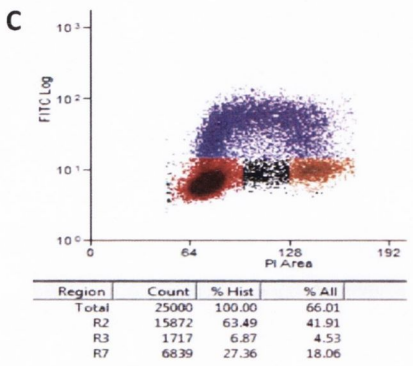


| Region | Count | % Hist | % All |
|---|---|---|---|
| Total | 25000 | 100.00 | 66.01 |
| R2 | 15872 | 63.49 | 41.91 |
| R3 | 1717 | 6.87 | 4.53 |
| R7 | 6839 | 27.36 | 18.06 |

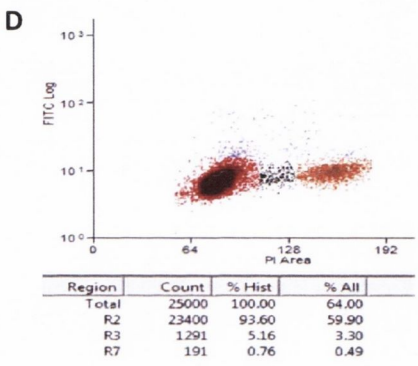


| Region | Count | % Hist | % All |
|---|---|---|---|
| Total | 25000 | 100.00 | 64.00 |
| R2 | 23400 | 93.60 | 59.90 |
| R3 | 1291 | 5.16 | 3.30 |
| R7 | 191 | 0.76 | 0.49 |

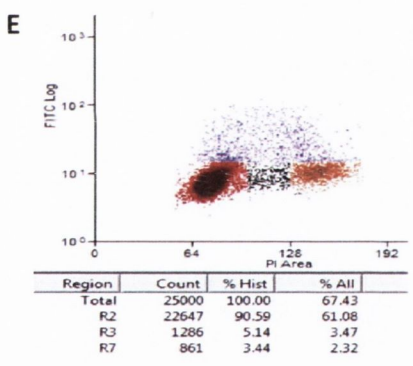


| Region | Count | % Hist | % All |
|---|---|---|---|
| Total | 25000 | 100.00 | 67.43 |
| R2 | 22647 | 90.59 | 61.08 |
| R3 | 1286 | 5.14 | 3.47 |
| R7 | 861 | 3.44 | 2.32 |

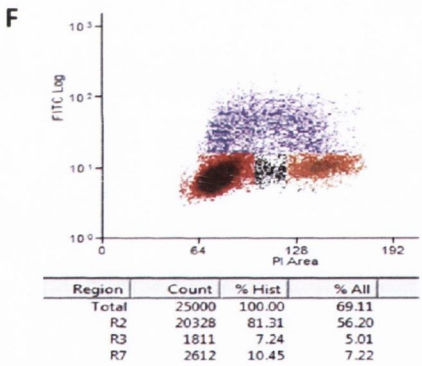


| Region | Count | % Hist | % All |
|---|---|---|---|
| Total | 25000 | 100.00 | 69.11 |
| R2 | 20328 | 81.31 | 56.20 |
| R3 | 1811 | 7.24 | 5.01 |
| R7 | 2612 | 10.45 | 7.22 |

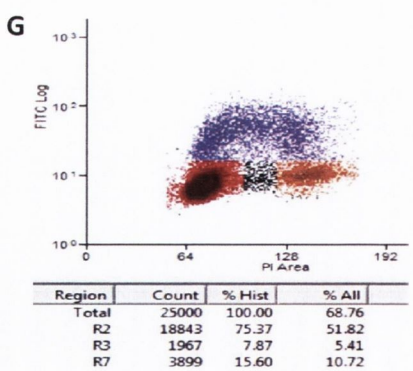


| Region | Count | % Hist | % All |
|---|---|---|---|
| Total | 25000 | 100.00 | 68.76 |
| R2 | 18843 | 75.37 | 51.82 |
| R3 | 1967 | 7.87 | 5.41 |
| R7 | 3899 | 15.60 | 10.72 |

**Figure 3.14: Representative fluorocytograms of cell cycle analysis on SiHa cells 48hrs post E7 siRNA transfection.** SiHa cells were left untreated **(A)**, mock-transfected **(B)**, transfected with negative control **(C)**, or transfected with E7 siRNA #1 **(D)**, #2 **(E)**, #3 **(F)** or #4 **(G)**. After 48hrs, BrdU was added to the cell culture media. Following 2hrs incubation, all cells (adherent and non-adherent) were collected and stained with both FITC labelled anti-BrdU antibody and PI. Finally, the cells were analysed by flow cytometry. The dual parametric dot plots combining FITC labelled anti-BrdU antibody and PI fluorescence shows the G1 phase (**red**; R2), S phase (**purple**; R7) and the G2/M phase (**orange**; R3) of the cell cycle. Data from one complete experiment of three performed is presented as a representation of data obtained.

### *3.4.4 E7 siRNA do not induce apoptosis in SiHa cells*

There is much controversy in the literature over whether the removal of E6 and/or E7 expression can induce apoptosis. To evaluate the situation in SiHa cells post transfection with the E7 siRNA, flow cytometry analysis was performed on samples using annexin V and propidium iodide (PI) dual staining. There was no significant change in apoptotic profile of the cells 48hrs post transfection as compared to negative and mock-transfected controls (Figure 3.15 A). The analysis was extended out to the 96hr time point, as the prior cell viability assay had demonstrated that the rate of cell proliferation was significantly reduced by this point (Figure 3.12). However, even though there is a continuous decrease in cell viability from 48hrs to 96hrs post transfection, this does equate to an increase in the apoptosis (Figure 3.15). While there was a modest trend towards increased levels of early and late apoptotic cells with both E7#1 and E7#2 compared to the controls, it was not significant and was not observed with the other two siRNA (Figure 3.15 B). One noticeable difference between the cells treated with some of the E7 siRNA and the controls was a shift in the fluorescent profile of the cells, which can be observed in the lower left quadrant of the fluorocytograms in Figure 3.16 and 3.17. The effect was evident with the E7#1 and E7#2 siRNA and to a lesser extent with E7#3 and more prominent at 96hrs than 48hrs. There appeared to be little change in the profile of the cells transfected with the E7#4 siRNA, having the same profile as the controls. A possible interpretation of this result is that there is increased autofluorescence of the cells after treatment with the siRNA. The fact that this occurs with multiple siRNA targeting different regions of the E7 gene, i.e. multiplicity control, and appears to correspond with their potency, indicates it is a true phenomena resulting from the suppression of E6 and E7 oncogenes.

Furthermore, the flow cytometry analysis showed very obvious differences in the forward and side scatter profiles of cells transfected with E7#1, E7#2 and E7#3 siRNA compared to the controls (Figure 3.18 – 3.21). The side and forward scatter profile was increased. Again the efficiency of the siRNA appeared to equate to the extent of the observation. Side scatter is proportional to cellular granularity/complexity; the

more organelles/bits inside the cytoplasm, the more light scatter and the higher the detected signal. While forward scatter is proportional to the size of the cell, the larger the cell the more light scatter and the higher the detected signal. Therefore, the data suggests that the cells transfected with the more potent E7 siRNA, E7#1 and E7#2, have an increased size and granularity compared to their control counterparts. Figure 3.22 to 3.25 show the morphological changes of the SiHa cells over 96hrs period post transfection. At 96hrs it is very obvious that the cells treated with E7 siRNA have considerably different morphological characteristics to the untreated and negative control cells (Figure 3.25). The cells are not forming tight cell-cell contacts, appear larger, more granular and even to have adopted a slightly more elongated morphology. This is consistent with the observations of the flow cytometry side and forward scatter analysis. It is interesting to note that these morphology characteristics are observed in senescent cells and that cells in senescence are known to autofluorescence (Goodwin and DiMaio 2001).

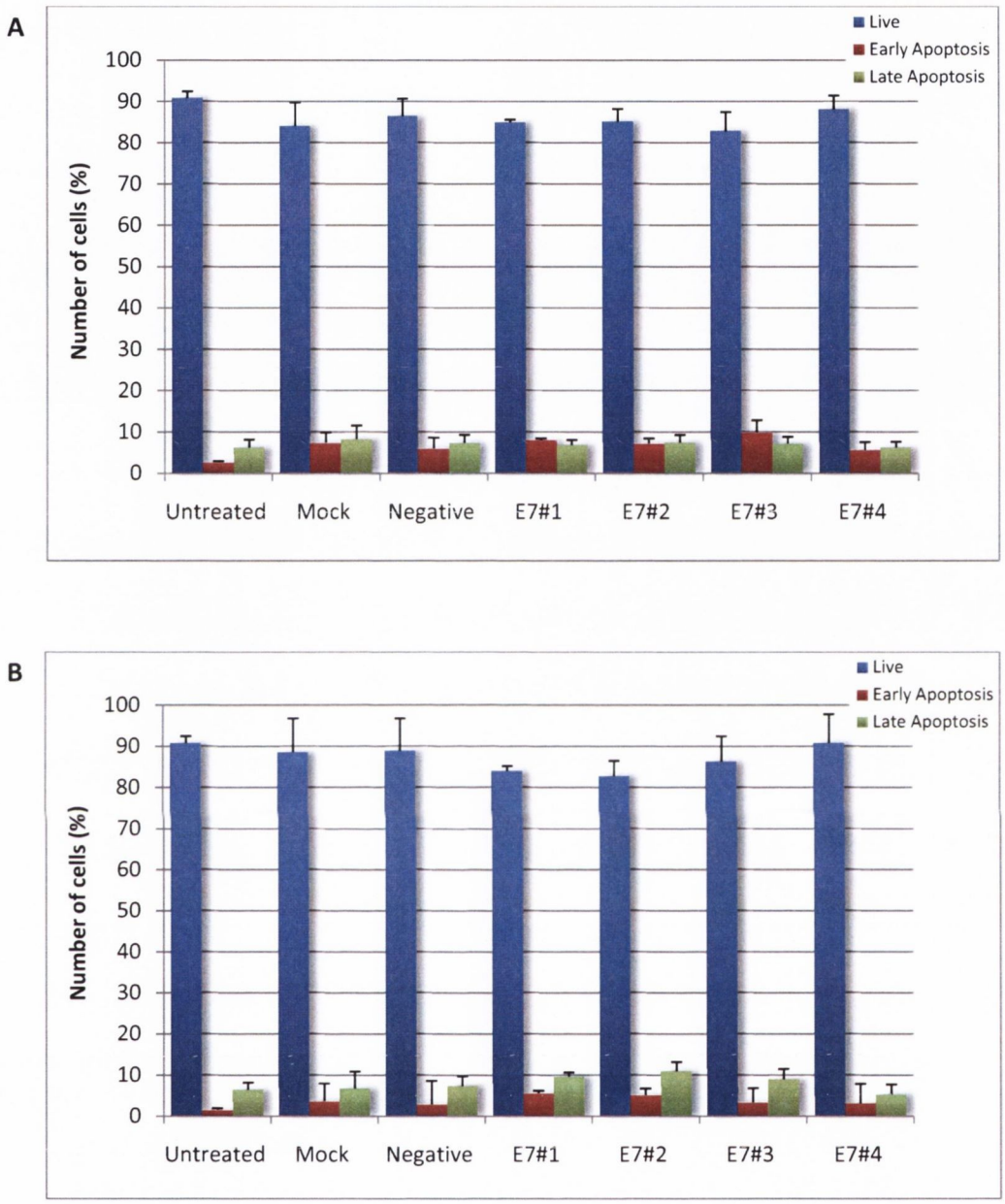


**Figure 3.15**: **E7 siRNA do not induce apoptosis by 96hrs.** SiHa ($1.5x10^5$) cells were left untreated (Unt), mock-transfected, transfected with negative control siRNA or transfected with E7 targeting siRNA (#1 - #4). After 48hrs **(A)** or 96hrs **(B)** incubation all cells (adherent and non-adherent) were collected and stained with both FITC labelled annexin V and PI. Finally the cells were analysed by flow cytometry. The Histograms represent the apoptotic profile distribution post transfection. Results are representative of three independent experiments. Values are expressed as mean + SD. P values were calculated compared to negative control but no samples reached statistical significance.

A

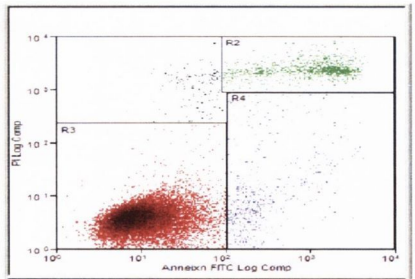


| Region | Count | % Hist | % All |
|---|---|---|---|
| Total | 20000 | 100.00 | 76.95 |
| R2 | 1067 | 5.34 | 4.11 |
| R3 | 18362 | 91.81 | 70.65 |
| R4 | 497 | 2.48 | 1.91 |

B

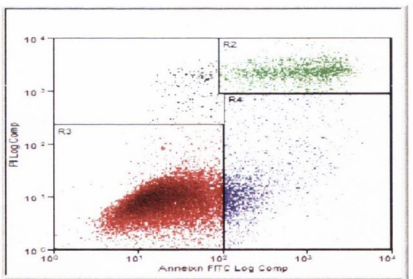


| Region | Count | % Hist | % All |
|---|---|---|---|
| Total | 20000 | 100.00 | 75.24 |
| R2 | 1707 | 8.54 | 6.42 |
| R3 | 16447 | 82.23 | 61.87 |
| R4 | 1801 | 9.01 | 6.78 |

C

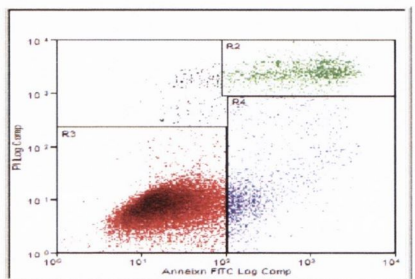


| Region | Count | % Hist | % All |
|---|---|---|---|
| Total | 20000 | 100.00 | 77.35 |
| R2 | 1308 | 6.54 | 5.06 |
| R3 | 17412 | 87.06 | 67.34 |
| R4 | 1230 | 6.15 | 4.76 |

D

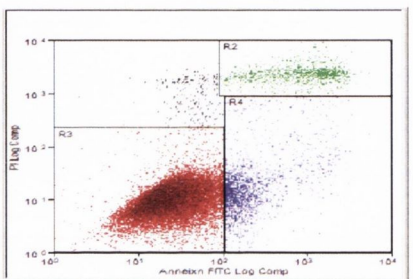


| Region | Count | % Hist | % All |
|---|---|---|---|
| Total | 20000 | 100.00 | 72.15 |
| R2 | 1109 | 5.54 | 4.00 |
| R3 | 17151 | 85.76 | 61.87 |
| R4 | 1682 | 8.41 | 6.07 |

E

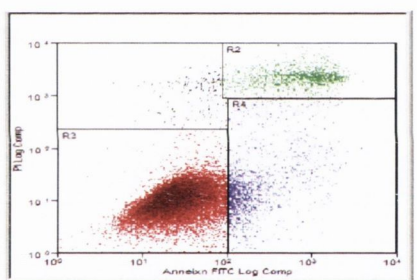


| Region | Count | % Hist | % All |
|---|---|---|---|
| Total | 20000 | 100.00 | 75.77 |
| R2 | 1365 | 6.83 | 5.17 |
| R3 | 17212 | 86.06 | 65.20 |
| R4 | 1394 | 6.97 | 5.28 |

F

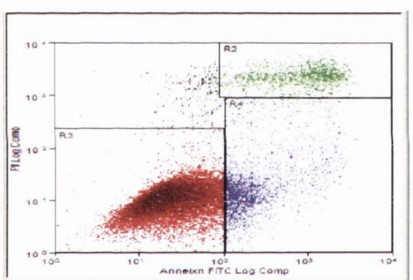


| Region | Count | % Hist | % All |
|---|---|---|---|
| Total | 20000 | 100.00 | 72.29 |
| R2 | 1634 | 8.17 | 5.91 |
| R3 | 16134 | 80.67 | 58.31 |
| R4 | 2162 | 10.81 | 7.81 |

G

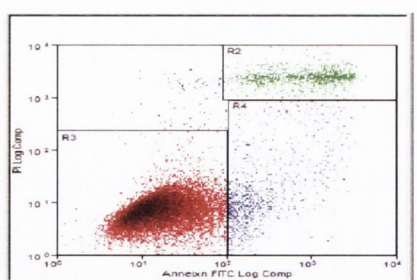


| Region | Count | % Hist | % All |
|---|---|---|---|
| Total | 20000 | 100.00 | 73.44 |
| R2 | 1154 | 5.77 | 4.24 |
| R3 | 17842 | 89.21 | 65.52 |
| R4 | 984 | 4.92 | 3.61 |

**Figure 3.16: Representative fluorocytograms of apoptosis analysis of SiHa cells 48hrs post siRNA treatment.** SiHa cells ($1.5x10^5$) were left untreated **(A)**, mock-transfected **(B)**, transfected with negative control **(C)**, or transfected with E7 siRNA #1 **(D)**, #2 **(E)**, #3 **(F)** or #4 **(G)**. After 48hrs incubation all cells (adherent and non-adherent) were collected, stained with FITC labelled annexin V and PI and analysed by flow cytometry. The dual parametric dot plots combining annexin V-FITC and PI fluorescence shows the viable cell population in the lower left quadrant (**red**; R3; annexin $V^-PI^-$), the early apoptotic cells in the lower right quadrant (**purple**; R4; annexin $V^+PI^-$), and the late apoptotic cells in the upper right quadrant (green; R2; annexin $V^+PI^+$). Data from one complete experiment is presented.

A

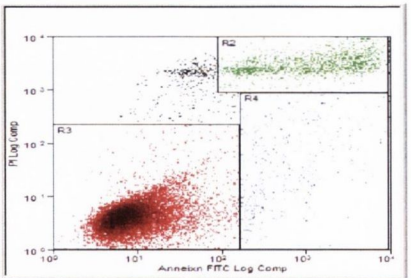


| Region | Count | % Hist | % All |
|---|---|---|---|
| Total | 20000 | 100.00 | 69.90 |
| R2 | 1560 | 7.80 | 5.45 |
| R3 | 17890 | 89.45 | 62.52 |
| R4 | 298 | 1.49 | 1.04 |

B

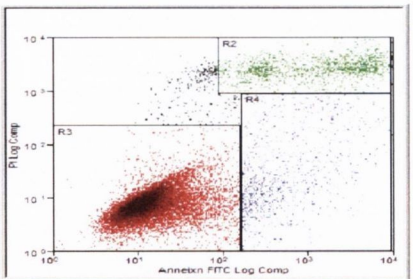


| Region | Count | % Hist | % All |
|---|---|---|---|
| Total | 20000 | 100.00 | 71.20 |
| R2 | 1498 | 7.49 | 5.33 |
| R3 | 17606 | 88.03 | 62.68 |
| R4 | 716 | 3.58 | 2.55 |

C

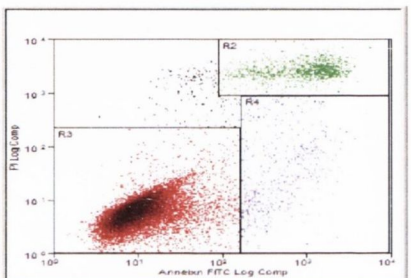


| Region | Count | % Hist | % All |
|---|---|---|---|
| Total | 20000 | 100.00 | 70.86 |
| R2 | 1315 | 6.58 | 4.66 |
| R3 | 18138 | 90.69 | 64.26 |
| R4 | 453 | 2.27 | 1.61 |

D

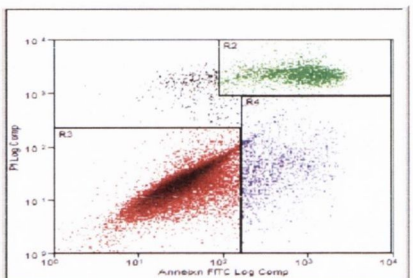


| Region | Count | % Hist | % All |
|---|---|---|---|
| Total | 20000 | 100.00 | 70.02 |
| R2 | 2214 | 11.07 | 7.75 |
| R3 | 16366 | 81.83 | 57.30 |
| R4 | 1254 | 6.27 | 4.39 |

E

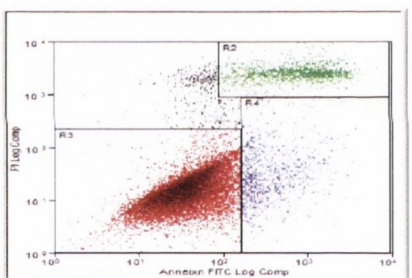


| Region | Count | % Hist | % All |
|---|---|---|---|
| Total | 20000 | 100.00 | 68.57 |
| R2 | 1813 | 9.06 | 6.22 |
| R3 | 17018 | 85.09 | 58.35 |
| R4 | 989 | 4.95 | 3.39 |

F

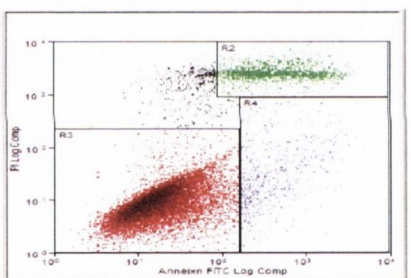


| Region | Count | % Hist | % All |
|---|---|---|---|
| Total | 20000 | 100.00 | 69.94 |
| R2 | 2062 | 10.31 | 7.21 |
| R3 | 17101 | 85.50 | 59.80 |
| R4 | 551 | 2.76 | 1.93 |

G

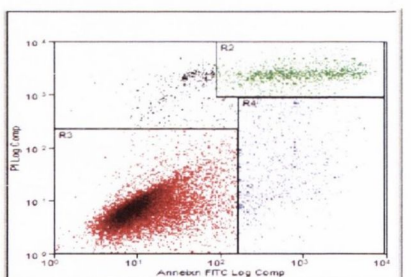


| Region | Count | % Hist | % All |
|---|---|---|---|
| Total | 20000 | 100.00 | 70.82 |
| R2 | 1278 | 6.39 | 4.53 |
| R3 | 17949 | 89.74 | 63.56 |
| R4 | 572 | 2.86 | 2.03 |

**Figure 3.17: Representative fluorocytograms of apoptosis analysis of SiHa cells 96hrs post siRNA treatment.** SiHa cells ($1.5x10^5$) were left untreated **(A)**, mock-transfected **(B)**, transfected with negative control **(C)**, or transfected with E7 siRNA #1 **(D)**, #2 **(E)**, #3 **(F)** or #4 **(G)**. After 96hrs incubation all cells (adherent and non-adherent) were collected, stained with FITC labelled annexin V and PI and analysed by flow cytometry. The dual parametric dot plots combining annexin V-FITC and PI fluorescence shows the viable cell population in the lower left quadrant (**red**; R3; annexin $V^-PI^-$), the early apoptotic cells in the lower right quadrant (**purple**; R4; annexin $V^+PI^-$), and the late apoptotic cells in the upper right quadrant (green; R2; annexin $V^+PI^+$). Data from one complete experiment is presented.

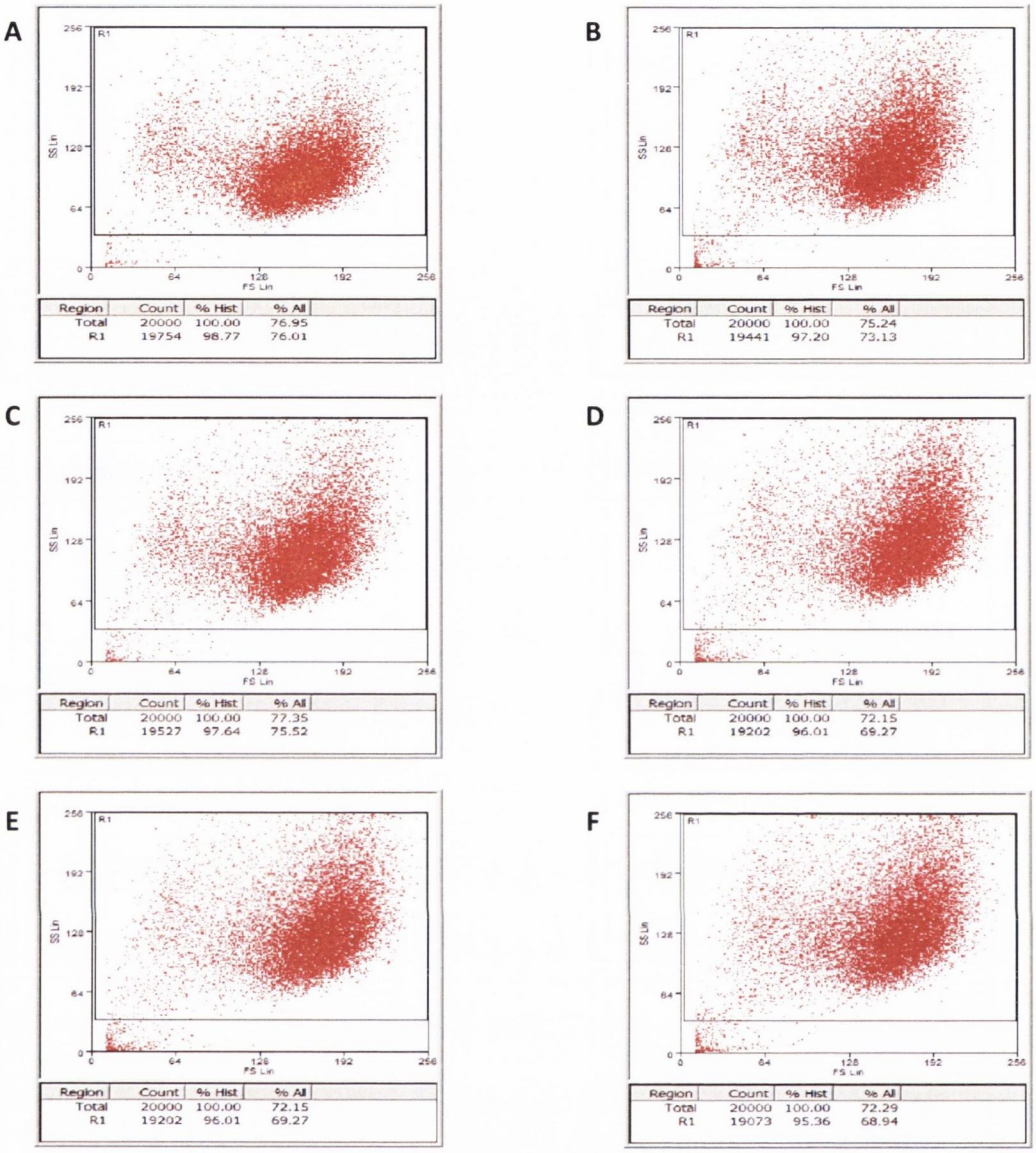


**Figure 3.18: Representative fluorocytograms of side versus forward scatter analysis of SiHa cells 48hrs post siRNA treatment.** SiHa cells ($1.5x10^5$) were left untreated **(A)**, mock-transfected **(B)**, transfected with negative control **(C)**, or transfected with E7 siRNA #1 **(D)**, #2 **(E)**, #3 **(F)** or #4 **(G)**. After 48hrs incubation all cells were collected, stained with FITC labelled annexin V and PI and analysed by flow cytometry. The dual parametric dot plots combine side and forward scatter profiles of the cells. Side scatter (vertical axis) is proportional to cellular granularity/complexity, the more within the cell, the greater the light scatter and the higher the detected signal. Cell size is proportional to Forward scatter (horizontal axis), the larger the cell the greater the light scatter and the higher the detected signal. Data from one complete experiment is presented.

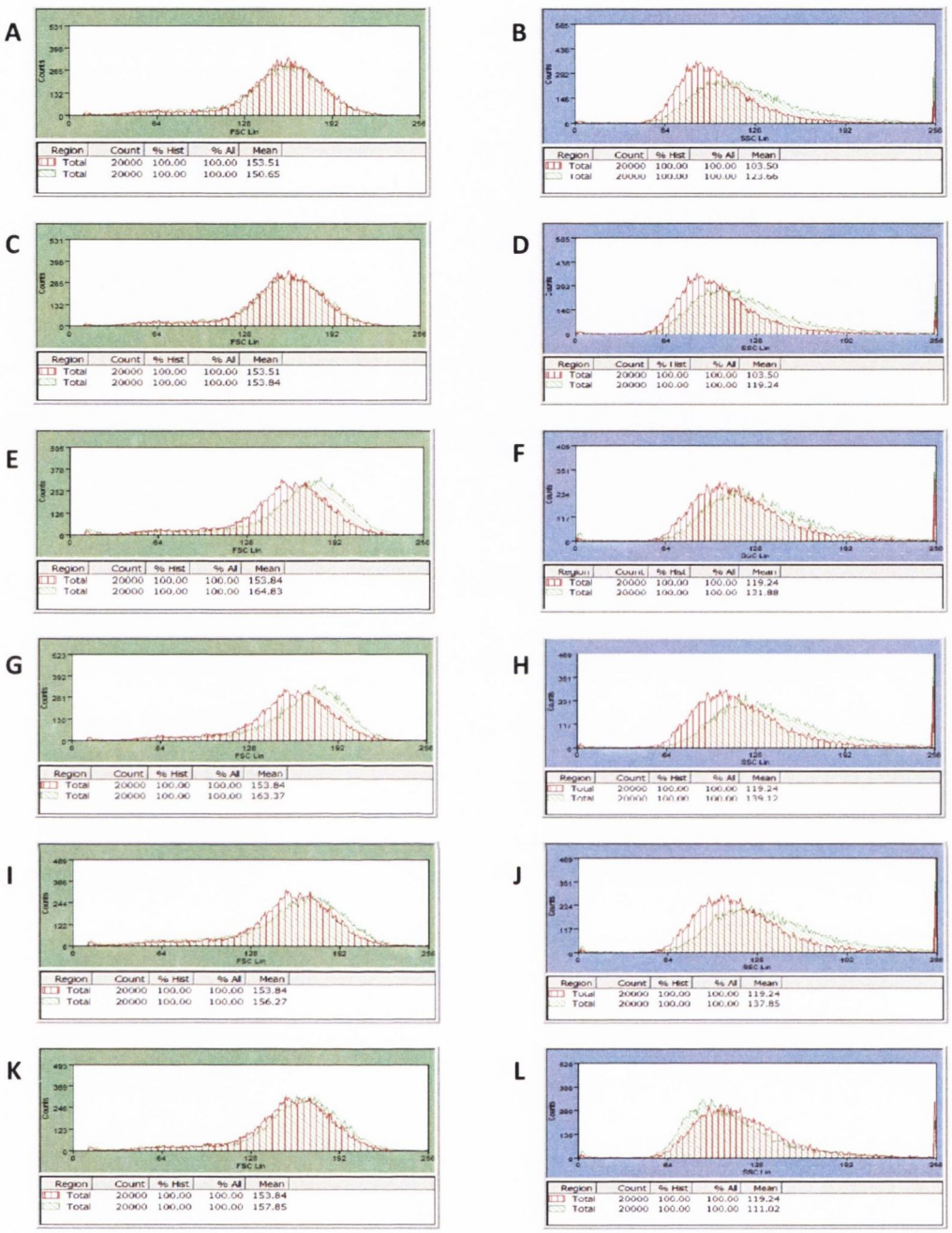


**Figure 3.19: Representative graphs of side scatter and forward scatter profiles of SiHa cells 48hrs post siRNA treatment.** SiHa cells ($1.5x10^5$) were left untreated, mock-transfected, transfected with negative control or transfected with E7 siRNA (#1 - #4). After 48hrs incubation all cells were collected, stained with FITC labelled annexin V and PI and analysed by flow cytometry. Figures **A** and **C** represent forward scatter and **B** and **D** represent side scatter profiles, comparing untreated (red) and mock-transfected (green; **A**, **B**) or negative control (green; **C**, **D**) samples. Figures **E, G , I** and **K** represent forward scatter and **F, H, J** and **L** represent side scatter profiles, comparing negative control (red) and E7#1 (green; **E, F**), E7#2 (green; **G, H**), E7#3 (green; **I, J**) or E7#4 (green; **K, L**) siRNA samples. Forward scatter is proportional to cell size, increased cell size increased forward scatter signal. Side scatter is proportional to cellular granularity, increased granularity increased side scatter signal. Data from one experiment of three performed is presented as a representation of data obtained.

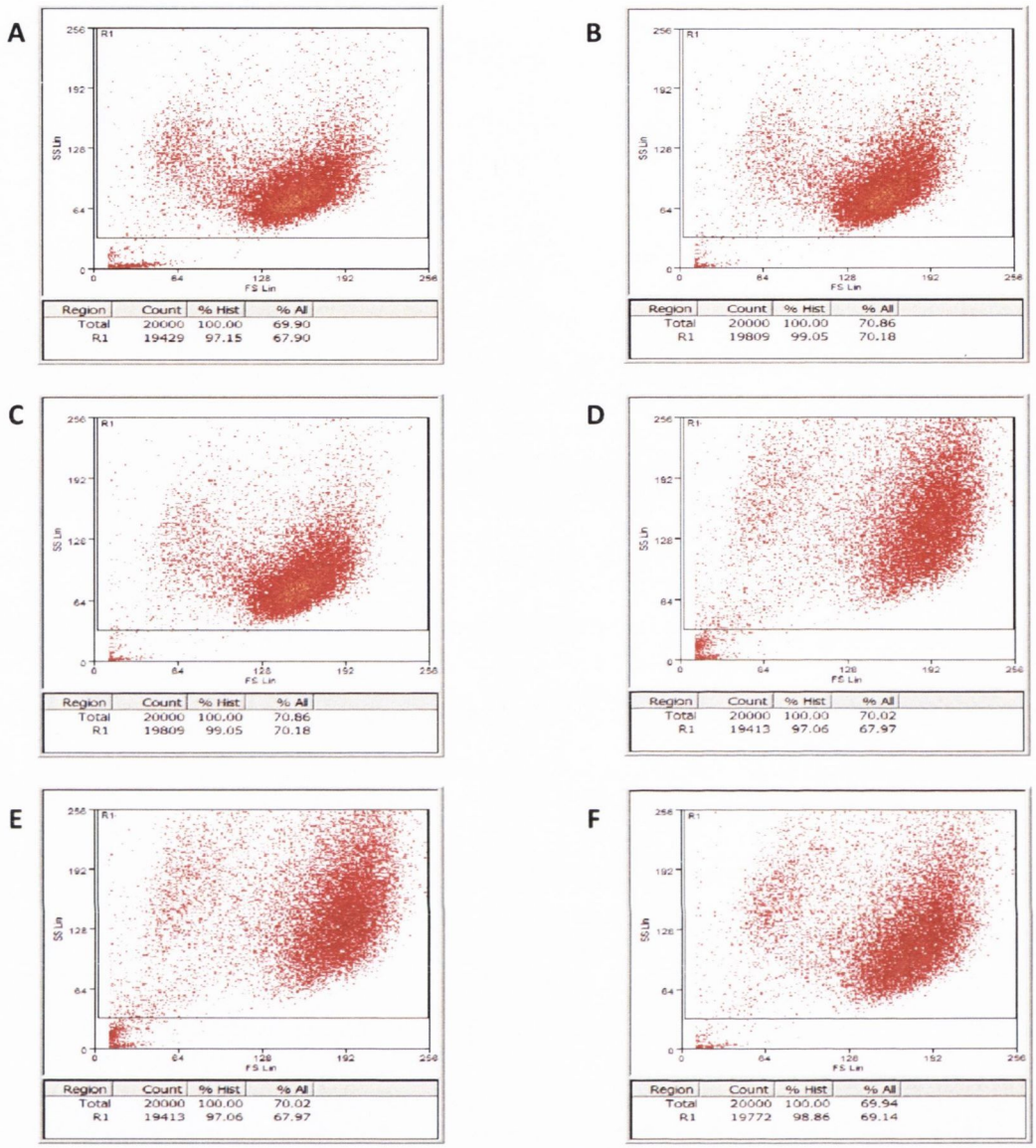


**Figure 3.20: Representative fluorocytograms of side versus forward scatter analysis of SiHa cells 96hrs post siRNA treatment.** SiHa cells ($1.5x10^5$) were left untreated **(A)**, mock-transfected **(B)**, transfected with negative control **(C)**, or transfected with E7 siRNA #1 **(D)**, #2 **(E)**, #3 **(F)** or #4 **(G)**. After 96hrs incubation all cells were collected, stained with FITC labelled annexin V and PI and analysed by flow cytometry. The dual parametric dot plots combine side and forward scatter profiles of the cells. Side scatter (vertical axis) is proportional to cellular granularity/complexity, the more within the cell, the greater the light scatter and the higher the detected signal. Cell size is proportional to Forward scatter (horizontal axis), the larger the cell the greater the light scatter and the higher the detected signal. Data from one complete experiment is presented.

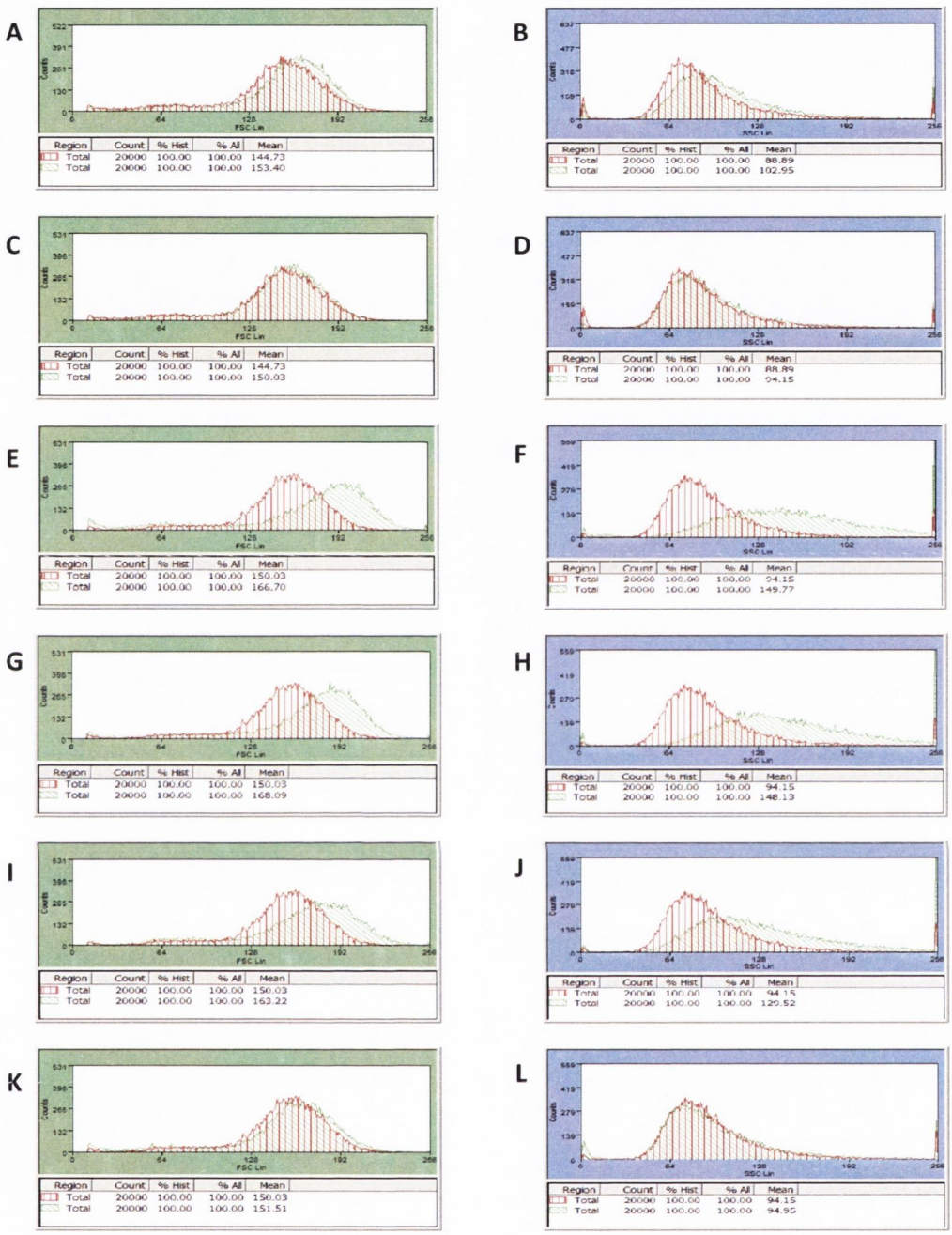


**Figure 3.21: Representative graphs of side scatter and forward scatter profiles of SiHa cells 96hrs post siRNA treatment.** SiHa cells ($1.5x10^5$) were left untreated, mock-transfected, transfected with negative control or transfected with E7 siRNA (#1 - #4). After 96hrs incubation all cells were collected, stained with FITC labelled annexin V and PI and analysed by flow cytometry. Figures **A** and **C** represent forward scatter and **B** and **D** represent side scatter profiles, comparing untreated (red) and mock-transfected (green; **A, B**) or negative control (green; **C, D**) samples. Figures **E, G , I** and **K** represent forward scatter and **F, H, J** and **L** represent side scatter profiles, comparing negative control (red) and E7#1 (green; **E, F**), E7#2 (green; **G, H**), E7#3 (green; **I, J**) or E7#4 (green; **K, L**) siRNA samples. Forward scatter is proportional to cell size, increased cell size increased forward scatter signal. Side scatter is proportional to cellular granularity, increased granularity increased side scatter signal. Data from one experiment of three performed is presented as a representation of data obtained.

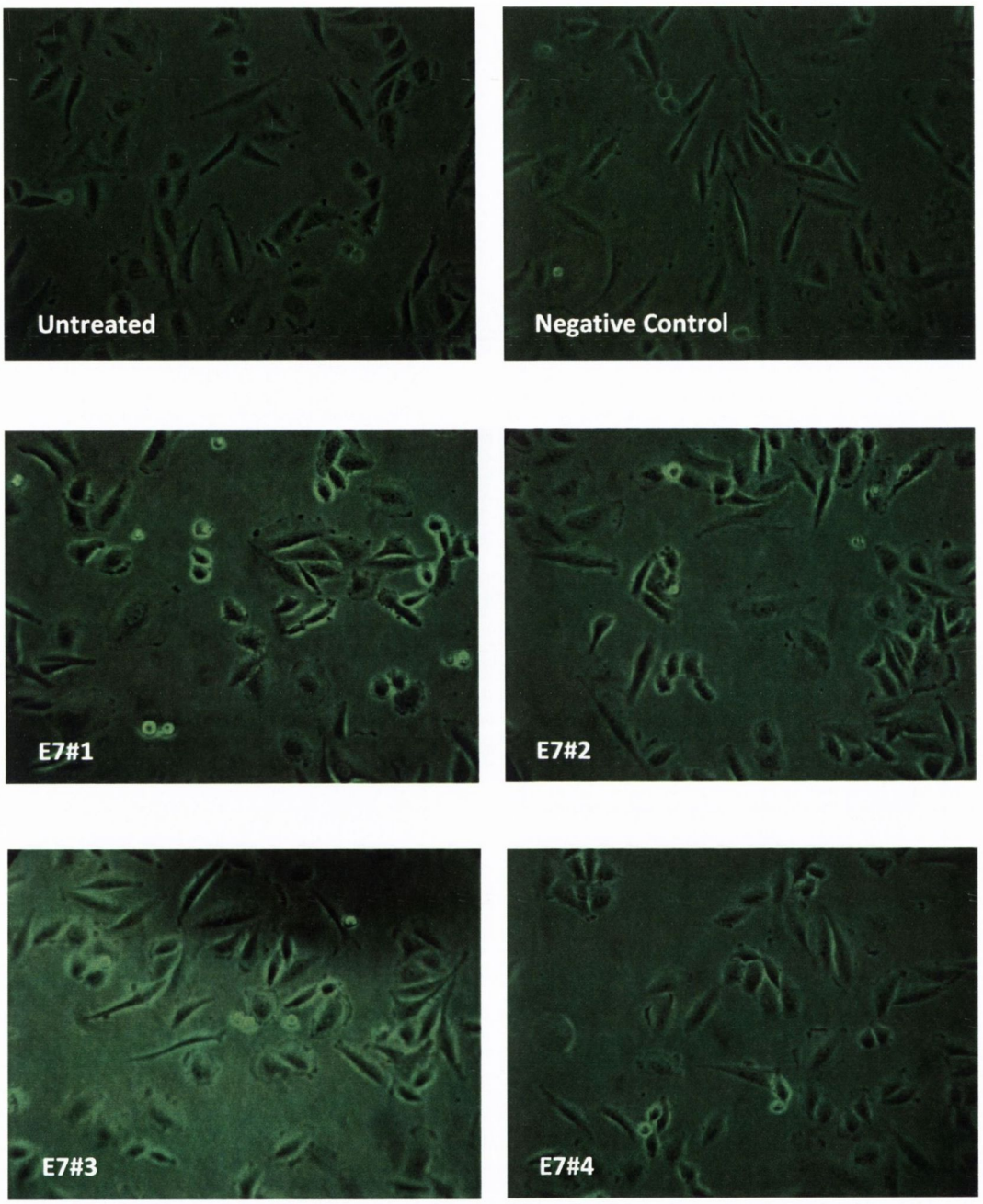


**Figure 3.22: Light microscopic findings 24hrs post transfection.** SiHa cells ($1.5x10^5$) were left untreated, mock-transfected, transfected with negative control or transfected with E7 siRNA (#1 - #4). After 25hrs incubation, cells were examined by light microscopy. There are no major morphology differences between any of the cells at this time point. All appear to have similar morphological characteristics. (Magnification 200x)

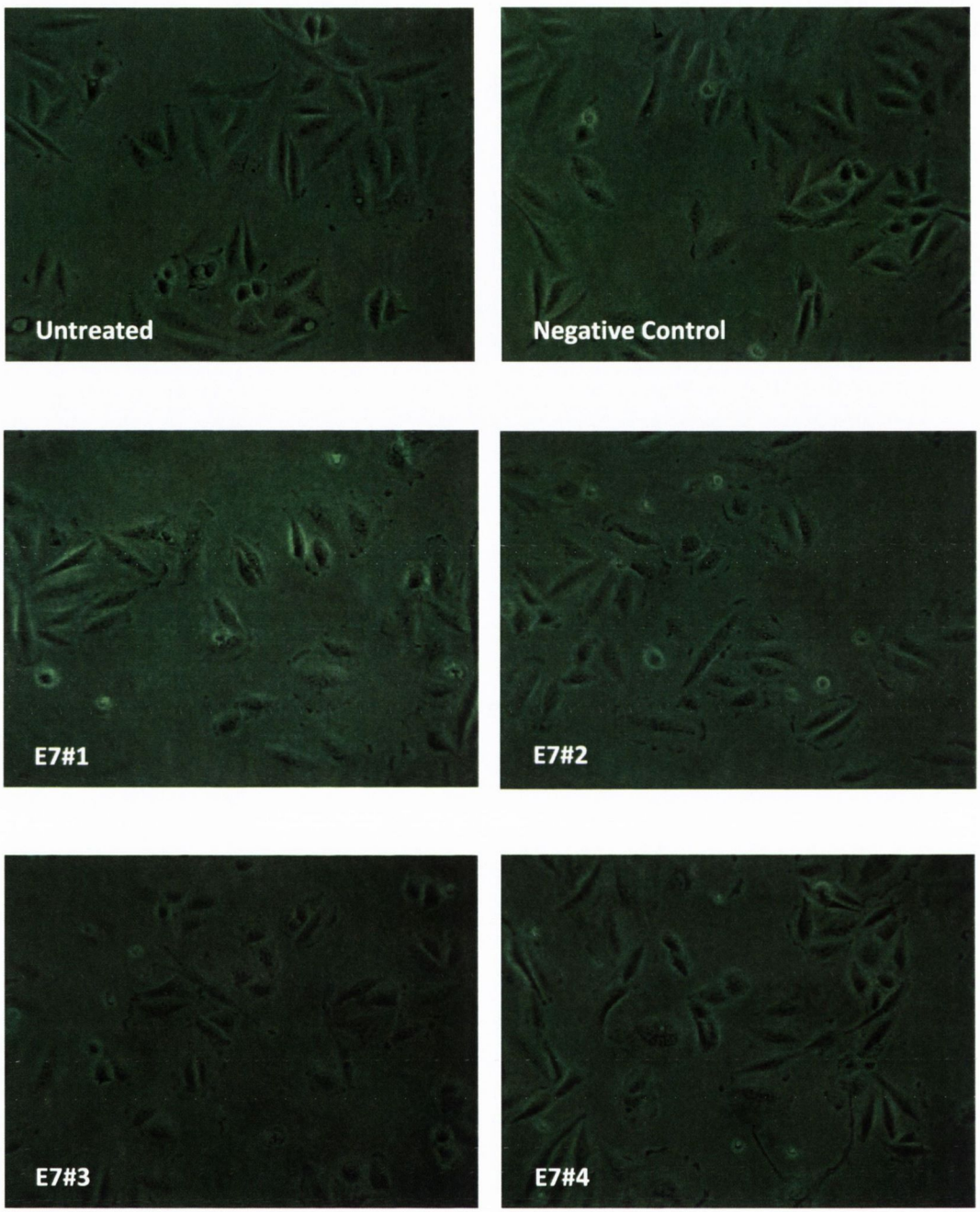


**Figure 3.23: Light microscopic findings 48hrs post transfection.** SiHa cells ($1.5x10^5$) were left untreated, mock-transfected, transfected with negative control or transfected with E7 siRNA (#1 - #4). After 48hrs incubation, cells were examined by light microscopy. There are no morphology differences between untreated and negative control transfected cells. Cells treated with E7#1 and E7#2 siRNA seem to have slightly altered morphological phenotype compared to those of untreated and negative control cells. The cytoplasm of these cells appears more granular and fewer cells are forming tight cell-cell contacts. The morphology of cells transfected with E7#3 and E7#4 appears similar to that of the negative control. (Magnification 200x)

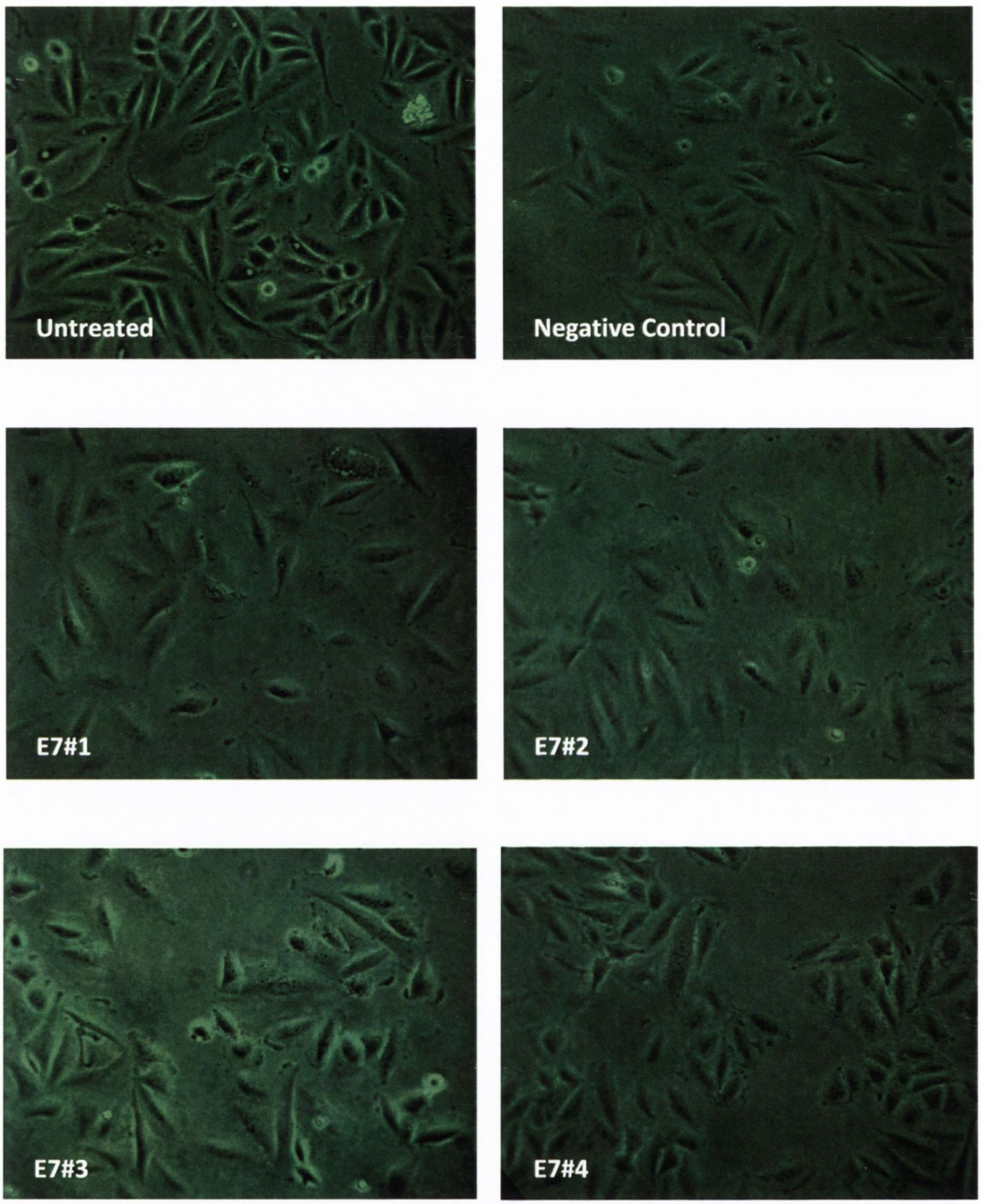


**Figure 3.24: Light microscopic findings 72hrs post transfection.** SiHa cells ($1.5x10^5$) were left untreated, mock-transfected, transfected with negative control or transfected with E7 siRNA (#1 - #4). After 72hrs incubation, cells were examined by light microscopy. There are no morphology differences between untreated and negative control transfected cells. Cells treated with E7#1 and E7#2 siRNA have significantly altered morphological characteristics to those of untreated and negative control cells. These cells are no longer forming tight cell-cell contacts; appear larger, flatter and more granular. Cells transfected with E7#3 and E7#4 neither have the morphology of the control cells or that of E7#1 and E7#2 transfected cells. In comparison to the negative control their cytoplasm appears more granular and fewer cells are forming tight cell-cell contacts. (Magnification 200x)

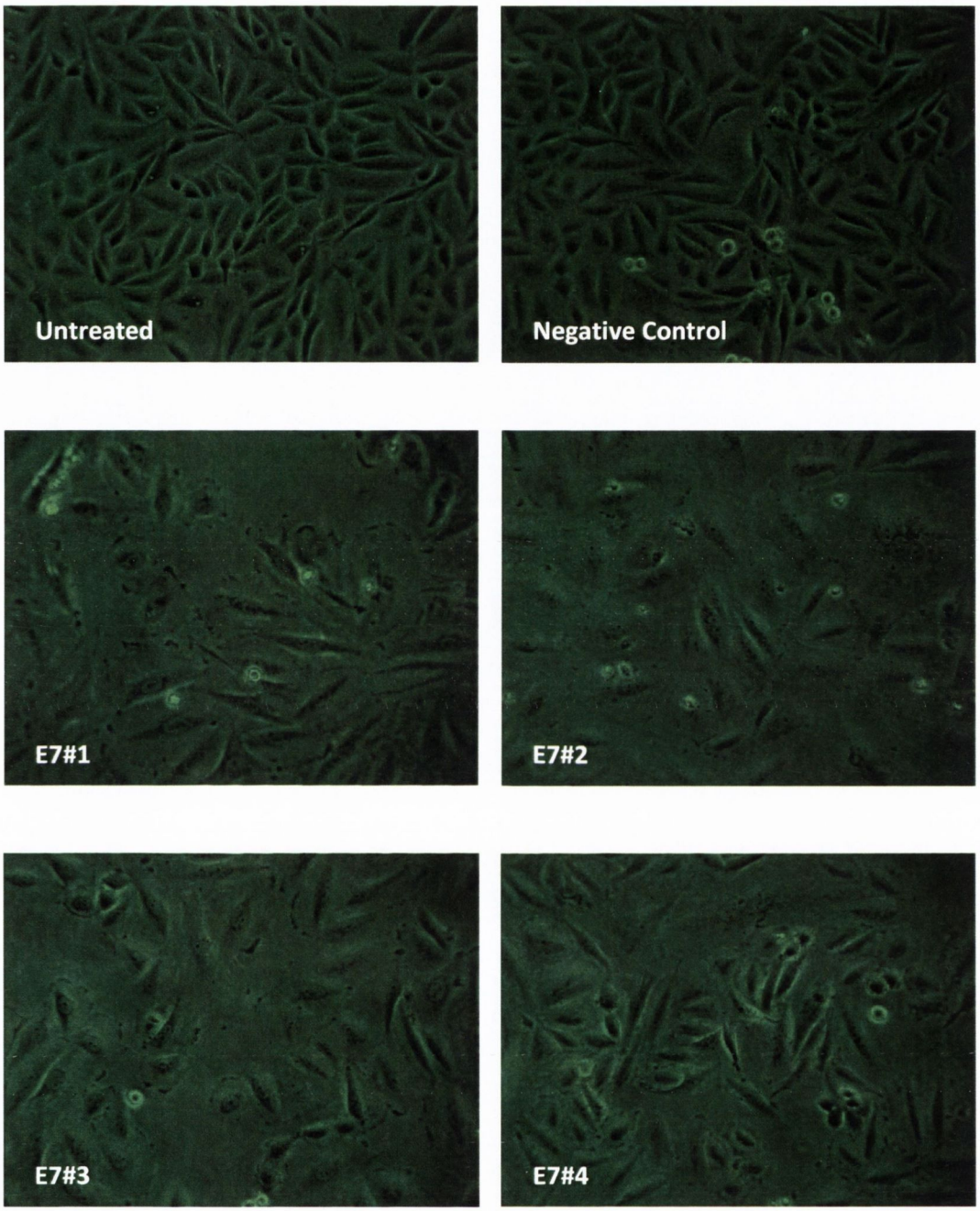


**Figure 3.25: Light microscopic findings 96hrs post transfection.** SiHa cells ($1.5x10^5$) were left untreated, mock-transfected, transfected with negative control or transfected with E7 siRNA (#1 - #4). After 96hrs, incubation cells were examined by light microscopy. There are no morphology differences between untreated and negative control transfected cells. Cells treated with E7 siRNA have significantly altered morphological characteristics to those of untreated and negative control cells. The cells are no longer forming tight cell-cell contacts, appear larger, flatter, more granular and have even adopted a slightly more elongated morphology. (Magnification 200x)

## 3.5 Discussion

The objective of this work, was to develop an *in vitro* system to concomitantly suppress the expression of the HPV oncogenes, E6 and E7. It was proposed that the established system would then become the basis for future studies, for example to identify novel intracellular functions of E6 and E7 (as described in Chapter 4). The system developed needed to specifically target the HPV oncogenes and be highly reproducible. Since its discovery in 1998, RNAi technology has rapidly become the cornerstone of gene functional studies due to its unparalleled specificity and reproducibility, and thus was deemed the ideal technology base for this work.

Throughout this study, particular consideration was given to control utilisation, as off-target effects, due to non-specific activities of siRNA, have become an increasingly important issue when using RNAi technology (discussed in Section 3.1). It is accepted that the lower the concentration of siRNA introduced into a system the lower the relative risk of inducing an off-target event. As transfection agent efficiency impacts directly on the concentration of siRNA necessary to achieve efficient silencing and since no prior transfection protocols had been performed in this laboratory, an initial step in this study was to identify an optimal transfection agent for both high risk HPV16 and 18 infected cervical cancer cell line systems. As described in section 3.4.1.1 Lipofectamine™ RNAiMax produced a high level of transfection efficiency with minimal toxicity. The second consideration was a negative control, which is seen as an essential control to establish for RNAi experiments. A negative control siRNA should activate the RNAi machinery but have no sequence similarity to any gene within the system. By comparing experimental siRNA to negative control siRNA results, one can eliminate intracellular changes associated with the activation of the RNAi pathway rather than the specific suppression of the target gene. Many commercially available human negative controls exist and through careful assessment, one such siRNA was identified which did not impact on HPV infected cervical cancer systems. Having established the optimal basic requirements for RNAi, transfection agent and negative control siRNA, in both HPV16 and 18 infected cells, it was decided to focus on silencing the HPV

oncogenes in a HPV16 infected cervical cell system, as it is the predominant HPV type identified in cervical cancer neoplasia (Clifford *et al.*, 2003; Muñoz *et al.*, 2003). Since different siRNA of the same gene have dramatically variable silencing capabilities, multiple siRNA were designed towards the HPV16 E7 oncogene. In total, five siRNA were synthesised; a set of three that were designed in-house by means of multiple online predication tools in combination with criteria set out in the literature and a set of two that were designed by Ambion® using their Silencer® Select design protocol. By designing multiple siRNA, it was anticipated that at least two would be functional and therefore it would be possible to implement a multiplicity control.

Of the five siRNA designed, three demonstrated significant suppression of E7 expression at the RNA level; greater than 70% reduction. E7#4 induced approximately a 50% reduction in expression and E7#5 was found to be non-functional. By designing the siRNA to target the E7 oncogene, the intention was to induce a concomitant silencing of E6 and E7. In 2002, Jiang and Milner published the very first report in which siRNA were applied to HPV infected cervical cancer cells. In this study, E6 and E7 siRNA were demonstrated to specifically inhibit the expression of the particular oncogene to which they were targeted without any crossover effect. Since this initial study, several papers have been published examining the consequence of treating either HPV18 or HPV16 infected cells with E6 and/or E7 siRNA both *in vitro* and *in vivo* (Bai *et al.*, 2006; Koivusalo *et al.*, 2006; Lea *et al.*, 2007; Sima *et al.*, 2008; Yamato *et al.*, 2003; Yamato *et al.*, 2008; Yoshinouchi *et al.*, 2003). While some have induced exclusive silencing of E6 (Koivusalo *et al.*, 2006; Yamato *et al.*, 2003) none have been able to repeat the specific suppression of E7 (Lea *et al.*, 2007; Sima *et al.*, 2008; Yamato *et al.*, 2008; Yoshinouchi *et al.*, 2003). The selective silencing of E7 observed by Jiang and Milner is hard to resolve and in fact the results of the subsequent studies are far easier to explain, as E7 mRNA is unspliced and stems from the bicistonic E6/E7 mRNA transcript (Stacey *et al.*, 2000; Stacey *et al.*, 1995). The four active siRNA in this study reduced the expression levels of E6 to the same degree as E7. Thus this work supports the previous findings that targeting E7 results in an effective concomitant silencing of E7 and E6 mRNA.

While it has been demonstrated that E7 can be translated equally and efficiently from either E6 or its splice variant E6*I (Stacey *et al.*, 1995), recent evidence suggest that E6*I mRNA transcripts of high-risk HPV are predominantly responsible for the production of E7 (Tang *et al.*, 2006). In addition, it has been demonstrated *in vivo* and *in vitro* that the majority of E6 transcripts are E6*I mRNAs, although unspliced full-length E6 mRNAs can also be detected (Smotkin and Wettstein 1986; Tang *et al.*, 2006; Zheng and Baker 2006). To confirm that the E7 siRNA suppressed the expression of full-length E6, TaqMan® RT-PCR primers and probes specific for full-length E6 were designed. Figure 3.10 demonstrates that though there is an increase in the remaining expression levels of full-length E6 compared to E6/E6*I expression, it is minor and that the majority of full-length E6 is lost. Therefore the system developed, silences both HPV oncogenes with equal efficiency at the transcriptome level.

No high-quality anti-E6 or E7 antibodies for HPV16 were available during the course of the study. Instead, accumulation of hypophosphorylated Rb and stabilization of cellular p53 protein was used as an indication of the siRNA mediated suppression of E7 and E6 respectively. In addition, the expression level of p21 a transcriptional target and effector molecule of p53 was also determined. All four active siRNA induced an accumulation of hypophosphorylated Rb, p53 and p21. There was however, considerable variation to the extent to which this occurred, particularly evident with p53 and p21 accumulation. As was anticipated from their activity at the RNA level, the E7#4 siRNA had the smallest effect, with the Ambion® designed siRNA E7#1 and E7#2 having a significant effect at the protein level. Surprisingly, E7#3 though it induced the largest reduction in E7 and E6 mRNA expression, did not have a corresponding significant effect at the protein level. Indeed, the activity of this siRNA at the protein level appeared to be close to half that of the E7#1 and E7#2 siRNA. This observation was substantiated by the flow cytometry analysis, where the impact of the E7#3 siRNA was always higher than E7#4, but considerably less than that of E7#1 and E7#2. This result was not anticipated and thus far no definitive explanation has been identified. The accuracy of the TaqMan® RT-PCR data is evidenced by the low standard deviation across six biological replicates (Figure 3.10). One possibility is that in comparison to the

E7#1 and E7#2 siRNA, E7#3 does not reach its maximum activity as efficiently and/or rapidly, such that by 48hrs post-transfection while having induced a highly significant reduction in mRNA expression, this has not yet been translated to the proteome. A reason for this might be, that instead of solely incorporating the antisense strand into the RISC complex, the sense strand is also been incorporated thus reducing the number of RISC/antisense complexes capable of inducing oncogene suppression. Perhaps in addition, secondary structure either relating to the siRNA itself or the target mRNA is delaying the speed at which the silencing events can occur. However, it is less likely to be an mRNA secondary structure issue as E7#3 and E7#2 target overlapping regions.

Studies using antisense oligonucleotides, ribozymes, E2 expression vectors, and siRNAs have revealed that inhibition of E6 and E7 expression is sufficient to cause growth suppression of HPV-related cancer cells (Alvarez-Salas *et al.*, 1998; Butz *et al.*, 2003; Chen *et al.*, 1996; DeFilippis *et al.*, 2003; Gu *et al.*, 2006; Hall and Alexander 2003; Hwang *et al.*, 1993; Jiang an Milner 2002; Niu *et al.*, 2006; Thierry and Howley 1991; Venturini *et al.*, 1999). In this present study, all four functional siRNA induced a reduction in cellular proliferation, which was associated with an increase in the cell numbers in the G1 phase of the cell cycle and a decrease in the S phase. The Ambion® designed siRNA, E7#1 and E7#2, had the most pronounced effect, nearly completely obliterating the S phase of the cell cycle. Parallel with this G1 arrest were alterations in the morphology of the cells transfected with the E7 siRNA. These cells appeared larger, flatter, and more granular, and they were no longer forming tight cell-cell contacts as compared to their negative control counterparts. These findings were supported by flow cytometry analysis where there was an increase in both forward and side scatter profiles of E7 siRNA transfected cells, indicating an increase in size and cellular granularity respectively. By 96hrs post-transfection, all four siRNA were demonstrating very different phenotype characteristics. However, similar to the cell cycle analysis performed, these morphological changes were more pronounced in cells transfected with the E7#1 and E7#2 siRNA. Indeed at 48hrs post-transfection, it was becoming evident that the cells transfected with these siRNA had an altered phenotype to the

negative control, but it was not until 72hrs that the other two siRNA, E7#3 and E7#4, showed signs of a difference. Thus, there was an interlinking time and potency dependent increase in these morphological effects. The time dependent increase in the level of change would suggest that the silencing of E6 and E7 initiates an irreversible process of change within these cells. The fact that siRNA with minimal activity, i.e. E7#4, can also induce this time dependent process, would indicate that this is a preferential phenotype for the cells which is inhibited normally by the expression of E6 and E7.

While over a 96hr period there were decreases in the cell proliferation and alterations in cellular morphology in cells transfected with E7 targeting siRNA, there was no equivalent increase in the apoptotic profile of the cells. However, the annexin V-FITC and PI flow cytometry analysis performed to determine the apoptotic profile of the cells did demonstrate that there was a shift in the fluorescent profile of the cells. The level of this alteration corresponded with the observed potency of the siRNA at the protein level and increased with time. A study in 2003, by DeFilippis *et al.* demonstrated that in HPV18 infected cervical cancer cells, the re-introduction of bovine papillomavirus (BPV) E2 gene repressed the expression of E6 and E7. This inhibition of oncogene expression induced cell growth arrest and markers of senescence, including autofluorescence of the cells. This study also performed annexin V-FITC and PI counter staining of the cells and observed a similar shift in the fluorescent profile of the cells in the lower left quadrant after the suppression of E6 and E7 expression as was seen in this study (Figure 3.26). This shift was attributed to the higher fluorescence of senescent cells. It is interesting to postulate that the change observed in this study is also due to cellular autofluorescence and potentially the result of cellular senescence.

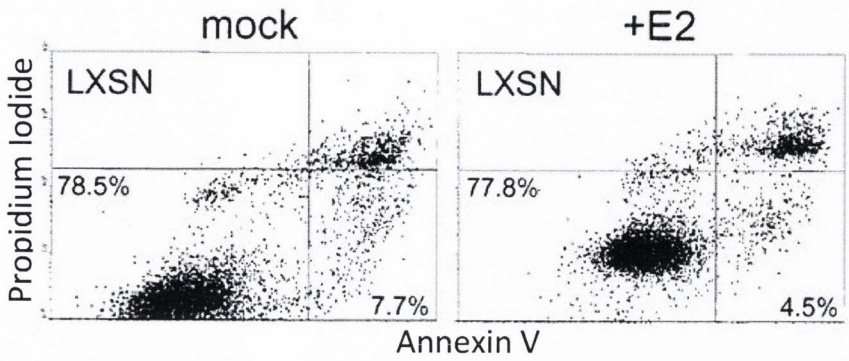


**Figure 3.26: Effect of repressing HPV E6 and E7 genes on apoptosis.** HeLa were assayed by flow cytometry for annexin V-FITC binding and propidium iodide staining 6 days after infection with the BPV E2 viral gene or mock transfected. Reproduced and modified from DeFilippis *et al.*, 2003.

Cellular senescence, is the phenomenon by which cells permanently and irreversibly lose the ability to undergo cell division. Senescent cells are observed to arrest in the G1 phase of the cell cycle and display distinctive phenotypic and biochemical properties; including an enlarged and flattened morphology, loss of contact inhibition, increased cytoplasmic granularity, cell autofluorescence, expression of senescence-associated-β-galactosidase (SA-β-gal) and resistance to apoptotic stimuli (Campisi *et al.*, 2007; Dimri *et al.*, 1995; Sedivy, 1998). Many of these characteristics are observed in this study in the SiHa cells post-transfection with the E7 siRNA. Senescence is a potent anti-cancer mechanism, controlled by tumour suppressor genes, in particular p53 and Rb (Shay *et al.*, 1991), and induced by DNA damage, oncogenic stimulation or excessive mitogenic signalling (Bartek *et al.*, 2007; Bartkova *et al.*, 2006). Therefore, it would seem plausible that such a phenotype would be induced upon suppression of HPV oncogene expression. Indeed, in addition to the numerous studies that have demonstrated senescence post E2 re-expression and E6/E7 repression (DeFilippis *et al.* 2003; Goodwin and DiManio, 2001; Lee *et al.*, 2002; Wells *et al.*, 2000; Wells *et al.*, 2003), a number of studies that silenced the expression of the HPV oncogenes simultaneously with siRNA, also observed senescent properties in these cells (Hall and Alexander,

2003; Kuner *et al.*, 2007; Putral *et al.*, 2005; Yamato *et al.*, 2008). These findings are not unexpected, as they are consistent with the situation in normal cervical epithelial cells, which undergo irreversible senescence and differentiation as part of their normal life cycle.

There is much debate in the literature over the phenotypic outcome post knockdown of either or both HPV oncogenes. This study has demonstrated that the concurrent silencing of HPV16 E6 and E7 decreases cell proliferation through a G1 cell cycle arrest but does not induce an apoptotic response. Therefore, it falls in line with several previous studies that demonstrated E6 and/or E7 silencing results in inhibition of cellular proliferation but not apoptosis (Bai *et al.*, 2006; Hall and Alexander, 2003; Koivusalo *et al.*, 2005; Kuner *et al.*, 2007; Putral *et al.*, 2005; Yamato *et al.*, 2008; Yoshinouchi *et al.*, 2003) and is in contrast to others which have demonstrated that siRNA targeting one or both HPV oncogenes induces apoptosis in the transfected cells (Butz *et al.*, 2003; Jiang and Milner,2002; Jonson *et al.*, 2008; Lea *et al.*, 2007; Sima *et al.*, 2008; Yamato *et al.*, 2006). The discrepancy between these studies has not yet been deciphered conclusively, but several suggestions have been put forward. Firstly, the range of the cell lines used as well as the use of *in vivo* models would eliminate the idea that HPV type specific consequences maybe involved. An initial suggestion was that for apoptosis to occur, the specific silencing of E6 is required, allowing continuous E7 expression which would maintain a pro-apoptotic environment (Butz *et al.*, 2003). However, in conflict with this theory, is the fact that a number of the pro-apoptotic studies are based on the silencing of both oncogenes (Jonson *et al.*, 2008; Lea *et al.*, 2007; Sima *et al.*, 2008). Nonetheless, this premise may be partially correct; potentially rather than requiring the expression of E7, what is necessary is a pro-apoptotic signal. Koivusalo *et al.*, found that if E6 is inhibited under non-stress conditions, the p53 degradation machinery quickly reverses the activation of this increase in p53 function, therefore reducing the possibility of an apoptotic phenotype (Koivusalo *et al.*, 2003; Koivusalo *et al.*, 2006). One mechanism which may potentiate a stress environment is the exposure of cells to high doses of siRNA. Indeed Gu *et al.*, demonstrated *in vivo* that the delivery of high doses and not low doses of siRNA inhibited tumour growth via

apoptosis (Gu *et al.*, 2006). The above mentioned studies which induced apoptosis post transient transfection with siRNA targeting E6 and/or E7 expression all used doses in the 100nM range, which would be consider high by today's standards and as "harsh" conditions of cell transfection.

The results of this chapter demonstrate, as other studies have, that silencing of the HPV viral oncogenes, E6 and E7, induces cell cycle arrest and potentially cellular senescence. This study has used only 10nM of siRNA, which is considerably less than most of the previous studies and has also paid particular consideration to the inclusion of appropriate controls. Since for the purpose of applying siRNA technology to therapy it is mandatory to select siRNA sequences targeting E6 and E7 that have high levels of RNAi activity and minimal off-target effects. These siRNA meet these criteria and lend further support to the concept of RNAi therapy in a cervical cancer setting. It would be optimal to use siRNA targeted towards these oncogenes as a sole therapeutic, eliminating the need for traditional non-HPV therapies. However if the efficacy was not optimal, a combinational approach between siRNA and traditional therapies could be another alternative. Indeed, two independent studies have taken this approach, pretreating cells with E6 siRNA before applying chemotherapeutic agents (Koivusalo *et al.*, 2005; Putral *et al.*, 2005). They found that reactivation of the dormant p53 pathway by RNAi, sensitised cervical cancer cells to the antitumour activity of the chemotherapeutic agents. These findings suggest RNAi may have potential in the treatment of cervical cancer when used as an adjunct to chemotherapy.

## 3.6 References

Amarzguioui, Mohammed, and Hans Prydz. 2004. An algorithm for selection of functional siRNA sequences. *Biochemical and Biophysical Research Communications* 316, no. 4 (April 16): 1050-1058.

Anon. 2003. Whither RNAi? *Nature Cell Biology* 5, no. 6 (June): 489-490.

Bagga, Shveta, John Bracht, Shaun Hunter, Katlin Massirer, Janette Holtz, Rachel Eachus, and Amy E Pasquinelli. 2005. Regulation by let-7 and lin-4 miRNAs results in target mRNA degradation. *Cell* 122, no. 4 (August 26): 553-563.

Bai, L, L Wei, J Wang, X Li, and P He. 2006. Extended effects of human papillomavirus 16 E6-specific short hairpin RNA on cervical carcinoma cells. *International Journal of Gynecological Cancer: Official Journal of the International Gynecological Cancer Society* 16, no. 2 (April): 718-729.

Bartek, J, J Bartkova, and J Lukas. 2007. DNA damage signalling guards against activated oncogenes and tumour progression. *Oncogene* 26, no. 56 (December 10): 7773-7779.

Bertrand, Jean-Rémi, Mireille Pottier, Antoine Vekris, Paule Opolon, Andrei Maksimenko, and Claude Malvy. 2002. Comparison of antisense oligonucleotides and siRNAs in cell culture and in vivo. *Biochemical and Biophysical Research Communications* 296, no. 4 (August 30): 1000-1004.

Birmingham, Amanda, Emily M Anderson, Angela Reynolds, Diane Ilsley-Tyree, Devin Leake, Yuriy Fedorov, Scott Baskerville, et al. 2006. 3' UTR seed matches, but not overall identity, are associated with RNAi off-targets. *Nature Methods* 3, no. 3 (March): 199-204.

Butz, Karin, Tutik Ristriani, Arnd Hengstermann, Claudia Denk, Martin Scheffner, and Felix Hoppe-Seyler. 2003. siRNA targeting of the viral E6 oncogene efficiently kills human papillomavirus-positive cancer cells. *Oncogene* 22, no. 38 (September 4): 5938-5945.

Campisi, Judith, and Fabrizio d'Adda di Fagagna. 2007. Cellular senescence: when bad things happen to good cells. *Nature Reviews. Molecular Cell Biology* 8, no. 9 (September): 729-740.

Cerutti, Heriberto. 2003. RNA interference: traveling in the cell and gaining functions? *Trends in Genetics: TIG* 19, no. 1 (January): 39-46.

Chen, Po Yu, Lasse Weinmann, Dimos Gaidatzis, Yi Pei, Mihaela Zavolan, Thomas Tuschl, and Gunter Meister. 2008. Strand-specific 5'-O-methylation of siRNA duplexes controls guide strand selection and targeting specificity. *RNA (New York, N.Y.)* 14, no. 2 (February): 263-274.

Chen, Z, P Kamath, S Zhang, L St John, K Adler-Storthz, and E J Shillitoe. 1996. Effects on tumor cells of ribozymes that cleave the RNA transcripts of human papillomavirus type 18. *Cancer Gene Therapy* 3, no. 1 (February): 18-23.

Cullen, Bryan R. 2006. Enhancing and confirming the specificity of RNAi experiments. *Nature Methods* 3, no. 9 (September): 677-681.

Dahlgren, Cecilia, Hong-Yan Zhang, Quan Du, Maria Grahn, Gunnar Norstedt, Claes Wahlestedt, and Zicai Liang. 2008. Analysis of siRNA specificity on targets with double-nucleotide mismatches. *Nucleic Acids Research* 36, no. 9 (May): e53.

DeFilippis, Rosa Anna, Edward C Goodwin, Lingling Wu, and Daniel DiMaio. 2003. Endogenous human papillomavirus E6 and E7 proteins differentially regulate proliferation, senescence, and apoptosis in HeLa cervical carcinoma cells. *Journal of Virology* 77, no. 2 (January): 1551-1563.

Denli, Ahmet M, and Gregory J Hannon. 2003. RNAi: an ever-growing puzzle. *Trends in Biochemical Sciences* 28, no. 4 (April): 196-201.

Dimri, G P, X Lee, G Basile, M Acosta, G Scott, C Roskelley, E E Medrano, M Linskens, I Rubelj, and O Pereira-Smith. 1995. A biomarker that identifies senescent human cells in culture and in aging skin in vivo. *Proceedings of the National Academy of Sciences of the United States of America* 92, no. 20 (September 26): 9363-9367.

Doench, John G, Christian P Petersen, and Phillip A Sharp. 2003. siRNAs can function as miRNAs. *Genes & Development* 17, no. 4 (February 15): 438-442.

Du, Quan, Håkan Thonberg, Jue Wang, Claes Wahlestedt, and Zicai Liang. 2005. A systematic analysis of the silencing effects of an active siRNA at all single-nucleotide mismatched target sites. *Nucleic Acids Research* 33, no. 5: 1671-1677.

Dyson, J E, J Daniel, and C R Surrey. 1992. The effect of sodium butyrate on the growth characteristics of human cervix tumour cells. *British Journal of Cancer* 65, no. 6 (June): 803-808.

Elbashir, S M, W Lendeckel, and T Tuschl. 2001. RNA interference is mediated by 21- and 22-nucleotide RNAs. *Genes & Development* 15, no. 2 (January 15): 188-200.

Elbashir, S M, J Martinez, A Patkaniowska, W Lendeckel, and T Tuschl. 2001. Functional anatomy of siRNAs for mediating efficient RNAi in Drosophila melanogaster embryo lysate. *The EMBO Journal* 20, no. 23 (December 3): 6877-6888.

Grimm, Dirk, Konrad L Streetz, Catherine L Jopling, Theresa A Storm, Kusum Pandey, Corrine R Davis, Patricia Marion, Felix Salazar, and Mark A Kay. 2006. Fatality in mice due to oversaturation of cellular microRNA/short hairpin RNA pathways. *Nature* 441, no. 7092 (May 25): 537-541.

Grünweller, Arnold, Eliza Wyszko, Birgit Bieber, Ricarda Jahnel, Volker A Erdmann, and Jens Kurreck. 2003. Comparison of different antisense strategies in mammalian cells using locked nucleic acids, 2'-O-methyl RNA, phosphorothioates and small interfering RNA. *Nucleic Acids Research* 31, no. 12 (June 15): 3185-3193.

Guapillo, Mario R, Miguel A Márquez, María L Benítez-Hess, and Luis M Alvarez-Salas. 2006. A bacterial reporter system for the evaluation of antisense oligodeoxynucleotides directed against human papillomavirus type 16 (HPV-16). *Archives of Medical Research* 37, no. 5 (July): 584-592.

Hall, Allison H S, and Kenneth A Alexander. 2003. RNA interference of human papillomavirus type 18 E6 and E7 induces senescence in HeLa cells. *Journal of Virology* 77, no. 10 (May): 6066-6069.

Heil, Florian, Hiroaki Hemmi, Hubertus Hochrein, Franziska Ampenberger, Carsten Kirschning, Shizuo Akira, Grayson Lipford, Hermann Wagner, and Stefan Bauer. 2004. Species-specific recognition of single-stranded RNA via toll-like receptor 7 and 8. *Science (New York, N.Y.)* 303, no. 5663 (March 5): 1526-1529.

Hornung, Veit, Margit Guenthner-Biller, Carole Bourquin, Andrea Ablasser, Martin Schlee, Satoshi Uematsu, Anne Noronha, et al. 2005. Sequence-specific potent induction of IFN-alpha by short interfering RNA in plasmacytoid dendritic cells through TLR7. *Nature Medicine* 11, no. 3 (March): 263-270.

Hsieh, Andrew C, Ronghai Bo, Judith Manola, Francisca Vazquez, Olivia Bare, Anastasia Khvorova, Stephen Scaringe, and William R Sellers. 2004. A library of siRNA duplexes targeting the phosphoinositide 3-kinase pathway: determinants of gene silencing for use in cell-based screens. *Nucleic Acids Research* 32, no. 3: 893-901.

Jackson, Aimee L, Steven R Bartz, Janell Schelter, Sumire V Kobayashi, Julja Burchard, Mao Mao, Bin Li, Guy Cavet, and Peter S Linsley. 2003. Expression profiling reveals off-target gene regulation by RNAi. *Nature Biotechnology* 21, no. 6 (June): 635-637.

Jagla, Bernd, Nathalie Aulner, Peter D Kelly, Da Song, Allen Volchuk, Andrzej Zatorski, David Shum, et al. 2005. Sequence characteristics of functional siRNAs. *RNA (New York, N.Y.)* 11, no. 6 (June): 864-872.

Jiang, Ming, and Jo Milner. 2002. Selective silencing of viral gene expression in HPV-positive human cervical carcinoma cells treated with siRNA, a primer of RNA interference. *Oncogene* 21, no. 39 (September 5): 6041-6048.

Judge, Adam D, Vandana Sood, Janet R Shaw, Dianne Fang, Kevin McClintock, and Ian MacLachlan. 2005. Sequence-dependent stimulation of the mammalian innate immune response by synthetic siRNA. *Nature Biotechnology* 23, no. 4 (April): 457-462.

Khvorova, Anastasia, Angela Reynolds, and Sumedha D Jayasena. 2003. Functional siRNAs and miRNAs exhibit strand bias. *Cell* 115, no. 2 (October 17): 209-216.

Kittler, Ralf, Laurence Pelletier, Chunling Ma, Ina Poser, Steffi Fischer, Anthony A Hyman, and Frank Buchholz. 2005. RNA interference rescue by bacterial artificial chromosome transgenesis in mammalian tissue culture cells. *Proceedings of the National Academy of Sciences of the United States of America* 102, no. 7 (February 15): 2396-2401.

Kleinman, Mark E, Kiyoshi Yamada, Atsunobu Takeda, Vasu Chandrasekaran, Miho Nozaki, Judit Z Baffi, Romulo J C Albuquerque, et al. 2008. Sequence- and target-independent angiogenesis suppression by siRNA via TLR3. *Nature* 452, no. 7187 (April 3): 591-597.

Koivusalo, Riku, Eberhard Krausz, Hans Helenius, and Sakari Hietanen. 2005. Chemotherapy compounds in cervical cancer cells primed by reconstitution of p53 function after short interfering RNA-mediated degradation of human papillomavirus 18 E6 mRNA: opposite effect of siRNA in combination with different drugs. *Molecular Pharmacology* 68, no. 2 (August): 372-382.

Koivusalo, Riku, Eberhard Krausz, Pertti Ruotsalainen, Hans Helenius, and Sakari Hietanen. 2002. Chemoradiation of cervical cancer cells: targeting human papillomavirus E6 and p53 leads to either augmented or attenuated apoptosis depending on the platinum carrier ligand. *Cancer Research* 62, no. 24 (December 15): 7364-7371.

Koivusalo, Riku, Antoine Mialon, Hanna Pitkänen, Jukka Westermarck, and Sakari Hietanen. 2006. Activation of p53 in cervical cancer cells by human papillomavirus E6 RNA interference is transient, but can be sustained by inhibiting endogenous nuclear export-dependent p53 antagonists. *Cancer Research* 66, no. 24 (December 15): 11817-11824.

Lea, Jayanthi S, Noriaki Sunaga, Mitsuo Sato, Geetha Kalahasti, David S Miller, John D Minna, and Carolyn Y Muller. 2007. Silencing of HPV 18 oncoproteins With RNA interference causes growth inhibition of cervical cancer cells. *Reproductive Sciences (Thousand Oaks, Calif.)* 14, no. 1 (January): 20-28.

Marques, Joao T, and Bryan R G Williams. 2005. Activation of the mammalian immune system by siRNAs. *Nature Biotechnology* 23, no. 11 (November): 1399-1405.

Marques, Joao Trindade, Thalie Devosse, Die Wang, Maryam Zamanian-Daryoush, Paul Serbinowski, Rune Hartmann, Takashi Fujita, Mark A Behlke, and Bryan R G Williams. 2006. A structural basis for discriminating between self and nonself double-stranded RNAs in mammalian cells. *Nature Biotechnology* 24, no. 5 (May): 559-565.

Martinez, Javier, Agnieszka Patkaniowska, Henning Urlaub, Reinhard Lührmann, and Thomas Tuschl. 2002. Single-stranded antisense siRNAs guide target RNA cleavage in RNAi. *Cell* 110, no. 5 (September 6): 563-574.

Miyagishi, Makoto, Mariko Hayashi, and Kazunari Taira. 2003. Comparison of the suppressive effects of antisense oligonucleotides and siRNAs directed against the same targets in mammalian cells. *Antisense & Nucleic Acid Drug Development* 13, no. 1 (February): 1-7.

Muñoz, Nubia, F Xavier Bosch, Silvia de Sanjosé, Rolando Herrero, Xavier Castellsagué, Keerti V Shah, Peter J F Snijders, and Chris J L M Meijer. 2003. Epidemiologic classification of human papillomavirus types associated with cervical cancer. *The New England Journal of Medicine* 348, no. 6 (February 6): 518-527.

Nature editorial. 2003. Whither RNAi? *Nature Cell Biology* 5, no. 6 (June): 489-490. doi:10.1038/ncb0603-490.

Patzel, Volker, Sascha Rutz, Isabell Dietrich, Christian Köberle, Alexander Scheffold, and Stefan H E Kaufmann. 2005. Design of siRNAs producing unstructured guide-RNAs results in improved RNA interference efficiency. *Nature Biotechnology* 23, no. 11 (November): 1440-1444.

Phipps, Krista M, Alejandro Martinez, Jin Lu, Beverly A Heinz, and Genshi Zhao. 2004. Small interfering RNA molecules as potential anti-human rhinovirus agents: in vitro potency, specificity, and mechanism. *Antiviral Research* 61, no. 1 (January): 49-55.

Putral, Lisa N, Megan J Bywater, Wenyi Gu, Nicholas A Saunders, Brian G Gabrielli, Graham R Leggatt, and Nigel A J McMillan. 2005. RNA interference against human papillomavirus oncogenes in cervical cancer cells results in increased sensitivity to cisplatin. *Molecular Pharmacology* 68, no. 5 (November): 1311-1319.

Reynolds, Angela, Devin Leake, Queta Boese, Stephen Scaringe, William S Marshall, and Anastasia Khvorova. 2004. Rational siRNA design for RNA interference. *Nature Biotechnology* 22, no. 3 (March): 326-330.

Saxena, Sandeep, Zophonías O Jónsson, and Anindya Dutta. 2003. Small RNAs with imperfect match to endogenous mRNA repress translation. Implications for off-target activity of small inhibitory RNA in mammalian cells. *The Journal of Biological Chemistry* 278, no. 45 (November 7): 44312-44319.

Scheffner, M, B A Werness, J M Huibregtse, A J Levine, and P M Howley. 1990. The E6 oncoprotein encoded by human papillomavirus types 16 and 18 promotes the degradation of p53. *Cell* 63, no. 6 (December 21): 1129-1136.

Schlee, Martin, Veit Hornung, and Gunther Hartmann. 2006. siRNA and isRNA: two edges of one sword. *Molecular Therapy: The Journal of the American Society of Gene Therapy* 14, no. 4 (October): 463-470.

Schwarz, Dianne S, György Hutvágner, Tingting Du, Zuoshang Xu, Neil Aronin, and Phillip D Zamore. 2003a. Asymmetry in the assembly of the RNAi enzyme complex. *Cell* 115, no. 2 (October 17): 199-208.

Sedivy, J M. 1998. Can ends justify the means?: telomeres and the mechanisms of replicative senescence and immortalization in mammalian cells. *Proceedings of the National Academy of Sciences of the United States of America* 95, no. 16 (August 4): 9078-9081.

Shabalina, Svetlana A, Alexey N Spiridonov, and Aleksey Y Ogurtsov. 2006. Computational models with thermodynamic and composition features improve siRNA design. *BMC Bioinformatics* 7: 65.

Shay, J W, O M Pereira-Smith, and W E Wright. 1991. A role for both RB and p53 in the regulation of human cellular senescence. *Experimental Cell Research* 196, no. 1 (September): 33-39.

Sima, Ni, Wei Wang, Debo Kong, Dongrui Deng, Qian Xu, Jianfeng Zhou, Gang Xu, et al. 2008. RNA interference against HPV16 E7 oncogene leads to viral E6 and E7 suppression in cervical cancer cells and apoptosis via upregulation of Rb and p53. *Apoptosis: An International Journal on Programmed Cell Death* 13, no. 2 (February): 273-281.

Sioud, Mouldy, and Dag R Sørensen. 2003. Cationic liposome-mediated delivery of siRNAs in adult mice. *Biochemical and Biophysical Research Communications* 312, no. 4 (December 26): 1220-1225.

Smotkin, D, and F O Wettstein. 1986. Transcription of human papillomavirus type 16 early genes in a cervical cancer and a cancer-derived cell line and identification of the E7 protein. *Proceedings of the National Academy of Sciences of the United States of America* 83, no. 13 (July): 4680-4684.

Stacey, S N, D Jordan, P J Snijders, M Mackett, J M Walboomers, and J R Arrand. 1995. Translation of the human papillomavirus type 16 E7 oncoprotein from bicistronic mRNA is independent of splicing events within the E6 open reading frame. *Journal of Virology* 69, no. 11 (November): 7023-7031.

Stein, C A. 2001. Antisense that comes naturally. *Nature Biotechnology* 19, no. 8 (August): 737-738.

Tang, Shuang, Mingfang Tao, J Philip McCoy, and Zhi-Ming Zheng. 2006. The E7 oncoprotein is translated from spliced E6*I transcripts in high-risk human papillomavirus type 16- or type 18-positive cervical cancer cell lines via translation reinitiation. *Journal of Virology* 80, no. 9 (May): 4249-4263.

Thierry, F, and P M Howley. 1991. Functional analysis of E2-mediated repression of the HPV18 P105 promoter. *The New Biologist* 3, no. 1 (January): 90-100.

Wells, Susanne I, Bruce J Aronow, Trisha M Wise, Sarah S Williams, Jennifer A Couget, and Peter M Howley. 2003. Transcriptome signature of irreversible senescence in human papillomavirus-positive cervical cancer cells. *Proceedings of the National Academy of Sciences of the United States of America* 100, no. 12 (June 10): 7093-7098.

Werk, Denise, Steffen Schubert, Vanessa Lindig, Hans-Peter Grunert, Heinz Zeichhardt, Volker A Erdmann, and Jens Kurreck. 2005. Developing an effective RNA interference strategy against a plus-strand RNA virus: silencing of coxsackievirus B3 and its cognate coxsackievirus-adenovirus receptor. *Biological Chemistry* 386, no. 9 (September): 857-863.

Werness, B A, A J Levine, and P M Howley. 1990. Association of human papillomavirus types 16 and 18 E6 proteins with p53. *Science (New York, N.Y.)* 248, no. 4951 (April 6): 76-79.

White, A E, E M Livanos, and T D Tlsty. 1994. Differential disruption of genomic integrity and cell cycle regulation in normal human fibroblasts by the HPV oncoproteins. *Genes & Development* 8, no. 6 (March 15): 666-677.

Wilson, Joyce A, Sumedha Jayasena, Anastasia Khvorova, Sarah Sabatinos, Ian Gaël Rodrigue-Gervais, Sudha Arya, Farida Sarangi, Marees Harris-Brandts, Sylvie Beaulieu, and Christopher D Richardson. 2003. RNA interference blocks gene expression and RNA synthesis from hepatitis C replicons propagated in human liver cells. *Proceedings of the National Academy of Sciences of the United States of America* 100, no. 5 (March 4): 2783-2788.

Wu, Weilin, Emily Hodges, and Christer Höög. 2006. Thorough validation of siRNA-induced cell death phenotypes defines new anti-apoptotic protein. *Nucleic Acids Research* 34, no. 2: e13.

Yamato, K, J Fen, H Kobuchi, Y Nasu, T Yamada, T Nishihara, Y Ikeda, M Kizaki, and M Yoshinouchi. 2006. Induction of cell death in human papillomavirus 18-positive cervical cancer cells by E6 siRNA. *Cancer Gene Therapy* 13, no. 3 (March): 234-241. doi:10.1038/sj.cgt.7700891.

Yamato, K, T Yamada, M Kizaki, K Ui-Tei, Y Natori, M Fujino, T Nishihara, et al. 2008. New highly potent and specific E6 and E7 siRNAs for treatment of HPV16 positive cervical cancer. *Cancer Gene Therapy* 15, no. 3 (March): 140-153. doi:10.1038/sj.cgt.7701118.

Yoshinouchi, Mitsuo, Taketo Yamada, Masahiro Kizaki, Jin Fen, Takeyoshi Koseki, Yasuo Ikeda, Tatsuji Nishihara, and Kenji Yamato. 2003. In vitro and in vivo growth suppression of human papillomavirus 16-positive cervical cancer cells by E6 siRNA. *Molecular Therapy: The Journal of the American Society of Gene Therapy* 8, no. 5 (November): 762-768.

zur Hausen, H, and E M de Villiers. 1994. Human papillomaviruses. *Annual Review of Microbiology* 48: 427-447. doi:10.1146/annurev.mi.48.100194.002235.

Zheng, Zhi-Ming, and Carl C Baker. 2006. Papillomavirus genome structure, expression, and post-transcriptional regulation. *Frontiers in Bioscience: A Journal and Virtual Library* 11: 2286-2302.

# Chapter Four

# Genome expression profiling of E6/E7 silenced cervical cancer cells

## 4.1 Introduction

Cervical cancer is preceded by a well defined pre-malignant phase, with a series of dysplastic changes occurring in cells of the cervical epithelium over a period of many years (Wright *et al.*, 1994). Cervical screening, using the PAP smear technique allows assessment of these dysplastic changes and enables early diagnosis, making cervical cancer a potentially preventable disease. Nevertheless, it remains the second most common malignancy in women worldwide (Parkin And Bray, 2006). This is primarily due to two interrelated factors: one a lack of screening programmes worldwide and two diagnosis occurring at late-stage invasive cervical carcinoma. While most cases of early-stage invasive cervical carcinoma can be cured by a combination of surgery, radiotherapy and chemotherapy (Gerbault *et al.*, 1992; Landoni *et al.*, 1997; Morris *et al.*, 1999), treatment results for advanced metastatic disease are poor (Omura *et al.*, 1997). The introduction of prophylactic HPV vaccines will no doubt reduce the burden of this disease, however its high cost means it will not be available where it is most needed, i.e. resource-constraint developing nations, and even in countries where it is available, the effect will not be seen for several decades. Therefore, in order to combat this high incidence rate of cervical cancer what is required are novel biomarkers, to facilitate more high-throughput and objective diagnosis, and tailored therapeutic agents, to improve upon the existing treatment options.

The development of the prophylactic vaccine came from our understanding of the contribution of HPV infection to the development of cervical cancer and on the molecular knowledge of the structure of the HPV virus. This demonstrates the impact increased molecular knowledge of a disease process can have in a clinical setting. Therefore, it would seem rational to suggest that a deeper understanding of the molecular activities of the two HPV oncogenes, E6 and E7, known to be necessary for the neoplastic progression of cervical cancer (Pett and Coleman 2007; Snijders *et al.*, 2006; zur Hausen and deVillers, 1994), may lead to the identification of novel biomarkers and potentially also papillomavirus-specific therapies. After 25 years of research, many biological activities have been attributed to E6 and E7, including

adverse interactions with the major tumour suppressor proteins, p53 and Rb (Dyson *et al.*, 1992; Scheffner *et al.*, 1991; Werness *et al.*, 1990). However, a complete view of their oncogenic potential still eludes us. It has been established that *in vivo* E6 and E7 work in a cooperative manner to induce genomic instability through the induction of chromosomal rearrangements and abnormal centrosome numbers (Duensing *et al.*, 2000; Plug-DeMaggio *et al.*, 2004). It has also been demonstrated that high-risk HPV E7 contributes to this activity by inducing centrosome over-duplication, however, it is unknown how exactly it induces this effect (Duensing *et al.*, 2000). Furthemore, E6 and/or E7 oncoprotein expressing cells have been observed to exhibit centrosome independent mechanisms of genomic instability through chromosomal rearrangements (Duensing and Munger, 2002; Plug-DeMaggio *et al.*, 2004), primarily anaphase bridges. While it is presumed that this occurs due to abrogation of multiple checkpoint controls and DNA damage responses, this has not been substantiated and evidently pathways intrinsic to this activity of E6 and E7 have not been defined.

Reverse genetic studies are often employed to evaluate the function of a gene. This is where a gene is disrupted and the downstream consequences of this activity are studied in order to determine how it works. Large-scale gene expression analyses such as high-density DNA microarrays are a powerful partner in such studies. The simultaneous analysis of numerous mRNA expression patterns by microarray-based technology allows an unbiased approach to study downstream effects on gene expression alterations induced by disruption of the gene of interest, which in turn allows aspects of gene function to be determined. Without this technology base, only a few genes could be studied at any one time and this means interactions between different genes or genetic pathways could be overlooked.

Reverse genetic studies utilising microarray technology have previously been applied to examine the activity of the HPV E6 and E7 oncogenes in cervical cancer (Johung *et al.*, 2006; Kelley *et al.*, 2005; Kuner *et al.*, 2007; Min *et al.*, 2009; Thierry *et al.*, 2004; Wells *et al.*, 2003). Two main approaches have been taken to disrupt the expression of

viral oncogenes, ectopic expression of the HPV E2 protein (Johung *et al.*, 2006; Thierry *et al.*, 2004; Wells *et al.*, 2003) and RNAi (Kelley *et al.*, 2006; Kuner *et al.*, 2007; Min *et al.*, 2009). HPV E2 has been established to regulate the expression of the HPV E6 and E7 oncogenes both by transcriptional blockage and direct interaction (Gammoh *et al.*, 2006; Grm *et al.*, 2005; Longworth and Laimins, 2004). While HPV E2 has been demonstrated to efficiently repress the expression of integrated E6 and E7 (DeFilippis *et al.*, 2003; Goodwin and DiMaio 2001), there are some concerns with applying this approach. Besides its activity as a negative regulator of HPV transcription, the E2 protein has been found to affect crucial cellular processes even in HPV-negative cells, such as the control of proliferation, mitosis and/or apoptosis (Demeret *et al.*, 2003; Webster *et al.*, 2000). RNAi would appear a more promising approach since it has the potential to specifically target the expression of E6 and/or E7. However, careful consideration must be given to controls as an ongoing issue in RNAi studies is the possibility of "off-target" effects (see chapter 3 for a comprehensive discussion on this topic).

Unlike most cancers, the cell regulatory machinery in cervical cancer cells is not broken, but instead through the activity of E6 and E7 has been made dormant, and therefore the loss of E6 and E7 expression has been demonstrated to re-impose growth control (Goodwin and DiMaio, 2000). Thus these approaches, combining the use of gene silencing techniques, microarray screening, and functional classification of differential genes, have the potential to elucidate the role of E6/E7 oncogene in the carcinogenesis of HPV and provide some possible targets for clinical utility in the diagnosis and eventual treatment of cervical cancer.

## 4.2 Chapter Aim

The aim of this chapter, was to identity cellular targets that are affected by the action of HPV16 E6 and E7 oncogenes. This was achieved, by determining the genome-wide alterations induced at the transcriptome level in HPV16 infected cervical cells by the simultaneous silencing of E6 and E7. The suppression of the viral oncogenes was accomplished through the use of E7 targeting siRNA as described in chapter 3. Validated HPV16 E6 and E7 knockdown samples were applied to Affymetrix GenChip® microarrays. This facilitated an unbiased analysis of gene expression alterations that occurred upon silencing of E6 and E7.

## 4.3 Materials and Methods

### *4.3.1 Samples*

The experiments in this chapter were all based on the analysis of total RNA from the HPV16 positive cervical cell line SiHa. All samples used originated from the validated E6 and E7 knockdown experiments of chapter 3. Specifically, they were obtained from SiHa cells ($1.5x10^5$cells/well) that were left untreated or transfected with 10nM of negative control or experimental siRNA, E7#1, E7#2 or E7#3, for 48hrs in 6 well dishes. In each case, total RNA was isolated using the Ambion MirVanna kit (section 2.3.2), subjected to DNase digestion (section 2.3.3) and purified using the Qiagen RNeasy mini kit (section 2.3.3). It should be noted that the same three biological replicates for each sample group, i.e. untreated, negative control, E7#1, E7#2 and E7#3 siRNA, were used for all analyses performed in this chapter.

### *4.3.2 RNA quantity and quality*

RNA quantity and purity was determined using the NanoDrop® ND-100 spectrophotometer (section 2.4.1). RNA integrity was assessed using the 2100 Bioanlayzer (section 2.4.2).

### *4.3.3 Affymetrix GenChip® Gene 1.0 ST microarray*

Microarray analysis was carried out as described in section 2.6. Briefly, 200ng of total RNA was reverse transcribed, fragmented and biotin labelled following recommended Affymetrix protocols. Single stranded fragmented, biotin labelled DNA was hybridised to GeneChip® Human Gene 1.0 ST Arrays (Affymetrix, Santa Clara, CA, USA). Hybridised arrays were scanned on an Affymetrix GeneChip® Scanner 3000 7G (Affymetrix, Santa Clara, CA, USA). Nine microarray experiments were performed; three biological replicates of SiHa cells transfected with siRNA E7#1, three transfected with siRNA E7#3 and three transfected with the negative control siRNA.

### *4.3.4 Quality control analysis of microarrays*

Quality Control analysis was performed using the Expression Console ™ (EC) software (Affymetrix, Santa Clara, CA, USA). The objective of this analysis was to identify any outlying microarrays. Initial analysis involved visual inspection of the array images for hybridization artefacts and for the performance of the positive hybridisation control, B2 oligo. Subsequently, analysis was based on quality control metrics that were generated by the EC software. The EC software calculates various quality assessment metrics. Some are based on probe intensities others on probeset intensities. Probe intensities were summarised into probeset intensities using the Robust Multiplechip Analysis (RMA) summarisation method. A summary of the different quality control metrics, their meanings and functions is given below.

I. **Probe Level Metrics:** This quality assessment metric is based on the probe signal level data.

**pm_mean** is the mean of the raw intensity for all of the perfect match (PM) probes on the array prior to any intensity transformations (e.g. quantile normalization). This value can be used to ascertain whether certain arrays are unusually dim or bright. Dim or bright arrays may not be a problem *per se*. It does however indicate that closer inspection of the probeset based metrics is required to ensure further irregularities are not present (e.g. unusually high median absolute deviation of residuals, unusually high mean absolute relative log expression values when looking within replicates, etc.).

II. **Probeset Summarisation Based Metrics:** This set of metrics is based on the summarised probeset intensities. The majority of these metrics are performed for different categories of probesets; for instance the hybridization or 'bac spike' controls.

**pos_vs_neg_auc** is the area under the curve (AUC) for a plot comparing signal values for the positive controls to the negative controls. The curve is generated by evaluating how well the signals separate the positive controls from the

negative controls, with the assumption that the negative controls are a measure of false positives and the positive controls are a measure of true positives. An AUC of 1 reflects perfect separation, whereas, as an AUC value of 0.5 would reflect no separation. The expected value for this metric is tissue type specific and may be sensitive to the quality of the RNA sample; values between 0.80 and 0.90 are typical.

**X_mean** is the mean signal value for all the probesets analyzed from category "X".

**X_mad_residual_mean** is the mean of the absolute deviation of the residuals from the median, for all probesets analysed from category "X". Different probes return different intensities when hybridised to a common target. To account for these relative differences in intensity, the RMA algorithm creates a model for individual probe responses. The difference between the actual signal intensity value and the predicted value is the residual. If the residual for a probe on any given array is very different from the median, it means that it is a poorer fit to the model. Thus, calculating the mean of the absolute value of all the deviations produces a measure of how well or poor all of the probes on a given array fit the model. An unusually high mean absolute deviation of the residuals from the median suggests problematic data for that array.

**X_rle_mean** is the mean absolute relative log expression (RLE) for all the probesets analyzed from category "X". This metric is generated by taking the signal estimate for a given probeset on a given array and calculating the difference in log base 2 from the median signal value of that probeset over all the chips. The mean is then computed from the absolute RLE for all the probe sets analyzed from category "X". When only replicates from a tissue or cell line are analysed together, the mean absolute RLE should be consistently low, reflecting the low biological variability of the replicates.

III. **Probeset signals as quality metrics:** These sets of quality assessment metrics are individual probe set signal values for various controls. These include the bacterial spike and polyA spike probesets. The main use in looking at specific probeset values is to determine if expected behaviours for these probesets are observed, i.e. constant expression levels for housekeeping genes, rank order of signal values between spike probe sets.

As is apparent from the above descriptions, many of the quality assessment metrics are reported not just for all the probe sets analyzed, but also for particular subsets of probesets. The group specific metrics are particularly useful when troubleshooting a poorer performing sample. The different categories of probesets are described below.

I. **all_probeset** is all the probe sets analyzed. In most cases, this category is the bulk of probesets that will be carried into downstream statistical analysis. Thus the metrics reported for this category will be the most representative of the quality of the data being used downstream.

II. **bac_spike** is the set of probesets which hybridise to the pre-labelled bacterial spike controls (BioB, BioC, BioD, and Cre). This category is useful in identifying problems with the hybridisation and/or array. Metrics in this category have more variability than other categories (i.e. positive controls, all probesets) due to the limited number of spikes and probesets for this category.

III. **polya_spike** is the set of polyadenylated RNA spikes (Lys, Phe, Thr, and Dap). This category is useful in identifying problems with the target preparation. As with the bacterial spike controls, metrics in this category have more variability than other categories due to the limited number of spikes and probesets for this category.

IV. **neg_control** is the set of putative intron-based probesets from putative housekeeping genes. Multiple species-specific probesets were selected against putative intronic regions in genes that were previously shown to have constitutive expression over a large number of samples. Thus in any given sample, some (or many) of these putative intronic regions may be transcribed

and retained. These probesets form a moderately large collection which generally has very low signal values. They are used to estimate the false positive rate for the pos_vs_neg_auc metric.

V. **pos_control** is the set of putative exon-based probe sets from putative housekeeping genes. Multiple species-specific probesets were selected against the putative exonic regions in these genes as they were previously shown to have constitutive expression over a large number of samples. These probesets form a moderately large collection of probesets with target present which generally have moderate to high signal values. These probesets are used to estimate the true positive rate for the pos_vs_neg_auc metric.

### *4.3.5 Data analysis of microarrays*

Microarray data was analysed using the XRAY version 3.99 software from Biotique Systems Inc. (Reno, NV, USA).

#### 4.3.5.1 Probe transformation and summarisation

The expression score for each probeset was derived by application of standard RMA normalisation and probe summarisation methods. The RMA algorithm consists of three steps; normalisation, transformation and background correction of the probe scores. The RMA algorithm fits a robust linear model at the probe level to minimize the effect of probe-specific affinity differences. Using this approach (as opposed to other algorithms such as PLIER) increases sensitivity to small changes between experiment and control samples and minimises variance across the dynamic range, but does compress calculated fold change values (Irizarry *et al*, 2003). Each probe score was normalised with full quantile normalisation. Next, normalised probe scores were filtered and probes with a GC content less than 6 and greater than 17 were excluded from further analysis (Figure 4.1 demonstrates the limited number of probes removed by this filter). The remaining probes were transformed by taking the natural logarithm of 1 plus their scores. This was followed by background correction, which was performed by subtracting from the individual probe scores the median probe expression score of the antigenomic background probes of similar GC content. Summarisation of probes into probe sets, which represent exons, was achieved by application of the Tukey's Median Polish method.

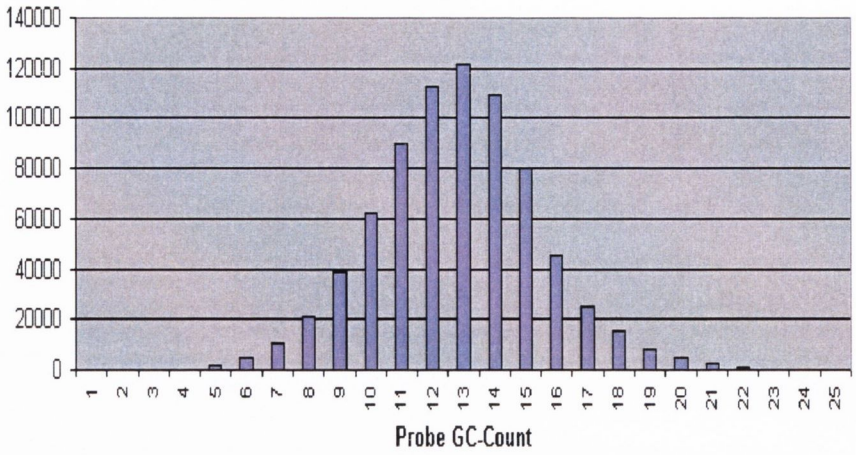


**Figure 4.1: A histogram of the GC content range of the probes on the Affymetrix GeneChip® Gene 1.0 ST microarray.** Represented on the x-axis of the histogram is the probe GC count and on the y-axis the frequency on the input 1.0 ST microarrays. The diagram demonstrates that filtering out probes with less than 6 and more than 17 G/C bases does not significantly alter the number of probes analysed. Approximately 10,000 probes are removed by this filter.

### 4.3.5.2 Identification of expressed genes

To establish the presence or absence of a particular gene in a group, i.e. E7#1, E7#3 or negative control group, a p-value to investigate the null hypothesis was derived using a one-sided t-test. The null hypothesis was that in a particular group, the probes are not expressed above the level of the background probes of similar GC content. Rejection of the null hypothesis occurs when the p-value is less than the significance level (set at 0.05) in which case it is inferred that the gene is most likely expressed in given group.

### 4.3.5.3 Comparative analysis between groups

Mixed model, nested ANOVA (Montgomery, 2006) was used to identify genes that were differentially expressed between the experimental groups (SiHa cells transfected with E7#1 or E7#3 siRNA) and the control group (negative control siRNA). The nested model is appropriate, because data is not sampled in a truly randomized fashion because expression points are harvested in batches defined by hybridisations. The mixed model is used since hybridisations are random factors (i.e. we are not interested in the effect of individual hybridisations since we are sampling from the many arrays that have been manufactured). On the other hand, groups are fixed effects. To justify

the designation of states as fixed or random, consider that if the experiment was redone, the same groups would be used but there would be different arrays. The mixed model, nested ANOVA is a non-parametric analysis which generates unadjusted p-values. The basic principle behind this test is that it considers the mean and variance of the experimental sample and the control sample distributions and calculates the probability that the observed difference in mean occurs when the null hypothesis is true. The null hypothesis states that the mean of the two distributions is equal. The aim is to look for genes that show a distinct difference in expression between the groups.

When microarrays are performed, thousands of genes are analysed, generally in a small number of biological replicates. In the main, the aim is to select the relevant genes corresponding to the transcriptional changes which are related to a clinical or biological outcome. In such a case, a major multiplicity problem arises. The p-value (0.05 or 0.01) has been used classically to control the type I error rate (i.e. the false positive rate). Its interpretation is that from 100 tests, 5 tests would nevertheless be significant in the case of p=0.05 (i.e. false positives). Although useful in most experiments, the use of the same p-value on a microarray with 30,000 genes would yield 1,500 false positive genes, which is an unacceptable amount (Glantz, 1996). Therefore additional measures need to be taken to correct for this effect. There are several different methods that can be applied such as those of Bonferroni and Sidak. However, these two are generally considered to be too conservative and to have low power in microarray experiments. Instead the Benjamini and Hochberg False Discovery Rate (FDR) method outlined by Benjamini and Hochberg (1995) and originally proposed by Simes (1986) that controls the family wide error rate in a weak sense was used.

Fold change for detected probes were also calculated. Fold change compares the expression level of the same gene in both groups and assesses the degree to which the gene is up- or down-regulated in one group compared to the other. On initial analysis,

genes were deemed to be differentially expressed between the experimental groups and the control group if they possessed a FDR ≤ 0.05 and a fold change ≥ 2. In a second round of analysis, genes were deemed to be differentially expressed between the experimental groups and the control group if they possessed a p-value ≤ 0.05 and a fold change ≥ 1.5.

#### 4.3.5.4 Analysis of gene target lists

The online databases PANTHER and DAVID (Database for Annotation, Visualization and Integrated Discovery) 2008 were used to classify genes according to function and pathways. Both databases adopt a common core strategy to systematically map a large number of interesting genes in a list to the associated biological annotation (e.g., gene ontology terms), and then statistically highlight the most overrepresented (enriched) biological annotation out of thousands of linked terms and contents. One of the key features of PANTHER is a simplified ontology of protein function, which allows browsing of the database by biological functions (Thomas *et al.,* 2003). Biologist curators have associated the ontology terms with groups of protein sequences rather than individual sequences. Statistical models (Hidden Markov Models, or HMMs) are built from each of these groups. The key feature of DAVID is its knowledgebase, which is based on more than 20 gene identifier types and more than 40 functional annotation categories from dozens of heterogeneous public databases, including PANTHER (Dennis *et al.,* 2003). This annotation data is comprehensively integrated by a unique single linkage method. These 40 annotation categories include GO terms, protein-protein interactions, protein functional domains, disease associations, bio-pathways, sequence general features, homologies, gene functional summaries, gene tissue expressions and literatures.

### *4.3.6 TaqMan® low density arrays*

TaqMan® RT-PCR was performed using custom designed TLDAs (Applied Biosystems, Foster City, CA, USA). RNA was reverse transcribed into cDNA as per section 2.5.2.1. TLDA RT-PCR experiments were performed as detailed in section 2.5.3. The relative quantity of gene expression was calculated using the $2^{-\Delta\Delta CT}$ comparative $C_T$ method as described in section 2.5.3.1, where GAPDH gene expression was used as the endogenous control and gene expression of untreated or negative control cells were used as the calibrator sample.

## 4.4 Results

### *4.4.1 Microarray quality control*

#### 4.4.1.1 RNA for microarray gene expression analysis

For gene expression analysis, the quality of the extracted RNA is essential, as RNA of low or even moderate quality can result in highly variable or un-interpretable data. The purity and integrity of RNA samples was established using the NanoDrop® ND-100 and the Agilent 2100 Bioanlayzer, respectively. The purity of each sample was assessed based on the calculated 260/280 ratio, where a value between 1.9 and 2.1 was considered pure, i.e. free from contaminants, e.g. proteins, phenol chloroform, etc. All samples fell within this range and therefore were deemed to be of high purity. For each sample, RNA integrity was determined by visual assessment of their 28S and 18S RNA bands on a gel image (Figure 4.2) and by evaluation of the calculated RIN numbers (Table 4.1). For a full explanation on the RIN number calculation see section 2.4.2. Figure 4.2 demonstrates that the 28S and 18S bands for each sample were of high quality and consequently that there was little to no RNA degradation. Supporting this finding was the fact that all the RIN numbers were above 7. Based on the purity and the integrity analyses all samples were deemed of sufficient quality to be used in microarray experiments.

**Table 4.1: 260/280 ratios and RIN numbers of RNA samples deemed suitable for microarray analysis.**

| Sample | 260/280 Ratio | RIN |
|---|---|---|
| E7#1 Rep1 | 2.02 | 7.6 |
| E7#1 Rep2 | 1.96 | 8.8 |
| E7#1 Rep3 | 2.05 | 7.3 |
| E7#2 Rep1 | 2.01 | 7.5 |
| E7#2 Rep2 | 2.02 | 7.5 |
| E7#2 Rep3 | 2.08 | 7.4 |
| Negative Control Rep1 | 2.04 | 8.5 |
| Negative Control Rep2 | 2.00 | 8.2 |
| Negative Control Rep3 | 2.05 | 7.6 |

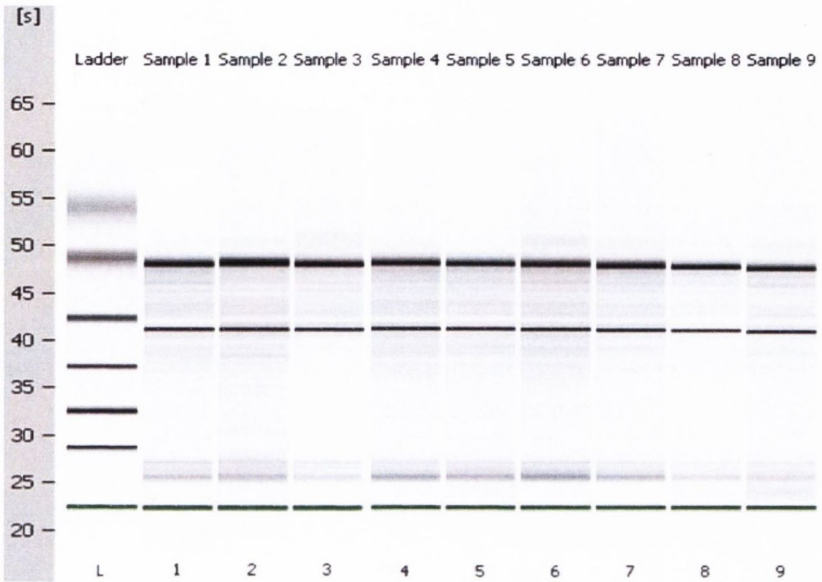


**Figure 4.2: Assessment of the RNA quality.** Lanes 1-3 represents RNA samples from three biological replicates of E7#1, lanes 4-6 represents three biological replicates of E7#3 RNA samples and lanes 7-9 represents three biological replicates of negative control RNA extracts. This is the output gel-like image produced by analysis of these RNA samples on the Agilent 2100Bioanalyzer. The clear 18S and 28S RNA bands evident in each sample demonstrate the high-quality of the RNA.

#### 4.4.1.2 Initial quality control assessment of microarrays

Initial quality checks were performed by direct visual inspection of the microarray images. Step one is to check for the presence of image artefacts on the arrays, i.e., high/low intensity spots, scratches, high regional or overall background. Step two the performance of the positive hybridisation control, the B2 oligo, is assessed. Hybridisation of B2 is highlighted on array images as depicted in Figure 5.3. Of particular importance is the B2 intensity at the checkerboard corners (Figure 5.3 A), as if this is either too low or high, or skewed due to image artefacts, the grid over the microarray image will not align automatically. All arrays passed these initial quality controls, i.e. there were no artefacts and the B2 oligos appeared correctly on all images.

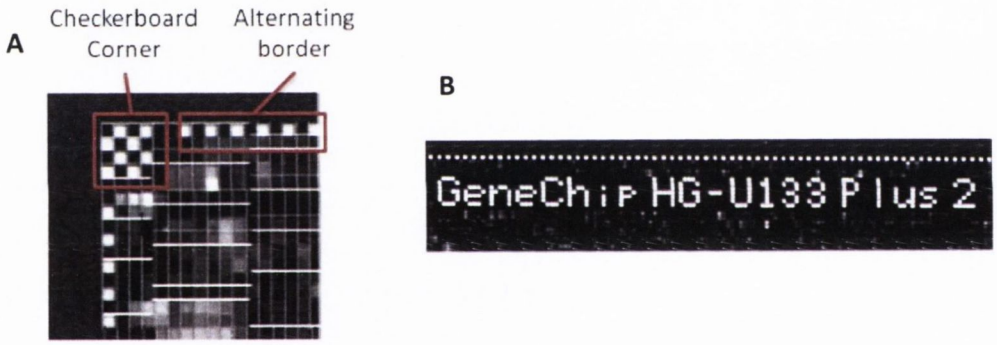


**Figure 4.3: Diagrammatic representation of B2 illuminated regions of an Affymetrix GeneChip microarray.** B2 oligos, which are spiked into each hybridization cocktail, serve as a positive hybridization control and are used by the GCOS software to place a grid over the microarray image. They are visualised on the microarray images as an alternating pattern of intensities on the border (**A**), a checkerboard pattern at each corner (**A**), and in the lower-left of the array as the array name (**B**). (adapted from www.affymetrix.com)

#### 4.4.1.3 Quality control assessment of microarrays by calculated quality metrics

The quality of the arrays was further evaluated to ensure no outliers or defective arrays were present that might skew the results of downstream analysis. The quality assessment procedures entail computing summary statistics for each array and then comparing the level of the summary statistics across all the arrays. The Affymetrix EC software was used to calculate the quality assessment metrics and to generate graphs to facilitate data quality assessment. The different metrics that were utilised are comprehensively described in section 4.3.4.

Figure 4.4 depicts several of the critical quality control metrics assessed. There was a low level of variation in all of the quality control metrics. This is anticipated when microarrays using RNA from the same cell line are assessed together. The pos_control and all_probeset categories are used to assess the overall quality of the data from each array (Figure 4.4 A – C). Metrics based on these categories reflect the quality of the whole experiment including RNA quality, target preparation, chip, hybridization, scanning and griding. Thus, they are useful to assess the nature of the data being used in downstream statistical analysis. The area under the curve for the signal discrimination of the positive and negative controls was above 0.80 for all arrays and showed only a low amount of variation between samples (Figure 4.4 A the red line). This means that there is good separation between the positive and negative controls, which are a measure of true and false positives respectively, and indicates that the entire microarray experiment of all of the samples analysed was successful. Another example of the similarity of the samples is the box plots of the relative log expression (RLE) of the probesets (Figure 4.4 B). The median RLEs should be zero, and all samples are very close to 0. Deviations from zero typically indicate a skew in the raw intensities of an array that were not properly corrected by normalisation. If the RLE box plots indicate a skew, visual inspection of the array image with non-zero median RLE often reveals dense areas of unusually bright or unusually dim intensities. The pm_mean of an array can also reveal an unusually dim or bright chip. In figure 5.7 C the pm_mean appears to vary a lot between microarrays, however when the range of the signal

intensity of this metric is viewed, it is low (630 - 354) and so again reaffirms the low levels of inter-array variation.

Figure 4.4 E-D represents metrics for the bac_spike and polya_spike controls, which are useful in evaluating different points along the experimental protocol. The bac_spike category identifies potential problems with the hybridization stage of the experiment and the quality of the chip (Figure 4.4 D). The polya_spike category is useful for identifying potential problems with the target preparation phase of the experiment (Figure 4.4 E). The bacterial spikes display the expected rank order (BioB < BioC < BioD < Cre) indicating that no problem occurred during the hybridization phase (Figure 4.4 D), and the polyA spikes display the expected rank order (lys < phe < thr < dap) indicating that there was no problem with the RNA sample or the target preparation (Figure 4.4 E). The quality control metrics discussed above indicated that the microarray experiments were successful and that no outlier arrays were present.

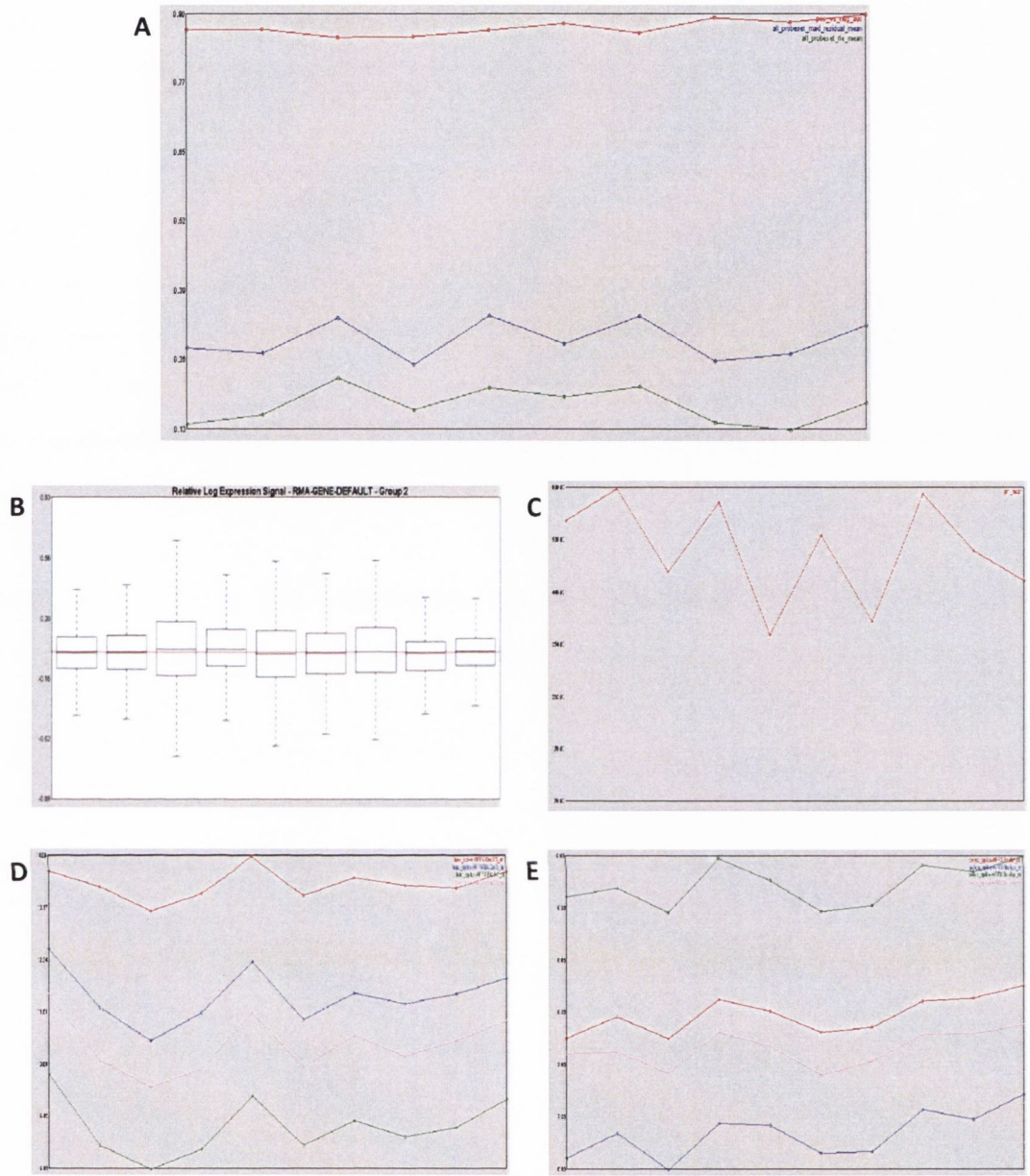


**Figure 4.4: Quality control metrics of microarrays performed on siRNA transfected SiHa cells.** Each point in the diagrams represents the value of a metric for a particular microarray. (**A**) Shows a graph of the mean absolute deviation of residuals (blue), mean absolute relative log expression (RLE) (green), and the area under the curve for signal discrimination of the positive and negative controls (red). (**B**) Box plots of the RLE for all the probesets analyzed. The mean absolute RLE is proportional to the width of the box plots, or the inter-quartile range of RLE values. The middle bar in each box is the median RLE. (**C**) The mean probe level intensity (prior to normalization or background correction). (**D**) Depicts the signal values of the bacterial spikes and (**E**) the signal values of the poly A spikes.

### *4.4.4 Differential gene expression analysis*

To characterise the gene expression alterations induced by siRNA silencing of the viral oncogenes E6 and E7 in HPV16 positive cervical cancer SiHa cells, whole-genome transcriptional profiling was performed. In chapter 3 the design, validation and selected functional analysis of siRNA targeting the HPV16 E7 coding region was described. Five siRNAs were designed and of these, four were deemed functional. In particular, three were determined to induce similar levels of significant knockdown in the RNA expression of the E6 and E7 oncogenes; these were siRNA E7#1, E7#2 and E7#3. Two of these siRNAs, E7#1 and E7#2, had been designed commercially by Ambion using their Silencer® Select design process, while the third, E7#3, was in-house designed. In order to facilitate the application of a multiplicity control, it was decided the transcriptional response induced in the SiHa cells by two of these three siRNAs would be investigated. The E7#2 and E7#3 siRNAs target overlapping regions of the HPV16 E7 coding sequence. Therefore, it was concluded that E7#1 would be examined along with one of the other two. As E7#3 was in-house designed, and gave a more potent and consistent result at the RNA level than E7#2 (see section 3.4.2, Figure 3.10), it was chosen for analysis. To identify changes in gene expression patterns, comparisons were made between the experimental samples, where E6 and E7 expression had been knocked down, and samples transfected with negative control siRNA.

The RNA samples utilised in this study originated from three independent experiments in which SiHa cells had been transfected for 48hrs with E7#1, E7#3 or negative control siRNA and where E6/E7 RNA knockdown was validated by TaqMan® RT-PCR (section 3.4.2). Biotinylated DNA was hybridised to Affymetrix Human GenChip® Gene ST 1.0 microarrays, which contains 818,005 probes that correspond to 28,869 gene transcripts. Data analysis was performed using XRAY version 3.99 software. Probe intensities were transformed and summarised via application of standard RMA normalisation and summarisation methods. The XRAY software uses a one sided t-test to evaluate the presence or absence of gene transcripts. The total number of

transcripts present according to the XRAY presence/absence call criteria were as follows: 6,617 (E7#1), 6,747 (E7#3) and 6,600 (negative control). The relative change in abundance for each transcript between the baseline sample (negative control) and the experimental samples (E7#1 and E7#3) was determined using mixed model, nested ANOVA analysis. To adjust for multiple comparisons, a false discovery rate (FDR) was also calculated using the method outlined by Benjamini and Hochberg (1995). Genes were deemed to be differentially expressed if they possessed a FDR≤ 0.05 and fold change ≥2. Table 4.2 shows the number of genes differentially expressed in the E7#1 and E7#3 transfected SiHa cells.

**Table 4.2: Genes differentially regulated upon E7#1 or E7#3 siRNA induced silencing of the E6/E7 oncogenes in SiHa cells.**

| | Significant* differentially regulated genes | Significant* down-regulated genes | Significant* up-regulated genes |
|---|---|---|---|
| siRNA E7#1 | 253 | 236 | 17 |
| siRNA E7#3 | 221 | 196 | 25 |

*FDR ≤0.05, Fold Change ≥2

### *4.4.5 Comparative analysis of the differentially expressed genes*

Table 4.2 indicates that the number of significantly differentially regulated genes between the two experimental groups does not vary considerably. To evaluate whether this was the result of similar gene expression profiles, analysis was performed using both Pearson's correlation and hierarchical clustering. Pearson's correlation coefficient, represented in calculations as r, reflects the degree of linear relationship between two variables. The correlation coefficient ranges from +1 to -1, with a correlation of 0 inferring there is no relationship and a correlation of ±1 inferring there is a perfect linear relationship.

Figure 4.5 A is a Pearson's correlation plot of normalised, non-background corrected data. It is in the form of a heat map representing all possible pair-wise combinations of samples used in the microarray analysis. Examination of the plot illustrates that the most highly correlated samples are the biological replicates within each array grouping, with correlation coefficients ranging from 0.994 to 0.990. This result validates the data analysis approach undertaken where the expression profile of biological replicates were combined as one outcome. If viewed at group level, this plot demonstrates that the most highly related gene expression profiles are those of the E7#1 and E7#3 transfected cells, thus indicating that the gene expression changes induced at the transcriptome level by the E7#1 and E7#3 siRNA are comparable. Furthermore, this analysis shows that the difference in the gene expression patterns between the experimental groups and the negative control is low. For example, the highest observed variation is between the E7#1 and negative control siRNA gene sets, with a correlation coefficient of 0.98. In reality, this value signifies a highly significant positive correlation between these two groups. The fact that there is a low amount of variation between the groups indicates that the silencing of the viral oncogenes does not cause transcriptome wide modifications but instead induces alterations in a small subset of genes. Indeed for both E7#1 and E7#3 the number of identified differentially expressed genes, 253 and 223 respectively, represents less than 4% of the overall number of genes expressed on either array set, 6,617 and 6,747 respectively. Figure

4.5B depicts the hierarchal clustering of normalised, background corrected data from the E7#1, E7#3 and negative control groups. The findings of this analysis support the previous results of the Pearson's correlation heat map, with all biological replicates clustering within their designated groups and the experimental groups (E7#1 and E7#3) also clustering together.

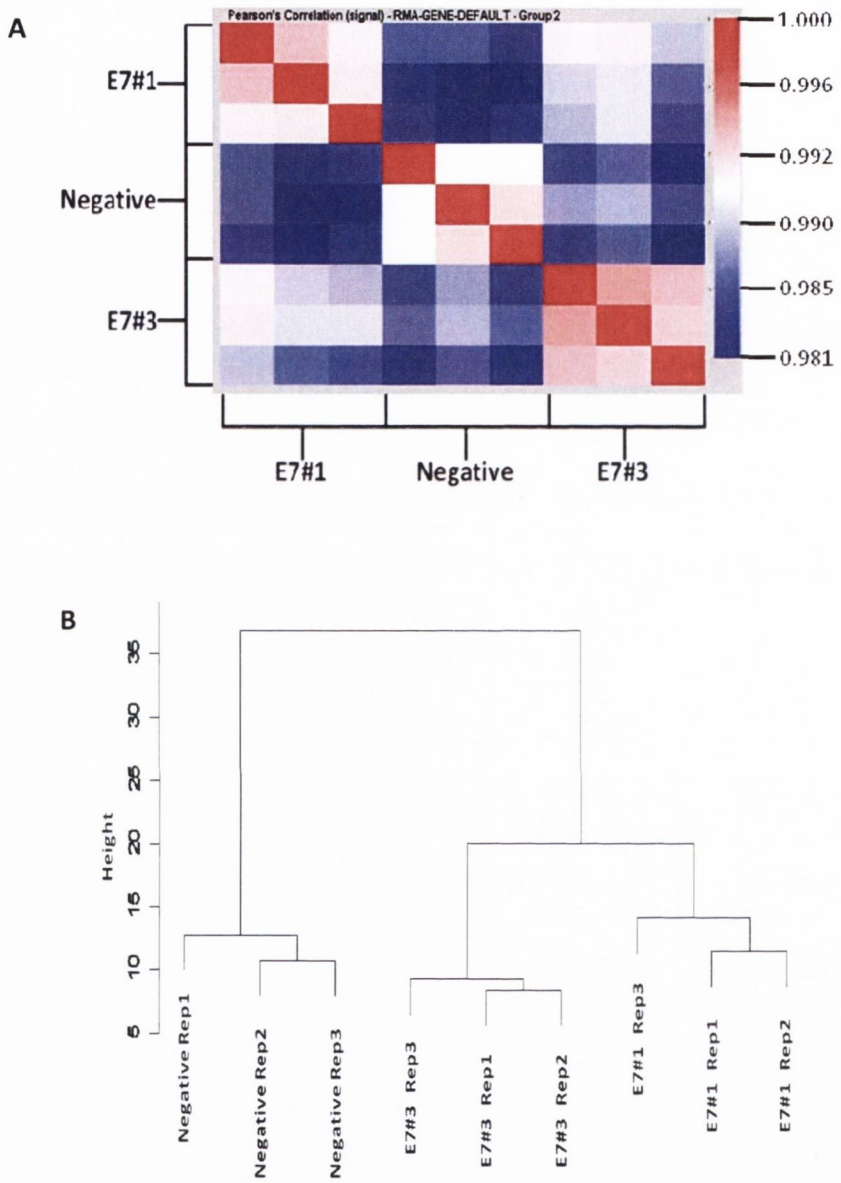


**Figure 4.5: Correlation between the gene expression profiles of SiHa cells transfected with E7#1, E7#3 or negative control siRNA.** (**A**) Pearson's correlation plot of normalised, non-background corrected data. This plot is in the form of a heat map representing all possible pair-wise combinations of samples used in the analysis. [Pearson's correlation coefficient ranges from +1 to -1, with a correlation of 0 inferring there is no relationship and a correlation of ±1 inferring there is a perfect linear relationship.] (**B**) Denogram was created from hierarchical clustering of the transcriptional profiles of normalised, background corrected data.

To evaluate whether the correlation between the transcriptional profiles of SiHa cells transfected with E7#1 and E7#3 siRNA was also evident in genes deemed to be significantly differentially expressed post E6/E7 knockdown, a cross comparison analysis of the differentially expressed gene lists for E7#1 and E7#3 was performed. Compared to the negative control group, there were 253 genes differentially expressed at ≥2 fold and with a FDR ≤0.05 in the E7#1 set and 223 in the E7#3 set. Of these, 168 were represented on both array sets. This corresponds to 66% and 75% of the genes noted to be significantly altered by E7#1 and E7#3 respectively, therefore implying there is a high degree of similarity between these two groups of differentially expressed genes. To conclusively demonstrate that these 168 genes were correlated, the fold change in expression of these genes in both groups was compared (Figure 4.6). A highly significant positive correlation ($r = 0.88$) was obtained indicating both E7#1 and E7#3 induced an equivalent pattern of gene expression alterations within the HPV16 positive cervical cancer cell line SiHa. Of the 168 genes, 10 were up-regulated, Table 4.3, and 158 were down-regulated (Figure 4.7). The 20 genes showing the greatest down-regulation after E7 siRNA induced silencing of the viral oncogenes are listed in Table 4.4. For a complete list of the 168 common significantly differentially regulated genes see Table 1 in the appendix.

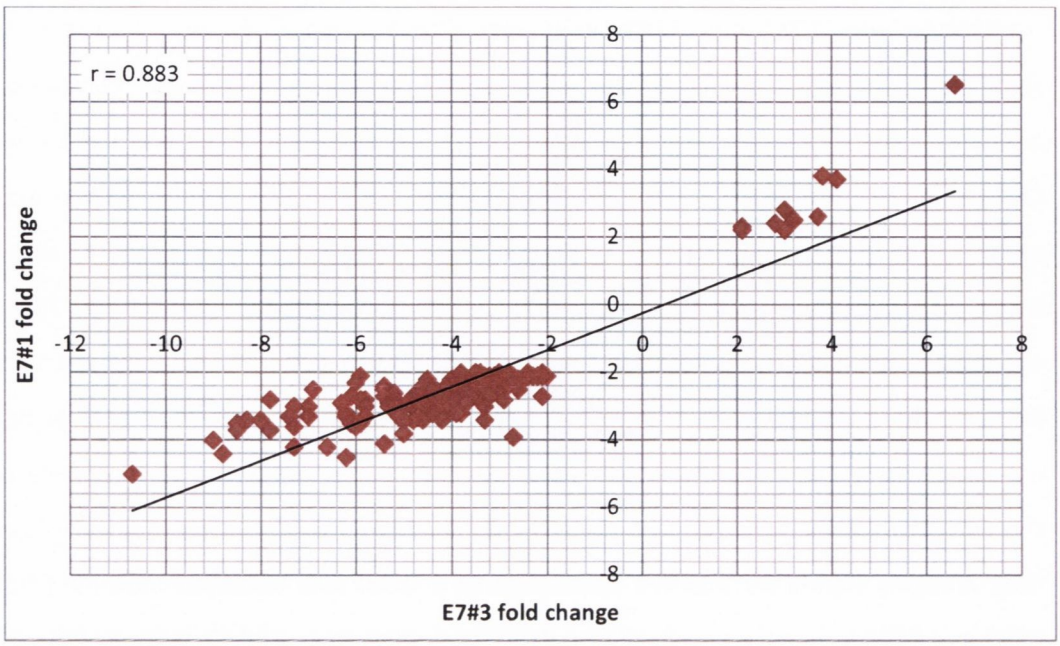


**Figure 4.6: Comparison of the 168 differentially expressed genes identified on both the E7#1 and E7#3 microarrays.** The fold change values of the 168 differentially regulated genes identified in both E7#1 (compared with negative control) and E7#3 (compared with negative control) were plotted against each other and the Pearson correlation coefficient (r) was calculated. There is a highly significant positive relationship between the common differentially expressed genes on both arrays ($r=0.883$, $p<0.0001$ (two –tailed)).

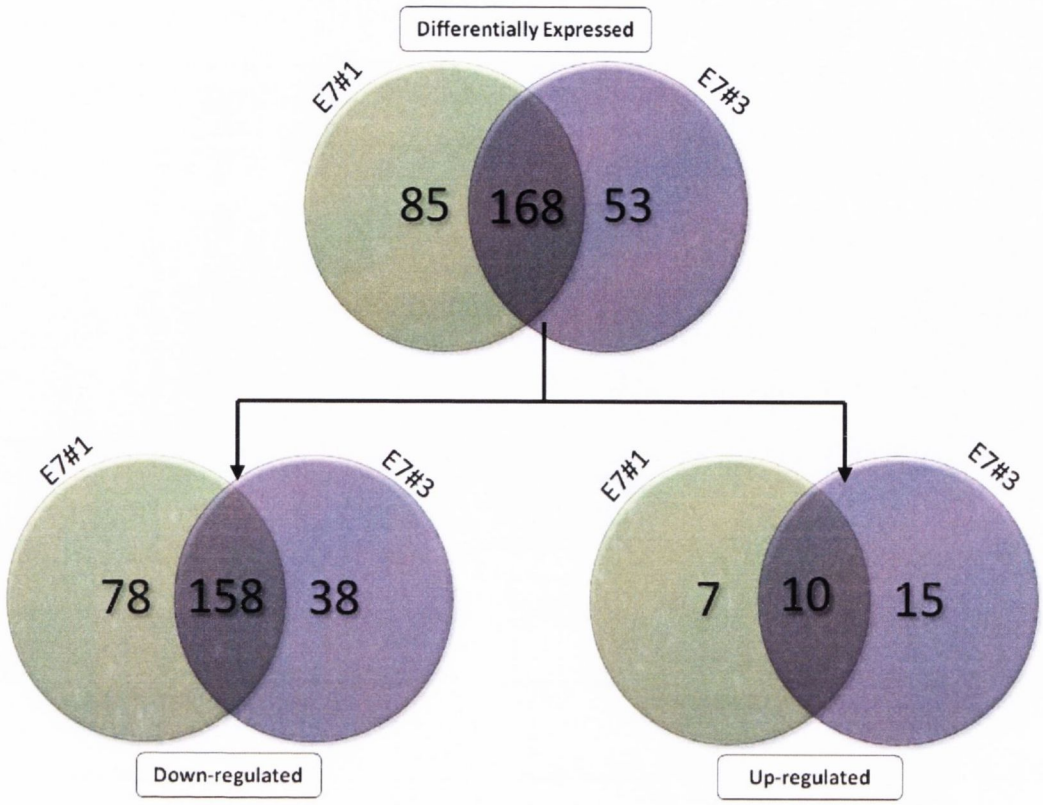


**Figure 4.7: Venn diagrams illustrating the number of differentially expressed unique and common genes between E7#1 and E7#3 transfection in SiHa cells.** Compared to the negative control group there were 253 genes differentially expressed (236 down-regulated and 17 up-regulated), at ≥2 fold and with a FDR ≤0.05, in the E7#1 set and 223 (196 down-regulated and 25 up-regulated) in the E7#3 set, of these 168 (158 down-regulated and 10 up-regulated) were represented on both array sets.

**Table 4.3: The 10 genes up-regulated by both E7#1 and E7#3 siRNA induced silencing of E6/E7.**

| Gene Symbol | Gene Annotation | NCBI Link | E7#1 | | | E7#3 | | |
|---|---|---|---|---|---|---|---|---|
| | | | FC | P-value | FDR | FC | P-value | FDR |
| SPATA18 | spermatogenesis associated 18 homolog (rat) | NM_145263 | 6.61 | 4.1E-04 | 3.7E-02 | 6.51 | 1.9E-04 | 1.7E-02 |
| ACTA2 | actin alpha 2 smooth muscle aorta | NM_001613 | 4.11 | 2.6E-04 | 3.0E-02 | 3.71 | 1.7E-04 | 1.7E-02 |
| BTG2 | BTG family member 2 | NM_006763 | 3.81 | 3.8E-04 | 3.5E-02 | 3.81 | 9.6E-05 | 1.3E-02 |
| MDM2 | Mdm2 p53 binding protein homolog (mouse) | NM_002392 | 3.71 | 8.0E-05 | 2.5E-02 | 2.61 | 3.1E-04 | 2.2E-02 |
| CDKN1A | cyclin-dependent kinase inhibitor 1A (p21 Cip1) | NM_078467 | 3.21 | 9.2E-05 | 2.5E-02 | 2.51 | 6.8E-06 | 6.1E-03 |
| RPS27L | ribosomal protein S27-like | NM_015920 | 3.01 | 9.4E-04 | 4.9E-02 | 2.81 | 7.9E-05 | 1.2E-02 |
| TRIM22 | tripartite motif-containing 22 | NM_006074 | 3.01 | 7.8E-04 | 4.6E-02 | 2.21 | 7.5E-04 | 3.7E-02 |
| FDXR | ferredoxin reductase | NM_024417 | 2.81 | 8.2E-04 | 4.7E-02 | 2.41 | 6.9E-04 | 3.5E-02 |
| BLOC1S2 | Biogenesis of lysosomal organelles complex-1 subunit 2 | NM_001001342 | 2.11 | 7.1E-05 | 2.5E-02 | 2.31 | 4.9E-04 | 2.9E-02 |
| RAB4B | RAB4B member RAS oncogene family | NM_016154 | 2.11 | 7.7E-04 | 4.6E-02 | 2.21 | 5.3E-04 | 3.0E-02 |

**Table 4.4: The top 20 genes down-regulated by both E7#1 and E7#3 siRNA silencing of E6/E7.**

| Gene Symbol | Gene Annotation | NCBI Link | E7#1 | | | E7#3 | | |
|---|---|---|---|---|---|---|---|---|
| | | | FC | P-value | FDR | FC | P-value | FDR |
| EXO1 | exonuclease 1 | NM_130398 | -10.71 | 4.3E-05 | 3.0E-02 | -5.01 | 1.4E-05 | 7.8E-03 |
| ASPM | asp (abnormal spindle) homolog microcephaly associated (Drosophila) | NM_018136 | -9.01 | 8.4E-04 | 4.8E-02 | -4.01 | 4.3E-06 | 5.1E-03 |
| DTL | denticleless homolog (Drosophila) | NM_016448 | -8.81 | 3.1E-04 | 3.3E-02 | -4.41 | 1.9E-05 | 7.5E-03 |
| HIST1H3G | histone cluster 1 H3g | NM_003534 | -8.51 | 9.3E-04 | 4.9E-02 | -3.71 | 5.7E-04 | 3.1E-02 |
| CDC6 | cell division cycle 6 homolog (S. cerevisiae) | NM_001254 | -8.51 | 2.2E-04 | 3.1E-02 | -3.51 | 4.9E-05 | 1.0E-02 |
| NCAPG | non-SMC condensin I complex subunit G | NM_022346 | -8.31 | 7.8E-04 | 4.6E-02 | -3.41 | 2.5E-05 | 8.4E-03 |
| CENPI | centromere protein I | NM_006733 | -8.01 | 4.0E-04 | 3.6E-02 | -3.41 | 1.9E-05 | 7.7E-03 |
| MKI67 | antigen identified by monoclonal antibody Ki-67 | NM_002417 | -7.81 | 6.5E-04 | 4.3E-02 | -2.81 | 5.2E-05 | 1.0E-02 |
| C15orf42 | chromosome 15 open reading frame 42 | NM_152259 | -7.81 | 5.8E-05 | 2.5E-02 | -3.71 | 1.9E-05 | 7.6E-03 |
| KIFC1 | kinesin family member C1 | NM_002263 | -7.41 | 2.3E-04 | 3.1E-02 | -3.31 | 7.6E-06 | 6.1E-03 |
| RAD51AP1 | RAD51 associated protein 1 | NM_001130862 | -7.31 | 9.2E-05 | 2.5E-02 | -3.61 | 7.1E-06 | 6.0E-03 |
| DLGAP5 | discs large (Drosophila) homolog-associated protein 5 | NM_014750 | -7.31 | 8.9E-04 | 4.8E-02 | -3.01 | 9.2E-05 | 1.3E-02 |
| CDCA7 | cell division cycle associated 7 | NM_031942 | -7.31 | 6.8E-04 | 4.3E-02 | -4.21 | 8.7E-04 | 4.0E-02 |
| SHCBP1 | SHC SH2-domain binding protein 1 | NM_024745 | -7.01 | 7.1E-04 | 4.4E-02 | -3.01 | 1.6E-05 | 7.6E-03 |
| KIF4A | kinesin family member 4A | NM_012310 | -7.01 | 3.2E-04 | 3.3E-02 | -3.31 | 3.2E-05 | 9.0E-03 |
| CDCA2 | cell division cycle associated 2 | NM_152562 | -7.01 | 2.4E-05 | 2.4E-02 | -3.31 | 1.4E-05 | 7.3E-03 |
| MYBL2 | v-myb myeloblastosis viral oncogene homolog (avian)-like 2 | NM_002466 | -6.91 | 2.9E-04 | 3.3E-02 | -2.51 | 3.8E-04 | 2.5E-02 |
| BUB1 | budding uninhibited by benzimidazoles 1 homolog (yeast) | NM_004336 | -6.31 | 2.4E-04 | 3.1E-02 | -2.91 | 7.5E-05 | 1.1E-02 |
| TOP2A | topoisomerase (DNA) II alpha 170kDa | NM_001067 | -6.21 | 7.4E-04 | 4.5E-02 | -3.21 | 6.6E-05 | 1.1E-02 |
| ORC1L | origin recognition complex subunit 1-like (yeast) | NM_004153 | -6.21 | 2.4E-04 | 3.1E-02 | -4.51 | 3.7E-06 | 5.4E-03 |

While 168 genes were established to be differentially expressed by both the E7#1 and E7#3 induced loss of E6/E7, there were a second set of genes whose expression was significantly altered by one siRNA but not the other. In total, 85 genes were demonstrated to be differentially regulated, ≥2 fold change and ≤0.05 FDR, by the introduction of E7#1 into SiHa cells but not by E7#3 and 53 by E7#3 but not by E7#1 (Figure 4.7). To try and determine whether these 85 and 53 genes represented true biological events post knockdown of E6/E7, re-analysis of the microarray expression profiles of each group was performed.

The comparative analysis between the gene expression profiles of the baseline sample (negative control) and the experimental samples (E7#1 and E7#3) was re-calculated with relaxed analysis parameters, such that genes were deemed to be differentially expressed if they possessed a p-value ≤0.05 and a fold change ≥1.5. The new differentially expressed genes lists produced by this analysis were then examined for the presence or absence of the above mentioned 85 and 53 genes. For example the analysis of E7#3 with the relaxed criteria produced a differentially expressed gene list of 586 genes (Table 4.5), of the 85 genes differentially regulated based on ≥2 fold change and ≤0.05 FDR criteria by E7#1 but not by E7#3, 51 were identified on the E7#3 ≥1.5 fold change and ≤0.05 p-value list. A similar analysis was performed for the 53 genes differentially regulated based on ≥2 fold change and ≤0.05 FDR criteria by E7#3 but not by E7#1, with 34 being identified on the E7#1 ≥1.5 fold change and ≤0.05 p-value list. Therefore of the 253 genes identified as significantly differentially expressed post E7#1 transfection, by the ≥2 fold change and ≤0.05 FDR criteria, 86% (219 genes) were also altered by E7#3. Similarly, of the 221 genes altered by the activity of E7#3, based on the ≥2 fold change and ≤0.05 FDR criteria, it was demonstrated that 91% (200 genes) were differentially regulated by E7#1. This comparative analysis establishes a list of 251 genes that are unquestionably altered by the loss of E6 and E7 expression in the SiHa cell line.

**Table 4.5: Genes differentially regulated upon E7#1 or E7#3 siRNA induced silencing of the E6/E7 oncogenes in SiHa cells.**

| | Significant* Differentially Regulated Genes | Significant* Down-Regulated Genes | Significant* Up-regulated Genes |
|---|---|---|---|
| siRNA E7#1 | 744 | 560 | 184 |
| siRNA E7#3 | 586 | 425 | 161 |

*p-value ≤0.05, Fold Change ≥1.5

As outlined in Table 4.6 after the above comparative analysis, three sets of differentially expressed genes can be described: those that were significantly altered by the activity of both E7#1 and E7#3, those that were differentially regulated by both E7#1 and E7#3 but only significantly by one and those that were only altered by one of the siRNA (significant is defined as ≥2 fold change and ≤0.05 FDR). For a complete list of genes represented in each of these groups see Table 1 - 5 in the appendix.

**Table 4.6: Three groups of differentially expressed genes upon E7#1 or E7#3 siRNA induced silencing of the E6/E7 oncogenes in SiHa cells.**

| Group | | Number of genes | Total number of genes within group |
|---|---|---|---|
| I | Met ≥2 fold change and ≤0.05 FDR criteria on both E7#1 and E7#3 lists | 168 | 168 |
| II | Met ≥2 fold change and ≤0.05 FDR criteria on E7#1 list **Plus** Met ≥1.5 fold change ≤0.05 p-value criteria on E7#3 list | 51 | 83 |
| | Met ≥2 fold change and ≤0.05 FDR criteria on E7#3 list **Plus** Met ≥1.5 fold change ≤0.05 p-value criteria on E7#1 list | 32 | |
| III | Met ≥2 fold change and ≤0.05 FDR criteria on E7#1 list **But** was not differentially expressed by E7#3 | 34 | 55 |
| | Met ≥2 fold change and ≤0.05 FDR criteria on E7#3 list **But** was not differentially expressed by E7#1 | 21 | |

### *4.4.6 Validation of microarray results by TaqMan® RT-PCR*

To confirm the microarray expression measurements, TaqMan® RT-PCR analysis was performed. In total 55 genes were selected from the group I differential gene expression list for validation. The analysis revealed excellent agreement with the microarray data, with a highly significant positive correlation obtained between microarray and TaqMan® data (Table 4.7). In the majority of cases, the amplitude of the change was greater according to RT-PCR (Figure 4.8 - 4.10). This was not unexpected, as the normalisation method used was quantile normalisation. This system of normalisation is known to slightly compress values of relative expression, which results in a systematic under-evaluation of alterations, as compared with quantitative RT-PCR. All 8 genes examined that were significantly up-regulated and 47 that were significantly down-regulated in both the E7#1 and E7#3 microarray analyses were also induced and repressed, respectively, when assessed by RT-PCR (Figure 4.8 - 4.10). One caveat to this analysis was, that though a downward trend was always observed in the expression of the 47 repressed genes when investigated by either microarray or RT-PCR analysis, for 8 of these genes RT-PCR expression levels in E7#3 RNA samples did not indicate a significant difference, i.e. it did not have a fold change $\geq 2$ as detected in the microarray analysis.

**Table 4.7: Pearson correlation between expression values as determined by Affymetrix microarrays and TaqMan® RT-PCR.**

| | Array E7#1 | TaqMan® E7#3 |
|---|---|---|
| Array E7#3 | 0.95 | 0.92 |
| TaqMan® E7#1 | 0.90 | 0.94 |

$p<0.0001$ (two –tailed).

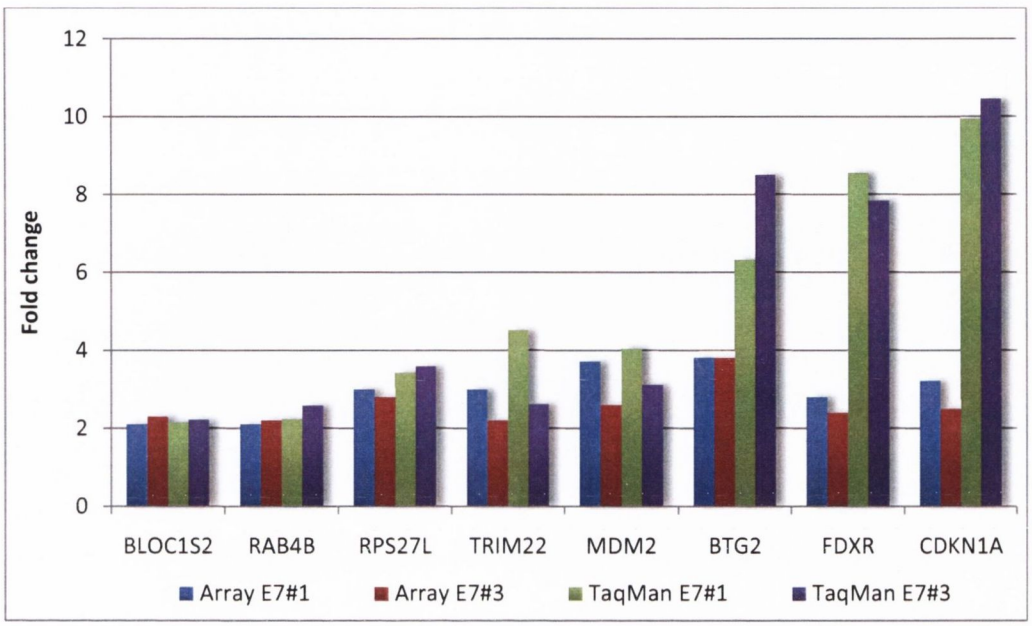


**Figure 4.8: Evaluating the correlation between Affymetrix microarray derived and TaqMan® RT-PCR derived gene expression values for 8 up-regulated genes.** SiHa ($1.5x10^5$) cells were transfected with negative control siRNA or transfected with E7 targeting siRNA (labelled #1 and #3) for 48hrs. Total RNA was extracted and mRNA expression levels were evaluated by both Affymetrix microarray analysis (labelled array) and by TaqMan® RT-PCR (labelled TaqMan). For Affymetrix microarray analysis, differential genes expression was determined using the XRAY software, where the negative control treated cells were used as a calibrator. For TaqMan® RT-PCR the mRNA gene expression values for each gene were normalised to that of GAPDH and calibrated to that of negative control cells to establish differential gene expression.

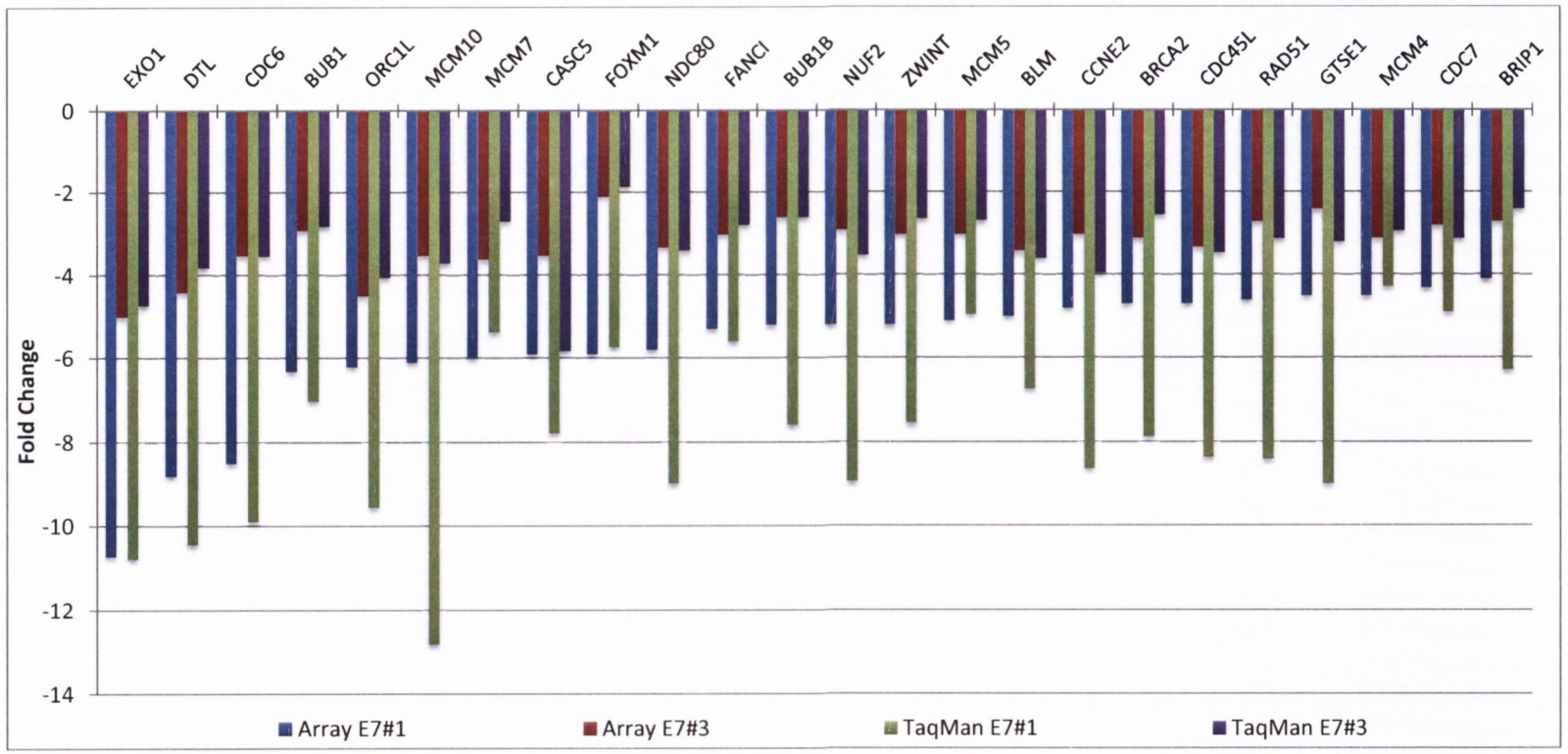


**Figure 4.9: Evaluating the correlation between Affymetrix microarray derived and TaqMan® RT-PCR derived gene expression values for 24 down-regulated genes.** SiHa ($1.5x10^5$) cells were transfected with negative control siRNA or transfected with E7 targeting siRNA (labelled #1 and #3) for 48hrs. Total RNA was extracted and mRNA expression levels were evaluated by both Affymetrix microarray analysis (labelled array) and by TaqMan® RT-PCR (labelled TaqMan). For Affymetrix microarray analysis, differential genes expression was determined using the XRAY software, where the negative control treated cells were used as a calibrator. For TaqMan® RT-PCR the mRNA gene expression values for each gene were normalised to that of GAPDH and calibrated to that of negative control cells to establish differential gene expression.

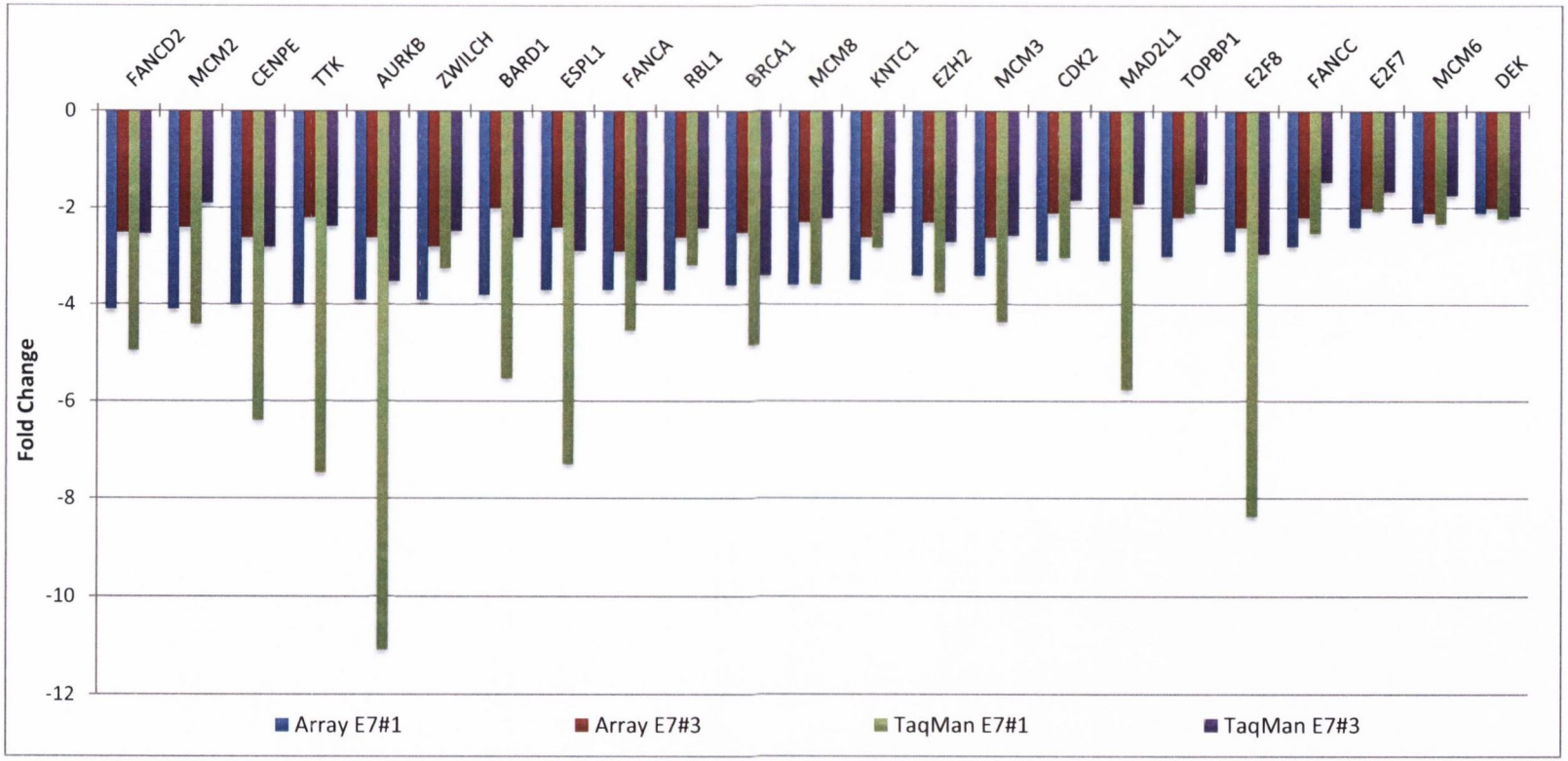


**Figure 4.10: Evaluating the correlation between Affymetrix microarray derived and TaqMan® RT-PCR derived gene expression values for 23 down-regulated genes.** SiHa ($1.5x10^5$) cells were transfected with negative control siRNA or transfected with E7 targeting siRNA (labelled #1 and #3) for 48hrs. Total RNA was extracted and mRNA expression levels were evaluated by both Affymetrix microarray analysis (labelled array) and by TaqMan® RT-PCR (labelled TaqMan). For Affymetrix microarray analysis, differential genes expression was determined using the XRAY software, where the negative control treated cells were used as a calibrator. For TaqMan® RT-PCR the mRNA gene expression values for each gene were normalised to that of GAPDH and calibrated to that of negative control cells to establish differential gene expression.

As mentioned in section 4.4.5, there was an additional HPV16 E7 targeting siRNA, E7#2, that altered the RNA expression of E6/E7 to a similar extent as E7#1 and E7#3. To further evaluate the above mentioned, 8 genes and their expression in RNA isolated from E7#2 transfected SiHa cells, where E6/E7 silencing had been confirmed (section 3.4.2), was assessed (Figure 4.11). For 4 of the 8 genes, FOXMI, MCM2, MAD2L1 and cdk2, a significant down-regulation in their expression was demonstrated. For the remaining 4 there was a decrease in their expression as had been noted for both E7#1 and E7#3 and while it was greater than that seen with E7#3, it did not go beyond the significance threshold of 2. The analysis with E7#2 was extended to all 55 genes and this showed a high correlation with both TaqMan and array data from the other two siRNA (Table 4.8). Overall these results indicate that the microarray results are an accurate reflection of gene expression changes in response to the E6/E7 silencing by E7 siRNA.

**Table 4.8: Pearson correlation between expression values as determined by Affymetrix microarrays and TaqMan® RT-PCR for E7 siRNA transfected SiHa cells.**

| | Array E7#1 | Array E7#3 | TaqMan® E7#1 | TaqMan® E7#3 |
|---|---|---|---|---|
| TaqMan® E7#2 | 0.87 | 0.91 | 0.94 | 0.96 |
| TaqMan® E7#3 | 0.87 | 0.92 | 0.94 | |
| TaqMan® E7#1 | 0.90 | 0.89 | | |

$p<0.0001$ (two –tailed).

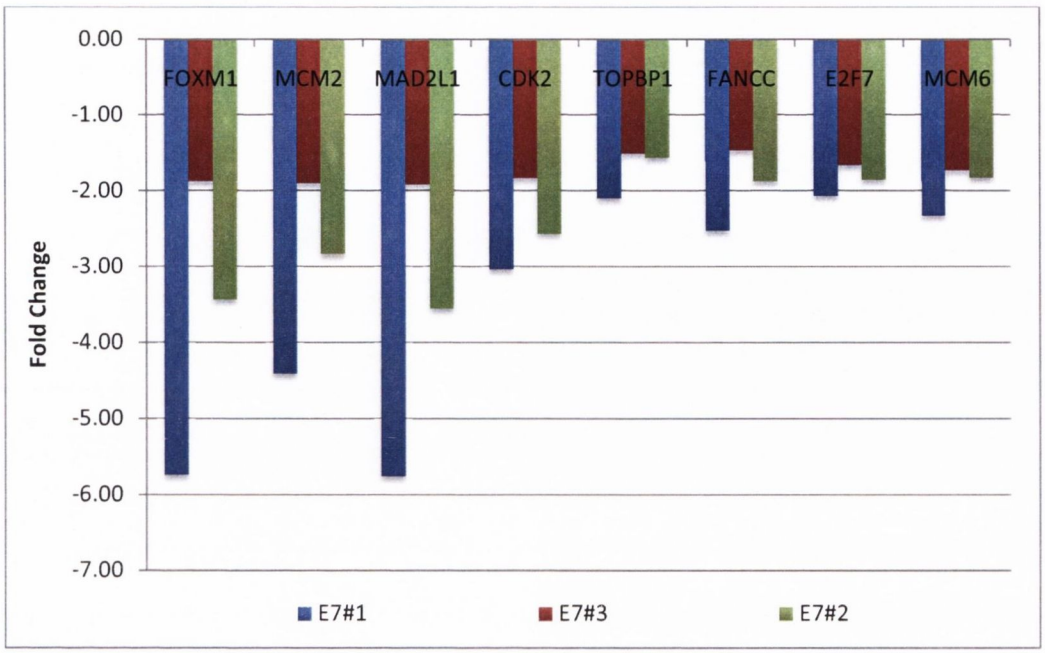


**Figure 4.11: Evaluating the validity of 8 genes which did not meet significance parameters in E7#3 samples when analysed by TaqMan® RT-PCR but did when analysed by Affymetrix microarray analysis.** SiHa ($1.5x10^5$) cells were transfected with negative control siRNA or transfected with E7 targeting siRNA (labelled #1, #2 and #3) for 48hrs. Total RNA was extracted and mRNA expression levels were evaluated by both Affymetrix microarray analysis and by TaqMan® RT-PCR. The mRNA gene expression values for each genes was normalised to that of GAPDH and calibrated to that of negative control cells to establish differential gene expression.

To further evaluate the microarray results, it was decided that a subset of group II and group III genes would be assessed by TaqMan® RT-PCR. The analysis would not only be performed in RNA isolates from cells transfected with E7#1 and E7#3, but also with E7#2. The aim of taking this approach, was to try and determine in the case of group II genes whether the observed expression in the E7#1 or the E7#3 array sets was more representative of the cellular response, and in the case if group III genes to ascertain whether the results were true effects of E7 silencing or potentially were off-target effects.

The 6 group III genes analysed were determined by the microarray analysis to be significantly altered in E7#1 transfected cells but not E7#3. RT-PCR demonstrated that these were all true biological consequences of the loss of E6/E7 expression, with all 6 genes being significantly altered in both E7#1 and E7#2 transfected cells (Table 4.9; Figure 4.12 B). In addition, all 6 were observed to be down-regulated in the E7#3 RNA sample correlating with the trend seen in the E7#1 and E7#2 data and 2 were even detected as significantly differential expressed (>2 foldchange), CDCA8 and FANCB.

Of the 7 group II genes analysed, all were determined to be significantly altered by E7#1, including 4 that did not meet the significance criteria in the array analysis (Table 4.9; Figure 4.12 A). In the majority of cases, the E7#2 expression profile of these 7 genes resembled that of E7#1, with the one exception of USP1, which fell just below the 2 fold change significance limit. For cells treated with E7#3, the array and RT-PCR results were comparable with the exception of BIRC5. On the whole, this analysis would suggest that where a significant difference is observed with the array analysis that this is a true event.

**Table 4.9: Differential gene expression of group II and III gens as determined by Affymetrix microarrays and TaqMan® RT-PCR for E7 siRNA transfected SiHa cells.**

| | Genes | Array Analysis | | TaqMan Analysis | | |
|---|---|---|---|---|---|---|
| | | E7#1 | E7#3 | E7#1 | E7#2 | E7#3 |
| Group II | SULF2 | 5.51 | 4.11 | 10.55 | 9.29 | 7.45 |
| | TP53INP1 | 4.41 | 3.61 | 6.43 | 5.14 | 5.05 |
| | KIF2C | -4.41 | -2.91 | -6.66 | -3.77 | -3.30 |
| | CCNA2 | -6.11 | -3.81 | -8.22 | -3.87 | -3.57 |
| | USP1 | -2.71 | -2.31 | -2.52 | -1.98 | -1.94 |
| | CDKN2C | -3.01 | -2.41 | -2.69 | -2.46 | -1.96 |
| | BIRC5 | -4.01 | -1.91 | -4.74 | -6.56 | -5.72 |
| Group III | CHEK1 | -2.51 | 0.00 | -2.36 | -2.04 | -1.88 |
| | RPA2 | -2.51 | 0.00 | -2.34 | -2.12 | -1.46 |
| | FANCB | -2.61 | 0.00 | -2.69 | -2.10 | -1.56 |
| | CDCA8 | -2.81 | 0.00 | -7.25 | -3.83 | -2.43 |
| | E2F1 | -3.01 | 0.00 | -6.04 | -3.33 | -2.94 |
| | FANCM | -3.01 | 0.00 | -3.04 | -2.21 | -1.91 |

Blue represents significant alterations and red represents non-significant alterations. For microarray analysis significance was defined as ≥ 2 fold change and ≤ 0.05 FDR. For microarray analysis significance was defined as ≥ 2 fold change.

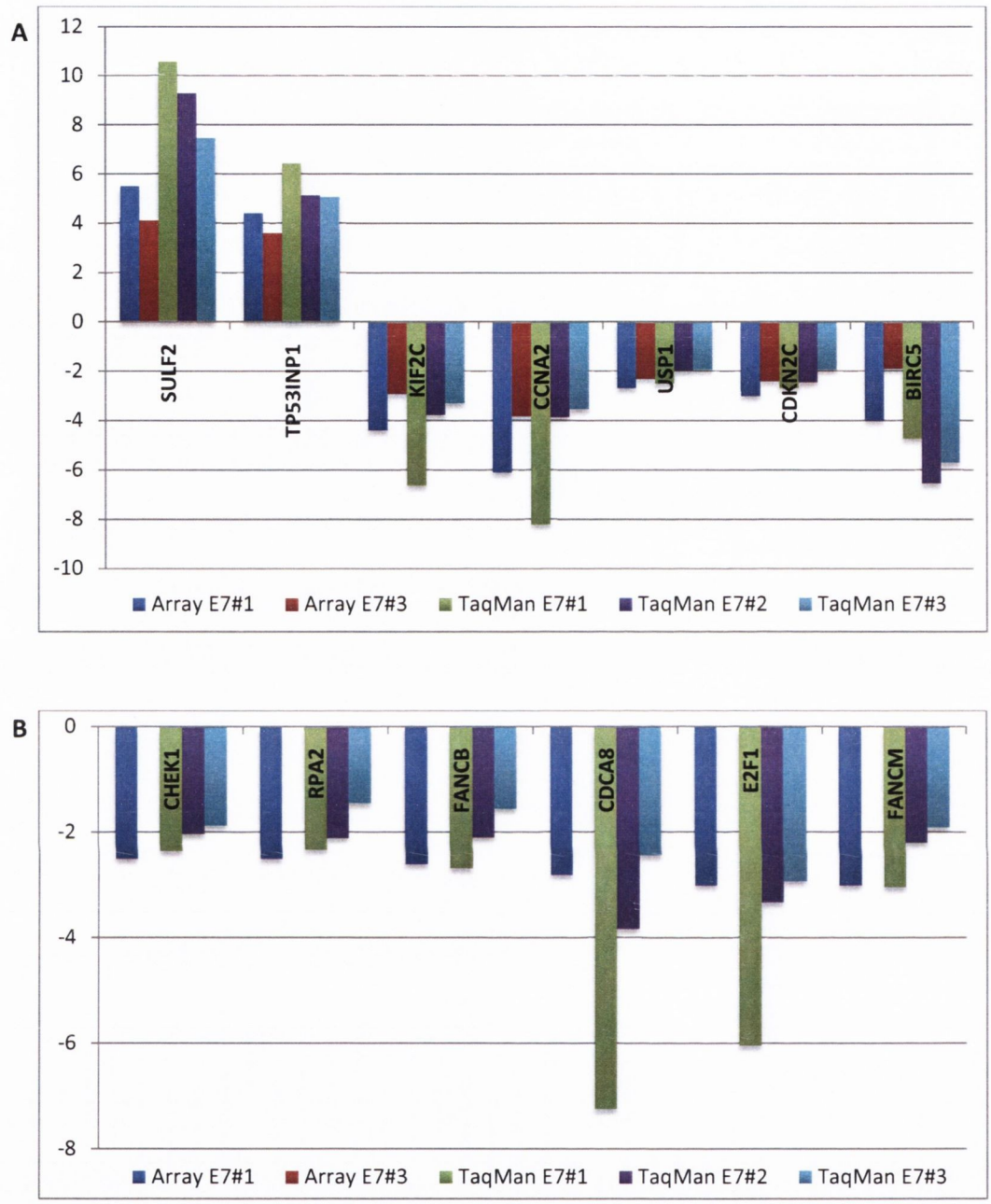


**Figure 4.12: Evaluating the validity of Group II and Group III differentially expressed genes.** SiHa ($1.5x10^5$) cells were transfected with negative control siRNA or transfected with E7 targeting siRNA (labelled #1, #2 and #3) for 48hrs. Total RNA was extracted and mRNA expression levels were evaluated by both Affymetrix microarray analysis (labelled array) and by TaqMan® RT-PCR (labelled TaqMan). For Affymetrix microarray analysis, differential genes expression was determined using the XRAY software, where the negative control treated cells were used as a calibrator. For TaqMan® RT-PCR, the mRNA gene expression values were normalised to that of GAPDH and calibrated to that of negative control cells to establish differential gene expression. (**A**) Represents 7 Group II genes, and (**B**) 6 Group III genes.

Finally, it was decided to use the expression of all of the above described genes (68 in total) to evaluate whether the cells treated with the negative control siRNA were a true reflection of the normal SiHa transcriptome profile. All the above presented data was calculated using the expression profile of cells transfected with negative control siRNA. The expression values for each of the 68 genes were re-calculated using untreated cells as the calibrator sample. The fold change in expression of these genes when the negative control and when the untreated samples were used as calibrators were compared (Figure 4.13). This analysis demonstrated that there was a highly significant correlation between the expression values in both groups. In addition, the fold change between the negative control expression value and the untreated expression value was calculated. As illustrated in figure 4.14, all fold change value fell within the limits of biological variation. Therefore, these results indicate that the negative control siRNA does not significantly alter the transcriptional profile of the SiHa cells.

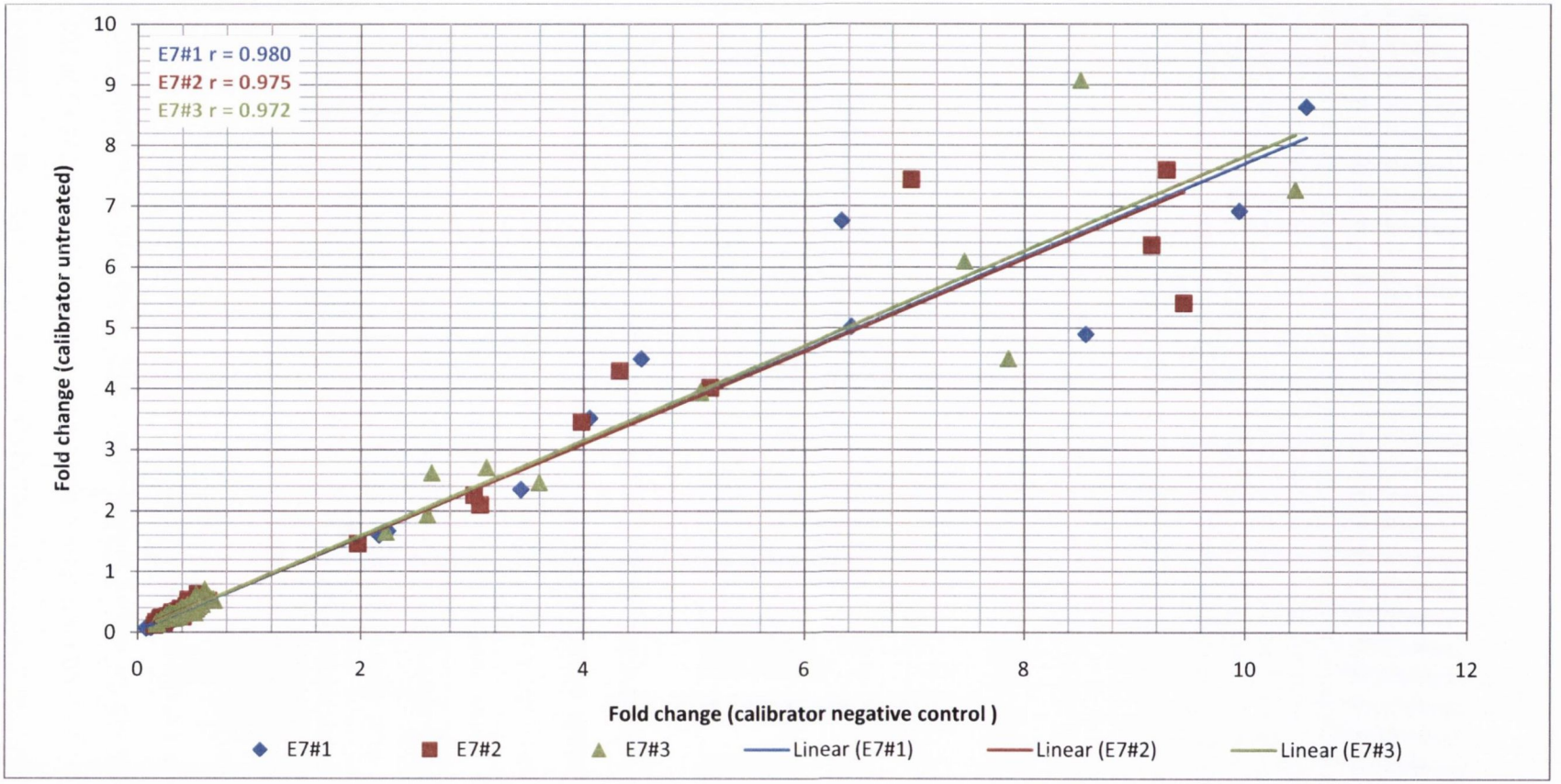


**Figure 4.13: Evaluating the correlation between TaqMan® fold change values when untreated cells were applied as a calibrator and when negative control cells were applied as the calibrator.** The fold change values as calculated using untreated and negative control cells for 68 genes from E7 siRNA transfected cells were plotted against each other and the Pearson correlation coefficient was calculated. There is a highly significant positive relationship between the common differentially expressed genes on both arrays ($r=0.883$, $p<0.0001$ (two –tailed)).

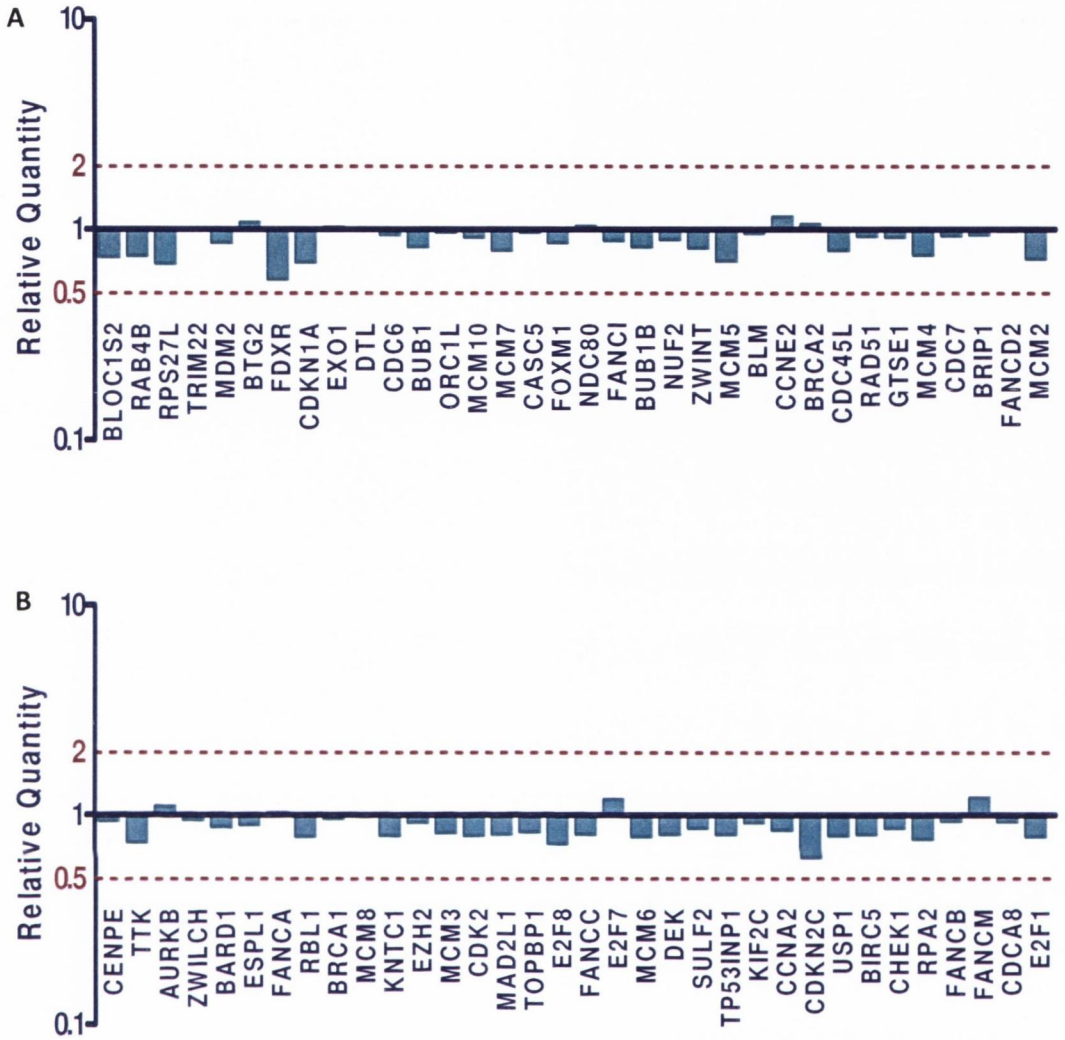


**Figure 4.14: Evaluation of the gene expression profile of 68 genes in SiHa cells transfected with negative control siRNA compared to untreated SiHa cells.** SiHa ($1.5x10^5$) cells were left untreated or transfected with negative control siRNA. After 48hours, total RNA was extracted and mRNA expression was evaluated for each of the 68 genes by TaqMan® RT-PCR. The mRNA expression for each gene was normalised to that of GAPDH and calibrated to that of the untransfected cells to establish the relative level of mRNA expression. Marked on the graphs are the considered limits of biological variation, from 0.5 to 2. (**A**) Represent a group of 34 of the 68 genes analysed and (**B**) represent the remaining 34.

### *4.4.7 Gene ontology analysis*

To investigate what key genes and processes were altered by the loss of E6/E7 expression, the group I gene list was uploaded and analysed in the two online gene ontology databases, DAVID and PANTHER. Both software statistically compare the input list to a reference list to look for under and over-represented molecular functions and biological processes. A total of 159 of the 168 genes in the group I were present in the PANTHER database and 161 were present in the DAVID database. Significance, a measure of the overrepresentation of a functional category compared to its representation in the Homo sapiens proteome, was set at p-value $\leq 0.05$ in PANTHER and FDR $\leq 0.05$ in DAVID. Tables 4.10 and 4.11 represent the biological processes identified by DAVID and PANTHER, respectively, as overrepresented. While the PANTHER data base output is considerably less, due to the algorithm used in this database (see section 4.3.5.4), the major biological processes highlighted by this analysis are also highly significant on the DAVID output. For the pathway analysis, DAVID determined the over-representation of cellular pathways within in the 161 genes identified based on data from both the publically available KEGG and Biocarta databases. Again, the output from the DAVID database was considerably more than from Panther. For the purposes of clarity, in any future discussion in relation to gene ontology analysis, the data discussed will be from the more comprehensive DAVID outputs.

**Table 4.10: Significantly over-represented biological processes as defined by the DAVID database.**

| Biological Process | Count | % | P value | FDR |
|---|---|---|---|---|
| cell cycle | 77 | 47.8 | 4.90E-57 | 2.60E-53 |
| cell cycle process | 64 | 39.8 | 1.40E-45 | 3.60E-42 |
| cell cycle phase | 50 | 31.1 | 4.50E-45 | 7.80E-42 |
| mitotic cell cycle | 47 | 29.2 | 3.40E-43 | 4.50E-40 |
| M phase | 45 | 28 | 2.20E-42 | 2.30E-39 |
| cell division | 42 | 26.1 | 5.10E-41 | 4.50E-38 |
| mitosis | 41 | 25.5 | 6.20E-41 | 4.60E-38 |
| M phase of mitotic cell cycle | 41 | 25.5 | 9.00E-41 | 5.90E-38 |
| DNA metabolic process | 57 | 35.4 | 5.30E-34 | 3.10E-31 |
| DNA replication | 35 | 21.7 | 1.00E-30 | 5.50E-28 |
| response to DNA damage stimulus | 34 | 21.1 | 1.20E-25 | 5.70E-23 |
| chromosome segregation | 20 | 12.4 | 1.80E-24 | 7.90E-22 |
| mitotic sister chromatid segregation | 16 | 9.9 | 2.70E-23 | 1.10E-20 |
| sister chromatid segregation | 16 | 9.9 | 5.10E-23 | 1.90E-20 |
| response to endogenous stimulus | 34 | 21.1 | 1.30E-22 | 4.50E-20 |
| DNA repair | 28 | 17.4 | 6.10E-21 | 2.00E-18 |
| regulation of progression through cell cycle | 35 | 21.7 | 5.10E-20 | 1.60E-17 |
| regulation of cell cycle | 35 | 21.7 | 6.10E-20 | 1.80E-17 |
| DNA-dependent DNA replication | 20 | 12.4 | 2.00E-19 | 5.40E-17 |
| chromosome organization and biogenesis | 29 | 18 | 1.30E-17 | 3.50E-15 |
| organelle organization and biogenesis | 44 | 27.3 | 1.10E-15 | 2.80E-13 |
| DNA replication initiation | 12 | 7.5 | 1.60E-15 | 3.70E-13 |
| cell cycle checkpoint | 14 | 8.7 | 8.70E-15 | 2.00E-12 |
| nucleobase, nucleoside, nucleotide and nucleic acid metabolic process | 80 | 49.7 | 2.60E-14 | 5.60E-12 |
| spindle organization and biogenesis | 9 | 5.6 | 4.20E-12 | 8.90E-10 |
| biopolymer metabolic process | 89 | 55.3 | 7.00E-12 | 1.40E-09 |
| microtubule-based process | 18 | 11.2 | 1.40E-11 | 2.80E-09 |
| regulation of mitosis | 12 | 7.5 | 3.10E-11 | 5.80E-09 |
| response to stress | 34 | 21.1 | 3.90E-10 | 7.10E-08 |
| chromosome condensation | 8 | 5 | 4.50E-10 | 7.80E-08 |
| interphase | 12 | 7.5 | 1.30E-09 | 2.20E-07 |
| cell proliferation | 28 | 17.4 | 2.20E-09 | 3.70E-07 |
| mitotic chromosome condensation | 7 | 4.3 | 3.70E-09 | 5.80E-07 |
| microtubule cytoskeleton organization and biogenesis | 11 | 6.8 | 3.70E-09 | 5.70E-07 |
| interphase of mitotic cell cycle | 11 | 6.8 | 1.00E-08 | 1.50E-06 |
| mitotic cell cycle checkpoint | 8 | 5 | 1.50E-08 | 2.20E-06 |
| cellular process | 138 | 85.7 | 2.00E-08 | 2.80E-06 |
| cellular component organization and biogenesis | 53 | 32.9 | 2.60E-08 | 3.70E-06 |
| traversing start control point of mitotic cell cycle | 5 | 3.1 | 2.20E-07 | 3.00E-05 |
| cytoskeleton organization and biogenesis | 20 | 12.4 | 2.70E-07 | 3.60E-05 |

| Biological Process | Count | % | P value | FDR |
|---|---|---|---|---|
| regulation of progression through mitotic cell cycle | 7 | 4.3 | 3.70E-07 | 4.70E-05 |
| macromolecule metabolic process | 95 | 59 | 6.50E-07 | 8.10E-05 |
| regulation of cellular process | 67 | 41.6 | 2.20E-06 | 2.70E-04 |
| mitotic spindle organization and biogenesis | 5 | 3.1 | 3.00E-06 | 3.60E-04 |
| regulation of DNA metabolic process | 7 | 4.3 | 8.00E-06 | 9.30E-04 |
| double-strand break repair | 6 | 3.7 | 1.50E-05 | 1.70E-03 |
| cellular metabolic process | 100 | 62.1 | 1.90E-05 | 2.10E-03 |
| S phase | 5 | 3.1 | 2.80E-05 | 3.00E-03 |
| G1 phase of mitotic cell cycle | 5 | 3.1 | 2.80E-05 | 3.00E-03 |
| meiosis | 7 | 4.3 | 2.90E-05 | 3.00E-03 |
| M phase of meiotic cell cycle | 7 | 4.3 | 2.90E-05 | 3.00E-03 |
| regulation of biological process | 67 | 41.6 | 3.20E-05 | 3.20E-03 |
| meiotic cell cycle | 7 | 4.3 | 3.40E-05 | 3.40E-03 |
| primary metabolic process | 99 | 61.5 | 4.70E-05 | 4.50E-03 |
| G1 phase | 5 | 3.1 | 5.00E-05 | 4.70E-03 |
| recombinational repair | 4 | 2.5 | 1.50E-04 | 1.40E-02 |
| double-strand break repair via homologous recombination | 4 | 2.5 | 1.50E-04 | 1.40E-02 |
| DNA integrity checkpoint | 5 | 3.1 | 1.90E-04 | 1.70E-02 |
| cytokinesis | 5 | 3.1 | 2.10E-04 | 1.90E-02 |
| regulation of nucleobase, nucleoside, nucleotide and nucleic acid metabolic process | 42 | 26.1 | 2.60E-04 | 2.20E-02 |
| DNA unwinding during replication | 4 | 2.5 | 3.00E-04 | 2.60E-02 |
| phosphoinositide-mediated signaling | 7 | 4.3 | 4.00E-04 | 3.30E-02 |
| DNA geometric change | 4 | 2.5 | 4.50E-04 | 3.60E-02 |
| DNA duplex unwinding | 4 | 2.5 | 4.50E-04 | 3.60E-02 |
| cytokinesis during cell cycle | 3 | 1.9 | 4.80E-04 | 3.80E-02 |
| microtubule-based movement | 7 | 4.3 | 5.40E-04 | 4.20E-02 |

Highlighted in red are the biological processes that overlap with the PANTHER database output, Table 4.11.

**Table 4.11: Significantly over-represented biological processes as defined by the PANTHER database.**

| Biological Process | Count | Percentage | P-value |
|---|---|---|---|
| Cell cycle | 69 | 43.4 | 1.97E-51 |
| DNA metabolism | 37 | 23.3 | 2.22E-31 |
| DNA replication | 24 | 15.1 | 8.01E-24 |
| Mitosis | 28 | 17.6 | 2.17E-19 |
| Nucleoside, nucleotide and nucleic acid metabolism | 59 | 37.1 | 7.25E-13 |
| DNA repair | 15 | 9.4 | 7.13E-11 |
| Cell cycle control | 19 | 11.9 | 3.66E-09 |
| Chromosome segregation | 12 | 7.5 | 4.98E-09 |
| Chromatin packaging and remodeling | 11 | 6.9 | 5.45E-05 |
| Cell proliferation and differentiation | 21 | 13.2 | 6.45E-05 |
| Cytokinesis | 7 | 4.4 | 1.87E-03 |

**Table 4.12: Significantly over-represented pathways as defined by the PANTHER and DAVID databases.**

| Source | Pathway | Count | Percentage | P-value |
|---|---|---|---|---|
| PANTHER | DNA replication | 4 | 2.5 | 3.52E-03 |
| | p53 pathway | 6 | 3.8 | 3.94E-02 |
| DAVID-KEGG | Cell cycle | 20 | 12.4 | 2.80E-20 |
| | DNA polymerase | 7 | 4.3 | 5.90E-08 |
| | Pyrimidine metabolism | 8 | 5 | 1.50E-05 |
| | Purine metabolism | 7 | 4.3 | 2.20E-03 |
| | p53 signaling pathway | 5 | 3.1 | 3.70E-03 |
| | Prostate cancer | 4 | 2.5 | 4.90E-02 |
| DAVID-BioCarta | BRCA1-dependent Ub-ligase activity | 5 | 3.1 | 1.70E-06 |
| | Role of BRCA1, BRCA2 and ATR in Cancer Susceptibility | 6 | 3.7 | 7.70E-06 |
| | ATM Signaling Pathway | 4 | 2.5 | 2.40E-03 |
| | Cyclins and Cell Cycle Regulation | 4 | 2.5 | 3.20E-03 |
| | CDK Regulation of DNA Replication | 3 | 1.9 | 4.60E-03 |
| | p53 Signaling Pathway | 3 | 1.9 | 1.90E-02 |
| | Cell Cycle | 3 | 1.9 | 4.00E-02 |

## 4.5 Discussion

HPV infection has been established as the main etiological factor in the pathogenesis of cervical cancer (Kirwan and Herrington, 2001). Therefore, it would seem logical in order to gain further insight into the disease process that an understanding of the oncogenic activities of HPV in the host cell is required. A crucial event in the carcinogenic progression of cervical cancer is the integration and subsequent un-regulated expression of the viral oncogenes E6 and E7 (zur Hause and deVillers, 1994; Snijders *et al.*, 2006; Pett and Coleman 2007). Some functions of these oncoproteins are well classified, such as their interaction with the cell regulatory molecules p53 and Rb (Scheffner *et al.*, 1991; Werness *et al.*, 1990; Dyson *et al.*, 1992), however there are still many unanswered questions when it comes to their role in carcinogenesis. In this chapter a reverse genetic study was performed to examine the activity of high-risk HPV16 E6 and E7 oncogenes. This entailed a combination of microarray screening and functional classification of genes differentially expressed after the concomitant silencing of E6 and E7 expression. A disadvantage of this approach, is that it is known that some functions of E6 and E7 are not manifested at the level of gene expression alterations. For example the inhibitory activity of E6 on p53 is mediated through is interaction with E6AP, where the E6/E6AP complex functions as an ubiquitin ligase inducing p53 degradation (Huibregtse *et al.*, 1993a; Huibregtse *et al.*, 1993b). Therefore, it would clearly be desirable to also examine alterations in global protein levels upon E6 or E7 silencing. However, until protein array technology becomes available that allows for the surveillance of a significant fraction of the proteome (Zhu *et al.*, 2003), gene expression analysis provides the most comprehensive and unbiased method for analysing the response of HPV-positive cells to the depletion of E6/E7.

Chapter 3 describes the establishment of an *in vitro* system to concomitantly suppress the expression of the viral oncogenes E6 and E7. This was achieved through the transfection of SiHa cells, a HPV16 positive cervical carcinoma cell line, with siRNA specific for the E7 coding region. Three of the designed siRNA were deemed highly functional at the RNA level, denoted E7#1, E7#2 and E7#3. The transcriptional profile

induced by two of these siRNA, E7#1 and E7#3, was analysed by microarray analysis in this study. The reason it was decided to evaluate the activity of two siRNA was based on the ongoing issue in RNAi experiments of siRNA induced off-target effects. As discussed thoroughly in chapter 3, these events can be mediated by the binding of siRNA with unintended target genes, hence suppressing their expression (Jackson *et al.*, 2003; Birmingham *et al.*, 2006; Jackson *et al.*, 2006), or by activation of the innate immune response by type I interferon and inflammatory cytokines (Heil etal., 2004; Judge *et al.*, 2005; Hornung *et al.*, 2005). There are several methods being pursued to try and eliminate the potential of off-target effects, including the use of chemical modifications (Hornung *et al.*, 2005; Chen *et al.*, 2008). Indeed the E7#1 and the E7#2 siRNA, which were designed by Ambion, included a LNA modification for such purposes. To ensure that the observed effects at the transcriptome were specific to the targeted silencing of E6 and E7 and not due to unconnected events, multiple controls were utilised. All analyses were compared to negative control siRNA transfected cells to ensure that none of the effects identified were due to the activation of the RNAi pathway or the transfection procedure. The analysis of the transcriptional profile of two siRNA meant, that it was possible to implement a multiplicity control, i.e. the application of two different siRNA targeting different regions of the same gene, which should given identical end results. The experimental approach taken in this study should avoid the analysis of genes, the modulation of which is irrelevant to E6/E7 silencing.

Interestingly, the initial analysis of the transcriptional profiles produced by the microarray experiments demonstrated that there was high correlation in the gene expression pattern between the cells transfected with E7 targeting siRNA and negative control siRNA. This indicated that the silencing of the HPV16 E6 and E7 oncogenes by the E7 siRNA did not mediate transcriptome wide changes, but that a discrete group of genes were altered in expression. Indeed, when the gene expression profiles of E7#1 and E7#3 were compared to that of the negative control, the number of differential expressed genes represented 3.8% and 3.3%, respectively, of the total number of

genes expressed in these cells. In later analysis using TaqMan® RT-PCR, it was possible to demonstrate that the expression profile of 68 genes, identified as differentially expressed by either E7#1 and/or E7#3 by microarray analysis, had the same expression profile post E6/E7 silencing whether they were analysed in comparison to the negative control cells or untreated cells. Furthermore, it was possible to demonstrate that the expression levels of these 68 genes were similar in the cells left untreated and in those treated with negative control siRNA; a comparative analysis demonstrated all values fell within biological variation limits. This signifies that the negative control is not having any major consequences on the expression profile of the SiHa cells and that the low variance between the groups is a true reflection of the level of change in the cells post E6/E7 silencing.

Since the experimental premise for performing microarray experiments on two siRNA was to implement a multiplicity control to ensure the events described by the analysis were a true phenomenon, a cross comparison was made between the genes significantly differentially regulated by E7#1 and E7#3 siRNA. The parameters used to define significant differential expression were fold changes $\geq 2$ and FDR $\leq 0.05$. 168 genes were identified as meeting these criteria both on the E7#1 and E7#3 differentially expressed gene sets. This corresponded to 66% and 75% of the total number genes, whose expression was differentially regulated by the introduction of E7#1 and E7#3 siRNA, respectively. This, along with the fact that the fold change values between these 168 genes are highly correlated (r=0.88), demonstrates that E7#1 and E7#3 induce similar alterations in the transcriptional profile of SiHa cells. Further analysis of these gene lists demonstrated that the commonality between the activities of the two siRNA was even higher. It was possible to shown that of the 253 genes demonstrated to be significantly differentially expressed by E7#1 (fold change $\geq 2$ and FDR $\leq 0.05$) that 219 were altered by E7#3 by at least 1.5 fold with a significance level of at least p-value $\leq 0.05$. A similar analysis with the 221 genes significantly differentially expressed by E7#3 demonstrated that 200 were altered by E7#1 by at least 1.5 fold, p-value $\leq 0.05$. This analysis adds further assurance that the data sets

derived by microarray analysis are truly representative of events specific to E6/E7 silencing. In the reminder of this discussion, analysis is presented in relation to the 168 genes whose differential expression was identified as $\geq 2$ fold and $\leq 0.05$ FDR by both the activity of E7#1 and E7#3.

TaqMan® RT-PCR was performed on 55 targets from the list of 168 differentially expressed genes using the same E7#1 and E7#3 samples as in the microarray analysis. The correlation between the TaqMan® and the microarray result over these 55 genes was highly significant ($\geq 0.90$), thus validating the microarray results. Furthermore, these 55 genes were evaluated in the third highly functional siRNA, E7#2, and not only was there a highly significantly correlation between these results and those of the TaqMan® data from the other two siRNA samples, but also with their microarray data ($\geq 0.87$). This provides conclusive evidence that the gene signature identified by the microarray analysis was truly representative of the effect of E6/E7 silencing in SiHa cells.

Three previous studies took a similar reverse genetic approach, combining siRNA and microarray analysis to elucidate genes targeted by the high-risk HPV oncogenes. However, only one study by Kuner *et al.* (2007) evaluated the concomitant loss of E6 and E7. A cross comparison between the 168 genes identified as significantly altered in this study and the 648 identified by Kuner *et al.* (2007) demonstrates that 19% of the 168 genes were also represented on the Kuner study (see Table 6 in the appendix for cross comparison of gene lists). This overlap is not particularly sizeable, but there are several differences between the two studies, in particular the *in vitro* system used was the HPV18 positive cervical cancer cell line HeLa. A study by Kelley *et al.* (2005) specifically targeted E6 expression by RNAi in HeLa and SiHa cell lines prior to microarray analysis. It was found that E6 silencing had a greater impact on the transcriptional profile of HeLa cells than SiHa cells. The differences could not be explained by transfection efficiencies and therefore it was concluded to be due to inherent differences among the cell lines. A potential explanation is the different tissue

types from which the original tumours arose, HeLa cells were derived from an adenocarcinoma and SiHa cells from a squamous cell carcinoma. Indeed a study by Rosty *et al.* (2005) where gene expression profiling of cervical cancer tumour biopsies was performed demonstrated that there was a clear distinction between the gene transcriptional profiles of tumour types depending on their histology, i.e. adenocarcinoma versus squamous cell carcinoma. These studies provide a potential explanation for the variation seen between this analysis and that of Kuner *et al.* (2007). It should be noted, that while there is discourse between the exact results of this study and that of Kuner *et al.* (2007), the gene ontology classifications of the differential regulated genes sets were highly similar. The top five categories indentified in the Kuner study were cell cycle, DNA replication, DNA metabolic process, M phase of the mitotic cell cycle and DNA repair, which closely corresponds with those identified in this study (Table 4.10 and 4.11).

As mentioned above in 2005 Rosty *et al.* published a paper in relation to gene expression profiling of cervical cancer tumour samples. They demonstrated that compared to normal cervix there were 1206 transcripts showing over-expression in tumour samples. A comparative analysis between the genes identified in this study and the 1206 of Rosty *et al.* demonstrated a high similarity, with 80 of the 168 identified (48%; see Table 6 of the appendix for cross comparison of gene lists). As was anticipated, none of the 10 up-regulated genes described within the 168 differentially expressed featured on the Rosty over-expression data set. Again, there was high correlation in the categories identified by gene ontology analysis. For the 1206 probe sets, the major and most significant functional groups were: DNA metabolism (n=96), mitotic cell cycle (n=93), regulation of cell cycle (n=59), DNA replication and chromosome cycle (n=56), and DNA repair (n=35). This demonstrates the relevance of the E6 and E7 targets identified in the present analysis for HPV-associated tumourigenesis *in vivo.*

Several other studies examining the transcriptional profile of cervical cancer have been published (Ahn *et al.*, 2004; Garner-Hamrick *et al.*, 2004; Thierry *et al.*, 2004; Santin *et*

*al.*, 2005; Johung *et al.*, 2006; Kelley *et al.*, 2006). While it was not possible to evaluate the correlation between these data sets and the one described in this study, where gene ontology data was provided, there was a high degree of overlap between the functional categories represented. Importantly, these previous microarray experiments have lead to the identification of several biomarkers, the altered expression of which is believed to be induced by HPV infection and mediated carcinogenesis. A number of these markers have been tested to identify dysplastic cells in cervical cancer and several are represented on the list of a 168 differentially expressed genes.

For example, an over-representation of DNA replication genes was observed according to the gene ontology analysis. Included within this group were many of the genes known to be involved in the DNA licensing complex, all of which were observed to be down-regulated. These included the origin recognition complex subunit 1-like (yeast) (Orc1), cell division cycle protein 6 (cdc6), chromatin licensing and DNA replication factor 1 (cdt1) and the minichromosome maintenance proteins (MCM's) 2 to 8. The DNA licensing complex is involved in the initiation of DNA replication and ensures that replication occurs only once in a single cell cycle (Figure 4.15). Over-expression of MCM 2,4,5 and 6, cdc6 and cdt1 have all been identified in gene expression profiling experiments (Chen *et al.*, 2003; Santin *et al.*, 2005) in keeping with the theory that cell cycle dysregulation is a key factor in the development of cervical cancer. Both immunohistochemical analysis and PCR studies have demonstrated over expression of cdc6, MCM3 and MCM5 in cervical cancer (Ishimi *et al.*, 2003; Ha *et al.*, 2004; Murhpy *et al.*, 2005). This study demonstrates that upon silencing of viral oncogene expression, there is a complete shutdown in this cellular activity. The association between the observed of over-expression these biomarkers in cervical cancer and their down-regulation post E6/E7 silencing, provides support for the relevance of this data set to the clinical setting. In addition it clearly demonstrates that the over-expression of these biomarkers in the setting of cervical cancer is due to the presence and activity of

the viral oncogenes E6 and E7. This capacity to switch off the biomarkers, used to detect the disease state, is a unique finding in a cancer system.

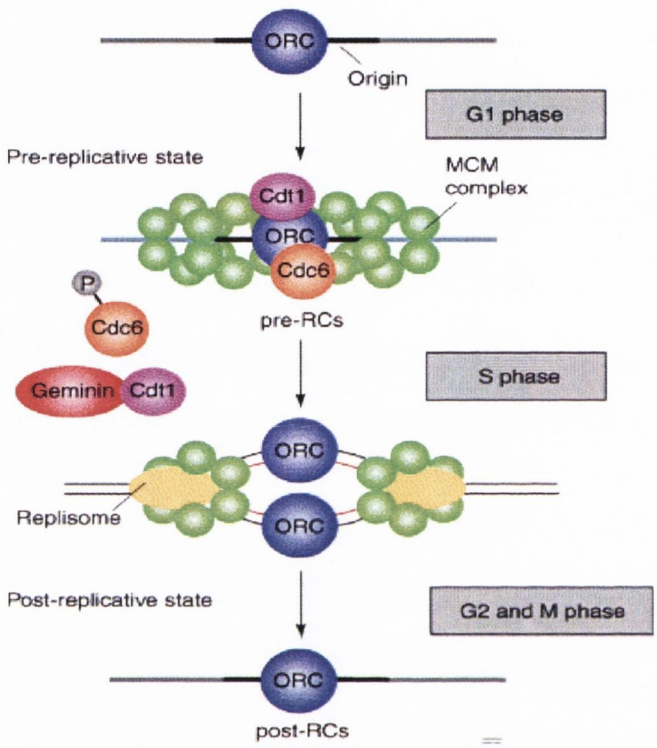


**Figure 4.15: DNA replication – the formation of the licensing complex.** Initiation of DNA replication requires the regulated assembly of pre-replicative complexes (pre-RC) consisting of MCM proteins, cell division cycle protein 6 (cdc6) and cdt1, onto the origins of replication, e.g. ORC1L, scattered along each chromosome. Cdc6 and cdt1 act as MCM loading proteins. Once loaded onto the origin of replication, the MCM complex forms a hexameric ring, which may act as a rotary motor that pumps DNA along its helicase axis, comparable to the movement of a threaded bolt through a nut. As DNA replication proceeds, MCM proteins are phosphorylated, the MCM complex becomes dissociated from the chromatin and is prevented from re-binding DNA until late mitosis, by the inactivation of its loading factors, cdc6 and cdt1. Cdc6 inactivation is achieved by phosphorylation, whereas cdt1 is inactivated via binding to its inhibitor, geminin. (reproduced Pelizon, 2003)

The molecular biomarkers identified within the set of 168 differentially expressed genes are not limited to the DNA licensing genes. Other examples include Topoisomerase IIa, v-myb myeloblastosis viral oncogene homolog (avian)-like 2 (MYBL2) and survivin (Martin *et al.*, 2007), all of which were demonstrated to decrease in expression upon E7 siRNA mediated E6/E7 silencing. However noticeably absent was $p16^{INK4A}$, which is probably the best established biomarker for cervical dysplasia and HPV infection (Martin *et al.*, 2007). This in fact, though an unexpected result, is not an unusual finding. Several microarray studies and gene specific studies which have de-regulated the expression of HPV E6 and/or E7 have not observed any effect on $p16^{INK4A}$ (DeFillipis *et al.*, 2003; Thierry *et al.*, 2004; Kuner *et al.*, 2007). It has been suggested, that events that occur during the carcinogenic progression uncouple $p16^{INK4A}$ expression from that of the oncogenes, in particular E7 (DeFillipis *et al.*, 2003). Indeed, a recent body of work by a colleague in our laboratorty indicates that after HPV infection $p16^{INK4A}$ expression becomes autonomous, as it is uncoupled from its natural antisense molecule, ANRIL, and from regulatory miRNA molecules.

The gene ontology analysis performed using the DAVID database, demonstrated that the repression of E6/E7 affected a number of pathways. However, it is not possible to discuss each in detail, but it is worthwhile to point out a number of interesting insights that these results have provided.

The p53 pathway was highlighted as over-represented within the 168 differentially expressed genes. This was anticipated and provides further validation for the experimental approach taken in the initial siRNA experiments (chapter 3), i.e. that in targeting E7 there was a concomitant repression of E6. Of the 10 genes whose expression was up-regulated by the repression of E6/E7, 7 were identified as p53 responsive genes, this included well characterised targets such as p21 and MDM2 and less well established targets like tripartite motif-containing 22 (TRIM22) and BTG family member 2 (BTG2). In addition, 4 of the 158 down regulated genes represented proteins whose activity is known to interfere with p53 fuction, including the DEK

oncogene (DEK), denticleless homolog (Drosophila) (DTL), forkhead box M1 (FOXM1), enhancer of zeste homolog 2 (Drosophila) (EZH2) and G-2 and S-phase expressed 1 (GTSE1); providing further evidence of an activation of the p53 pathways post E7#1 and E7#3 transfection into SiHa cells. Importantly, though there was a re-activation of the p53 pathway, there were no signs that its pro-apoptotic activities were being mediated. No well characterised apoptotic genes were identified within the 168 differentially expressed genes. In addition, the gene ontology analysis, even if the significance parameters were relaxed to $p \leq 0.1$, did not highlight an apoptotic functional category. This result corroborates the findings of chapter 3, where flow cytometry analysis using dual Annexin V and PI staining demonstrated that the introduction of any of the E7 siRNA into the SiHa cells did not induce an apoptotic response over the 96hr time period studied.

Significant over-representation of genes involved in the mitotic phase of the cell cycle was observed. Given the fact that in chapter 3, it was demonstrated that the introduction of E7 targeting siRNA into SiHa cells resulted in a cell cycle arrest in G1, with a strong reduction in S phase, it was anticipated that a major representation of repressed S phase genes would be observed. However, only 5 genes specific for the S phase were identified, and the FDR for this classification was 3.0E-3, in comparison to 45 genes within the M phase, with a FDR of 2.3E-39. These results strongly suggest that the viral oncogenes not only influence the G1/S phase transition of the cell cycle but also the M phase. While this result was unexpected, given the functional analysis performed on the system, it is in fact in agreement with several previously published studies (Garner-Hamerick *et al.*, 2004; Thierry *et al.*, 2004; Rosty *et al.*, 2005; Johung *et al.*, 2007). The consensus from the literature appears to be that this effect is mediated in an E7 dependent manner. For instance, Thierry *et al.* (2004) demonstrated that the majority of mitotic genes indentified in their study, post ectopic expression of E2 in HPV18 positive cells, were E2F responsive and Johung *et al.* (2005) who only repressed HPV E7 also identified an over-representation of mitotic genes in their gene cohort (p-value of 2.1E-27). The emerging view is that E7 oncogene, through its interaction with Rb, reactivates a mitotic pathway regulated by E2F in addition to the activity these

proteins have on the G1/S genes. Supporting this view, is recent microarray data that has demonstrated that E2F responsive genes have a role to play in the regulation of mitotic genes (Ishida *et al.*, 2001 ; Muller *et al.*, 2001; Weinmann *et al.*, 2001; Markey *et al.*, 2002; Polager *et al.*, 2002).

What was evident from the gene ontology analysis, is that many of the mitotic genes identified in this study were involved in chromosomal segregation, specifically there were many centromeric proteins, kinetochore associated proteins and members of the spindle checkpoint (Table 4.13). The functions of these three groups of proteins are highly interconnected. Kinetochores are specialised structures that form at centromers and serve as the site of microtubule attachment in eukaryotic chromosomes (Pluta *et al.*, 1995; Rieder and Salmon, 1998). The spindle assembly checkpoint monitors events that occur at the kinetochore to verify that all the chromosomes are properly orientated on the mitotic spindle before anaphase can begin (Elledge, 1998; Rieder and Salmon, 1998; Wells, 1996; Scaerou *et al.*, 1999). The mitotic checkpoint ensures that chromosomes are divided equally between daughter cells and is the primary mechanism preventing the chromosome instability often seen in aneuploid human tumours (Kops *et al.*, 2005).

**Table 4.13: Centromeric proteins, kinetochore associated proteins and members of the spindle checkpoint identified within the list of 168 differentially expressed genes.**

| Gene Symbol | Gene description |
|---|---|
| **Aurora B** | aurora kinase B |
| **Bub1** | budding uninhibited by benzimidazoles 1 homolog (yeast) |
| **BubR1/Bub1B** | budding uninhibited by benzimidazoles 1 homolog beta (yeast) |
| **CASC5/KNL1** | cancer susceptibility candidate 5 |
| **CENPA** | centromere protein A |
| **CENPE** | centromere protein E 312kDa |
| **CENPI** | centromere protein I |
| **CENPJ** | centromere protein J |
| **CENPK** | centromere protein K |
| **CENPL** | centromere protein L |
| **CENPN** | centromere protein N |
| **Esp1/Seperain** | extra spindle pole bodies homolog 1 (S. cerevisiae) |
| **HEC1** | NDC80 homolog kinetochore complex component (S. cerevisiae) |
| **MAD2** | MAD2 mitotic arrest deficient-like 1 (yeast) |
| **MCAK** | kinesin family member 2C |
| **Mps1/TTK** | TTK protein kinase |
| **NEK2** | NIMA (never in mitosis gene a)-related kinase 2 |
| **NUF2** | NUF2 NDC80 kinetochore complex component homolog (S. cerevisiae) |
| **Nup 160** | nucleoporin 160kDa |
| **Nup107** | nucleoporin 107kDa |
| **Rough Deal/ROD** | kinetochore associated 1 |
| **Sgo2** | shugoshin-like 2 (S. pombe) |
| **Smc1/Cohesin** | structural maintenance of chromosomes 1A |
| **Survivin** | baculoviral IAP repeat-containing 5 |
| **Topolla** | topoisomerase (DNA) II alpha 170kDa |
| **Zwilch** | Zwilch kinetochore associated homolog (Drosophila) |
| **ZWINT1** | ZW10 interactor |

As discussed in chapter one, the HPV oncogenes E6 and E7 are sufficient to immortalize cells (White *et al.*, 1994; Song *et al.*, 2000), but an accumulation of genetic events following infection is required for malignant progression. While the high-risk oncogenes may not be able to fully transform cells, potentially they may facilitate the acquisition of the additional genetic changes required to drive neoplastic procession. For instance, both high-risk E6 and E7 have been demonstrated *in vivo* to work in a cooperative manner to induce genomic instability in normal cells (White *et al* 1994) through the induction of chromosomal rearrangements and abnormal centrosome numbers, which results in the generation of mitotic defects and aneuploidy (Duensing *et al.*, 2000; Plug-DeMaggio *et al.*, 2004). What is of particular interest here is the fact that centrosome duplication has been solely attributed to the activity of high-risk E7 (Duensing *et al.*, 2000). It has been proposed that this activity of E7 is Rb independent, and mediated through E7's deregulatory activity on the cyclinA and E/cdk2 complexes (Duensing *et al.*, 2006; Duensing and Munger, 2003; Southern *et al.*, 2004). However, recent publications have demonstrated that direct inactivation of Rb can lead to supernumerary centrosomes (Lentini *et al.*, 2006; Amato *et al.*, 2009). In light of the over-representation of mitotic checkpoint proteins, the emerging view is that as a result of Rb suppression, and the specific role of E7 in centrosome duplication events, it is interesting to speculate that this overexpression of mitotic proteins may in fact be inducing centrosome multiplicity. Indeed overexpression of mitotic checkpoint protein TTK (also known as Mps1), the activity of which was inhibited in this study by the repression of E6/E7, has been shown to be sufficient to promote centrosome duplication (Norman *et al.*, 1999; Fisk *et al.*, 2001).

Another interesting observation came from the pathway analysis performed using the DAVID database, focusing on the Biocarta pathway. This demonstrated two particular pathways as highly overrepresented (p-value $\leq$ 1.0E-5), the 'BRCA1-dependent Ub-ligase activity' and the 'Role of BRCA1, BRCA2 and ATR in Cancer Susceptibility' (Figure 4.16). When these pathways were examined, it was established that a similar set of genes were identifying these pathways as over-represented. These genes are members of the Fanconi Anaemia (FA) - breast cancer associated gene (BRCA) pathway.

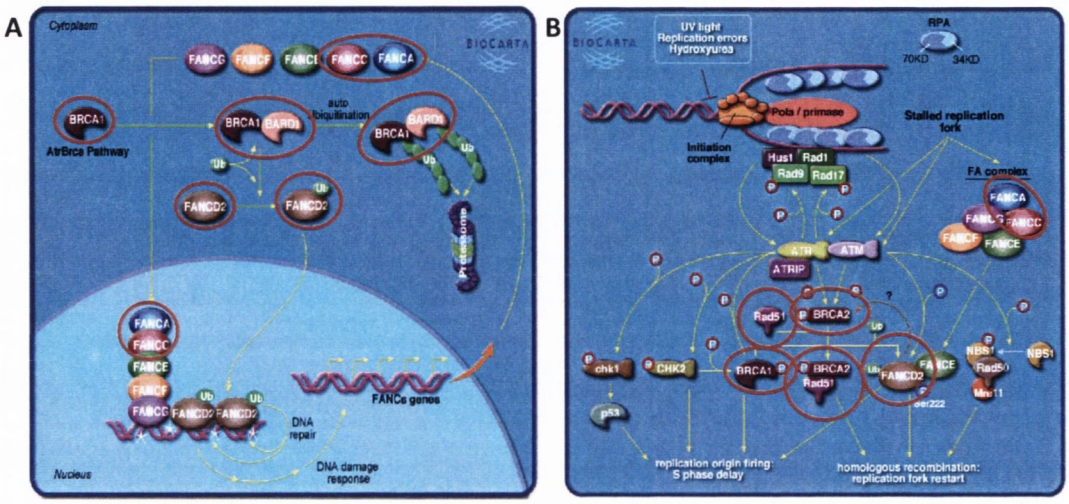


**Figure 4.16: Representative illustrations of (A) the BRCA1-dependent ubiquitin-ligase activity pathway and (B) the role of BRCA1, BRCA2 and ATR in cancer susceptibility pathway.** Represented within the red circles are genes that were found to be differentially expressed after siRNA induced silencing of E6/E7 in SiHa cells.

The FA-BRCA pathway was discovered through the identification of proteins involved in a rare autosomal recessive chromosomal instability disorder, known as Fanconi anaemia (Alter, 2003). Thirteen fanconi anemia, complementation group (FANC) genes have been identified based on their mutated status FA patients (Hannenberg *et al.*, 2002; Chandra *et al.*, 2005; Wang, 2007). These proteins, along with two others known to be involved in the pathway (but as yet have not been identified as mutated in FA patients), have been subdivided into 3 groups depending on their function within in the FA pathway (Wang *et al.*, 2007). The first group comprises eight FA proteins (FANCA, B, C, E, F, G, L, FAAP100) that associate to form the inactive FANC core subcomplex, and two proteins which form a heterodimer, FANCM/FAAP24, that possesses DNA translocase activity (Meetei et al., 2005; Gari *et al.*, 2008; Xue *et al.*, 2008). The FANCM/FAAP24 heterodimer interacts with the core subcomplex to form the larger active core complex (Kim *et al.*, 2008), containing the FANCL E3 ubiquitin ligase (Meetei *et al.*, 2004; Seki et val., 2007). The E3 ubiquitin ligase activity of the core complex is responsible for the monoubiquitylation of both FANCD2 and FANCI components of the second group (Garcia-Higuera *et al.*, 2001; Smogorzewska *et al.*,

2007; Sims *et al.*, 2007). The third FA protein group is comprised of the breast cancer-associated proteins FANCD1 or BRCA2, FANCN or PALB2 (partner and localizer for BRCA2) and FANCJ or BRIP1 (BRCA1-interacting protein 1). This third group is dispensable for FANCD2/FANCI monoubiquitylation and therefore is believed to function downstream of this complex (Wang *et al.*, 2007). Other proteins also associated with the downstream activities of the FA pathway are BRCA1, topoisomerase (DNA) II binding protein 1 (TOPBP1) and RAD51 homolog (RAD51) (Garcia-Higuera *et al.*, 2001; Meetei *et al.*, 2003).

A comprehensive examination of the differentially expressed genes in this study, demonstrated that E6/E7 silencing induced a down-regulation of components of each FA pathway grouping, including the downstream components mentioned above. In total 9 proteins, FANCA, FANCC, FACD2 FANCI, BRCA2, BRIP1, BRCA1, RAD51 and TOPBP1, were identified as significantly down-regulated, fold change $\geq 2$ and FDR $\leq$ 0.05, by both E7#1 and E7#3 transfection, with an additional two group one FA proteins, FANCB and FANCM, significantly down-regulated by E7#1. Though these last two were not identified as differentially regulated by E7#3 mediated silencing of E6/E7, TaqMan® analysis did show that E7#2 induced a significant reduction in their expression. These results demonstrate that the repression of E6 and E7 expression in the HPV16 positive SiHa cells results in a down-regulation of the FA pathway.

FA is characterized by developmental abnormalities, progressive aplastic anemia, and cancer proneness (Alter, 2003; Tischkowitz and Hodgson, 2003; Mathew, 2006). In particular, FA patients are predisposed to leukaemia but also prone to various solid maliganacies, including squamous cell carcinoma of the cervix (Kutler *et al.*, 2003a). The lifetime risk for FA patients developing cervical cancer is significantly higher than in control population (Kuntler *et al.*, 2003a). Interestingly, recently a potential link has been suggested between FA- and HPV-associated disease states. Specifically, in one study, 84% of FA-associated SCCs were reported to contain genomic DNA from high-risk human papillomaviruses compared with only 36% of SCCs in the general

population (Kutler *et al.*, 2003b). Two additional reports have provided further support for a link between FA and HPV, one demonstrated that HPV E7 could activate the FA pathway and that in FA-deficient, HPV16 E7 oncogene-expressing cells, accelerated chromosomal instability was evident (Spardy *et al.*, 2007). The second showed that in FA patient derived, high-risk HPV immortalised keratinocytes, there was increased rates of epithelial hyperplasia, which was attenuated by FA complementation (Hoskins *et al.*, 2009). The finding by Spardy *et al.* (2007) that HPV E7 could activate the FA pathway would seem to be corroborated by the results of this study where there was a down-regulation in the pathway. However, a study published in 2004 demonstrated that there was the potential for the FA pathway to be inactivated in cervical cancer (Narayan *et al.*, 2004). In that study, it was observed that in a number of cervical cancer patient samples, there was hypermethylation of FANCF, a member of the core complex. While overall the findings were not significant, what was interesting was that there was a statically significant over-representation of this phenotype in younger patients ($\leq$ 45 years of age). In addition, they demonstrated that in many cervical cancer cell lines, six of nine examined, there was down-regulation in the expression of FANCF, including in SiHa cells. It should be mentioned, that hypermethylation of the FANCF promoter has previously been demonstrated to disrupt the FA pathway in ovarian cancer (Taniguchi *et al.*, 2003). These studies pose an interesting question as to whether FA mutations may be selected for during HPV associated cancer development in the general population or whether inactivation of the FA pathway is part of the disease process.

Of particular interest with the FA pathway is the fact that it has been implicated in the regulation of common fragile site stability (Howlett *et al.*, 2005; Chan *et al.*, 2009; Naim and Rosselli, 2009), which are suggested to represent preferred regions for HPV genome integration (Wentzensen *et al.*, 2004; Yu *et al.*, 2005; Thorland *et al.*, 2003). The FA pathway has been demonstrated to have a key role in maintaining chromosome stability. Primarily, this has been demonstrated to be mediated through its activation in the response to S phase DNA replication stress and to DNA damage

(Howlett *et al.*, 2005; Thompson and Hinz, 2009). However, recently two publications have described a role for the FA pathway in preventing instability and aneuploidy during mitosis (Chan *et al.*, 2009; Naim and Rosselli, 2009). It appears there may be some overlap between these functions, as induced DNA replication stress was seen to increase the number of FANCD2/FANCI foci on mitotic chromosomes and this was proven to be a consequence of unresolved foci induced by fork stalling during the S phase (Chan *et al.*, 2009; Naim and Rosselli, 2009). Potentialy important in relation to HPV infection, is that both these functions of the FA pathway were observed to specifically target common fragile sites (CFS; Howlett *et al.*, 2005; Chan *et al.*, 2009; Naim and Rosselli, 2009).

This chapter describes for the first time, the combined application of concomitant silencing of E6 and E7 by siRNA and microarray gene expression profiling in a HPV16 cervical cancer model. The analysis demonstrated that the silencing of E6/E7 did not reveal whole transcriptome wide alterations but the differential expression a discrete subset of genes. In total, 168 genes were identified as differential expressed by the suppression of E6/E7 activity. The relevance of this approach to HPV-induced malignant transformation *in vivo* was demonstrated by the substantial overlap between the data set described in this study and that of Rosty et al (2005), where microarray technology was used to evaluate the gene expression profile of cervical cancer biopsies. In addition many of the previously described biomarkers for the identification of dysplastic cells in cervical cancer were also identified within the group of 168 differentially expressed genes. The future challenge with this data set, will be to identify novel functions of E6 and E7 which are key to their oncogenic role in cervical cancer. The functional classification performed in this study should provide a strong basis for this work. The ultimate goal will be to identify genes that are specific biomarkers for cervical cancer or hold the potential to be new therapeutic targets for drug discovery.

## 4.6 References

Ahn, Woong Shick, Su Mi Bae, Joon Mo Lee, Sung Eun Namkoong, Sei-Jun Han, Young Lae Cho, Gye Hyun Nam, Jeong-Sun Seo, Chong Kook Kim, and Yong-Wan Kim. 2004. Searching for pathogenic gene functions to cervical cancer. *Gynecologic Oncology* 93, no. 1 (April): 41-48.

Alter, Blanche P. 2003. Cancer in Fanconi anemia, 1927-2001. *Cancer* 97, no. 2 (January 15): 425-440.

Amato, Angela, Laura Lentini, Tiziana Schillaci, Flora Iovino, and Aldo Di Leonardo. 2009. RNAi mediated acute depletion of retinoblastoma protein (pRb) promotes aneuploidy in human primary cells via micronuclei formation. *BMC Cell Biology* 10: 79.

Benjamin, Jacqueline M, and W James Nelson. 2008. Bench to bedside and back again: molecular mechanisms of alpha-catenin function and roles in tumorigenesis. *Seminars in Cancer Biology* 18, no. 1 (February): 53-64.

Birmingham, Amanda, Emily M Anderson, Angela Reynolds, Diane Ilsley-Tyree, Devin Leake, Yuriy Fedorov, Scott Baskerville, et al. 2006. 3' UTR seed matches, but not overall identity, are associated with RNAi off-targets. *Nature Methods* 3, no. 3 (March): 199-204.

Chan, Kok Lung, Timea Palmai-Pallag, Songmin Ying, and Ian D Hickson. 2009. Replication stress induces sister-chromatid bridging at fragile site loci in mitosis. *Nature Cell Biology* 11, no. 6 (June): 753-760.

Chandra, Saurabh, Orna Levran, Ingrid Jurickova, Chiel Maas, Rick Kapur, Detlev Schindler, Rashida Henry, et al. 2005. A rapid method for retrovirus-mediated identification of complementation groups in Fanconi anemia patients. *Molecular Therapy: The Journal of the American Society of Gene Therapy* 12, no. 5 (November): 976-984.

Chen, Po Yu, Lasse Weinmann, Dimos Gaidatzis, Yi Pei, Mihaela Zavolan, Thomas Tuschl, and Gunter Meister. 2008. Strand-specific 5'-O-methylation of siRNA duplexes controls guide strand selection and targeting specificity. *RNA (New York, N.Y.)* 14, no. 2 (February): 263-274.

Chen, Yan, Christine Miller, Rebecca Mosher, Xumei Zhao, Jim Deeds, Mike Morrissey, Barb Bryant, et al. 2003. Identification of cervical cancer markers by cDNA and tissue microarrays. *Cancer Research* 63, no. 8 (April 15): 1927-1935.

DeFilippis, Rosa Anna, Edward C Goodwin, Lingling Wu, and Daniel DiMaio. 2003. Endogenous human papillomavirus E6 and E7 proteins differentially regulate proliferation, senescence, and apoptosis in HeLa cervical carcinoma cells. *Journal of Virology* 77, no. 2 (January): 1551-1563.

Demeret, Caroline, Alejandro Garcia-Carranca, and Françoise Thierry. 2003. Transcription-independent triggering of the extrinsic pathway of apoptosis by human papillomavirus 18 E2 protein. *Oncogene* 22, no. 2 (January 16): 168-175.

Dennis, Glynn, Brad T Sherman, Douglas A Hosack, Jun Yang, Wei Gao, H Clifford Lane, and Richard A Lempicki. 2003. DAVID: Database for Annotation, Visualization, and Integrated Discovery. *Genome Biology* 4, no. 5: P3.

Duensing, A, Y Liu, M Tseng, M Malumbres, M Barbacid, and S Duensing. 2006. Cyclin-dependent kinase 2 is dispensable for normal centrosome duplication but required for oncogene-induced centrosome overduplication. *Oncogene* 25, no. 20 (May 11): 2943-2949.

Duensing, S, L Y Lee, A Duensing, J Basile, S Piboonniyom, S Gonzalez, C P Crum, and K Munger. 2000. The human papillomavirus type 16 E6 and E7 oncoproteins cooperate to induce mitotic defects and genomic instability by uncoupling centrosome duplication from the cell division cycle. *Proceedings of the National Academy of Sciences of the United States of America* 97, no. 18 (August 29): 10002-10007.

Duensing, Stefan, and Karl Münger. 2002. The human papillomavirus type 16 E6 and E7 oncoproteins independently induce numerical and structural chromosome instability. *Cancer Research* 62, no. 23 (December 1): 7075-7082.

Duensing, Stefan, and Karl Münger. 2003. Human papillomavirus type 16 E7 oncoprotein can induce abnormal centrosome duplication through a mechanism independent of inactivation of retinoblastoma protein family members. *Journal of Virology* 77, no. 22 (November): 12331-12335.

Dyson, J E, J Daniel, and C R Surrey. 1992. The effect of sodium butyrate on the growth characteristics of human cervix tumour cells. *British Journal of Cancer* 65, no. 6 (June): 803-808.

Elledge, S J. 1998. Mitotic arrest: Mad2 prevents sleepy from waking up the APC. *Science (New York, N.Y.)* 279, no. 5353 (February 13): 999-1000.

Fisk, H A, and M Winey. 2001. The mouse Mps1p-like kinase regulates centrosome duplication. *Cell* 106, no. 1 (July 13): 95-104.

Gammoh, Noor, Helena Sterlinko Grm, Paola Massimi, and Lawrence Banks. 2006. Regulation of human papillomavirus type 16 E7 activity through direct protein interaction with the E2 transcriptional activator. *Journal of Virology* 80, no. 4 (February): 1787-1797.

Garcia-Higuera, I, T Taniguchi, S Ganesan, M S Meyn, C Timmers, J Hejna, M Grompe, and A D D'Andrea. 2001. Interaction of the Fanconi anemia proteins and BRCA1 in a common pathway. *Molecular Cell* 7, no. 2 (February): 249-262.

Gari, Kerstin, Chantal Décaillet, Mathieu Delannoy, Leonard Wu, and Angelos Constantinou. 2008. Remodeling of DNA replication structures by the branch point translocase FANCM. *Proceedings of the National Academy of Sciences of the United States of America* 105, no. 42 (October 21): 16107-16112.

Garner-Hamrick, Peggy A, J M Fostel, Wei-Ming Chien, N Sanjib Banerjee, Louise T Chow, Thomas R Broker, and Chris Fisher. 2004. Global effects of human papillomavirus type 18 E6/E7 in an organotypic keratinocyte culture system. *Journal of Virology* 78, no. 17 (September): 9041-9050.

Gerbaulet, A, C Haie, G Michel, D Castaigne, M Prade, I Kunkler, J Pomp, J Masselot, C Lhomme, and D Chassagne. 1992. Combined radio-surgical treatment in early invasive cervix carcinoma according to prognostic factors. Experience of the Gustave-Roussy Institute. *European Journal of Gynaecological Oncology* 13, no. 3: 256-261.

Goodwin, E C, and D DiMaio. 2000. Repression of human papillomavirus oncogenes in HeLa cervical carcinoma cells causes the orderly reactivation of dormant tumor suppressor pathways. *Proceedings of the National Academy of Sciences of the United States of America* 97, no. 23 (November 7): 12513-12518.

Grm, Helena Sterlinko, Paola Massimi, Noor Gammoh, and Lawrence Banks. 2005. Crosstalk between the human papillomavirus E2 transcriptional activator and the E6 oncoprotein. *Oncogene* 24, no. 33 (August 4): 5149-5164.

Ha, Seon-Ah, Seung Min Shin, Hong Namkoong, Heejeong Lee, Goang Won Cho, Soo Young Hur, Tae Eung Kim, and Jin Woo Kim. 2004. Cancer-associated expression of minichromosome maintenance 3 gene in several human cancers and its involvement in tumorigenesis. *Clinical Cancer Research: An Official Journal of the American Association for Cancer Research* 10, no. 24 (December 15): 8386-8395.

Hanenberg, Helmut, Sat Dev Batish, Karen E Pollok, Lydia Vieten, Peter C Verlander, Cordula Leurs, Ryan J Cooper, et al. 2002. Phenotypic correction of primary Fanconi anemia T cells with retroviral vectors as a diagnostic tool. *Experimental Hematology* 30, no. 5 (May): 410-420.

Heil, Florian, Hiroaki Hemmi, Hubertus Hochrein, Franziska Ampenberger, Carsten Kirschning, Shizuo Akira, Grayson Lipford, Hermann Wagner, and Stefan Bauer. 2004. Species-specific recognition of single-stranded RNA via toll-like receptor 7 and 8. *Science (New York, N.Y.)* 303, no. 5663 (March 5): 1526-1529.

Hornung, Veit, Margit Guenthner-Biller, Carole Bourquin, Andrea Ablasser, Martin Schlee, Satoshi Uematsu, Anne Noronha, et al. 2005. Sequence-specific potent induction of IFN-alpha by short interfering RNA in plasmacytoid dendritic cells through TLR7. *Nature Medicine* 11, no. 3 (March): 263-270.

Hoskins, E E, T A Morris, J M Higginbotham, N Spardy, E Cha, P Kelly, D A Williams, K A Wikenheiser-Brokamp, S Duensing, and S I Wells. 2009. Fanconi anemia deficiency stimulates HPV-associated hyperplastic growth in organotypic epithelial raft culture. *Oncogene* 28, no. 5 (February 5): 674-685.

Howlett, Niall G, Toshiyasu Taniguchi, Sandra G Durkin, Alan D D'Andrea, and Thomas W Glover. 2005. The Fanconi anemia pathway is required for the DNA replication stress response and for the regulation of common fragile site stability. *Human Molecular Genetics* 14, no. 5 (March 1): 693-701.

Huibregtse, J M, M Scheffner, and P M Howley. 1993. Cloning and expression of the cDNA for E6-AP, a protein that mediates the interaction of the human papillomavirus E6 oncoprotein with p53. *Molecular and Cellular Biology* 13, no. 2 (February): 775-784.

Irizarry, Rafael A, Siew Loon Ooi, Zhijin Wu, and Jef D Boeke. 2003. Use of mixture models in a microarray-based screening procedure for detecting differentially represented yeast mutants. *Statistical Applications in Genetics and Molecular Biology* 2: Article1.

Ishida, S, E Huang, H Zuzan, R Spang, G Leone, M West, and J R Nevins. 2001. Role for E2F in control of both DNA replication and mitotic functions as revealed from DNA microarray analysis. *Molecular and Cellular Biology* 21, no. 14 (July): 4684-4699.

Ishimi, Yukio, Isao Okayasu, Chieko Kato, Hyun-Ju Kwon, Hiroshi Kimura, Kouichi Yamada, and Si-Young Song. 2003. Enhanced expression of Mcm proteins in cancer cells derived from uterine cervix. *European Journal of Biochemistry / FEBS* 270, no. 6 (March): 1089-1101.

Jackson, Aimee L, Steven R Bartz, Janell Schelter, Sumire V Kobayashi, Julja Burchard, Mao Mao, Bin Li, Guy Cavet, and Peter S Linsley. 2003. Expression profiling reveals off-target gene regulation by RNAi. *Nature Biotechnology* 21, no. 6 (June): 635-637.

Jackson, Aimee L, Julja Burchard, Devin Leake, Angela Reynolds, Janell Schelter, Jie Guo, Jason M Johnson, et al. 2006. Position-specific chemical modification of siRNAs reduces "off-target" transcript silencing. *RNA (New York, N.Y.)* 12, no. 7 (July): 1197-1205.

Johung, Kimberly, Edward C Goodwin, and Daniel DiMaio. 2007. Human papillomavirus E7 repression in cervical carcinoma cells initiates a transcriptional cascade driven by the retinoblastoma family, resulting in senescence. *Journal of Virology* 81, no. 5 (March): 2102-2116.

Judge, Adam D, Vandana Sood, Janet R Shaw, Dianne Fang, Kevin McClintock, and Ian MacLachlan. 2005. Sequence-dependent stimulation of the mammalian innate immune response by synthetic siRNA. *Nature Biotechnology* 23, no. 4 (April): 457-462.

Kelley, Melissa L, Kerri E Keiger, Chan Jae Lee, and Jon M Huibregtse. 2005. The global transcriptional effects of the human papillomavirus E6 protein in cervical carcinoma cell lines are mediated by the E6AP ubiquitin ligase. *Journal of Virology* 79, no. 6 (March): 3737-3747.

Kim, Jung Min, Younghoon Kee, Allan Gurtan, and Alan D D'Andrea. 2008. Cell cycle-dependent chromatin loading of the Fanconi anemia core complex by FANCM/FAAP24. *Blood* 111, no. 10 (May 15): 5215-5222.

Kirwan, J M, and C S Herrington. 2001. Human papillomavirus and cervical cancer: where are we now? *BJOG: An International Journal of Obstetrics and Gynaecology* 108, no. 12 (December): 1204-1213.

Kops, Geert J P L, Beth A A Weaver, and Don W Cleveland. 2005. On the road to cancer: aneuploidy and the mitotic checkpoint. *Nature Reviews. Cancer* 5, no. 10 (October): 773-785.

Kuner, Ruprecht, Markus Vogt, Holger Sultmann, Andreas Buness, Susanne Dymalla, Julia Bulkescher, Mark Fellmann, Karin Butz, Annemarie Poustka, and Felix Hoppe-Seyler. 2007. Identification of cellular targets for the human papillomavirus E6 and E7 oncogenes by RNA interference and transcriptome analyses. *Journal of Molecular Medicine (Berlin, Germany)* 85, no. 11 (November): 1253-1262.

Kutler, David I, Bhuvanesh Singh, Jaya Satagopan, Sat Dev Batish, Marianne Berwick, Philip F Giampietro, Helmut Hanenberg, and Arleen D Auerbach. 2003a. A 20-year perspective on the International Fanconi Anemia Registry (IFAR). *Blood* 101, no. 4 (February 15): 1249-1256.

Kutler, David I, Arleen D Auerbach, Jaya Satagopan, Philip F Giampietro, Sat Dev Batish, Andrew G Huvos, Andy Goberdhan, Jatin P Shah, and Bhuvanesh Singh. 2003b. High incidence of head and neck squamous cell carcinoma in patients with Fanconi anemia. *Archives of Otolaryngology--Head & Neck Surgery* 129, no. 1 (January): 106-112.

Landoni, F, A Maneo, A Colombo, F Placa, R Milani, P Perego, G Favini, L Ferri, and C Mangioni. 1997. Randomised study of radical surgery versus radiotherapy for stage Ib-IIa cervical cancer. *Lancet* 350, no. 9077 (August 23): 535-540.

Lentini, Laura, Flora Iovino, Angela Amato, and Aldo Di Leonardo. 2006. Centrosome amplification induced by hydroxyurea leads to aneuploidy in pRB deficient human and mouse fibroblasts. *Cancer Letters* 238, no. 1 (July 8): 153-160.

Longworth, Michelle S, and Laimonis A Laimins. 2004. Pathogenesis of human papillomaviruses in differentiating epithelia. *Microbiology and Molecular Biology Reviews: MMBR* 68, no. 2 (June): 362-372.

Ma, Yihong, Rhonda Croxton, Ronnie L Moorer, and W Douglas Cress. 2002. Identification of novel E2F1-regulated genes by microarray. *Archives of Biochemistry and Biophysics* 399, no. 2 (March 15): 212-224.

Markey, Michael P, Steven P Angus, Matthew W Strobeck, Sarah L Williams, Ranjaka W Gunawardena, Bruce J Aronow, and Erik S Knudsen. 2002. Unbiased analysis of RB-mediated transcriptional repression identifies novel targets and distinctions from E2F action. *Cancer Research* 62, no. 22 (November 15): 6587-6597.

Martin, Cara M, Louise Kehoe, Cathy O Spillane, and John J O'Leary. 2007. Gene discovery in cervical cancer : towards diagnostic and therapeutic biomarkers. *Molecular Diagnosis & Therapy* 11, no. 5: 277-290.

Mathew, C G. 2006. Fanconi anaemia genes and susceptibility to cancer. *Oncogene* 25, no. 43 (September 25): 5875-5884.

Meetei, Amom R, Zhijiang Yan, and Weidong Wang. 2004. FANCL replaces BRCA1 as the likely ubiquitin ligase responsible for FANCD2 monoubiquitination. *Cell Cycle (Georgetown, Tex.)* 3, no. 2 (February): 179-181.

Meetei, Amom Ruhikanta, Annette L Medhurst, Chen Ling, Yutong Xue, Thiyam Ramsing Singh, Patrick Bier, Jurgen Steltenpool, et al. 2005. A human ortholog of archaeal DNA repair protein Hef is defective in Fanconi anemia complementation group M. *Nature Genetics* 37, no. 9 (September): 958-963.

Meetei, Amom Ruhikanta, Salvatore Sechi, Michael Wallisch, Dafeng Yang, Mary K Young, Hans Joenje, Maureen E Hoatlin, and Weidong Wang. 2003. A multiprotein nuclear complex connects Fanconi anemia and Bloom syndrome. *Molecular and Cellular Biology* 23, no. 10 (May): 3417-3426.

Min, Wei, Ma Wen-li, Sun Zhao-hui, Li Ling, Zhang Bao, and Zheng Wen-ling. 2009. Microarray analysis identifies differentially expressed genes induced by human papillomavirus type 18 E6 silencing RNA. *International Journal of Gynecological Cancer: Official Journal of the International Gynecological Cancer Society* 19, no. 4 (May): 547-563.

Morris, M, P J Eifel, J Lu, P W Grigsby, C Levenback, R E Stevens, M Rotman, D M Gershenson, and D G Mutch. 1999. Pelvic radiation with concurrent chemotherapy compared with pelvic and para-aortic radiation for high-risk cervical cancer. *The New England Journal of Medicine* 340, no. 15 (April 15): 1137-1143.

Müller, H, A P Bracken, R Vernell, M C Moroni, F Christians, E Grassilli, E Prosperini, E Vigo, J D Oliner, and K Helin. 2001. E2Fs regulate the expression of genes involved in differentiation, development, proliferation, and apoptosis. *Genes & Development* 15, no. 3 (February 1): 267-285.

Murphy, N, M Ring, C C B B Heffron, B King, A G Killalea, C Hughes, C M Martin, E McGuinness, O Sheils, and J J O'Leary. 2005. p16INK4A, CDC6, and MCM5: predictive biomarkers in cervical preinvasive neoplasia and cervical cancer. *Journal of Clinical Pathology* 58, no. 5 (May): 525-534.

Naim, Valeria, and Filippo Rosselli. 2009. The FANC pathway and BLM collaborate during mitosis to prevent micro-nucleation and chromosome abnormalities. *Nature Cell Biology* 11, no. 6 (June): 761-768.

Narayan, Gopeshwar, Hugo Arias-Pulido, Subhadra V Nandula, Katia Basso, Dorcas D Sugirtharaj, Hernan Vargas, Mahesh Mansukhani, et al. 2004. Promoter hypermethylation of FANCF: disruption of Fanconi Anemia-BRCA pathway in cervical cancer. *Cancer Research* 64, no. 9 (May 1): 2994-2997.

Norman, T C, D L Smith, P K Sorger, B L Drees, S M O'Rourke, T R Hughes, C J Roberts, S H Friend, S Fields, and A W Murray. 1999. Genetic selection of peptide inhibitors of biological pathways. *Science (New York, N.Y.)* 285, no. 5427 (July 23): 591-595.

Omura, G A, J A Blessing, L Vaccarello, M L Berman, D L Clarke-Pearson, D G Mutch, and B Anderson. 1997. Randomized trial of cisplatin versus cisplatin plus mitolactol versus cisplatin plus ifosfamide in advanced squamous carcinoma of the cervix: a Gynecologic Oncology Group study. *Journal of Clinical Oncology: Official Journal of the American Society of Clinical Oncology* 15, no. 1 (January): 165-171.

Parkin, D Maxwell, and Freddie Bray. 2006. Chapter 2: The burden of HPV-related cancers. *Vaccine* 24 Suppl 3 (August 31): S3/11-25.

Pelizon, Cristina. 2003. Down to the origin: Cdc6 protein and the competence to replicate. *Trends in Cell Biology* 13, no. 3 (March): 110-113.

Pett, M, and N Coleman. 2007. Integration of high-risk human papillomavirus: a key event in cervical carcinogenesis? *The Journal of Pathology* 212, no. 4 (August): 356-367.

Plug-DeMaggio, Annemieke W, Terri Sundsvold, Michelle A Wurscher, Jennifer I Koop, Aloysius J Klingelhutz, and James K McDougall. 2004. Telomere erosion and chromosomal instability in cells expressing the HPV oncogene 16E6. *Oncogene* 23, no. 20 (April 29): 3561-3571.

Pluta, A F, A M Mackay, A M Ainsztein, I G Goldberg, and W C Earnshaw. 1995. The centromere: hub of chromosomal activities. *Science (New York, N.Y.)* 270, no. 5242 (December 8): 1591-1594.

Polager, Shirley, Yael Kalma, Eli Berkovich, and Doron Ginsberg. 2002. E2Fs up-regulate expression of genes involved in DNA replication, DNA repair and mitosis. *Oncogene* 21, no. 3 (January 17): 437-446.

Rieder, C L, and E D Salmon. 1998. The vertebrate cell kinetochore and its roles during mitosis. *Trends in Cell Biology* 8, no. 8 (August): 310-318.

Rosty, Christophe, Michal Sheffer, Dafna Tsafrir, Nicolas Stransky, Ilan Tsafrir, Martine Peter, Patricia de Crémoux, et al. 2005. Identification of a proliferation gene cluster associated with HPV E6/E7 expression level and viral DNA load in invasive cervical carcinoma. *Oncogene* 24, no. 47 (October 27): 7094-7104.

Santin, Alessandro D, Fenghuang Zhan, Eliana Bignotti, Eric R Siegel, Stefania Cané, Stefania Bellone, Michela Palmieri, et al. 2005. Gene expression profiles of primary HPV16- and HPV18-infected early stage cervical cancers and normal cervical epithelium: identification of novel candidate molecular markers for cervical cancer diagnosis and therapy. *Virology* 331, no. 2 (January 20): 269-291.

Scaërou, F, I Aguilera, R Saunders, N Kane, L Blottière, and R Karess. 1999. The rough deal protein is a new kinetochore component required for accurate chromosome segregation in Drosophila. *Journal of Cell Science* 112 ( Pt 21) (November): 3757-3768.

Scheffner, M, K Münger, J C Byrne, and P M Howley. 1991. The state of the p53 and retinoblastoma genes in human cervical carcinoma cell lines. *Proceedings of the National Academy of Sciences of the United States of America* 88, no. 13 (July 1): 5523-5527.

Seki, Sohsuke, Mioko Ohzeki, Akiko Uchida, Seiki Hirano, Nobuko Matsushita, Hiroyuki Kitao, Tsukasa Oda, et al. 2007. A requirement of FancL and FancD2 monoubiquitination in DNA repair. *Genes to Cells: Devoted to Molecular & Cellular Mechanisms* 12, no. 3 (March): 299-310.

Simes, R J, M H Tattersall, A S Coates, D Raghavan, H J Solomon, and H Smartt. 1986. Randomised comparison of procedures for obtaining informed consent in clinical trials of treatment for cancer. *British Medical Journal (Clinical Research Ed.)* 293, no. 6554 (October 25): 1065-1068.

Sims, Ashley E, Elizabeth Spiteri, Robert J Sims, Adriana G Arita, Francis P Lach, Thomas Landers, Melanie Wurm, et al. 2007. FANCI is a second monoubiquitinated member of the Fanconi anemia pathway. *Nature Structural & Molecular Biology* 14, no. 6 (June): 564-567.

Smogorzewska, Agata, Shuhei Matsuoka, Patrizia Vinciguerra, E Robert McDonald, Kristen E Hurov, Ji Luo, Bryan A Ballif, et al. 2007. Identification of the FANCI protein, a monoubiquitinated FANCD2 paralog required for DNA repair. *Cell* 129, no. 2 (April 20): 289-301.

Snijders, Peter J F, Renske D M Steenbergen, Daniëlle A M Heideman, and Chris J L M Meijer. 2006. HPV-mediated cervical carcinogenesis: concepts and clinical implications. *The Journal of Pathology* 208, no. 2 (January): 152-164.

Song, S, A Liem, J A Miller, and P F Lambert. 2000. Human papillomavirus types 16 E6 and E7 contribute differently to carcinogenesis. *Virology* 267, no. 2 (February 15): 141-150.

Southern, S A, M H Lewis, and C S Herrington. 2004. Induction of tetrasomy by human papillomavirus type 16 E7 protein is independent of pRb binding and disruption of differentiation. *British Journal of Cancer* 90, no. 10 (May 17): 1949-1954.

Spardy, Nicole, Anette Duensing, Domonique Charles, Nathan Haines, Tomomi Nakahara, Paul F Lambert, and Stefan Duensing. 2007. The human papillomavirus type 16 E7 oncoprotein activates the Fanconi anemia (FA) pathway and causes accelerated chromosomal instability in FA cells. *Journal of Virology* 81, no. 23 (December): 13265-13270.

Taniguchi, Toshiyasu, Marc Tischkowitz, Najim Ameziane, Shirley V Hodgson, Christopher G Mathew, Hans Joenje, Samuel C Mok, and Alan D D'Andrea. 2003. Disruption of the Fanconi anemia-BRCA pathway in cisplatin-sensitive ovarian tumors. *Nature Medicine* 9, no. 5 (May): 568-574.

Thierry, Françoise, Mohammed Abderrafi Benotmane, Caroline Demeret, Marcella Mori, Sébastien Teissier, and Christian Desaintes. 2004. A genomic approach reveals a novel mitotic pathway in papillomavirus carcinogenesis. *Cancer Research* 64, no. 3 (February 1): 895-903.

Thomas, Paul D, Michael J Campbell, Anish Kejariwal, Huaiyu Mi, Brian Karlak, Robin Daverman, Karen Diemer, Anushya Muruganujan, and Apurva Narechania. 2003. PANTHER: a library of protein families and subfamilies indexed by function. *Genome Research* 13, no. 9 (September): 2129-2141.

Thompson, Larry H, and John M Hinz. 2009. Cellular and molecular consequences of defective Fanconi anemia proteins in replication-coupled DNA repair: mechanistic insights. *Mutation Research* 668, no. 1-2 (July 31): 54-72.

Thorland, Erik C, Shannon L Myers, Bobbie S Gostout, and David I Smith. 2003. Common fragile sites are preferential targets for HPV16 integrations in cervical tumors. *Oncogene* 22, no. 8 (February 27): 1225-1237.

Tischkowitz, M D, and S V Hodgson. 2003. Fanconi anaemia. *Journal of Medical Genetics* 40, no. 1 (January): 1-10.

Wang, Weidong. 2007. Emergence of a DNA-damage response network consisting of Fanconi anaemia and BRCA proteins. *Nature Reviews. Genetics* 8, no. 10 (October): 735-748.

Webster, K, A Taylor, and K Gaston. 2001. Oestrogen and progesterone increase the levels of apoptosis induced by the human papillomavirus type 16 E2 and E7 proteins. *The Journal of General Virology* 82, no. Pt 1 (January): 201-213.

Weinmann, A S, S M Bartley, T Zhang, M Q Zhang, and P J Farnham. 2001. Use of chromatin immunoprecipitation to clone novel E2F target promoters. *Molecular and Cellular Biology* 21, no. 20 (October): 6820-6832.

Wells, Susanne I, Bruce J Aronow, Trisha M Wise, Sarah S Williams, Jennifer A Couget, and Peter M Howley. 2003. Transcriptome signature of irreversible senescence in human papillomavirus-positive cervical cancer cells. *Proceedings of the National Academy of Sciences of the United States of America* 100, no. 12 (June 10): 7093-7098.

Wells, W A. 1996. The spindle-assembly checkpoint: aiming for a perfect mitosis, every time. *Trends in Cell Biology* 6, no. 6 (June): 228-234.

Wentzensen, Nicolas, Svetlana Vinokurova, and Magnus von Knebel Doeberitz. 2004. Systematic review of genomic integration sites of human papillomavirus genomes in epithelial dysplasia and invasive cancer of the female lower genital tract. *Cancer Research* 64, no. 11 (June 1): 3878-3884.

Werness, B A, A J Levine, and P M Howley. 1990. Association of human papillomavirus types 16 and 18 E6 proteins with p53. *Science (New York, N.Y.)* 248, no. 4951 (April 6): 76-79.

White, A E, E M Livanos, and T D Tlsty. 1994. Differential disruption of genomic integrity and cell cycle regulation in normal human fibroblasts by the HPV oncoproteins. *Genes & Development* 8, no. 6 (March 15): 666-677.

Wright, T C, T V Ellerbrock, M A Chiasson, N Van Devanter, and X W Sun. 1994. Cervical intraepithelial neoplasia in women infected with human immunodeficiency virus: prevalence, risk factors, and validity of Papanicolaou smears. New York Cervical Disease Study. *Obstetrics and Gynecology* 84, no. 4 (October): 591-597.

Xue, Yutong, Yongjiang Li, Rong Guo, Chen Ling, and Weidong Wang. 2008. FANCM of the Fanconi anemia core complex is required for both monoubiquitination and DNA repair. *Human Molecular Genetics* 17, no. 11 (June 1): 1641-1652.

Yu, Tingxi, Matthew J Ferber, Tak Hong Cheung, Tong Kwok Hung Chung, Yick Fu Wong, and David I Smith. 2005. The role of viral integration in the development of cervical cancer. *Cancer Genetics and Cytogenetics* 158, no. 1 (April 1): 27-34.

zur Hausen, H, and E M de Villiers. 1994. Human papillomaviruses. *Annual Review of Microbiology* 48: 427-447.

Zhu, Wei, Xuena Wang, Yeming Ma, Manlong Rao, James Glimm, and John S Kovach. 2003. Detection of cancer-specific markers amid massive mass spectral data. *Proceedings of the National Academy of Sciences of the United States of America* 100, no. 25 (December 9): 14666-14671.

# Chapter Five

# Sulindac induces apoptosis & E7 degradation in HPV18 positive cervical cancer cells

## 5.1 Introduction

Although there has been a decrease in the incidence of cervical cancer in developed countries (Bray *et al.*, 2005; Parkin *et al*, 2005; Wang *et al.*, 2004), mainly due to screening programmes, this is not true worldwide (Parkin *et al.*, 2001; Pisani *et al.*, 1999). In developing countries where access to screening is limited cervical cancer is often only diagnosed at an advanced stage and for women presenting with advanced stage disease the survival rate is less than 50% (Jemal *et al.*, 2007). Current therapeutic options for invasive disease include surgery, radiotherapy and chemotherapy. In general, a complex treatment regime including combination therapies is utilised. In developing countries low survival rates not only reflect cost limited access to screening and therapies but also poor protocol adherence (Magrath, 2003). As therapy regimes are complex with toxic side effects, monitoring and support of patients is required. Generally this exceeds the capabilities of the medical staff in these countries, due to a lack of resources such as facilities, accesses to products required to reduce the burden of the toxicity and training. In such circumstances, the toxic death rate may be so high as to outweigh any advantage that the therapy might otherwise bring (Magrath, 2003). Therefore, research is needed to elucidate effective treatment modalities with reduced toxicity and simpler treatment regimes.

Chemotherapeutics with low levels of toxicity may also be beneficial as chemopreventative agents in cervical cancer. Chemoprevention is the use of a drug or compound to interfere with pathogenesis of the disease to prevent that disease. In cancer the aim is to inhibit, delay or reverse the process of carcinogenesis. CIN II and III are defined as a precancerous lesions of cervical cancer and immediate treatment is generally warranted (Kietpeerakool *et al.*, 2007; Mitchel *et al.*, 1994; Ostor, 1993). There has been a trend toward more conservative management for CIN II, III, with loop excision of transformation zone (Leitz) and cervical conisation becoming the two major forms of standard treatment. However, a certain number of CIN II and III cases are diagnosed in reproductive-age women. Possibly, neither cervical conisation nor Leitz would be an appropriate treatment options due to their association with adverse

reproductive consequences (Jakobsson *et al.*, 2007; Kyrgiou *et al.*, 2006). Since CIN has a well defined pre-invasive stage and clinicians can follow the lesion without using a significantly invasive technique, theoretically, medical treatment is possible and may be an attractive alternative, particularly in the treatment of reproductive-age women.

It is now clear that proliferation of cells alone does not cause cancer, exemplified by the fact that though E6 and E7 oncogenes drive proliferation and can immortalise cells (White et al., 1994; Song et al., 2000), they are not sufficient for cervical cancer pathogenesis (DiPaolo et al., 1989; Durst et al., 1989; Hurlin 1991; Pei et al., 1993). Instead it is recognised that a multi-component microenvironment rich in inflammatory cells, growth factors, activated stroma, and DNA-damage-promoting agents is required to potentiate and/or promote neoplastic progression (Coussens and Werb, 2002). The causal link between inflammation and cancer is of particular interest. Epidemiological studies have shown that chronic inflammation predisposes individuals to various types of cancer. It is estimated that underlying infections and inflammatory responses are linked to 15-20% of all deaths from cancer worldwide (Balkwill and Mantvani, 2001). The hallmarks of cancer-related inflammation include the presence of inflammatory cells and inflammatory mediators (for example prostaglandins) in tumour tissues, tissue remodelling and angiogenesis similar to that seen in chronic inflammation, and tissue repair (Balkwill et al., 2005). Significantly these signs are not only present in tumours for which a causal link to inflammation has been established but also in tumour where a firm causal link to inflammation has not been established (Mantovani et al., 2008).

Over the last thirty years, non steroidal anti-inflammatory drugs (NSAIDs) have attracted a great deal of interest as promising anticancer agents, as they have been shown to inhibit the growth of tumour cells *in vitro* and *in vivo* (Adolphie *et al.* in 1972; Hial *et al.*, 1976; Piazza *et al.*, 1997; Subbegowda and Frommel, 1998; Tanaka *et al.*, 1989; Tanaka 1991). NSAIDs are some of the most commonly used drugs worldwide; examples are aspirin, ibuprofen and sulindac. They are predominantly used to provide

symptomatic relief from pain and swelling in chronic inflammatory disorders such as osteoarthritis and rheumatoid arthritis. The anti-inflammatory properties of NSAIDs are known to be mediated through the inhibition of the cyclooxygenase (COX) enzymes, and many have attributed their antineoplastic activity to this property also. COX is the rate limiting enzyme in the arachidonic cascade, where arachidonic acid is converted to prostaglandins (PGs), for example $PGE_2$ (Figure 5.1). There are two main isoforms of the COX enzyme, COX-1 and COX-2. COX-1 is constitutively expressed in many tissues and is responsible for producing PGs involved in maintaining biological homeostasis, such as cytoprotection of the gastric mucosa, regulation of the renal blood flow and platelet aggregation (Vane *et al.*, 1998). In contrast, COX-2 is not detectable in most normal tissues (Vane *et al.*, 1998). Instead, it is rapidly induced in response to mitogenic and inflammatory stimuli including growth factors, cytokines and oncogenes (DuBois *et al.*, 1994; Subbaramaiah *et al.*, 1996; Smith *et al.*, 2000; Williams and DuBois 1996).

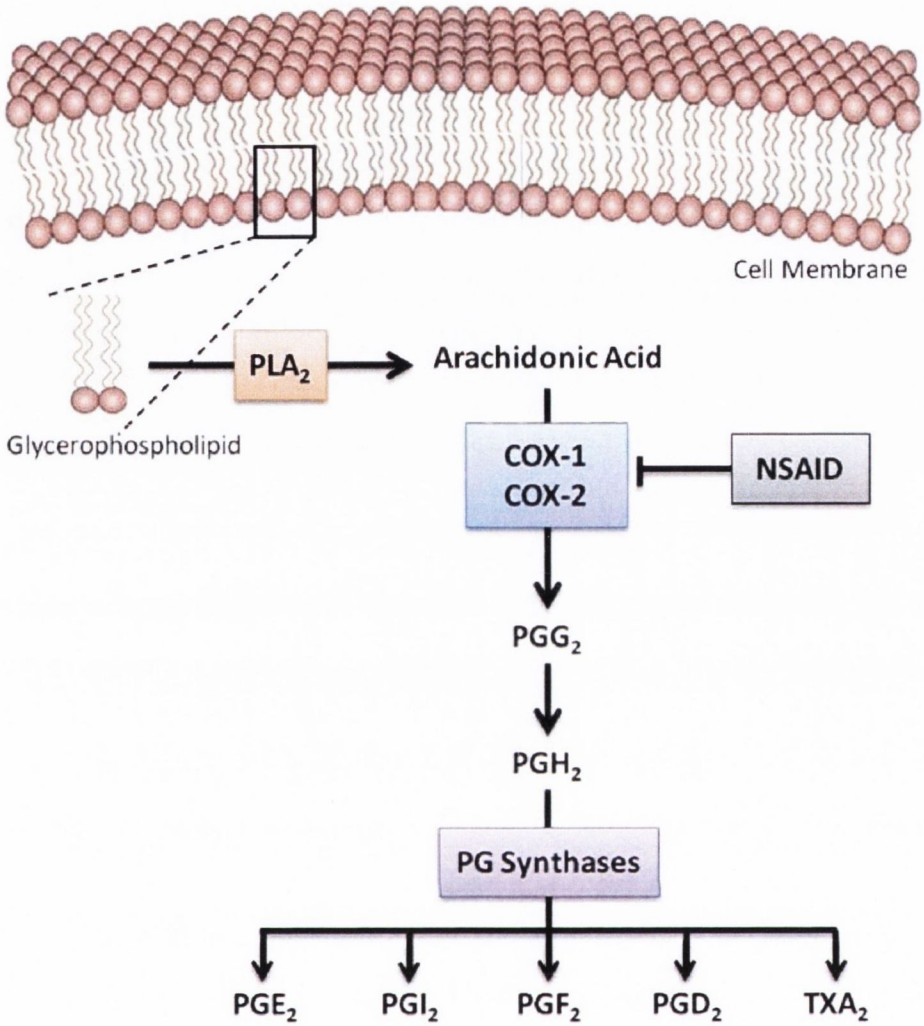


**Figure 5.1: Representative diagram of arachadonic acid cascade.** Arachidonic acid is first liberated from membrane glycerophospholipids by the actions of the phospholipase $A_2$ ($PLA_2$) family of enzymes. The cyclooxygenase (COX) enzymes then catalyse the biosynthesis of the bicyclic endoperoxide intermediate $PGG_2$, followed by reduction to $PGH_2$. $PGH_2$ is subsequently converted to one of several structurally related prostaglandins (PGs), including $PGE_2$, $PGD_2$, $PGF_2$, $PGI_2$ and thromboxane A2 ($TXA_2$), by the activity of specific PG synthases. Non-steroidal anti-inflammatory drugs (NSAIDs) inhibit the activity of both COX-1 and COX-2. COX-1 is responsible for 'housekeeping' PG biosynthesis and is constitutively produced in most tissues in the body. COX-2, on the other hand, is not normally produced in most tissues but is induced by a wide spectrum of growth factors and pro-inflammatory cytokines in specific pathphysiological conditions.

NSAIDs are under investigation both as novel chemopreventative and chemotherapeutic agents. Early evidence for their antineoplastic properties came from rodent models of carcinogenesis that demonstrated that certain NSAIDs could inhibit the growth of transplanted tumours and/or chemical and radiation induced carcinogenesis (Hial *et al.*, 1976; Tanaka *et al.*, 1989; Tanaka 1991). Much of this work took place in colon cancer models and was further substantiated by the observations in the 1980's that the NSAID sulindac caused regression of and prevented recurrence of adenomatous colorectal polyps in patients with familial adenomatous polyposis (FAP) (Waddel and Loughry,1983; Waddel *et al.*, 1989). Subsequent clinical trials confirmed these observations and demonstrated the utility of sulindac for treating precancerous lesions in FAP patients (Giardiello *et al.*, 1993; Nugent *et al.*, 1993). In 1991, a population based study reported that the risk of colon cancer decreased in people who took aspirin daily (Thun *et al.*, 1991). Since then, numerous epidemiology studies have confirmed that NSAIDs have chemopreventive activity against cancer (Kamijo *et al.*, 2001; Kim *et al.*, 2004; Thun *et al.*, 2002; Ding *et al.*, 2000). Recently a meta-analysis was performed examining all existing epidemiology studies relating to the exposure to traditional over the counter NSAIDs such as aspirin and ibuprofen and the risk of developing cancers of the colon, breast, prostate and lung (Harris, 2009). It found that regular intake of these NSAIDs inferred a significant reduction in the risk of colon (43%), breast (25%), lung (28%) and prostate (27%) cancer. This study gives a further degree of validation to the individual epidemiology studies and to the concept that NSAIDs have chemopreventive properties. Unfortunately, the prolonged use of NSAIDs for cancer chemoprevention is limited due to the association with gastrointestinal, renal and cardiovascular toxicities as a result of the depletion of physiologically important PGs (Mukherjee, 2002; Vane and Botting, 1998; Vane *et al.*, 1998). Therefore, there are now intense research efforts into understanding the underlying antineoplastic activity of NSAIDs with the aim of developing agents with the same potential but without the side effects.

An explanation for the antineoplastic properties of NSAIDs was first suggested by Adolphie *et al.* in 1972, who reported that certain NSAIDs were capable of inhibiting

the proliferation of cultured cervical cells, HeLa, by causing cell cycle arrest. From this original report many studies have been published demonstrating that in various *in vitro* and *in vivo* cancer models NSAIDs can cause cell cycle arrest and in addition can induce apoptosis (Castonguay and Rioux, 1997; Karl *et al.*, 2007; Kim *et al.*, 2003; Lim *et al.*, 1999; Lovebridge *et al.*, 2008; Piazza *et al.*, 1997; Seo *et al.*, 2009; Subbegowda and Frommel, 1998). Although there has been no direct *in situ* evidence of NSAIDs inducing apoptosis, regressing adenomas of FAP patients treated with sulindac have been demonstrated to display increased rates of apoptosis (Pasricha *et al.*, 1995). To date, several molecular mechanisms underlying the pro-apoptotic effects of NSAIDs have been described, however the exact mechanism is still unknown.

Many investigators have attributed the anti-cancer efficacy of NSAIDs to their anti-inflammatory COX inhibitory activity. In particular COX-2 has received much attention, as there are multiple lines of evidence suggesting it has a significant role to play in carcinogenesis. For example molecular studies have revealed that overexpression of COX-2 is a prominent feature of premalignant and malignant neoplasia (Brown *et al.*, 2005; Eberhart *et al.*, 1994; Half *et al.*, 2002; Hwang *et al.*, 1998; Rozic *et al.*, 2001;Williams *et al.*, 1997; Wolff *et al.*, 1998). In addition, the overexpression of COX-2 in transgenic mice leads to neoplastic changes (Muller-Decker *et al.*, 2006; Neufang *et al.*, 2001), while conversely, tumour formation and growth are reduced in animals that were engineered to be COX-2 deficient (Chulada *et al.*, 2000; Howe *et al.*, 2005; Oshima *et al.*, 1996; Tiano *et al.*, 2002; Williams *et al.*, 2000). In HPV-related diseases, including cervical cancer, COX-2 overexpression is well documented (Golijanin *et al.*, 2004; Kulkarni *et al.*, 2001; Ryu *et al.*, 2000). Moreover, several groups have shown that COX-2 expression enhances the progression of cervical cancer by increasing lymph node metastasis and resistance to radiation therapy (Ferrandina *et al.*, 2002; Gaffney *et al.*, 2001; Ryu *et al.*, 2000). Until recently, it was unclear whether the overexpression of COX-2 in cervical dysplasia was the result of a direct effect of HPV oncogenes or simply due to the consequence of cell transformation. In 2008, Subbaramaiah and Dannenberg demonstrated that HPV16 E6 and E7 were capable of stimulating COX-2 transcription by activating the epithelial growth factor receptor (EGFR) pathway.

Subsequent work by this group also established that HPV16 E5 has the ability to increase the transcription of COX-2 through activation of the EGFR pathway (Kim *et al.*, 2009). The E5 protein is generally considered to act early in the oncogenic process therefore this result suggests that altered COX-2 expression is an early event in cervical carcinogenesis.

The link between COX-2 and malignancy could be due to increased levels of prostaglandins in tumours. Indeed COX-2 expression and the PG biosynthesis are known to stimulate cell proliferation, promote angiogenesis, increase invasiveness, inhibit immune surveillance and prevent apoptosis all key features of carcinogenesis (Dohadwala *et al.*, 2001; Harris, 2007; Sheng *et al.*, 1998; Sheng *et al.*, 2001;Tsujii *et al.*, 1997; Tsujii *et al.*, 1998). $PGE_2$ is of particular interest as it is the predominant prostaglandin produced in an inflammatory response and the primary pro-carcinogenic mediator of inflammation (Subbaramaiah and Dannenberg, 2003). In human cervical cancer tissue $PGE_2$ mediated inflammatory changes have been observed (Mori *et al.*, 1990) and like COX-2 expression have been shown to increase with severity of malignancy. Of particular interest is the fact that these pro-inflammatory alterations have been demonstrated to decrease the cell-mediated immune response necessary to eradicate HPV transformed cells (Castle and Giuliano, 2003). Therefore, there appears to be a direct association between HPV infection, overexpression of COX-2 and $PGE_2$ the development of cervical carcinogenesis, making COX-2 and ideal therapeutic target.

Although COX inhibition of prostaglandins synthesis can explain part of the anti-tumour activity of certain NSAIDs there are some inconsistencies. For example NSAIDs also suppress the growth and induce apoptosis of cancer cells that do not express COX-1 or COX-2 (Grosch *et al.* 2001; Hanif *et al.*, 1996; Kim *et al.*, 2004; Kim *et al.*, 2009; Subbaramaiah and Dannenberg, 2007; Waskewich *et al.* 2002; Zhang *et al.*, 1999). In addition, the NSAID sulindac is a sulfoxide prodrug that is converted *in vivo* into sulfide and sulfone derivatives. The sulfone derivative does not inhibit COX enzymatic activity

(Riendeau *et al.*, 1997) or contribute to the anti-inflammatory activity of sulindac (Duggan *et al.*, 1978). However there are numerous studies where direct administration of this form of the drug has been shown to result in a chemoprotective benefits similar to that of the parent form (Andrews *et al.*, 2008; Goluboff *et al.*, 1999; Mahmoud *et al.*, 1998; Malkinson *et al.*, 1998; Piazza *et al.*, 2001; Scheper *et al.*, 2007; Thompson *et al.*, 1997; Willimas *et al*, 1999). Based on these observations, investigators have concluded that a COX independent mechanism may be involved and suggest this off-target effect of NSAIDs may either contribute to or be fully responsible for their antineoplastic activities. A number of COX-independent targets have been implicated including ceramide (Chan *et al.*, 1998), NFκB (Yamamoto *et al.*, 1999), 15-lipoxygenase (Shereiqi wt al., 2000), Ras (Herrmann *et al.*, 1998), peroxisome proliferator-activated receptor (He *et al.*, 1999), PDK-1/Akt (Zhu *et al.*, 2004), phosphodiesterase (Thompson *et al.*, 2000) and survivin (Zhang *et al.*, 2004). If COX inhibition is not necessary for the antineoplastic properties of NSAIDs, then it should be feasible to develop safer and more efficacious NSAID-like drugs for treating patients.

In this study, the effect of the NSAID sulindac on cervical cancer cell lines was examined. Sulindac was one of the early NSAIDs and it equally affects COX-1 and COX-2 activity. As mentioned earlier, for more than two decades now, sulindac has also been of interest as a chemopreventative treatment for adenomatous colorectal polyps and colon cancer, particularly in patients with FAP (Waddel and Loughry, 1983; Waddel *et al.*, 1989). However its utility is not limited to colon cancer. It has been reported to have inhibitory effects on cellular proliferation both *in vivo* and *in vitro* in a variety of cancers, including cervical cancer (Karl *et al.*, 2007; Yasui *et al.*, 2003). As with other NSAIDs, the mechanism by which sulindac mediates in anticancer activity is unknown and could involve COX dependent or independent mechanisms. Sulindac has a distinct advantage over other NSAIDs in answering this question, owing to its two derivatives, sulfide and sulfone. Sulfide has been attributed to mediating the COX inhibitory action of sulfide (Davies and Watson 1997) and as previously described sulfone lacks any anti-inflammatory activity (Duggan *et al.*, 1978; Riendeau *et al.*, 1997). Therefore, the

sulindac derivatives provided a useful method to determine if COX inhibition is required for its antineoplastic properties. A particularly interesting paper was published in 2007 by Karl *et al* in relation to sulindac treatment of cervical cancer cells. This study demonstrated the anti-proliferative activity of sulindac on HPV18 infected cervical cells, which was found to be mediated though a G1 arrest and apoptosis. In addition, it was found that the sulindac-induced G1 arrest was preceded by suppression of cyclins E and A, inactivation of cdk2, and complete loss of the viral oncoprotein E7, despite ongoing HPV transcription (including E7). Since E7 is essential for the maintenance of the carcinogenic phenotype of cervical cancer cells, this results suggest that sulindac has the potential to become an E7 oncogene specific therapeutic agent.

## 5.2 Chapter Aim

The objectives of this chapter were three fold:

- To determine the anti-proliferative efficacy of sulindac on a number of cervical cancer cell lines with varying origins, HPV status and viral DNA content. This was facilitated by measuring a number of criteria post treatment, including rate of cellular growth, cell cycle distribution and apoptotic profile.

- To establish whether any observed anti-proliferative activity of sulindac involved COX inhibition. This was achieved by examining the anti-proliferative capabilities of the two sulindac derivatives (sulfide and sulfone) and additionally by monitoring COX-2 activity and expression.

- To examine whether sulindac had the ability to alter the expression of the HPV viral oncogenes, E6 and E7. This was accomplished by monitoring transcriptomic and proteomic expression of E6 and E7 post treatment.

## 5.3 Methods

### *5.3.1Cell culture*

The cervical cancer cell lines used in this chapter were the HPV18 positive HeLa, the HPV16 positive SiHa and the HPV negative C33A (see section 2.1 for a detailed description). All cell lines were grown at 37°C in a humidified 5% $CO_2$ atmosphere and cultured as described in section 2.1.1.

### *5.3.2 Drug treatment of cells*

The NSAID drug sulindac and its derivatives, sulindac sulfide and sulindac sulfone were obtained from Sigma-Aldrich (St. Louis, MO, USA). Stock solutions for each drug were prepared by dissolving the powder formulations in dimethyl sulfoxide (DMSO). Stock solutions were prepared individually for 96-well and 6-well plate experiments, such that the final concentration of DMSO per well in the 96-well plates would not exceed 0.2% and in 6-well plates would not exceed 0.1%. The difference between these two set ups was due to the requirement for higher concentrations of drug in the 96-well plate experiments.

Briefly, the drug treatment protocol for the cells involved seeding the cells in complete growth media and allowing them to grow for 24hrs. The cells were seeded such that they were in an exponential growth phase and after 24hrs were 70-80% confluent. Following this initial 24hr incubation period, the media was removed, the cells were washed with PBS and fresh complete growth media was applied. The cells were then treated with various concentrations of the drug solutions. For each experimental set up, the controls included were: untreated cells and cells treated with DMSO, known as a vehicle control. The volume of DMSO used for the vehicle control depended on the set up; for 96-well plates the final volume was 0.2% and for 6-well plates the final volume was 0.1%.

### *5.3.3 MTT assay*

#### 5.3.3.1 Defining the exponential growth phase

Exponential growth curves were established for each cell line using the standard MTT assay. HeLa, SiHa and C33A cells were seeded at increasing concentrations ranging from $1x10^2$ to $3x10^6$ cells per well in 200µl of complete growth medium. To allow the cells to adhere, they were incubated for 1hr at 37°C in a humidified 5% $CO_2$ atmosphere before performing a MTT assay (described in section 2.10). Exponential growth curves were constructed using the GraphPad Prim version5 software (GraphPad Software, CA, USA). All assays were performed in triplicate and repeated three times.

#### 5.3.3.2 Cell viability

The effect of sulindac and its derivatives on the viability of the cervical cell lines was determined using the standard MTT assay. HeLa, SiHa and C33A cells were plated at $1x10^4$, $1x10^4$ and $2x10^4$ cells per well in 200µl of complete growth medium, respectively. After 24hrs growth the cells were treated with varying concentrations of sulindac from 1.5µM to 1.5mM. Following incubation for 24, 48 or 72hrs at 37°C in a humidified 5% $CO_2$ atmosphere, cell viability was determined by means of the MTT assay, as described in section 2.10. Cell viability rate was calculated as the percentage MTT absorption as follows: % cell viability = (mean absorbance/mean vehicle control absorbance) x 100. Dose response curves were generated and $IC_{50}$ values calculated using the GraphPad Prim version5 software (GraphPad Software, CA, USA). All assays were performed in triplicate and repeated three times.

### *5.3.4 Cell cycle analysis*

Cell cycle status was evaluated by flow cytometry by means of dual BrdU and PI staining. HeLa cells were seeded in a 6-well plate at a density of $1.5x10^5$ cells per well, after 24hrs growth they were treated with sulindac at various concentrations. The cells were incubated for a further 24 or 48hrs prior to the addition of BrdU. After 2hrs growth in the presence of BrdU, all cells were collected (adherent and non adherent). Subsequent cell staining procedures and flow cytometry analysis was performed as described in section 2.8.2.

### *5.3.5 Apoptosis analysis*

The apoptotic profile of cells was determined by flow cytometry by means of annexin V-FITC and PI counter staining. All HeLa cells were collected (adherent and non adherent) after 24 or 48hrs sulindac treatment and subjected to annexin V-FITC/PI staining and flow cytometry analysis as described in section 2.8.1.

### *5.3.6 Determination of COX activity*

After 48hrs treatment with sulindac, the culture medium was collected from HeLa cells and used to determine the level of secreted $PGE_2$. The quantity of $PGE_2$ was measured by a competitive ELISA technique ($PGE_2$ enzyme immunoassay kit, R&D Systems, Minn., USA) according to the manufacturer's instructions. Results were calculated as per section 2.9.1 and are expressed as pg/ml. All assays were performed in duplicate (as per manufacturer's instructions) and repeated three times.

### *5.3.7 TaqMan® RT-PCR*

Total RNA was extracted from HeLa cells after 48hrs treatment with sulindac, 48hr time point was chosen based on the results of the cell viability assay. Total RNA was extracted using the Ambion MirVanna kit (section 2.3.2) and subjected to DNase digestion (section 2.3.3). The 260/280 nm ratio and the concentration of the extracted total RNA was determined using the NanoDrop® ND-1000 (section 2.4.1). TaqMan® two step RT-PCR was performed as per section 2.5.2 using the below primer and probe sets. The relative quantity of gene expression was calculation using the $2^{-\Delta\Delta Ct}$ comparative CT method as described in section 2.5.4.1, where B2M gene expression was used as the endogenous control and gene expression of untreated cells were used as the calibrator sample.

PCR primers and probes towards HPV16 E6 and E7 were designed using Primer Express Software Version 3.0 (Applied Biosystems, Foster City, CA USA) as described in section 2.5.1. Primers and probes towards E6 were designed based on the E6 coding region (nucleotides 105-581) of the HPV18 complete genomic sequence (Genbank accession number X05015). Primers and probes towards E7 were designed based on the E7 coding region (nucleotides 590-907) of the HPV18 complete genomic sequence (Genbank accession number X05015). Table 5.1 shows the HPV18 E6 and E7 primer and probe sequences and amplicon sizes. The concentration of HPV18 E6 and E7 primers and probes used in each assay was optimised on controls by performing PCR titrations of each primer set, 50-900nM, and probe, 50-250nM. The optimal combination of primer and probes for the TaqMan® RT-PCR assay were chosen based on those that generated the lowest threshold cycle and maximum ΔRn, see Table 5.1 for optimal concentrations.

The utilised primers and probes specific for COX-2 and B2M were commercial pre-designed sets obtained from Applied Biosystems (Foster City, CA, USA). They were provided in 20X mixes and were used as per manufacturer's instructions at a concentration of 1X.

**Table 5.1: HPV18 E6 and E7 primer and probe sequences.**

| PCR Target | Nucleotide position | Amplicon size | Sequence | Concentrations | |
|---|---|---|---|---|---|
| | | | | Primers | Probes |
| E6 | 404-468 | 65 | F: 5'-GAGGCCAGTGCCATTCGT-3'<br>R: 5'-TCCAACGACGCAGAGAAACA-3'<br>P: 5'-CAACCGAGCACGACAG-3' | 300nM | 200nM |
| E7 | 153-211 | 60 | F:5'-CCGACGAGCCGAACCA-3'<br>R:5'-TGTATGTGTTGTAAGTGTGAAGCCA-3'<br>P:5'-AACGTCACACAATGTT-3' | 300nM | 250nM |

Symbols: F represents forward primer, R represents reverse primer and P represents probe.

### *5.3.8 Western blot analysis*

Protein cell extracts were prepared from HeLa cells 48hrs after sulindac treatment by lysing cells with 50µl of RIPA buffer (section 2.7.1). The concentration of recovered protein in each lysate was determined using the Pierce BCA™ protein assay kit (section 2.7.2). Equal amounts of protein (30µg/lane) were resolved by 10-12% SDS-PAGE and electrotransferred to PVDF membranes. After blocking, the membranes were incubated with anti-COX-2, anti-p53, anti-HPV18 E7 or anti-GAPDH antibodies (Table 5.2). Subsequently the membranes were washed and incubated with the appropriate peroxidise-conjugated secondary antibody (Table 5.2). The immunoreactivity was detected with the ECL system. GAPDH was used to asses protein loading.

**Table 5.2: Antibody and corresponding dilutions used in the study.**

| Primary Antibodies | Supplied by | Antibody Type | Species Raised in | Dilution factor |
|---|---|---|---|---|
| **GAPDH** | Abcam (Cambridge, CB4 0WN, UK) | Monoclonal | Mouse | 1/250000 |
| **COX-2** | Santa Cruz Biotechnology , Inc. (Santa Cruz, CA, USA) | Polyclonal | Rabbit | 1/100 |
| **HPV18 E7** | Santa Cruz Biotechnology , Inc. (Santa Cruz, CA, USA) | Polyclonal | Goat | 1/100 |
| **p53** | BD Pharmigen™ (at BD Biosciences, San Jose, CA, USA) | Monoclonal | Mouse | 1/1000 |
| **Secondary Antibodies** | | | | |
| **Mouse** | Jackson Immuno Research (West Grove, PA, USA) | | Goat | 1/1000 |
| **Rabbit** | Jackson Immuno Research (West Grove, PA, USA) | | Goat | 1/100 |
| **Goat** | Jackson Immuno Research (West Grove, PA, USA) | | Rabbit | 1/1000 |

### *5.3.9 Statistical analysis*

Data is expressed as means ± the standard deviation from at least three biological replicates. For all measurements as needed, a Student *t* test was used to assess the statistical significance of treated groups versus vehicle control groups. Student *t* test was performed using the GraphPad Prim version5 software (GraphPad Software, CA, USA). A statistically significant difference was considered to be present at $p < 0.05$.

## 5.4 Results

### *5.4.1 Sulindac decreases cell viability of cervical cancer cell lines*

To assess whether sulindac affected the growth of cervical cancer cells *in vitro,* dose response curves were established for its effect on three cervical cancer lines, HeLa, SiHa and C33A. The final concentrations of sulindac used ranged from 1.5μM to 1.5mM. To ensure that cells would be in an exponential growth phase for the work, an initial assessment was carried out to determine the correct seeding density for exponential growth of each cell line (Figure 5.2). Subsequently, exponentially growing, unsynchronized cells were co-cultured with sulindac for 24, 48 or 72hr time periods. A standard MTT assays was performed to establish any inhibitory activity of sulindac on cell viability. Dose response curves for the each time point were generated and where possible an $IC_{50}$ value was calculated. The $IC_{50}$ represents the concentration required for a particular drug to inhibit a biological function by half, in this case cell viability, and is considered a measure of the effectiveness of a compound.

Sulindac decreased cell viability in a dose and time dependent manner in all three cell lines (Figure 5.3). The most potent effect was observed with the HPV18 positive adenocarcinoma cell line HeLa, with an initial decrease in cell viability observed with 150μM of sulindac in comparison to 250μM for the other two cell lines (Figure 5.3 A & B). Furthermore, the $IC_{50}$ value for the HeLa cells was substantially lower (232μM) than that of the SiHa and C33A cells, 495μM and 389μM respectively (Figure 5.3 A & B).

To confirm these results, alterations in cell density were assessed visually by microscopic examination. The sulindac concentrations used corresponded to doses which were seen to have none (57.5μM), marginal (115μM) and significant (230μM and 400μM) inhibitory effects on HeLa cell growth (Figure 5.3).Treatment of HeLa cells, with 115μM, 230μM or 400μM of sulindac for 24 or 48hrs, resulted not only in lower cell density but also distinct changes in cellular shape (Figure 5.4 & 5.5). In particular cells incubated with 155μM, 230μM and 400μM developed a flattened-like

morphology with long spindle projections and there was a loss of tight cell-cell contact. These alterations were also observed with 57.5μM, but were less pronounced. Additionally, there was a dose dependant increase in the level of cell detachment and nuclear condensation, which is indicative of cell death being induced. In contrast to the HeLa cells, there were only marginal mitotic activity and morphological differences when SiHa cells were exposed to the equivalent concentrations of sulindac over the same time periods (Figure 5.6 & 5.7). It should be noted that there was no obvious proliferative or morphological differences between the untreated cells and the vehicle control (0.1% DMSO treated cells) for either cell line (Figure 5.4 – 5.7).

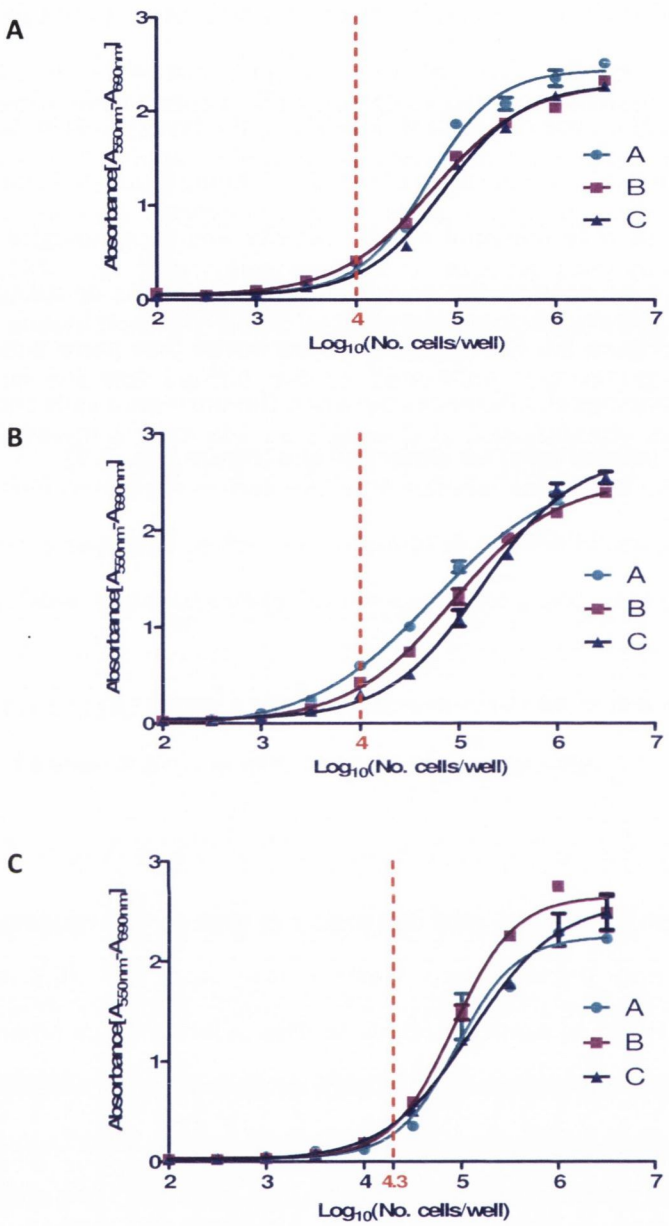


**Figure 5.2: Determining seeding concentration for exponential growth. (A)**HeLa, **(B)**SiHa, **(C)**C33A were established on a 96 well plate at seeding concentrations ranging from $1x10^2$ to $3x10^6$. After one hour growth, which allowed for the cells to adhere, cell viability was assessed by means of the MTT assay. All experiments were performed in triplicate, thrice. Marked on each plot, is the point at which the cells enter exponential growth. This occurs at the log cell concentration 4 (equivalent to $1x10^4$) for both the HeLa and SiHa cells and at the log cell concentration 4.3 (equivalent to $2x10^4$) for the C33A cells.

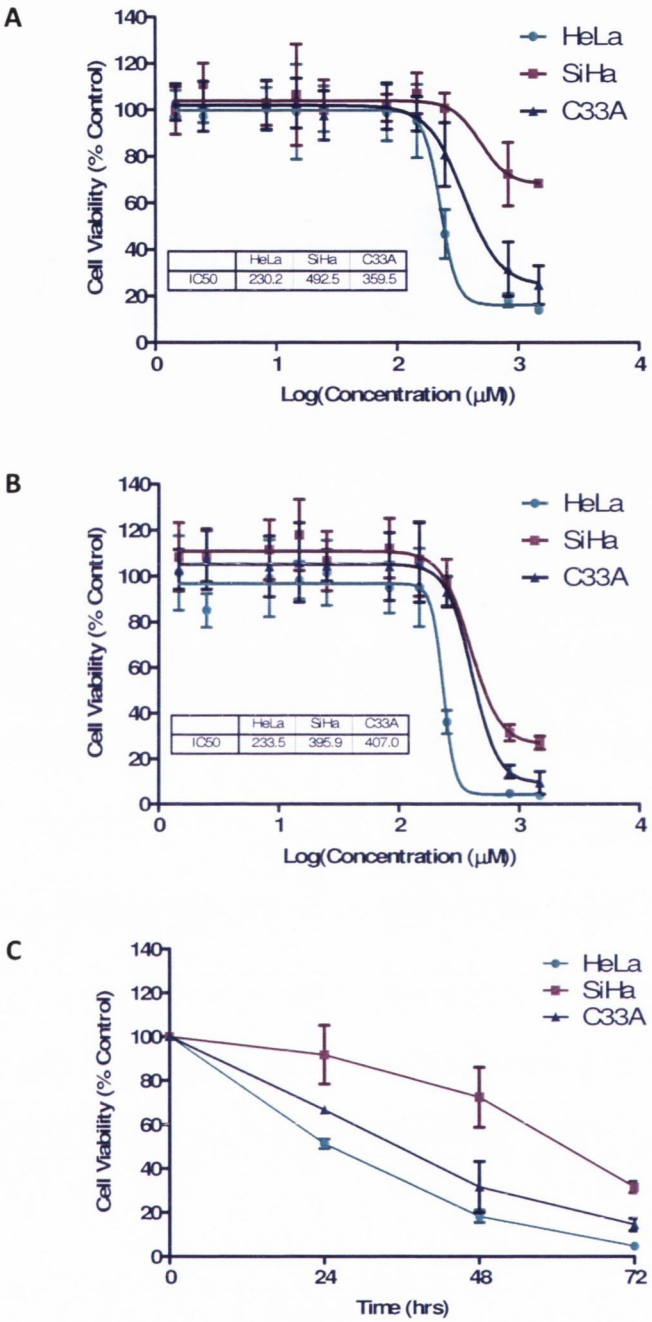


**Figure 5.3 Effect of sulindac on cervical cell lines.** HeLa ($1x10^4$), SiHa ($1x10^4$) and C33A ($2x10^4$) cells were established on a 96 well plate. After 24hrs, the cells were treated with increasing concentrations of Sulindac. **(A)** 48 or **(B)** 72 hours post treatment, cell viability was assessed by means of the MTT assay. **(C)** Cells were treated with 800μM and cell viability was monitored at 24hr intervals over a 72hr period. Cell viability rate was calculated as the percentage MTT absorption as follows: % cell viability = (mean experimental absorbance/mean vehicle control absorbance) x 100. All experiments were performed in triplicate, thrice (n=9).

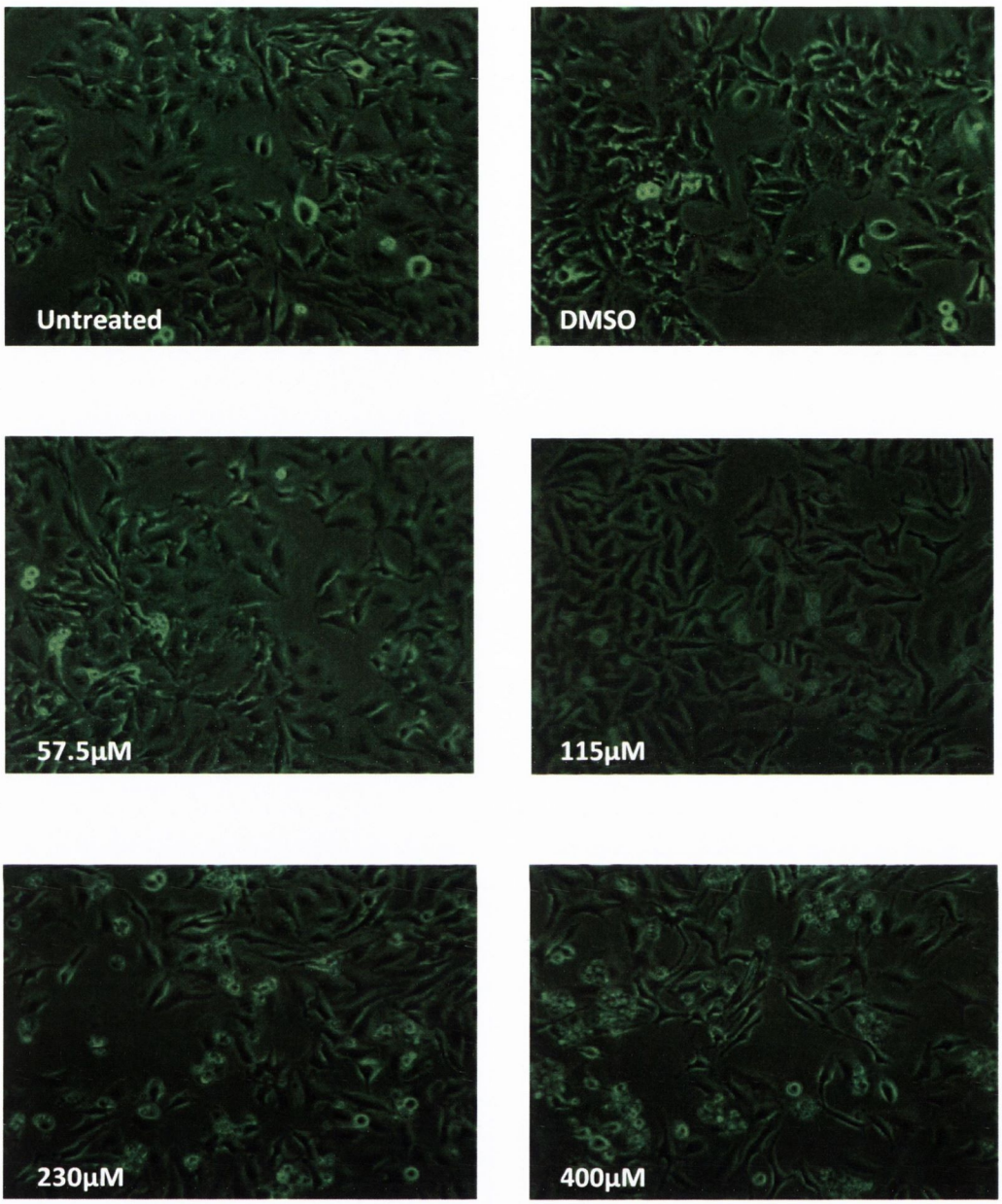


**Figure 5.4: HeLa cells 24hrs after treatment with sulindac.** HeLa cells were left untreated, treated with DMSO (0.1%) or treated with sulindac at the indicated concentrations. After 24hrs incubation, cells were examined by light microscopy. There are no differences between untreated cells, vehicle control (DMSO) cells and those treated with 57.5μM of sulindac. The most pronounced alterations are observed with 400μM of sulindac. The cell density has decreased and there are morphological alterations. These cells have elongated morphology with long spindle projections and are no longer forming tight cell-cell contacts. Cells treated with 115μM and 230μM appear to have a number of cells undergoing similar morphological alterations. (Magnification 200x)

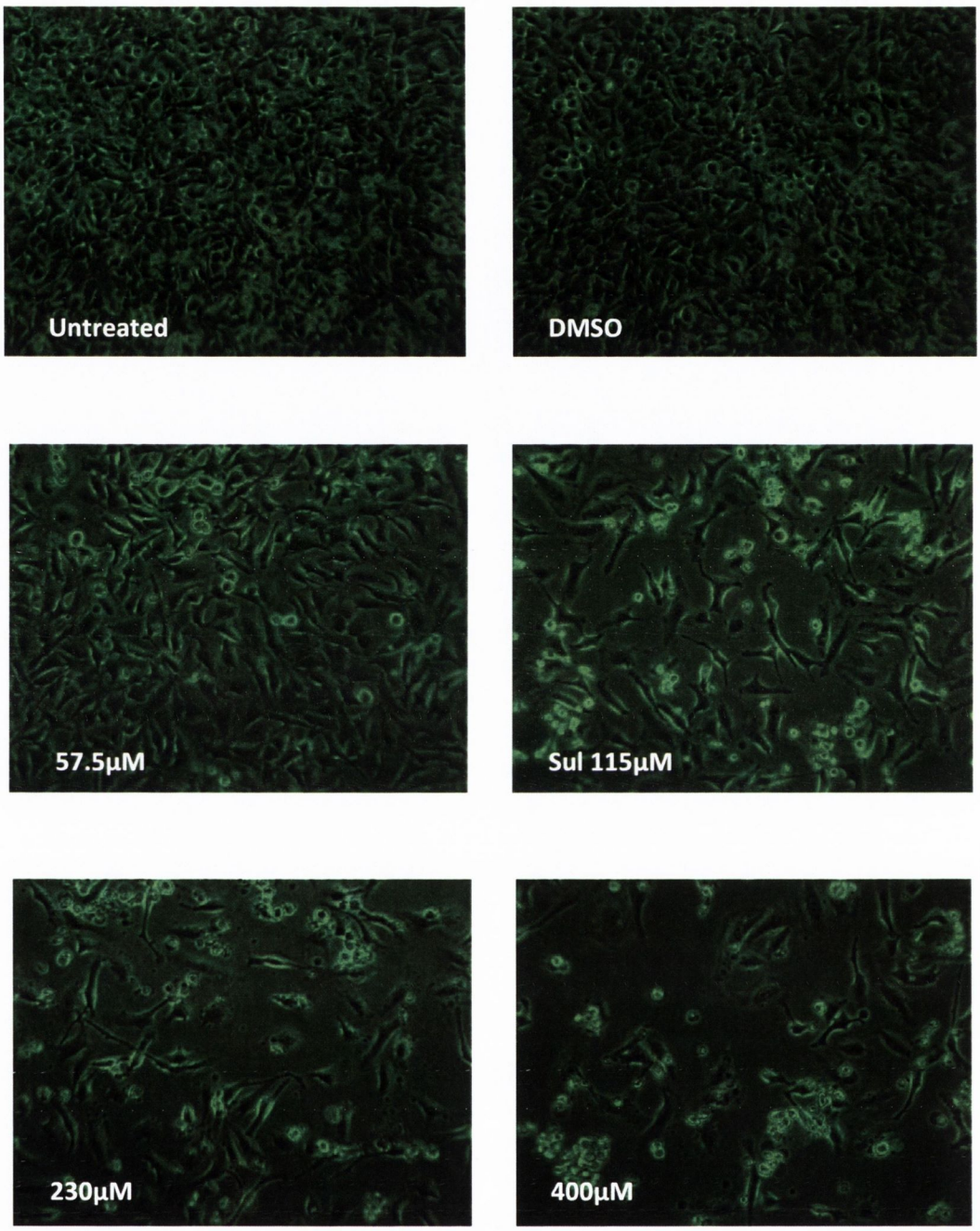


**Figure 5.5: HeLa cells 48hrs after treatment with sulindac.** HeLa cells were left untreated, treated with DMSO (0.1%) or treated with sulindac at the indicated concentrations. After 48hrs incubation, cells were examined by light microscopy. There are no differences between untreated and vehicle control (DMSO) cells. Sulindac reduced the cell density in all treatment groups and there was a dose dependent increase in the number of detached cells. Morphological alterations are observed in cell treated with 115μM, 230μM and 400μM of sulindac. These cells are no longer forming tight cell-cell contacts and have developed a flattened, elongated morphology with long spindle projections. (Magnification 200x)

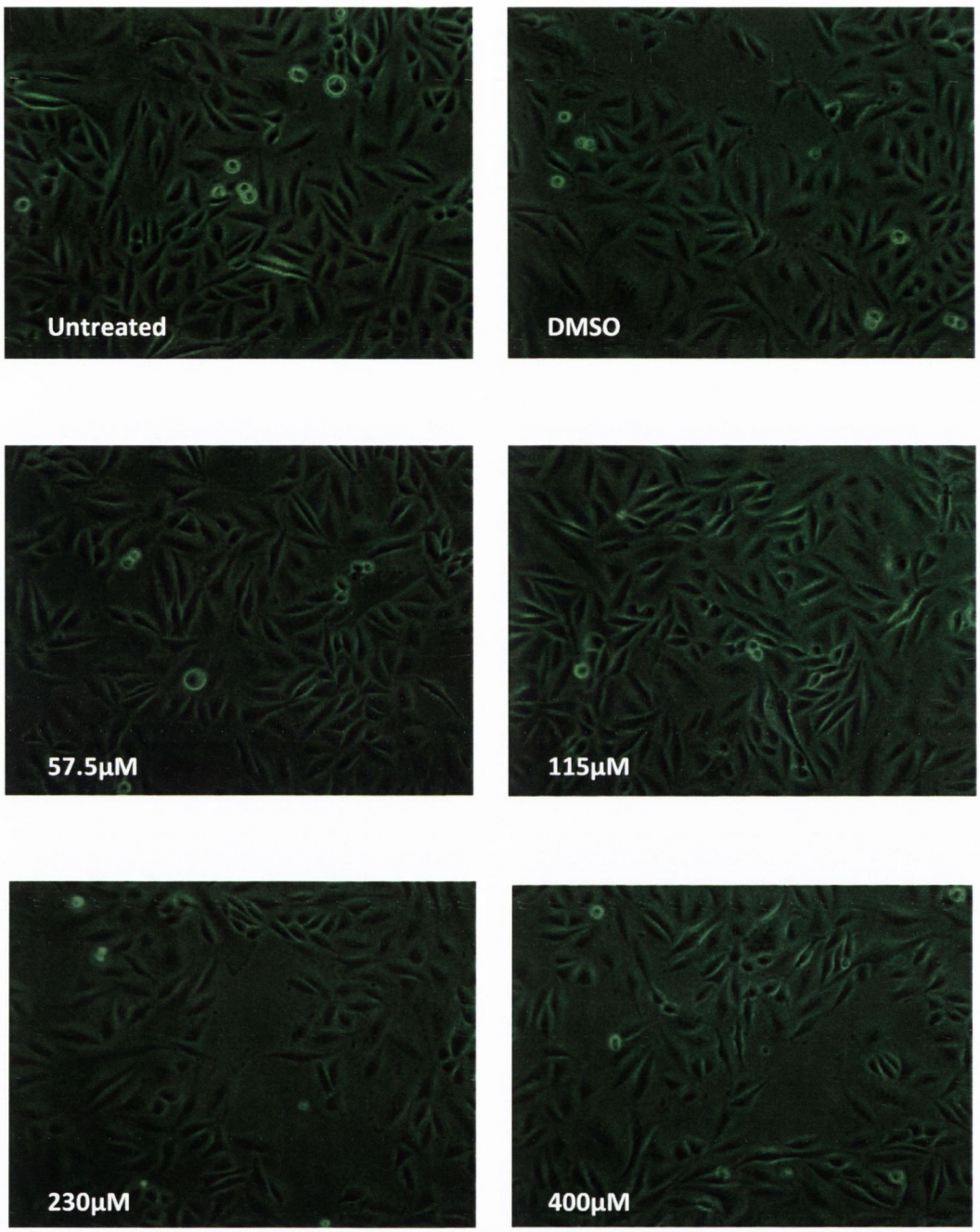


**Figure 5.6: SiHa cells 24hrs after treatment with sulindac.** SiHa cells were left untreated, treated with DMSO (0.1%) or treated with sulindac at the indicated concentrations. After 24hrs incubation, cells were examined by light microscopy. There are no major morphology or cell density differences between any of the cells at this time point. (Magnification 200x)

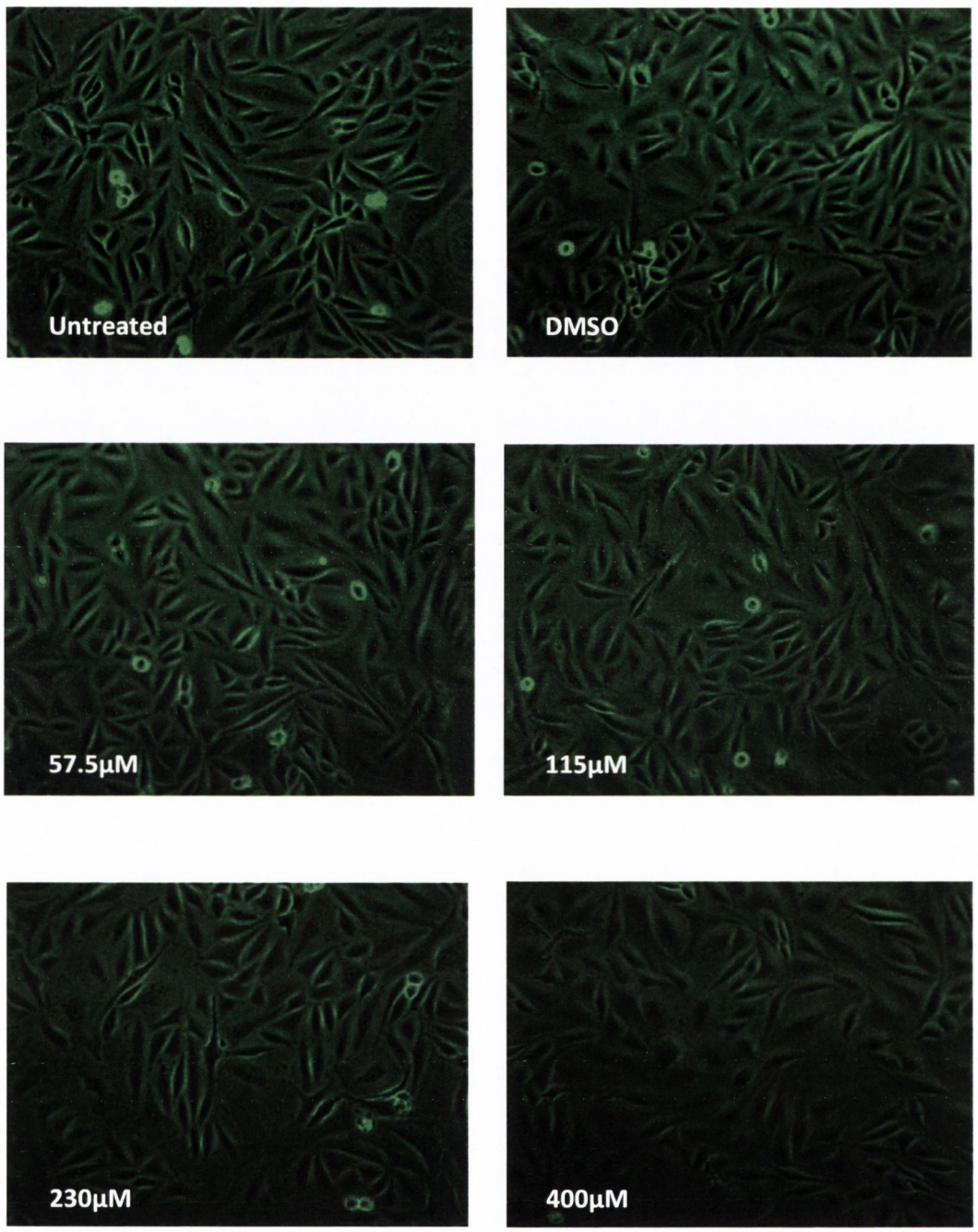


**Figure 5.7: SiHa cells 48hrs after treatment with sulindac.** SiHa cells were left untreated, treated with DMSO (0.1%) or treated with sulindac at the indicated concentrations. After 48hrs incubation, cells were examined by light microscopy. There are no major morphology or cell density differences between any of the cells at this time point. (Magnification 200x)

### *5.4.2 The effect of sulindac derivatives on the growth of cervical cancer cells*

To examine whether the growth inhibitory effect of sulindac was attributable specifically to either of its derivatives, additional dose response curves were established based on the activity of sulfide and sulfone. Again, the final concentrations of drug used ranged from 1.5μM to 1.5mM and exponentially growing, unsynchronized cells were co-cultured with the derivatives over either 48 or 72hrs. In contrast to previous studies in other cancer types (Han *et al.*, 1998; Malkinson *et al.*, 1998; Loveridge *et al.*, 2008; Thompson *et al.*, 1997), neither of the derivatives potentiated or equalled the original anti-proliferative effect observed with the parent drug (Figure 5.8). While there was a decrease in cell viability, the effect was minimal in many cases (Figure 5.8) and consistently less than that seen with the prodrug form (Figure 5.3). The efficacy of sulfide was considerably greater than that of sulfone. For example by 72hrs sulfide at concentrations of 1.5mM had inhibited proliferation in the SiHa and C33A (Figure 5.8 E), however, sulfone had no effect on the growth pattern of these cells (Figure 5.8 F). Consistent with the results of the prodrug form, the more significant findings were observed with HeLa cells, with both sulfide and sulfone decreasing the number of viable cells after 72hrs (Figure 5.8 A-B). Overall these results indicate that the growth inhibitory activity of sulindac on cervical cell line models does not rely solely on either the activity of its COX dependent or independent derivatives. The finding that sulfide, unlike sulfone, had a limited degree of efficacy towards the cervical cell lines in comparison to sulindac, indicates that part of the effect may be mediated through COX inhibition. Since the most potent growth inhibitory effects were observed with sulindac and in the HPV18 adenocarcinoma cells, the remainder of the study focused on analysing its effect in this cell line.

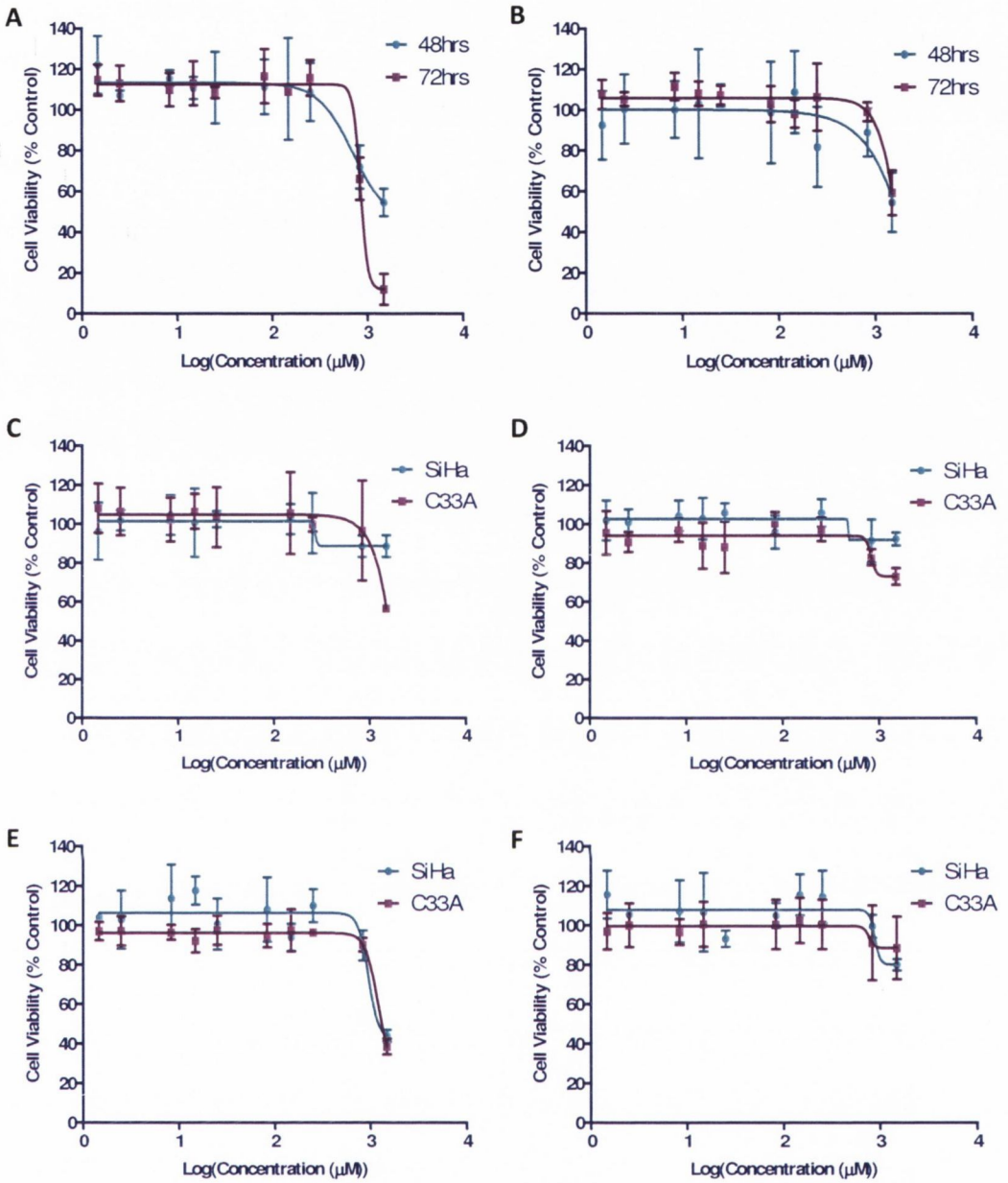


**Figure 5.8: The effect of sulfide and sulfone on cervical cancer cells.** (**A**, **B**) HeLa ($1x10^4$) were established on a 96 well plate. After 24hrs, the cells were treated with increasing concentrations of (**A**) sulfide or (**B**) sulfone. 48 or 72 hours post treatment cell viability was assessed by means of the MTT assay. (**C** - **F**) SiHa ($1x10^4$) and C33A ($2x10^4$) cells were established on a 96 well plate. After 24hrs the cells were treated with increasing concentrations of (**C**, **E**) sulfide or (**D**, **F**) sulfone. 48 (**C**, **D**) or 72 (**E**, **F**) hours post treatment cell viability was assessed by means of the MTT assay. Cell viability rate was calculated as the percentage MTT absorption as follows: cell viability (% control) = (mean experimental absorbance/mean vehicle control cell absorbance) x 100. All experiments were performed in triplicate, thrice (n=9).

### *5.4.3 Sulindac alters endogenous COX-2 activity and expression*

COX-2 overexpression in cervical cancer is well documented (Kulkarni *et al.*, 2001; Ryu *et al.*, 2000; Wu *et al.*, 2005) and has been demonstrated to enhance the progression of the disease (Ferrandina *et al.*, 2002; Gaffney *et al.*, 2001; Ryu *et al.*, 2000). The activity of sulfide, though limited, indicated that COX inhibition may account for part of the efficacy of sulindac (Figure 5.8). Based on these observations of the importance of COX-2 and the potential role in the system, it was decided to further evaluate the role of COX inhibition in the growth inhibitory activities of sulindac. This was achieved by establishing whether the parental form could alter endogenous COX-2 activity and expression.

Figure 5.9 C shows that sulindac reduces the production $PGE_2$ in a dose dependent manner from concentrations of 115μM and greater. As $PGE_2$ is a downstream product of COX enzymatic activity, this result indicates that sulindac can inhibit COX-2 activity. To assess whether this reduction in activity corresponded with changes at the transcriptome or proteome level TaqMan® RT-PCR and western blot analysis was performed. There was a decrease in the protein expression of COX-2. However this result does not correlate with the reduction in COX activity as it is only significantly observed with the higher concentrations of 230μM and 400μM of sulindac (Figure 5.9 B). Interestingly at the same concentrations there is an increase in the mRNA expression level (Figure 5.9 A), thus there is an inverse correlation between COX-2 mRNA and protein expression. This result indicates that COX-2 is being post-transcriptionally regulated at doses of 230μM and 400μM of sulindac. Overall these findings would indicate that sulindac has COX-2 inhibitory capabilities but that the mechanism by which they are mediated is predominantly independent of changes in its expression. Additionally, it would appear that a reduction in COX-2 activity is a more significant event than that of the expressional alterations, as it occurs at a lower dose.

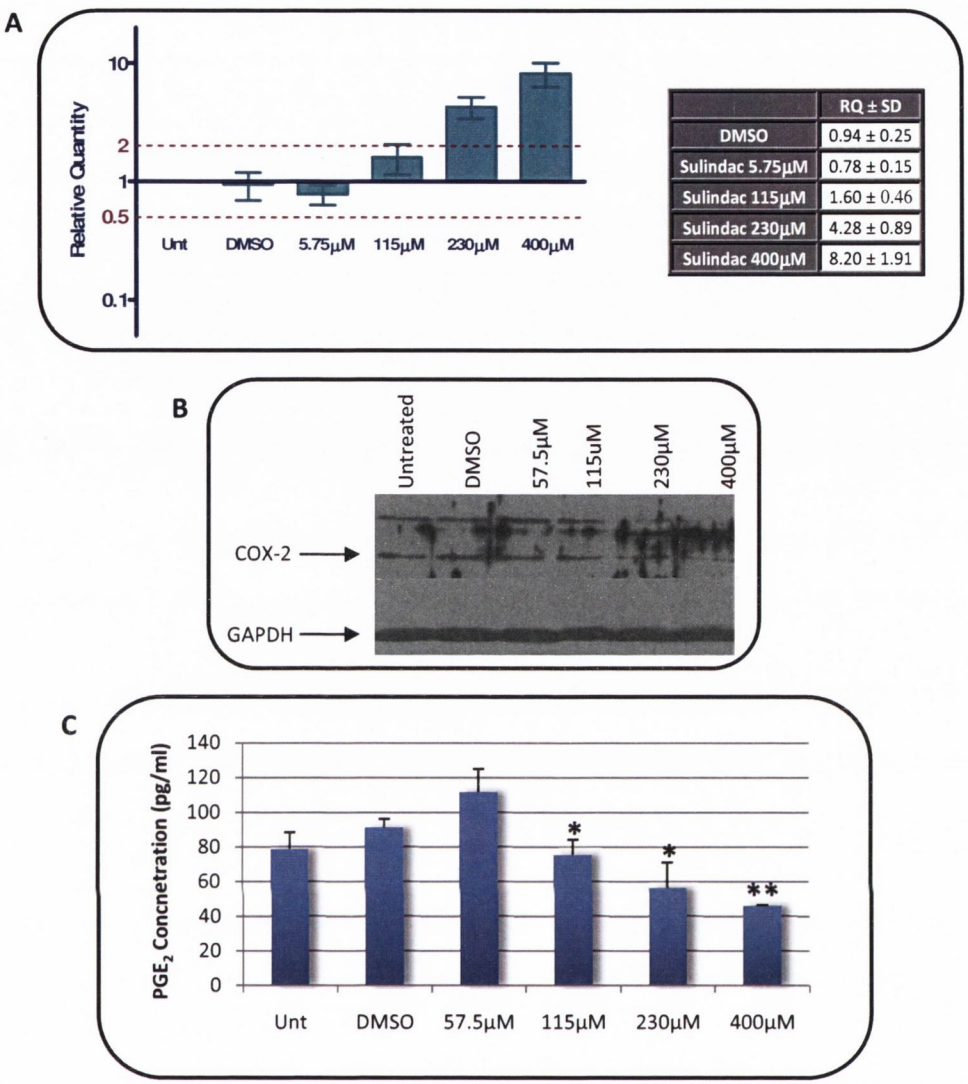


**Figure 5.9: Effect of sulindac on endogenous COX-2 expression and activity in HeLa cells.** HeLa cells were left untreated (Unt), treated with DMSO (0.1%; vehicle control) or treated with sulindac at the indicated concentrations for 48hrs. (**A**) Total RNA was extracted and mRNA expression was evaluated by TaqMan® RT-PCR using primers and probes selective for COX-2 mRNA. The COX-2 mRNA expression was normalised to that of B2M and calibrated to that of the untreated cells to establish the relative level of mRNA expression. Marked on the graphs are the considered limits of biological variation between two biological samples, from 0.5 to 2. (**B**) Cells were lysed with RIPA buffer. The lysate samples (30μg) were then resolved by SDS PAGE electrophoresis and transferred to a PVDF membrane. The membrane was firstly blocked in blocking buffer and then immunoblotted for COX-2 (top panel) and GAPDH (bottom panel). GAPDH was used as a loading control. (**C**) Secreted $PGE_2$ concentrations were determined in the cell growth media using a competitive ELISA technique. Values are expressed in as mean + SD. P values were calculated compared to the vehicle control; *p<0.05, **p<0.01.

### *5.4.4 Sulindac induces cell cycle dysregulation in HPV18 positive cells*

To try and understand the anti-proliferative action of sulindac, cell cycle distribution analysis was performed by flow cytometry based on dual BrdU and PI staining. HeLa cells were treated with different concentrations of sulindac (57.5μM, 115μM, 230μM and 400μM) over a 24 or 48hr time period and harvested for flow cytometry analysis. All data is discussed in comparison to the vehicle control.

The flow cytometry analysis clearly demonstrated that sulindac induces prolonged cell cycle arrest in HeLa cells at doses of 115μM and above. Figures 5.10 to 5.12 show there is a reduction in the number of cells entering the S phase of the cell cycle. At the higher concentrations of 230μM and 400μM this decline in the S phase is matched with an increase in the G2/M phase, and the extent of these alterations becomes more evident with time (Figure 5.10). At these concentrations, the number of cells in the G1 phase remains relatively constant in comparison to the vehicle control (Figure 5.10). On initial consideration, these findings would imply that the sulindac induced cell cycle arrest is mediated through a block in the G2/M phase. However, if we consider the observed reduction in the S phase and the cell cycle mechanism this is hard to reconcile. Normally with a pure G2/M arrest, there is an accumulation of cells in the G2/M phase with a corresponding decrease in the G1 phase and a smaller decrease in the S phase (Ceraline *et al*, 1998; Zhang *et al.*, 2006; Jin *et al.*, 2006; Selvendiran *et al.*, 2007; Shin *et al.*, 2008). This makes sense, as the blockage of cells in the G2/M phase directly impacts on the G1 phase and indirectly on the S Phase. For there to be a substantial decrease in the S phase due to a G2/M arrest, there would have to be a reciprocal significant change in the G1 phase. Since at no point does the G2/M arrest induced by sulindac correspond with a significant reduction in the G1 phase, it is unlikely that the observed significant decreases in the S phase are solely due to the G2/M arrest. An alternative explanation for this cell cycle distribution is that, not only is sulindac inducing a G2/M arrest in the treated cells but also a G1 arrest, and that it is this G1 arrest that is producing the significant decrease in the S phase. The G1 arrest is not clearly evident from the results as an accumulation of cells in this phase of the cell cycle does not occur. The reason for this is that cells are neither entering, due to the

G2/M arrest, nor leaving the G1 phase therefore the cell numbers remain relatively stagnant.

Figure 5.10 supports the idea that there is a dual G1 and G2/M arrest in cells treated with 230μM and 400μM of sulindac. It shows examples of representative fluorocytograms from the analysis of HeLa cells after 24hrs treatment with sulindac. In figures A-C, which represent untreated, vehicle control and 57.5μM respectively, it would appear that the cells are evenly distributed throughout the S phase (region highlighted in purple), if slightly denser at the upward arc in the curve. However, in figures D-F, which represent 115μM, 230μM and 400μM respectively, there appears to be a dose dependent decrease in the number of cell in this upward arc region of the curve. This indicates an inability of the cells to move from the G1 phase (region highlighted in orange) into the S phase. It is also visually apparent that there is an increase in the number of cells in the G2/M phase at these concentrations.

Sulindac at 115μM 24hrs post treatment has a more potent effect on the S Phase of the cell cycle than higher concentrations of sulindac. This alteration is matched with an increase in the G1 and also a marginal increase in the G2/M phase. This would indicate that at this concentration and time point the HeLa cells are arresting in the G1 phase. By 48hrs post treatment there is a reduction in the number of cells in the G1 phase and an increase in the S and G2/M phase. This could either mean that the cells are recovering for the initial treatment or that there phenotype is becoming similar to that of the higher concentrations. The idea that these cells may be recovering is supported by the results of the lower concentration of sulindac, 57.5μM. At 24hrs, its cells cycle distribution profile was similar to their of 115μM, but by 48hrs it is identical to that of the vehicle control, i.e. the cells have recovered. However arguing against this recovery theory is the microscopy analysis which demonstrates that from 24 to 48hrs the cell density and morphological abberations observed after treatment become more pronounced (Figure 5.4-5.5).

The findings of this analysis indicate that in the HeLa cells, sulindac is mediating an arrest in the cell cycle by targeting both the G1 and G2/M cell cycle checkpoints. The fact that the G1 arrest occurs initially with both the 57.5μM and 115μM concentration may indicate that it is an early event and that the G2/M arrest only occurs with extended length of exposure or increased concentration.

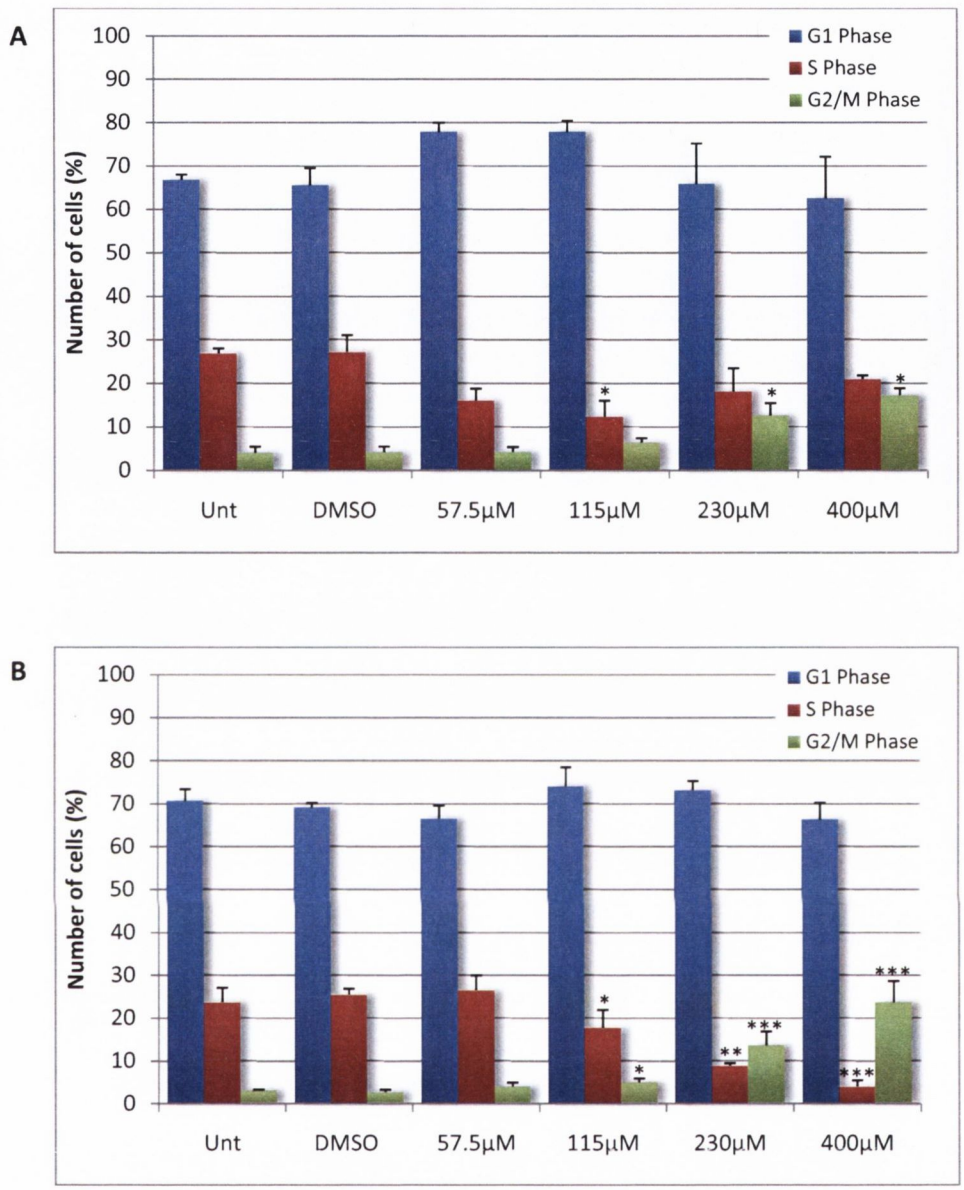


**Figure 5.10: Sulindac induces alterations in the cell cycle of HeLa cells.** HeLa cells were left untreated (Unt), treated with DMSO (0.1%; vehicle control), or treated with sulindac at the indicated concentrations. After 24hrs **(A)** or 48hrs **(B)** BrdU was added to the cell culture media. After 2hrs incubation all cells (adherent and non-adherent) were collected, stained with both FITC labelled anti-BrdU antibody and PI. Finally the cells were analysed by flow cytometry. The Histograms represent the cell cycle distribution after treatment with sulindac. Results are representative of three independent experiments. Values are expressed as mean +SD. P values were calculated compared to the vehicle control; *p<0.05, **p<0.01, ***p<0.001.

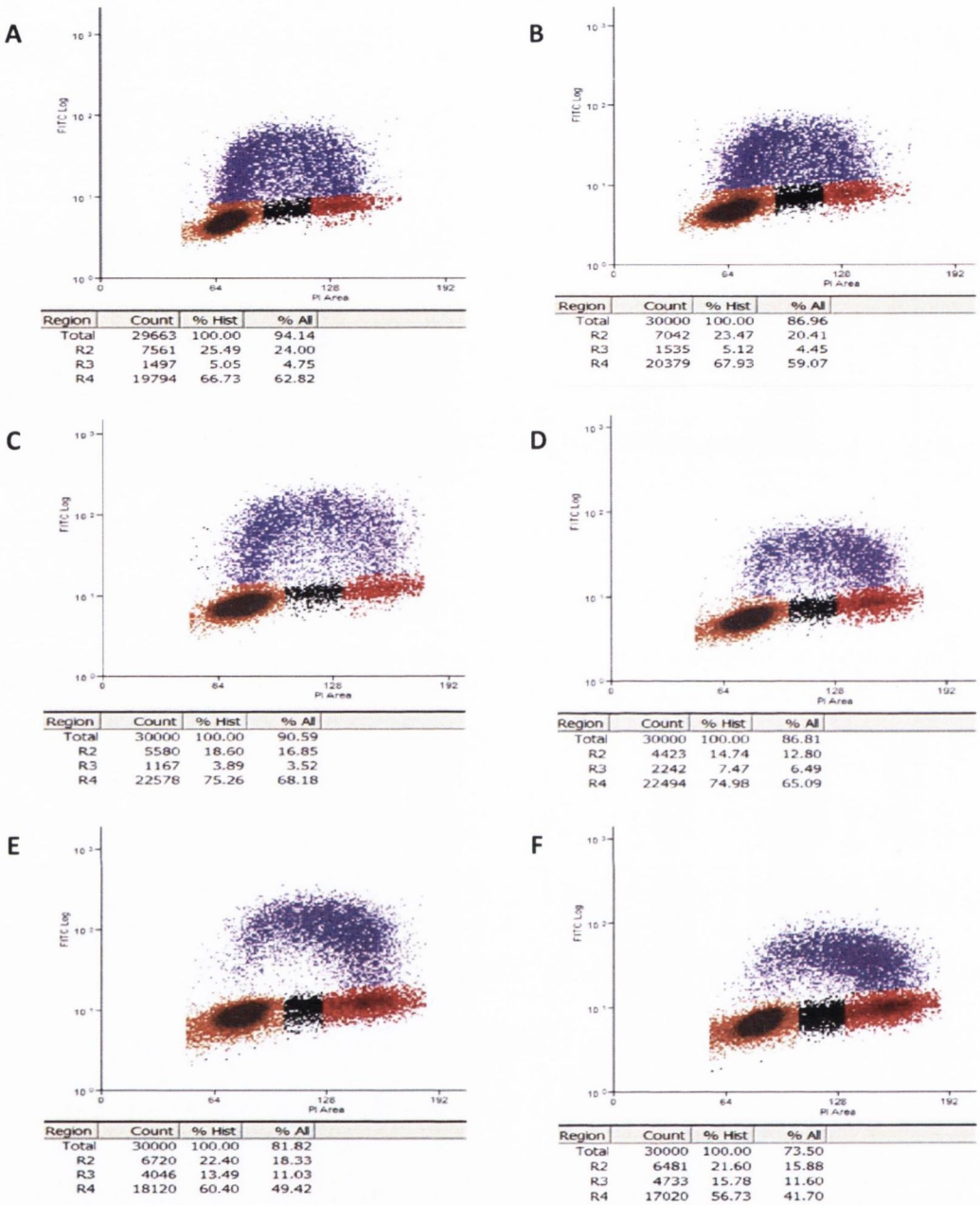


**Figure 5.11: Representative fluorocytograms of cell cycle analysis on HeLa cells 24hrs post sulindac treatment.** HeLa cells were left untreated **(A)**, treated with DMSO (vehicle control) **(B)** or treated with sulindac at concentrations of 57.5μM **(C)**, 115μM **(D)**, 230μM **(E)** and 400μM **(F)**. After 24hrs BrdU was added to the cell culture media. Following 2hrs incubation all cells (adherent and non-adherent) were collected and stained with both FITC labelled anti-BrdU antibody and PI. Finally the cells were analysed by flow cytometry. The dual parametric dot plots combining FITC labelled anti-BrdU antibody and PI fluorescence shows the G1 phase (orange; R4), S phase (purple; R2) and the G2/M phase (red; R3) of the cell cycle. Data from one complete experiment is presented.

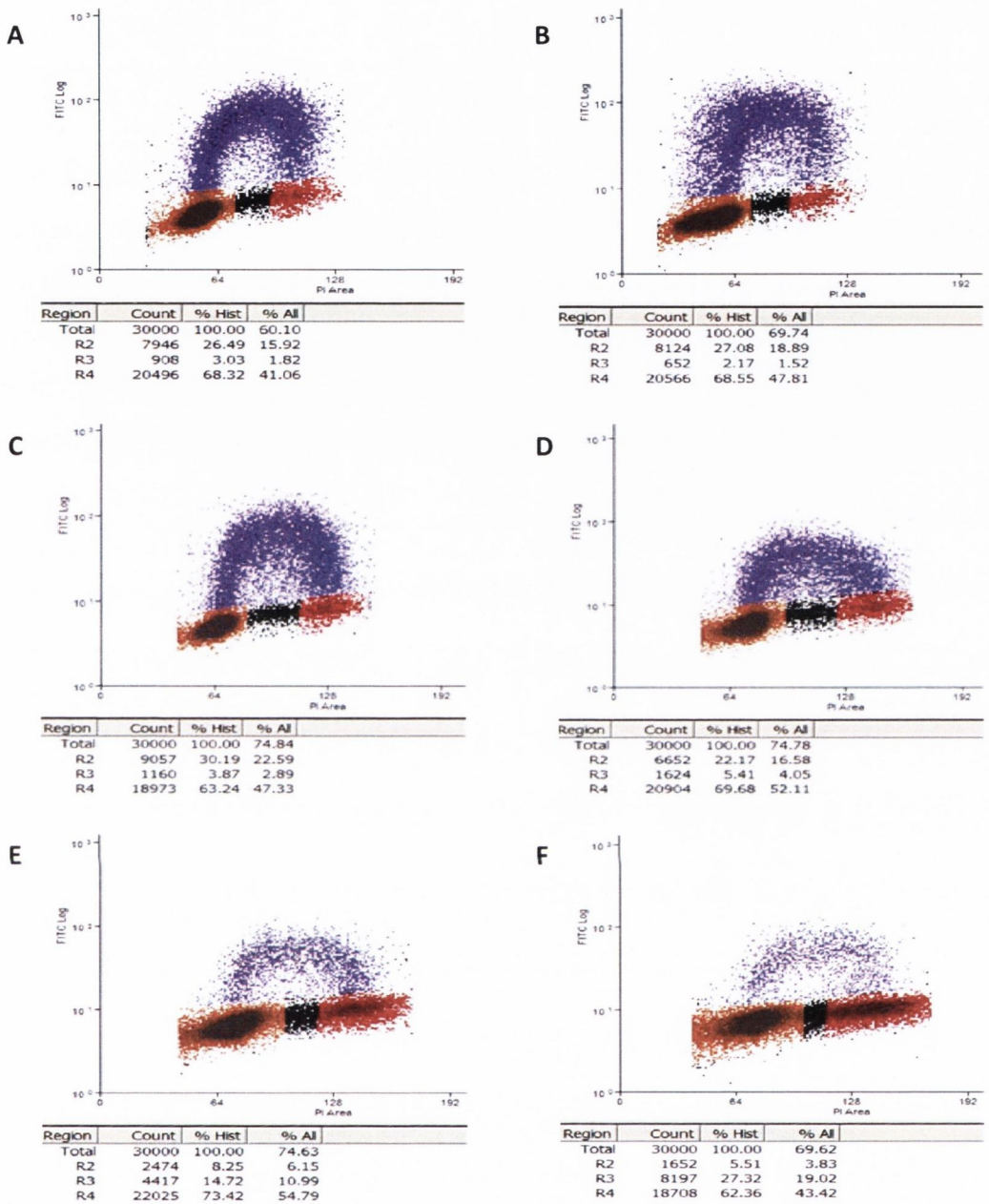


| Region | Count | % Hist | % All |
|---|---|---|---|
| Total | 30000 | 100.00 | 60.10 |
| R2 | 7946 | 26.49 | 15.92 |
| R3 | 908 | 3.03 | 1.82 |
| R4 | 20496 | 68.32 | 41.06 |

| Region | Count | % Hist | % All |
|---|---|---|---|
| Total | 30000 | 100.00 | 69.74 |
| R2 | 8124 | 27.08 | 18.89 |
| R3 | 652 | 2.17 | 1.52 |
| R4 | 20566 | 68.55 | 47.81 |

| Region | Count | % Hist | % All |
|---|---|---|---|
| Total | 30000 | 100.00 | 74.84 |
| R2 | 9057 | 30.19 | 22.59 |
| R3 | 1160 | 3.87 | 2.89 |
| R4 | 18973 | 63.24 | 47.33 |

| Region | Count | % Hist | % All |
|---|---|---|---|
| Total | 30000 | 100.00 | 74.78 |
| R2 | 6652 | 22.17 | 16.58 |
| R3 | 1624 | 5.41 | 4.05 |
| R4 | 20904 | 69.68 | 52.11 |

| Region | Count | % Hist | % All |
|---|---|---|---|
| Total | 30000 | 100.00 | 74.63 |
| R2 | 2474 | 8.25 | 6.15 |
| R3 | 4417 | 14.72 | 10.99 |
| R4 | 22025 | 73.42 | 54.79 |

| Region | Count | % Hist | % All |
|---|---|---|---|
| Total | 30000 | 100.00 | 69.62 |
| R2 | 1652 | 5.51 | 3.83 |
| R3 | 8197 | 27.32 | 19.02 |
| R4 | 18708 | 62.36 | 43.42 |

**Figure 5.12: Representative fluorocytograms of cell cycle analysis on HeLa cells 48hrs post sulindac treatment.** HeLa cells were left untreated **(A)**, treated with DMSO (vehicle control) **(B)** or treated with sulindac at concentrations of 57.5μM **(C)**, 115μM **(D)**, 230μM **(E)** and 400μM **(F)**. After 48hrs BrdU was added to the cell culture media. Following 2hrs incubation all cells (adherent and non-adherent) were collected and stained with both FITC labelled anti-BrdU antibody and PI. Finally the cells were analysed by flow cytometry. The dual parametric dot plots combining FITC labelled anti-BrdU antibody and PI fluorescence shows the G1 phase (orange; R4), S phase (purple; R2) and the G2/M phase (red; R3) of the cell cycle. Data from one complete experiment is presented.

### *5.4.5 Quantification of apoptosis*

Sulindac has been demonstrated to induce apoptosis in several different tumour cell lines including colon, breast, prostate, gastric and cervical (Karl *et al.*, 2007; Lim *et al.*, 1999; Piazza *et al.*, 1997; Seo *et al.*, 2009; Wu *et al.*, 2001). In addition, the morphological analysis of the HeLa cells (Figure 5.4 - 5.5) indicated that decreased cell viability correlated with increasing numbers of dead cells. Therefore, to examine whether sulindac induced inhibition of cell proliferation and cell cycle arrest lead to apoptosis, annexin V binding and PI permeability were analysed by flow cytometry. The results showed that there was a dose and time dependent increase in the number of cells undergoing apoptosis (Figure 5.13). In particular, highly significant changes were observed after just 24hrs treatment with 230μM and 400μM of sulindac (Figure 5.13 A; Figure 5.14 E-F), with a decrease (10% and 13.5% respectively) in the number of live cells and a reciprocal increase (9.5% and 13.5% respectively) in the number of cells in early apoptosis. While, the number of late apoptotic or necrotic cells was only marginally increased at 24hrs post treatment with these two concentrations, by 48hrs there was significant change (Figure 5.13 B; Figure 5.15 E-F). The apoptotic profile of cells treated with 115μM showed no significant alteration until 48hrs post treatment. At that point, the profile resembled that of the higher doses at 24hrs, with a decrease in the number of live cells and a significant increase in the number of early apoptotic cells (9% and 7% respectively) but no significant alteration in the number in late apoptosis (Figure 5.13 B; Figure 5.15 D). At 24 and 48hrs post treatment, there were no profile differences between the untreated cells, the vehicle control cells and those treated with 57.5μM of sulindac (Figure 5.13 A-B; Figure 5.14 A-C; Figure 5.15 A-C). These findings demonstrate that sulindac induced inhibition of cell proliferation correlates with an increase in apoptosis.

The fluorocytograms at 24 and 48hrs demonstrate a shift in the fluorescent profile of the HeLa cells after treatment with 115μM, 230μM and 400μM of sulindac (Figure 5.14 D-F; Figure 5.15 D-F). This result suggests that these cells have an increased level of fluorescence, which appears to be enhanced both with increasing concentration of sulindac and length of exposure. One explanation for this occurrence, is, that sulindac

itself has fluorescent properties. Sulindac is known to bind to serum albumin (Karl *et al.*, 2007) and the acryl hydrocarbon receptor (Ciolino *et al.*, 2006), therefore it is possible that it becomes associated with the cells through protein-protein interactions. If this was to occur and sulindac did indeed have fluorescent properties then it could increase the fluorescent profile of the cells. Alternatively, this trend is similar, though not as significant, to that observed with the SiHa cells after transfection with E7 siRNA (Chapter 3). Since a potential explanation for these findings was that the SiHa cells had gained increasing levels of autofluorescence this may also be true in this situation.

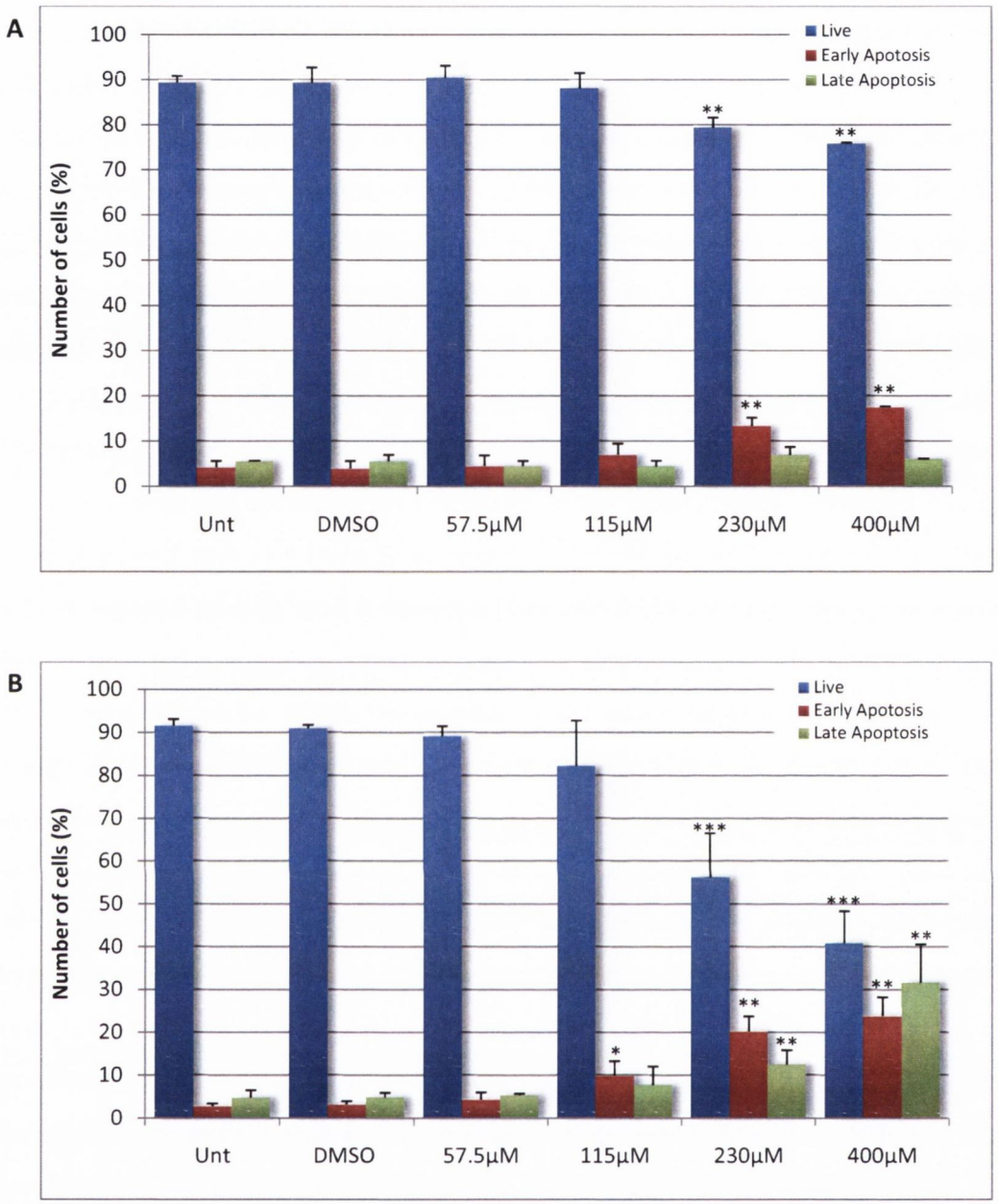


**Figure 5.13: Sulindac induces apoptosis in HeLa cells.** HeLa cells were left untreated (Unt), treated with DMSO (0.1%; vehicle control), or treated with sulindac at the indicated concentrations. After 24hrs **(A)** or 48hrs **(B)** incubation all cells (adherent and non-adherent) were collected and stained with both FITC labelled annexin V and PI. Finally the cells were analysed by flow cytometry. The Histograms represent the apoptotic profile distribution after treatment with sulindac. Results are representative of three independent experiments. Values are expressed as mean + SD. P values were calculated compared to the vehicle control; *p<0.05, **p<0.01.

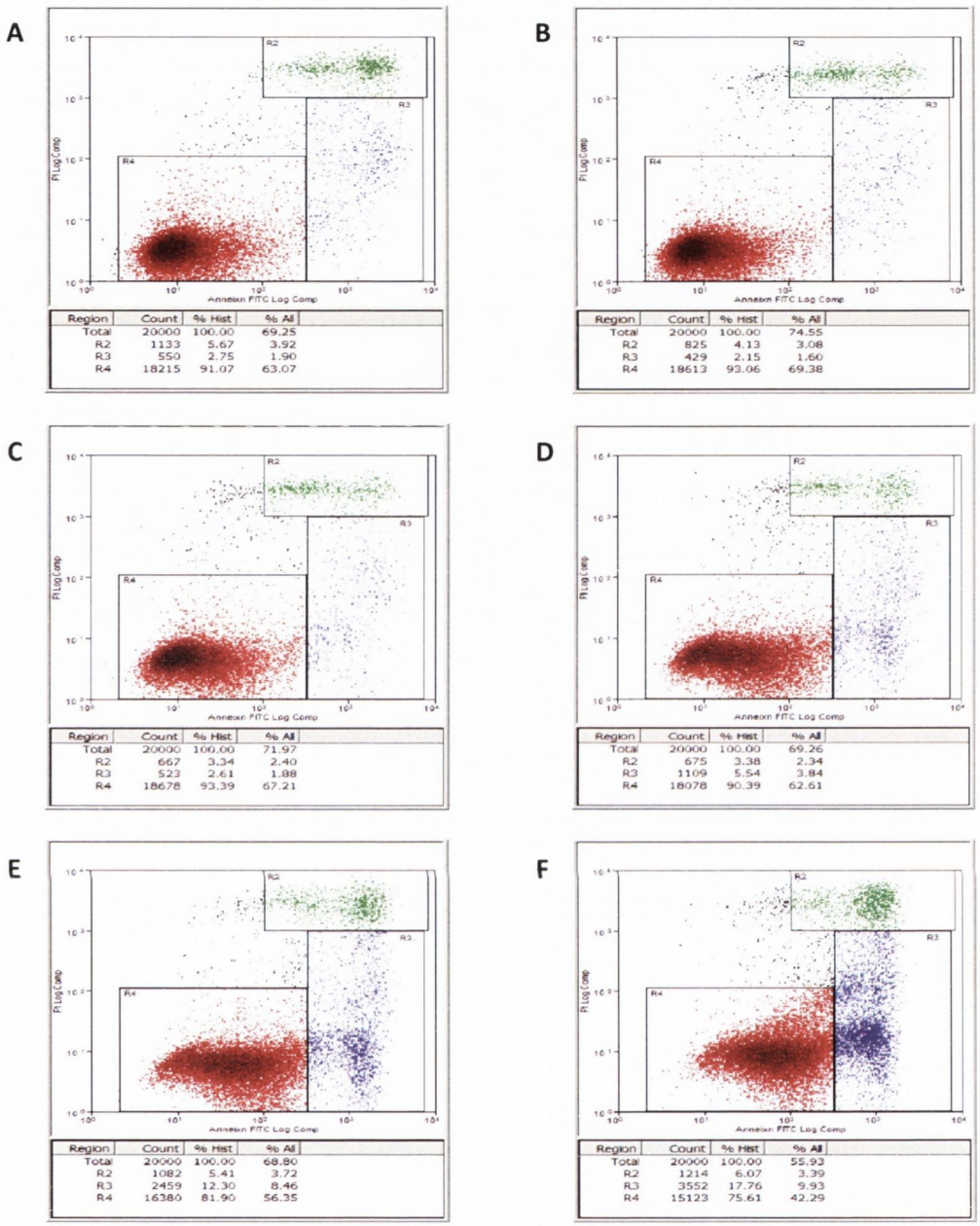


**Figure 5.14: Representative fluorocytograms of apoptosis analysis on HeLa cells 24hrs post sulindac treatment.** HeLa cells were left untreated **(A)**, treated with DMSO (vehicle control) **(B)** or treated with sulindac at concentrations of 57.5μM **(C)**, 115μM **(D)**, 230μM **(E)** and 400μM **(F)**. After 24hrs incubation all cells (adherent and non-adherent) were collected and stained with both FITC labelled annexin V and PI. Finally the cells were analysed by flow cytometry. The dual parametric dot plots combining annexin V-FITC and PI fluorescence shows the viable cell population in the lower left quadrant (**red**; R4; annexin $V^-PI^-$), the early apoptotic cells in the lower right quadrant (**purple**; R3; annexin $V^+PI^-$), and the late apoptotic cells in the upper right quadrant (green; R2; annexin $V^+PI^+$). Data from one experiment is presented.

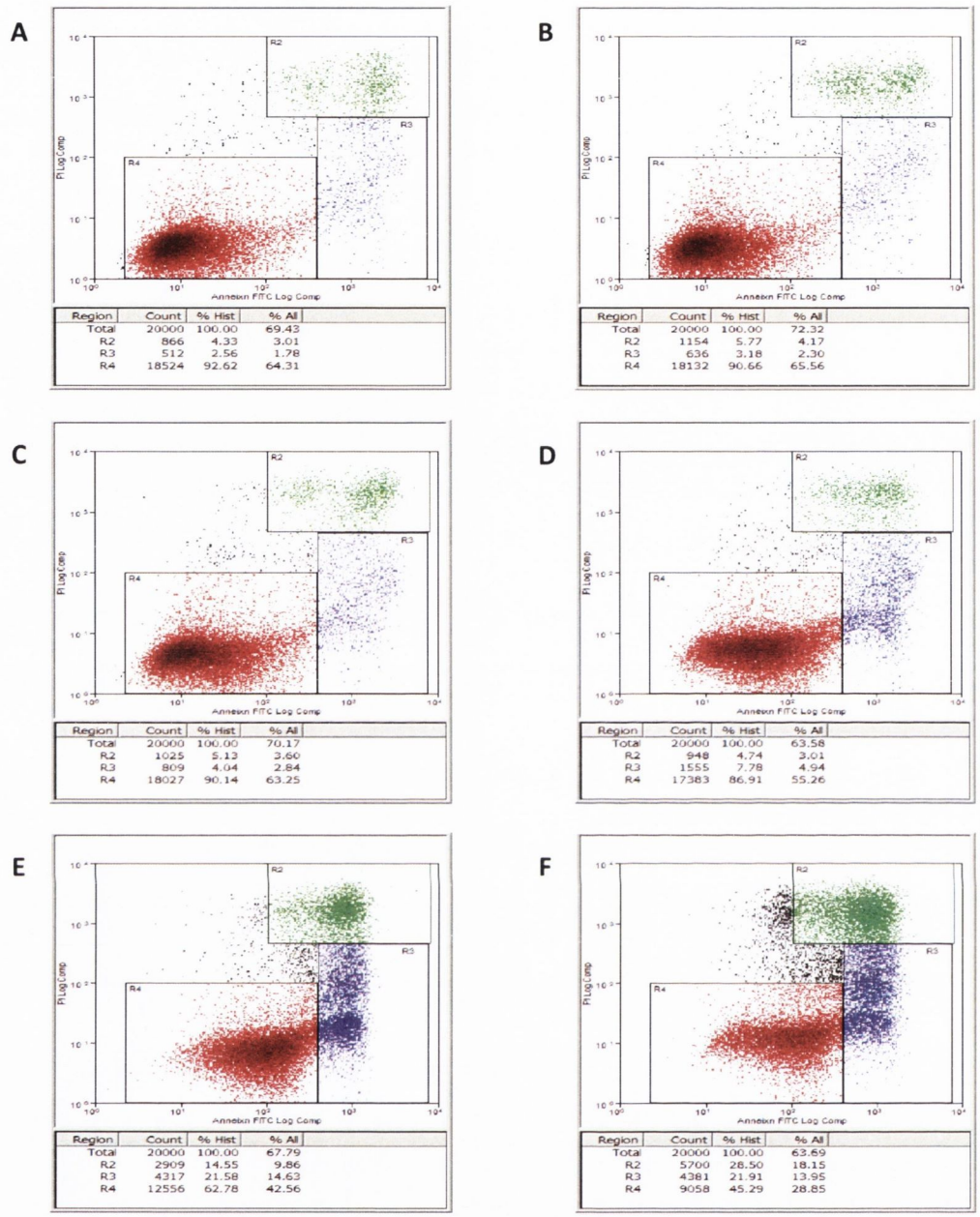


**Figure 5.15: Representative fluorocytograms of apoptosis analysis on HeLa cells 48hrs post sulindac treatment.** HeLa cells were left untreated **(A)**, treated with DMSO (vehicle control) **(B)** or treated with sulindac at concentrations of 57.5μM **(C)**, 115μM **(D)**, 230μM **(E)** and 400μM **(F)**. After 48hrs incubation all cells (adherent and non-adherent) were collected and stained with both FITC labelled annexin V and PI. Finally the cells were analysed by flow cytometry. The dual parametric dot plots combining annexin V-FITC and PI fluorescence shows the viable cell population in the lower left quadrant (**red**; R4; annexin $V^-PI^-$), the early apoptotic cells in the lower right quadrant (**purple**; R3; annexin $V^+PI^-$), and the late apoptotic cells in the upper right quadrant (green; R2; annexin $V^+PI^+$). Data from one experiment is presented.

### *5.4.6 Sulindac treatment induces altered HPV18 oncogene expression*

A previous report by Karl *et al.* (2007) demonstrated the ability of sulindac to induce a post-transcriptional loss of the HPV18 E7 oncoprotein. To establish whether sulindac induced cell cycle arrest and apoptotic phenotypes of the HeLa cells corresponded with alterations in the expression of HPV18 E6 and E7, TaqMan® RT-PCR and western blot analysis was performed. There are no high-affinity antibodies available to reliably detect HPV18 E6 and therefore its expression was assessed functionally by investigating the E6 targeted protein p53. After 48hrs treatment, there was an increase in the mRNA expression of both HPV18 E6 and E7 in cells treated with 230μM and 400μM of sulindac (Figure 5.16 A). This increase did not however translate to the proteome, where there was no decrease in p53 expression or increase in E7 expression (Figure 5.16 B-C). In fact the expression level of E6 appears to be relatively constant with increasing doses of sulindac with the exception of a minor increase at 230μM and 400μM doses (Figure 5.16 B). In contrast there was a significant dose dependent decrease in the E7 protein (Figure 5.16 C). It was most evident with concentrations of 115μM and above but could be observed with the lower dose of 57.5μM. This supports the previous findings of a post-transcriptional degradation of E7 (Karl *et al.*, 2007). The dose dependent manner in which it is observed to occur, corroborates this result, with the findings of growth arrest and apoptosis post sulindac treatment. Since alterations in the apoptotic profile of cells treated with 57.5μM of sulindac was not observed (Figure 5.13) but cell cycle disruption was (Figure 5.10) this would indicate that the loss of E7 expression may more closely correlate with the induction of cell cycle arrest results than apoptosis. Supporting this view is the microscopic analysis where there was no increase in the number of detached cells with 57.5μM of sulindac but there was a decrease in the cell density compared to the vehicle control (Figure 5.5).

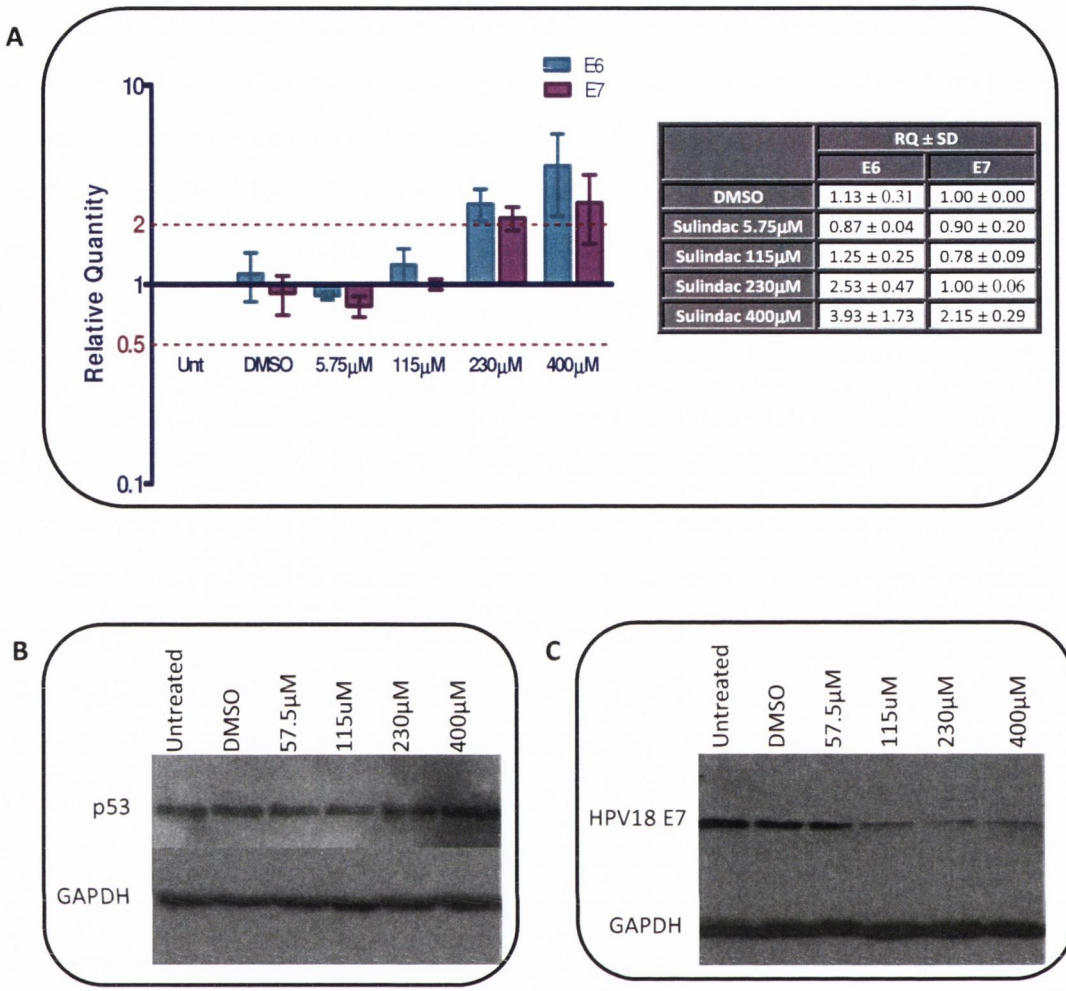


| | RQ ± SD | |
|---|---|---|
| | E6 | E7 |
| DMSO | 1.13 ± 0.31 | 1.00 ± 0.00 |
| Sulindac 5.75μM | 0.87 ± 0.04 | 0.90 ± 0.20 |
| Sulindac 115μM | 1.25 ± 0.25 | 0.78 ± 0.09 |
| Sulindac 230μM | 2.53 ± 0.47 | 1.00 ± 0.06 |
| Sulindac 400μM | 3.93 ± 1.73 | 2.15 ± 0.29 |

**Figure 5.16: Effect of sulindac on endogenous HPV18 E6 and E7 expression in HeLa cells.** HeLa cells were left untreated (Unt), treated with DMSO (0.1%; vehicle control) or treated with sulindac at the indicated concentrations for 48hrs. (**A**) Total RNA was extracted and mRNA expression was evaluated by TaqMan® RT-PCR using primers and probes selective for HPV18 E6, HPV18 E7 and B2M mRNA. The HPV18 E6 and E7 mRNA expression was normalised to that of B2M and calibrated to that of the untreated cells to establish the relative level of mRNA expression. Marked on the graphs are the considered limits of biological variation between two biological samples, from 0.5 to 2. (**B-C**) Cells were lysed with RIPA buffer. The lysate samples (30μg) were resolved by SDS PAGE electrophoresis and transferred to a PVDF membrane. The membrane was firstly blocked in blocking buffer and then immunoblotted for p53 (upper panel **B**) and HPV18 E7 (upper panel **C**). All membranes were stripped and re-immunoblotted for GAPDH (lower panel **B – C**), which was used as a loading control.

## 5.5 Discussion

Epidemiological, *in vitro* and *in vivo* studies have all demonstrated that many NSAIDs have antineoplastic activities. Since NSAIDs and their derivatives have anti-cancer properties and are significantly less toxic than traditional chemotherapeutic agents, they represent promising future alternatives for both the treatment and prevention of various types of cancers. Previous studies have demonstrated the ability of certain NSAIDs, such as celecoxib and sulindac, to inhibit the cellular growth of cervical cancer both *in vivo* and *in vitro* (Fukada *et al.*, 2007; Karl *et al.*, 2007; Kim *et al.*, 2003; Kim *et al.*, 2004; Yasui *et al.*, 2003). Sulindac is considered to be one of the most efficacious NSAIDs based on its ability to cause the regression of colonic adenomas in patients with FAP (Giardiello *et al.*, 1993; Matsuhashi *et al.*, 1997; Nugent *et al.*, 1993). An interesting study published in 2007 by Karl *et al.* demonstrated the ability of sulindac not only to inhibit cervical cancer cell growth *in vitro* but to induce a post-transcriptional degradation of HPV18 E7. Since a focus of this thesis was to establish techniques to suppress the expression of HPV viral oncogenes, it was decided to investigate the effect of sulindac on cervical cancer cells.

Previous studies that have evaluated the effect of sulindac on cervical cancer have focused on the HPV18 cervical adenocarcinoma cell line HeLa (Karl *et al.*, 2007; Kim *et al.*, 2004; Kim *et al.*, 2003; Yasui *et al.*, 2003). To get a broader view of the capabilities of sulindac in relation to cervical cancer, several cervical carcinoma cell lines with differing origins, HPV status and viral DNA content were examined. In addition, the effect of the derivatives of sulindac on these cell lines was also established. The sulindac derivatives have also been demonstrated to have anti-neoplastic capabilities and in some situations have been observed to be more potent than the prodrug form (Han *et al.*, 1998; Hanif *et al.*, 1996; Loveridge *et al.*, 2008; Piazza *et al.*, 1997). Sulindac had a time and dose dependent growth inhibitory effect on all three cell lines employed in this study. However, the most potent response was observed in the HeLa cell line, with the $IC_{50}$ value for these cells approximately 200μM less than that of the other two cell lines. There was also a time and dose dependent decrease in the level of

cell proliferation with the sulfide metabolite and once again the HeLa cells were more sensitive to this growth inhibitory activity. While sulfide successfully reduced the growth rate of all three cell lines, at no time was this activity as substantial as that of the parent drug. Moreover sulfone had little to no effect on any of the three cell lines. Therefore, it must be assumed, from these results that the prodrug form of sulindac has antineoplastic activities towards cervical cancer cells that are lost or significantly diminished once it becomes reduced to sulfide or oxidised to sulfone.

The fact that there was a differential sensitivity among the cell lines to sulindac is not an unusual result. For example, the efficacy of sulindac to inhibit cellular growth of breast cancer cell lines is seen to be dependent on their degree of malignancy, with the more potent response observed in the more aggressive phenotypes (Seo *et al.*, 2009). Interestingly HeLa cells have been demonstrated to have a higher transforming ability than either the SiHa or C33A cell lines (Nakamura *et al.*, 2000). This is almost certainly due to the fact that these cells are derived from an adenocarcinoma and have integrated HPV18 both of which have been linked with a higher degree of malignancy compared to squamous cell carcinomas and HPV16 respectively (Chen *et al.*, 1999; Hopkins and Morely, 1991; Kim *et al.*, 2004). The altered sensitivity in the breast cancer cell lines has been attributed at least in part to the level of IκK kinase β expression (Seo *et al.*, 2009). Examination of data from microarray experiments previously performed by this group comparing these three cervical cell lines did not establish an altered expression of this gene at the transcriptome level (Astbury *et al.*, manuscript in preparation). However it cannot be excluded as a possibility until verified by protein analysis. The microarray analysis did demonstrate that expression profiles of the SiHa and C33A cell lines were more closely related than either was to the HeLa cell line. The commonality between these two cell lines enhances the possibility that the reduced efficacy observed in comparison to the HeLa cell line is due to the expressional presence or absence of a common gene or set of genes.

The anti-proliferative activities of sulindac have been attributed to alterations in the cell cycle and to the induction of apoptosis (Castonguay and Rioux, 1997; Karl *et al.*,

2007; Kim *et al.*, 2002; Lovebridge *et al.*, 2007; Lim *et al.*, 1999; Piazza *et al.*, 1997; Seo *et al.*, 2009; Subbegowda and Frommel, 1998). In this study, sulindac at concentrations between 115μM and 400μM was found to both significantly induce a cell cycle arrest and apoptosis in HeLa cells. Similar to the growth inhibitory analysis performed, there was a dose and time dependent increase in the number of cells in the early or late stages of apoptosis. While apoptosis was the predominant phenotype post sulindac treatment, it did not account fully for the anti-proliferative activity towards the HeLa cells. For example a dose of 230μM caused a growth inhibition of approximately 50% in comparison to the vehicle control, however it only induced apoptosis by around 35%. This indicates that in this cell type, the apoptotic and cell cycle arrest effects of sulindac may be mediated by separate mechanisms.

The cell cycle analysis demonstrated that HeLa cells treated with doses from 115μM to 400μM of sulindac enter a stage of prolonged cell cycle arrest, established by the significant reduction in DNA synthesis. The process behind these cell cycle alterations is complex involving cells "stalling" both in the G1 and G2/M phases. At the higher concentrations of 230μM and 400μM, cells appear neither able to leave the G1 or the G2/M phase. The dose and time dependent accumulation of cells in the G2/M phase indicates that the G2/M arrest is the predominant cell cycle alteration at these concentrations of sulindac. In comparison, sulindac at 115μM appears to have a biphasic effect on the cell cycle pattern of the HeLa cells. At 24hrs, this concentration induces the largest decrease in the S phase, which is attributable to a G1 cell cycle arrest. By 48hrs, there is a partial reversal of both the S phase decrease and the G1 increase. There is a gradual increase in the G2/M phase over these time periods. The findings at 48hrs might suggest that the cells are recovering however both the apoptotic and the microscopic analysis indicate that the effect of sulindac at this concentration is becoming more pronounced with time. It can be concluded from these findings that at this concentration there is an initial G1 arrest, which is followed potentially by a G1 and G2/M arrest.

While sulindac has been demonstrated to induce apoptosis in a number of different cancer models, including cervical cancer (Goldberg *et al.*, 1996; Han *et al.*, 1996; Karl *et al.*, 2007; Piazza *et al.*, 1997), a G2/M arrest has not previously been described. However the concept that antineoplastic agents can induce apoptosis and stall the cell cycle in the G2/M phase has been documented. Chemotherapeutic agents, including cisplatin and placitaxel, have been demonstrated to induce a G2/M arrest in cancer cells and it is suggested that this alteration in the cell cycle is involved in mediating the apoptotic induction observed with these compounds (Candelaria *et al.*, 2006; Eastman and Rigas, 1999). This is an interesting observation since the predominant result of treating the HeLa cells with doses of sulindac of 230μM and 400μM was a G2/M cell cycle arrest and apoptosis.

Although there are differences between this study and the previous study by Karl *et al.* (2007) in relation to the overall cell phenotype post sulindac treatment, their finding that sulindac could induce a post-transcriptional degradation of E7 was substantiated in this study. The expression of both the HPV18 E6 and E7 viral oncogenes was observed to be altered by exposure of HeLa cells to sulindac. At the transcriptome there was an increase in their expression at the higher concentrations of 230μM and 400μM but not at 57.5μM and 115μM after 48hrs treatment. As 115μM induces both cell cycle alterations and apoptosis by 48hrs, this suggests that these alterations seen at the mRNA level are not a direct result of sulindac treatment but a consequence of significant levels of cell cycle arrest and/or apoptosis. There were no major alterations in the expression of p53, which is targeted for degradation by E6 therefore indicating that E6 protein expression is not altered by sulindac. Conversely, there was a dose dependent reduction in the expression level of the E7 protein. In comparison to the Karl *et al.* (2007) study, this was observed with significantly lower concentrations of sulindac. Karl *et al.* (2007) did not demonstrate any alterations in HPV18 E7 expression with 100μM of sulindac but did with 500μM. In contrast even the lowest concentration, 57.5μM, was observed to have an effect on E7 protein expression in this study.

It is interesting to note, that the only other alterations observed in the phenotype of the HeLa cells treated with 57.5μM of sulindac was a G1 arrest at 24hrs and a lower cell density at 48hrs. These findings suggest that the lower cell density may be the result of an initial G1 arrest, which in turn could be due to the reduction in E7 expression. The best characterised property of E7 is its ability to subvert the activity of Rb, which results in the uncontrolled entry into the S phase (Dyson *et al.*, 1992). Therefore unsurprisingly the loss of E7 has previously been demonstrated to induce a G1 arrest in the cell cycle of HPV infected cells (DeFilippis *et al.*, 2003). Karl *et al.* were able to show that sulindac induced G1 arrest correlated not only with the loss of E7 protein but in addition with the loss of cdk2, cyclin A and cyclin E. Cdk2 activity is essential for the G1 to S phase transition and is regulated by cyclin A and E. Furthermore, E7 can directly associate with these cyclin/cdk2 complexes (McIntyre *et al.*, 1996; Nguyen and Munger, 2008; Tommasino *et al.*, 1993), which results in increased cdk2 activity. Therefore, it would seem plausible in this cell type that degradation of HPV18 E7 is inducing a G1 arrest.

As mentioned earlier, though apoptosis is the principal phenotype post sulindac treatment it does not account fully for the anti-proliferative activity towards HeLa cells. This indicates that the apoptotic and cell cycle arrest effects of sulindac may not be entirely linked. Based on the above discussion, it is interesting to speculate that the separation in these mechanisms may be related to the two forms a cell cycle arrest observed in this cell type, G1 and G2/M. Since E7 loss, G1 arrest and a decrease in cell density is observed with 57.5μM without any alteration in the apoptotic profile of these cells, it is possible that the G1 arrest is solely involved in inducing the less significant cell cycle arrest phenotype. As apoptosis is observed to increase with dose and time like the G2/M arrest, potentially this alteration in the cell cycle is involved in mediating the apoptotic induction observed with this compound, similar to the observed activities of cisplatin and placitaxol.

As discussed in section 5.1, the mechanism underlying the antineoplastic properties of NSAIDs is still unknown. The general conclusion that can be drawn from the current literature is that these agents have a multifaceted action on cancer cells, as the inhibition of no one gene has been shown to completely diminish their anti-cancer activities. The overall findings of this study, would suggest, that both COX dependent and independent mechanisms of action may have a role to play in the anti-proliferative action of sulindac in cervical cancer cells. In HeLa cells, the COX inhibitory sulindac derivative, sulfide, decreased cellular growth post treatment. This activity was not as great as that seen with the parent form, but does indicate that part of the activity of sulindac may be mediated in a COX dependent manner. However, the fact that sulfide also induced growth inhibition in the C33A cell line, though to a smaller extent, contradicts this view, as it has been established that these cells do not expresses either COX enzymes (Kim *et al.*, 2004; Kim *et al.*, 2009; Subbaramaiah and Dannenberg 2007). Since HeLa cells show a more effective response to the sulfide derivative than C33A cells, it is still possible that while there is only a COX independent mechanism at work in the C33A cells, an additional COX dependent mechanism is potentiating the effect in HeLa cells. In addition to examining the efficacy of the COX inhibitory component of sulindac, this study also evaluated the ability of the parent form to alter COX activity. The activity of COX was seen to be diminished in a dose dependent manner after 48hrs treatment in HeLa cells with concentrations from 115μM to 400μM. This reduction in activity correlates with the increased level of apoptosis.

The results of this chapter establish the antineoplastic efficacy of sulindac towards cervical cancer cells of different origin, HPV status and viral DNA content. Analysis in the HeLa cell line, which was most sensitive to the anti-proliferative activity of sulindac, demonstrated that this activity predominantly occurred through the induction of apoptosis but additionally by cell cycle arrest. In addition, the previous findings that sulindac induced a post-transcriptional degradation of HPV18 viral oncogene E7 were validated. This decrease was dose dependent and appeared to correlate with the observed G1 arrest. Furthermore, it was demonstrated that a decrease in COX activity may be partially responsible for the anti-proliferative activity of sulindac. These observations indicate that the antineoplastic activities of sulindac are multifaceted. Since most cancers progress through the action of multiple pathways, drugs that simultaneously block several pathways might be particularly effective as therapeutic agents.

## 5.6 References

Astbuty K, Martin CM, Sheils O, O'Leary JJ. *Manuscript in prepartation.*

Balkwill, F, and A Mantovani. 2001. Inflammation and cancer: back to Virchow? *Lancet* 357, no. 9255 (February 17): 539-545.

Balkwill, Frances, Kellie A Charles, and Alberto Mantovani. 2005. Smoldering and polarized inflammation in the initiation and promotion of malignant disease. *Cancer Cell* 7, no. 3 (March): 211-217.

Bray, Freddie, Bendix Carstensen, Henrik Møller, Marco Zappa, Maja Primic Zakelj, Gill Lawrence, Matti Hakama, and Elisabete Weiderpass. 2005. Incidence trends of adenocarcinoma of the cervix in 13 European countries. *Cancer Epidemiology, Biomarkers & Prevention: A Publication of the American Association for Cancer Research, Cosponsored by the American Society of Preventive Oncology* 14, no. 9 (September): 2191-2199.

Candelaria, Myrna, Alicia Garcia-Arias, Lucely Cetina, and Alfonso Dueñas-Gonzalez. 2006. Radiosensitizers in cervical cancer. Cisplatin and beyond. *Radiation Oncology (London, England)* 1: 15.

Castle, Philip E, and Anna R Giuliano. 2003. Chapter 4: Genital tract infections, cervical inflammation, and antioxidant nutrients--assessing their roles as human papillomavirus cofactors. *Journal of the National Cancer Institute. Monographs*, no. 31: 29-34.

Castonguay, A, and N Rioux. 1997. Inhibition of lung tumourigenesis by sulindac: comparison of two experimental protocols. *Carcinogenesis* 18, no. 3 (March): 491-496.

Chan, T A, P J Morin, B Vogelstein, and K W Kinzler. 1998. Mechanisms underlying nonsteroidal antiinflammatory drug-mediated apoptosis. *Proceedings of the National Academy of Sciences of the United States of America* 95, no. 2 (January 20): 681-686.

Chen, R J, Y H Lin, C A Chen, S C Huang, S N Chow, and C Y Hsieh. 1999. Influence of histologic type and age on survival rates for invasive cervical carcinoma in Taiwan. *Gynecologic Oncology* 73, no. 2 (May): 184-190.

Chulada, P C, M B Thompson, J F Mahler, C M Doyle, B W Gaul, C Lee, H F Tiano, S G Morham, O Smithies, and R Langenbach. 2000. Genetic disruption of Ptgs-1, as well as Ptgs-2, reduces intestinal tumorigenesis in Min mice. *Cancer Research* 60, no. 17 (September 1): 4705-4708.

Ciolino, Henry P, Christopher J MacDonald, Omar S Memon, Sara E Bass, and Grace Chao Yeh. 2006. Sulindac regulates the aryl hydrocarbon receptor-mediated expression of Phase 1 metabolic enzymes in vivo and in vitro. *Carcinogenesis* 27, no. 8 (August): 1586-1592.

Coussens, Lisa M, and Zena Werb. 2002. Inflammation and cancer. *Nature* 420, no. 6917 (December 19): 860-867.

Dannenberg, Andrew J, and Kotha Subbaramaiah. 2003. Targeting cyclooxygenase-2 in human neoplasia: rationale and promise. *Cancer Cell* 4, no. 6 (December): 431-436.

Davies, N M, and M S Watson. 1997. Clinical pharmacokinetics of sulindac. A dynamic old drug. *Clinical Pharmacokinetics* 32, no. 6 (June): 437-459.

DeFilippis, Rosa Anna, Edward C Goodwin, Lingling Wu, and Daniel DiMaio. 2003. Endogenous human papillomavirus E6 and E7 proteins differentially regulate proliferation, senescence, and apoptosis in HeLa cervical carcinoma cells. *Journal of Virology* 77, no. 2 (January): 1551-1563.

Ding, X Z, W G Tong, and T E Adrian. 2000. Blockade of cyclooxygenase-2 inhibits proliferation and induces apoptosis in human pancreatic cancer cells. *Anticancer Research* 20, no. 4 (August): 2625-2631.

DiPaolo, J A, C D Woodworth, N C Popescu, V Notario, and J Doniger. 1989. Induction of human cervical squamous cell carcinoma by sequential transfection with human papillomavirus 16 DNA and viral Harvey ras. *Oncogene* 4, no. 4 (April): 395-399.

Dohadwala, M, J Luo, L Zhu, Y Lin, G J Dougherty, S Sharma, M Huang, M Pold, R K Batra, and S M Dubinett. 2001. Non-small cell lung cancer cyclooxygenase-2-dependent invasion is mediated by CD44. *The Journal of Biological Chemistry* 276, no. 24 (June 15): 20809-20812.

DuBois, R N, J Awad, J Morrow, L J Roberts, and P R Bishop. 1994. Regulation of eicosanoid production and mitogenesis in rat intestinal epithelial cells by transforming growth factor-alpha and phorbol ester. *The Journal of Clinical Investigation* 93, no. 2 (February): 493-498.

Duggan, D E, K F Hooke, R M Noll, H B Hucker, and C G Van Arman. 1978. Comparative disposition of sulindac and metabolites in five species. *Biochemical Pharmacology* 27, no. 19: 2311-2320.

Dürst, M, D Gallahan, G Jay, and J S Rhim. 1989. Glucocorticoid-enhanced neoplastic transformation of human keratinocytes by human papillomavirus type 16 and an activated ras oncogene. *Virology* 173, no. 2 (December): 767-771.

Dyson, N. 1998. The regulation of E2F by pRB-family proteins. *Genes & Development* 12, no. 15 (August 1): 2245-2262.

Eastman, A, and J R Rigas. 1999. Modulation of apoptosis signaling pathways and cell cycle regulation. *Seminars in Oncology* 26, no. 5 Suppl 16 (October): 7-16; discussion 41-42.

Eberhart, C E, R J Coffey, A Radhika, F M Giardiello, S Ferrenbach, and R N DuBois. 1994. Up-regulation of cyclooxygenase 2 gene expression in human colorectal adenomas and adenocarcinomas. *Gastroenterology* 107, no. 4 (October): 1183-1188.

Ferrandina, G, L Lauriola, M G Distefano, G F Zannoni, M Gessi, F Legge, N Maggiano, et al. 2002. Increased cyclooxygenase-2 expression is associated with chemotherapy resistance and poor survival in cervical cancer patients. *Journal of Clinical Oncology: Official Journal of the American Society of Clinical Oncology* 20, no. 4 (February 15): 973-981.

Fukada, Kazuhiro, Fumi Takahashi-Yanaga, Naoko Sakoguchi-Okada, Fumie Shiraishi, Yoshikazu Miwa, Sachio Morimoto, and Toshiyuki Sasaguri. 2007. Celecoxib induces apoptosis by inhibiting the expression of survivin in HeLa cells. *Biochemical and Biophysical Research Communications* 357, no. 4 (June 15): 1166-1171.

Gaffney, D K, J Holden, M Davis, K Zempolich, K J Murphy, and M Dodson. 2001. Elevated cyclooxygenase-2 expression correlates with diminished survival in carcinoma of the cervix treated with radiotherapy. *International Journal of Radiation Oncology, Biology, Physics* 49, no. 5 (April 1): 1213-1217.

Giardiello, F M, S R Hamilton, A J Krush, S Piantadosi, L M Hylind, P Celano, S V Booker, C R Robinson, and G J Offerhaus. 1993. Treatment of colonic and rectal adenomas with sulindac in familial adenomatous polyposis. *The New England Journal of Medicine* 328, no. 18 (May 6): 1313-1316.

Goldberg, Y, I I Nassif, A Pittas, L L Tsai, B D Dynlacht, B Rigas, and S J Shiff. 1996. The anti-proliferative effect of sulindac and sulindac sulfide on HT-29 colon cancer cells: alterations in tumor suppressor and cell cycle-regulatory proteins. *Oncogene* 12, no. 4 (February 15): 893-901.

Golijanin, Dragan, Jian-You Tan, Agnieszka Kazior, Erik G Cohen, Paul Russo, Guido Dalbagni, Karen J Auborn, Kotha Subbaramaiah, and Andrew J Dannenberg. 2004. Cyclooxygenase-2 and microsomal prostaglandin E synthase-1 are overexpressed in squamous cell carcinoma of the penis. *Clinical Cancer Research: An Official Journal of the American Association for Cancer Research* 10, no. 3 (February 1): 1024-1031.

Goluboff, E T, A Shabsigh, J A Saidi, I B Weinstein, N Mitra, D Heitjan, G A Piazza, R Pamukcu, R Buttyan, and C A Olsson. 1999. Exisulind (sulindac sulfone) suppresses growth of human prostate cancer in a nude mouse xenograft model by increasing apoptosis. *Urology* 53, no. 2 (February): 440-445.

Grösch, S, I Tegeder, E Niederberger, L Bräutigam, and G Geisslinger. 2001. COX-2 independent induction of cell cycle arrest and apoptosis in colon cancer cells by the selective COX-2 inhibitor celecoxib. *The FASEB Journal: Official Publication of the Federation of American Societies for Experimental Biology* 15, no. 14 (December): 2742-2744.

Half, Elizabeth, Xi Ming Tang, Karin Gwyn, Aysegul Sahin, Kyle Wathen, and Frank A Sinicrope. 2002. Cyclooxygenase-2 expression in human breast cancers and adjacent ductal carcinoma in situ. *Cancer Research* 62, no. 6 (March 15): 1676-1681.

Han, E K, N Arber, H Yamamoto, J T Lim, T Delohery, R Pamukcu, G A Piazza, W Q Xing, and I B Weinstein. 1998. Effects of sulindac and its metabolites on growth and apoptosis in human mammary epithelial and breast carcinoma cell lines. *Breast Cancer Research and Treatment* 48, no. 3 (April): 195-203.

Hanif, R, A Pittas, Y Feng, M I Koutsos, L Qiao, L Staiano-Coico, S I Shiff, and B Rigas. 1996. Effects of nonsteroidal anti-inflammatory drugs on proliferation and on induction of apoptosis in colon cancer cells by a prostaglandin-independent pathway. *Biochemical Pharmacology* 52, no. 2 (July 26): 237-245.

Harris, Randall E. 2007. Cyclooxygenase-2 (cox-2) and the inflammogenesis of cancer. *Sub-Cellular Biochemistry* 42: 93-126.

He, T C, T A Chan, B Vogelstein, and K W Kinzler. 1999. PPARdelta is an APC-regulated target of nonsteroidal anti-inflammatory drugs. *Cell* 99, no. 3 (October 29): 335-345.

Herrmann, C, C Block, C Geisen, K Haas, C Weber, G Winde, T Möröy, and O Müller. 1998. Sulindac sulfide inhibits Ras signaling. *Oncogene* 17, no. 14 (October 8): 1769-1776.

Howe, Louise R, Sung-Hee Chang, Kelly C Tolle, Rachelle Dillon, Lawrence J T Young, Robert D Cardiff, Robert A Newman, et al. 2005. HER2/neu-induced mammary tumorigenesis and angiogenesis are reduced in cyclooxygenase-2 knockout mice. *Cancer Research* 65, no. 21 (November 1): 10113-10119.

Hurlin, P J, P Kaur, P P Smith, N Perez-Reyes, R A Blanton, and J K McDougall. 1991. Progression of human papillomavirus type 18-immortalized human keratinocytes to a malignant phenotype. *Proceedings of the National Academy of Sciences of the United States of America* 88, no. 2 (January 15): 570-574.

Hwang, D, D Scollard, J Byrne, and E Levine. 1998. Expression of cyclooxygenase-1 and cyclooxygenase-2 in human breast cancer. *Journal of the National Cancer Institute* 90, no. 6 (March 18): 455-460.

Jakobsson, Maija, Mika Gissler, Susanna Sainio, Jorma Paavonen, and Anna-Maija Tapper. 2007. Preterm delivery after surgical treatment for cervical intraepithelial neoplasia. *Obstetrics and Gynecology* 109, no. 2 Pt 1 (February): 309-313.

Jemal, Ahmedin, Rebecca Siegel, Elizabeth Ward, Taylor Murray, Jiaquan Xu, and Michael J Thun. 2007. Cancer statistics, 2007. *CA: A Cancer Journal for Clinicians* 57, no. 1 (February): 43-66.

Kamijo, T, T Sato, Y Nagatomi, and T Kitamura. 2001. Induction of apoptosis by cyclooxygenase-2 inhibitors in prostate cancer cell lines. *International Journal of Urology: Official Journal of the Japanese Urological Association* 8, no. 7 (July): S35-39.

Karl, Theresia, Nadine Seibert, Michael Stöhr, Hans Osswald, Frank Rösl, and Patrick Finzer. 2007. Sulindac induces specific degradation of the HPV oncoprotein E7 and causes growth arrest and apoptosis in cervical carcinoma cells. *Cancer Letters* 245, no. 1-2 (January 8): 103-111.

Kietpeerakool, Chumnan, Jatupol Srisomboon, Prapaporn Suprasert, Chalong Cheewakriangkrai, Kittipat Charoenkwan, and Sitthicha Siriaree. 2007. Routine prophylactic application of Monsel's solution after loop electrosurgical excision procedure of the cervix: is it necessary? *The Journal of Obstetrics and Gynaecology Research* 33, no. 3 (June): 299-304.

Kim, Kye Young, Ji Yeon Seol, Geong-A Jeon, and Myeong Jin Nam. 2003. The combined treatment of aspirin and radiation induces apoptosis by the regulation of bcl-2 and caspase-3 in human cervical cancer cell. *Cancer Letters* 189, no. 2 (January 28): 157-166.

Kim, Su-Hyeong, Jung-Min Oh, Jae-Hong No, Yung-Jue Bang, Yong-Sung Juhnn, and Yong-Sang Song. 2009. Involvement of NF-kappaB and AP-1 in COX-2 upregulation by human papillomavirus 16 E5 oncoprotein. *Carcinogenesis* 30, no. 5 (May): 753-757.

Kim, Su-Hyeong, Sang-Hyun Song, Sang-Gyun Kim, Kyung-Soo Chun, So-Young Lim, Hye-Kyung Na, Jae Weon Kim, Young-Joon Surh, Yung-Jue Bang, and Yong-Sang Song. 2004. Celecoxib induces apoptosis in cervical cancer cells independent of cyclooxygenase using NF-kappaB as a possible target. *Journal of Cancer Research and Clinical Oncology* 130, no. 9 (September): 551-560.

Kulkarni, S, J S Rader, F Zhang, H Liapis, A T Koki, J L Masferrer, K Subbaramaiah, and A J Dannenberg. 2001. Cyclooxygenase-2 is overexpressed in human cervical cancer. *Clinical Cancer Research: An Official Journal of the American Association for Cancer Research* 7, no. 2 (February): 429-434.

Kyrgiou, M, G Koliopoulos, P Martin-Hirsch, M Arbyn, W Prendiville, and E Paraskevaidis. 2006. Obstetric outcomes after conservative treatment for intraepithelial or early invasive cervical lesions: systematic review and meta-analysis. *Lancet* 367, no. 9509 (February 11): 489-498.

Lim, J T, G A Piazza, E K Han, T M Delohery, H Li, T S Finn, R Buttyan, et al. 1999. Sulindac derivatives inhibit growth and induce apoptosis in human prostate cancer cell lines. *Biochemical Pharmacology* 58, no. 7 (October 1): 1097-1107.

Loveridge, C J, A D H MacDonald, H C Thoms, M G Dunlop, and L A Stark. 2008. The proapoptotic effects of sulindac, sulindac sulfone and indomethacin are mediated by nucleolar translocation of the RelA(p65) subunit of NF-kappaB. *Oncogene* 27, no. 18 (April 17): 2648-2655.

Magrath, I. 2003. Chemotherapy in developing countries--is less better? *European Journal of Cancer (Oxford, England: 1990)* 39, no. 11 (July): 1497-1500.

Mahmoud, N N, S K Boolbol, A J Dannenberg, J R Mestre, R T Bilinski, C Martucci, H L Newmark, A Chadburn, and M M Bertagnolli. 1998. The sulfide metabolite of sulindac prevents tumors and restores enterocyte apoptosis in a murine model of familial adenomatous polyposis. *Carcinogenesis* 19, no. 1 (January): 87-91.

Malkinson, A M, K M Koski, L D Dwyer-Nield, P L Rice, N Rioux, A Castonguay, D J Ahnen, H Thompson, R Pamukcu, and G A Piazza. 1998. Inhibition of 4-(methylnitrosamino)-1-(3-pyridyl)-1-butanone-induced mouse lung tumor formation by FGN-1 (sulindac sulfone). *Carcinogenesis* 19, no. 8 (August): 1353-1356.

Mantovani, Alberto, Paola Allavena, Antonio Sica, and Frances Balkwill. 2008. Cancer-related inflammation. *Nature* 454, no. 7203 (July 24): 436-444.

Matsuhashi, N, A Nakajima, Y Fukushima, Y Yazaki, and T Oka. 1997. Effects of sulindac on sporadic colorectal adenomatous polyps. *Gut* 40, no. 3 (March): 344-349.

McIntyre, M C, M N Ruesch, and L A Laimins. 1996. Human papillomavirus E7 oncoproteins bind a single form of cyclin E in a complex with cdk2 and p107. *Virology* 215, no. 1 (January 1): 73-82.

Mitchell, M F, W N Hittelman, W K Hong, R Lotan, and D Schottenfeld. 1994. The natural history of cervical intraepithelial neoplasia: an argument for intermediate endpoint biomarkers. *Cancer Epidemiology, Biomarkers & Prevention: A Publication of the American Association for Cancer Research, Cosponsored by the American Society of Preventive Oncology* 3, no. 7 (November): 619-626.

Mori, H, T Hanabayashi, Y Yamada, and T Tamaya. 1990. Decrease in interferon-gamma production by peripheral blood mononuclear cells in patients with uterine cervical cancer. *Journal of Clinical Immunology* 10, no. 1 (January): 45-51.

Mukherjee, Debabrata. 2002. Selective cyclooxygenase-2 (COX-2) inhibitors and potential risk of cardiovascular events. *Biochemical Pharmacology* 63, no. 5 (March 1): 817-821.

Müller-Decker, Karin, Gerhard Fürstenberger, Nadine Annan, Dagmar Kucher, Andrea Pohl-Arnold, Brigitte Steinbauer, Irene Esposito, et al. 2006. Preinvasive duct-derived neoplasms in pancreas of keratin 5-promoter cyclooxygenase-2 transgenic mice. *Gastroenterology* 130, no. 7 (June): 2165-2178.

Nakamura, K, A Hongo, J Kodama, Y Miyagi, M Yoshinouchi, and T Kudo. 2000. Down-regulation of the insulin-like growth factor I receptor by antisense RNA can reverse the transformed phenotype of human cervical cancer cell lines. *Cancer Research* 60, no. 3 (February 1): 760-765.

Nguyen, Christine L, and Karl Münger. 2008. Direct association of the HPV16 E7 oncoprotein with cyclin A/CDK2 and cyclin E/CDK2 complexes. *Virology* 380, no. 1 (October 10): 21-25.

Nugent, K P, K C Farmer, A D Spigelman, C B Williams, and R K Phillips. 1993. Randomized controlled trial of the effect of sulindac on duodenal and rectal polyposis and cell proliferation in patients with familial adenomatous polyposis. *The British Journal of Surgery* 80, no. 12 (December): 1618-1619.

Oshima, M, J E Dinchuk, S L Kargman, H Oshima, B Hancock, E Kwong, J M Trzaskos, J F Evans, and M M Taketo. 1996. Suppression of intestinal polyposis in Apc delta716 knockout mice by inhibition of cyclooxygenase 2 (COX-2). *Cell* 87, no. 5 (November 29): 803-809.

Ostör, A G. 1993. Natural history of cervical intraepithelial neoplasia: a critical review. *International Journal of Gynecological Pathology: Official Journal of the International Society of Gynecological Pathologists* 12, no. 2 (April): 186-192.

Parkin, D M, F I Bray, and S S Devesa. 2001. Cancer burden in the year 2000. The global picture. *European Journal of Cancer (Oxford, England: 1990)* 37 Suppl 8 (October): S4-66.

Parkin, D Max, Freddie Bray, J Ferlay, and Paola Pisani. 2005. Global cancer statistics, 2002. *CA: A Cancer Journal for Clinicians* 55, no. 2 (April): 74-108.

Pasricha, P J, A Bedi, K O'Connor, A Rashid, A J Akhtar, M L Zahurak, S Piantadosi, S R Hamilton, and F M Giardiello. 1995. The effects of sulindac on colorectal proliferation and apoptosis in familial adenomatous polyposis. *Gastroenterology* 109, no. 3 (September): 994-998.

Pei, X F, J M Meck, D Greenhalgh, and R Schlegel. 1993. Cotransfection of HPV-18 and v-fos DNA induces tumorigenicity of primary human keratinocytes. *Virology* 196, no. 2 (October): 855-860.

Piazza, G A, W J Thompson, R Pamukcu, H W Alila, C M Whitehead, L Liu, J R Fetter, et al. 2001. Exisulind, a novel proapoptotic drug, inhibits rat urinary bladder tumorigenesis. *Cancer Research* 61, no. 10 (May 15): 3961-3968.

Pisani, P, D M Parkin, F Bray, and J Ferlay. 1999. Estimates of the worldwide mortality from 25 cancers in 1990. *International Journal of Cancer. Journal International Du Cancer* 83, no. 1 (September 24): 18-29.

Riendeau, D, S Charleson, W Cromlish, J A Mancini, E Wong, and J Guay. 1997. Comparison of the cyclooxygenase-1 inhibitory properties of nonsteroidal anti-inflammatory drugs (NSAIDs) and selective COX-2 inhibitors, using sensitive microsomal and platelet assays. *Canadian Journal of Physiology and Pharmacology* 75, no. 9 (September): 1088-1095.

Rozic, J G, C Chakraborty, and P K Lala. 2001. Cyclooxygenase inhibitors retard murine mammary tumor progression by reducing tumor cell migration, invasiveness and angiogenesis. *International Journal of Cancer. Journal International Du Cancer* 93, no. 4 (August 15): 497-506.

Ryu, H S, K H Chang, H W Yang, M S Kim, H C Kwon, and K S Oh. 2000. High cyclooxygenase-2 expression in stage IB cervical cancer with lymph node metastasis or parametrial invasion. *Gynecologic Oncology* 76, no. 3 (March): 320-325.

Scheper, Mark A, Nikolaos G Nikitakis, Risa Chaisuparat, Silvia Montaner, and John J Sauk. 2007. Sulindac induces apoptosis and inhibits tumor growth in vivo in head and neck squamous cell carcinoma. *Neoplasia (New York, N.Y.)* 9, no. 3 (March): 192-199.

Seo, A-Mi, Seung-Woo Hong, Jae-Sik Shin, In-Chul Park, Nam-Joo Hong, Dae-Jin Kim, Won-Keun Lee, Wang-Jae Lee, Dong-Hoon Jin, and Myeong-Sok Lee. 2009. Sulindac induces apoptotic cell death in susceptible human breast cancer cells through, at least in part, inhibition of IKKbeta. *Apoptosis: An International Journal on Programmed Cell Death* 14, no. 7 (July): 913-922.

Sheng, H, J Shao, J D Morrow, R D Beauchamp, and R N DuBois. 1998. Modulation of apoptosis and Bcl-2 expression by prostaglandin E2 in human colon cancer cells. *Cancer Research* 58, no. 2 (January 15): 362-366.

Sheng, H, J Shao, M K Washington, and R N DuBois. 2001. Prostaglandin E2 increases growth and motility of colorectal carcinoma cells. *The Journal of Biological Chemistry* 276, no. 21 (May 25): 18075-18081.

Shiff, S J, L Qiao, L L Tsai, and B Rigas. 1995. Sulindac sulfide, an aspirin-like compound, inhibits proliferation, causes cell cycle quiescence, and induces apoptosis in HT-29 colon adenocarcinoma cells. *The Journal of Clinical Investigation* 96, no. 1 (July): 491-503.

Smith, W L, D L DeWitt, and R M Garavito. 2000. Cyclooxygenases: structural, cellular, and molecular biology. *Annual Review of Biochemistry* 69: 145-182.

Song, S, A Liem, J A Miller, and P F Lambert. 2000. Human papillomavirus types 16 E6 and E7 contribute differently to carcinogenesis. *Virology* 267, no. 2 (February 15): 141-150.

Subbaramaiah, K, N Telang, J T Ramonetti, R Araki, B DeVito, B B Weksler, and A J Dannenberg. 1996. Transcription of cyclooxygenase-2 is enhanced in transformed mammary epithelial cells. *Cancer Research* 56, no. 19 (October 1): 4424-4429.

Subbaramaiah, Kotha, and Andrew J Dannenberg. 2003. Cyclooxygenase 2: a molecular target for cancer prevention and treatment. *Trends in Pharmacological Sciences* 24, no. 2 (February): 96-102.

Subbaramaiah, Kotha, and Andrew J Dannenberg. 2007. Cyclooxygenase-2 transcription is regulated by human papillomavirus 16 E6 and E7 oncoproteins: evidence of a corepressor/coactivator exchange. *Cancer Research* 67, no. 8 (April 15): 3976-3985.

Tanaka, T, T Kojima, N Yoshimi, S Sugie, and H Mori. 1991. Inhibitory effect of the non-steroidal anti-inflammatory drug, indomethacin on the naturally occurring carcinogen, 1-hydroxyanthraquinone in male ACI/N rats. *Carcinogenesis* 12, no. 10 (October): 1949-1952.

Thompson, H J, C Jiang, J Lu, R G Mehta, G A Piazza, N S Paranka, R Pamukcu, and D J Ahnen. 1997. Sulfone metabolite of sulindac inhibits mammary carcinogenesis. *Cancer Research* 57, no. 2 (January 15): 267-271.

Thompson, W J, G A Piazza, H Li, L Liu, J Fetter, B Zhu, G Sperl, D Ahnen, and R Pamukcu. 2000. Exisulind induction of apoptosis involves guanosine 3',5'-cyclic monophosphate phosphodiesterase inhibition, protein kinase G activation, and attenuated beta-catenin. *Cancer Research* 60, no. 13 (July 1): 3338-3342.

Thun, Michael J, S Jane Henley, and Carlo Patrono. 2002. Nonsteroidal anti-inflammatory drugs as anticancer agents: mechanistic, pharmacologic, and clinical issues. *Journal of the National Cancer Institute* 94, no. 4 (February 20): 252-266.

Tiano, Howard F, Charles D Loftin, Jackie Akunda, Christopher A Lee, Judson Spalding, Alisha Sessoms, David B Dunson, et al. 2002. Deficiency of either cyclooxygenase (COX)-1 or COX-2 alters epidermal differentiation and reduces mouse skin tumorigenesis. *Cancer Research* 62, no. 12 (June 15): 3395-3401.

Tommasino, M, J P Adamczewski, F Carlotti, C F Barth, R Manetti, M Contorni, F Cavalieri, T Hunt, and L Crawford. 1993. HPV16 E7 protein associates with the protein kinase p33CDK2 and cyclin A. *Oncogene* 8, no. 1 (January): 195-202.

Tsujii, M, S Kawano, and R N DuBois. 1997. Cyclooxygenase-2 expression in human colon cancer cells increases metastatic potential. *Proceedings of the National Academy of Sciences of the United States of America* 94, no. 7 (April 1): 3336-3340.

Tsujii, M, S Kawano, S Tsuji, H Sawaoka, M Hori, and R N DuBois. 1998. Cyclooxygenase regulates angiogenesis induced by colon cancer cells. *Cell* 93, no. 5 (May 29): 705-716.

Vane, J R, Y S Bakhle, and R M Botting. 1998. Cyclooxygenases 1 and 2. *Annual Review of Pharmacology and Toxicology* 38: 97-120.

Vane, J R, and R M Botting. 1998. Mechanism of action of antiinflammatory drugs. *International Journal of Tissue Reactions* 20, no. 1: 3-15.

Waddell, W R, and R W Loughry. 1983. Sulindac for polyposis of the colon. *Journal of Surgical Oncology* 24, no. 1 (September): 83-87.

Wang, Sophia S, Mark E Sherman, Allan Hildesheim, James V Lacey, and Susan Devesa. 2004. Cervical adenocarcinoma and squamous cell carcinoma incidence trends among white women and black women in the United States for 1976-2000. *Cancer* 100, no. 5 (March 1): 1035-1044.

Waskewich, Chris, Rosalyn D Blumenthal, Honglan Li, Rhona Stein, David M Goldenberg, and Jack Burton. 2002. Celecoxib exhibits the greatest potency amongst cyclooxygenase (COX) inhibitors for growth inhibition of COX-2-negative hematopoietic and epithelial cell lines. *Cancer Research* 62, no. 7 (April 1): 2029-2033.

White, A E, E M Livanos, and T D Tlsty. 1994. Differential disruption of genomic integrity and cell cycle regulation in normal human fibroblasts by the HPV oncoproteins. *Genes & Development* 8, no. 6 (March 15): 666-677.

Williams, C S, and R N DuBois. 1996. Prostaglandin endoperoxide synthase: why two isoforms? *The American Journal of Physiology* 270, no. 3 Pt 1 (March): G393-400.

Williams, C S, A P Goldman, H Sheng, J D Morrow, and R N DuBois. 1999. Sulindac sulfide, but not sulindac sulfone, inhibits colorectal cancer growth. *Neoplasia (New York, N.Y.)* 1, no. 2 (June): 170-176.

Williams, C S, M Tsujii, J Reese, S K Dey, and R N DuBois. 2000. Host cyclooxygenase-2 modulates carcinoma growth. *The Journal of Clinical Investigation* 105, no. 11 (June): 1589-1594.

Wolff, H, K Saukkonen, S Anttila, A Karjalainen, H Vainio, and A Ristimäki. 1998. Expression of cyclooxygenase-2 in human lung carcinoma. *Cancer Research* 58, no. 22 (November 15): 4997-5001.

Wu, Y L, B Sun, X J Zhang, S N Wang, H Y He, M M Qiao, J Zhong, and J Y Xu. 2001. Growth inhibition and apoptosis induction of Sulindac on Human gastric cancer cells. *World Journal of Gastroenterology: WJG* 7, no. 6 (December): 796-800.

Yamamoto, Y, M J Yin, K M Lin, and R B Gaynor. 1999. Sulindac inhibits activation of the NF-kappaB pathway. *The Journal of Biological Chemistry* 274, no. 38 (September 17): 27307-27314.

Yasui, Hiroshi, Masaaki Adachi, and Kohzoh Imai. 2003. Combination of tumor necrosis factor-alpha with sulindac augments its apoptotic potential and suppresses tumor growth of human carcinoma cells in nude mice. *Cancer* 97, no. 6 (March 15): 1412-1420.

Young, Jennifer L, Amir A Jazaeri, Christopher J Darus, and Susan C Modesitt. 2008. Cyclooxygenase-2 in cervical neoplasia: a review. *Gynecologic Oncology* 109, no. 1 (April): 140-145.

Zhang, Bei, Jia-yin Liu, Jin-shun Pan, Su-ping Han, Xiao-xing Yin, Bing Wang, and Gang Hu. 2006. Combined treatment of ionizing radiation with genistein on cervical cancer HeLa cells. *Journal of Pharmacological Sciences* 102, no. 1 (September): 129-135.

Zhang, Tao, Jeremy Z Fields, Saundra M Ehrlich, and Bruce M Boman. 2004. The chemopreventive agent sulindac attenuates expression of the antiapoptotic protein survivin in colorectal carcinoma cells. *The Journal of Pharmacology and Experimental Therapeutics* 308, no. 2 (February): 434-437.

Zhang, X, S G Morham, R Langenbach, and D A Young. 1999. Malignant transformation and antineoplastic actions of nonsteroidal antiinflammatory drugs (NSAIDs) on cyclooxygenase-null embryo fibroblasts. *The Journal of Experimental Medicine* 190, no. 4 (August 16): 451-459.

Zhu, Jiuxiang, Jui-Wen Huang, Ping-Hui Tseng, Ya-Ting Yang, Joseph Fowble, Chung-Wai Shiau, Yeng-Jeng Shaw, Samuel K Kulp, and Ching-Shih Chen. 2004. From the cyclooxygenase-2 inhibitor celecoxib to a novel class of 3-phosphoinositide-dependent protein kinase-1 inhibitors. *Cancer Research* 64, no. 12 (June 15): 4309-4318.

# Chapter Six

# General Discussion

## 6.1 General discussion

The hypothesis behind this thesis was that while high-risk HPV E6 and E7 are not sufficient to induce malignant transformation in the cervix (White *et al.*, 1994; Song *et al.*, 2000), they do provide an environment whereby malignant transformation can occur at higher rates than normally observed. The overall objective of this thesis was to further substantiate this view, and to investigate novel pathways involved in the pathogenesis of cervical cancer. This was achieved by suppressing the expression of the endogenously expressed viral oncogenes. A two pronged approach was taken: i). the expression of E6 and E7 was concomitantly silenced at the RNA level by the use of RNAi technology, and ii). the protein product of the E7 oncogene was targeted using a pharmacological approach, involving the NSAID sulindac.

In chapter 3, siRNA targeted towards the HPV16 E7 coding region were designed and validated. It was demonstrated that three out of five designed siRNA were highly functional, denoted as E7#1, E7#2 and E7#3, inducing approximately a 70% reduction in the mRNA expression level of E7 and E6 simultaneously. The concomitant silencing of HPV E6 and E7 was anticipated due to the bicistonic nature of their mRNA transcript (Stacey *et al.*, 1995; Stacey *et al.*, 2000), and has previously been described in other studies examining the effect of E7 siRNA in HPV systems (Koivusalo *et al.*, 2006; Yamato *et al.*, 2006; Bai *et al.*, 2006; Yoshinouchi *et al.*, 2003; Lea *et al.*, 2007; Sima *et al.*, 2008; Yamato *et al.*, 2008). While all three siRNA induced a similar significant knockdown at RNA level their efficacy at the protein level varied. E7#1 and E7#2 induced a similar level of response, with E7#1 being slightly more potent, while E7#3 induced a significant but smaller response in comparison to the other two siRNA. These findings were initially observed through western blot analysis of downstream targets of E6 and E7 activity, p53, Rb and p21, but were confirmed in all further protein based analysis, e.g. flow cytometry analysis. Furthermore, the microarray and TaqMan® validation experiments of chapter 6 also highlighted a similar trend. The microarray data demonstrated that the effect of the E7#3 siRNA was less than that of E7#1; evident in the fold change expression values calculated for the differentially

expressed genes. The TaqMan data validated this trend between E7#1 and E7#3 siRNA and in addition, substantiated the original proteome based findings that the level of E7#2 activity fell in between that of the other two siRNA. To observe differences in the efficacy of siRNA is not an unusual or unexpected result, particularly when it is put in the context of the many considerations that must be made when designing siRNA (Amarzguioui and Prydz, 2004; Hsieh *et al.*, 2004; Jagla *et al.*, 2005; Patzel *et al.*, 2005; Reynolds *et al.*, 2004; Shabalina *et al.*, 2006; Ui-Tel *et al.*, 2004). Additionally one must appreciates that we do not yet have an exhaustive list of criteria for siRNA design (Hajeri and Singh, 2009). The important point to take from this analysis is that in order to identify highly effective siRNA, which is particularly important in the therapeutic setting, multiple siRNA targeting different regions of the siRNA should be examined.

The silencing of HPV16 E6 and E7 resulted in significant alterations in both the phenotype and the cell cycle distribution of the cells. In contrast, even though the western blot data demonstrated a stabilisation in the expression of the pro-apoptotic protein p53, there was no indication that apoptosis was occurring as a result of the knockdown of E6/E7. This finding was validated by our microarray data, where no differential expression of apoptotic genes was observed. While this lack of an apoptotic response to the silencing of E6/E7 is in contrast with several studies that have examined the effect of siRNA mediated HPV E6 and/or E7 knockdown in cervical cancer models (Jiang and Milner,2002; Butz *et al.*, 2003; Yamato *et al.*, 2006; Lea *et al.*, 2007; Jonson *et al.*, 2008; Sima *et al.*, 2008), it corroborates that of many others (Hall and Alexander, 2003; Yoshinouchi *et al.*, 2003; Putral *et al.*, 2005; Koivusalo *et al.*, 2005; Bai *et al.*, 2006; Kuner *et al.*, 2007; Yamato *et al.*, 2008). The discrepancy between these studies is an ongoing matter of discussion. However an emerging explanation is that under non-stress conditions, the knockdown of the HPV oncogenes does not induce pro-apoptotic signals, therefore the activation of any pro-apoptotic proteins due to the silencing of E6 and/or E7 is reversed and consequently apoptosis does not occur (Koivusalo *et al.*, 2005; Koivusalo *et al.*, 2006). This insinuates that where apoptosis did occur in conjunction with E6 and/or E7 silencing that these cells

were exposed to a cellular stressor. Interestingly all the studies where apoptosis was observed to occur used doses of siRNA in the 100nM range and high dosage is considered a potential stress factor (Gu *et al.*, 2006).

A particularly interesting finding from these RNAi experiment was that while no apoptotic profile changes were observed, there were many indications that senescence may be occurring post E6/E7 silencing. By 96hrs, after the introduction of the siRNA the cells displayed distinctive phenotypic properties of senescence; including an enlarged and flattened morphology, loss of contact inhibition and increased cytoplasmic granularity (Campisi *et al.*, 2007; Dimri *et al.*, 1995; Sedivy, 1998). This finding was supported by flow cytometry analysis where there was an increase in both forward and side scatter profiles of E7 siRNA transfected cells, indicating an increase in size and cellular granularity respectively. Additionally, the cells transfected with E7 targeting siRNA demonstrated one of the defining characteristics of a senescent cell a G1 arrest (Campisi *et al.*, 2007; Dimri *et al.*, 1995; Sedivy, 1998), which primarily resulted from the loss of the S phase. Furthermore, the flow cytometry analysis performed on annexin V and PI dual stained cells indicated that there was the possibility that E7 siRNA transfected cells were increasing in fluorescence, a known biochemical property of senescent cells (Campisi *et al.*, 2007; Dimri *et al.*, 1995; Sedivy, 1998). Cellular senescence is the phenomenon by which cells permanently and irreversibly lose the ability to undergo cell division and is a potent anti-cancer mechanism (Caino *et al.*, 2009). Naturally cervical basal epithelial cells will, as they move towards the mucosal surface, undergo irreversible senescence and differentiation. The function of HPV E6 and E7 is to inhibit this process, allowing the maintenance of a replicative competent environment (Doorbar, 2006). Therefore, it should not be entirely unexpected that the silencing of their expression would result in senescence. Indeed several other studies, where E6/E7 expression has been silenced, either by ectopic expression of E2 or by RNAi, have demonstrated a senescent phenotype (Goodwin and DiManio, 2001; Lee *et al.*, 2002; Wells *et al.*, 2000; Wells *et*

*al.*, 2003; DeFilippis *et al.* 2003; Hall and Alexander, 2003; Putral *et al.*, 2005; Kuner *et al.*, 2007; Yamato *et al.*, 2008).

There are two major signalling pathways in senescence, the $p16^{INk4A}$/Rb and the ARF/p53 pathways (Caino *et al.*, 2009), both of which could potentially be activated by the loss of E6/E7 expression. Although molecular cross-talk between these two pathways has been reported, the consensus is that senescence signalling primarily uses one of the pathways (Campisi, 2005; Wright and Shay 2002). A study by DeFillippis *et al.* (2003) demonstrated that in a HPV positive cervical cancer model system, senescence induced by the suppression of E6/E7, which was due to ectopic expression of E2, is primarily mediated by the loss of E7 rather than E6 expression. Since the best characterised activity of E7 is its interaction with Rb and as the DeFillippis *et al.* study demonstrated that stabilisation of p53, an E6 target protein, was not required for a senescent phenotype, it would appear that senescence which occurs due to the loss of HPV E6/E7 activity is mediated through the $p16^{INk4A}$/Rb pathway. The principle steps in this pathway are, the expression of $p16^{INk4A}$, which results in the activation of the Rb protein, i.e. it is found in its hypophosphorylated form, which in turn leads to silencing of E2F responsive genes through heterochromatin formation (Alcorta *et al.*, 1996; Lowe *et al.*, 2003; Stein *et al.*, 1999). In relation to our data, it would seem plausible that this pathway was being activated, as the western blot analysis of E7 siRNA transfected cells demonstrated that the principle form of Rb found in these cells was the hypophosphorylated form and the microarray data showed that $p16^{INk4A}$, which is well established to be overexpressed in cervical cancer, was not altered post E6/E7 knockdown.

While chapter 3 described the silencing of E6/E7 mRNA expression in a HPV16 positive cervical cancer model system, a complimentary study was performed in chapter 5 where the expression of the protein product of the E7 oncogene was degraded. This was achieved in a HPV18 positive cervical cancer model system by treating the cells with doses of 57.5μM and greater of the NSAID sulindac. The expressional loss of E7

was determined to be post-transcriptionally mediated, as there was no reciprocal decrease at the mRNA level. In addition, there was no corresponding decrease in E6 expression, which proves this activity must be post-transcriptionally mediated since, as discussed and proven earlier the bicistronic nature of the E6/E7 mRNA transcript means that it is not possible to silence E7 without having a corresponding effect on E6 (Stacey *et al.*, 1995; Stacey *et al.*, 2000). This result confirms that of a previous study by Karl *et al.* (2007) who also demonstrated that sulindac could induce a post-transcriptional degradation of HPV18 E7. In addition, the study by Karl *et al.* (2007) provided evidence to suggest the mechanism of action of sulindac on E7 was potentially mediated by the proteosomal pathway, a finding which we plan to verify in the future.

The activity of sulindac was not only examined in the HeLa cells but also in two other cell cervical cancer lines, HPV16 positive SiHa cells and the HPV negative C33A cells. While it was possible to demonstrate that sulindac had an anti-proliferative activity on all three cell lines examined, the efficacy was most profound in the HeLa cell line. The exact reason for this discrepancy was not established, however it was postulated that it was due to the different origins of these cells lines. We based this view on previous findings in breast cancer cells, where sulindac was observed to be more potent in cell lines with a higher transforming ability (Nakamura *et al.*, 2000). The HeLa cell line is derived from a HPV18 positive adenocarcinoma, both factors which are considered independently to infer a higher degree of malignancy compared to squamous cell carcinoma and HPV16, respectively. Nakamura *et al.* (2000) demonstrated that this variation in the breast cancer cells was due to the expression of IKκB. Presently there is no evidence to suggest that is the case in these cervical cancer cell lines, but it is potentially due to altered gene expression levels of one or several genes. Two sources lead us to make this supposition. One, work from this laboratory has demonstrated that there are particular gene expression profile differences between the HeLa adenocarcinoma cell line and the other two cell line, such that hierarchal clustering analysis shows a strong relationship between SiHa and C33A cells but not with HeLa

cells (Astbury *et al.*, manuscript in preparation). Secondly, in a clinical setting, it has been demonstrated that tumour biopsies from squamous cell carcinomas and adenocarcinoma have different gene expression profiles (Rosty *et al.*, 2005).

The anti-proliferative activity of sulindac in HeLa cells was further evaluated and it was established that it could be attributed to both a cell cycle arrest and to increased level of apoptosis. These effects were observed using a single dosage regime of sulindac at concentrations of 115μM to 400μM. The increase in apoptosis in HeLa cells, like the anti-proliferative effect was observed to be dose and time dependent. However, it was determined that though apoptosis was the predominant phenotype post sulindac treatment, it did not account for the entire anti-proliferative activity of sulindac, therefore indicating that, there were separate apoptotic and cell cycle arrest effects being mediated by sulindac.

The cell cycle analysis performed on sulindac treated HeLa cells indicated that while the predominant effect of this drug is a G2/M arrest, these cells are also stalling in G1. Although previous findings in other cancer cell types, including colon, breast and prostate, have demonstrated the ability of sulindac to both induce apoptosis and a cell cycle arrest (Castonguay and Rioux, 1997; Piazza *et al.*, 1997; Subbegowda and Frommel, 1998; Lim *et al.*, 1999; Kim *et al.*, 2002; Karl *et al.*, 2007; Love bridge *et al.*, 2007; Seo *et al.*, 2009), a G2/M arrest has not been previously described. However, chemotherapeutic agents, including cisplatin and paclitaxel, have been demonstrated to induce a G2/M arrest in cancer cells and it is suggested that this alteration in the cell cycle is involved in mediating the apoptotic induction observed with these compounds (Eastman and Rigas, 1999; Candelaria *et al.*, 2006). In particular, it has been proposed that this effect is mediated through the functional suppression of spindle checkpoint protein activity, as both cisplatin and paclitaxel require a functional spindle checkpoint for action (Cheung *et al.*, 2005; Chabalier *et al.*, 2003). Spindle checkpoint suppression results in apoptotic cell death arising from mitotic failure including, defective spindle formation, chromosome mis-segregation, and premature mitotic exit (Yun *et al.*,

2009). Since both apoptosis and G2/M arrest are the main phenotypic outcomes of sulindac treatment, based on the results from dosages of 115μM and above, it is interesting to speculate that this alteration in the cell cycle may mediate the apoptotic induction of this compound, similar to the potential mechanism of action for cisplatin and paclitaxel.

Supporting evidence for this view comes from the lowest dose of sulindac applied to the HeLa cells, 57.5μM. This concentration of sulindac was demonstrated to induce a G1 arrest in cells 24hrs after treatment and to decrease both cell density and E7 expression over a 48hr period, but there were no indications of an increase in the apoptotic profile of these cells. This result would indicate that the less significant outcome of sulindac treatment, an apoptotic independent cell cycle arrest, is mediated through a stalling of the cell cycle in the G1 phase. The involvement of E7 degradation at this point would also seem logical, as the best characterised property of E7 is its ability to drive the cell cycle from the G1 to the S phase. Furthermore, this result with the 57.5μM concentration of sulindac also demonstrates that the observed G1 arrest is an early response to the treatment of HeLa cells with sulindac.

Chapter 3 and 5 describe some of the cellular events mediated upon E6 and/or E7 suppression. However the molecular events induced by the suppression of oncogene expression were not examined in detail. Part of the objective of this study was to examine these events, with the aim of identifying novel pathways involved in the pathogenesis of cervical cancer. While it is appreciated that E6 and E7 mediate some of their activities at the protein level there are currently no high-throughput technologies available to study a significant fraction of the proteome. Therefore, in order to get a comprehensive and unbiased view of the response to the depletion of E6/E7 expression gene expression microarray analysis was performed. This analysis was carried out on the HPV16 positive SiHa cells that were transfected with E7 siRNA and will in the future be performed with sulindac treated cells.

The array analysis performed identified 168 genes as significantly differentially expressed in the SiHa cells post E7#1 and E7#3 siRNA transfection. Furthermore, a subset of these targets were validated by TaqMan® RT-PCR in E7#2 transfected cells and a high degree of correlation was established between the expression values of these genes across all three experimental sample types, therefore indicating that the genes identified by the microarray analysis were a true representation of the alterations induced at the transcriptome level by E7 siRNA mediated E6/E7 silencing.

Interestingly, just as had been observed in the sulindac study, differences between adenocarcinoma and squamous cell carcinoma were highlighted by this analysis. A study in 2007 by Kuner *et al.* had taken a similar combinatorial approach of siRNA mediated E6/E7 loss and microarray examination to study the activities of E6 and E7, albeit in the HPV18 positive cervical cancer cell line HeLa. When a cross comparison between these two differential gene expression lists was performed only 19% of the genes described in our study were also identified in the Kuner *et al.* study. We believe the low level of correlation is due to the different origins of the cell lines analysed. Indeed this view can be substantiated by the findings of Kelley *et al.*, (2005). Again a combination of RNAi and microarray technology was utilised but in this instance the focus was solely on the activity of E6. This study analysed the transcriptional profile of several different cervical cell lines including, SiHa and HeLa cell lines, and demonstrated that E6 silencing had a greater impact on the transcriptional profile of HeLa cells than SiHa cells and that there was only a low level of correlation between the differentially expressed genes from both cell types.

While the there was disagreement between the exact results of this study and that of Kuner *et al.* (2007) the gene ontology classification of the differential regulated gene sets were highly correlated. This correlation between gene classification groups was also observed in several other studies, which examined the transcriptional profile of both *in vitro* and *in vivo* cervical cancer systems (Ahn *et al.*, 2004; Garner-Hamrick *et al.*, 2004; Thierry *et al.*, 2004; Santin *et al.*, 2005; Johung *et al.*, 2006; Kelley *et al.*,

2006). In addition, a similarity between the data set described in this study and that of Rosty *et al.*, (2005) where gene expression profiling of cancer tumour samples was performed was identified. These findings establishing the relevance of the E6 and E7 targets identified in the present study to the pathogenesis of cervical cancer.

Gene ontology classification, of the 168 genes identified as altered in expression post E6/E7 knockdown, demonstrated that the most over-represented group were cell cycle related genes, which were predominantly down-regulated. G1, S and M phase genes were represented within this classification group, thus demonstrating that upon silencing of the viral oncogenes there is a dramatic repression in the proliferative process of the cell. This validates the findings of chapter 3, where a decrease in cellular proliferation, due to cells arresting in the G1 phase of the cell cycle, was demonstrated in response to the transfection of E7 siRNA into SiHa cells. Additionally represented within this group of cell cycle genes were many biomarkers used to detect the presence of dysplastic cells within the cervix, for example the MCMs, cdc6, cdt1 and Topoisomerase II A. The down-regulation of these genes in an E6/E7 knockdown system clearly demonstrates a link between the over-expression of these biomarkers and HPV oncogene expression.

Based on the analysis of chapter 3, it was anticipated that we would observe a significant over-representation of down-regulated S phase genes. However, while there was a significant number of S phase genes identified within the 168 differentially expressed genes, the most over-represented group of cell cycle genes were M phase genes. Although unexpected this result is in agreement with several recent studies (Garner-Hamerick *et al.*, 2004; Thierry *et al.*, 2004; Rosty *et al.*, 2005; Johung *et al.*, 2007). Based on these results, it would appear that not only do the viral oncogenes influence the G1/S phase transition of the cell cycle but also the mitotic phase. Furthermore, an emerging body of evidence suggests that this effect on the mitotic phase of the cell cycle is mediate by the E7 oncogene, through its interaction with Rb (Johung *et al.*, 2005; Thierry *et al.*, 2004). The interesting aspect of this data is that

many of the genes identified within this group relate to the mitotic spindle check point. The mitotic checkpoint ensures that chromosomes are divided equally between daughter cells and is the primary mechanism preventing the chromosome instability often seen in aneuploid human tumours (Kops *et al.*, 2005). Both high-risk E6 and E7 have been demonstrated *in vivo* to induce genomic instability in normal cells (White *et al* 1994), which results in the generation of mitotic defects and aneuploidy (Duensing *et al.*, 2000; Plug-DeMaggio *et al.*, 2004). Specifically, the activity of the E7 oncogene has been demonstrated to induce centrosome multiplicity, which results in the creation of multipolar mitotic spindle poles that give rise to aberrant chromosome segregation (Duensing *et al.*, 2000). Since a down-regulation was observed in mitotic spindle checkpoint proteins, and the activity of E7 has been linked to both this point in the cell cycle and centrosome multiplicity, is interesting to speculate that the overexpression of the mitotic checkpoint may be involved in inducing centrosome multiplicity. In support of this concept is the finding that the overexpression of mitotic checkpoint TTK (also known as Mps1), the activity of which was inhibited in this study by the repression of E6/E7, has been shown to be sufficient to promote centrosome duplication (Norman *et al.*, 1999; Fisk and Winey, 2001).

A second interesting genetic instability observation gleaned from the gene ontology analysis was in relation to the FA-BRCA pathway. There was a significant representation of down-regulated members of this pathway within the data set of 168 differentially expressed genes. The FA-BRCA pathway was discovered through the identification of proteins mutated in a rare autosomal recessive chromosomal instability disorder, Fanconi anemia (Alter, 2003; Chandra *et al.*, 2005; Wang *et al.*, 2007). Patients with FA are predisposed to developing leukaemia and various solid tumours, including cervical cancer (Kutler *et al.*, 2003a). There are several reports suggesting a potential link between FA and HPV associated disease states (Hoskins *et al.*, 2009; Kutler *et al.*, 2003b; Spardy *et al.*, 2007). However, this relationship has yet to be conclusively defined. In addition, the FA pathway has been demonstrated to have a key role in maintaining chromosome stability. Of particular interest is the fact

that it has been implicated in the regulation of common fragile site stability (Howlett *et al.*, 2005; Chan *et al.*, 2009; Naim and Rosselli, 2009), which are suggested to represent preferred regions for HPV genome integration (Wentzensen *et al.*, 2004; Yu *et al.*, 2004; Thorland *et al.*, 2003). These observations of a down-regulation of the FA pathway in our data set, a potential link between FA and HPV disease states and the role it plays in chromosomal stability, especially common fragile site stability, warrant further investigation into the functionality of this pathway in relation to cervical cancer.

## 6.2 Translational implications of this study

Currently, the main translational outcomes from this thesis are the potential application of both the RNAi and the pharmacological oncogene targeting approaches as HPV-specific therapeutics. However, further evaluation and functional assessment of the microarray data produced by this study has the potential to identify both novel biomarkers and therapeutic targets.

RNAi has rapidly progressed beyond use as an *in vitro* research tool and currently many pharmaceutical companies are undertaking RNAi-based drug trials targeting various diseases and disorders such as age-related maculodegeneration (AMD), choroidal neovascularisation, HIV infection, RSV infection, HSV2 infection among many others (Nguyen *et al.*, 2008). However, as with all other therapeutic nucleic acids (TNAs) the major obstacle in the development of siRNA-based therapeutics is one of delivery. It is not possible to use naked siRNAs as they do not freely diffuse across cell membranes, therefore a delivery system is required to facilitate their entry into the cell. Different strategies have been employed for the delivery of siRNAs into cells and these include, viral based approaches, plasmid based approaches and approaches using naked siRNAs in combination with liposomes, lipid and protein antibodies (Kim and Rossi, 2009). All current clinical trials are based on the local administration of naked siRNA. Local administration is favoured over systemic, as it avoids unwanted delivery to other organs and decreased elimination through renal filtration (Aigner, 2007). Local administration of siRNA complexed with a transfection lipid has been achieved in the cervix of mice (Palliser *et al.*, 2006). However there is an issue in applying this siRNA-therapy to cervical cancer as the siRNA would need to gain entry into parabasal cells in order to achieve an effective response. Perhaps a concept to be considered is to re-create the HPV entry method, i.e. create microabrasions on the cervix and then inject the siRNA into these abrasions. This could be achieved by staining the CIN lesion with iodine (as in normal colposcopy) and then making radial abrasions into the cervix and injecting the siRNA through these abrasions

In relation to the application of the NSAID, sulindac, in a clinical setting, chapter 5 identified the fact that oral administration is not a possibility, even if it was considered this may be an effective approach at targeting the cervix. This is because the antineoplastic capabilities of sulindac towards cervical cancer were demonstrated to be diminished when the derivaities, sulfide and sulfone, of the parent form were applied. It is proposed therefore that sulindac would be administered by local application to the cervix, avoiding the gut mediated reduction of sulindac to sulfide or the oxidation of sulindac to sulfone. Local application would also mean that higher concentrations of sulindac could be applied. In relation to dosage the plasma levels of sulindac are reported to be in the region of 50μM, approximately the same as the lowest dose utilised in this study. However, this concentration did not elicit an efficacious response. This is not a problem *per se* for two reasons. One, the cells were treated with a single dosage regime, therefore the possibility exists that increasing the dosage regime will increase the potency at lower concentrations. Secondly, if the drug is to be applied in a topical manner then the concentration of the drug can be much higher, potentially as high as 1mM.

## 6.3 Future Work

In this thesis it was observed that potentially the introduction of E7 siRNA into the HPV16 positive SiHa cells, and the subsequent reduction in the mRNA level of E6/E7, resulted in the induction of a senescent phenotype. In order to full substantiate this finding it is intended that these RNAi experiments will be repeated and that β-galactosidase activity in the cells will be assessed. In addition, an exact measurement of the auto-fluorescent levels of these cells will also be made by flow cytometry analysis. These two criteria if met would fully verify a senescent phenotype.

The gene expression profile analysis on the E7 siRNA transfected cells has identified a number of differentially regulated genes from different pathways. We believe that the FA pathway and its functionality in cervical cancer could potentially be of significant importance, given its role in maintaining chromosomal fragile sites. Therefore we propose to further investigate its involvement in cervical cancer. An initial step will be to examine the expression profile of members of this pathway in cervical cancer compared to a normal control. In particular, it will be interesting to evaluate the expression of components of the pathway that did not demonstrate alteration post E6/E7 silencing. This analysis will be performed at RNA and protein level, and additionally the cellular localisation of these proteins, in particular FANCD2 and FANCI which have been demonstrated to localise to discrete sites on mitotic chromosome, will be determined. This approach should ensure a comprehensive evaluation of the activity of the FA pathway in cervical cancer.

Additionally in order to try and delineate E6 and E7 specific activities in our differentially expressed gene set it is intended to repeat the functional genomics study, which incorporated the RNAi and microarray analysis, but to specifically target E6 expression. Subsequently, a cross comparison between gene lists can be performed and E6 and E7 specific activities identified.

This thesis demonstrated that the NSAID sulindac has antineoplastic activities towards cervical cancer. Further work will be performed to examine the exact nature of the activity of this compound. This will be achieved using microarray technology to dissect out the molecular components of its action. We proposed not only to carry this work out in cervical cancer lines, but also in at least one other cancer cell line type, which is demonstrated to be responsive to sulindac anti-cancer activity, for example the prostate cancer cell line LNCAP. Since sulindac has been demonstrated to have anti-cancer activities in several different cancer models this should establish whether there is a common mechanism of action in these different cancer cell types.

The antineoplastic activities of sulindac were demonstrated to induce E7 degradation. In order to further evaluate this result several experiments will be performed. The expression of HPV16 E6 expression will be assessed in the SiHa cell line to evaluate whether there is any effect on this protein. In addition, to evaluate the suggestion of Karl *et al.* (2007) that this effect is mediated by proteasomal degradation, the cell will be pre-treated with the proteasomal inhibitor MG132 and then sulindac's ability to degrade E7 will be investigated.

## 6.4 Conclusion

Since the seminal discovery by Harald zur Hausen and colleagues of the association between HPV infection and cervical cancer (Gissmann and zur Hausen, 1980), there has been a drive to understand the casual link between these two events. It is now accepted that high-risk forms of HPV are major contributors to the development of cervical cancer (Walboomers *et al.*, 1999) and that their oncogenic potential lies in the uncontrolled expression of the two late proteins E6 and E7 (zur Hausen and deVillers, 1994; Snijders *et al.*, 2006; Pett and Coleman 2007). The last three decades of work has culminated in the development of prophylactic vaccine towards cervical cancer. However, as alluded to throughout this thesis it is essential that work into understanding the molecular events in cervical cancer is continued. While the vaccine is a huge step forward, due to its high cost global coverage will not currently been achieved. Additionally at present there is no proof that these vaccines can accelerate HPV clearance. Therefore they are unlikely to be of significant benefit to the large number of individuals with established lesions who are already infected with oncogenic HPV (Hildesheim *et al.*, 2007). Thus, there is still a need for the development of novel biomarkers, to facilitate more high-throughput and objective diagnosis, and tailored therapeutic agents, to improve upon the existing treatment options.

With this in mind this study aimed to gain further insight into the involvement of the HPV viral oncogenes in cervical cancer pathogenesis. Two different mechanism were employed to specifically target HPV, one was targeted against both viral oncogenes and the second the E7 oncoprotein. Both approaches had a detrimental effect on the proliferative capabilities of the cervical cancer cells. The oncogene targeted approach stalled the cells in the G1 phase and potentially induced senescence (a supposition that will be verified in the future). The second, the oncoprotein approach induced both cell cycle arrest and apoptosis. Thus, demonstrating the potential utility in specifically targeting HPV oncogenes in a clinical setting.

The downstream effects of RNAi mediated silencing of the viral oncogenes was examined by transcriptome profiling. We were able to demonstrate relevance of the

E6 and E7 targets identified in the present study to the pathogenesis of cervical cancer, by comparing our result to those of previous studies. Interestingly there was a significant over-representation of both mitotic spindle genes and members of the FA-BRCA pathway, both of which play a role in chromosomal maintenance. This is potentially important as one mechanism by which E6 and E7 are believed to augment the accumulation of pro-oncogeneic alterations is through chromosomal instability. Since it is of interest to determine the factors by which E6 and E7 create a pro-oncogenic enviroment investigations into the role FA-BRCA and mitotic spindle proteins in this process will be pursued in future.

## 6.5 References

Ahn, Woong Shick, Su Mi Bae, Joon Mo Lee, Sung Eun Namkoong, Sei-Jun Han, Young Lae Cho, Gye Hyun Nam, Jeong-Sun Seo, Chong Kook Kim, and Yong-Wan Kim. 2004. Searching for pathogenic gene functions to cervical cancer. *Gynecologic Oncology* 93, no. 1 (April): 41-48.

Aigner, Achim. 2007. Applications of RNA interference: current state and prospects for siRNA-based strategies in vivo. *Applied Microbiology and Biotechnology* 76, no. 1 (August): 9-21.

Alcorta, D A, Y Xiong, D Phelps, G Hannon, D Beach, and J C Barrett. 1996. Involvement of the cyclin-dependent kinase inhibitor p16 (INK4a) in replicative senescence of normal human fibroblasts. *Proceedings of the National Academy of Sciences of the United States of America* 93, no. 24 (November 26): 13742-13747.

Alter, Blanche P. 2003. Cancer in Fanconi anemia, 1927-2001. *Cancer* 97, no. 2 (January 15): 425-440.

Amarzguioui, Mohammed, and Hans Prydz. 2004. An algorithm for selection of functional siRNA sequences. *Biochemical and Biophysical Research Communications* 316, no. 4 (April 16): 1050-1058.

Astbuty K, Martin CM, Sheils O, O'Leary JJ. *Manuscript in prepartation.*

Bai, L, L Wei, J Wang, X Li, and P He. 2006. Extended effects of human papillomavirus 16 E6-specific short hairpin RNA on cervical carcinoma cells. *International Journal of Gynecological Cancer: Official Journal of the International Gynecological Cancer Society* 16, no. 2 (April): 718-729.

Butz, Karin, Tutik Ristriani, Arnd Hengstermann, Claudia Denk, Martin Scheffner, and Felix Hoppe-Seyler. 2003. siRNA targeting of the viral E6 oncogene efficiently kills human papillomavirus-positive cancer cells. *Oncogene* 22, no. 38 (September 4): 5938-5945.

Caino, M Cecilia, John Meshki, and Marcelo G Kazanietz. 2009. Hallmarks for senescence in carcinogenesis: novel signaling players. *Apoptosis: An International Journal on Programmed Cell Death* 14, no. 4 (April): 392-408.

Campisi, Judith. 2005. Senescent cells, tumor suppression, and organismal aging: good citizens, bad neighbors. *Cell* 120, no. 4 (February 25): 513-522.

Campisi, Judith, and Fabrizio d'Adda di Fagagna. 2007. Cellular senescence: when bad things happen to good cells. *Nature Reviews. Molecular Cell Biology* 8, no. 9 (September): 729-740.

Candelaria, Myrna, Alicia Garcia-Arias, Lucely Cetina, and Alfonso Dueñas-Gonzalez. 2006. Radiosensitizers in cervical cancer. Cisplatin and beyond. *Radiation Oncology (London, England)* 1: 15.

Castonguay, A, and N Rioux. 1997. Inhibition of lung tumourigenesis by sulindac: comparison of two experimental protocols. *Carcinogenesis* 18, no. 3 (March): 491-496.

Chabalier, C, C Lamare, C Racca, M Privat, A Valette, and F Larminat. 2006. BRCA1 downregulation leads to premature inactivation of spindle checkpoint and confers paclitaxel resistance. *Cell Cycle (Georgetown, Tex.)* 5, no. 9 (May): 1001-1007.

Chan, Kok Lung, Timea Palmai-Pallag, Songmin Ying, and Ian D Hickson. 2009. Replication stress induces sister-chromatid bridging at fragile site loci in mitosis. *Nature Cell Biology* 11, no. 6 (June): 753-760.

Chandra, Saurabh, Orna Levran, Ingrid Jurickova, Chiel Maas, Rick Kapur, Detlev Schindler, Rashida Henry, et al. 2005. A rapid method for retrovirus-mediated identification of complementation groups in Fanconi anemia patients. *Molecular Therapy: The Journal of the American Society of Gene Therapy* 12, no. 5 (November): 976-984.

Cheung, Hiu Wing, Dong-Yan Jin, Ming-Tat Ling, Yong Chuan Wong, Qi Wang, Sai Wah Tsao, and Xianghong Wang. 2005. Mitotic arrest deficient 2 expression induces chemosensitization to a DNA-damaging agent, cisplatin, in nasopharyngeal carcinoma cells. *Cancer Research* 65, no. 4 (February 15): 1450-1458.

DeFilippis, Rosa Anna, Edward C Goodwin, Lingling Wu, and Daniel DiMaio. 2003. Endogenous human papillomavirus E6 and E7 proteins differentially regulate proliferation, senescence, and apoptosis in HeLa cervical carcinoma cells. *Journal of Virology* 77, no. 2 (January): 1551-1563.

Dimri, G P, X Lee, G Basile, M Acosta, G Scott, C Roskelley, E E Medrano, M Linskens, I Rubelj, and O Pereira-Smith. 1995. A biomarker that identifies senescent human cells in culture and in aging skin in vivo. *Proceedings of the National Academy of Sciences of the United States of America* 92, no. 20 (September 26): 9363-9367.

Doorbar, John. 2006. Molecular biology of human papillomavirus infection and cervical cancer. *Clinical Science (London, England: 1979)* 110, no. 5 (May): 525-541.

Duensing, S, L Y Lee, A Duensing, J Basile, S Piboonniyom, S Gonzalez, C P Crum, and K Munger. 2000. The human papillomavirus type 16 E6 and E7 oncoproteins cooperate to induce mitotic defects and genomic instability by uncoupling centrosome duplication from the cell division cycle. *Proceedings of the National Academy of Sciences of the United States of America* 97, no. 18 (August 29): 10002-10007.

Eastman, A, and J R Rigas. 1999. Modulation of apoptosis signaling pathways and cell cycle regulation. *Seminars in Oncology* 26, no. 5 Suppl 16 (October): 7-16; discussion 41-42.

Fisk, H A, and M Winey. 2001. The mouse Mps1p-like kinase regulates centrosome duplication. *Cell* 106, no. 1 (July 13): 95-104.

Garner-Hamrick, Peggy A, J M Fostel, Wei-Ming Chien, N Sanjib Banerjee, Louise T Chow, Thomas R Broker, and Chris Fisher. 2004. Global effects of human papillomavirus type 18 E6/E7 in an organotypic keratinocyte culture system. *Journal of Virology* 78, no. 17 (September): 9041-9050.

Gissmann, L, and H zur Hausen. 1980. Partial characterization of viral DNA from human genital warts (Condylomata acuminata). *International Journal of Cancer. Journal International Du Cancer* 25, no. 5 (May 15): 605-609.

Goodwin, E C, and D DiMaio. 2001. Induced senescence in HeLa cervical carcinoma cells containing elevated telomerase activity and extended telomeres. *Cell Growth & Differentiation: The Molecular Biology Journal of the American Association for Cancer Research* 12, no. 11 (November): 525-534.

Gu, W, L Putral, K Hengst, K Minto, N A Saunders, G Leggatt, and N A J McMillan. 2006. Inhibition of cervical cancer cell growth in vitro and in vivo with lentiviral-vector delivered short hairpin RNA targeting human papillomavirus E6 and E7 oncogenes. *Cancer Gene Therapy* 13, no. 11 (November): 1023-1032.

Hajeri, Praveensingh B, and Sunit Kumar Singh. 2009. siRNAs: their potential as therapeutic agents--Part I. Designing of siRNAs. *Drug Discovery Today* 14, no. 17-18 (September): 851-858.

Hall, Allison H S, and Kenneth A Alexander. 2003. RNA interference of human papillomavirus type 18 E6 and E7 induces senescence in HeLa cells. *Journal of Virology* 77, no. 10 (May): 6066-6069.

zur Hausen, H, and E M de Villiers. 1994. Human papillomaviruses. *Annual Review of Microbiology* 48: 427-447.

Hildesheim, Allan, Rolando Herrero, Sholom Wacholder, Ana C Rodriguez, Diane Solomon, M Concepcion Bratti, John T Schiller, et al. 2007. Effect of human papillomavirus 16/18 L1 viruslike particle vaccine among young women with preexisting infection: a randomized trial. *JAMA: The Journal of the American Medical Association* 298, no. 7 (August 15): 743-753.

Hoskins, E E, T A Morris, J M Higginbotham, N Spardy, E Cha, P Kelly, D A Williams, K A Wikenheiser-Brokamp, S Duensing, and S I Wells. 2009. Fanconi anemia deficiency stimulates HPV-associated hyperplastic growth in organotypic epithelial raft culture. *Oncogene* 28, no. 5 (February 5): 674-685.

Howlett, Niall G, Toshiyasu Taniguchi, Sandra G Durkin, Alan D D'Andrea, and Thomas W Glover. 2005. The Fanconi anemia pathway is required for the DNA replication stress response and for the regulation of common fragile site stability. *Human Molecular Genetics* 14, no. 5 (March 1): 693-701.

Hsieh, Andrew C, Ronghai Bo, Judith Manola, Francisca Vazquez, Olivia Bare, Anastasia Khvorova, Stephen Scaringe, and William R Sellers. 2004. A library of siRNA duplexes targeting the phosphoinositide 3-kinase pathway: determinants of gene silencing for use in cell-based screens. *Nucleic Acids Research* 32, no. 3: 893-901.

Jagla, Bernd, Nathalie Aulner, Peter D Kelly, Da Song, Allen Volchuk, Andrzej Zatorski, David Shum, et al. 2005. Sequence characteristics of functional siRNAs. *RNA (New York, N.Y.)* 11, no. 6 (June): 864-872.

Johung, Kimberly, Edward C Goodwin, and Daniel DiMaio. 2007. Human papillomavirus E7 repression in cervical carcinoma cells initiates a transcriptional cascade driven by the retinoblastoma family, resulting in senescence. *Journal of Virology* 81, no. 5 (March): 2102-2116.

Jonson, Amy L, Lisa M Rogers, Sundaram Ramakrishnan, and Levi S Downs. 2008. Gene silencing with siRNA targeting E6/E7 as a therapeutic intervention in a mouse model of cervical cancer. *Gynecologic Oncology* 111, no. 2 (November): 356-364.

Karl, Theresia, Nadine Seibert, Michael Stöhr, Hans Osswald, Frank Rösl, and Patrick Finzer. 2007. Sulindac induces specific degradation of the HPV oncoprotein E7 and causes growth arrest and apoptosis in cervical carcinoma cells. *Cancer Letters* 245, no. 1-2 (January 8): 103-111.

Kelley, Melissa L, Kerri E Keiger, Chan Jae Lee, and Jon M Huibregtse. 2005. The global transcriptional effects of the human papillomavirus E6 protein in cervical carcinoma cell lines are mediated by the E6AP ubiquitin ligase. *Journal of Virology* 79, no. 6 (March): 3737-3747.

Kim, Daniel, and John Rossi. 2008. RNAi mechanisms and applications. *BioTechniques* 44, no. 5 (April): 613-616.

Kim, Kye Young, Ji Yeon Seol, Geong-A Jeon, and Myeong Jin Nam. 2003. The combined treatment of aspirin and radiation induces apoptosis by the regulation of bcl-2 and caspase-3 in human cervical cancer cell. *Cancer Letters* 189, no. 2 (January 28): 157-166.

Koivusalo, Riku, Eberhard Krausz, Hans Helenius, and Sakari Hietanen. 2005. Chemotherapy compounds in cervical cancer cells primed by reconstitution of p53 function after short interfering RNA-mediated degradation of human papillomavirus 18 E6 mRNA: opposite effect of siRNA in combination with different drugs. *Molecular Pharmacology* 68, no. 2 (August): 372-382.

Koivusalo, Riku, Antoine Mialon, Hanna Pitkänen, Jukka Westermarck, and Sakari Hietanen. 2006. Activation of p53 in cervical cancer cells by human papillomavirus E6 RNA interference is transient, but can be sustained by inhibiting endogenous nuclear export-dependent p53 antagonists. *Cancer Research* 66, no. 24 (December 15): 11817-11824.

Kops, Geert J P L, Beth A A Weaver, and Don W Cleveland. 2005. On the road to cancer: aneuploidy and the mitotic checkpoint. *Nature Reviews. Cancer* 5, no. 10 (October): 773-785.

Kuner, Ruprecht, Markus Vogt, Holger Sultmann, Andreas Buness, Susanne Dymalla, Julia Bulkescher, Mark Fellmann, Karin Butz, Annemarie Poustka, and Felix Hoppe-Seyler. 2007. Identification of cellular targets for the human papillomavirus E6 and E7 oncogenes by RNA interference and transcriptome analyses. *Journal of Molecular Medicine (Berlin, Germany)* 85, no. 11 (November): 1253-1262.

Kutler, David I, Arleen D Auerbach, Jaya Satagopan, Philip F Giampietro, Sat Dev Batish, Andrew G Huvos, Andy Goberdhan, Jatin P Shah, and Bhuvanesh Singh. 2003. High incidence of head and neck squamous cell carcinoma in patients with Fanconi anemia. *Archives of Otolaryngology--Head & Neck Surgery* 129, no. 1 (January): 106-112.

Kutler, David I, Bhuvanesh Singh, Jaya Satagopan, Sat Dev Batish, Marianne Berwick, Philip F Giampietro, Helmut Hanenberg, and Arleen D Auerbach. 2003. A 20-year perspective on the International Fanconi Anemia Registry (IFAR). *Blood* 101, no. 4 (February 15): 1249-1256.

Lea, Jayanthi S, Noriaki Sunaga, Mitsuo Sato, Geetha Kalahasti, David S Miller, John D Minna, and Carolyn Y Muller. 2007. Silencing of HPV 18 oncoproteins With RNA interference causes growth inhibition of cervical cancer cells. *Reproductive Sciences (Thousand Oaks, Calif.)* 14, no. 1 (January): 20-28.

Lee, Chan Jae, Eun Jung Suh, Hyun Tae Kang, Jun Sub Im, Soo Jong Um, Jong Sup Park, and Eun Seong Hwang. 2002. Induction of senescence-like state and suppression of telomerase activity through inhibition of HPV E6/E7 gene expression in cells immortalized by HPV16 DNA. *Experimental Cell Research* 277, no. 2 (July 15): 173-182.

Lim, J T, G A Piazza, E K Han, T M Delohery, H Li, T S Finn, R Buttyan, et al. 1999. Sulindac derivatives inhibit growth and induce apoptosis in human prostate cancer cell lines. *Biochemical Pharmacology* 58, no. 7 (October 1): 1097-1107.

Loveridge, C J, A D H MacDonald, H C Thoms, M G Dunlop, and L A Stark. 2008. The proapoptotic effects of sulindac, sulindac sulfone and indomethacin are mediated by nucleolar translocation of the RelA(p65) subunit of NF-kappaB. *Oncogene* 27, no. 18 (April 17): 2648-2655.

Naim, Valeria, and Filippo Rosselli. 2009. The FANC pathway and BLM collaborate during mitosis to prevent micro-nucleation and chromosome abnormalities. *Nature Cell Biology* 11, no. 6 (June): 761-768.

Nakamura, K, A Hongo, J Kodama, Y Miyagi, M Yoshinouchi, and T Kudo. 2000. Down-regulation of the insulin-like growth factor I receptor by antisense RNA can reverse the transformed phenotype of human cervical cancer cell lines. *Cancer Research* 60, no. 3 (February 1): 760-765.

Narita, Masashi, Sabrina Nũnez, Edith Heard, Masako Narita, Athena W Lin, Stephen A Hearn, David L Spector, Gregory J Hannon, and Scott W Lowe. 2003. Rb-mediated heterochromatin formation and silencing of E2F target genes during cellular senescence. *Cell* 113, no. 6 (June 13): 703-716.

Nguyen, Thu, Ellen M Menocal, Jens Harborth, and Johannes H Fruehauf. 2008. RNAi therapeutics: an update on delivery. *Current Opinion in Molecular Therapeutics* 10, no. 2 (April): 158-167.

Norman, T C, D L Smith, P K Sorger, B L Drees, S M O'Rourke, T R Hughes, C J Roberts, S H Friend, S Fields, and A W Murray. 1999. Genetic selection of peptide inhibitors of biological pathways. *Science (New York, N.Y.)* 285, no. 5427 (July 23): 591-595.

Palliser, Deborah, Dipanjan Chowdhury, Qing-Yin Wang, Sandra J Lee, Roderick T Bronson, David M Knipe, and Judy Lieberman. 2006. An siRNA-based microbicide protects mice from lethal herpes simplex virus 2 infection. *Nature* 439, no. 7072 (January 5): 89-94.

Patzel, Volker, Sascha Rutz, Isabell Dietrich, Christian Köberle, Alexander Scheffold, and Stefan H E Kaufmann. 2005. Design of siRNAs producing unstructured guide-RNAs results in improved RNA interference efficiency. *Nature Biotechnology* 23, no. 11 (November): 1440-1444.

Pett, M, and N Coleman. 2007. Integration of high-risk human papillomavirus: a key event in cervical carcinogenesis? *The Journal of Pathology* 212, no. 4 (August): 356-367.

Piazza, G A, A K Rahm, T S Finn, B H Fryer, H Li, A L Stoumen, R Pamukcu, and D J Ahnen. 1997. Apoptosis primarily accounts for the growth-inhibitory properties of sulindac metabolites and involves a mechanism that is independent of cyclooxygenase inhibition, cell cycle arrest, and p53 induction. *Cancer Research* 57, no. 12 (June 15): 2452-2459.

Plug-DeMaggio, Annemieke W, Terri Sundsvold, Michelle A Wurscher, Jennifer I Koop, Aloysius J Klingelhutz, and James K McDougall. 2004. Telomere erosion and chromosomal instability in cells expressing the HPV oncogene 16E6. *Oncogene* 23, no. 20 (April 29): 3561-3571.

Putral, Lisa N, Megan J Bywater, Wenyi Gu, Nicholas A Saunders, Brian G Gabrielli, Graham R Leggatt, and Nigel A J McMillan. 2005. RNA interference against human papillomavirus oncogenes in cervical cancer cells results in increased sensitivity to cisplatin. *Molecular Pharmacology* 68, no. 5 (November): 1311-1319.

Reynolds, Angela, Devin Leake, Queta Boese, Stephen Scaringe, William S Marshall, and Anastasia Khvorova. 2004. Rational siRNA design for RNA interference. *Nature Biotechnology* 22, no. 3 (March): 326-330.

Rosty, Christophe, Michal Sheffer, Dafna Tsafrir, Nicolas Stransky, Ilan Tsafrir, Martine Peter, Patricia de Crémoux, et al. 2005. Identification of a proliferation gene cluster associated with HPV E6/E7 expression level and viral DNA load in invasive cervical carcinoma. *Oncogene* 24, no. 47 (October 27): 7094-7104.

Santin, Alessandro D, Fenghuang Zhan, Eliana Bignotti, Eric R Siegel, Stefania Cané, Stefania Bellone, Michela Palmieri, et al. 2005. Gene expression profiles of primary HPV16- and HPV18-infected early stage cervical cancers and normal cervical epithelium: identification of novel candidate molecular markers for cervical cancer diagnosis and therapy. *Virology* 331, no. 2 (January 20): 269-291.

Sedivy, J M. 1998. Can ends justify the means?: telomeres and the mechanisms of replicative senescence and immortalization in mammalian cells. *Proceedings of the National Academy of Sciences of the United States of America* 95, no. 16 (August 4): 9078-9081.

Seo, A-Mi, Seung-Woo Hong, Jae-Sik Shin, In-Chul Park, Nam-Joo Hong, Dae-Jin Kim, Won-Keun Lee, Wang-Jae Lee, Dong-Hoon Jin, and Myeong-Sok Lee. 2009. Sulindac induces apoptotic cell death in susceptible human breast cancer cells through, at least in part, inhibition of IKKbeta. *Apoptosis: An International Journal on Programmed Cell Death* 14, no. 7 (July): 913-922.

Shabalina, Svetlana A, Alexey N Spiridonov, and Aleksey Y Ogurtsov. 2006. Computational models with thermodynamic and composition features improve siRNA design. *BMC Bioinformatics* 7: 65.

Sima, Ni, Wei Wang, Debo Kong, Dongrui Deng, Qian Xu, Jianfeng Zhou, Gang Xu, et al. 2008. RNA interference against HPV16 E7 oncogene leads to viral E6 and E7 suppression in cervical cancer cells and apoptosis via upregulation of Rb and p53. *Apoptosis: An International Journal on Programmed Cell Death* 13, no. 2 (February): 273-281.

Snijders, Peter J F, Renske D M Steenbergen, Daniëlle A M Heideman, and Chris J L M Meijer. 2006. HPV-mediated cervical carcinogenesis: concepts and clinical implications. *The Journal of Pathology* 208, no. 2 (January): 152-164.

Song, S, A Liem, J A Miller, and P F Lambert. 2000. Human papillomavirus types 16 E6 and E7 contribute differently to carcinogenesis. *Virology* 267, no. 2 (February 15): 141-150.

Spardy, Nicole, Anette Duensing, Domonique Charles, Nathan Haines, Tomomi Nakahara, Paul F Lambert, and Stefan Duensing. 2007. The human papillomavirus type 16 E7 oncoprotein activates the Fanconi anemia (FA) pathway and causes accelerated chromosomal instability in FA cells. *Journal of Virology* 81, no. 23 (December): 13265-13270.

Stacey, S N, D Jordan, P J Snijders, M Mackett, J M Walboomers, and J R Arrand. 1995. Translation of the human papillomavirus type 16 E7 oncoprotein from bicistronic mRNA is independent of splicing events within the E6 open reading frame. *Journal of Virology* 69, no. 11 (November): 7023-7031.

Stacey, S N, D Jordan, A J Williamson, M Brown, J H Coote, and J R Arrand. 2000. Leaky scanning is the predominant mechanism for translation of human papillomavirus type 16 E7 oncoprotein from E6/E7 bicistronic mRNA. *Journal of Virology* 74, no. 16 (August): 7284-7297.

Stein, G H, L F Drullinger, A Soulard, and V Dulić. 1999. Differential roles for cyclin-dependent kinase inhibitors p21 and p16 in the mechanisms of senescence and differentiation in human fibroblasts. *Molecular and Cellular Biology* 19, no. 3 (March): 2109-2117.

Subbegowda, R, and T O Frommel. 1998. Aspirin toxicity for human colonic tumor cells results from necrosis and is accompanied by cell cycle arrest. *Cancer Research* 58, no. 13 (July 1): 2772-2776.

Thierry, Françoise, Mohammed Abderrafi Benotmane, Caroline Demeret, Marcella Mori, Sébastien Teissier, and Christian Desaintes. 2004. A genomic approach reveals a novel mitotic pathway in papillomavirus carcinogenesis. *Cancer Research* 64, no. 3 (February 1): 895-903.

Thorland, Erik C, Shannon L Myers, Bobbie S Gostout, and David I Smith. 2003. Common fragile sites are preferential targets for HPV16 integrations in cervical tumors. *Oncogene* 22, no. 8 (February 27): 1225-1237.

Ui-Tei, Kumiko, Yuki Naito, Fumitaka Takahashi, Takeshi Haraguchi, Hiroko Ohki-Hamazaki, Aya Juni, Ryu Ueda, and Kaoru Saigo. 2004. Guidelines for the selection of highly effective siRNA sequences for mammalian and chick RNA interference. *Nucleic Acids Research* 32, no. 3: 936-948.

Walboomers, J M, M V Jacobs, M M Manos, F X Bosch, J A Kummer, K V Shah, P J Snijders, J Peto, C J Meijer, and N Muñoz. 1999. Human papillomavirus is a necessary cause of invasive cervical cancer worldwide. *The Journal of Pathology* 189, no. 1 (September): 12-19.

Wang, Weidong. 2007. Emergence of a DNA-damage response network consisting of Fanconi anaemia and BRCA proteins. *Nature Reviews. Genetics* 8, no. 10 (October): 735-748.

Wells, S I, D A Francis, A Y Karpova, J J Dowhanick, J D Benson, and P M Howley. 2000. Papillomavirus E2 induces senescence in HPV-positive cells via pRB- and p21(CIP)-dependent pathways. *The EMBO Journal* 19, no. 21 (November 1): 5762-5771.

Wells, Susanne I, Bruce J Aronow, Trisha M Wise, Sarah S Williams, Jennifer A Couget, and Peter M Howley. 2003. Transcriptome signature of irreversible senescence in human papillomavirus-positive cervical cancer cells. *Proceedings of the National Academy of Sciences of the United States of America* 100, no. 12 (June 10): 7093-7098.

Wentzensen, Nicolas, Svetlana Vinokurova, and Magnus von Knebel Doeberitz. 2004. Systematic review of genomic integration sites of human papillomavirus genomes in epithelial dysplasia and invasive cancer of the female lower genital tract. *Cancer Research* 64, no. 11 (June 1): 3878-3884.

White, A E, E M Livanos, and T D Tlsty. 1994. Differential disruption of genomic integrity and cell cycle regulation in normal human fibroblasts by the HPV oncoproteins. *Genes & Development* 8, no. 6 (March 15): 666-677.

Wright, Woodring E, and Jerry W Shay. 2002. Historical claims and current interpretations of replicative aging. *Nature Biotechnology* 20, no. 7 (July): 682-688.

Yamato, K, J Fen, H Kobuchi, Y Nasu, T Yamada, T Nishihara, Y Ikeda, M Kizaki, and M Yoshinouchi. 2006. Induction of cell death in human papillomavirus 18-positive cervical cancer cells by E6 siRNA. *Cancer Gene Therapy* 13, no. 3 (March): 234-241.

Yamato, K, T Yamada, M Kizaki, K Ui-Tei, Y Natori, M Fujino, T Nishihara, et al. 2008. New highly potent and specific E6 and E7 siRNAs for treatment of HPV16 positive cervical cancer. *Cancer Gene Therapy* 15, no. 3 (March): 140-153.

Yoshinouchi, Mitsuo, Taketo Yamada, Masahiro Kizaki, Jin Fen, Takeyoshi Koseki, Yasuo Ikeda, Tatsuji Nishihara, and Kenji Yamato. 2003. In vitro and in vivo growth suppression of human papillomavirus 16-positive cervical cancer cells by E6 siRNA. *Molecular Therapy: The Journal of the American Society of Gene Therapy* 8, no. 5 (November): 762-768.

Yu, Tingxi, Matthew J Ferber, Tak Hong Cheung, Tong Kwok Hung Chung, Yick Fu Wong, and David I Smith. 2005. The role of viral integration in the development of cervical cancer. *Cancer Genetics and Cytogenetics* 158, no. 1 (April 1): 27-34.

Yun, Miyong, Young-Hoon Han, Sun Hee Yoon, Hee Young Kim, Bu-Yeo Kim, Yeun-Jin Ju, Chang-Mo Kang, et al. 2009. p31comet Induces cellular senescence through p21 accumulation and Mad2 disruption. *Molecular Cancer Research: MCR* 7, no. 3 (March): 371-382.

# Appendix

**Table 1: Group I - List of 168 common differentially expressed genes (≥2 fold change and ≤0.05 FDR).**

| Gene Symbol | Gene Annotation | NCBI Link | E7#1 | | | E7#3 | | |
|---|---|---|---|---|---|---|---|---|
| | | | FC | P-value | FDR | FC | P-value | FDR |
| SPATA18 | spermatogenesis associated 18 homolog (rat) | NM_145263 | 6.61 | 4.12E-04 | 3.65E-02 | 6.51 | 1.94E-04 | 1.73E-02 |
| ACTA2 | actin alpha 2 smooth muscle aorta | NM_001613 | 4.11 | 2.55E-04 | 3.05E-02 | 3.71 | 1.71E-04 | 1.65E-02 |
| BTG2 | BTG family member 2 | NM_006763 | 3.81 | 3.77E-04 | 3.53E-02 | 3.81 | 9.55E-05 | 1.28E-02 |
| MDM2 | Mdm2 p53 binding protein homolog (mouse) | NM_002392 | 3.71 | 8.00E-05 | 2.50E-02 | 2.61 | 3.12E-04 | 2.24E-02 |
| CDKN1A | cyclin-dependent kinase inhibitor 1A (p21 Cip1) | NM_078467 | 3.21 | 9.21E-05 | 2.52E-02 | 2.51 | 6.82E-06 | 6.07E-03 |
| RPS27L | ribosomal protein S27-like | NM_015920 | 3.01 | 9.44E-04 | 4.94E-02 | 2.81 | 7.86E-05 | 1.17E-02 |
| TRIM22 | tripartite motif-containing 22 | NM_006074 | 3.01 | 7.82E-04 | 4.59E-02 | 2.21 | 7.52E-04 | 3.68E-02 |
| FDXR | ferredoxin reductase | NM_024417 | 2.81 | 8.19E-04 | 4.67E-02 | 2.41 | 6.93E-04 | 3.54E-02 |
| BLOC1S2 | Biogenesis of lysosomal organelles complex-1 subunit 2 | NM_001001342 | 2.11 | 7.05E-05 | 2.51E-02 | 2.31 | 4.91E-04 | 2.93E-02 |
| RAB4B | RAB4B member RAS oncogene family | NM_016154 | 2.11 | 7.66E-04 | 4.57E-02 | 2.21 | 5.31E-04 | 3.00E-02 |
| EXO1 | exonuclease 1 | NM_130398 | -10.71 | 4.26E-05 | 3.03E-02 | -5.01 | 1.40E-05 | 7.80E-03 |
| ASPM | asp (abnormal spindle) homolog microcephaly associated (Drosophila) | NM_018136 | -9.01 | 8.42E-04 | 4.76E-02 | -4.01 | 4.31E-06 | 5.11E-03 |
| DTL | denticleless homolog (Drosophila) | NM_016448 | -8.81 | 3.13E-04 | 3.32E-02 | -4.41 | 1.94E-05 | 7.52E-03 |
| HIST1H3G | histone cluster 1 H3g | NM_003534 | -8.51 | 9.25E-04 | 4.89E-02 | -3.71 | 5.74E-04 | 3.13E-02 |
| CDC6 | cell division cycle 6 homolog (S. cerevisiae) | NM_001254 | -8.51 | 2.20E-04 | 3.08E-02 | -3.51 | 4.86E-05 | 1.04E-02 |
| NCAPG | non-SMC condensin I complex subunit G | NM_022346 | -8.31 | 7.82E-04 | 4.61E-02 | -3.41 | 2.54E-05 | 8.38E-03 |
| CENPI | centromere protein I | NM_006733 | -8.01 | 4.01E-04 | 3.64E-02 | -3.41 | 1.86E-05 | 7.69E-03 |
| MKI67 | antigen identified by monoclonal antibody Ki-67 | NM_002417 | -7.81 | 6.54E-04 | 4.31E-02 | -2.81 | 5.21E-05 | 1.03E-02 |

| Gene Symbol | Gene Annotation | NCBI Link | E7#1 | | | E7#3 | | |
|---|---|---|---|---|---|---|---|---|
| | | | FC | P-value | FDR | FC | P-value | FDR |
| C15orf42 | chromosome 15 open reading frame 42 | NM_152259 | -7.81 | 5.82E-05 | 2.52E-02 | -3.71 | 1.88E-05 | 7.62E-03 |
| KIFC1 | kinesin family member C1 | NM_002263 | -7.41 | 2.34E-04 | 3.13E-02 | -3.31 | 7.55E-06 | 6.11E-03 |
| RAD51AP1 | RAD51 associated protein 1 | NM_001130862 | -7.31 | 9.21E-05 | 2.48E-02 | -3.61 | 7.06E-06 | 5.98E-03 |
| DLGAP5 | discs large (Drosophila) homolog-associated protein 5 | NM_014750 | -7.31 | 8.87E-04 | 4.77E-02 | -3.01 | 9.24E-05 | 1.27E-02 |
| CDCA7 | cell division cycle associated 7 | NM_031942 | -7.31 | 6.80E-04 | 4.34E-02 | -4.21 | 8.67E-04 | 4.02E-02 |
| SHCBP1 | SHC SH2-domain binding protein 1 | NM_024745 | -7.01 | 7.11E-04 | 4.41E-02 | -3.01 | 1.62E-05 | 7.61E-03 |
| KIF4A | kinesin family member 4A | NM_012310 | -7.01 | 3.23E-04 | 3.32E-02 | -3.31 | 3.19E-05 | 9.02E-03 |
| CDCA2 | cell division cycle associated 2 | NM_152562 | -7.01 | 2.42E-05 | 2.39E-02 | -3.31 | 1.43E-05 | 7.26E-03 |
| MYBL2 | v-myb myeloblastosis viral oncogene homolog (avian)-like 2 | NM_002466 | -6.91 | 2.86E-04 | 3.25E-02 | -2.51 | 3.78E-04 | 2.54E-02 |
| BUB1 | budding uninhibited by benzimidazoles 1 homolog (yeast) | NM_004336 | -6.31 | 2.43E-04 | 3.14E-02 | -2.91 | 7.54E-05 | 1.18E-02 |
| TOP2A | topoisomerase (DNA) II alpha 170kDa | NM_001067 | -6.21 | 7.44E-04 | 4.50E-02 | -3.21 | 6.61E-05 | 1.13E-02 |
| ORC1L | origin recognition complex subunit 1-like (yeast) | NM_004153 | -6.21 | 2.36E-04 | 3.11E-02 | -4.51 | 3.66E-06 | 5.44E-03 |
| NCAPH | non-SMC condensin I complex subunit H | NM_015341 | -6.21 | 5.87E-04 | 4.15E-02 | -3.31 | 1.22E-04 | 1.42E-02 |
| NCAPG2 | non-SMC condensin II complex subunit G2 | NM_017760 | -6.11 | 7.15E-04 | 4.42E-02 | -3.41 | 4.19E-06 | 5.32E-03 |
| MCM10 | minichromosome maintenance complex component 10 | NM_182751 | -6.11 | 2.97E-05 | 2.40E-02 | -3.51 | 2.46E-06 | 3.98E-03 |
| CIT | citron (rho-interacting serine/threonine kinase 21) | NM_007174 | -6.11 | 5.79E-04 | 4.11E-02 | -2.71 | 1.54E-06 | 3.42E-03 |
| PRC1 | protein regulator of cytokinesis 1 | NM_003981 | -6.01 | 8.94E-04 | 4.78E-02 | -2.31 | 1.65E-04 | 1.63E-02 |
| MCM7 | minichromosome maintenance complex component 7 | NM_005916 | -6.01 | 2.18E-04 | 3.09E-02 | -3.61 | 1.67E-04 | 1.62E-02 |
| GAS2L3 | growth arrest-specific 2 like 3 | NM_174942 | -5.91 | 2.73E-04 | 3.18E-02 | -2.81 | 3.68E-04 | 2.52E-02 |
| FOXM1 | forkhead box M1 | NM_202002 | -5.91 | 1.70E-04 | 2.77E-02 | -2.11 | 2.81E-05 | 8.62E-03 |

| Gene Symbol | Gene Annotation | NCBI Link | E7#1 | | | E7#3 | | |
|---|---|---|---|---|---|---|---|---|
| | | | FC | P-value | FDR | FC | P-value | FDR |
| CASC5 | cancer susceptibility candidate 5 | NM_170589 | -5.91 | 1.68E-04 | 2.82E-02 | -3.51 | 1.47E-05 | 7.25E-03 |
| UHRF1 | ubiquitin-like with PHD and ring finger domains 1 | NM_001048201 | -5.81 | 4.51E-04 | 3.75E-02 | -3.01 | 9.55E-04 | 4.28E-02 |
| SPAG5 | sperm associated antigen 5 | NM_006461 | -5.81 | 3.71E-04 | 3.49E-02 | -2.81 | 4.86E-04 | 2.93E-02 |
| NDC80 | NDC80 homolog kinetochore complex component (S. cerevisiae) | NM_006101 | -5.81 | 4.39E-04 | 3.76E-02 | -3.31 | 5.50E-05 | 1.04E-02 |
| TROAP | trophinin associated protein (tastin) | NM_005480 | -5.41 | 8.23E-04 | 4.68E-02 | -2.51 | 7.64E-04 | 3.71E-02 |
| MELK | maternal embryonic leucine zipper kinase | NM_014791 | -5.41 | 4.87E-04 | 3.91E-02 | -4.11 | 3.75E-04 | 2.53E-02 |
| LMNB1 | lamin B1 | NM_005573 | -5.41 | 4.26E-04 | 3.74E-02 | -2.41 | 2.34E-04 | 1.90E-02 |
| CEP55 | centrosomal protein 55kDa | NM_018131 | -5.41 | 4.34E-04 | 3.74E-02 | -2.71 | 9.47E-05 | 1.28E-02 |
| KIF14 | kinesin family member 14 | NM_014875 | -5.31 | 1.77E-04 | 2.81E-02 | -2.91 | 1.58E-05 | 7.62E-03 |
| FANCI | Fanconi anemia complementation group I | NM_001113378 | -5.31 | 7.34E-05 | 2.42E-02 | -3.01 | 5.75E-06 | 5.69E-03 |
| ZWINT | ZW10 interactor | NM_032997 | -5.21 | 7.56E-04 | 4.54E-02 | -3.01 | 6.14E-04 | 3.26E-02 |
| NUF2 | NUF2 NDC80 kinetochore complex component homolog (S. cerevisiae) | NM_145697 | -5.21 | 7.82E-04 | 4.62E-02 | -2.91 | 6.62E-04 | 3.44E-02 |
| BUB1B | budding uninhibited by benzimidazoles 1 homolog beta (yeast) | NM_001211 | -5.21 | 2.89E-04 | 3.24E-02 | -2.61 | 1.89E-04 | 1.72E-02 |
| POLQ | polymerase (DNA directed) theta | NM_199420 | -5.11 | 1.42E-04 | 2.64E-02 | -3.31 | 1.15E-04 | 1.38E-02 |
| MCM5 | minichromosome maintenance complex component 5 | NM_006739 | -5.11 | 4.70E-04 | 3.86E-02 | -3.01 | 2.01E-04 | 1.77E-02 |
| FBXO5 | F-box protein 5 | NM_012177 | -5.11 | 5.94E-04 | 4.14E-02 | -2.91 | 4.98E-04 | 2.95E-02 |
| TMEM194A | transmembrane protein 194A | NM_001130963 | -5.01 | 3.13E-04 | 3.33E-02 | -3.81 | 3.07E-07 | 5.46E-03 |
| NUSAP1 | nucleolar and spindle associated protein 1 | NM_016359 | -5.01 | 6.32E-04 | 4.24E-02 | -3.01 | 2.04E-04 | 1.77E-02 |
| BLM | Bloom syndrome | NM_000057 | -5.01 | 1.09E-04 | 2.45E-02 | -3.41 | 3.42E-05 | 8.94E-03 |
| NEIL3 | nei endonuclease VIII-like 3 (E. coli) | NM_018248 | -4.91 | 6.29E-05 | 2.49E-02 | -2.91 | 1.02E-05 | 6.49E-03 |

| Gene Symbol | Gene Annotation | NCBI Link | E7#1 | | | E7#3 | | |
|---|---|---|---|---|---|---|---|---|
| | | | FC | P-value | FDR | FC | P-value | FDR |
| KIF15 | kinesin family member 15 | NM_020242 | -4.91 | 9.16E-05 | 2.55E-02 | -2.91 | 3.84E-05 | 9.50E-03 |
| TCF19 | transcription factor 19 (SC1) | NM_007109 | -4.81 | 7.60E-04 | 4.55E-02 | -2.71 | 2.17E-04 | 1.86E-02 |
| NEK2 | NIMA (never in mitosis gene a)-related kinase 2 | NM_002497 | -4.81 | 9.45E-05 | 2.40E-02 | -2.81 | 9.02E-04 | 4.10E-02 |
| MASTL | microtubule associated serine/threonine kinase-like | NM_032844 | -4.81 | 1.18E-04 | 2.47E-02 | -3.41 | 3.29E-05 | 8.88E-03 |
| ESCO2 | establishment of cohesion 1 homolog 2 (S. cerevisiae) | NM_001017420 | -4.81 | 2.37E-04 | 3.10E-02 | -3.01 | 4.32E-05 | 9.86E-03 |
| CCNE2 | cyclin E2 | NM_057749 | -4.81 | 2.49E-04 | 3.03E-02 | -3.01 | 5.04E-04 | 2.92E-02 |
| CLSPN | claspin homolog (Xenopus laevis) | NM_022111 | -4.71 | 2.07E-04 | 3.04E-02 | -3.01 | 1.37E-05 | 7.86E-03 |
| CENPK | centromere protein K | NM_022145 | -4.71 | 3.31E-04 | 3.33E-02 | -2.91 | 1.75E-06 | 3.45E-03 |
| CDC45L | CDC45 cell division cycle 45-like (S. cerevisiae) | NM_003504 | -4.71 | 8.11E-04 | 4.72E-02 | -3.31 | 9.24E-05 | 1.28E-02 |
| CDC25C | cell division cycle 25 homolog C (S. pombe) | NM_001790 | -4.71 | 1.21E-04 | 2.48E-02 | -2.71 | 4.38E-05 | 9.87E-03 |
| BRCA2 | breast cancer 2 early onset | NM_000059 | -4.71 | 2.04E-04 | 3.05E-02 | -3.11 | 1.78E-05 | 7.53E-03 |
| RAD51 | RAD51 homolog (RecA homolog E. coli) (S. cerevisiae) | NM_002875 | -4.61 | 2.18E-05 | 2.42E-02 | -2.71 | 4.88E-05 | 1.03E-02 |
| PHF19 | PHD finger protein 19 | NM_015651 | -4.61 | 9.91E-05 | 2.35E-02 | -2.91 | 6.46E-05 | 1.13E-02 |
| KIAA1524 | KIAA1524 | NM_020890 | -4.61 | 3.00E-04 | 3.32E-02 | -3.41 | 7.31E-05 | 1.15E-02 |
| DIAPH3 | diaphanous homolog 3 (Drosophila) | NM_001042517 | -4.61 | 3.02E-04 | 3.32E-02 | -2.41 | 9.44E-05 | 1.28E-02 |
| STIL | SCL/TAL1 interrupting locus | NM_001048166 | -4.51 | 7.06E-05 | 2.46E-02 | -2.81 | 8.85E-05 | 1.25E-02 |
| PRR11 | proline rich 11 | NM_018304 | -4.51 | 5.56E-04 | 4.04E-02 | -2.81 | 3.25E-04 | 2.29E-02 |
| MCM4 | minichromosome maintenance complex component 4 | NM_005914 | -4.51 | 3.27E-04 | 3.30E-02 | -3.11 | 5.01E-06 | 5.25E-03 |
| KIF23 | kinesin family member 23 | NM_138555 | -4.51 | 4.11E-04 | 3.66E-02 | -2.21 | 4.22E-04 | 2.69E-02 |
| GTSE1 | G-2 and S-phase expressed 1 | NM_016426 | -4.51 | 5.30E-04 | 4.08E-02 | -2.41 | 9.98E-05 | 1.28E-02 |

| Gene Symbol | Gene Annotation | NCBI Link | E7#1 | | | E7#3 | | |
|---|---|---|---|---|---|---|---|---|
| | | | FC | P-value | FDR | FC | P-value | FDR |
| RACGAP1 | Rac GTPase activating protein 1 | NM_013277 | -4.41 | 1.77E-04 | 2.79E-02 | -2.41 | 1.66E-05 | 7.40E-03 |
| KIF11 | kinesin family member 11 | NM_004523 | -4.41 | 3.42E-04 | 3.35E-02 | -2.51 | 1.02E-04 | 1.29E-02 |
| FAM72A | family with sequence similarity 72 member A | BC035696 | -4.41 | 6.59E-04 | 4.31E-02 | -3.21 | 2.69E-05 | 8.70E-03 |
| CENPA | centromere protein A | NM_001809 | -4.41 | 8.93E-04 | 4.79E-02 | -3.11 | 1.87E-04 | 1.71E-02 |
| C14orf145 | chromosome 14 open reading frame 145 | NM_152446 | -4.41 | 2.15E-04 | 3.06E-02 | -2.91 | 1.48E-04 | 1.52E-02 |
| DEPDC1B | DEP domain containing 1B | NM_018369 | -4.31 | 3.43E-04 | 3.34E-02 | -3.11 | 4.01E-06 | 5.49E-03 |
| CDC7 | cell division cycle 7 homolog (S. cerevisiae) | NM_003503 | -4.31 | 7.78E-05 | 2.52E-02 | -2.81 | 9.52E-06 | 6.52E-03 |
| TIMELESS | timeless homolog (Drosophila) | NM_003920 | -4.21 | 7.99E-05 | 2.54E-02 | -2.81 | 1.42E-05 | 7.45E-03 |
| RRM1 | ribonucleotide reductase M1 | NM_001033 | -4.21 | 6.29E-04 | 4.25E-02 | -3.01 | 2.51E-05 | 8.42E-03 |
| PRIM1 | primase DNA polypeptide 1 (49kDa) | NM_000946 | -4.21 | 1.20E-04 | 2.49E-02 | -3.41 | 1.59E-04 | 1.59E-02 |
| WDHD1 | WD repeat and HMG-box DNA binding protein 1 | NM_007086 | -4.11 | 1.28E-04 | 2.59E-02 | -3.11 | 1.25E-06 | 3.70E-03 |
| MCM2 | minichromosome maintenance complex component 2 | NM_004526 | -4.11 | 5.73E-04 | 4.10E-02 | -2.41 | 1.24E-04 | 1.41E-02 |
| FANCD2 | Fanconi anemia complementation group D2 | NM_033084 | -4.11 | 4.49E-05 | 2.96E-02 | -2.51 | 6.69E-05 | 1.12E-02 |
| BRIP1 | BRCA1 interacting protein C-terminal helicase 1 | NM_032043 | -4.11 | 8.68E-05 | 2.57E-02 | -2.71 | 4.60E-06 | 5.12E-03 |
| TTK | TTK protein kinase | NM_003318 | -4.01 | 2.44E-04 | 3.12E-02 | -2.21 | 3.09E-04 | 2.23E-02 |
| TMEM48 | transmembrane protein 48 | NM_018087 | -4.01 | 4.10E-04 | 3.67E-02 | -3.01 | 2.72E-04 | 2.09E-02 |
| MLF1IP | MLF1 interacting protein | NM_024629 | -4.01 | 1.05E-04 | 2.40E-02 | -2.91 | 1.48E-04 | 1.52E-02 |
| IQGAP3 | IQ motif containing GTPase activating protein 3 | NM_178229 | -4.01 | 1.17E-04 | 2.48E-02 | -2.41 | 2.76E-05 | 8.61E-03 |
| CENPE | centromere protein E 312kDa | NM_001813 | -4.01 | 4.44E-04 | 3.76E-02 | -2.61 | 5.28E-04 | 3.01E-02 |
| ZWILCH | Zwilch kinetochore associated homolog (Drosophila) | NR_003105 | -3.91 | 1.39E-04 | 2.61E-02 | -2.81 | 5.53E-07 | 4.92E-03 |

| Gene Symbol | Gene Annotation | NCBI Link | E7#1 | | | E7#3 | | |
|---|---|---|---|---|---|---|---|---|
| | | | FC | P-value | FDR | FC | P-value | FDR |
| RAD54L | RAD54-like (S. cerevisiae) | NM_003579 | -3.91 | 1.33E-05 | 3.39E-02 | -2.81 | 5.13E-05 | 1.05E-02 |
| AURKB | aurora kinase B | NM_004217 | -3.91 | 2.67E-04 | 3.14E-02 | -2.61 | 8.25E-04 | 3.91E-02 |
| ATAD5 | ATPase family AAA domain containing 5 | NM_024857 | -3.91 | 1.09E-04 | 2.43E-02 | -3.21 | 8.50E-05 | 1.23E-02 |
| ATAD2 | ATPase family AAA domain containing 2 | NM_014109 | -3.91 | 5.47E-04 | 4.04E-02 | -2.51 | 2.49E-04 | 1.97E-02 |
| PRIM2 | primase DNA polypeptide 2 (58kDa) | NM_000947 | -3.81 | 1.69E-04 | 2.79E-02 | -2.41 | 7.11E-05 | 1.14E-02 |
| BARD1 | BRCA1 associated RING domain 1 | NM_000465 | -3.81 | 1.01E-04 | 2.37E-02 | -2.01 | 4.35E-04 | 2.74E-02 |
| RBL1 | retinoblastoma-like 1 (p107) | NM_002895 | -3.71 | 1.06E-05 | 4.72E-02 | -2.61 | 2.73E-05 | 8.67E-03 |
| FANCA | Fanconi anemia complementation group A | NM_000135 | -3.71 | 3.78E-04 | 3.53E-02 | -2.91 | 1.82E-04 | 1.69E-02 |
| ESPL1 | extra spindle pole bodies homolog 1 (S. cerevisiae) | NM_012291 | -3.71 | 5.35E-04 | 4.02E-02 | -2.41 | 1.22E-04 | 1.41E-02 |
| MCM8 | minichromosome maintenance complex component 8 | NM_032485 | -3.61 | 5.69E-05 | 2.60E-02 | -2.31 | 1.38E-04 | 1.47E-02 |
| GINS4 | GINS complex subunit 4 (Sld5 homolog) | NM_032336 | -3.61 | 1.58E-05 | 2.56E-02 | -2.31 | 3.24E-05 | 8.88E-03 |
| DNA2 | DNA replication helicase 2 homolog (yeast) | NM_001080449 | -3.61 | 1.28E-05 | 3.80E-02 | -2.71 | 1.99E-05 | 7.54E-03 |
| DDX11 | DEAD/H (Asp-Glu-Ala-Asp/His) box polypeptide 11 (CHL1-like helicase homolog S. cerevisiae) | NM_030653 | -3.61 | 2.72E-05 | 2.42E-02 | -2.61 | 1.84E-04 | 1.71E-02 |
| BRCA1 | breast cancer 1 early onset | NM_007296 | -3.61 | 2.04E-05 | 2.60E-02 | -2.51 | 7.88E-06 | 6.10E-03 |
| SMC2 | structural maintenance of chromosomes 2 | NM_001042551 | -3.51 | 3.66E-04 | 3.48E-02 | -2.71 | 6.12E-05 | 1.09E-02 |
| KNTC1 | kinetochore associated 1 | NM_014708 | -3.51 | 1.35E-04 | 2.59E-02 | -2.61 | 1.31E-04 | 1.43E-02 |
| HELLS | helicase lymphoid-specific | NM_018063 | -3.51 | 3.24E-04 | 3.31E-02 | -2.51 | 1.37E-04 | 1.47E-02 |
| ECT2 | epithelial cell transforming sequence 2 oncogene | NM_018098 | -3.51 | 4.22E-04 | 3.71E-02 | -2.01 | 2.30E-04 | 1.89E-02 |
| RFC5 | replication factor C (activator 1) 5 36.5kDa | NM_001130113 | -3.41 | 5.53E-05 | 2.59E-02 | -2.61 | 5.08E-05 | 1.05E-02 |

| Gene Symbol | Gene Annotation | NCBI Link | E7#1 | | | E7#3 | | |
|---|---|---|---|---|---|---|---|---|
| | | | FC | P-value | FDR | FC | P-value | FDR |
| MCM3 | minichromosome maintenance complex component 3 | NM_002388 | -3.41 | 2.11E-04 | 3.06E-02 | -2.61 | 1.44E-06 | 3.65E-03 |
| EZH2 | enhancer of zeste homolog 2 (Drosophila) | NM_004456 | -3.41 | 5.76E-05 | 2.56E-02 | -2.31 | 5.41E-05 | 1.04E-02 |
| CCNF | cyclin F | NM_001761 | -3.41 | 2.81E-04 | 3.21E-02 | -2.01 | 3.73E-05 | 9.36E-03 |
| ZNF367 | zinc finger protein 367 | NM_153695 | -3.31 | 2.92E-05 | 2.48E-02 | -2.51 | 6.04E-04 | 3.25E-02 |
| SMC4 | structural maintenance of chromosomes 4 | NM_005496 | -3.31 | 6.33E-04 | 4.22E-02 | -2.21 | 3.16E-05 | 9.08E-03 |
| FBXO43 | F-box protein 43 | NM_001077528 | -3.31 | 4.78E-05 | 2.84E-02 | -2.11 | 1.32E-04 | 1.44E-02 |
| CDCA7L | cell division cycle associated 7-like | NM_018719 | -3.31 | 1.33E-04 | 2.57E-02 | -3.41 | 1.66E-05 | 7.58E-03 |
| C6orf167 | chromosome 6 open reading frame 167 | NM_198468 | -3.31 | 2.25E-04 | 3.08E-02 | -3.01 | 2.33E-04 | 1.90E-02 |
| TMPO | thymopoietin | NM_001032283 | -3.21 | 6.97E-04 | 4.40E-02 | -2.51 | 6.75E-05 | 1.11E-02 |
| RTKN2 | rhotekin 2 | NM_145307 | -3.21 | 6.12E-04 | 4.19E-02 | -2.41 | 1.47E-04 | 1.52E-02 |
| RFC4 | replication factor C (activator 1) 4 37kDa | NM_002916 | -3.21 | 4.77E-04 | 3.89E-02 | -2.61 | 1.60E-04 | 1.59E-02 |
| POLE2 | polymerase (DNA directed) epsilon 2 (p59 subunit) | NM_002692 | -3.21 | 1.38E-05 | 3.08E-02 | -2.11 | 1.32E-05 | 7.84E-03 |
| POLE | polymerase (DNA directed) epsilon | NM_006231 | -3.21 | 5.41E-05 | 2.60E-02 | -2.11 | 1.20E-04 | 1.41E-02 |
| POLA2 | polymerase (DNA directed) alpha 2 (70kD subunit) | NM_002689 | -3.21 | 1.53E-04 | 2.66E-02 | -2.21 | 3.23E-04 | 2.29E-02 |
| POLA1 | polymerase (DNA directed) alpha 1 catalytic subunit | NM_016937 | -3.21 | 6.99E-06 | 4.15E-02 | -2.51 | 1.05E-05 | 6.43E-03 |
| GPSM2 | G-protein signaling modulator 2 (AGS3-like C. elegans) | NM_013296 | -3.21 | 3.37E-04 | 3.35E-02 | -2.21 | 7.56E-05 | 1.17E-02 |
| MYBL1 | v-myb myeloblastosis viral oncogene homolog (avian)-like 1 | NM_001080416 | -3.11 | 3.40E-04 | 3.34E-02 | -2.21 | 8.31E-04 | 3.91E-02 |
| MAD2L1 | MAD2 mitotic arrest deficient-like 1 (yeast) | NM_002358 | -3.11 | 3.20E-04 | 3.31E-02 | -2.21 | 2.40E-05 | 8.22E-03 |
| ITGB3BP | integrin beta 3 binding protein (beta3-endonexin) | NM_014288 | -3.11 | 2.47E-04 | 3.06E-02 | -2.21 | 1.78E-04 | 1.69E-02 |
| GINS1 | GINS complex subunit 1 (Psf1 homolog) | NM_021067 | -3.11 | 6.08E-05 | 2.52E-02 | -2.51 | 2.27E-04 | 1.88E-02 |

| Gene Symbol | Gene Annotation | NCBI Link | E7#1 | | | E7#3 | | |
|---|---|---|---|---|---|---|---|---|
| | | | FC | P-value | FDR | FC | P-value | FDR |
| CDK2 | cyclin-dependent kinase 2 | NM_001798 | -3.11 | 4.58E-05 | 2.91E-02 | -2.11 | 2.18E-04 | 1.85E-02 |
| CDC25A | cell division cycle 25 homolog A (S. pombe) | NM_001789 | -3.11 | 8.69E-05 | 2.54E-02 | -2.31 | 5.90E-04 | 3.21E-02 |
| CCDC77 | coiled-coil domain containing 77 | NM_032358 | -3.11 | 6.26E-05 | 2.53E-02 | -2.11 | 5.03E-04 | 2.93E-02 |
| TOPBP1 | topoisomerase (DNA) II binding protein 1 | NM_007027 | -3.01 | 6.51E-05 | 2.46E-02 | -2.21 | 8.65E-06 | 6.16E-03 |
| CHAF1B | chromatin assembly factor 1 subunit B (p60) | NM_005441 | -3.01 | 3.25E-04 | 3.31E-02 | -2.11 | 1.05E-04 | 1.32E-02 |
| CHAF1A | chromatin assembly factor 1 subunit A (p150) | NM_005483 | -3.01 | 5.35E-05 | 2.65E-02 | -2.61 | 2.24E-04 | 1.88E-02 |
| C13orf3 | chromosome 13 open reading frame 3 | NM_145061 | -3.01 | 5.11E-04 | 4.03E-02 | -2.01 | 1.66E-04 | 1.63E-02 |
| E2F8 | E2F transcription factor 8 | NM_024680 | -2.91 | 1.12E-04 | 2.46E-02 | -2.41 | 3.98E-05 | 9.56E-03 |
| CENPJ | centromere protein J | NM_018451 | -2.91 | 3.68E-04 | 3.49E-02 | -2.51 | 4.87E-04 | 2.93E-02 |
| C6orf173 | chromosome 6 open reading frame 173 | NM_001012507 | -2.91 | 6.98E-04 | 4.39E-02 | -2.81 | 7.57E-05 | 1.16E-02 |
| RAD18 | RAD18 homolog (S. cerevisiae) | NM_020165 | -2.81 | 1.48E-04 | 2.67E-02 | -2.21 | 1.53E-04 | 1.55E-02 |
| NCAPD2 | non-SMC condensin I complex subunit D2 | NM_014865 | -2.81 | 8.18E-05 | 2.47E-02 | -2.11 | 1.43E-04 | 1.49E-02 |
| MSH2 | mutS homolog 2 colon cancer nonpolyposis type 1 (E. coli) | NM_000251 | -2.81 | 9.34E-04 | 4.92E-02 | -2.01 | 3.00E-05 | 8.90E-03 |
| FANCC | Fanconi anemia complementation group C | NM_000136 | -2.81 | 1.42E-05 | 2.81E-02 | -2.21 | 7.01E-05 | 1.13E-02 |
| TYMS | thymidylate synthetase | NM_001071 | -2.71 | 6.90E-04 | 4.37E-02 | -3.91 | 1.80E-04 | 1.69E-02 |
| C4orf21 | chromosome 4 open reading frame 21 | BC044799 | -2.71 | 2.46E-04 | 3.08E-02 | -2.11 | 4.68E-04 | 2.89E-02 |
| C18orf24 | chromosome 18 open reading frame 24 | NM_001039535 | -2.71 | 5.32E-05 | 2.71E-02 | -2.21 | 9.70E-05 | 1.29E-02 |
| RTTN | rotatin | NM_173630 | -2.61 | 2.32E-04 | 3.15E-02 | -2.21 | 1.36E-04 | 1.47E-02 |
| C18orf54 | chromosome 18 open reading frame 54 | NM_173529 | -2.61 | 5.95E-04 | 4.13E-02 | -2.51 | 7.67E-04 | 3.72E-02 |
| SMC1A | structural maintenance of chromosomes 1A | NM_006306 | -2.51 | 4.87E-05 | 2.80E-02 | -2.21 | 2.18E-05 | 7.91E-03 |

| Gene Symbol | Gene Annotation | NCBI Link | E7#1 | | | E7#3 | | |
|---|---|---|---|---|---|---|---|---|
| | | | FC | P-value | FDR | FC | P-value | FDR |
| SGOL2 | shugoshin-like 2 (S. pombe) | NM_152524 | -2.41 | 6.49E-04 | 4.29E-02 | -2.11 | 8.81E-05 | 1.25E-02 |
| E2F7 | E2F transcription factor 7 | NM_203394 | -2.41 | 6.42E-04 | 4.26E-02 | -2.01 | 5.22E-05 | 1.02E-02 |
| C6orf182 | chromosome 6 open reading frame 182 | NM_001083535 | -2.41 | 6.57E-04 | 4.32E-02 | -2.11 | 1.92E-04 | 1.73E-02 |
| MCM6 | minichromosome maintenance complex component 6 | NM_005915 | -2.31 | 3.47E-04 | 3.35E-02 | -2.11 | 4.96E-05 | 1.04E-02 |
| IL17RB | interleukin 17 receptor B | NM_018725 | -2.21 | 8.08E-05 | 2.48E-02 | -2.11 | 1.86E-04 | 1.71E-02 |
| UBR7 | ubiquitin protein ligase E3 component n-recognin 7 (putative) | NM_175748 | -2.11 | 9.54E-05 | 2.39E-02 | -2.71 | 8.45E-05 | 1.24E-02 |
| SUV39H2 | suppressor of variegation 3-9 homolog 2 (Drosophila) | NM_024670 | -2.11 | 2.24E-04 | 3.10E-02 | -2.01 | 1.28E-04 | 1.42E-02 |
| DHTKD1 | dehydrogenase E1 and transketolase domain containing 1 | NM_018706 | -2.11 | 4.84E-04 | 3.93E-02 | -2.11 | 6.11E-04 | 3.27E-02 |
| DEK | DEK oncogene | NM_003472 | -2.11 | 2.66E-04 | 3.16E-02 | -2.01 | 1.21E-03 | 4.96E-02 |
| BLMH | bleomycin hydrolase | NM_000386 | -2.11 | 6.62E-04 | 4.29E-02 | -2.11 | 2.81E-05 | 8.48E-03 |
| SUZ12 | suppressor of zeste 12 homolog (Drosophila) | NM_015355 | -2.01 | 2.79E-04 | 3.21E-02 | -2.11 | 4.14E-04 | 2.66E-02 |

**Table 2: Group II A - Significant differentially expressed by E7#1 (≥2 fold change and ≤0.05 FDR), differentially expressed by E7#3.**

| Gene Symbol | Gene Annotation | NCBI Link | E7#1 | | | E7#3 | | |
|---|---|---|---|---|---|---|---|---|
| | | | FC | P-value | FDR | FC | P-value | FDR |
| SPC25 | SPC25 NDC80 kinetochore complex component homolog (S. cerevisiae) | NM_020675 | -4.91 | 4.96E-04 | 3.96E-02 | -2.81 | 1.62E-03 | 5.96E-02 |
| HIST1H2BJ | histone cluster 1 H2bj | NM_021058 | -4.51 | 7.07E-04 | 4.43E-02 | -2.71 | 3.11E-03 | 9.29E-02 |
| BIRC5 | baculoviral IAP repeat-containing 5 | NM_001168 | -4.01 | 6.90E-05 | 2.51E-02 | -1.91 | 2.85E-04 | 2.16E-02 |
| GINS2 | GINS complex subunit 2 (Psf2 homolog) | NM_016095 | -3.91 | 6.30E-04 | 4.25E-02 | -2.81 | 1.68E-03 | 6.08E-02 |
| PSMC3IP | PSMC3 interacting protein | NM_013290 | -3.91 | 6.02E-05 | 2.55E-02 | -2.91 | 1.37E-03 | 5.33E-02 |
| PTTG1 | pituitary tumor-transforming 1 | NM_004219 | -3.91 | 4.08E-04 | 3.67E-02 | -1.81 | 1.07E-02 | 2.13E-01 |
| VRK1 | vaccinia related kinase 1 | NM_003384 | -3.41 | 1.62E-04 | 2.78E-02 | -1.81 | 4.50E-04 | 2.82E-02 |
| CENPO | centromere protein O | NM_024322 | -3.31 | 5.99E-04 | 4.15E-02 | -2.21 | 2.45E-03 | 7.75E-02 |
| HIST1H2BD | histone cluster 1 H2bd | NM_021063 | -3.31 | 6.10E-04 | 4.20E-02 | -2.21 | 1.55E-03 | 5.88E-02 |
| KIF20B | kinesin family member 20B | NM_016195 | -3.31 | 3.52E-04 | 3.37E-02 | -2.01 | 1.29E-03 | 5.17E-02 |
| POLD3 | polymerase (DNA-directed) delta 3 accessory subunit | NM_006591 | -3.31 | 1.54E-05 | 2.75E-02 | -1.91 | 1.67E-04 | 1.63E-02 |
| OVOS | ovostatin | ENST00000334227 | -3.21 | 8.60E-04 | 4.75E-02 | -2.61 | 4.17E-03 | 1.13E-01 |
| HICE1 | HEC1/NDC80 interacting centrosome associated 1 | NM_033417 | -3.11 | 7.37E-04 | 4.49E-02 | -1.81 | 1.68E-03 | 6.07E-02 |
| KIF18A | kinesin family member 18A | NM_031217 | -3.11 | 6.82E-04 | 4.34E-02 | -1.71 | 9.63E-04 | 4.29E-02 |
| C15orf23 | chromosome 15 open reading frame 23 | NM_033286 | -3.01 | 1.76E-04 | 2.82E-02 | -1.71 | 9.10E-04 | 4.10E-02 |
| CCDC99 | coiled-coil domain containing 99 | NM_017785 | -3.01 | 8.62E-04 | 4.72E-02 | -2.11 | 1.28E-03 | 5.16E-02 |
| FANCM | Fanconi anemia complementation group M | NM_020937 | -3.01 | 9.65E-05 | 2.35E-02 | -1.91 | 3.70E-05 | 9.40E-03 |
| OVOS2 | ovostatin 2 | NM_001080502 | -3.01 | 1.90E-04 | 2.92E-02 | -2.61 | 2.94E-03 | 8.89E-02 |
| WDR51A | WD repeat domain 51A | NM_015426 | -2.91 | 9.24E-05 | 2.45E-02 | -2.41 | 1.48E-03 | 5.65E-02 |
| MYO19 | myosin XIX | NM_025109 | -2.61 | 8.89E-05 | 2.55E-02 | -1.91 | 5.28E-04 | 2.99E-02 |
| NCAPD3 | non-SMC condensin II complex subunit D3 | NM_015261 | -2.61 | 3.04E-05 | 2.35E-02 | -1.91 | 6.08E-06 | 5.70E-03 |
| SASS6 | spindle assembly 6 homolog (C. elegans) | NM_194292 | -2.61 | 7.20E-05 | 2.42E-02 | -1.81 | 9.98E-05 | 1.29E-02 |

| Gene Symbol | Gene Annotation | NCBI Link | E7#1 | | | E7#3 | | |
|---|---|---|---|---|---|---|---|---|
| | | | FC | P-value | FDR | FC | P-value | FDR |
| TMEM97 | transmembrane protein 97 | NM_014573 | -2.61 | 3.39E-04 | 3.36E-02 | -1.91 | 2.22E-03 | 7.25E-02 |
| CEP78 | centrosomal protein 78kDa | NM_001098802 | -2.51 | 1.15E-04 | 2.48E-02 | -1.91 | 9.71E-05 | 1.28E-02 |
| CHEK1 | CHK1 checkpoint homolog (S. pombe) | NM_001274 | -2.51 | 9.58E-05 | 2.37E-02 | -1.91 | 4.64E-05 | 1.01E-02 |
| DSN1 | DSN1 MIND kinetochore complex component homolog (S. cerevisiae) | NM_024918 | -2.51 | 1.39E-04 | 2.63E-02 | -1.81 | 3.00E-04 | 2.22E-02 |
| LIN9 | lin-9 homolog (C. elegans) | NM_173083 | -2.51 | 5.67E-04 | 4.08E-02 | -1.91 | 5.80E-05 | 1.06E-02 |
| SMC1B | structural maintenance of chromosomes 1B | NM_148674 | -2.51 | 5.06E-06 | 4.51E-02 | -2.31 | 2.60E-03 | 8.07E-02 |
| FKBP5 | FK506 binding protein 5 | NM_004117 | -2.41 | 3.80E-04 | 3.51E-02 | -1.81 | 4.84E-03 | 1.24E-01 |
| DCK | deoxycytidine kinase | NM_000788 | -2.31 | 1.30E-04 | 2.59E-02 | -1.81 | 7.06E-03 | 1.61E-01 |
| MTBP | Mdm2 transformed 3T3 cell double minute 2 p53 binding protein (mouse) binding protein 104kDa | NM_022045 | -2.31 | 2.35E-04 | 3.12E-02 | -1.91 | 2.19E-04 | 1.86E-02 |
| WDR79 | WD repeat domain 79 | NM_018081 | -2.31 | 5.69E-04 | 4.09E-02 | -1.61 | 3.54E-03 | 1.02E-01 |
| WHSC1 | Wolf-Hirschhorn syndrome candidate 1 | NM_133330 | -2.31 | 8.72E-04 | 4.72E-02 | -1.71 | 1.77E-03 | 6.25E-02 |
| CENPN | centromere protein N | NM_001100624 | -2.21 | 6.78E-04 | 4.34E-02 | -1.61 | 1.05E-03 | 4.54E-02 |
| GEN1 | Gen homolog 1 endonuclease (Drosophila) | NM_182625 | -2.21 | 1.73E-04 | 2.80E-02 | -1.91 | 1.91E-05 | 7.54E-03 |
| NUP205 | nucleoporin 205kDa | NM_015135 | -2.21 | 1.52E-04 | 2.69E-02 | -1.61 | 2.75E-04 | 2.09E-02 |
| RBBP8 | retinoblastoma binding protein 8 | NM_002894 | -2.21 | 2.47E-04 | 3.08E-02 | -1.61 | 1.14E-03 | 4.80E-02 |
| NUP107 | nucleoporin 107kDa | NM_020401 | -2.11 | 3.19E-04 | 3.32E-02 | -1.81 | 2.14E-04 | 1.85E-02 |
| NUP85 | nucleoporin 85kDa | NM_024844 | -2.11 | 4.85E-04 | 3.91E-02 | -1.61 | 3.94E-04 | 2.60E-02 |
| ANKRD32 | ankyrin repeat domain 32 | NM_032290 | -2.01 | 2.95E-04 | 3.28E-02 | -1.61 | 8.98E-04 | 4.09E-02 |
| CASP2 | caspase 2 apoptosis-related cysteine peptidase | NM_032982 | -2.01 | 7.26E-04 | 4.44E-02 | -1.51 | 5.38E-05 | 1.04E-02 |
| CCDC18 | coiled-coil domain containing 18 | NM_206886 | -2.01 | 3.11E-04 | 3.35E-02 | -1.71 | 4.78E-04 | 2.91E-02 |
| CENPL | centromere protein L | NM_001127181 | -2.01 | 1.49E-04 | 2.65E-02 | -1.61 | 4.71E-04 | 2.90E-02 |
| CP110 | CP110 protein | NM_014711 | -2.01 | 6.61E-04 | 4.29E-02 | -1.71 | 1.85E-04 | 1.71E-02 |
| DONSON | downstream neighbor of SON | NM_017613 | -2.01 | 2.50E-04 | 3.03E-02 | -1.51 | 4.31E-04 | 2.73E-02 |

| Gene Symbol | Gene Annotation | NCBI Link | E7#1 | | | E7#3 | | |
|---|---|---|---|---|---|---|---|---|
| | | | FC | P-value | FDR | FC | P-value | FDR |
| SPATA5 | spermatogenesis associated 5 | NM_145207 | -2.01 | 4.85E-04 | 3.92E-02 | -1.91 | 1.05E-04 | 1.33E-02 |
| UBE2S | ubiquitin-conjugating enzyme E2S | NM_014501 | -2.01 | 1.48E-04 | 2.69E-02 | -1.61 | 5.76E-03 | 1.39E-01 |
| ABCC3 | ATP-binding cassette sub-family C (CFTR/MRP) member 3 | NM_003786 | 2.21 | 7.90E-04 | 4.61E-02 | 1.81 | 3.60E-04 | 2.49E-02 |
| GADD45A | growth arrest and DNA-damage-inducible alpha | NM_001924 | 2.31 | 5.92E-04 | 4.15E-02 | 1.71 | 4.48E-03 | 1.18E-01 |
| CLDN1 | claudin 1 | NM_021101 | 3.01 | 4.02E-04 | 3.63E-02 | 2.21 | 2.68E-03 | 8.24E-02 |
| SULF2 | sulfatase 2 | NM_018837 | 5.51 | 5.54E-04 | 4.06E-02 | 4.11 | 1.29E-03 | 5.18E-02 |
| SPC25 | SPC25 NDC80 kinetochore complex component homolog (S. cerevisiae) | NM_020675 | -4.91 | 4.96E-04 | 3.96E-02 | -2.81 | 1.62E-03 | 5.96E-02 |
| HIST1H2BJ | histone cluster 1 H2bj | NM_021058 | -4.51 | 7.07E-04 | 4.43E-02 | -2.71 | 3.11E-03 | 9.29E-02 |

**Table 3: Group II B - Significant differentially expressed by E7#3 (≥2 fold change and ≤0.05 FDR), differentially expressed by E7#1.**

| Gene Symbol | Gene Annotation | NCBI Link | E7#1 | | | E7#3 | | |
|---|---|---|---|---|---|---|---|---|
| | | | FC | P-value | FDR | FC | P-value | FDR |
| AEN | apoptosis enhancing nuclease | NM_022767 | 2.01 | 6.68E-03 | 1.72E-01 | 2.81 | 3.89E-04 | 2.58E-02 |
| S100A16 | S100 calcium binding protein A16 | NM_080388 | 2.71 | 9.99E-04 | 5.14E-02 | 2.81 | 1.57E-04 | 1.58E-02 |
| NINJ1 | ninjurin 1 | NM_004148 | 2.21 | 1.25E-03 | 5.98E-02 | 2.61 | 5.44E-04 | 3.05E-02 |
| FAM174A | family with sequence similarity 174 member A | NM_198507 | 2.21 | 4.41E-03 | 1.30E-01 | 2.21 | 3.07E-04 | 2.23E-02 |
| LAMB3 | laminin beta 3 | NM_001017402 | 1.71 | 4.15E-02 | 5.97E-01 | 2.21 | 5.62E-04 | 3.11E-02 |
| CTDSPL2 | CTD (carboxy-terminal domain RNA polymerase II polypeptide A) small phosphatase like 2 | NM_016396 | -1.51 | 2.07E-02 | 3.68E-01 | -2.01 | 7.66E-05 | 1.17E-02 |
| LBR | lamin B receptor | NM_002296 | -2.51 | 9.40E-03 | 2.16E-01 | -2.01 | 1.69E-05 | 7.35E-03 |
| RCCD1 | RCC1 domain containing 1 | NM_033544 | -1.71 | 4.49E-06 | 7.98E-02 | -2.01 | 7.28E-04 | 3.65E-02 |
| TPX2 | TPX2 microtubule-associated homolog (Xenopus laevis) | NM_012112 | -5.11 | 1.20E-03 | 5.82E-02 | -2.01 | 2.00E-04 | 1.77E-02 |
| DNMT3B | DNA (cytosine-5-)-methyltransferase 3 beta | NM_006892 | -2.31 | 4.94E-03 | 1.39E-01 | -2.11 | 6.92E-04 | 3.55E-02 |
| PHGDH | phosphoglycerate dehydrogenase | NM_006623 | -2.71 | 4.34E-03 | 1.29E-01 | -2.11 | 2.52E-04 | 1.98E-02 |
| CEP152 | centrosomal protein 152kDa | NM_014985 | -2.51 | 9.86E-04 | 5.09E-02 | -2.21 | 6.70E-05 | 1.11E-02 |
| HLTF | helicase-like transcription factor | NM_003071 | -1.81 | 4.45E-04 | 3.75E-02 | -2.21 | 5.70E-05 | 1.06E-02 |
| UBE2T | ubiquitin-conjugating enzyme E2T (putative) | NM_014176 | -3.31 | 1.00E-03 | 5.12E-02 | -2.21 | 3.03E-04 | 2.21E-02 |
| CKAP2L | cytoskeleton associated protein 2-like | NM_152515 | -3.91 | 1.02E-03 | 5.18E-02 | -2.31 | 3.92E-04 | 2.60E-02 |
| CCNB2 | cyclin B2 | NM_004701 | -5.31 | 1.29E-03 | 6.04E-02 | -2.41 | 6.74E-04 | 3.48E-02 |
| FLJ35848 | hypothetical protein FLJ35848 | AK302001 | -3.31 | 1.71E-03 | 7.15E-02 | -2.41 | 1.14E-03 | 4.79E-02 |
| CDT1 | chromatin licensing and DNA replication factor 1 | NM_030928 | -4.81 | 2.84E-03 | 9.66E-02 | -2.51 | 8.00E-04 | 3.82E-02 |
| STK17B | serine/threonine kinase 17b | NM_004226 | -1.51 | 2.10E-02 | 3.72E-01 | -2.51 | 5.25E-04 | 3.00E-02 |
| C5orf34 | chromosome 5 open reading frame 34 | BC036867 | -3.61 | 1.29E-03 | 6.06E-02 | -2.61 | 6.98E-07 | 4.14E-03 |
| PLK1 | polo-like kinase 1 (Drosophila) | NM_005030 | -6.51 | 1.12E-03 | 5.55E-02 | -2.71 | 2.92E-04 | 2.17E-02 |

| Gene Symbol | Gene Annotation | NCBI Link | E7#1 | | | E7#3 | | |
|---|---|---|---|---|---|---|---|---|
| | | | FC | P-value | FDR | FC | P-value | FDR |
| ARHGAP11A | Rho GTPase activating protein 11A | NM_014783 | -4.91 | 2.08E-03 | 8.08E-02 | -2.81 | 2.45E-04 | 1.95E-02 |
| DEPDC1 | DEP domain containing 1 | NM_001114120 | -4.21 | 4.57E-03 | 1.33E-01 | -2.81 | 6.21E-04 | 3.28E-02 |
| GNB4 | guanine nucleotide binding protein (G protein) beta polypeptide 4 | NM_021629 | -2.61 | 3.03E-02 | 4.77E-01 | -2.91 | 4.06E-05 | 9.51E-03 |
| KIF20A | kinesin family member 20A | NM_005733 | -7.21 | 1.99E-03 | 7.90E-02 | -2.91 | 3.24E-04 | 2.29E-02 |
| KIF2C | kinesin family member 2C | NM_006845 | -4.41 | 1.91E-03 | 7.69E-02 | -2.91 | 3.15E-04 | 2.24E-02 |
| WDR76 | WD repeat domain 76 | NM_024908 | -4.61 | 9.86E-04 | 5.10E-02 | -2.91 | 1.26E-04 | 1.42E-02 |
| CENPF | centromere protein F 350/400ka (mitosin) | NM_016343 | -7.21 | 1.01E-03 | 5.12E-02 | -3.01 | 7.69E-05 | 1.16E-02 |
| PBK | PDZ binding kinase | NM_018492 | -6.91 | 1.54E-03 | 6.82E-02 | -3.21 | 8.88E-05 | 1.24E-02 |
| CDC2 | cell division cycle 2 G1 to S and G2 to M | NM_001786 | -6.41 | 1.62E-03 | 6.98E-02 | -3.41 | 5.15E-05 | 1.04E-02 |
| ANLN | anillin actin binding protein | NM_018685 | -6.01 | 1.70E-03 | 7.13E-02 | -3.81 | 5.19E-05 | 1.04E-02 |
| CCNA2 | cyclin A2 | NM_001237 | -6.11 | 1.62E-03 | 6.97E-02 | -3.81 | 1.12E-04 | 1.37E-02 |

**Table 4: Group III A- Significant differentially expressed by E7#1 (≥2 fold change and ≤0.05 FDR) only.**

| Gene Symbol | Gene Annotation | NCBI Link | E7#3 | | |
|---|---|---|---|---|---|
| | | | FC | P-value | FDR |
| RIPK4 | receptor-interacting serine-threonine kinase 4 | NM_020639 | 2.61 | 8.51E-04 | 4.72E-02 |
| C17orf91 | chromosome 17 open reading frame 91 | NM_032895 | 2.11 | 3.89E-04 | 3.57E-02 |
| SDC4 | syndecan 4 | NM_002999 | 2.01 | 8.63E-04 | 4.71E-02 |
| NMU | neuromedin U | NM_006681 | -2.01 | 1.70E-05 | 2.53E-02 |
| LIN54 | lin-54 homolog (C. elegans) | NM_194282 | -2.01 | 6.08E-04 | 4.20E-02 |
| LMNB2 | lamin B2 | NM_032737 | -2.01 | 8.17E-04 | 4.69E-02 |
| USP37 | ubiquitin specific peptidase 37 | NM_020935 | -2.11 | 1.14E-04 | 2.48E-02 |
| TRAIP | TRAF interacting protein | NM_005879 | -2.11 | 2.03E-04 | 3.06E-02 |
| USP13 | ubiquitin specific peptidase 13 (isopeptidase T-3) | NM_003940 | -2.11 | 9.21E-04 | 4.88E-02 |
| LIG1 | ligase I DNA ATP-dependent | NM_000234 | -2.21 | 3.79E-04 | 3.51E-02 |
| LOC81691 | exonuclease NEF-sp | NM_030941 | -2.21 | 7.10E-04 | 4.42E-02 |
| CCDC5 | coiled-coil domain containing 5 (spindle associated) | NM_138443 | -2.31 | 1.31E-04 | 2.57E-02 |
| PPIL5 | peptidylprolyl isomerase (cyclophilin)-like 5 | NM_152329 | -2.31 | 5.06E-05 | 2.65E-02 |
| STAG1 | stromal antigen 1 | NM_005862 | -2.31 | 2.11E-04 | 3.08E-02 |
| RNFT2 | ring finger protein transmembrane 2 | NM_001109903 | -2.31 | 5.17E-04 | 4.02E-02 |
| RFWD3 | ring finger and WD repeat domain 3 | NM_018124 | -2.31 | 5.29E-04 | 4.09E-02 |
| RAD54B | RAD54 homolog B (S. cerevisiae) | NM_012415 | -2.41 | 2.16E-05 | 2.57E-02 |
| CCDC150 | coiled-coil domain containing 150 | NM_001080539 | -2.51 | 1.60E-04 | 2.76E-02 |
| RPA2 | replication protein A2 32kDa | NM_002946 | -2.51 | 4.34E-05 | 2.97E-02 |
| MNS1 | meiosis-specific nuclear structural 1 | NM_018365 | -2.51 | 2.78E-04 | 3.21E-02 |
| RIBC2 | RIB43A domain with coiled-coils 2 | NM_015653 | -2.51 | 5.03E-04 | 3.98E-02 |
| LOC91431 | prematurely terminated mRNA decay factor-like | NM_001099776 | -2.51 | 8.23E-04 | 4.67E-02 |
| CDC25B | cell division cycle 25 homolog B (S. pombe) | NM_021873 | -2.51 | 8.16E-04 | 4.70E-02 |
| FANCB | Fanconi anemia complementation group B | NM_001018113 | -2.61 | 5.43E-04 | 4.03E-02 |
| RFC2 | replication factor C (activator 1) 2 40kDa | NM_181471 | -2.61 | 5.41E-04 | 4.03E-02 |
| C1orf112 | chromosome 1 open reading frame 112 | BC091516 | -2.81 | 5.05E-05 | 2.72E-02 |
| CDCA8 | cell division cycle associated 8 | NM_018101 | -2.81 | 3.31E-04 | 3.31E-02 |
| KPNA2 | karyopherin alpha 2 (RAG cohort 1 importin alpha 1) | NM_002266 | -2.91 | 4.49E-04 | 3.75E-02 |
| E2F1 | E2F transcription factor 1 | NM_005225 | -3.01 | 2.45E-04 | 3.12E-02 |
| SPC24 | SPC24 NDC80 kinetochore complex component homolog | NM_182513 | -3.11 | 5.02E-04 | 3.99E-02 |
| AURKA | aurora kinase A | NM_198433 | -3.11 | 8.61E-04 | 4.73E-02 |
| CKS2 | CDC28 protein kinase regulatory subunit 2 | NM_001827 | -3.41 | 1.05E-04 | 2.42E-02 |
| KPNA2 | karyopherin alpha 2 (RAG cohort 1 importin alpha 1) | NM_002266 | -3.51 | 3.15E-04 | 3.30E-02 |
| STMN1 | stathmin 1/oncoprotein 18 | NM_203401 | -3.71 | 3.94E-04 | 3.60E-02 |

**Table 4: Group III B - Significant differentially expressed by E7#3 (≥2 fold change and ≤0.05 FDR) only.**

| Gene Symbol | Gene Annotation | NCBI Link | E7#3 | | |
|---|---|---|---|---|---|
| | | | FC | P-value | FDR |
| RHOF | ras homolog gene family member F (in filopodia) | NM_019034 | 2.61 | 3.60E-05 | 9.29E-03 |
| HMOX1 | heme oxygenase (decycling) 1 | NM_002133 | 2.51 | 2.41E-04 | 1.92E-02 |
| SERPINB5 | serpin peptidase inhibitor clade B (ovalbumin) member 5 | NM_002639 | 2.31 | 3.68E-04 | 2.53E-02 |
| LIPH | lipase member H | NM_139248 | 2.31 | 7.79E-04 | 3.77E-02 |
| SYNC | syncoilin intermediate filament protein | NM_030786 | 2.21 | 6.54E-04 | 3.42E-02 |
| CRYAB | crystallin alpha B | NM_001885 | 2.21 | 1.02E-03 | 4.47E-02 |
| PPP2R2C | protein phosphatase 2 (formerly 2A) regulatory subunit B gamma isoform | NM_020416 | 2.11 | 7.99E-04 | 3.82E-02 |
| IDUA | iduronidase alpha-L- | NM_000203 | 2.11 | 8.80E-04 | 4.04E-02 |
| LRFN3 | leucine rich repeat and fibronectin type III domain containing 3 | NM_024509 | 2.01 | 1.08E-04 | 1.34E-02 |
| SYNE2 | spectrin repeat containing nuclear envelope 2 | NM_182914 | -2.01 | 3.10E-04 | 2.24E-02 |
| TMEM181 | transmembrane protein 181 | NM_020823 | -2.11 | 1.26E-04 | 1.42E-02 |
| CNNM4 | cyclin M4 | NM_020184 | -2.11 | 1.30E-04 | 1.44E-02 |
| SORL1 | sortilin-related receptor L(DLR class) A repeats-containing | NM_003105 | -2.11 | 1.79E-04 | 1.69E-02 |
| H3F3B | H3 histone family 3B (H3.3B) | NM_005324 | -2.11 | 3.82E-04 | 2.55E-02 |
| TMEM209 | transmembrane protein 209 | NM_032842 | -2.11 | 4.55E-04 | 2.83E-02 |
| ACBD5 | acyl-Coenzyme A binding domain containing 5 | NM_145698 | -2.21 | 3.02E-05 | 8.81E-03 |
| GNPAT | glyceronephosphate O-acyltransferase | NM_014236 | -2.21 | 5.55E-05 | 1.04E-02 |
| PIGK | phosphatidylinositol glycan anchor biosynthesis class K | NM_005482 | -2.21 | 5.01E-04 | 2.93E-02 |
| TAF7L | TAF7-like RNA polymerase II TATA box binding protein (TBP)-associated factor 50kDa | NM_024885 | -2.21 | 1.14E-03 | 4.80E-02 |
| SFXN1 | sideroflexin 1 | NM_022754 | -2.41 | 9.22E-07 | 4.10E-03 |
| C14orf94 | chromosome 14 open reading frame 94 | BC001916 | -2.41 | 1.13E-04 | 1.37E-02 |

**Table 5: Genes identified on differentially expression list of Rosty *et al.* (2005) and Kuner *et al.* (2007).**

| Gene Symbol | NCBI Link | Fold change | | Present on: | |
|---|---|---|---|---|---|
| | | E7#1 | E7#3 | Rosty *et al.*, 2005 | Kuner *et al.*, 2007 |
| ASPM | NM_018136 | -9.01 | -4.01 | Yes | Yes |
| ATAD2 | NM_014109 | -3.91 | -2.51 | Yes | |
| AURKB | NM_004217 | -3.91 | -2.61 | Yes | |
| BLM | NM_000057 | -5.01 | -3.41 | Yes | |
| BRCA1 | NM_007296 | -3.61 | -2.51 | Yes | |
| BRCA2 | NM_000059 | -4.71 | -3.11 | Yes | |
| BUB1 | NM_004336 | -6.31 | -2.91 | Yes | Yes |
| BUB1B | NM_001211 | -5.21 | -2.61 | Yes | Yes |
| CCNE2 | NM_057749 | -4.81 | -3.01 | Yes | Yes |
| CCNF | NM_001761 | -3.41 | -2.01 | Yes | |
| CDC25A | NM_001789 | -3.11 | -2.31 | Yes | |
| CDC25C | NM_001790 | -4.71 | -2.71 | Yes | Yes |
| CDC45L | NM_003504 | -4.71 | -3.31 | Yes | Yes |
| CDC6 | NM_001254 | -8.51 | -3.51 | Yes | |
| CDC7 | NM_003503 | -4.31 | -2.81 | Yes | |
| CDK2 | NM_001798 | -3.11 | -2.11 | Yes | |
| CENPA | NM_001809 | -4.41 | -3.11 | Yes | |
| CENPE | NM_001813 | -4.01 | -2.61 | Yes | |
| CHAF1A | NM_005483 | -3.01 | -2.61 | Yes | |
| CHAF1B | NM_005441 | -3.01 | -2.11 | Yes | |
| CIT | NM_007174 | -6.11 | -2.71 | Yes | |
| DEK | NM_003472 | -2.11 | -2.01 | Yes | Yes |
| ECT2 | NM_018098 | -3.51 | -2.01 | Yes | |
| ESPL1 | NM_012291 | -3.71 | -2.41 | Yes | |
| EXO1 | NM_130398 | -10.71 | -5.01 | Yes | Yes |
| EZH2 | NM_004456 | -3.41 | -2.31 | Yes | Yes |
| FANCA | NM_000135 | -3.71 | -2.91 | Yes | |
| FANCC | NM_000136 | -2.81 | -2.21 | Yes | |
| FBXO5 | NM_012177 | -5.11 | -2.91 | Yes | |
| FOXM1 | NM_202002 | -5.91 | -2.11 | Yes | Yes |
| GPSM2 | NM_013296 | -3.21 | -2.21 | Yes | |
| GTSE1 | NM_016426 | -4.51 | -2.41 | Yes | |
| HELLS | NM_018063 | -3.51 | -2.51 | Yes | |
| KIF11 | NM_004523 | -4.41 | -2.51 | Yes | |
| KIF14 | NM_014875 | -5.31 | -2.91 | Yes | |
| KIF23 | NM_138555 | -4.51 | -2.21 | Yes | Yes |
| KIF4A | NM_012310 | -7.01 | -3.31 | Yes | |
| KIFC1 | NM_002263 | -7.41 | -3.31 | Yes | |
| KNTC1 | NM_014708 | -3.51 | -2.61 | Yes | |

| Gene Symbol | NCBI Link | Fold change | | Present on: | |
|---|---|---|---|---|---|
| | | E7#1 | E7#3 | Rosty *et al.*, 2005 | Kuner *et al.*, 2007 |
| LMNB1 | NM_005573 | -5.41 | -2.41 | Yes | Yes |
| MAD2L1 | NM_002358 | -3.11 | -2.21 | Yes | Yes |
| MCM10 | NM_182751 | -6.11 | -3.51 | Yes | |
| MCM2 | NM_004526 | -4.11 | -2.41 | Yes | Yes |
| MCM3 | NM_002388 | -3.41 | -2.61 | Yes | Yes |
| MCM4 | NM_005914 | -4.51 | -3.11 | Yes | |
| MCM5 | NM_006739 | -5.11 | -3.01 | Yes | |
| MCM6 | NM_005915 | -2.31 | -2.11 | Yes | Yes |
| MCM7 | NM_005916 | -6.01 | -3.61 | Yes | |
| MELK | NM_014791 | -5.41 | -4.11 | Yes | Yes |
| MKI67 | NM_002417 | -7.81 | -2.81 | Yes | |
| MLF1IP | NM_024629 | -4.01 | -2.91 | Yes | Yes |
| MSH2 | NM_000251 | -2.81 | -2.01 | Yes | |
| MYBL2 | NM_002466 | -6.91 | -2.51 | Yes | |
| NEK2 | NM_002497 | -4.81 | -2.81 | Yes | |
| NUSAP1 | NM_016359 | -5.01 | -3.01 | Yes | |
| POLA2 | NM_002689 | -3.21 | -2.21 | Yes | |
| POLE | NM_006231 | -3.21 | -2.11 | Yes | |
| POLE2 | NM_002692 | -3.21 | -2.11 | Yes | |
| POLQ | NM_199420 | -5.11 | -3.31 | Yes | |
| PRC1 | NM_003981 | -6.01 | -2.31 | Yes | Yes |
| PRIM1 | NM_000946 | -4.21 | -3.41 | Yes | |
| RACGAP1 | NM_013277 | -4.41 | -2.41 | Yes | |
| RAD51 | NM_002875 | -4.61 | -2.71 | Yes | |
| RAD51AP1 | NM_001130862 | -7.31 | -3.61 | Yes | Yes |
| RAD54L | NM_003579 | -3.91 | -2.81 | Yes | |
| RBL1 | NM_002895 | -3.71 | -2.61 | Yes | |
| RFC4 | NM_002916 | -3.21 | -2.61 | Yes | |
| RFC5 | NM_001130113 | -3.41 | -2.61 | Yes | |
| RRM1 | NM_001033 | -4.21 | -3.01 | Yes | |
| SHCBP1 | NM_024745 | -7.01 | -3.01 | Yes | |
| SPAG5 | NM_006461 | -5.81 | -2.81 | Yes | |
| TIMELESS | NM_003920 | -4.21 | -2.81 | Yes | Yes |
| TMPO | NM_001032283 | -3.21 | -2.51 | Yes | |
| TOP2A | NM_001067 | -6.21 | -3.21 | Yes | Yes |
| TOPBP1 | NM_007027 | -3.01 | -2.21 | Yes | |
| TROAP | NM_005480 | -5.41 | -2.51 | Yes | |
| TTK | NM_003318 | -4.01 | -2.21 | Yes | |
| TYMS | NM_001071 | -2.71 | -3.91 | Yes | |
| WDHD1 | NM_007086 | -4.11 | -3.11 | Yes | |
| ZWINT | NM_032997 | -5.21 | -3.01 | Yes | Yes |

| Gene Symbol | NCBI Link | Fold change | | Present on: | |
|---|---|---|---|---|---|
| | | E7#1 | E7#3 | Rosty *et al.*, 2005 | Kuner *et al.*, 2007 |
| BTG2 | NM_006763 | 3.81 | 3.81 | Yes | |
| CDKN1A | NM_078467 | 3.21 | 2.51 | | Yes |
| CEP55 | NM_018131 | -5.41 | -2.71 | | Yes |
| DTL | NM_016448 | -8.81 | -4.41 | | Yes |
| FAM72A | BC035696 | -3.81 | -3.21 | | Yes |
| FDXR | NM_024417 | 2.81 | 2.41 | | Yes |
| KIF15 | NM_020242 | -4.91 | -2.91 | | Yes |
| TMEM48 | NM_018087 | -4.01 | -3.01 | | Yes |
| ZWILCH | NR_003105 | -3.91 | -2.81 | | Yes |